U.PORTO

DOUTORAMENTO

CIÊNCIAS BIOMEDICAS

The signature of nucleus pulposus cells in homeostasis and aging

Maria Molinos

D

2017

U.PORTO

Maria Molinos. The signature of nucleus pulposus cells in homeostasis and aging

D.ICBAS **2017**

The signature of nucleus pulposus cells in homeostasis and aging Maria Cabral Maio Molinos

INSTITUTO DE CIÊNCIAS BIOMÉDICAS ABEL SALAZAR

Maria Cabral Maio Molinos

The signature of nucleus pulposus cells in homeostasis and aging

Tese de Candidatura ao grau de Doutor em Ciências Biomédicas, submetida ao Instituto de Ciências Biomédicas Abel Salazar da Universidade do Porto.

Orientador – Professor Doutor Mário Adolfo Barbosa
Categoria – Professor Catedrático
Afiliação – Instituto de Ciências Biomédicas Abel Salazar (ICBAS), Instituto de Investigação e Inovação em Saúde (i3S) e Instituto de Engenharia Biomédica (INEB), Universidade do Porto

Coorientador – Doutora Catarina Rodrigues Almeida
Categoria – Professora Auxiliar Convidada
Afiliação – Instituto de Biomedicina (iBiMED) e Departamento de Ciências Biomédicas da Universidade de Aveiro

Coorientador – Doutora Raquel Madeira Gonçalves
Categoria – Investigadora Assistente
Afiliação – Instituto de Investigação e Inovação em Saúde (i3S) e Instituto de Engenharia Biomédica (INEB), Universidade do Porto

This PhD thesis was financially supported by the FCT PhD fellowship SFRH/BD/80577/2011.

This work was financed by FEDER - Fundo Europeu de Desenvolvimento Regiona -l funds through the COMPETE 2020 - Operacional Programme for Competitiveness and Internationalisation (POCI), Portugal 2020, by Portuguese funds through FCT - Fundação para a Ciência e a Tecnologia/ Ministério da Ciência, Tecnologia e Ensino Superior in the framework of the project "Institute for Research and Innovation in Health Sciences" (POCI-01-0145-FEDER-007274), and by Norte Portugal Regional Operational Programme (NORTE 2020), under the PORTUGAL 2020 Partnership Agreement, through the European Regional Development Fund (ERDF) in the framework of the project NORTE-01-0145-FEDER-000012.

“O que se quer existe – só que está coberto: Por isso se chama à busca feita pelos Portugueses Descobrimentos.”

Agostinho da Silva in Espólio

AGRADECIMENTOS

Foi sem dúvida uma longa jornada que me trouxe até ao dia de hoje. São muitas as pessoas e casas a quem devo o mais sentido dos agradecimentos, por, de uma forma ou de outra, garantirem a conclusão desta importante etapa na minha vida profissional. Espero não me esquecer de ninguém!

Em primeiro lugar, devo agradecer à Universidade do Porto, ao Instituto de Ciências Biomédicas Abel Salazar (ISCBAS) e ao Instituto de Engenharia Biomédica (INEB) todo os meios que me providenciaram, o atendimento irrepreensível e o acolhimento caloroso.

Quero agradecer também à Invicta cidade do Porto a inspiração e o lindo fluir dos dias.

Ao meu orientador, Mário Barbosa, agradeço esta oportunidade de transcender intelectualmente. Obrigada professor pela confiança que depositou em mim desde o primeiro dia. Obrigada pelo INEB que me (nos) deu. Obrigada por estar atento ao desalento e saber oferecer as palavras mais desejadas no momento certeiro. Obrigada pelo seu abraço amigo sempre que a hora foi de festejo. Obrigada por todas as portas que deixou entreabertas para eu empurrar. Findo este capítulo, sinto que desperdicei conversas ricas de uma vida tão vivida, fruto do meu jeito tímido, ou talvez contemplativo. Desculpe esta minha vergonha teimosa e natureza fugidia, de quem já resolveu tudo, quando o tudo é ainda esboço! Felizmente, ainda temos o amanhã!

Para as minhas co-orientadoras, Catarina Almeida e Raquel Gonçalves, não haverá obrigada que baste, pois a elas devo todas as pequenas conquistas desta investida. Obrigada pela paciência, pelo ouvido atento, pelo otimismo e alegria contantes. Obrigada pela compreensão e obrigada pela amizade que cultivamos, e que para sempre nutrirei com carinho. Obrigada por semearem tão bem a sede de saber e orientarem os ramos desta era desgovernada. Obrigada pela liberdade que me deram para crescer ao meu ritmo tosco. Encherei a boca de orgulho e o coração de gratidão sempre que falar o vosso nome. Obrigada.

Ao longo destes quase 7 anos (9 de INEB), foram várias as casas por onde passei. Sem exceção, todas me acolheram como membro da sua família científica, no mais caloroso dos abraços. Conheci pessoas fabulosas – no seu génio e na sua humanidade. Foi extremamente gratificante poder esticar as raízes e tocar outros

mundos aqui tão perto. Obrigada à família INEB, à família IPATIMUP, à família IBMC e à família ICBAS.

Em particular, obrigada à Ana Paula Filipe, por ser a nossa mãe e nunca deixar nada falhar, à Virgínia Fonseca, à Dulce Novo, à Daniela Azevedo e à Gabriela Afonso, por sempre atenderem com tanto carinho os meus pedidos. Agradeço também à Eliana Vale, ao Ricardo Vidal, à Manuela Brás e à Susana Carrilho toda a paciência, profissionalismo e acima de tudo a amizade.

Ao núcleo duro das discas suricatas, Joana Antunes, Catarina Pereira, Inês Odila, Joana Caldeira – obrigada amigas, companheiras, cúmplices, parceiras, guerreiras! O sentimento de gratidão por ter integrado esta equipa instalou-se desde muito cedo, e desde então cresceu desmesuradamente. Sei que vou ter muitas saudades vossas e do extraordinário ambiente de trabalho do qual vocês são muito responsáveis. Obrigada. Mil vezes obrigada por tudo.

Obrigada ao meu grupinho dos almoços (na cantina ou no cantinho), por tornarem os dias ainda mais completos e felizes. Pelas conversetas, pelas risotas, pelos programas que daí derivaram, pelas surpresas que me fizeram, pelo companheirismo do dia-a-dia. Gosto tanto de vocês! Joana Antunes, Catarina Almeida, Fabíola Moutinho, Maria Lázaro, Nilza Ribeiro, Daniel Vasconcelos, Sidónio Freitas, Joana Maciel, Daniela Rocha, Sílvia Bidarra, Daniela Sousa, Inês Gonçalves, Ana Freire, Ana Lopes, Pedro Moreno, Cláudia Monteiro, e todas as pessoas que comigo lá se cruzaram afim de partilhar energia boa.

Não poderia deixar de agradecer às minhas parceiras do Science Club, Inês Odila e Mariana Valente. Gostei imenso de trabalhar e crescer convosco. Guardo só boas memórias desses dias.

Obrigada à minha equipa do ICBAS, Andreia Silva, Inês Almeida, Daniel Vasconcelos, José Henrique Teixeira, Susana Santos, Graciosa Teixeira, Joana Ferreira, João Brás, Ana Almeida, Marisa Castro e Carla Oliveira. Demos vida àquele laboratório sobre o Douro plantado e sinto um orgulho imenso em tê-lo partilhado convosco.

Obrigada Raquel Seruca pelo cantinho ao sol e pela mulher inspiradora que é. À Joana Caldeira, à Renata, à Cecília, ao André, à Marta Pinto, à Marta T. Pinto, à Ana Pinto, à Maria Oliveira, à Marta Oliveira, ao Hugo Caires, à Ângela, à Joana Figueiredo, à Ana Margarida, ao Sr Oliveira, ao Sr Mendes e a todas as pessoas do

IPATIMUP que me integraram desde o primeiro dia naquela linda casa, o meu profundo obrigada também.

Agradeço ainda ao Dr. Rui Vaz, ao Dr. Paulo Pereira, ao Dr. Pedro Silva e às suas equipas do Hospital de São João e do Hospital CUF Porto, extraordinários profissionais que admiro com o maior dos apreços. Obrigada por embarcarem nesta aventura e pela vossa tão importante contribuição para este trabalho. Obrigada por toda a atenção e pronta disponibilidade para esclarecerem as nossas dúvidas do foro clínico.

Por fim, obrigada à minha família do coração. À minha Mãe. Ao meu Pai. Ao meu Irmão. Ao meu Filho. Pela rede que nunca me deixou cair. Pelo tempo que vos roubei. Pela confiança cega na minha integridade e valores. Pelo vosso amor.

Obrigada a ti Sérgio, a paciência interminável dos dias e tudo o resto que nunca caberá nas palavras...

PUBLICATIONS

The work performed in the frame of this Thesis resulted in the following publications:

Molinos M, Almeida CR, Caldeira J, Cunha C, Gonçalves RM, Barbosa MA. *Inflammation in intervertebral disc degeneration and regeneration.* J R Soc Interface. 2015 Mar 6;12(104):20141191. doi: 10.1098/rsif.2014.1191.
(parts included in Chapter I)

Molinos M, Almeida CR, Gonçalves RM, Barbosa MA. *Improvement of Bovine Nucleus Pulposus Cells Isolation Leads to Identification of Three Phenotypically Distinct Cell Subpopulations.* Tissue Eng Part A. 2015 Aug;21(15-16):2216-27. doi: 10.1089/ten.TEA.2014.0461. (Chapter II)

Molinos M, Cunha C, Almeida CR, Gonçalves RM, Santos OS, Pereira PM, Vaz R. *Age-Correlated phenotypic alterations in cells Isolated from human degenerated intervertebral discs with Contained hernias.* Spine (Phila Pa 1976). 2017 Jul 3. doi: 10.1097/BRS.0000000000002311. (Chapter IV)

Molinos M, Almeida CR, Teixeira GQ, Gonçalves RM, Barbosa MA. *Profiling nucleus pulposus cells aging using a bovine model.* Manuscript in preparation**.** (Chapter III)

Caldeira, J., C. Santa, H. Osório, **M. Molinos**, B. Manadas, et al. (2017) *Matrisome Profiling During Intervertebral Disc Development And Aging.* Scientific Reports. 2017 Sep 14; 7(1):11629. doi: 10.1038/s41598-017-11960-0.

Cunha C, Almeida CR, Almeida MI, Silva AM, **Molinos M**, Lamas S, Pereira CL, Teixeira GQ, Monteiro A, Santos SG, Gonçalves RM, Barbosa MA. *Systemic delivery of bone marrow MSCs for in situ intervertebral disc regeneration.* Stem Cellls Translational Medicine. 2016. doi: 10.5966/sctm.2016-0033

Silva AM, Varela-Moreira A, Pereira Gomes C, **Molinos M**, Leite M, Almeida M, Ribeiro D, Schrader M, Figueiredo C, Barbosa M, Gonçalves R, Almeida C, Pêgo A, Santos SG, Gomez-Lazaro M. *Integrated Analysis of Biological Samples by Imaging Flow*

Cytometry. Microsc Microanal. 2015 Aug;21 Suppl 5:95-6. doi: 10.1017/S1431927615014282.

AUTHOR CONTRIBUTION

As first author, Maria Molinos performed the laboratory work, sample collection, data analysis and statistical analysis, contributed to the study design and drafted the manuscripts.

Regarding the three co-authored publications, Maria Molinos was involved in data collection and final approval of the manuscripts.

ABSTRACT

Intervertebral disc (IVD) degeneration is an age-dependent process resulting from successive biomolecular and functional failures, highly correlated with low back pain (LBP) - the world's leading cause of years lived with disability. Primarily seeking symptomatic relief, clinical approaches targeting disc-related LBP are interventive in nature and do not address the underlying pathophysiology, ultimately failing to restore tissue function or to slow down IVD disease (IDD) progression. Nonetheless, fundamental scientific research on this field has grown tremendously in recent years, and major efforts are being put on regenerative therapies. As such, understanding the cellular and molecular mechanisms behind disturbance of IVD homeostasis, and particularly addressing early age-correlated degenerative changes, will foster the creation of safer and more effective therapies to combat IDD.

The dissertation presented herein aimed to move forward the basic knowledge on IVD cell biology, by thoroughly characterizing the phenotypic signature of its endemic cell populations, more specifically the ones found within the nucleus pulposus (NP), both in homeostasis and aging. For this purpose, novel approaches to this field were introduced, namely high-throughput methods of cell analysis, such as flow cytometry (FC) and imaging flow cytometry (IFC).

Firstly, driven by the lack of standardized protocols to isolate and profile primary NP cells, an improved method, guarantying high cell yields and viability, was established, along with a systematic FC gating procedure. This study demonstrated that collagenase-type-XI is an efficient enzyme to obtain single-NP cells suspensions in a short-time period. Furthermore, it highlighted the presence of three phenotypically distinct subpopulations of cells within young bovine NP in homeostasis.

The second part of the work focused on the effects of aging on the signature of bovine NP cells both at protein and gene levels. Results revealed striking differences between young (12 months old) and old (10-16 years old) cells, namely a decrease with aging on the prevalence of the mesenchymal stem cells (MSC)-related (CD29 and CD44), hematopoietic (CD45) and NP-progenitor (Tie2) markers, along with an increase in $GD2^+$ cells (NP-progenitor marker as well), and a stable expression of CD146 (MSC marker). Moreover, by changing the analytical system, a fourth distinct subpopulation was discovered, and the signature of the subpopulations was also found to be altered with aging. Evidence gathered supports the bovine animal model as a

valuable tool to explore age-induced modifications on NP cells, and to identify potential anti-aging targets, towards the prevention of IVD degeneration.

Finally, to validate previous results in the human scenario, IVD cells retrieved from patients undergoing microdiscectomy were analysed. Findings from this part of the work highlighted remarkable morphological alterations that occur on primary human IVD cells with aging and degeneration, namely the gradual shift in cells diameter due to deposition of an aberrant pericellular matrix (PCM). Importantly, gradual disappearance of an endogenous progenitor cell population expressing either CD73, CD90 and Tie2, already reinforced by other reports, was questioned by the maintenance of the expression profile of CD146 and GD2 with aging, similar to that found in bovine NP cells. This brought renewed hope on the capability of IVD cells to pro-actively respond to damage.

Overall, this doctoral thesis significantly contributed to the advance of knowledge on nucleus pulposus cell biology, applying novel cell characterization techniques. Importantly, by comparatively exploring cells phenotype in homeostasis and aging, it identifies potential anti-aging molecular targets to combat IVD disease.

RESUMO

A degeneração do disco intervertebral (DIV) é um processo intrinsecamente associado à idade, resultante de falhas biomoleculares e funcionais sucessivas, e significativamente correlacionado com a dor lombar – a principal causa de anos vividos com incapacidade em todo o mundo. Procurando alivio sintomático, as abordagens clínicas atuais focadas na dor lombar de origem discal são interventivas por natureza e não direcionadas para a patofisiologia subjacente, consequentemente impedindo o restauro da função do tecido ou o abrandar da progressão da doença degenerativa do disco intervertebral (DDD). Todavia, nos últimos anos a investigação fundamental nesta área científica tem crescido consideravelmente, com um grande empenho em torno das terapias regenerativas. Deste modo, compreender os mecanismos celulares e moleculares responsáveis pela destabilização da homeostasia do DIV, e particularmente as alterações degenerativas associadas à idade, promoverá a criação de terapias mais seguras e mais efetivas no combate à DDD.

A presente dissertação procura contribuir para o avanço do conhecimento básico da biologia celular do DIV, através da caracterização aprofundada da assinatura fenotípica do disco e das suas populações celulares endémicas, especificamente as que se encontram no nucleus pulposo (NP), em homeostasia e no envelhecimento. Neste sentido, foram aplicadas técnicas inovadoras e pouco utilizadas até agora nesta área, como a citometria de fluxo e a citometria de fluxo com imagem.

Motivados pela falta de estandardização dos protocolos de isolamento e caracterização das células primárias do NP, na primeira fase deste trabalho foi estabelecido um método otimizado de isolamento daquelas células, garantindo elevado rendimento e viabilidade celular, assim como uma classificação sistemática dos eventos na análise de citometria. Este estudo permitiu destacar a collagenase-tipo-XI como uma enzima eficaz na dissociação do NP e consequente obtenção de suspensões unicelulares, bem como descobrir a existência de três subopulações celulares fenotipicamente distintas no NP bovino jovem em homeostasia.

Numa segunda fase estudou-se o efeito do envelhecimento na assinatura das células bovinas do NP ao nível da proteína e do gene. Os resultados revelaram diferenças evidentes entre células jovens (12 meses) e as envelhecidas (10-16 anos),

nomeadamente uma diminuição na prevalência de marcadores associados a células mesenquimais estaminais (MSCs) (CD29 e CD44), hematopoiéticas (CD45) e progenitoras do NP (Tie2), acompanhada de um aumento de células $GD2^+$ (também marcador de células progenitoras do NP) e manutenção de células $CD146^+$ (marcador de MSCs). Adicionalmente, na sequência da mudança de sistema analítico, uma quarta subpopulação celular foi identificada. A assinatura das subpopulações foi também significativamente afetada pela idade. De notar, os resultados obtidos permitiram concluir que o modelo animal bovino representa uma ferramenta de grande utilidade no estudo das alterações induzidas nas células do NP pela idade, e consequentemente na identificação de potenciais alvos terapêuticos anti envelhecimento, tendo em vista a prevenção da degeneração do DIV.

Finalmente, procurando validar os resultados anteriormente obtidos, células isoladas de DIVs humanos, recolhidos após microdiscectomia foram analisadas, e os resultados permitiram registar as alterações notáveis que ocorrem a nível morfológico nas células humanas do DIV com a idade e a degeneração, mais precisamente a gradual transição no diâmetro das células, devida à deposição de uma matrix pericelular aberrante. De destacar, o desaparecimento gradual de uma população de células progenitoras incluindo células $CD73^+$, CD90+ e $Tie2^+$, suportado por outros estudos prévios, foi questionado pela manutenção células $CD146^+$ e $GD2^+$ com a idade, semelhante ao averiguado em células do NP bovino. Este facto deposita renovada confiança na capacidade das células do DIV responderam proactivamente face à lesão do tecido.

Em resumo, esta tese doutoral vem contribuir significativamente para o avanço do conhecimento da biologia celular do nucleus pulposo, utilizando técnicas inovadoras de caracterização das células. Adicionalmente, explorando comparativamente o fenótipo celular em homeostasia e no envelhecimento, identifica potenciais alvos moleculares de combate à doença degenerativa do disco.

TABLE OF CONTENTS

LIST OF ABBREVIATIONS

AARD	A5D3 protein
AC	articular cartilage
ACAN	aggrecan
ADAMTS	a disintegrin and metalloproteinase with thrombospondin motifs
AF	annulus fibrosus
Agg	aggrecan
APC	allophycocyanin
BASP	brain abundant membrane signal protein
bFGF	basic fibroblast growth factor
CA	carbonic anhydrase
CCL	chemokine ligand
CD	cluster of differentiation
CD14	pan-monocytic antigen
CD19	pan-B-cell marker
CD34	hematopoietic stem cell marker
CD45	pan-hematopoietic marker
CEP	cartilaginous endplate
CK	cytokeratin
COL2A1	collagen type-II
Coll	collagen
COMP	cartilage oligomeric matrix protein
COX	cyclooxygenase
C_T	threshold cycle
CXCL	monokine induced by gamma interferon
DDD	degenerative disc disease
DNA	deoxyribonucleic acid
DPP	dipeptidylpeptidase
ECM	extracellular matrix
FACIT	fibril associated collagens with interrupted triple helices
FBLN	fibromodulin
FC	flow cytometry
FITC	fluorescein isothiocyanate

FOX	forkhead box
FSC-H(A)	forward scatter-height (area)
GAG	glycosaminoglycan
GAL	galectin
GAPDH	glyceraldehyde 3-phosphate dehydrogenase
GLUT	glucose transporter
GM-CSF	granulocyte macrophage colony-stimulating factor
HIF	hypoxia inducible factor
HLA-DR	class 2 HLA antigen
IBSP	integrin binding sialoprotein
ICE	IL-1β-converting enzyme
ID	inhibitor of DNA binding
IDD	intervertebral disc disease
IFC	imaging flow cytometry
IFN-γ	interferon gamma
Ig	immunoglobulin
IGFBP3	Insulin-like growth factor binding protein 3
IHC	immunohistochemistry
IL	interleukine
IL-1Ra	IL-1 receptor antagonist
IL-1RI	IL-1 receptor, type I
IVD	intervertebral disc
LAM	laminin
LBP	low back pain
LPS	lipopolysaccharide
LRRN	leucine rich repeat protein
MGP	matrix gla protein
MMP	metalloproteinase
mRNA	messenger RNA
MSC	mesenchymal stem cell
N:C	nuclear to cytoplasmic ratio
NC	notochordal cells
NCDN	neurochondrin
NDN	necdin

NGF	nerve growth factor
NP	nucleus pulposus
NRP	neuropilin
NSAIDs	nonsteroidal anti-inflammatory drugs
OVO	ovostatin
PAX	paired box
PCM	pericellular matrix
PE	phycoerythrin
PG	proteoglycan
PGE2	prostaglandin E2
PI	propidium iodide
PLA2	calcium-dependent phospholipase 2
PRELP	proline arginine-rich end leucine-rich repeat protein
RNA	ribonucleic acid
SHH	sonic hedgehog
SNAP	synaptosomal-associated protein
SSC-H(A)	side scatter-height (area)
SSRIs	serotonin reuptake inhibitors
TCAs	tricyclic antidepressants
TGF-β	transforming growth factor beta
TNF-α	tumor necrosis factor alpha
TNMD	tenomodulin
TrkA	high affinity NGF receptor
TSP	thrombospondin
VCAN	versican
VEGF	vascular endothelial growth factor

CHAPTER I

General Introduction

This chapter included some material from the review article published in
The Journal of the Royal Society Interface 12(104):20141191, 2015
doi: 10.1098/rsif.2014.1191

LOW BACK PAIN, INTERVERTEBRAL DISC DEGENERATION AND DISEASE: EPIDEMIOLOGY AND AETIOLOGY

Low back pain (LBP) remains the world's leading cause of years leaved with disability, in both developed and developing countries, according to the Lancet Global Burden of disease study 2015 [1]. The estimate costs of LBP are difficult to compare between different countries, but its heavy socio-economic impact is evident in modern society [2]. Nearly everyone is affected by LBP at some moment in life (70-80% of lifetime prevalence) and about 4–33 % of the population at any given point (point prevalence) [3-5]. In Portugal, the recent EpiReumaPt study revealed that 26.4% of the population self-reported LBP at a given point [6] and 10.4% actually suffered from active chronic LBP [7]. This pathology promotes a high consumption of healthcare resources, since subjects present a higher likelihood for anxiety symptoms, early retirement due to disease and more physician visits [7].

The aetiology of LPB is still unclear and in 90% of cases the pathoanatomical cause is non-specific, i.e. no known disorder that causes LBP can be directly identified, such as cancer, vertebral infection, cauda equina syndrome, vertebral compression fracture, axial spondyloarthritis, radicular pain or radiculopathy (sciatica), or spinal canal stenosis [2]. However, and despite no causal link has been confirmed yet [8], the literature suggests that there is a strong positive correlation between degenerative disc changes and LBP [9-11]. Physiologically, the pain may arise from the disc per se (discogenic), since nerve fibers are present on the surface of the posterior aspect of the IVD, or from secondary changes, which may affect adjacent anatomical structures [8].

Whether symptomatic or not, IVD degeneration begins in youth and is ubiquitous in adulthood, despite the wide variation in degenerative findings (i.e. MRI signal intensity, disc height narrowing, annular tears, disc buldging, herniation and osteophytes) between different disc levels and age groups [11-13]. Prevalence rates are difficult to estimate based on reported clinical observations, due to the different case definitions, methodologies and samples used [13]. The same happens with intervertebral disc disease (IDD) [or degenerative disc disease (DDD)]. Albeit considered the most common reason for lumbar fusion in the USA [14], this pathology does not have a universally accepted definition, nor it is clearly measurable [13].

Moreover, IDD or DDD are many times synonyms with IVD degeneration. However, this may be misleading, since the word disease implies symptoms, and most degenerated discs are actually asymptomatic [13, 15, 16]. Hence, one should be precise when using the terms IDD or DDD, which should designate painful disc-related disorders, comprising naturally aged disc, as well as prematurely degenerated ones [17], the latest as a result of hereditary predisposition and/or environmental insults (e.g. mechanical trauma, high body weight, tabagism, diabetes or oxidative stress) [18].

CURRENT TREATMENT MODALITIES FOR DEGENERATIVE DISC DISEASE

First stage treatments for DDD rely on physiotherapy and medications. If symptoms are not relived after conservative approaches, patients are indicated for surgery (Table 1.1). However, spine surgeries have a high risk of complications associated [19, 20], and recurrent interventions are many times needed (15-30% of cases)[21], increasing the personal and financial costs even further [22]. Crucially, the underlying pathophysiology is not being addressed, nor is the restoration of IVD's function or the slowing down of disease progression.

Alternative biological approaches focusing on IVD regeneration or IVD-associated pain relief begun in the early 1990s, and have since increased in number and diversity, including gene and biomolecular therapies, cell-based therapies and tissue engineering solutions for total or partial IVD replacement [23-25]. Indeed, researchers are seeking to regenerate the IVD by restoring its native properties, namely by: 1) recovering IVD biomechanics; 2) re-establishing cells biological activity, including production of healthy ECM; and 3) reducing IVD-associated pain. However, such sophisticated solutions are still on its infancy and very few have reached Phase-I clinical trials [26, 27]. Indeed, the lack of fundamental knowledge on IVD cell biology and its intrinsic aging and degenerative mechanisms has been hindering the discovery of more effective therapeutic targets.

Table 1.1: Current treatment modalities to manage back pain. Adapted from [28].

	Treatment modality	To address	Designation	Disadvantages/Complications
Non-surgical	Education, activity modification, behavioural therapy and exercise therapy	Back pain	Promotion of healthier life-style (e.g. reduce weight, no smoking); limit activity for a short period of time; confrontation of the fear of pain; trunk or core stabilization and low-impact aerobic activity	Not proven effective
	Oral and topical medication	Back pain	Non-narcotic analgesics (acetaminophen, tramadol) narcotic analgesics, nonsteroidal anti-inflammatory drugs (NSAIDs – COX inhibitors), muscle relaxants (diazepam, carisoprodol) oral corticosteroids, antidepressants (TCAs and SSRIs), topical treatments (NSAIDS or anesthetics)	Do not address underling disease mechanisms. Only postpones surgical intervention by temporarily alleviating pain.
	Injected medication	Back pain	Epidural corticosteroids, soft tissue, facet-joint, sacroiliac joint	
	Physical modalities	Back pain	Manipulation, traction, acupuncture, transcutaneous electrical nerve stimulation, orthoses	Not proven effective
Surgical	Arthrodesis (+ decompressive laminectomy)	Discogenic pain (and spondylolisthesis)		Failure to achieve solid fusion, stiffness, persistent back pain, stiffness, possible increased degeneration on adjacent segments, consequent facet arthrosis
	Total disc arthroplasty or dynamic stabilization	Discogenic pain	ProDisc-C, Prestige, Bryan, SB Charité III, ProDisc-L, Nuclear replacement, facet replacement	No available long-term clinical results, durability and complications remain unknown
	Microdiscectomy	Disc herniation (normally with radiculopathy symptoms)		Inadvertent durotomy, nerve root injury, infection, postoperative instability, recurrent disc herniation, fibrosis
	Decompressive laminectomy	Lumbar stenosis (neurogenic claudication)	Lamina excision, X-STOP spacer	Incidental dural tears, postoperative instability, persistent back pain, persistent radiculopathy, recurrence of stenosis

NSAIDs: Nonsteroidal anti-inflammatory drugs; **COX:** cyclooxygenase; **SSRIs:** serotonin reuptake inhibitors; **TCAs:** tricyclic antidepressants

INTERVERTEBRAL DISC ANATOMY AND PHYSIOLOGY

The IVD is a fibrocartilage with a roughly cylindrical structure, which comprises 1) a well-hydrated central nucleus pulposus (NP), 2) a firm and flexible annulus fibrosus (AF) surrounding the NP, and 3) inferior and superior cartilaginous endplates (CEP) forming the interface between the disc and the adjacent vertebrae (Figure 1.1). During embryogenesis, the NP originates from the notochord, whereas the AF and the CEP derive from the somites (scleretome) [29, 30]. As such, distinct cell populations are found within these structures, which are responsible for the regional variations and for the specialized physiological function of each anatomical part [31, 32]. Overall, the IVD guarantees the flexibility of the spine, allowing movements between the axial and appendicular skeleton and the head, and also absorbing applied loads [33].

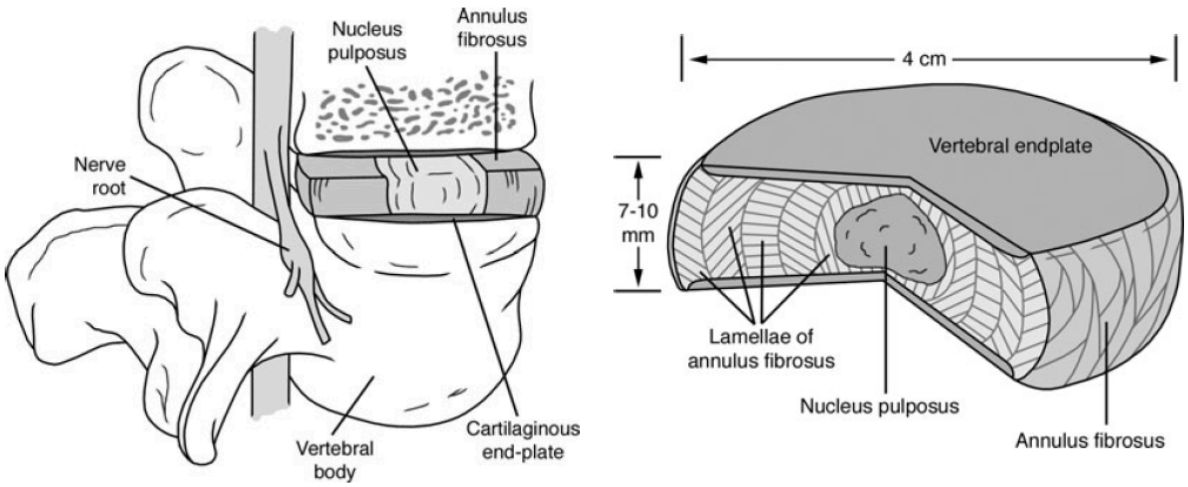

Figure 1.1: Intervertebral disc anatomy and physiology. The intervertebral discs are fibrocartilaginous cushions acting as shock absorbers between each of the vertebrae. The human spinal column is composed of a total of 23 intervertebral discs, which allow extension and flexion of the spine to some extent, while also guarantying protection to the vertebrae, brain, and other surrounding structures (i.e. arthrodial, ligamentous, muscular, vascular, lymphatic and neural elements). Adapted from [34].

The nucleus pulposus. The healthy NP is highly rich in proteoglycans and contains collagen fibers randomly organized [35] and elastin fibers arranged radially [36]. Daily pressure applied to the nucleus is passed on to both the annulus and the endplates. When loaded from above, the height of the nucleus is reduced, as it attempts to expand radially. As a consequence, the collagen rings of the annulus are

stretched and the pressure exerted by the nucleus is quickly balanced by the elastic tension that develops in the lengthening fibers of the annulus. On the other hand, the pressure exerted on the endplates transmits part of the load from one vertebra to the next, although other structures of the spine also take some of the strain (i.e. ligaments, tendons, muscles, thoracolumbar fascia, facet joints) to resist compressive forces.

The annulus fibrosus. The AF has a laminate structure ranging from 15 (posterior) to 25 (lateral) concentric layers, with collagen fibers of various diameters lying parallel within each lamella [37]. The spaces between the separate lamellae are called interlamellar septae, and contain proteoglycan aggregates and a complex structure of linking elements creating interlamellar cohesion. At the periphery, some of the annulus fibers, i.e. Sharpey's fibers, pass the endplates to penetrate into the apophysial ring. The outermost fibers blend with overlying periosteum and longitudinal ligaments. Central fibers either insert into the cartilage of both endplates or bend with the NP. Based on structural and cellular differences, the AF can be further differentiated into an inner and an outer part. The inner AF is a broad transition zone between the highly organized collagenous structure of the outer AF and the highly hydrated NP, and consists of a mixture of extracellular matrix (ECM) components of both. Mechanically, the inner AF is more subjected to the high hydrostatic pressures from the NP than to the tensile forces from the outer AF. These differences have major consequences on ECM synthesis and turnover. The proportion of type I collagen increases from the inner part towards the outer annulus, whereas type II collagen follows a counter wise distribution [38]. This highly organized bioactive structure results in a complex anisotropic behaviour, with the tensile, compressive, and shear properties differing in the axial, circumferential, and radial directions. The forces experienced by the AF tissue can be quite high and therefore an intact AF is critical to proper disc function [39].

The cartilaginous endplates. Each CEP constitutes a thin horizontal layer, usually less than 1 mm thick of hyaline cartilage and fibrocartilage, with collagen fibers running parallel to the vertebral bodies, and continuing into the disc [40, 41]. Hyaline cartilage occurs towards the vertebral body and is most evident in neonatal and young discs, while fibrocartilage occurs towards the nucleus pulposus, being formed by

invading collagen fibres from the annulus fibrosus. In older individuals the end plates become entirely made of fibrocartilage [42]. Although tightly bound to the disc by the collagen fibers of the annulus, the endplates are only loosely bound to the vertebral bodies, for which they are considered an anatomic part of the IVD. The CEP fills the concave depression within the surface of the bony vertebral end plate up to the level of the apophyseal ring (outermost part made of cortical bone) (Figure 1.2). The central portion of the bony endplate is made of cancellous bone, being less resistant than the surrounding apophyseal ring, and is perforated by marrow contact channels, through which blood capillaries emerge, connecting the trabecular spaces to the cartilaginous endplate [43].

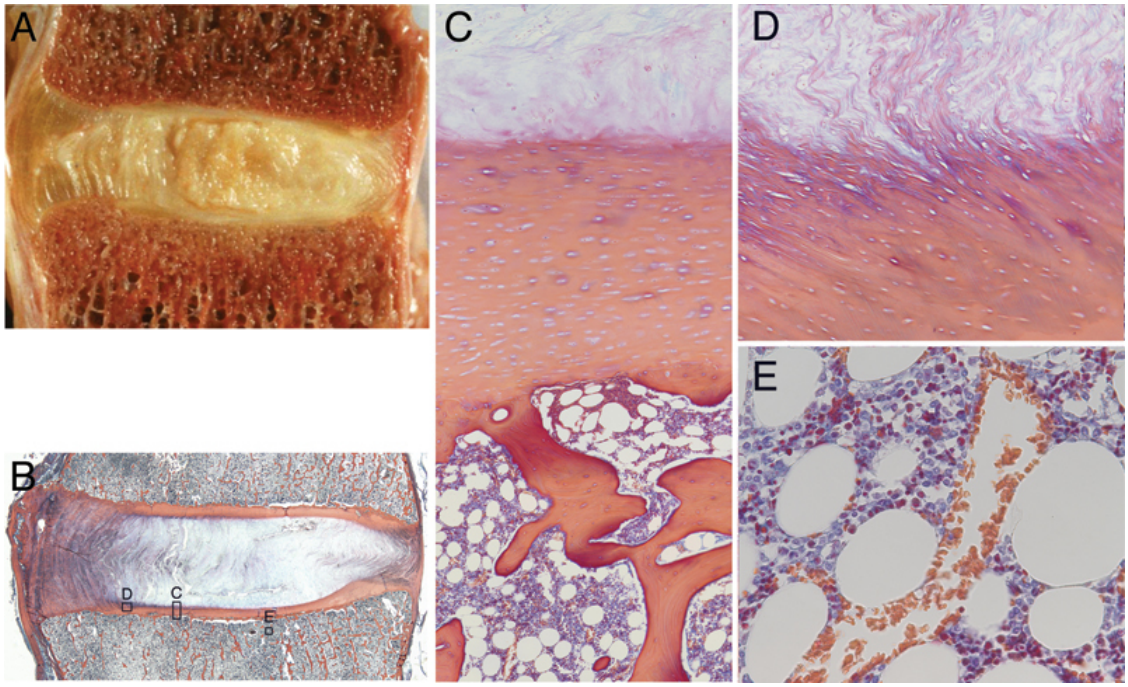

Figure 1.2: End-plates anatomy. A | Gross morphology of the lumbar intervertebral joint. **B |** Histology section showing regions of interest for panels C, D, and E. **C |** End plate detail showing cartilaginous and bony components with hematopoietic marrow elements. **D |** Insertion of annular fibers into the end plate cartilage at the inner annulus junction. **E |** Vascular sinusoids in the marrow space adjacent to the end plate. Note for panels A and B, left side is anterior. From [44].

Biomolecular components of the IVD. The disc is primarily comprised of water, proteoglycans, collagens, and other proteins. Table 1.2 groups the main ECM components found within the IVD, and Table 1.3 the main proteinases. Altogether, these molecules have a fundamental role in maintaining disc homeostasis.

Proteoglycans, particularly aggrecan, maintain matrix hydration and provide the appropriate osmotic pressure to facilitate nutrient transport and allow the plastic deformation required to disperse compressive forces. Others, such as versican, control disc cell differentiation and proliferation in the annulus, whereas leucine-rich proteoglycans regulate collagen fibril assembly, transport, and incorporation into ECM [45].

The different biomolecules distribution varies along the depth of the disc (Figure 1.3), and this correlates with the distinct biomechanical roles of its different anatomical parts [42]. The NP, rich in type II collagen, is more subjected to pressure, while the annulus fibrosus, containing both type I and type II collagen, is more involved in both tension-related and pressure-related processes [42]. In general, collagen fibers are densest in regions at the periphery of the disc [46]. On the other hand, PG content increases towards the center of the disc, which confers a large negative charge and hence high osmotic potential to the NP, attracting cations (mainly Na^+, K^+ and Ca^{2+}) and associated water, causing the tissue to swell [47]. The interaction between the proteoglycans and water is critically important, not only with regard to the mechanical properties of the disc (acting as a shock absorber), but also in determining the environment through which diffusion of nutrients and waste must occur [48]. The ECM is composed of many other components, the exact function of which in maintaining the biomechanical and biochemical balance in the disc are still unknown. However, ECM remodelling is critical to maintain IVD homeostasis. Nutrient supply and correct mechanical loading provide a proper environment for cells, which in turn control ECM turnover, needed for cell anchorage and to provide loading resistance.

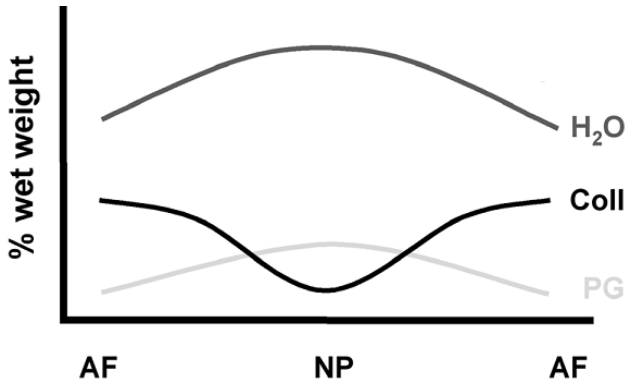

Figure 1.3: Variation of the main disc constituents' concentration within the tissue. From [49].

Table 1.2: Main extracellular matrix components of a young and healthy IVD. From [50].

			Name	Distribution/Localization	Putative/Possible Function
Collagens			***Fibril-forming collagens***		
			Type I	AF and NP	Confers tensile stiffness allowing torsion and flexion [51-54]
			Type II	AF and NP	Confines PG within the matrix to retain more water to allow larger deformations and withstand greater compressive loads [55, 56]
			Type III	NP and outer AF	Organizes pericellular environment; allows extensibility of tissue [57-59]
			Type V	AF and NP (increased in AF cells when compared to NP cells	Regulates fibril diameter (smaller if this collagen is more abundant) influencing mechanical properties [59, 60]
			Type XI	All over, mostly NP	Regulates fibril diameter (smaller if this collagen is more abundant) influencing mechanical properties [59, 61, 62]
			Beaded-filament forming collagens		
			Type VI	All over, mostly NP	Helps cell fixation to the matrix and facilitates collagen bundles' sliding and lubrication [63, 64]
			FACIT collagens		
			Type IX	NP	Maintains matrix integrity [65, 66]
			Type XII	AF	Might regulate fibrillogenesis [53, 67]
			Type XIV	AF	Might regulate fibrillogenesis [53, 67]
Proteoglycans			***Aggregating PGs***		
			Aggrecan	AF and NP	Maintains IVD's osmotic pressure; may act as an anti-angiogenic factor due to its inhibition of endothelial cell migration [64, 68, 69]
			Versican	All over, mostly AF	Favors the attachment of adjacent lamellae, contributes to resistance to compressive forces and facilitates cell migration, since it is an anti-adhesive molecule [59, 64]
			Non-aggregating PGs		
	Small Leucine-rich Proteoglycans (SLRPs)			Outer AF and fibrillar NP	Regulates collagen fibril diameter and spacing, maintaining uniform patterning; GFs' reservoir (TGF-β), modulating ECM metabolism [70-72]
			Biglycan	Outer AF and NP (fibrillar and pericellular region)	GFs' reservoir (TGF-β), modulating ECM metabolism [70, 71]
			Asporin	Outer and inner AF, rarely NP	GFs' reservoir (TGF-β), modulating ECM metabolism; may play a major role in modulating chondrocyte matrix homeostasis [73, 74]
			Fibromodulin	AF and NP	Regulates collagen fibril diameter and spacing, maintaining uniform patterning; GFs' reservoir (TGF-β), modulating ECM metabolism [68, 71]
			Lumican	AF and NP	Regulates collagen fibril diameter and spacing, maintaining uniform patterning [68, 75]
			Prolargin (encoded by PRELP*)	allover, mostly AF	Anchors basement membranes to the underlying connective tissue [68, 76]
			Chondroadherin	AF and NP	Binds integrin ad collagen; regulates cell metabolism and ECM structure, promoting matrix homeostasis [68, 77, 78]
			Osteoglycin/Mimecan	AF and NP	Unknown [68]
	Other PGs		Perlecan	AF and NP	Has a role in cell proliferation and differentiation by acting as co-receptor for FGFs; matrix organization and stabilization; role in FGF signalling [64, 79]
Other matrix proteins			Fibronectin	All over the disc	Preserves structural integrity of the ECM; involved in cell adhesion through interaction with integrins [80-82]
			Elastin	All over the disc	Preserves structural integrity of the ECM; help to regain disc height and shape after deformation [83-85]
			COMP	All over, mostly AF	Preserves structural integrity of the ECM; binds other matrix proteins and catalyzes polymerization of type II collagen fibrils; prevents vascularization of cartilage [86, 87]

Thrombospondin	AF	Preserves structural integrity of the ECM. Mediates cell adhesion, matrix-matrix interactions, cell migration and proliferation in other tissues; might prevent vascularization of the tissue; activates TGF-β complex [88, 89]

COMP: cartilage oligomeric matrix protein; **ECM:** extracellular matrix; **FACIT:** fibril associated collagens with interrupted triple helices; **NP:** nucleus pulposus; **AF:** Annulus fibrosus; **PG:** Proteoglycan; **PRELP:** proline arginine-rich end leucine-rich repeat protein; **TGF-β:** transforming growth factor beta

Table 1.3: Main IVD proteinases. From [50].

Name	Distribution/Localization	Putative/Possible Function
Aggrecanases		
ADAMTS1, 4, 5, 9 and 15	*ADAMTS1:* NP and AF; *ADAMTS4:* low levels NP and AF; *ADAMTS5:* low levels NP and AF; *ADAMTS9:* NP and AF; *ADAMTS15:* low levels NP and AF	Degrades aggrecan [90-93], as well as versican, biglycan, fibromodulin, COMP, TSP1, TSP2, nidogen, among other substrates [94]
Collagenases		
MMP1, 8 and 13	*MMP1:* low levels, mostly inner AF and NP; *MMP8:* low levels; *MMP13:* low levels, mostly NP	Cleaves fibrillar collagen [90-92]
Gelatinases		
MMP2 and 9	*MMP2:* low levels, mostly inner AF and NP; *MMP9:* low levels AF and NP	Degrades denatured collagen and basement membrane collagen [92]
Stromelysin		
MMP3 and 10	*MMP3:* low levels, mostly in the adult NP; *MMP10:* only checked in the NP	Digests noncollagenous matrix proteins and denatured collagen [90, 92, 95]
Matrilysin		
MMP7	NP and inner AF	Degrades aggrecan and collagen type II cleaves aggrecan, COMP, types I and IV collagen, and fibronectin and acts on tenascin; can interfere with stabilization of capillary-like structures, possibly playing a role on the avascular status of the disc [96, 97]
Other MMPs		
MMP19	AF and NP	Regulates IGF-mediated proliferation in other tissues by proteolysis of IGFBP3 [97]

ADAMTS: a disintegrin and metalloproteinase with thrombospondin motifs; **AF:** Annulus fibrosus; **IGFBP3:** Insulin-like growth factor binding protein 3; **MMP:** metalloproteinase; **NP:** nucleus pulposus; **TSP:** Thrombospondin

IVD nutrition and cell metabolism. The IVD is the largest avascular structure in the human body [98]. As such, glycolysis is the main mechanism of cellular metabolism in the disc [99]. Nutrients such as glucose and oxygen are supplied to the disc by blood vessels at its margins. The outer annulus is supplied by blood vessels surrounding the disc's periphery, while the nucleus and inner annulus are supplied with nutrients by a capillary bed which arises in the vertebral body, penetrates the subchondral plate and terminates at the junction between the cartilaginous end plate and bone [100]. Small solutes (e.g. oxygen, glucose, lactate) move primarily by diffusion under gradients set up by cellular activity, and are additionally oriented along the IVD according to the permeability and diffusion properties of the disc and end plate [101]. On the other hand, large proteins move in and out of the disc attached to water

molecules, according to a load induced flow. As a result of the limited blood supply and hypoxic conditions, the tissue is more acidic in the inner regions compared to the outer regions (Figure 1.4). The pH within the IVD ranges from 6.9 to 7.2, reflecting the importance of cell specialization within the IVD [41, 102]. For cell-based regenerative strategies, one of the most challenging microenvironment condition of the intervertebral disc is its matrix acidity [103], which increases with degeneration [104]. In general, three main factors are responsible for the acidic conditions in the normal IVD:

i. Diffusion of lactic acid (the product from anaerobic glycolysis) across the thick and dense matrix (up to 8 mm for adult lumbar discs) is slow, resulting in elevated acidity within the matrix and around the cells, particularly in the centre of the disc [105, 106];

ii. Due to the presence of many COO^- and $SO4^{2-}$ groups on the constituent glycosaminoglycan chains of the proteoglycans, the IVD has a high negative charge density, which attracts high amounts of free cations [105, 107];

iii. Although to a lesser extent, acid extrusion mechanisms will acidify the pericellular matrix further. The maintenance of a constant intracellular pH is of paramount importance for cell viability and function, and therefore disc cells possess acid extruding proteins of which the Na^+ x H^+ exchanger is the most prominent [105].

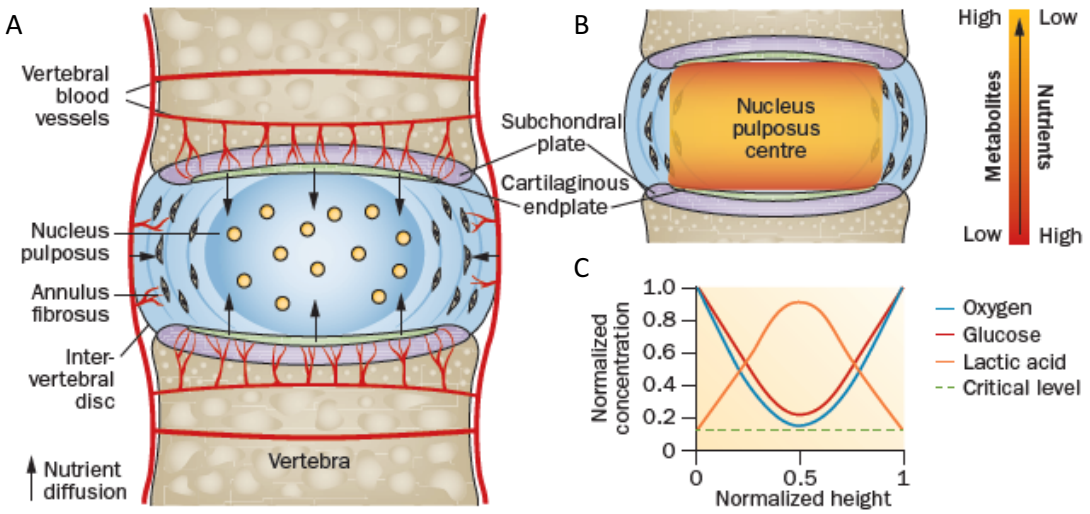

Figure 1.4: Intervertebral disc nutrition pathways. **A |** Cells of the avascular disc nucleus pulposus and inner annulus fibrosus are supplied by vertebral blood vessels. Capillaries penetrate the

subchondral plate through marrow spaces and terminate in loops at the junction of the subchondral plate and cartilaginous endplate. Nutrients (e.g. oxygen and glucose) diffuse from the capillary bed through the cartilaginous endplate under gradients arising from metabolic demands of disc cells, while metabolic wastes (e.g. lactic acid) diffuse in the reverse direction. Cells of the outer annulus fibrosus are supplied by capillaries from blood vessels in the surrounding soft tissues that penetrate a few millimetres into the disc. **B |** The centre of the disc has the lowest levels of nutrients and highest concentration of metabolites. **C |** Schematic showing normalized concentration gradients of glucose, oxygen and lactic acid across the nucleus, endplate–endplate. Nutrient concentrations must remain above the critical levels to maintain cell viability and activity. From [108].

However, matrix acidification may be even more exacerbated during degenerative processes [101], leading to a decrease in cell proliferation and viability, a shift towards matrix catabolism and an increase in pro-inflammatory cytokines and pain-related factors expression [104].

INTERVERTEBRAL DISC CELL POPULATIONS

Although all the cells of the mature disc are derived from mesenchymal cells, the cells of the OAF, IAF and the NP produce distinct extracellular matrices [109-111]. These differences are maintained in vitro, when cells are isolated from the tissue, and reflect distinct cellular phenotypes rather than environmentally induced differences [112, 11end3]. The molecular profile of IVD cells has been subject of intensive research in recent years. In order to develop more effective biological strategies that address the underlying pathogenesis, ideally by overcoming age-dependent degenerative processes, there is the need to better understand the cellular and molecular mechanisms behind IVD development, homeostasis and healthy aging. An overview on the phenotypic characteristics of the distinct cell populations found within the human (unless otherwise stated) IVD is given in next sections.

CEP cells. During IVD development, once Sox9 expression and chondrogenesis are initiated in the axial skeleton, chondrocyte differentiation and endochondral bone formation occur in the vertebral bodies. When the vertebrae are formed, hyaline cartilage is maintained at the end, in close contact with the IVD. Alike the articular cartilage, the CEP contains round chondrocytes, at a density of around

$14x10^6$ cells.cm^{-3} [114], embedded in a collagen II and proteoglycan-rich ECM, with collagen fibers mainly aligned horizontally. Although cells do not undergo terminal differentiation, collagen X may also be found in central areas of healthy CEP, possibly constituting focal areas of endochondral ossification. In aged or scoliotic discs, collagen X staining can be localized across the whole disc surrounding cells, and is mainly associated with abnormal calcifications [115, 116]. Contrarily to cells of the AF and NP, reports on CEP phenotype are few and essentially based on immunostaining of matrix proteins [117-119]. Only recently, Thorpe and colleagues included the CEP on their investigation on the regional variations in the expression of the previously proposed NP markers [120]. However, only negative discriminating protein markers were highlighted, such as KRT-19, as compared with NP cells, and LAM-5, PAX1 and FOXF1, as compared with both AF and NP cells. However, alike other mesoderm-derived tissues, CEPs were recently found to be home for stem cells (CESCs), which have been thoroughly characterized. These cells had the ability to form clusters, containing similar cells to BM-MSCs, namely, in their morphology, when adhered to tissue culture plates, and in their surface markers expression: positive for CD105, CD73, CD90, CD44, CD166, Stro-1 and CD133, and negative for CD14, CD34, CD19, CD45, and HLA-DR. Moreover, CESCs also exhibited differentiation potential into the three mesenchymal lineages [121, 122].

Fibroblast-like cells. Within the adult AF, cell density stays around 9000 cell/mm^3 [123], with higher cell densities registered in the OAF [110]. AF cells, particularly in the outer region, tend to be fibroblast-like, elongated, thin, and aligned parallel to the collagen fibers [124, 125]. Towards the IAF, some cells become more oval (Figure 1.5 A) [126]. In bovine OAF, cells show a complex morphology with sinuous processes woven into the extracellular matrix, and some interconnections via functional gap junctions [127, 128]. Often, linear cell arrays are found extending throughout the lamellae, embedded in an extensive pericellular matrix of collagen VI (Figure 1.5 B) [127]. Noteworthy, in pigs, AF cells were shown to exhibit a metabolic pathway distinct from that of cells with notochordal origin (i.e. NP cells), with higher lactate production and glucose consumption [109]. Numerous studies have assessed the phenotype of AF cells, either alone [129-133] or in comparison with NP, CEP or AC cells, in various species, including human, bovine, rat, ovine, canine, porcine and

rabbit [87, 134, 135]. Importantly, interspecies variations at the gene level were sometimes evident, empathizing the value of human samples in this field. For instance, in bovine AF cells, higher expression of versican (VACAN), tenomodulin (TNMD), alpha-induced protein 6 (TNFAIP6), forkhead box-1 and -2 (FOXF1 and FOXF2) and aquaporin (AQP1) was detected, when compared to NP or AC cells. However, from this report, only tenomodulin was further validated in normal human AF cells [135]. Also seeking validation of previously proposed AF marker genes selected from microarray analysis, van der Akker *et al.*, confirmed by qPCR that COL1A1, COL5A1, COL12A1, SFRP-2 and ADAMTS17 expression levels positively discriminate AF from NP cell cultures [133]. However, these results were retrieved after standardized cell culturing and conditioning with TGFß3, which may have forced cells to adopt a phenotype *in vitro* that does not resemble the one *in vivo*. Hence, further validation using different conditioning is required. Moreover, the fact that the AF tissue under study was from two scoliotic discs may constitute an additional concern. Further work from the same group, with bovine samples, exposed the different transcripts within the IAF and OAF in comparison with the NP and AC [132]. COL5A1, COL12A1, SFRP-2 and ADAMTS17 were again positive markers for OAF cells when compared to NP cell, but also in relation to IAF cells. As expected, aggrecan (ACAN) and COL2A1 expression was higher in the NP, while COL1A1 was higher in the OAF (no differences between OAF and IAF). Also, both the IAF and OAF showed less GAG content than the NP, while only the OAF showed significant higher DNA content.

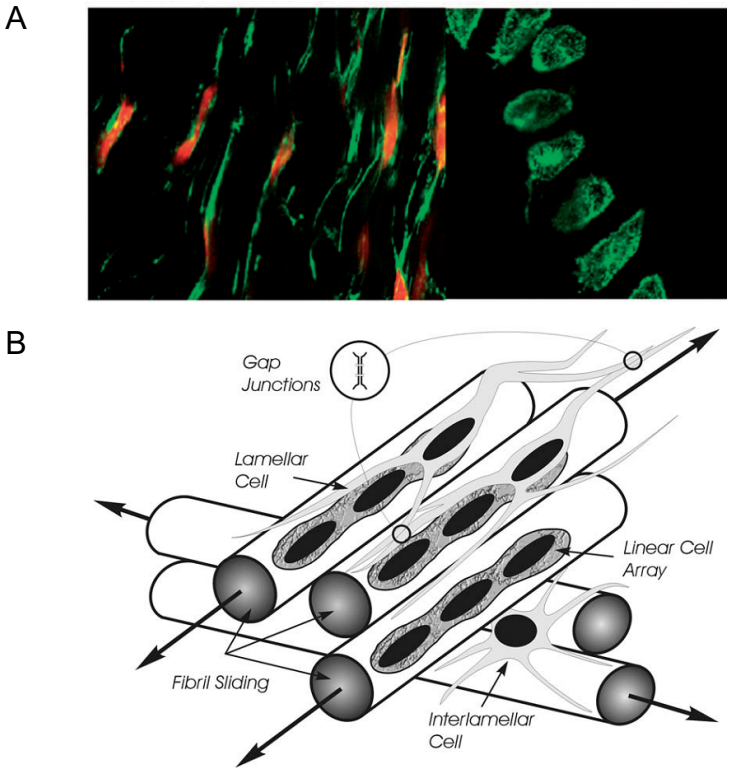

Figure 1.5: Annulus fibrosus cells morphology across the disc. A | AF cells are elongated in the periphery (left) and more rounded near the frontier with the NP (right). Adapted from [126]. **B |** Schematic illustration of the complex disposition and interconnectivity of OAF cells along and within the lamellae. Lamellar linear cell arrays are protected from tensile strains through fibril sliding, transferring shear strains to the cellular processes and interlamellar cells. Adapted from [127].

Chondrocyte-like or mature NP cells. The NP, considered the epicentre of IVD degeneration [136], as well as home for progenitor cells [137, 138], has attracted special attention from the scientific community. In the adult human NP, chondrocyte-like cells are interspersed at a low density - near 4000 cells/mm^3 [123], around 1% of the total NP volume [139]. These cells possess Golgi cisternae and a well-developed endoplasmic reticulum, indicating their capability to produce and maintain the ECM. With age, lipid droplets can be found in the cytoplasm, as well as a distinct pericellular matrix around most cells, as identified by electron microscopy, possibly due to accumulation of cell products [140]. Frequently two or more cells can assemble in a fibrous capsule, forming chondrons similar to those found in articular cartilage [141]. While these cells have many times been confounded with AC chondrocytes in the past, due to some phenotypic similarities [142], it is now known that they produce a distinct kind of ECM, with different aggrecan/collagen II ratios [143], proteoglycan structure

[144], collagen network [145], and glycosignature [146]. These differences may as well be anticipated by their distinct transcriptional profiles [135, 147, 148]. Besides their distinct ontogeny (AC: lateral mesoderm; NP: notochord), the specialized biomechanical solicitation and behaviour [149], allied to the particularly challenging microenvironment, could be the driving forces behind such differences. During the last decade, a plethora of microarray studies have been conducted in different species in order to establish a panel of marker genes that distinguish NP cells from AF, CEP and AC cells [120, 134, 135, 137, 147, 148, 150]. Generally, the markers proposed are not exclusive to any of those cell types, but rather follow an on-off fashion between them. Importantly, following the consensus paper by Risbud *et al.* to define the phenotype of young NP cells [151] (Table 1.4), a special interest has arisen on the relevance of the proposed markers to NP physiology (prompting more studies at protein level), as well as on their evolution with age and degeneration (stimulating the use of human samples) [120, 137, 152]. On another front, the exact origin of mature NP cells remains subject of debate. Some believe they may migrate from neighbouring tissues, such as the AF [153], CEPs [154, 155] or perichondrium [156], while others consider that the transition from a notochordal to a fibrocartilaginous tissue is not an exogenous replacement, but an endogenous development, in which NC cells terminally differentiate into mature NP cells [157-160]. The latter hypothesis is supported by experimental evidence in mouse showing that NP cells express the signalling molecule sonic hedgehog (Shh) and the transcription factor brachyury (T), which are otherwise not expressed by cells derived from the sclerotome [160], and by lineage-tracing studies in mice that established that during normal development and aging all cells of the NP are notochord-derived (from E15.5 until 21 months of age) [161-163]. Notwithstanding, recent contrasting evidence poses the possibility that the mature NP may have a heterogeneous cell population, including both notochordal and non-notochordal cells [137, 153, 164-167]. Overall, wide-genome analysis alone is not fulfilling the need for specific cell markers to aid cell-based therapies on restoring an NP-like phenotype [120, 168]. Hence, future research on the phenotypic characterization of IVD cells is warranted, particularly regarding the signature of each subpopulation in terms of its ontogeny, physiology and function.

Table 1.4: Markers proposed by Risbud *et al.* to define the young healthy NP cells phenotype. Adapted from [151].

Phenotypic marker	Relevance to NP physiology
Primary markers [†*]	
Stabilized HIF-1/2α	Transactivate many pro-survival genes in NP. Necessary for post-natal NP survival.
GLUT-1	Glucose transporter expressed in hypoxic tissues. Expression controlled by HIF-1.
Shh	Signalling ligand necessary for post-natal function of NP cells.
Brachyury	Transcription factor necessary for notochordal morphogenesis and patterning.
Aggr/Col II ratio >20	High PG content maintains hydration to resist loads.
CA3 and 12	Acid-base balance
CD24	Unknown
CK-8, -18 and -19[**]	Cellular structural integrity and possibly signalling
Secondary markers [‡]	
Integrins α3, α6 and β4[*]	Cell-matrix adhesion
Annexin A3	Unknown
α2-macroglobulin[*]	
Glypican 3	
Democollin-2	
CD56	
CD155	
CD221	
SNAP25[*]	
CDH2[*]	
BASP1	
PAX1[*]	
SOSTDC1	
FOXF1[*]	
Hemoglobin β-chain[*]	
Ovostatin[*]	
Neurochondrin	
Neuropilin-1	
Lubricin (PRG4)[*]	
Progenitor markers [‡*]	
Tie2	Receptor for angiopoietin-1. Drives proliferation of progenitor cells.
GD2	Unknown

[†] Selection criteria: 1) specific expression in young healthy NP cells, 2) requirement for proper NP cell function and relevance to NP cell physiology, and 3) mRNA and protein expression validated across different species; [‡] Identified in the literature but less well validated than primary markers; [*] Identified in human; [**] Indicate a notochordal ontogeny to the NP cells.

Notochordal cells. Notochordal cells (NC) are much larger (30-40 μm in diameter) than NP mature cells (~10 μm in diameter), with significantly higher intracellular glycogen and cellular processes [140, 169, 170]. Additionally, they present

large ECM-containing inclusions [170], believed to be fast-acting osmoregulatory elements within the cells [171]. During human foetal development, these cells switch from a cluster-packed format to being totally separated by the twenty-first week of fetal life [140, 170]. In many animal species, with no evidence of IVD degeneration (e.g. non-chondrodystrophic dogs, rabbits, pigs, mice and rat), NCs persist throughout life [169, 172], and several reports suggest that they have an important role in regulating disc cell function [173-177]. In humans, as well as in other species, such as horses, cows, sheep, and chondrodystrpphic dogs, NCs gradually decrease with age, and seem to be replaced by chondrocyte-like cells. This is already significant around the age of 3 years old for humans [170, 178]. When compared to mature NP cells, NCs are also more active metabolically and less resistant to nutrient deprivation [179], which could foster their disappearance as the vascular supply retracts gradually with age. Furthermore, even though they exhibit some gene-expression profile similarities, clear differences can also be found. For instance, in a porcine model, while both cell types express common chondrogenic markers (aggrecan, collagen II and *Sox9*), the relative expression of collagen I, as well as biglycan, decorin and lumican was found to be higher for mature NP cells [180]. Also, markers such as CK8, -18 and -19, cadherin-2 and SOSTDC1, are expressed by both bovine NCs and NP cells, but at higher levels in the former [135]. However, there is a growing belief that these differences found between NCs and the replacing mature NP cells may be due to different stages of cellular activity [180], differentiation [181] or pathological stages of aging and degeneration [182, 183], rather than imply different cell lineages. Indeed, recent studies have shown that a NC population may still exist within the adult and degenerated human NP, given the expression of notochord-specific markers, both at gene and protein levels [120, 135, 137, 158, 165, 166]. Nevertheless, these cells represent a small subset within the whole adult NP population, and thus the already referred hypothesis that some of the existing cells may have migrated from other neighbouring areas [137, 153, 164-167] cannot be ruled out. NCs exclusively express CK8, -18, -19 and CD24, as recently confirmed in human embryos and foetuses (3.5-18 weeks post-conception) [184]. Importantly, in this same report, other previously proposed NC markers in other species, such as T (a so far widely accepted indicator of the common notochordal ancestry [158, 160]), GAL-3, CD55, BASP1 and CTGF, where not further validated in human, because of their co-expression with the

sclerotome at some point post-conception [184] (Figure 1.6). Hence, if used alone, these molecules are unsuitable NC-specific markers.

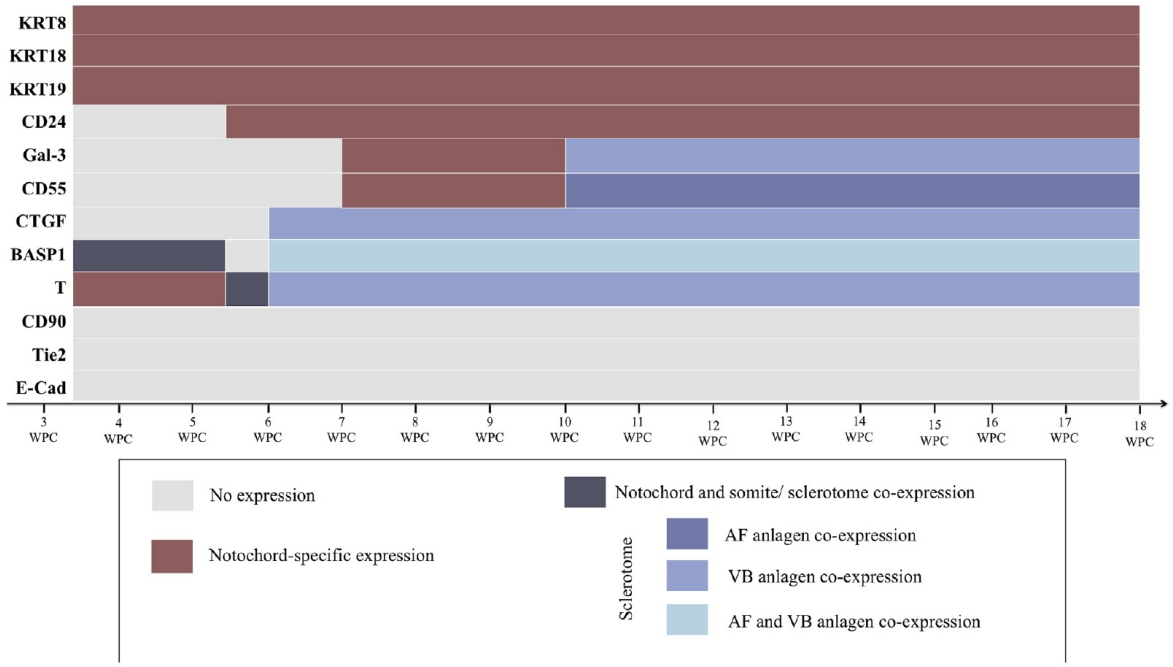

Figure 1.6: Schematic representation of the IHC staining of NC cells in the developing human spine. CK-8, -18, and -19 are notochord-specific markers at all stages, while CD24 is notochord-specific between 5.5 and 18 WPC. GAL3, CD55, CTGF, BASP1, and T expression varies with development stage. CD90, Tie2, and E-Cad are not expressed by any developing spine cell anlagen. Modified from [179].

Progenitor cells. The presence of progenitor cells has been reported in the human NP [152, 185-188], AF [186, 187, 189] and CEP [121, 186], as well as in several other species, such as dog [190], rat [191-193], mice [138], rabbit [193-195], Rhesus monkey [196], minipig [193, 197]. Despite some diversity found across the different species in terms of cell phenotypic signature and functional response, typically, these cells are plastic adherent and present the MSC surface markers profile $CD105^{+}CD73^{+}CD90^{+}CD45^{-}CD34^{-}CD14^{-}CD11b^{-}CD79^{-}CD19^{-}HLA\text{-}DR^{-}$ after liquid cell culture, while being capable of multi-lineage differentiation. When compared to bone marrow MSCs, degenerate NP-derived MSCs are less adiponegic [185], while CEP-derived MSCs show greater osteogenic and chondrogenic potential [121]. This observation was also true in relation to AF or NP derived MSCs, as recently confirmed

[186]. Of note, NP, AF and CEP derived MSCs had similar morphology and proliferation ability between them, and when compared to BM-MSCs, but the latter had significantly higher immunophenotypic expression of CD105 [186]. Notably, NP-derived MSCs are more resistant to the hypoxic [198], hypertonic[191] and acidic culture conditions [199], as opposed to adipose-derived MSCs, when both are cultured on a IVD-like microenvironment. On a different perspective, areas of proliferative cells (BrdU+) expressing migration markers (SNAI1, β1-Integrin) were found within the rabbit IVD, as well as expression of progenitor specific markers (e.g. Stro-1, Oct3/4, CD105, CD73, CD90, and Notch-1) [193, 200]. Most recently, Sakai *et al.* identified a population of progenitor cells within the NP, with multipotency and self-renewal capacity, which changed expression of specific cell-surface markers sequentially from angiopoietin-1 receptor (Ti2) positive, to disialoganglioside 2 (GD2) positive, to CD24 positive cells as they differentiate and lose their proliferative capacity. Also, they showed a negative correlation between Tie2 expression and age in human tissue [138]. Interestingly, new evidence shows that human notochordal cells do not express Tie2, suggesting that the cells isolated by Sakai and colleagues may indeed be of mesenchymal and not of notochordal origin [184]. Finally, in a more functional view, cell cultures of human degenerated discs positively responded to conditioned medium from MSCs, by displaying a more undifferentiated appearance and increasing the expression of the multipotency marker POU5F1, the cell-fate regulator Notch-1 and the MSC markers CD105, CD90 and Stro-1 [201]. Taken together, these findings indicate that degenerated human discs may exhibit an endogenous regenerative capacity, with possible paracrine on set, although some evidence shows there might be an age-limit for the efficient activation of those native progenitors [138, 148].

Inflammatory cells. Some studies suggest that the IVD might endogenously include inflammatory-like cells [202, 203]. In particular, it has been shown *in vitro* that a population of bovine IVD cells can phagocytize beads and apoptotic bodies [202]. In turn, human surgical non-herniated nucleus pulposus (NP) samples presented a high number of resident CD68+ cells [203]. The question of whether these cells could be resident macrophages or macrophage-like cells remains. Also, infiltrated leukocytes (CD11b positive cells) were found in prolapsed IVDs as well, where NP is supposedly intact and isolated from any vascular source of immune cells [204]. Most notably, a

range of cytokines have been found in human IVDs in varying amounts, presenting clear evidence that IVD cells, or at least some of them, are producers of specific inflammation-associated molecules, even in basal conditions (non-degenerated NP). Table 1.5 groups some of the most important observational studies, which have clarified which inflammatory factors are expressed either during homeostasis and with degeneration. Importantly, the identity of the cells producing these mediators (i.e. NP cells, AF cells, native IVD cells only, native cells plus infiltrating inflammatory cells) is highlighted. Although pleiotropic, cytokines and chemokines have three modes of action: 1) stimulating the production of other inflammatory mediators and MMPs; 2) enhancing matrix degradation; and 3) recruiting inflammatory cells and activating phagocytosis [205-210]. Together, these effects can contribute to disease progression in the IVD.

Table 1.5: Inflammatory mediators found in the human IVD. Adapted from [50].

	Mediator	Producing cells	Ref
inflammatory factors that are expressed during homeostasis			
Post-mortem and non-degenerate samples	TNF-α	IVD cells	[95, 211, 212]
	IL-1β	IVD cells	[95, 212-215]
	IL-1α, IL-1Ra, IL-1RI, and ICE	NP and AF cells	[215]
	IL-6, IL-8, RANTES	AF and NP cells	[214]
	NGF	NP and AF cells in monolayer and alginate bead culture	[95, 216]
	NGF receptor (trkA)	NP and AF cells in monolayer and alginate bead culture	[216]
	Substance P		[95]
	PLA2	NP and AF cells	[217]
	CCL3 and CCL4	IVD cells	[218]
	NOTCH	IVD cells	[212]
	MMPs	IVD cells	[95, 208]
inflammatory factors that are expressed with degeneration			
Herniations (including subligamentous and transligamentous, protrusion, extrusion, sequestration, spondylosis, scoliosis, degenerated or dicogenic pain)	TNF-α	IVD cells and infiltrating cells	[95, 193, 211, 219-223]
	IL-1β		[95, 193, 213, 220, 221, 223]
	IL-1α		[220-222]
	IL1-Ra, NO		[220]
	IL-6		[220, 221, 224, 225]
	IL-8		[222, 225]
	IL-12, IL-17, IFN-γ		[224]
	IL-20 (and its receptors)		[206]
	IL-10, TGF-β, RANTES		[222]
	IL-16, CCL2, CCL7, CXCL8		[204]
	Substance P		[95, 220]
	PGE_2		[220, 225]
	COX-2		[223]
	PLA2		[217, 223]
	NGF		[95]
	VEGF, bFGF		[219]
	GM-CSF		[221]
	CD20, CD45RO, CD68		[226]
	MMPs		[95, 219, 220, 226]

bFGF: basic fibroblast growth factor; **CCL:** chemokine ligand; **CXCL:** monokine induced by gamma interferon; **GM-CSF:** granulocyte macrophage colony-stimulating factor;; **ICE:** IL-1β-converting enzyme; **IFN-γ:** interferon gamma; **IL-1Ra:** IL-1 receptor antagonist; **IL-1RI:** IL-1 receptor, type I; **IL:** interleukin; **LPS:** lipopolysaccharide; **MMPs**: metalloproteinases; **NGF:** nerve growth factor **PGE2:** prostaglandin E2; **PLA2:** calcium-dependent phospholipase 2; **TGF-β**: transforming growth factor beta; **TNF-α**: tumor necrosis factor alpha; **TrkA:** high affinity NGF receptor; **VEGF:** vascular endothelial growth factor; **NP:** nucleus pulposus; **AF:** Annulus fibrosus; **IVD:** intervertebral disc.

THE HALLMARKS OF INTERVERTEBRAL DISC AGING

Alike every other organ of the human body, the IVD also faces the recognised hallmarks of aging [227]: genomic instability [228], telomere attrition[229], epigenetic alterations [230], loss of proteostasis [231-235], deregulated nutrient sensing [236], mitochondrial dysfunction [237, 238], cellular senescence [239], stem cell exhaustion [138], and intercellular communication [146, 240, 241]. Although these features may not have all been as thoroughly studied in the disc as in other tissues, particularly with regards to epigenetic alterations and deregulated nutrient sensing pathways, it is well accepted that systemic disc aging is generally characterized by an initial ossification and thinning of the CEP, with marrow contact channels occlusion, and a further drastic reduction in the vascular supply to the disc [178, 242]. The consequent compromised cell nutrition, accumulation of metabolites and increased acidity of the environment is then followed by a decrease in the native cell population together with alterations in cell phenotype and response to damage, which hinders the deposition and maintenance of healthy ECM, ultimately compromising tissue function. Macroscopically, an increased number and size of tissue fissures is detected, along with deposition of granular debris and neovascularization inwards the OAF, the tissue turns yellowish due to age-related accumulation of oxidized matrix proteins, and the NP becomes more fibrous due to a decrease in water and proteoglycan content, leading to a loss on NP osmotic pressure and overall disc height. The main degenerative findings related to disc aging are grouped in Table 1.6.

Animal models of IVD aging. Together with findings in humans, several animal species have served as models to investigate the aging features alterations mentioned above, including mouse [243-248], hamster [249], rat [250], sand rat [251-254], rabbit [255], pig [256], dog [257], sheep [258], alpaca [259], baboon [260, 261] and rhesus monkey [262, 263]. With exception of mouse models, which are genetically modified to express an aged phenotype, these animals present naturally occurring (spontaneous) and age-correlated disc degeneration, alike what happens with humans. However, interspecies variations are obvious [172], hindering the direct translation of results to the human scenario. Ideally, studies would be performed exclusively in human tissue, either from pathological, cadaveric or organ donor source.

Yet, ethical concerns often limit the access to such biological material, slowing down the pace of clinically relevant scientific discoveries. As we stand, work with animal models is an insurmountable fact, particularly in translational research leading to clinical trials. Much depending on the specific question do be addressed, some animal models adequate better than others [172, 264, 265]. Intriguingly, despite readily available, and commonly used to study the molecular phenotype of IVD cells [36, 132, 135, 166, 265-270], as well to serve as model for disc degeneration [271-276], bovine discs have not yet been posed as potential aging models. Indeed, there is one famous study by Demers at al. that concluded that bovine coccygeal discs could be useful to study young healthy (< 40 years old) human lumbar discs, but were not suitable to address aging [277]. However, the range of ages covered was only 8 months to 4 years. Demers *et al*. also suggest that the 8- to 20-month-old bovine coccygeal discs appear more representative of the human discs in their growth phase (less than 15 years old), whereas the older 2- to 4-year-old bovine coccygeal discs appear more biochemically comparable to human lumbar discs undergoing maturation and aging (15–40 years of age), but without significant degrees of degeneration [277]. Hence, changes in elder disc specimens were not covered (> 50 years old), despite the higher incidence of degenerative disc changes (and thus substantial clinical relevance) registered in this age group [12, 178]. Moreover, although interspecies differences may naturally occur, bovine coccygeal discs are becoming increasingly accepted tissues for large animal organ culture, majorly because of their large size and similar aspect ratios, transport distances, and composition, to study human discs. At the biomolecular level, similar types and distribution of aggrecan and collagen are found in human lumbar and bovine coccygeal discs [278, 279], as well as rates of in vitro PG synthesis [278] and matrix deposition in response to hydrostatic pressure [280, 281]. Also, although bovine tails support a lower load than human lumbar discs, the swelling pressure of bovine coccygeal discs has been shown to be similar to that of human discs in in the prone position. In terms of cellular content, cell density is comparable between mature bovine and human NPs [98] and both loose notochordal cells early in life (at birth in cattle [282] and at 11-16 years old in human [178], which are replaced by chondrocyte-like NP cells). The presence or not of notochordal cells may have a profound impact on ECM composition, since the phenotype of these two kinds of cells is very different [134]. In terms of aging, similarities between the two species were

reported, namely in terms of increased denatured collagen II and decreased proteoglycan content in the NP, although age-dependent alterations seem to affect the aging human discs more sharply within the young age window selected [277]. Still, more studies are owed on the overall hallmarks of aging, before the bovine coccygeal disc can be established as a useful tool to investigate age-dependent degenerative alterations.

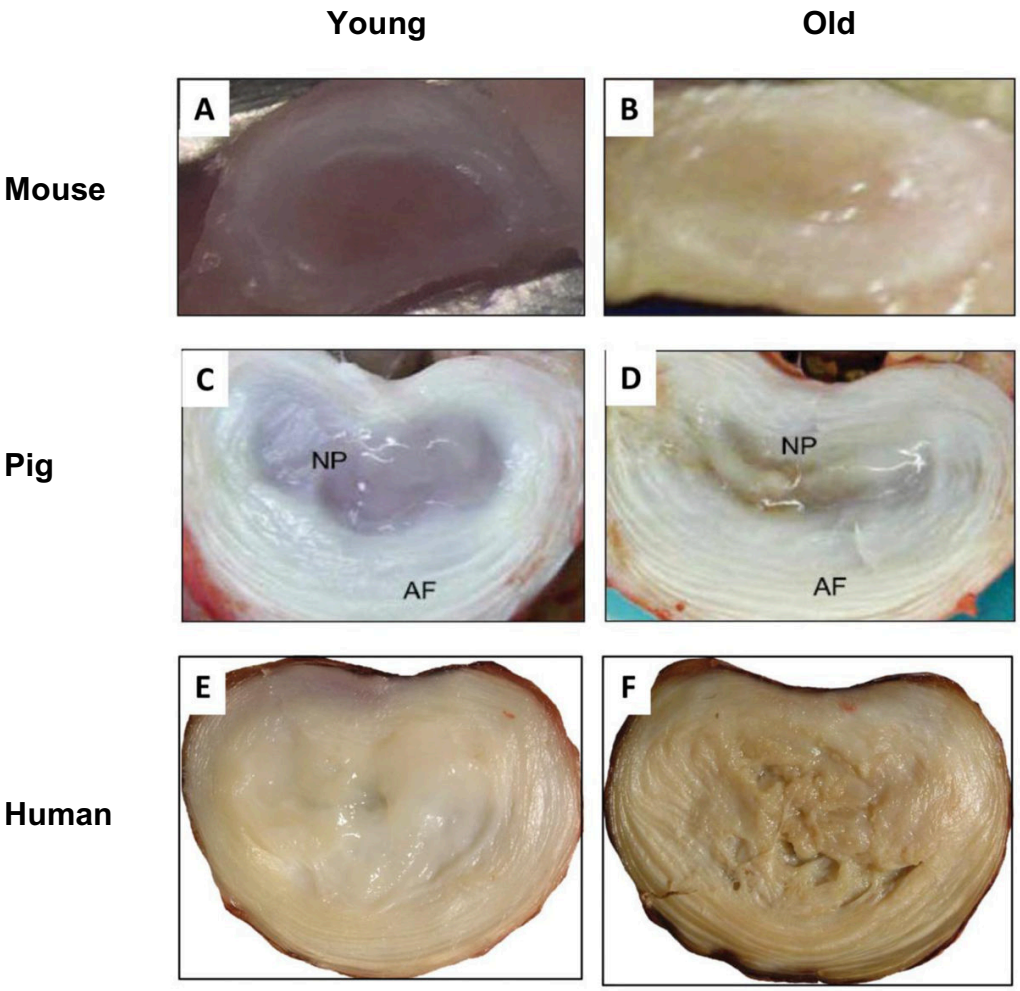

Figure 1.7: Gross features of aged mammalian discs. Pictures show axial sections of young and aged lumbar discs of 3 months- vs 24 months-old mice (A, B), 3 weeks- vs 3 years-old pigs (C, D), and 16 years- vs 55 years-old humans (E, F). Old discs exhibit an overall loss of hydration, loss of demarcation between the AF and NP boundary, and tissue discoloration (old disc more yellowish). Adapted from [283].

Table 1.6: Main features of age-related IVD degeneration. Collected from [239, 283-285].

Degenerative features
Gross anatomy changes (Histopathological/MRI findings)
End-plate sclerosis (calcification and occlusion of marrow contact channels)
Nurturing blood vessel retraction
↓ Water content (decreased signal intensity on MRI)
↓ Disc height
Inward bulging of AF lamellae
Loss of demarcation between NP and AF
Tears and clefts formation
Vascular and nerve ingrowth (inwards the tears)
Osteophyte formation
Altered nutrition and oxygen tension
↓ diffusion of essential nutrients
↓ oxygen levels (hypoxia)
↑ Lactic acid production and accumulation (drop in pH)
Altered cell response
↑ cell clusters (with proliferative cells - damage response)
↑ cell senescence (specially within clusters – secrete pro-aging and catabolic factors)
↑ autophagy and phagocytosis
↑ apoptosis
↑ aberrant deposition of ECM layers around cells
Deregulation of soluble factors
↑ pro-inflammatory cytokines (e.g. TNF-a, IL-1a, IL-1β, IL-1R1, IFN-g, PGE2, NOX)
↑ pro-agiogenic factors (Pleitrophin, VEGF, FGF-2, TGF-b, osteonectin, NGF, BDNF)
↓ semaphorin in OAF (axonal growth repellent)
↑ neurotrophic factors (NGF, BDNF)
Altered ECM composition
↓ Collagen II (specially in the NP)
↑ Collagen I (by NP and IAF cells)
↑ Collagen X (particularly in advanced degeneration, around clefts and clusters)
↑ Collagen VI (particularly around clusters)
↓ Collagen crosslinking
↑ Non-enzymatic glycosilation (AGEs) (tissue becomes more stiff and susceptible to damage)
↑Nonaggregating proteoglycans (from proteolytic degradation of aggrecan)
↑ Keratan sulfate and ↓ chondroitin sulfate
↑ Versican, decorin and biglycan
↑ Fibronectin
↑ Fibronectin fragments and ECM breakdown products (induce inflammation)
↑ Crystal deposits of calcium pyrophosphate dihydrate (CPPD), cuboid microstructures and hydroxyapatite (HA) (may induce inflammation)
Deregulation of proteostasis
↑ MMP-1, 2, 3, 7, 8, 9, and 13 (cleave the majority of ECM constituents)
Occurrence of cathepsin D, G, K, L in the AF (proteolytic enzymes)
↑ ADAMTSs 1, 4, 5, 9 and 15 (high degrading activity against aggrecan)
↑ TIMPs 1, 2 (broad inhibitors of the MMP family)
TIMP 3 is not altered (aggrecanase inhibitor - imbalance)

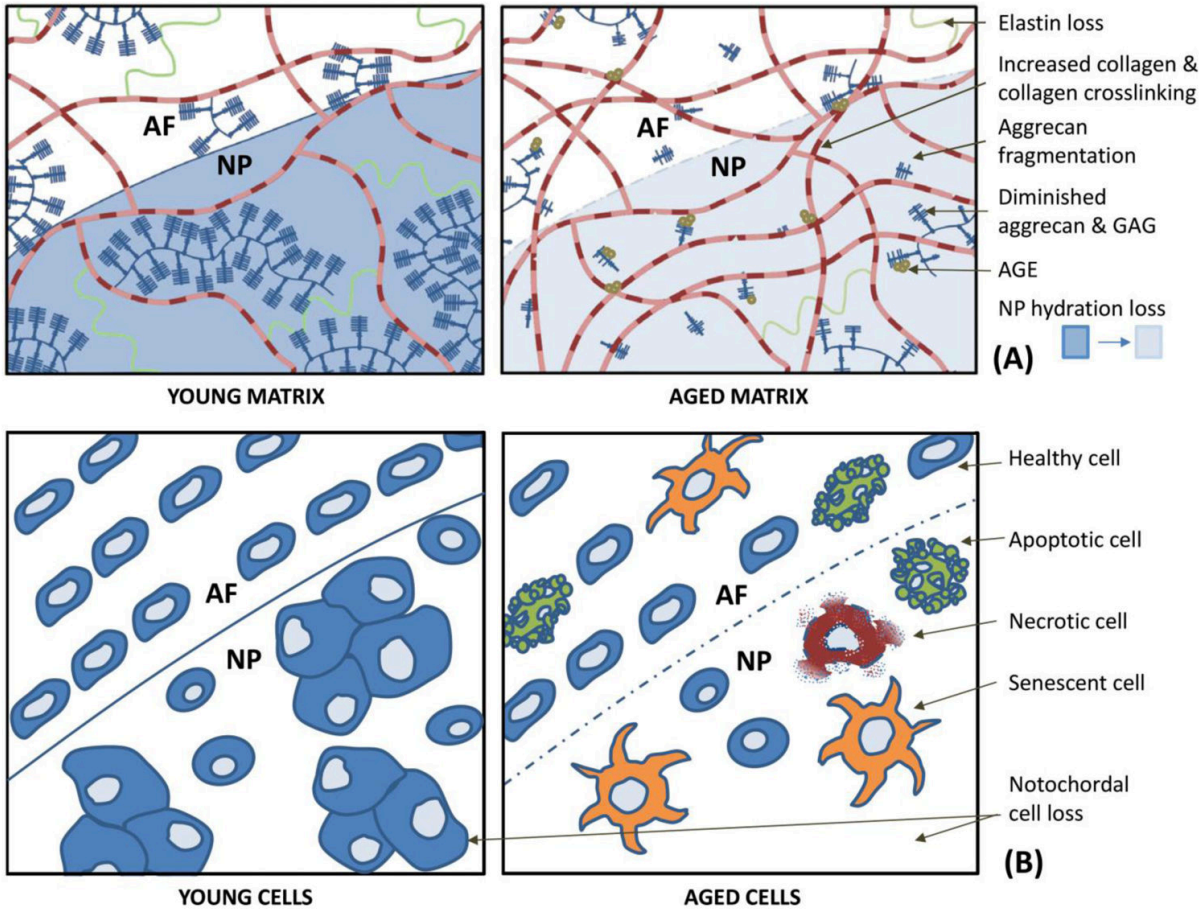

Figure 1.8: Molecular and cellular features of the aging disc. Young and aged extracellular matrix and cells are schematically compared to summarize important changes that occur during disc aging. **A |** Young matrix is rich in elastin (green, coiled fiber), aggregated aggrecan (dark blue, bottle-brush aggregate), and collagen fibers (banded fibers). Aged matrix shows loss of elastin, increased collagen and collagen crosslinking, fragmented aggregan, diminished GAG quality, reduced aggregan aggregates, increased accumulation of advanced glycation end-products (AGEs) along with lower hydration. **B |** Young AF cells are elongated fibrochondrocytes and NP cells are a mixture of large, clustering, notochordal cells and smaller, chondrocyte-like cells. Aged discs show reduced cellularity, loss of notchordal cells, and incidence of senescence, apoptosis, and necrosis. Adapted from [283].

Changes in NP cells molecular profile with age. Since aging and degeneration are two faces of a same coin, the majority of molecular alterations reported cannot be exclusively attributed to age. Indeed, one inherent struggle when studying human disc aging is that young healthy discs available for research purposes are seldom (post mortem samples are an example, but are generally difficult to obtain), and aged tissue is majorly from diseased samples collected upon microdiscectomies, where the degree of degeneration may be exacerbated due to other etiological factors

besides age. Additional challenges, such as 1) separating NP from AF tissue upon discectomy (the loss on demarcation between AF and NP in elder tissue is evident), and 2) in the case of herniated tissues (e.g. extruded, sequestered), avoiding contamination by other cell types, make the analysis of molecules released by regions of the IVD poorly accurate. Hence, few reports exist on molecular profile alterations of NP cells with age. A summary is given in Table 1.7. Interestingly, it was not until very recently that researchers started to confirm at protein level (e.g. IHC, FC) previous results obtained at mRNA level (microarrays and RT-PCR). Tang *et al*. confirmed the differential expression of 8 genes (Brachyury, CD24, CD90, CD155, CD221, Basp-1, Ncdn, Nrp-1) between NP and AF cells, yet, the comparative analysis between the different ages was rather difficult to read, as well as the bridging of the different methods used. Nrp-1 and CD90 staining were decreased in aged NP and AF, respectively, versus immature and mature tissues, and this followed a same genetic trend. Brachyury, however, which gene expression was not statistically different between immature and aged discs, but was up-regulated in mature disc, at the protein level showed an obvious decay on both mature and aged NP. Recently, the same author published new data, this time on human samples, allying IHC to flow cytometry, and probing the similarity of results between the different species. Nrp-1 and brachyury expression were also proven to be decreased during aging and degeneration in human NP, but in contrast, CD24, which was found to be highly expressed in the rat NP irrespective of age, in the human NP was shown to be decreased in the adult tissue (39-69 years old), when compared to juvenile (6-16 years old). Interestingly, new cell surface markers, such as CD166 and CD54, were for the first time shown to be increased in the human NP during aging and degeneration. However, with exception of two patients, the cohort selected for this study included only scoliotic discs, which cells were recently shown to express a molecular dysregulated profile when compared to normal discs [286, 287]. Hence, further validation is required. Besides studying IVD region-specific markers, Thorpe *et al.* also assessed the expression profile of NP samples with degeneration. Within a large cohort of surgical samples (101), FOXF1 and PAX1 mRNA expression in NP, while differential from AF and AC samples, was not increased with degeneration grade (further confirmed by qIHC), which indicate these could be good candidate markers for both young and mature NP cells. Unfortunately, and although the data was available, no correlation was stablished with

patient's age [120]. Finally, early this year, Richardson and colleagues published new data aiming to confirm expression of previously identified NP and NC marker genes in adult human NP from a range of ages and degenerate states. Combining gene expression analysis with IHC, they confirmed that both NP (FoxF1, Pax-1, KRT8, KRT18 and CA12) and NC markers (brachyury, galectin-3 and CD24) are expressed consistently by the NP cell population, regardless of age or grade of degeneration [137]. Interestingly, they verified that changes at the transcript level in NP markers FoxF1 and Pax-1with age find a parallel with changes with degeneration: both are significantly decreased with age (study range: 20-80 years old) and histological grade of tissue degeneration [grading system according to Sive *et al.* [142]: non-degenerate (grade 0–4); moderately degenerate (grade 5–7); and severely degenerate (grade 8–12)]. In contrast, KTR19 shows significant increase in expression in elderly adults when compared to mature adults, and NC marker LGALS3 is decreased only in mature adults (40-59 years old) when compared to young adults (20-39 years old), but no difference with degeneration. On the other hand, CD24 is only expressed in severely degenerate when compared to moderately degenerate discs, but not altered with aging. Noteworthy, IHC findings did not follow the same trend observed at mRNA level, where only brachyury showed decreased expression with both age and degeneration. Interestingly, opposite to the gene expression profile, Galectin-3 immunopositivity was increased in mature adults. Also, CA12 was highly immunoreactive within the NP when compared to the AF, and particularly in severely degenerate samples, while not altered with aging. This supports previous results pointing CA12 as a marker for IVD degeneration [148]. Overall these results represent a substantial contribute to a better understanding of the biological phenomena behind disc aging and degeneration, particularly in the poorly explored field of IVD epigenetics. Indeed, studies to detail the NP phenotype at the protein level are few [87, 120, 137, 148, 152, 288, 289] and validation of gene markers is required, since alterations at the transcriptome level do not necessarily translate into changes at the functional level. Crucially, at this point, standardization of tissue collection and processing techniques, as well as of primary cell isolation and culture is mandatory, so that comparison of results between different labs is feasible and a greater consensus regarding IVD cells phenotype can be achieved.

Table 1.7: Changes in nucleus pulposus cells molecular profile with age.

	SPECIES	BOVINE	RAT			HUMAN					
MOLECULE TYPE	Age / Molecule	Y:A	3M:24M	1M:12M	1M:21M	Y:A	Y:A	ND:D (Age: 45-60 yo)	Y:A	ND:D (Age: NA)	Y:A
INTERMIDIATE FILAMENT PROTEINS	CK- 8	-						↓			- -
	CK-18							↓		-	- -
	CK-19						↓ ↓	-		-	↑
CELL SURFACE RECEPTORS	CD24			-	H	↓ ↓				-	- - ↑
	CD54			-		↑ -					
	CD166			-		↑ ↑					
	CD155/PVR			↓ ↓	↑	↓ -					
	CD325/CDH2			↓				↓			
	CD221/IGF-1R			- ↑	↓ H	↓ -					
	CD168/RHAMM			↓							
	CD90/Thy-1			↓	N	↓ H					
	CD138/SDC1			↓							
	Gal-1/LGAS1,			↓							
	Gal-3/LGAS3,										↓ ↑ ↑
	CA12								↑	-	- H H
	GLUT-1									-	
TRANSCRIPTION FACTORS	Brachyury			**NA** ↑	- ↓	↓ ↓		-		-	- ↓ ?
	FoxF1							-		- -	↓ -
	FoxA2			-							-
	PAX1									- -	↓ -
	HIF1α			-						H	
	ID3			↓							
	ID2			↓							
	OVO-2									-	

SIGNALLING MOLECULES	SHH													?						
	NOGGIN																	-		
NEURONAL-RELATED PROTEINS	NCDN			↑	-	↑	H	↓												
	LRRN3			↓																
	DPP6			↓																
	AARD			↓																
	BASP1			-	-	↑	H	↓				-								
	NDN			↓																
	NRP-1			↓	-	↓	↓	↓												
	SNAP25											↓								
ECM-RELATED PROTEINS	COL2A1											-								
	ACAN											-								
	VCAN											-								
	IBSP											-		-						
	TNMD											-								
	LAMA5													-						
	LAMC2													-						
	FBLN1											↑								
	COMP		↑																	
	MGP		↑							↑	-									
	Method (sample size)	IHC (6)	RT-PCR (3-6)	MA (4)	RT-PCR (4)	RT-PCR (4)	IHC (3)	IHC (11)	FC* (5)	RT-PCR (11)	IHC (41)	MA (10)		IHC (6)	MA (71)	qIHC (30)	RT-PCR (60)	qIHC (56)	FC* (5)	
	Reference	[288]	[150]	[289]				[152]		[87]		[135]		[148]	[120]		[137]			

***FC:** flow cytometry after cell expansion in 2D liquid culture; **IHC:** immunohistochemistry; **M:** months; Y young; **A**: adult; **D**: degenerate; **ND**: non-degenerate; **N**: not detected; **H**: always high; **NA**: not available; ↓ Decreased; ↑ Increased; **-** maintained**?** contradictory findings

PRO-REGENERATIVE THERAPIES TARGETING DETRIMENTAL AGE EFFECTS ON INTERVERTEBRAL DISC CELLS

Age-related degenerative changes within the IVD can be found already in adolescence, with formation of clefts and tears, particularly in the centre of the disc, with substantial loss of notochordal cells and nurturing blood vessels, extensive cell death and proliferation of chondrocyte-like cells [178]. Hence, preventive therapies to address disc degeneration should take place very early in life. As such, there is a growing awareness that a healthier life-style (e.g. muscle-strengthening physical activities, un-physiological or excessive loadings avoidance, no smoking, balanced nutrition and low body weight) should be the starting point to delay age-accelerated disc degeneration [13]. On the other hand, biological approaches to treat IVD degeneration are still on its infancy and are mainly focused on counter acting age-occurring endogenous stressors, such as metabolic malfunctioning, DNA replication errors and inflammation. Thus, novel anti-aging strategies to IVD include reducing reactive oxygen species (ROS) production [237], minimizing aberrant damage response from cells (i.e. targeting intracellular signalling pathways) [290, 291], or addressing changes within the ECM or on cells, through protein-, gene- or cell-based therapies [27], although the latter have been essentially pursued in the context of disc degeneration and not specifically aging [27].

As a result of various exogenous stimuli, such as mechanical loading, high oxygen tension, high glucose stress, and proinflammatory cytokines, excessive mitochondria-derived ROS production has been reported in degenerative discs [292], as well as in an accelerated aging mice model [293], disturbing the redox homeostasis in IVD microenvironment. ROS are responsible for the activation of important signalling molecules on disc cells, which are involved in matrix metabolism, inflammation and autophagy (e.g ERK, JNK, p38, p65, p53, Akt, Nrf2, ATM, and Chk2) [292, 294-297]. Thus, various antioxidants, such as N-acetylcysteine (NAC), resveratrol, ROS scavengers, herbal components and growth factors, are under investigation, and were already proven effective on preventing the deleterious effects of ROS on human disc cells *in vitro* [237]. Indeed, although their effect on relieving IDD-associated LBP or on retarding the establishment and progression of IDD remains unknown, antioxidants hold great potential as anti-aging therapeutics.

Aging is per-se one of the major risk factors for IDD, implying a time-dependent accumulation of cell replication and replicative senescence. In young organisms, cellular senescence prevents the proliferation of damaged cells, thus protecting from other age-associated diseases as cancer and contributing to tissue homeostasis. In old organisms, the gradual systemic damage and the deficient clearance of senescent cells result in their accumulation, and this has a number of deleterious effects on tissue homeostasis, ultimately contributing to aging. Bearing in mind that senescent cells are also producers of ROS, along with catabolic cytokines and degrading enzymes, their presence is not desirable. Studies have shown that when the gel-like NP undergoes fibrosis, cells proliferate in an attempt to produce new ECM and re-establishing the hypertonic microenvironment. However, cells fail to self-repair the damaged tissue and replicative senescence is promoted, resulting in accumulation of senescent cell clusters [239, 298-300]. Hence, restoring the hydrated aggrecan-rich healthy NP matrix, as well as applying overall anti-senescence therapies (e.g. telomerase transduction, supply of growth factors and blocking cell cycle inhibitors) may delay aging effects on disc cells.

Research into the specific roles of intracellular signalling pathways in the disc has risen sharply in recent years. However, while many different pathways where found to be involved in disease progression, only the Nf-κB pathway was directly associated with disc aging [301]. Effectively, in two studies using a rodent model of accelerated aging, NF-κB signalling was suppressed genetically and pharmacologically, and the onset of age-related disc proteoglycan loss, as well as other degenerative changes, was delayed [290, 291]. Thus, NF-κB may also be a promising target to minimize the aberrant damage response, which exacerbates disc damage associated with age, even though its implication in many other biological processes [302] would certainly complicate the quest.

At the intercellular level, inflammaging, i.e., an installed proinflammatory phenotype, even in the absence of infection [303], is another prominent aging-associated alteration, in which the NOD-like receptor family pyrin domain containing 3 (NLRP3) inflammasome, together with other proinflammatory pathways are activated, leading to increased production of IL-1β, TNF-α and interferons. In the disc, while IL-1β is a recognized proinflammatory promoter of degeneration [211], by eliciting ECM degradation and inducing angiogenesis and neo-innervation, the molecular

mechanisms associated with its maturation and release remain unclear. Recently, the expression level of the NLRP3 inflammasome was shown to be markedly increased in the NP of human degenerate IVDs when compared to non-degenerate ones [304]. Furthermore, correlation studies from this report suggest that excessive activation of this molecule results in overproduction of downstream IL-1β [304]. One hypothesis behind this inflammatory response relies on the presence of crystals and ECM breakdown products [305]. Crystal deposits of calcium pyrophosphate dihydrate (CPPD), cuboid microstructures (characterized as magnesium whitlockite) and hydroxyapatite (HA) have been observed in degenerated IVD specimens [287, 306-308]. In articular cartilage, regions with crystals showed altered amounts of collagen, calcium-binding proteins, decorin and large proteoglycan content, as well as abnormal pericellular matrix deposition [309, 310]. Phagocytosis of crystals present in joints and pericellular tissues can prompt the activation of the NLRP3 inflammasome [311]. This cytoplasmic multimolecular protein complex regulates activity of caspase-1 and maturation and release of IL-1β [305, 312]. Most recently, another hypothesis points the accumulation of advanced glycation end-products (AGEs) within the NP as a possible initiator of inflammation-related degeneration, also via NLRP3 activation [313]. AGEs are formed by non-enzymatic glycation of macromolecules and accumulate in long-lived proteins during aging and degeneration. These have been previously identified throughout the disc and are more abundant with increasing age [314-316], eliciting oxidative stress and contributing to stiffness, brittleness and biomechanical alterations in collagen-rich tissues [317].

Overall, these findings highlight novel and exciting potential therapeutic targets for the prevention of premature age-related disc degeneration, while also proving the prompt need for a better understanding on IVD cells phenotypic signature in homeostasis, degeneration and aging. Importantly, methodological standardization in in field of research is also lacking, particularly regarding IVD primary cells isolation and manipulation.

AIMS OF THE THESIS

Regenerative medicine-based approaches to degenerated IVD are increasing, although with a profound lacuna on the scientific knowledge addressing basic cellular and molecular-related phenomena. While the main treatments targeting disc-related back pain are interventive in nature, seeking to guarantee symptomatic relief, preventive therapies could revolutionize this field of medicine. IVD degeneration is a gradual and long-lasting process of successive biomolecular and functional failures, starting earlier in life than in other organs, due to the exclusive and harsh microenvironment the native cells need to endure, and to their high susceptibility to exogenous stressors. Strategies aiming to restore IVD homeostasis, particularly addressing early age-correlated degenerative changes, could be more successful in combating IDD and contribute to an overall decrease in the estimated years lived with disability by the global population.

The aim of this PhD thesis is to better characterize the phenotypic signature of the endemic cell populations of the IVD, more specifically the ones found within the Nucleus Pulposus, and shed light on the cellular changes that occur with aging.

Therefore, the main objectives of the thesis are organized as follows:

1 **Improvement of nucleus pulposus primary cells isolation and dissection of their main phenotypic characteristics in homeostasis.**

In order to achieve this objective, bovine coccygeal discs were chosen as a model, and cells from the NP were harvested following three distinct protocols. This allowed to establish an improved method for bovine NP (bNP) cell isolation, whose procedure is still not consensual among the literature, and the subsequent thorough characterization of the cell (sub)populations that exist in the young NP. The results, which contribute to a better understanding of NP cell biology and its potential endogenous regenerative capacity, are presented in Chapter II, and demonstrate that collagenase-type-XI is an efficient enzyme to digest bNP, while highlighting the discovery of three phenotypically distinct subpopulations of cells within the bNP.

2 Study of aging effects on primary bovine NP cells phenotypic and genotypic signature.

Following the rational of previous work, primary cells from bovine coccygeal discs were further characterized, this time comparing cells from young (12 months old) and old (10-16 years old) animals, in order to uncover age-related alterations that occur on cells surface receptors expression, subpopulations signature, cells morphology and gene expression. Results from this study are gathered in Chapter III, revealing significant changes between the different age groups at both protein and gene levels. Importantly, we prove that the bovine animal model is a valuable tool to explore age-induced modifications on NP cell and to identify potential anti-aging targets, towards the prevention of IVD degeneration.

3 Dissection of age-correlated phenotypic alteration in cells isolated from human degenerated intervertebral discs with contained hernias.

This part of the work was conducted in collaboration with a team of neurosurgeons from Hospital de S. João, Porto, who gave us access to human IVD tissue from patients undergoing microdiscectomy. This task was performed taking advantage of a multiparameter image analysis tool (Imaging flow cytometry), which guaranteed robust quantitation of morphological features. Hence, parameters such as IVD cells size, prevalence of clusters and pericellular matrix (PCM) area were correlated with age, while changes in expression of known stem cell-related and NP-progenitor markers were also monitored. These findings are presented in Chapter IV and highlight the remarkable morphological alterations that occur on primary human IVD cells with aging and degeneration, while reinforcing previous reports on the gradual disappearance of an endogenous progenitor cell population.

References

[1] Global Burden of Disease Study, C. (2015) *Global, regional, and national incidence, prevalence, and years lived with disability for 301 acute and chronic diseases and injuries in 188 countries, 1990-2013: a systematic analysis for the Global Burden of Disease Study 2013.* Lancet, 386(9995): p. 743-800.

[2] Maher, C., M. Underwood, and R. Buchbinder (2017) *Non-specific low back pain.* Lancet, 389(10070): p. 736-747.

[3] Andersson, G.B. (1999) *Epidemiological features of chronic low-back pain.* Lancet, 354(9178): p. 581-5.

[4] Hoy, D., P. Brooks, F. Blyth, and R. Buchbinder (2010) *The Epidemiology of low back pain.* Best Pract Res Clin Rheumatol, 24(6): p. 769-81.

[5] Woolf, A.D. and B. Pfleger (2003) *Burden of major musculoskeletal conditions.* Bull World Health Organ, 81(9): p. 646-56.

[6] Branco, J.C., A.M. Rodrigues, N. Gouveia, M. Eusebio, S. Ramiro, et al. (2016) *Prevalence of rheumatic and musculoskeletal diseases and their impact on health-related quality of life, physical function and mental health in Portugal: results from EpiReumaPt- a national health survey.* RMD Open, 2(1): p. e000166.

[7] Gouveia, N., A. Rodrigues, M. Eusebio, S. Ramiro, P. Machado, et al. (2016) *Prevalence and social burden of active chronic low back pain in the adult Portuguese population: results from a national survey.* Rheumatol Int, 36(2): p. 183-97.

[8] Olmarker, K., (2014) *Back pain and disc degeneration: are they really linked?*, in *The intervertebral disc: molecular and structural studies of the disc in health and disease*, I.M. Shapiro and M.V. Risbud, Editors. Springer: Wien. p. 261-275.

[9] Schwarzer, A.C., C.N. Aprill, R. Derby, J. Fortin, G. Kine, et al. (1995) *The prevalence and clinical features of internal disc disruption in patients with chronic low back pain.* Spine (Phila Pa 1976), 20(17): p. 1878-83.

[10] Cheung, K.M., J. Karppinen, D. Chan, D.W. Ho, Y.Q. Song, et al. (2009) *Prevalence and pattern of lumbar magnetic resonance imaging changes in a population study of one thousand forty-three individuals.* Spine (Phila Pa 1976), 34(9): p. 934-40.

[11] Teraguchi, M., N. Yoshimura, H. Hashizume, S. Muraki, H. Yamada, et al. (2014) *Prevalence and distribution of intervertebral disc degeneration over the entire spine in a population-based cohort: the Wakayama Spine Study.* Osteoarthritis Cartilage, 22(1): p. 104-10.

[12] Battie, M.C., T. Videman, and E. Parent (2004) *Lumbar disc degeneration: epidemiology and genetic influences.* Spine (Phila Pa 1976), 29(23): p. 2679-90.

[13] Wang, Y. and M.C. Battie, (2014) *Epidemiology of lumbar disc degeneration*, in *The intervertebral disc: molecular and structural studies of the disc in health and disease*, I.M. Shapiro and M.V. Risbud, Editors. Springer: Wien. p. 139-156.

[14] Rajaee, S.S., H.W. Bae, L.E. Kanim, and R.B. Delamarter (2012) *Spinal fusion in the United States: analysis of trends from 1998 to 2008.* Spine (Phila Pa 1976), 37(1): p. 67-76.

[15] Boden, S.D., P.R. McCowin, D.O. Davis, T.S. Dina, A.S. Mark, et al. (1990) *Abnormal magnetic-resonance scans of the cervical spine in asymptomatic subjects. A prospective investigation.* J Bone Joint Surg Am, 72(8): p. 1178-84.

[16] Boden, S.D., D.O. Davis, T.S. Dina, N.J. Patronas, and S.W. Wiesel (1990) *Abnormal magnetic-resonance scans of the lumbar spine in asymptomatic subjects. A prospective investigation.* J Bone Joint Surg Am, 72(3): p. 403-8.

[17] Adams, M.A. and P.J. Roughley (2006) *What is intervertebral disc degeneration, and what causes it?* Spine (Phila Pa 1976), 31(18): p. 2151-61.

[18] Battie, M.C., T. Videman, J. Kaprio, L.E. Gibbons, K. Gill, et al. (2009) *The Twin Spine Study: contributions to a changing view of disc degeneration.* The spine journal : official journal of the North American Spine Society, 9(1): p. 47-59.

[19] Nasser, R., S. Yadla, M.G. Maltenfort, J.S. Harrop, D.G. Anderson, et al. (2010) *Complications in spine surgery.* J Neurosurg Spine, 13(2): p. 144-57.

[20] Swann, M.C., K.S. Hoes, S.G. Aoun, and D.L. McDonagh (2016) *Postoperative complications of spine surgery.* Best Pract Res Clin Anaesthesiol, 30(1): p. 103-20.

[21] Swartz, K.R. and G.R. Trost (2003) *Recurrent lumbar disc herniation.* Neurosurg Focus, 15(3): p. E10.

[22] Onesti, S.T. (2004) *Failed back syndrome.* Neurologist, 10(5): p. 259-64.

[23] Sakai, D. and G.B. Andersson (2015) *Stem cell therapy for intervertebral disc regeneration: obstacles and solutions.* Nat Rev Rheumatol, 11(4): p. 243-56.

[24] Richardson, S.M., G. Kalamegam, P.N. Pushparaj, C. Matta, A. Memic, et al. (2016) *Mesenchymal stem cells in regenerative medicine: Focus on articular cartilage and intervertebral disc regeneration.* Methods, 99: p. 69-80.

[25] Hughes, S.P., A.J. Freemont, D.W. Hukins, A.H. McGregor, and S. Roberts (2012) *The pathogenesis of degeneration of the intervertebral disc and emerging therapies in the management of back pain.* J Bone Joint Surg Br, 94(10): p. 1298-304.

[26] Sakai, D. and J. Schol (2017) *Cell therapy for intervertebral disc repair: Clinical perspective.* Journal of Orthopaedic Translation, 9: p. 8-18.

[27] Pennicooke, B., Y. Moriguchi, I. Hussain, L. Bonssar, and R. Hartl (2016) *Biological Treatment Approaches for Degenerative Disc Disease: A Review of Clinical Trials and Future Directions.* Cureus, 8(11): p. e892.

[28] Moss, I.L., H.S. An, F.H. Shen, Z. Li, G. Andersson, et al., (2014) *The nonsurgical treatment of back pain*, in *The intervertebral disc: molecular and structural studies of the disc in health and disease*, I.M. Shapiro and M.V. Risbud, Editors. Springer. p. 247-259.

[29] Smith, L.J., N.L. Nerurkar, K.S. Choi, B.D. Harfe, and D.M. Elliott (2010) *Degeneration and regeneration of the intervertebral disc: lessons from development.* Disease Models & Mechanisms, 4(1): p. 31-41.

[30] Henriksson, H.B. and H. Brisby (2012) *Development and Regeneration Potential of the Mammalian Intervertebral Disc.* Cells, tissues, organs.

[31] Horner, H.A., S. Roberts, R.C. Bielby, J. Menage, H. Evans, et al. (2002) *Cells from different regions of the intervertebral disc: effect of culture system on matrix expression and cell phenotype.* Spine (Phila Pa 1976), 27(10): p. 1018-28.

[32] Hayes, A.J., M. Benjamin, and J.R. Ralphs (1999) *Role of actin stress fibres in the development of the intervertebral disc: cytoskeletal control of extracellular matrix assembly.* Dev Dyn, 215(3): p. 179-89.

[33] Humzah, M.D. and R.W. Soames (1988) *Human intervertebral disc: structure and function.* Anat Rec, 220(4): p. 337-56.

[34] Raj, P.P. (2008) *Intervertebral disc: anatomy-physiology-pathophysiology-treatment.* Pain Pract, 8(1): p. 18-44.

[35] Inoue, H. (1981) *Three-dimensional architecture of lumbar intervertebral discs.* Spine, 6(2): p. 139-46.

[36] Yu, J., P.C. Winlove, S. Roberts, and J.P. Urban (2002) *Elastic fibre organization in the intervertebral discs of the bovine tail.* Journal of anatomy, 201(6): p. 465-75.

[37] Marchand, F. and A.M. Ahmed (1990) *Investigation of the laminate structure of lumbar disc anulus fibrosus.* Spine, 15(5): p. 402-10.

[38] Bron, J.L., M.N. Helder, H.J. Meisel, B.J. Van Royen, and T.H. Smit (2009) *Repair, regenerative and supportive therapies of the annulus fibrosus: achievements and challenges.* Eur Spine J, 18(3): p. 301-13.

[39] Nerurkar, N.L., D.M. Elliott, and R.L. Mauck (2010) *Mechanical design criteria for intervertebral disc tissue engineering.* J Biomech, 43(6): p. 1017-30.

[40] Plessis, B., M. Goldberg, R. Dillon, J. Tombaugh, J. Robertson, et al. (1989) *Context-dependent enhancements for radiological images.* Journal of digital imaging :

the official journal of the Society for Computer Applications in Radiology, 2(2): p. 114-22.

[41] An, H.S., P.A. Anderson, V.M. Haughton, J.C. Iatridis, J.D. Kang, et al. (2004) *Introduction: disc degeneration: summary.* Spine, 29(23): p. 2677-8.

[42] Bogduk, N. (2005) *Clinical Anatomy of the Lumbar Spine and Sacrum*. 4th edition ed, ed. E.C. Livingstone.

[43] Nachemson, A., T. Lewin, A. Maroudas, and M.A. Freeman (1970) *In vitro diffusion of dye through the end-plates and the annulus fibrosus of human lumbar inter-vertebral discs.* Acta Orthop Scand, 41(6): p. 589-607.

[44] Lotz, J.C., A.J. Fields, and E.C. Liebenberg (2013) *The role of the vertebral end plate in low back pain.* Global Spine J, 3(3): p. 153-64.

[45] Melrose, J., P. Ghosh, and T.K. Taylor (2001) *A comparative analysis of the differential spatial and temporal distributions of the large (aggrecan, versican) and small (decorin, biglycan, fibromodulin) proteoglycans of the intervertebral disc.* J Anat, 198(Pt 1): p. 3-15.

[46] Lewis, N.T., M.A. Hussain, and J.J. Mao (2008) *Investigation of nano-mechanical properties of annulus fibrosus using atomic force microscopy.* Micron, 39(7): p. 1008-19.

[47] Richardson, S.M., R. Knowles, D. Marples, J.A. Hoyland, and A. Mobasheri (2008) *Aquaporin expression in the human intervertebral disc.* Journal of Molecular Histology, 39(3): p. 303-309.

[48] Ishihara, H., K. Warensjo, S. Roberts, and J.P. Urban (1997) *Proteoglycan synthesis in the intervertebral disk nucleus: the role of extracellular osmolality.* Am J Physiol, 272(5 Pt 1): p. C1499-506.

[49] Bibby, S.R., D.A. Jones, R.B. Lee, J. Yu, and J.P.G. Urban (2001) *The pathophysiology of the intervertebral disc.* Joint Bone Spine, 68(6): p. 537-42.

[50] Molinos, M., C.R. Almeida, J. Caldeira, C. Cunha, R.M. Goncalves, et al. (2015) *Inflammation in intervertebral disc degeneration and regeneration.* J R Soc Interface, 12(104): p. 20141191.

[51] Eyre, D.R. and H. Muir (1977) *Quantitative analysis of types I and II collagens in human intervertebral discs at various ages.* Biochimica et biophysica acta, 492(1): p. 29-42.

[52] Eyre, D.R., I.R. Dickson, and K. Van Ness (1988) *Collagen cross-linking in human bone and articular cartilage. Age-related changes in the content of mature hydroxypyridinium residues.* The Biochemical journal, 252(2): p. 495-500.

[53] Sivan, S.S., A.J. Hayes, E. Wachtel, B. Caterson, Y. Merkher, et al. (2014) *Biochemical composition and turnover of the extracellular matrix of the normal and degenerate intervertebral disc.* Eur Spine J, 23 Suppl 3: p. S344-53.

[54] Eyre, D.R. and H. Muir (1976) *Types I and II collagens in intervertebral disc. Interchanging radial distributions in annulus fibrosus.* Biochem J, 157(1): p. 267-70.

[55] Brinckmann, J., H. Notbohm, and P.K. Müller (2005) *Collagen: Primer in Structure, Processing and Assembly*. Topics in Current Chemistry. Vol. 247. Springer.

[56] Ippolito, E. and I.V. Ponseti (1981) *Juvenile kyphosis: histological and histochemical studies.* J Bone Joint Surg Am, 63(2): p. 175-82.

[57] Gruber, H.E., J.A. Ingram, and E.N. Hanley, Jr. (2007) *Morphologic complexity of the pericellular matrix in the annulus of the human intervertebral disc.* Biotech Histochem, 82(4-5): p. 217-25.

[58] Roberts, S., J. Menage, V. Duance, and S.F. Wotton (1991) *Type III collagen in the intervertebral disc.* The Histochemical journal, 23(11-12): p. 503-8.

[59] Culav, E.M., C.H. Clark, and M.J. Merrilees (1999) *Connective tissues: matrix composition and its relevance to physical therapy.* Phys Ther, 79(3): p. 308-19.

[60] Clouet, J., G. Grimandi, M. Pot-Vaucel, M. Masson, H.B. Fellah, et al. (2009) *Identification of phenotypic discriminating markers for intervertebral disc cells and articular chondrocytes.* Rheumatology, 48(11): p. 1447-1450.

[61] Mio, F., K. Chiba, Y. Hirose, Y. Kawaguchi, Y. Mikami, et al. (2007) *A functional polymorphism in COL11A1, which encodes the alpha 1 chain of type XI collagen, is associated with susceptibility to lumbar disc herniation.* Am J Hum Genet, 81(6): p. 1271-7.

[62] Tow, B.P., W.K. Hsu, and J.C. Wang (2007) *Disc regeneration: a glimpse of the future.* Clin Neurosurg, 54: p. 122-8.

[63] Roberts, S., S. Ayad, and P.J. Menage (1991) *Immunolocalisation of type VI collagen in the intervertebral disc.* Annals of the rheumatic diseases, 50(11): p. 787-91.

[64] Melrose, J., S.M. Smith, R.C. Appleyard, and C.B. Little (2008) *Aggrecan, versican and type VI collagen are components of annular translamellar crossbridges in the intervertebral disc.* European spine journal : official publication of the European Spine Society, the European Spinal Deformity Society, and the European Section of the Cervical Spine Research Society, 17(2): p. 314-24.

[65] Eyre, D.R., J.J. Wu, R.J. Fernandes, T.A. Pietka, and M.A. Weis (2002) *Recent developments in cartilage research: matrix biology of the collagen II/IX/XI heterofibril network.* Biochem Soc Trans, 30(Pt 6): p. 893-9.

[66] Brinckmann, J., S. Kim, J. Wu, D.P. Reinhardt, C. Batmunkh, et al. (2005) *Interleukin 4 and prolonged hypoxia induce a higher gene expression of lysyl hydroxylase 2 and an altered cross-link pattern: important pathogenetic steps in early and late stage of systemic scleroderma?* Matrix Biol, 24(7): p. 459-68.

[67] Eyre, D.R., Y. Matsui, and J.J. Wu (2002) *Collagen polymorphisms of the intervertebral disc.* Biochem Soc Trans, 30(Pt 6): p. 844-8.

[68] Onnerfjord, P., A. Khabut, F.P. Reinholt, O. Svensson, and D. Heinegard (2012) *Quantitative proteomic analysis of eight cartilaginous tissues reveals characteristic*

differences as well as similarities between subgroups. J Biol Chem, 287(23): p. 18913-24.

[69] Johnson, W.E., B. Caterson, S.M. Eisenstein, and S. Roberts (2005) *Human intervertebral disc aggrecan inhibits endothelial cell adhesion and cell migration in vitro.* Spine (Phila Pa 1976), 30(10): p. 1139-47.

[70] Gotz, W., S. Barnert, R. Bertagnoli, N. Miosge, H. Kresse, et al. (1997) *Immunohistochemical localization of the small proteoglycans decorin and biglycan in human intervertebral discs.* Cell and tissue research, 289(1): p. 185-90.

[71] Hildebrand, A., M. Romaris, L.M. Rasmussen, D. Heinegard, D.R. Twardzik, et al. (1994) *Interaction of the small interstitial proteoglycans biglycan, decorin and fibromodulin with transforming growth factor beta.* The Biochemical journal, 302 (Pt 2): p. 527-34.

[72] Reed, C.C. and R.V. Iozzo (2002) *The role of decorin in collagen fibrillogenesis and skin homeostasis.* Glycoconj J, 19(4-5): p. 249-55.

[73] Gruber, H.E., J.A. Ingram, G.L. Hoelscher, N. Zinchenko, E.N. Hanley, Jr., et al. (2009) *Asporin, a susceptibility gene in osteoarthritis, is expressed at higher levels in the more degenerate human intervertebral disc.* Arthritis Res Ther, 11(2): p. R47.

[74] Kizawa, H., I. Kou, A. Iida, A. Sudo, Y. Miyamoto, et al. (2005) *An aspartic acid repeat polymorphism in asporin inhibits chondrogenesis and increases susceptibility to osteoarthritis.* Nat Genet, 37(2): p. 138-44.

[75] Chakravarti, S. (2002) *Functions of lumican and fibromodulin: lessons from knockout mice.* Glycoconjugate journal, 19(4-5): p. 287-93.

[76] Bengtsson, E., M. Morgelin, T. Sasaki, R. Timpl, D. Heinegard, et al. (2002) *The leucine-rich repeat protein PRELP binds perlecan and collagens and may function as a basement membrane anchor.* J Biol Chem, 277(17): p. 15061-8.

[77] Haglund, L., J. Ouellet, and P. Roughley (2009) *Variation in chondroadherin abundance and fragmentation in the human scoliotic disc.* Spine (Phila Pa 1976), 34(14): p. 1513-8.

[78] Akhatib, B., P. Onnerfjord, R. Gawri, J. Ouellet, P. Jarzem, et al. (2013) *Chondroadherin fragmentation mediated by the protease HTRA1 distinguishes human intervertebral disc degeneration from normal aging.* J Biol Chem, 288(26): p. 19280-7.

[79] Melrose, J., S. Smith, P. Ghosh, and J. Whitelock (2003) *Perlecan, the multidomain heparan sulfate proteoglycan of basement membranes, is also a prominent component of the cartilaginous primordia in the developing human fetal spine.* J Histochem Cytochem, 51(10): p. 1331-41.

[80] Oegema, T.R., Jr., S.L. Johnson, D.J. Aguiar, and J.W. Ogilvie (2000) *Fibronectin and its fragments increase with degeneration in the human intervertebral disc.* Spine, 25(21): p. 2742-7.

[81] Kadler, K.E., A. Hill, and E.G. Canty-Laird (2008) *Collagen fibrillogenesis: fibronectin, integrins, and minor collagens as organizers and nucleators.* Current opinion in cell biology, 20(5): p. 495-501.

[82] Leiss, M., K. Beckmann, A. Giros, M. Costell, and R. Fassler (2008) *The role of integrin binding sites in fibronectin matrix assembly in vivo.* Current opinion in cell biology, 20(5): p. 502-7.

[83] Yu, J., J.C. Fairbank, S. Roberts, and J.P. Urban (2005) *The elastic fiber network of the anulus fibrosus of the normal and scoliotic human intervertebral disc.* Spine (Phila Pa 1976), 30(16): p. 1815-20.

[84] Yu, J., P.C. Winlove, S. Roberts, and J.P. Urban (2002) *Elastic fibre organization in the intervertebral discs of the bovine tail.* J Anat, 201(6): p. 465-75.

[85] Johnson, E.F., K. Chetty, I.M. Moore, A. Stewart, and W. Jones (1982) *The distribution and arrangement of elastic fibres in the intervertebral disc of the adult human.* J Anat, 135(Pt 2): p. 301-9.

[86] Ishii, Y., A.O. Thomas, X.E. Guo, C.T. Hung, and F.H. Chen (2006) *Localization and distribution of cartilage oligomeric matrix protein in the rat intervertebral disc.* Spine (Phila Pa 1976), 31(14): p. 1539-46.

[87] Rutges, J., L.B. Creemers, W. Dhert, S. Milz, D. Sakai, et al. (2010) *Variations in gene and protein expression in human nucleus pulposus in comparison with annulus fibrosus and cartilage cells: potential associations with aging and degeneration.* Osteoarthritis and Cartilage, 18(3): p. 416-423.

[88] Gruber, H.E., P. Bornstein, E.H. Sage, J.A. Ingram, N. Zinchenko, et al. (2008) *Disruption of the thrombospondin-2 gene alters the lamellar morphology but does not permit vascularization of the adult mouse lumbar disc.* Arthritis Res Ther, 10(4): p. R96.

[89] DiCesare, P.E., M. Morgelin, K. Mann, and M. Paulsson (1994) *Cartilage oligomeric matrix protein and thrombospondin 1. Purification from articular cartilage, electron microscopic structure, and chondrocyte binding.* Eur J Biochem, 223(3): p. 927-37.

[90] Le Maitre, C.L., A.J. Freemont, and J.A. Hoyland (2004) *Localization of degradative enzymes and their inhibitors in the degenerate human intervertebral disc.* The Journal of Pathology, 204(1): p. 47-54.

[91] Vo, N.V., R.A. Hartman, T. Yurube, L.J. Jacobs, G.A. Sowa, et al. (2013) *Expression and regulation of metalloproteinases and their inhibitors in intervertebral disc aging and degeneration.* Spine J, 13(3): p. 331-41.

[92] Weiler, C., A.G. Nerlich, J. Zipperer, B.E. Bachmeier, and N. Boos (2002) *2002 SSE Award Competition in Basic Science: expression of major matrix metalloproteinases is associated with intervertebral disc degradation and resorption.* Eur Spine J, 11(4): p. 308-20.

[93] Pockert, A.J., S.M. Richardson, C.L. Le Maitre, M. Lyon, J.A. Deakin, et al. (2009) *Modified expression of the ADAMTS enzymes and tissue inhibitor of metalloproteinases 3 during human intervertebral disc degeneration.* Arthritis Rheum, 60(2): p. 482-91.

[94] Nagase, H., (2012) *The ADAMTS family of metalloproteinases*, in *Extracellular Matrix: Pathobiology and Signalling*, N. Karamanos, Editor. De Gruyter: Berlin.

[95] Richardson, S.M., P. Doyle, B.M. Minogue, K. Gnanalingham, and J.A. Hoyland (2009) *Increased expression of matrix metalloproteinase-10, nerve growth factor and substance P in the painful degenerate intervertebral disc.* Arthritis Res Ther, 11(4): p. R126.

[96] Le Maitre, C.L., A.J. Freemont, and J.A. Hoyland (2006) *Human disc degeneration is associated with increased MMP 7 expression.* Biotech Histochem, 81(4-6): p. 125-31.

[97] Gruber, H.E., J.A. Ingram, and E.N. Hanley, Jr. (2005) *Immunolocalization of MMP-19 in the human intervertebral disc: implications for disc aging and degeneration.* Biotech Histochem, 80(3-4): p. 157-62.

[98] Maroudas, A., R.A. Stockwell, A. Nachemson, and J. Urban (1975) *Factors involved in the nutrition of the human lumbar intervertebral disc: cellularity and diffusion of glucose in vitro.* J Anat, 120(Pt 1): p. 113-30.

[99] Agrawal, A., A. Guttapalli, S. Narayan, T.J. Albert, I.M. Shapiro, et al. (2007) *Normoxic stabilization of HIF-1alpha drives glycolytic metabolism and regulates aggrecan gene expression in nucleus pulposus cells of the rat intervertebral disk.* Am J Physiol Cell Physiol, 293(2): p. C621-31.

[100] Urban, J.P., S. Smith, and J.C. Fairbank (2004) *Nutrition of the intervertebral disc.* Spine (Phila Pa 1976), 29(23): p. 2700-9.

[101] Urban, J.P. (2002) *The role of the physicochemical environment in determining disc cell behaviour.* Biochem Soc Trans, 30(Pt 6): p. 858-64.

[102] Holm, S., A. Maroudas, J.P. Urban, G. Selstam, and A. Nachemson (1981) *Nutrition of the intervertebral disc: solute transport and metabolism.* Connect Tissue Res, 8(2): p. 101-19.

[103] Wuertz, K., K. Godburn, and J.C. Iatridis (2009) *MSC response to pH levels found in degenerating intervertebral discs.* Biochem Biophys Res Commun, 379(4): p. 824-9.

[104] Gilbert, H.T., N. Hodson, P. Baird, S.M. Richardson, and J.A. Hoyland (2016) *Acidic pH promotes intervertebral disc degeneration: Acid-sensing ion channel -3 as a potential therapeutic target.* Sci Rep, 6: p. 37360.

[105] Razaq, S., R.J. Wilkins, and J.P. Urban (2003) *The effect of extracellular pH on matrix turnover by cells of the bovine nucleus pulposus.* Eur Spine J, 12(4): p. 341-9.

[106] Bibby, S.R., D.A. Jones, R.M. Ripley, and J.P. Urban (2005) *Metabolism of the intervertebral disc: effects of low levels of oxygen, glucose, and pH on rates of energy metabolism of bovine nucleus pulposus cells.* Spine (Phila Pa 1976), 30(5): p. 487-96.

[107] Richardson, S.M., R. Knowles, D. Marples, J.A. Hoyland, and A. Mobasheri (2008) *Aquaporin expression in the human intervertebral disc.* J Mol Histol, 39(3): p. 303-9.

[108] Huang, Y.C., J.P. Urban, and K.D. Luk (2014) *Intervertebral disc regeneration: do nutrients lead the way?* Nat Rev Rheumatol, 10(9): p. 561-6.

[109] Salvatierra, J.C., T.Y. Yuan, H. Fernando, A. Castillo, W.Y. Gu, et al. (2011) *Difference in Energy Metabolism of Annulus Fibrosus and Nucleus Pulposus Cells of the Intervertebral Disc.* Cell Mol Bioeng, 4(2): p. 302-310.

[110] Hastreiter, D., R.M. Ozuna, and M. Spector (2001) *Regional variations in certain cellular characteristics in human lumbar intervertebral discs, including the presence of alpha-smooth muscle actin.* J Orthop Res, 19(4): p. 597-604.

[111] Bruehlmann, S.B., J.B. Rattner, J.R. Matyas, and N.A. Duncan (2002) *Regional variations in the cellular matrix of the annulus fibrosus of the intervertebral disc.* Journal of anatomy, 201(2): p. 159-71.

[112] Iu, J., J.P. Santerre, and R.A. Kandel (2014) *Inner and outer annulus fibrosus cells exhibit differentiated phenotypes and yield changes in extracellular matrix protein composition in vitro on a polycarbonate urethane scaffold.* Tissue Eng Part A, 20(23-24): p. 3261-9.

[113] Gorensek, M., C. Jaksimovic, N. Kregar-Velikonja, M. Gorensek, M. Knezevic, et al. (2004) *Nucleus pulposus repair with cultured autologous elastic cartilage derived chondrocytes.* Cell Mol Biol Lett, 9(2): p. 363-73.

[114] Roughley, P.J. (2004) *Biology of intervertebral disc aging and degeneration: involvement of the extracellular matrix.* Spine (Phila Pa 1976), 29(23): p. 2691-9.

[115] Aigner, T., K.R. Gresk-otter, J.C. Fairbank, K. von der Mark, and J.P. Urban (1998) *Variation with age in the pattern of type X collagen expression in normal and scoliotic human intervertebral discs.* Calcif Tissue Int, 63(3): p. 263-8.

[116] Illien-Junger, S., O.M. Torre, W.F. Kindschuh, X. Chen, D.M. Laudier, et al. (2016) *AGEs induce ectopic endochondral ossification in intervertebral discs.* Eur Cell Mater, 32: p. 257-270.

[117] Johnstone, B., M. Markopoulos, P. Neame, and B. Caterson (1993) *Identification and characterization of glycanated and non-glycanated forms of biglycan and decorin in the human intervertebral disc.* Biochem J, 292 (Pt 3): p. 661-6.

[118] Roberts, S., B. Caterson, H. Evans, and S.M. Eisenstein (1994) *Proteoglycan components of the intervertebral disc and cartilage endplate: an immunolocalization study of animal and human tissues.* Histochem J, 26(5): p. 402-11.

[119] Inkinen, R.I., M.J. Lammi, U. Agren, R. Tammi, K. Puustjarvi, et al. (1999) *Hyaluronan distribution in the human and canine intervertebral disc and cartilage endplate.* Histochem J, 31(9): p. 579-87.

[120] Thorpe, A.A., A.L. Binch, L.B. Creemers, C. Sammon, and C.L. Le Maitre (2016) *Nucleus pulposus phenotypic markers to determine stem cell differentiation: fact or fiction?* Oncotarget, 7(3): p. 2189-200.

[121] Liu, L.T., B. Huang, C.Q. Li, Y. Zhuang, J. Wang, et al. (2011) *Characteristics of stem cells derived from the degenerated human intervertebral disc cartilage endplate.* PLoS One, 6(10): p. e26285.

[122] Huang, B., L.T. Liu, C.Q. Li, Y. Zhuang, G. Luo, et al. (2012) *Study to determine the presence of progenitor cells in the degenerated human cartilage endplates.* Eur Spine J, 21(4): p. 613-22.

[123] Liebscher, T., M. Haefeli, K. Wuertz, A.G. Nerlich, and N. Boos (2011) *Age-related variation in cell density of human lumbar intervertebral disc.* Spine, 36(2): p. 153-9.

[124] Walter, B.A., O.M. Torre, D. Laudier, T.P. Naidich, A.C. Hecht, et al. (2015) *Form and function of the intervertebral disc in health and disease: a morphological and stain comparison study.* J Anat, 227(6): p. 707-16.

[125] Wei, A., B. Shen, L. Williams, and A. Diwan (2014) *Mesenchymal stem cells: potential application in intervertebral disc regeneration.* Transl Pediatr, 3(2): p. 71-90.

[126] Setton, L.A., L. Bonassar, and K. Masuda (2007) *Regeneration and Replacement of the Intervertebral Disc.* Principles of Tissue Engineering: p. 875-894.

[127] Duncan, N.A. (2006) *Cell deformation and micromechanical environment in the intervertebral disc.* J Bone Joint Surg Am, 88 Suppl 2: p. 47-51.

[128] Errington, R.J., K. Puustjarvi, I.R. White, S. Roberts, and J.P. Urban (1998) *Characterisation of cytoplasm-filled processes in cells of the intervertebral disc.* Journal of anatomy, 192 (Pt 3): p. 369-78.

[129] Gruber, H.E., G.L. Hoelscher, J.A. Ingram, N. Zinchenko, and E.N. Hanley, Jr. (2010) *Senescent vs. non-senescent cells in the human annulus in vivo: cell harvest with laser capture microdissection and gene expression studies with microarray analysis.* BMC Biotechnol, 10: p. 5.

[130] Gruber, H.E., G.L. Hoelscher, and E.N. Hanley, Jr. (2010) *Annulus cells from more degenerated human discs show modified gene expression in 3D culture compared with expression in cells from healthier discs.* Spine J, 10(8): p. 721-7.

[131] Gruber, H.E., J.A. Watts, G.L. Hoelscher, S.F. Bethea, J.A. Ingram, et al. (2011) *Mitochondrial gene expression in the human annulus: in vivo data from annulus cells and selectively harvested senescent annulus cells.* Spine J, 11(8): p. 782-91.

[132] van den Akker, G.G.H., M.I. Koenders, F.A.J. van de Loo, P. van Lent, E. Blaney Davidson, et al. (2017) *Transcriptional profiling distinguishes inner and outer annulus fibrosus from nucleus pulposus in the bovine intervertebral disc.* Eur Spine J.

[133] van den Akker, G.G., D.A. Surtel, A. Cremers, S.M. Richardson, J.A. Hoyland, et al. (2016) *Novel Immortal Cell Lines Support Cellular Heterogeneity in the Human Annulus Fibrosus.* PLoS One, 11(1): p. e0144497.

[134] Sakai, D., T. Nakai, J. Mochida, M. Alini, and S. Grad (2009) *Differential phenotype of intervertebral disc cells: microarray and immunohistochemical analysis of canine nucleus pulposus and anulus fibrosus.* Spine, 34(14): p. 1448-56.

[135] Minogue, B.M., S.M. Richardson, L.A.H. Zeef, A.J. Freemont, and J.A. Hoyland (2010) *Transcriptional profiling of bovine intervertebral disc cells: implications for identification of normal and degenerate human intervertebral disc cell phenotypes.* Arthritis Research & Therapy, 12(1): p. R22.

[136] Antoniou, J., T. Steffen, F. Nelson, N. Winterbottom, A.P. Hollander, et al. (1996) *The human lumbar intervertebral disc: evidence for changes in the biosynthesis and denaturation of the extracellular matrix with growth, maturation, ageing, and degeneration.* J Clin Invest, 98(4): p. 996-1003.

[137] Richardson, S.M., F.E. Ludwinski, K.K. Gnanalingham, R.A. Atkinson, A.J. Freemont, et al. (2017) *Notochordal and nucleus pulposus marker expression is maintained by sub-populations of adult human nucleus pulposus cells through aging and degeneration.* Sci Rep, 7(1): p. 1501.

[138] Sakai, D., Y. Nakamura, T. Nakai, T. Mishima, S. Kato, et al. (2012) *Exhaustion of nucleus pulposus progenitor cells with ageing and degeneration of the intervertebral disc.* Nat Commun, 3: p. 1264.

[139] Roberts, S., H. Evans, J. Trivedi, and J. Menage (2006) *Histology and pathology of the human intervertebral disc.* J Bone Joint Surg Am, 88 Suppl 2: p. 10-4.

[140] Trout, J.J., J.A. Buckwalter, and K.C. Moore (1982) *Ultrastructure of the human intervertebral disc: II. Cells of the nucleus pulposus.* Anat Rec, 204(4): p. 307-14.

[141] Roberts, S., J. Menage, V. Duance, S. Wotton, and S. Ayad (1991) *1991 Volvo Award in basic sciences. Collagen types around the cells of the intervertebral disc and cartilage end plate: an immunolocalization study.* Spine, 16(9): p. 1030-8.

[142] Sive, J.I., P. Baird, M. Jeziorsk, A. Watkins, J.A. Hoyland, et al. (2002) *Expression of chondrocyte markers by cells of normal and degenerate intervertebral discs.* Mol Pathol, 55(2): p. 91-7.

[143] Mwale, F., P. Roughley, and J. Antoniou (2004) *Distinction between the extracellular matrix of the nucleus pulposus and hyaline cartilage: a requisite for tissue engineering of intervertebral disc.* European Cells & Materials, 8: p. 58-63; discussion 63-4.

[144] Buckwalter, J.A., K.C. Smith, L.E. Kazarien, L.C. Rosenberg, and R. Ungar (1989) *Articular cartilage and intervertebral disc proteoglycans differ in structure: an electron microscopic study.* J Orthop Res, 7(1): p. 146-51.

[145] Vonk, L.A., R.J. Kroeze, B.Z. Doulabi, R.J. Hoogendoorn, C. Huang, et al. (2010) *Caprine articular, meniscus and intervertebral disc cartilage: an integral analysis of collagen network and chondrocytes.* Matrix Biol, 29(3): p. 209-18.

[146] Collin, E.C., M. Kilcoyne, S.J. White, S. Grad, M. Alini, et al. (2016) *Unique glycosignature for intervertebral disc and articular cartilage cells and tissues in immaturity and maturity.* Sci Rep, 6: p. 23062.

[147] Minogue, B.M., S.M. Richardson, L.A.H. Zeef, A.J. Freemont, and J.A. Hoyland (2010) *Characterization of the human nucleus pulposus cell phenotype and evaluation of novel marker gene expression to define adult stem cell differentiation.* Arthritis & Rheumatism, 62(12): p. 3695-3705.

[148] Power, K.A., S. Grad, J.P. Rutges, L.B. Creemers, M.H. van Rijen, et al. (2011) *Identification of cell surface-specific markers to target human nucleus pulposus cells: expression of carbonic anhydrase XII varies with age and degeneration.* Arthritis Rheum, 63(12): p. 3876-86.

[149] Iatridis, J.C., M. Weidenbaum, L.A. Setton, and V.C. Mow (1996) *Is the nucleus pulposus a solid or a fluid? Mechanical behaviors of the nucleus pulposus of the human intervertebral disc.* Spine (Phila Pa 1976), 21(10): p. 1174-84.

[150] Lee, C.R., D. Sakai, T. Nakai, K. Toyama, J. Mochida, et al. (2007) *A phenotypic comparison of intervertebral disc and articular cartilage cells in the rat.* European spine journal : official publication of the European Spine Society, the European Spinal Deformity Society, and the European Section of the Cervical Spine Research Society, 16(12): p. 2174-85.

[151] Risbud, M.V., Z.R. Schoepflin, F. Mwale, R.A. Kandel, S. Grad, et al. (2015) *Defining the phenotype of young healthy nucleus pulposus cells: recommendations of the Spine Research Interest Group at the 2014 annual ORS meeting.* J Orthop Res, 33(3): p. 283-93.

[152] Tang, X., L. Jing, W.J. Richardson, R.E. Isaacs, R.D. Fitch, et al. (2016) *Identifying molecular phenotype of nucleus pulposus cells in human intervertebral disc with aging and degeneration.* J Orthop Res, 34(8): p. 1316-26.

[153] Tanaka, M., D. Sakai, A. Hiyama, F. Arai, D. Nakajima, et al. (2017) *Evidence of Nonnotochordal Origin in Chondrocyte-like Cells of the Nucleus Pulposus Appearing in Early Stage Disk Degeneration in the Mouse Model.* Global Spine Journal.

[154] Kim, K.W., T.H. Lim, J.G. Kim, S.T. Jeong, K. Masuda, et al. (2003) *The origin of chondrocytes in the nucleus pulposus and histologic findings associated with the transition of a notochordal nucleus pulposus to a fibrocartilaginous nucleus pulposus in intact rabbit intervertebral discs.* Spine (Phila Pa 1976), 28(10): p. 982-90.

[155] Kim, K.W., K.Y. Ha, J.S. Lee, S.W. Nam, Y.K. Woo, et al. (2009) *Notochordal cells stimulate migration of cartilage end plate chondrocytes of the intervertebral disc in in vitro cell migration assays.* Spine J, 9(4): p. 323-9.

[156] Henriksson, H.B., E. Svala, E. Skioldebrand, A. Lindahl, and H. Brisby (2012) *Support of concept that migrating progenitor cells from stem cell niches contribute to normal regeneration of the adult mammal intervertebral disc: a descriptive study in the New Zealand white rabbit.* Spine, 37(9): p. 722-32.

[157] Smith, L.J., N.L. Nerurkar, K.S. Choi, B.D. Harfe, and D.M. Elliott (2011) *Degeneration and regeneration of the intervertebral disc: lessons from development.* Dis Model Mech, 4(1): p. 31-41.

[158] Risbud, M.V. and I.M. Shapiro (2011) *Notochordal cells in the adult intervertebral disc: new perspective on an old question.* Crit Rev Eukaryot Gene Expr, 21(1): p. 29-41.

[159] Risbud, M.V., T.P. Schaer, and I.M. Shapiro (2010) *Toward an understanding of the role of notochordal cells in the adult intervertebral disc: From discord to accord.* Developmental Dynamics, 239(8): p. 2141-2148.

[160] Choi, K.S., M.J. Cohn, and B.D. Harfe (2008) *Identification of nucleus pulposus precursor cells and notochordal remnants in the mouse: implications for disk degeneration and chordoma formation.* Dev Dyn, 237(12): p. 3953-8.

[161] McCann, M.R., O.J. Tamplin, J. Rossant, and C.A. Seguin (2012) *Tracing notochord-derived cells using a Noto-cre mouse: implications for intervertebral disc development.* Dis Model Mech, 5(1): p. 73-82.

[162] Sakai, D., K. Nishimura, M. Tanaka, D. Nakajima, S. Grad, et al. (2015) *Migration of bone marrow-derived cells for endogenous repair in a new tail-looping disc degeneration model in the mouse: a pilot study.* Spine J, 15(6): p. 1356-65.

[163] Colombier, P., A. Camus, L. Lescaudron, J. Clouet, and J. Guicheux (2014) *Intervertebral disc regeneration: a great challenge for tissue engineers.* Trends Biotechnol, 32(9): p. 433-5.

[164] van den Akker, G.G., D.A. Surtel, A. Cremers, R. Rodrigues-Pinto, S.M. Richardson, et al. (2014) *Novel immortal human cell lines reveal subpopulations in the nucleus pulposus.* Arthritis Res Ther, 16(3): p. R135.

[165] Weiler, C., A.G. Nerlich, R. Schaaf, B.E. Bachmeier, K. Wuertz, et al. (2010) *Immunohistochemical identification of notochordal markers in cells in the aging human lumbar intervertebral disc.* European Spine Journal, 19(10): p. 1761-1770.

[166] Gilson, A., M. Dreger, and J.P.G. Urban (2010) *Differential expression level of cytokeratin 8 in cells of the bovine nucleus pulposus complicates the search for specific intervertebral disc cell markers.* Arthritis Research & Therapy, 12(1): p. R24.

[167] Rodrigues-Pinto, R., S.M. Richardson, and J.A. Hoyland (2014) *An understanding of intervertebral disc development, maturation and cell phenotype provides clues to direct cell-based tissue regeneration therapies for disc degeneration.* Eur Spine J, 23(9): p. 1803-14.

[168] Boyle, E.A., Y.I. Li, and J.K. Pritchard (2017) *An Expanded View of Complex Traits: From Polygenic to Omnigenic.* Cell, 169(7): p. 1177-1186.

[169] Hunter, C.J., J.R. Matyas, and N.A. Duncan (2004) *Cytomorphology of notochordal and chondrocytic cells from the nucleus pulposus: a species comparison.* J Anat, 205(5): p. 357-62.

[170] Trout, J.J., J.A. Buckwalter, K.C. Moore, and S.K. Landas (1982) *Ultrastructure of the human intervertebral disc. I. Changes in notochordal cells with age.* Tissue Cell, 14(2): p. 359-69.

[171] Hunter, C.J., S. Bianchi, P. Cheng, and K. Muldrew (2007) *Osmoregulatory function of large vacuoles found in notochordal cells of the intervertebral disc running title: an osmoregulatory vacuole.* Mol Cell Biomech, 4(4): p. 227-37.

[172] Alini, M., S.M. Eisenstein, K. Ito, C. Little, A.A. Kettler, et al. (2008) *Are animal models useful for studying human disc disorders/degeneration?* Eur Spine J, 17(1): p. 2-19.

[173] Aguiar, D.J., S.L. Johnson, and T.R. Oegema (1999) *Notochordal cells interact with nucleus pulposus cells: regulation of proteoglycan synthesis.* Exp Cell Res, 246(1): p. 129-37.

[174] Cappello, R., J.L. Bird, D. Pfeiffer, M.T. Bayliss, and J. Dudhia (2006) *Notochordal cell produce and assemble extracellular matrix in a distinct manner, which may be responsible for the maintenance of healthy nucleus pulposus.* Spine (Phila Pa 1976), 31(8): p. 873-82; discussion 883.

[175] Erwin, W.M. and R.D. Inman (2006) *Notochord cells regulate intervertebral disc chondrocyte proteoglycan production and cell proliferation.* Spine, 31(10): p. 1094-9.

[176] Erwin, W.M., D. Islam, R.D. Inman, M.G. Fehlings, and F.W. Tsui (2011) *Notochordal cells protect nucleus pulposus cells from degradation and apoptosis: implications for the mechanisms of intervertebral disc degeneration.* Arthritis Res Ther, 13(6): p. R215.

[177] Gantenbein, B., E. Calandriello, K. Wuertz-Kozak, L.M. Benneker, M.J. Keel, et al. (2014) *Activation of intervertebral disc cells by co-culture with notochordal cells, conditioned medium and hypoxia.* BMC Musculoskelet Disord, 15: p. 422.

[178] Boos, N., S. Weissbach, H. Rohrbach, C. Weiler, K.F. Spratt, et al. (2002) *Classification of age-related changes in lumbar intervertebral discs: 2002 Volvo Award in basic science.* Spine (Phila Pa 1976), 27(23): p. 2631-44.

[179] Guehring, T., G. Wilde, M. Sumner, T. Grünhagen, G.B. Karney, et al. (2009) *Notochordal intervertebral disc cells: Sensitivity to nutrient deprivation.* Arthritis & Rheumatism, 60(4): p. 1026-1034.

[180] Chen, J., W. Yan, and L.A. Setton (2006) *Molecular phenotypes of notochordal cells purified from immature nucleus pulposus.* Eur Spine J, 15 Suppl 3: p. S303-11.

[181] Kim, J.H., B.M. Deasy, H.Y. Seo, R.K. Studer, N.V. Vo, et al. (2009) *Differentiation of intervertebral notochordal cells through live automated cell imaging system in vitro.* Spine (Phila Pa 1976), 34(23): p. 2486-93.

[182] Purmessur, D., C.C. Guterl, S.K. Cho, M.C. Cornejo, Y.W. Lam, et al. (2013) *Dynamic pressurization induces transition of notochordal cells to a mature phenotype while retaining production of important patterning ligands from development.* Arthritis Res Ther, 15(5): p. R122.

[183] Yang, F., V.Y. Leung, K.D. Luk, D. Chan, and K.M. Cheung (2009) *Injury-induced sequential transformation of notochordal nucleus pulposus to chondrogenic and fibrocartilaginous phenotype in the mouse.* J Pathol, 218(1): p. 113-21.

[184] Rodrigues-Pinto, R., A. Berry, K. Piper-Hanley, N. Hanley, S.M. Richardson, et al. (2016) *Spatiotemporal analysis of putative notochordal cell markers reveals CD24 and keratins 8, 18, and 19 as notochord-specific markers during early human intervertebral disc development.* J Orthop Res, 34(8): p. 1327-40.

[185] Blanco, J.F., I.F. Graciani, F.M. Sanchez-Guijo, S. Muntion, P. Hernandez-Campo, et al. (2010) *Isolation and characterization of mesenchymal stromal cells from human degenerated nucleus pulposus: comparison with bone marrow mesenchymal stromal cells from the same subjects.* Spine (Phila Pa 1976), 35(26): p. 2259-65.

[186] Wang, H., Y. Zhou, T.W. Chu, C.Q. Li, J. Wang, et al. (2016) *Distinguishing characteristics of stem cells derived from different anatomical regions of human degenerated intervertebral discs.* Eur Spine J, 25(9): p. 2691-704.

[187] Risbud, M.V., A. Guttapalli, T.T. Tsai, J.Y. Lee, K.G. Danielson, et al. (2007) *Evidence for skeletal progenitor cells in the degenerate human intervertebral disc.* Spine, 32(23): p. 2537-44.

[188] Turner, S., B. Balain, B. Caterson, C. Morgan, and S. Roberts (2014) *Viability, growth kinetics and stem cell markers of single and clustered cells in human intervertebral discs: implications for regenerative therapies.* Eur Spine J, 23(11): p. 2462-72.

[189] Feng, G., X. Yang, H. Shang, I.W. Marks, F.H. Shen, et al. (2010) *Multipotential differentiation of human anulus fibrosus cells: an in vitro study.* J Bone Joint Surg Am, 92(3): p. 675-85.

[190] Mark Erwin, W., D. Islam, E. Eftekarpour, R.D. Inman, M.Z. Karim, et al. (2012) *Intervertebral disc-derived stem cells: Implications for regenerative medicine and neural repair.* Spine.

[191] Tao, Y.Q., C.Z. Liang, H. Li, Y.J. Zhang, F.C. Li, et al. (2013) *Potential of co-culture of nucleus pulposus mesenchymal stem cells and nucleus pulposus cells in hyperosmotic microenvironment for intervertebral disc regeneration.* Cell Biol Int, 37(8): p. 826-34.

[192] Saraiya, M., R. Nasser, Y. Zeng, S. Addya, R.K. Ponnappan, et al. (2010) *Reversine enhances generation of progenitor-like cells by dedifferentiation of annulus fibrosus cells.* Tissue Eng Part A, 16(4): p. 1443-55.

[193] Henriksson, H., M. Thornemo, C. Karlsson, O. Hagg, K. Junevik, et al. (2009) *Identification of cell proliferation zones, progenitor cells and a potential stem cell niche in the intervertebral disc region: a study in four species.* Spine, 34(21): p. 2278-87.

[194] Yasen, M., Q. Fei, W.C. Hutton, J. Zhang, J. Dong, et al. (2013) *Changes of number of cells expressing proliferation and progenitor cell markers with age in rabbit intervertebral discs.* Acta Biochim Biophys Sin (Shanghai), 45(5): p. 368-76.

[195] Liu, C., Q. Guo, J. Li, S. Wang, Y. Wang, et al. (2014) *Identification of rabbit annulus fibrosus-derived stem cells.* PLoS One, 9(9): p. e108239.

[196] Huang, S., V.Y. Leung, D. Long, D. Chan, W.W. Lu, et al. (2013) *Coupling of small leucine-rich proteoglycans to hypoxic survival of a progenitor cell-like subpopulation in Rhesus Macaque intervertebral disc.* Biomaterials, 34(28): p. 6548-58.

[197] Mizrahi, O., D. Sheyn, W. Tawackoli, S. Ben-David, S. Su, et al. (2013) *Nucleus pulposus degeneration alters properties of resident progenitor cells.* Spine J, 13(7): p. 803-14.

[198] Li, H., Y. Tao, C. Liang, B. Han, F. Li, et al. (2013) *Influence of hypoxia in the intervertebral disc on the biological behaviors of rat adipose- and nucleus pulposus-derived mesenchymal stem cells.* Cells Tissues Organs, 198(4): p. 266-77.

[199] Han, B., H.C. Wang, H. Li, Y.Q. Tao, C.Z. Liang, et al. (2014) *Nucleus pulposus mesenchymal stem cells in acidic conditions mimicking degenerative intervertebral discs give better performance than adipose tissue-derived mesenchymal stem cells.* Cells Tissues Organs, 199(5-6): p. 342-52.

[200] Henriksson, H., Svala, E, Skioldebrand, E, Lindahl,A MD, Brisby,H (2012) *Support of Concept That Migrating Progenitor Cells From Stem Cell Niches Contribute*

to Normal Regeneration of the Adult Mammal Intervertebral Disc. Spine, 37(9): p. 722-732.

[201] Brisby, H., N. Papadimitriou, C. Brantsing, P. Bergh, A. Lindahl, et al. (2013) *The presence of local mesenchymal progenitor cells in human degenerated intervertebral discs and possibilities to influence these in vitro: a descriptive study in humans.* Stem Cells Dev, 22(5): p. 804-14.

[202] Jones, P., L. Gardner, J. Menage, G.T. Williams, and S. Roberts (2008) *Intervertebral disc cells as competent phagocytes in vitro: implications for cell death in disc degeneration.* Arthritis Research & Therapy, 10(4): p. -.

[203] Nerlich, A.G., C. Weiler, J. Zipperer, M. Narozny, and N. Boos (2002) *Immunolocalization of phagocytic cells in normal and degenerated intervertebral discs.* Spine, 27(22): p. 2484-2490.

[204] Phillips, K.L., N. Chiverton, A.L. Michael, A.A. Cole, L.M. Breakwell, et al. (2013) *The cytokine and chemokine expression profile of nucleus pulposus cells: implications for degeneration and regeneration of the intervertebral disc.* Arthritis Res Ther, 15(6): p. R213.

[205] Gabr, M.A., L. Jing, A.R. Helbling, S.M. Sinclair, K.D. Allen, et al. (2011) *Interleukin-17 synergizes with IFNgamma or TNFalpha to promote inflammatory mediator release and intercellular adhesion molecule-1 (ICAM-1) expression in human intervertebral disc cells.* J Orthop Res, 29(1): p. 1-7.

[206] Huang, K.Y., R.M. Lin, W.Y. Chen, C.L. Lee, J.J. Yan, et al. (2008) *IL-20 may contribute to the pathogenesis of human intervertebral disc herniation.* Spine (Phila Pa 1976), 33(19): p. 2034-40.

[207] Smith, L.J., J.A. Chiaro, N.L. Nerurkar, D.H. Cortes, S.D. Horava, et al. (2011) *Nucleus pulposus cells synthesize a functional extracellular matrix and respond to inflammatory cytokine challenge following long-term agarose culture.* Eur Cell Mater, 22: p. 291-301.

[208] Hoyland, J.A., C. Le Maitre, and A.J. Freemont (2008) *Investigation of the role of IL-1 and TNF in matrix degradation in the intervertebral disc.* Rheumatology (Oxford), 47(6): p. 809-14.

[209] Seguin, C.A., R.M. Pilliar, P.J. Roughley, and R.A. Kandel (2005) *Tumor necrosis factor-alpha modulates matrix production and catabolism in nucleus pulposus tissue.* Spine (Phila Pa 1976), 30(17): p. 1940-8.

[210] Seguin, C.A., R.M. Pilliar, J.A. Madri, and R.A. Kandel (2008) *TNF-alpha induces MMP2 gelatinase activity and MT1-MMP expression in an in vitro model of nucleus pulposus tissue degeneration.* Spine (Phila Pa 1976), 33(4): p. 356-65.

[211] Weiler, C., A.G. Nerlich, B.E. Bachmeier, and N. Boos (2005) *Expression and distribution of tumor necrosis factor alpha in human lumbar intervertebral discs: a study in surgical specimen and autopsy controls.* Spine (Phila Pa 1976), 30(1): p. 44-53; discussion 54.

[212] Wang, H., Y. Tian, J. Wang, K.L. Phillips, A.L. Binch, et al. (2013) *Inflammatory cytokines induce NOTCH signaling in nucleus pulposus cells: implications in intervertebral disc degeneration.* J Biol Chem, 288(23): p. 16761-74.

[213] Le Maitre, C., J. Hoyland, and A. Freemont (2007) *Catabolic cytokine expression in degenerate and herniated human intervertebral discs: IL-1beta and TNFalpha expression profile.* Arthritis Research & Therapy, 9(4): p. R77.

[214] Kepler, C.K., D.Z. Markova, F. Dibra, S. Yadla, A.R. Vaccaro, et al. (2013) *Expression and relationship of proinflammatory chemokine RANTES/CCL5 and cytokine IL-1beta in painful human intervertebral discs.* Spine (Phila Pa 1976), 38(11): p. 873-80.

[215] Le Maitre, C.L., A.J. Freemont, and J.A. Hoyland (2005) *The role of interleukin-1 in the pathogenesis of human intervertebral disc degeneration.* Arthritis Research & Therapy, 7(4): p. R732-R745.

[216] Abe, Y., K. Akeda, H.S. An, Y. Aoki, R. Pichika, et al. (2007) *Proinflammatory cytokines stimulate the expression of nerve growth factor by human intervertebral disc cells.* Spine (Phila Pa 1976), 32(6): p. 635-42.

[217] Miyahara, K., T. Ishida, S. Hukuda, K. Horiike, M. Okamoto, et al. (1996) *Human group II phospholipase A2 in normal and diseased intervertebral discs.* Biochim Biophys Acta, 1316(3): p. 183-90.

[218] Wang, J., Y. Tian, K.L. Phillips, N. Chiverton, G. Haddock, et al. (2013) *Tumor necrosis factor alpha- and interleukin-1beta-dependent induction of CCL3 expression by nucleus pulposus cells promotes macrophage migration through CCR1.* Arthritis Rheum, 65(3): p. 832-42.

[219] Kokubo, Y., K. Uchida, S. Kobayashi, T. Yayama, R. Sato, et al. (2008) *Herniated and spondylotic intervertebral discs of the human cervical spine: histological and immunohistological findings in 500 en bloc surgical samples. Laboratory investigation.* J Neurosurg Spine, 9(3): p. 285-95.

[220] Kang, J.D., H.I. Georgescu, L. McIntyre-Larkin, M. Stefanovic-Racic, W.F. Donaldson, 3rd, et al. (1996) *Herniated lumbar intervertebral discs spontaneously produce matrix metalloproteinases, nitric oxide, interleukin-6, and prostaglandin E2.* Spine (Phila Pa 1976), 21(3): p. 271-7.

[221] Takahashi, H., T. Suguro, Y. Okazima, M. Motegi, Y. Okada, et al. (1996) *Inflammatory cytokines in the herniated disc of the lumbar spine.* Spine (Phila Pa 1976), 21(2): p. 218-24.

[222] Ahn, S.H., Y.W. Cho, M.W. Ahn, S.H. Jang, Y.K. Sohn, et al. (2002) *mRNA expression of cytokines and chemokines in herniated lumbar intervertebral discs.* Spine (Phila Pa 1976), 27(9): p. 911-7.

[223] Miyamoto, H., R. Saura, T. Harada, M. Doita, and K. Mizuno (2000) *The role of cyclooxygenase-2 and inflammatory cytokines in pain induction of herniated lumbar intervertebral disc.* Kobe J Med Sci, 46(1-2): p. 13-28.

[224] Shamji, M.F., L.A. Setton, W. Jarvis, S. So, J. Chen, et al. (2010) *Proinflammatory cytokine expression profile in degenerated and herniated human intervertebral disc tissues.* Arthritis Rheum, 62(7): p. 1974-82.

[225] Burke, J.G., R.W. Watson, D. McCormack, F.E. Dowling, M.G. Walsh, et al. (2002) *Intervertebral discs which cause low back pain secrete high levels of proinflammatory mediators.* J Bone Joint Surg Br, 84(2): p. 196-201.

[226] Matsui, Y., M. Maeda, W. Nakagami, and H. Iwata (1998) *The involvement of matrix metalloproteinases and inflammation in lumbar disc herniation.* Spine (Phila Pa 1976), 23(8): p. 863-8; discussion 868-9.

[227] Lopez-Otin, C., M.A. Blasco, L. Partridge, M. Serrano, and G. Kroemer (2013) *The hallmarks of aging.* Cell, 153(6): p. 1194-217.

[228] Feng, Y., B. Egan, and J. Wang (2016) *Genetic Factors in Intervertebral Disc Degeneration.* Genes Dis, 3(3): p. 178-185.

[229] Le Maitre, C.L., A.J. Freemont, and J.A. Hoyland (2007) *Accelerated cellular senescence in degenerate intervertebral discs: a possible role in the pathogenesis of intervertebral disc degeneration.* Arthritis Res Ther, 9(3): p. R45.

[230] Tajerian, M., S. Alvarado, M. Millecamps, T. Dashwood, K.M. Anderson, et al. (2011) *DNA methylation of SPARC and chronic low back pain.* Mol Pain, 7: p. 65.

[231] Sarath Babu, N., S. Krishnan, C.V. Brahmendra Swamy, G.P. Venkata Subbaiah, A.V. Gurava Reddy, et al. (2016) *Quantitative proteomic analysis of normal and degenerated human intervertebral disc.* Spine J, 16(8): p. 989-1000.

[232] Ye, D., W. Liang, L. Dai, L. Zhou, Y. Yao, et al. (2015) *Comparative and quantitative proteomic analysis of normal and degenerated human annulus fibrosus cells.* Clin Exp Pharmacol Physiol, 42(5): p. 530-6.

[233] Gilson, A., M. Dreger, and J.P. Urban (2010) *Differential expression level of cytokeratin 8 in cells of the bovine nucleus pulposus complicates the search for specific intervertebral disc cell markers.* Arthritis Res Ther, 12(1): p. R24.

[234] Purmessur, D., R.M. Schek, R.D. Abbott, B.A. Ballif, K.E. Godburn, et al. (2011) *Notochordal conditioned media from tissue increases proteoglycan accumulation and promotes a healthy nucleus pulposus phenotype in human mesenchymal stem cells.* Arthritis Res Ther, 13(3): p. R81.

[235] Erwin, W.M., L. DeSouza, M. Funabashi, G. Kawchuk, M.Z. Karim, et al. (2015) *The biological basis of degenerative disc disease: proteomic and biomechanical analysis of the canine intervertebral disc.* Arthritis Res Ther, 17: p. 240.

[236] Zhang, F., X. Zhao, H. Shen, and C. Zhang (2016) *Molecular mechanisms of cell death in intervertebral disc degeneration (Review).* Int J Mol Med, 37(6): p. 1439-48.

[237] Feng, C., M. Yang, M. Lan, C. Liu, Y. Zhang, et al. (2017) *ROS: Crucial Intermediators in the Pathogenesis of Intervertebral Disc Degeneration.* Oxid Med Cell Longev, 2017: p. 5601593.

[238] Gruber, H.E., J.A. Watts, F.E. Riley, M.B. Fulkerson, H.J. Norton, et al. (2013) *Mitochondrial bioenergetics, mass, and morphology are altered in cells of the degenerating human annulus.* J Orthop Res, 31(8): p. 1270-5.

[239] Wang, F., F. Cai, R. Shi, X.H. Wang, and X.T. Wu (2016) *Aging and age related stresses: a senescence mechanism of intervertebral disc degeneration.* Osteoarthritis Cartilage, 24(3): p. 398-408.

[240] Hwang, P.Y., L. Jing, J. Chen, F.L. Lim, R. Tang, et al. (2016) *N-cadherin is Key to Expression of the Nucleus Pulposus Cell Phenotype under Selective Substrate Culture Conditions.* Sci Rep, 6: p. 28038.

[241] Dahia, C.L., E.J. Mahoney, A.A. Durrani, and C. Wylie (2009) *Intercellular signaling pathways active during intervertebral disc growth, differentiation, and aging.* Spine (Phila Pa 1976), 34(5): p. 456-62.

[242] Benneker, L.M., P.F. Heini, M. Alini, S.E. Anderson, and K. Ito (2005) *2004 Young Investigator Award Winner: vertebral endplate marrow contact channel*

occlusions and intervertebral disc degeneration. Spine (Phila Pa 1976), 30(2): p. 167-73.

[243] Vo, N., H.Y. Seo, A. Robinson, G. Sowa, D. Bentley, et al. (2010) *Accelerated aging of intervertebral discs in a mouse model of progeria.* J Orthop Res, 28(12): p. 1600-7.

[244] Bedore, J., W. Sha, M.R. McCann, S. Liu, A. Leask, et al. (2013) *Impaired intervertebral disc development and premature disc degeneration in mice with notochord-specific deletion of CCN2.* Arthritis Rheum, 65(10): p. 2634-44.

[245] Furukawa, T., K. Ito, S. Nuka, J. Hashimoto, H. Takei, et al. (2009) *Absence of biglycan accelerates the degenerative process in mouse intervertebral disc.* Spine (Phila Pa 1976), 34(25): p. E911-7.

[246] Mason, R.M. and A.J. Palfrey (1984) *Intervertebral disc degeneration in adult mice with hereditary kyphoscoliosis.* J Orthop Res, 2(4): p. 333-8.

[247] Semba, K., K. Araki, Z. Li, K. Matsumoto, M. Suzuki, et al. (2006) *A novel murine gene, Sickle tail, linked to the Danforth's short tail locus, is required for normal development of the intervertebral disc.* Genetics, 172(1): p. 445-56.

[248] Holguin, N., R. Aguilar, R.A. Harland, B.A. Bomar, and M.J. Silva (2014) *The aging mouse partially models the aging human spine: lumbar and coccygeal disc height, composition, mechanical properties, and Wnt signaling in young and old mice.* J Appl Physiol (1985), 116(12): p. 1551-60.

[249] Silberberg, R. and G. Gerritsen (1976) *Aging changes in intervertebral discs and spondylosis in Chinese hamsters.* Diabetes, 25(6): p. 477-83.

[250] Laing, A.C., R. Cox, W. Tetzlaff, and T. Oxland (2011) *Effects of advanced age on the morphometry and degenerative state of the cervical spine in a rat model.* Anat Rec (Hoboken), 294(8): p. 1326-36.

[251] Gruber, H.E., J.A. Ingram, H.J. Norton, and E.N. Hanley, Jr. (2007) *Senescence in cells of the aging and degenerating intervertebral disc: immunolocalization of*

senescence-associated beta-galactosidase in human and sand rat discs. Spine (Phila Pa 1976), 32(3): p. 321-7.

[252] Gruber, H.E., B. Gordon, C. Williams, H.J. Norton, and E.N. Hanley, Jr. (2007) *Vertebral endplate and disc changes in the aging sand rat lumbar spine: cross-sectional analyses of a large male and female population.* Spine (Phila Pa 1976), 32(23): p. 2529-36.

[253] Gruber, H.E., B. Gordon, H.J. Norton, J. Kilburn, C. Williams, et al. (2008) *Analysis of cell death and vertebral end plate bone mineral density in the annulus of the aging sand rat.* Spine J, 8(3): p. 475-81.

[254] Moskowitz, R.W., I. Ziv, C.W. Denko, B. Boja, P.K. Jones, et al. (1990) *Spondylosis in sand rats: a model of intervertebral disc degeneration and hyperostosis.* J Orthop Res, 8(3): p. 401-11.

[255] Sowa, G., G. Vadala, R. Studer, J. Kompel, C. Iucu, et al. (2008) *Characterization of intervertebral disc aging: longitudinal analysis of a rabbit model by magnetic resonance imaging, histology, and gene expression.* Spine (Phila Pa 1976), 33(17): p. 1821-8.

[256] Cho, H., S.H. Park, S. Lee, M. Kang, K.A. Hasty, et al. (2011) *Snapshot of degenerative aging of porcine intervertebral disc: a model to unravel the molecular mechanisms.* Exp Mol Med, 43(6): p. 334-40.

[257] Bergknut, N., J.P. Rutges, H.J. Kranenburg, L.A. Smolders, R. Hagman, et al. (2012) *The dog as an animal model for intervertebral disc degeneration?* Spine (Phila Pa 1976), 37(5): p. 351-8.

[258] Wade, K.R., P.A. Robertson, and N.D. Broom (2014) *Influence of maturity on nucleus-endplate integration in the ovine lumbar spine.* Eur Spine J, 23(4): p. 732-44.

[259] Stolworthy, D.K., A.E. Bowden, B.L. Roeder, T.F. Robinson, J.G. Holland, et al. (2015) *MRI evaluation of spontaneous intervertebral disc degeneration in the alpaca cervical spine.* J Orthop Res, 33(12): p. 1776-83.

[260] Lauerman, W.C., R.C. Platenberg, J.E. Cain, and V.F. Deeney (1992) *Age-related disk degeneration: preliminary report of a naturally occurring baboon model.* J Spinal Disord, 5(2): p. 170-4.

[261] Platenberg, R.C., G.B. Hubbard, W.J. Ehler, and C.J. Hixson (2001) *Spontaneous disc degeneration in the baboon model: magnetic resonance imaging and histopathologic correlation.* J Med Primatol, 30(5): p. 268-72.

[262] Duncan, A.E., R.J. Colman, and P.A. Kramer (2011) *Longitudinal study of radiographic spinal osteoarthritis in a macaque model.* J Orthop Res, 29(8): p. 1152-60.

[263] Nuckley, D.J., P.A. Kramer, A. Del Rosario, N. Fabro, S. Baran, et al. (2008) *Intervertebral disc degeneration in a naturally occurring primate model: radiographic and biomechanical evidence.* J Orthop Res, 26(9): p. 1283-8.

[264] Daly, C., P. Ghosh, G. Jenkin, D. Oehme, and T. Goldschlager (2016) *A Review of Animal Models of Intervertebral Disc Degeneration: Pathophysiology, Regeneration, and Translation to the Clinic.* Biomed Res Int, 2016: p. 5952165.

[265] Miyazaki, T., S. Kobayashi, K. Takeno, A. Meir, J. Urban, et al. (2009) *A phenotypic comparison of proteoglycan production of intervertebral disc cells isolated from rats, rabbits, and bovine tails; which animal model is most suitable to study tissue engineering and biological repair of human disc disorders?* Tissue Eng Part A, 15(12): p. 3835-46.

[266] Johnson, W.E., S. Stephan, and S. Roberts (2008) *The influence of serum, glucose and oxygen on intervertebral disc cell growth in vitro: implications for degenerative disc disease.* Arthritis Res Ther, 10(2): p. R46.

[267] Stephan, S., W.E. Johnson, and S. Roberts (2011) *The influence of nutrient supply and cell density on the growth and survival of intervertebral disc cells in 3D culture.* Eur Cell Mater, 22: p. 97-108.

[268] Yu, J., U. Tirlapur, J. Fairbank, P. Handford, S. Roberts, et al. (2007) *Microfibrils, elastin fibres and collagen fibres in the human intervertebral disc and bovine tail disc.* J Anat, 210(4): p. 460-71.

[269] Mavrogonatou, E. and D. Kletsas (2010) *Effect of varying osmotic conditions on the response of bovine nucleus pulposus cells to growth factors and the activation of the ERK and Akt pathways.* Journal of Orthopaedic Research, 28(10): p. 1276-1282.

[270] Chujo T, A.H., Akeda K, Miyamoto K, Muehleman C, Attawia M, Andersson G, Masuda K. (2006) *Effects of growth differentiation factor-5 on the intervertebral disc--in vitro bovine study and in vivo rabbit disc degeneration model study.* Spine, 31(25): p. 2909-17.

[271] Roberts, S., J. Menage, S. Sivan, and J.P. Urban (2008) *Bovine explant model of degeneration of the intervertebral disc.* BMC Musculoskelet Disord, 9: p. 24.

[272] Pereira, C.L., R.M. Goncalves, M. Peroglio, G. Pattappa, M. D'Este, et al. (2014) *The effect of hyaluronan-based delivery of stromal cell-derived factor-1 on the recruitment of MSCs in degenerating intervertebral discs.* Biomaterials, 35(28): p. 8144-53.

[273] Kazezian, Z., Z. Li, M. Alini, S. Grad, and A. Pandit (2017) *Injectable hyaluronic acid down-regulates interferon signaling molecules, IGFBP3 and IFIT3 in the bovine intervertebral disc.* Acta Biomater, 52: p. 118-129.

[274] Teixeira, G.Q., A. Boldt, I. Nagl, C.L. Pereira, K. Benz, et al. (2016) *A Degenerative/Proinflammatory Intervertebral Disc Organ Culture: An Ex Vivo Model for Anti-inflammatory Drug and Cell Therapy.* Tissue Eng Part C Methods, 22(1): p. 8-19.

[275] Krupkova, O., M. Hlavna, J. Amir Tahmasseb, J. Zvick, D. Kunz, et al. (2016) *An Inflammatory Nucleus Pulposus Tissue Culture Model to Test Molecular Regenerative Therapies: Validation with Epigallocatechin 3-Gallate.* Int J Mol Sci, 17(10).

[276] Arkesteijn, I.T., V.H. Mouser, F. Mwale, B.G. van Dijk, and K. Ito (2016) *A Well-Controlled Nucleus Pulposus Tissue Culture System with Injection Port for Evaluating Regenerative Therapies.* Ann Biomed Eng, 44(5): p. 1798-807.

[277] Demers, C.N., J. Antoniou, and F. Mwale (2004) *Value and limitations of using the bovine tail as a model for the human lumbar spine.* Spine (Phila Pa 1976), 29(24): p. 2793-9.

[278] Oshima, H., H. Ishihara, J.P. Urban, and H. Tsuji (1993) *The use of coccygeal discs to study intervertebral disc metabolism.* J Orthop Res, 11(3): p. 332-8.

[279] Roberts, S., J. Menage, V. Duance, S. Wotton, and S. Ayad (1991) *1991 Volvo Award in basic sciences. Collagen types around the cells of the intervertebral disc and cartilage end plate: an immunolocalization study.* Spine (Phila Pa 1976), 16(9): p. 1030-8.

[280] Ishihara, H., D.S. McNally, J.P. Urban, and A.C. Hall (1996) *Effects of hydrostatic pressure on matrix synthesis in different regions of the intervertebral disk.* J Appl Physiol (1985), 80(3): p. 839-46.

[281] Ohshima, H., J.P. Urban, and D.H. Bergel (1995) *Effect of static load on matrix synthesis rates in the intervertebral disc measured in vitro by a new perfusion technique.* Journal of orthopaedic research : official publication of the Orthopaedic Research Society, 13(1): p. 22-9.

[282] Hansen, H.J. (1956) *Studies on the pathology of the lumbosacral disc in female cattle.* Acta Orthop Scand, 25(3): p. 161-82.

[283] Vo, N.V., R.A. Hartman, P.R. Patil, M.V. Risbud, D. Kletsas, et al. (2016) *Molecular mechanisms of biological aging in intervertebral discs.* J Orthop Res, 34(8): p. 1289-306.

[284] Richardson, S., A.J. Freemont, and J.A. Hoyland, (2014) *Pathogenesis of intervertebral disc degeneration*, in *The intervertebral disc: molecular and structural studies of the disc in health and disease*, I.M. Shapiro and M.V. Risbud, Editors. Springer. p. 177-200.

[285] Sivan, S.S., E. Wachtel, and P. Roughley (2014) *Structure, function, aging and turnover of aggrecan in the intervertebral disc.* Biochim Biophys Acta, 1840(10): p. 3181-9.

[286] Grad, S., Y. Zhang, O. Rozhnova, E. Shelkunova, M. Mikhailovsky, et al., *Differential Gene Expression Profiles of Cells from Normal, Traumatic and Idiopathic Scoliotic Discs Identify Molecular Dysregulation in Scoliosis*, in *Global Spine Journal*. 2016: Dubai.

[287] Hristova, G.I., P. Jarzem, J.A. Ouellet, P.J. Roughley, L.M. Epure, et al. (2011) *Calcification in human intervertebral disc degeneration and scoliosis.* J Orthop Res, 29(12): p. 1888-95.

[288] Gilson, A., M. Dreger, and J.P. Urban (2010) *Differential expression level of cytokeratin 8 in cells of the bovine nucleus pulposus complicates the search for specific intervertebral disc cell markers.* Arthritis Research & Therapy, 12(1): p. R24.

[289] Tang, X., L. Jing, and J. Chen (2012) *Changes in the molecular phenotype of nucleus pulposus cells with intervertebral disc aging.* PLoS One, 7(12): p. e52020.

[290] Nasto, L.A., H.Y. Seo, A.R. Robinson, J.S. Tilstra, C.L. Clauson, et al. (2012) *ISSLS prize winner: inhibition of NF-kappaB activity ameliorates age-associated disc degeneration in a mouse model of accelerated aging.* Spine (Phila Pa 1976), 37(21): p. 1819-25.

[291] Tilstra, J.S., A.R. Robinson, J. Wang, S.Q. Gregg, C.L. Clauson, et al. (2012) *NF-kappaB inhibition delays DNA damage-induced senescence and aging in mice.* J Clin Invest, 122(7): p. 2601-12.

[292] Suzuki, S., N. Fujita, N. Hosogane, K. Watanabe, K. Ishii, et al. (2015) *Excessive reactive oxygen species are therapeutic targets for intervertebral disc degeneration.* Arthritis Res Ther, 17: p. 316.

[293] Nasto, L.A., A.R. Robinson, K. Ngo, C.L. Clauson, Q. Dong, et al. (2013) *Mitochondrial-derived reactive oxygen species (ROS) play a causal role in aging-related intervertebral disc degeneration.* J Orthop Res, 31(7): p. 1150-7.

[294] Dimozi, A., E. Mavrogonatou, A. Sklirou, and D. Kletsas (2015) *Oxidative stress inhibits the proliferation, induces premature senescence and promotes a catabolic phenotype in human nucleus pulposus intervertebral disc cells.* Eur Cell Mater, 30: p. 89-102; discussion 103.

[295] Mavrogonatou, E., M.T. Angelopoulou, and D. Kletsas (2014) *The catabolic effect of TNFalpha on bovine nucleus pulposus intervertebral disc cells and the restraining role of glucosamine sulfate in the TNFalpha-mediated up-regulation of MMP-3.* J Orthop Res, 32(12): p. 1701-7.

[296] Poveda, L., M. Hottiger, N. Boos, and K. Wuertz (2009) *Peroxynitrite induces gene expression in intervertebral disc cells.* Spine (Phila Pa 1976), 34(11): p. 1127-33.

[297] Chen, J.W., B.B. Ni, B. Li, Y.H. Yang, S.D. Jiang, et al. (2014) *The responses of autophagy and apoptosis to oxidative stress in nucleus pulposus cells: implications for disc degeneration.* Cell Physiol Biochem, 34(4): p. 1175-89.

[298] Sharp, C.A., S. Roberts, H. Evans, and S.J. Brown (2009) *Disc cell clusters in pathological human intervertebral discs are associated with increased stress protein immunostaining.* European spine journal : official publication of the European Spine Society, the European Spinal Deformity Society, and the European Section of the Cervical Spine Research Society, 18(11): p. 1587-94.

[299] Johnson, W.E., S.M. Eisenstein, and S. Roberts (2001) *Cell cluster formation in degenerate lumbar intervertebral discs is associated with increased disc cell proliferation.* Connect Tissue Res, 42(3): p. 197-207.

[300] Melrose, J. (2016) *A Global Pictorial Assessment of the Intervertebral Disc Cell in Several Species Reveals a Remarkable Biodiversity in this Cell Type which should be taken into Account in Experimental Studies on Intervertebral Disc Repair.* Spine Research, 2(1:13): p. 1-14.

[301] Nerlich, A.G., B.E. Bachmeier, E. Schleicher, H. Rohrbach, G. Paesold, et al. (2007) *Immunomorphological analysis of RAGE receptor expression and NF-kappaB activation in tissue samples from normal and degenerated intervertebral discs of various ages.* Ann N Y Acad Sci, 1096: p. 239-48.

[302] Oeckinghaus, A., M.S. Hayden, and S. Ghosh (2011) *Crosstalk in NF-kappaB signaling pathways.* Nat Immunol, 12(8): p. 695-708.

[303] Salminen, A., K. Kaarniranta, and A. Kauppinen (2012) *Inflammaging: disturbed interplay between autophagy and inflammasomes.* Aging (Albany NY), 4(3): p. 166-75.

[304] Chen, Z.H., S.H. Jin, M.Y. Wang, X.L. Jin, C. Lv, et al. (2015) *Enhanced NLRP3, caspase-1, and IL- 1beta levels in degenerate human intervertebral disc and their association with the grades of disc degeneration.* Anat Rec (Hoboken), 298(4): p. 720-6.

[305] Medzhitov, R. (2008) *Origin and physiological roles of inflammation.* Nature, 454(7203): p. 428-35.

[306] Lee, R.S., M.V. Kayser, and S.Y. Ali (2006) *Calcium phosphate microcrystal deposition in the human intervertebral disc.* J Anat, 208(1): p. 13-9.

[307] Gruber, H.E., H.J. Norton, Y.B. Sun, and E.N. Hanley (2007) *Crystal deposits in the human intervertebral disc: implications.* Spine Journal, 7(4): p. 444-450.

[308] Feinberg, J., O. Boachie-Adjei, P.G. Bullough, and A.L. Boskey (1990) *The distribution of calcific deposits in intervertebral discs of the lumbosacral spine.* Clin Orthop Relat Res, (254): p. 303-10.

[309] Kalya, S. and A.K. Rosenthal (2005) *Extracellular matrix changes regulate calcium crystal formation in articular cartilage.* Curr Opin Rheumatol, 17(3): p. 325-9.

[310] Masuda, I., K. Ishikawa, and G. Usuku (1991) *A histologic and immunohistochemical study of calcium pyrophosphate dihydrate crystal deposition disease.* Clin Orthop Relat Res, (263): p. 272-87.

[311] Sharma, D. and T.D. Kanneganti (2016) *The cell biology of inflammasomes: Mechanisms of inflammasome activation and regulation.* J Cell Biol, 213(6): p. 617-29.

[312] Stutz, A., D.T. Golenbock, and E. Latz (2009) *Inflammasomes: too big to miss.* J Clin Invest, 119(12): p. 3502-11.

[313] Song, Y., Y. Wang, Y. Zhang, W. Geng, W. Liu, et al. (2017) *Advanced glycation end products regulate anabolic and catabolic activities via NLRP3-inflammasome activation in human nucleus pulposus cells.* J Cell Mol Med.

[314] Sivan, S.S., E. Tsitron, E. Wachtel, P. Roughley, N. Sakkee, et al. (2006) *Age-related accumulation of pentosidine in aggrecan and collagen from normal and degenerate human intervertebral discs.* Biochem J, 399(1): p. 29-35.

[315] Pokharna, H.K. and F.M. Phillips (1998) *Collagen crosslinks in human lumbar intervertebral disc aging.* Spine (Phila Pa 1976), 23(15): p. 1645-8.

[316] Yokosuka, K., J.S. Park, K. Jimbo, K. Yamada, K. Sato, et al. (2006) *Advanced glycation end-products downregulating intervertebral disc cell production of proteoglycans in vitro.* J Neurosurg Spine, 5(4): p. 324-9.

[317] Wagner, D.R., K.M. Reiser, and J.C. Lotz (2006) *Glycation increases human annulus fibrosus stiffness in both experimental measurements and theoretical predictions.* J Biomech, 39(6): p. 1021-9.

CHAPTER II

Improvement of bovine nucleus pulposus cells isolation leads to identification of three phenotypically distinct cell subpopulations

Article 2
Published in TISSUE ENGINEERING: Part A
Volume 21, Numbers 15 and 16, 2015
doi: 10.1089/ten.TEA.2014.0461

Improvement of bovine nucleus pulposus cells isolation leads to identification of three phenotypically distinct cell subpopulations

Maria Molinos [1,2,3], Catarina R Almeida[1,2], Raquel M Gonçalves[1,2], Mário A Barbosa[1,2,3]

[1] i3S - Instituto de Investigação e Inovação em Saúde, Universidade do Porto, Rua Alfredo Allen, 208, 4200-135 Porto, Portugal

[2] INEB - Instituto de Engenharia Biomédica, Universidade do Porto, Portugal

[3] ICBAS - Instituto de Ciências Biomédicas Abel Salazar, Universidade do Porto, Rua de Jorge Viterbo Ferreira n.º 228, 4050-313 Portugal

Abstract

Strategies to promote intervertebral disc (IVD) regeneration have been hindered by the lack of knowledge of IVD fundamental cellular/molecular components. One of the key points to address is the characterization of nucleus pulposus (NP) cell population(s). This study establishes an improved method for bovine NP (bNP) cells isolation, whose procedure is still not consensual amongst the literature, allowing a thorough characterization of cell (sub)populations that exist in the young NP. bNP was digested with distinct enzymes (collagenase-type-I, collagenase-type-II and collagenase-type-XI) at different concentrations (0.5, 1.0 and 2.0 mg/ml), for 4 and 19 h. Cell yield, viability/apoptosis and morphology were analysed by flow cytometry and imaging flow cytometry. Identification of cell subpopulations within NP and its phenotype was investigated by assessing expression of CD29, CD44, CD45, CD34, CD146 and Brachyury. It was found that bNP cells present similar morphology independently of the digestive enzyme used. However, cell yield was greatly improved by Coll-XI (2 mg/ml) treatment for a short digestion period. Interestingly, three subpopulations, with different sizes and auto-fluorescence, were consistently identified by flow cytometry. And crucially, differential expression of cell markers was found among these subpopulations. This study demonstrated that collagenase-type-XI is an efficient enzyme to digest bNP. And most importantly, three phenotypically distinct subpopulations of cells where identified within the bovine NP. Such knowledge is key for a better understanding of NP cell biology and its potential endogenous regenerative capacity.

Improvement of bovine nucleus pulposus cells isolation leads to identification of three phenotypically distinct cell subpopulations

Introduction

The intervertebral disc (IVD) is a complex and bioactive structure within the spine. Continuous multidirectional mechanical forces allied to aging activate degenerative pathways in the IVD, which are responsible for many disabling back diseases, and ultimately imply a heavy socio-economic impact.

Current treatments include rest, anti-inflammatory medication, physical therapy, and, as a last resort, spinal fusion, total disc replacement or discectomy. These treatments focus on symptomatic management and do not address the underlying pathophysiology of the diseased tissue, resulting in long-term suboptimal outcomes. Alternative strategies, such as cell-based therapies, growth factor injection, gene therapy, and tissue engineering (TE), aiming to stop or reduce degeneration of the IVD, or to promote its regeneration, are being pursued [1, 2]. Recently, our group has shown that delivery of a chemoattractor in the IVD can recruit mesenchymal stem cells towards the NP, which opened new perspectives for IVD regenerative strategies [3]. However, success of current strategies has been hindered by the lack of knowledge on the cellular and molecular components of the IVD.

Cells in the adult IVD are usually divided in two populations, according to the different embryonic origin of the tissue where they reside: 1) the fibroblast-like cells in the annulus fibrosus (AF), which develop from the somites (sclerotome), and 2) the chondrocyte-like cells in the nucleus pulposus (NP), which derive from the notochord (both mesenchyme-derived tissues) [4]. NP cells share typical markers of extracellular matrix (ECM) with AF cells or articular cartilage (AC) cells, such as type-II-collagen, aggrecan and versican [5]. Expression of specific NP markers has been also described but is species-dependent. For instance, bovine NP (bNP) cells express synaptosomal-associated protein, 25 kDa (SNAP25), tenomodulin (TNMD), cytokeratin-8 (CK8) [5, 6], while human NP cells express carbonic anhydrase-12 (CA12), paired box 1 (PAX-1), haemoglobin β–chain (HBB) and ovostatin 2 (OVOS2). Rat NP cells exclusively express CD24, while rabbit NP cells express type V collagen, matrix Gla protein (MGP) and Htra serine peptidase 1 (Htra1). Most recently, a selection of markers has been proposed to define the phenotype of NP cells [7].

Cells isolated from degenerated and non-degenerated human discs can

differentiate into adipogenic, osteogenic and chondrogenic lineages, indicating that the IVD may include progenitor cells within its population [8-14]. Also, expression of markers associated with progenitors (e.g. Tie2, GD2, Stro-1, Oct3/4, CD105, CD90 and Notch-1) suggests that precursor cell populations might be present within degenerated human discs [8, 9]. These findings indicate that degenerated human discs may count on an endogenous regenerative capacity, although the exact nature and origin of the participating cells remains unknown.

Bovine IVDs have been proposed as a suitable model to study Tissue Engineering and biological repair of human IVD [15], and many studies have been published culturing bovine IVD cells as a model [3, 5, 6, 16-18]. However, the nonexistence of a definitive cell marker or clear phenotypic assays to distinguish NP cells from other cell types, the lack of standardization of NP cell isolation methods, together with differences in NP markers expression among distinct species, raises questions concerning the proper identification of cell types in IVD, establishment of *in vitro* cell cultures from these cells, and comparison of results obtained from different labs. A more standardized characterization of cell populations within IVD, and particularly in NP, is crucial when studying biological phenomena that might contribute to both IVD degeneration and its potential regenerative capacity.

Hence, in this study a bovine model was used to evaluate different isolation methods of NP cells. A new isolation method was explored, guarantying high cell yield and viability. Moreover, bNP cells morphology and phenotypic expression was thoroughly characterized immediately after isolation by image analysis and flow cytometry.

Materials and Methods

Bovine nucleus pulposus cells isolation

Caudal intervertebral discs from 10 to 13-month-old bovine steers were dissected until 3h hours after death. NP was harvested from 7-8 IVDs. With a scalpel blade, NP was separated from AF and vertebral endplates and finely chopped. Tissue digestion was performed in Dulbeccos's modified Eagle's medium (DMEM, 21885 Gibco), supplemented with 5% v/v Penicillin Streptomycin (PAA), 10% v/v

Amphotericin B. (PAA), 2.5% (v/v) of HEPES Buffer 1 mM (Lonza), 1.5% (v/v) of NaCl 5M and KCl 0.4M solution (to adjust osmolarity to 400 mOsm), 1.3 U/mL DNAse, as described elsewhere [19], and one of three different enzymatic formulations: collagenase-type-I (Coll-I), collagenase-type-II (Coll-II) or collagenase-type-XI (Coll-XI) (C0130, C6885 and C7657, respectively, Sigma Aldrich), at different concentrations (0.5, 1.0 and 2.0 mg/mL). All enzymatic preparations contain a mixture of the type I and II forms of the purified collagenase enzyme, which differ in their affinity for different substrates, as assessed by the manufacturer (see http://www.sigmaaldrich.com/life-science/metabolomics/enzyme-explorer/learning-center/collagenase-guide.html).

Tissue/medium ratio was set at 10% w/v to prevent the pH dropping below 6.8 during incubation. Tissue was digested for 4 h (minimum time required to totally digest tissue from at least one of the protocols used) or 19 h (overnight digestion – tissue totally digested in all protocols), in a humidified atmosphere at 37°C/5% CO_2, and under gentle stirring. ECM contaminants were filtered with a 70 µm cell strainer.

Assessing bNP cell yield, viability and apoptosis

Immediately upon digestion, cell yield was quantified by trypan blue exclusion and subsequently normalized by wet tissue weight. Cell viability and apoptosis were assessed by flow cytometry (FACS Calibur, BD Immunocytometry Systems), using FITC-Annexin V Apoptosis Detection Kit I (556547, eBioscience), according to manufacturer's instructions.

Characterization of bNP cell morphology by Imaging Flow Cytometry (IFC)

To examine the morphological features of freshly isolated NP cells, cells were fixed in 4% w/v paraformaldehyde (PFA) at room temperature (RT) for 15 min., washed with PBS, and then permeabilized with 0.2% v/v Triton, for 5 min. After washing again with PBS, cells were incubated for 20 min at RT, with Phalloidin-AlexaFluor®488 (1:40 Dil. per $2.0x10^5$ cells, A12379, Life Technologies), previously prepared in a PBS-1% w/v bovine serum albumin (BSA) solution, according to manufacturer's instructions. Shortly prior to acquisition, cells were labeled with DRAQ5 (1:1500 Dil. per $2.0x10^5$ cells, 65-0880, eBioscience), and run on ImageStream^X (IS, Millipore), and analysed

with IDEAS software for cell area, diameter, nuclear/cytoplasm ratio, and presence of vesicles. To quantify the percentage of cells with bright vesicles and the nuclear to cytoplasmic ratio, specific masks were developed and applied to brightfield and fluorescence images:

- Morphology (M01, Bightfield) - mask applied to calculate cell area based on brightfield;
- Morphology (M02, Actin) - to calculate cell area based on actin staining;
- Erode (M05, 5) - to calculate nucleus area;
- Spot (M01, Brightfield, Bright, 34, 1) - mask designed to mark bright vesicles within cells.

Characterization of bNP cells phenotype

Cell surface staining. The expression of surface markers (see Table 2.1) was analysed by flow cytometry immediately upon cells isolation, without fixation, to guaranty dead cells exclusion with PI staining. Firstly, cells were left to recover from digestion for 30 min in a humidified atmosphere at 37°C/5% CO_2. Cells were then washed with PBS-2% Fetal bovine Serum (FBS) and incubated with primary antibodies (Table 1), in the same solution, for 1h at RT. In the case of non-conjugated anti-CD34 antibody, cells were additionally incubated with a secondary goat anti-mouse-AlexaFluor488 antibody, in the same conditions. After labeling, cells were washed with 2mL PBS-2% FBS and run in FACSCalibur. Results were analysed with FlowJo software, Version 8.7.

Table 2.1: Antibodies used in flow cytometry analysis.

Antibodies	Fluorochrome	µg/mL	Clone	Catalog #, Manufacturer
Primary antibodies				
Mouse anti-bovine CD29	AlexaFluor®488		TS2/16	303015, Biolegend
Mouse anti-bovine CD44	FITC	10	IL-A118	MCA2433F, AbD Serotec
Mouse anti-bovine CD45	FITC	10	CC1	MCA832F, AbD Serotec
Mouse anti-human CD146	AlexaFluor®647	5	OJ79c	MCA2141A647T, AbD Serotec
Mouse anti-bovine CD34	-	24		Isotype N21, kindly provided by Sakurai M [20]
Mouse anti-human Brachyury	FITC	20	3E4.2	FCMAB302F, Millipore
Secondary antibody				
Goat Anti-Mouse IgG	AlexaFluor®488	20		A-11017, Life Technologies™
Isotype controls				
Mouse IgG1 k	AlexaFluor®488	10	MOPC-21	400132, Biolegend
Mouse IgG1 control	FITC	10	PPV-06	21275513, Immunotools
Mouse IgG1	AlexaFluor®647	5		sc-24636, Santa Cruz Biotechnology
Mouse IgG1 k Purified		20	P3.6.2.8.1	14-4714, eBioscience

Intracellular staining. To quantify brachyury intracellular expression, cells were fixed in 4% w/v PFA at RT for 15 min, and permeabilized with 0.2% v/v Triton for 5 min. Cells were then incubated with FITC-conjugate anti-Brachyury antibody, for 1h at 4°C, after which they were washed with PBS-2% FBS and analysed by IFC.

Cell senescence analysis by flow cytometry. The senescence of bNP cells was analysed by the detection of beta-galactosidase activity by flow cytometry, as described by Debacq-Chainiaux et al. [21]. Briefly, bNP cells were treated with Bafilomycin A1 (100 nM) for 1h in fresh culture medium at 37ºC, 5% CO_2, to induce lysossomal alkalinization. Then, the substrate dodecanoylaminofluorescein di-β-D-galactopyranoside (C_{12}FDG, 33 µM) was added to the cell suspension and incubated during 1-2h. This substrate, when hydrolyzed by beta-gal, becomes fluorescent. After incubation, the cells were washed in ice-cold PBS, stained with Propidium Iodide and analysed by flow cytometry in a FACSCalibur. C_{12}FDG was detected on the FL1 channel. Negative controls of bNP cells incubated only with Bafilomycin A1 or with C_{12}FDG were also performed. The data collected was analysed in FlowJo vs 8.7 software.

Statistical Analysis

Statistical analysis was performed using GraphPad Prism version 6.0a for Mac OS X. D'Agostino and Pearson omnibus normality test was used to assess Gaussian distribution of data. Results that did not follow a normal distribution (cell yield, viability, apoptosis, cell subpopulations sizes (P1, P2 and P3), and markers expression) were analysed for statistical differences using non-parametric Kruskal-Wallis and Dunn's multiple comparison tests. In the case of cell morphology data, which followed a Gaussian distribution, groups were compared using a two-way ANOVA (Bonferroni's multiple comparisons test). In all cases, a confidence level of at least 95% (*, $p < 0.05$) was considered.

Results

Isolation of bovine nucleus pulposus (bNP) cells

In order to characterize bNP cells, the cells isolation procedure was firstly optimized. For that, three different commercially available collagenase formulations were tested: 1) Coll-I, the formulation most used in the literature; 2) Coll-II, a mixture with augmented activity of type-II-collagenase; and 3) Coll-XI, with augmented activity of both type I and II collagenases. The effect of enzyme concentration (0.5, 1 and 2 mg/ml) and tissue digestion time (4 h and overnight) on cell yield, viability and apoptosis were addressed (Figure 2.1).

For shorter digestion periods (4 h), cell yield increased in a concentration-dependent manner with digestion by Coll-XI. In particular, the median cell yield obtained with Coll-XI digestion (2.0 mg/ml) ($(1.2\pm0.5) \times 10^6$ cells/mg of wet tissue) was significantly higher (*, $p<0.05$) than with Coll-I ($(6.3\pm5.8) \times 10^5$ cells/mg of wet tissue) or Coll-II ($(5.9\pm3.1) \times 10^5$ cells/mg of wet tissue) (Figure 1a, left). With a longer period of digestion (overnight) no significant differences could be found between the protocols tested, with a high variability being observed (Figure 1a, right). However, lower cell yields were observed at higher enzyme concentrations (except for Coll-I). In particular, overnight digestion with Coll-II at 2.0 mg/mL resulted in a drop in cell yield to $0.2\pm 1.6) \times 10^5$ cells/mg wet tissue.

In terms of cell viability, there was also an increase (79-85%) when using Coll-XI, for shorter incubation periods, and independently of enzyme concentration. Cell viability after 4 h digestion with different collagenases ranged from: i) 72±15 to 81±13 % for Coll-I; ii) 63±33 to 81±19 % for Coll-II; and iii) 79±22 to 85±16 % for Coll-XI (Figure 1b, right). With prolonged digestion time, cell viability showed a decrease, with exception of protocols using Coll-I, with viability around 80% (Figure 1b, right). Finally, the median percentage of apoptotic cells stood majorly below 5%, with no obvious differences between formulations (Figure 1c).

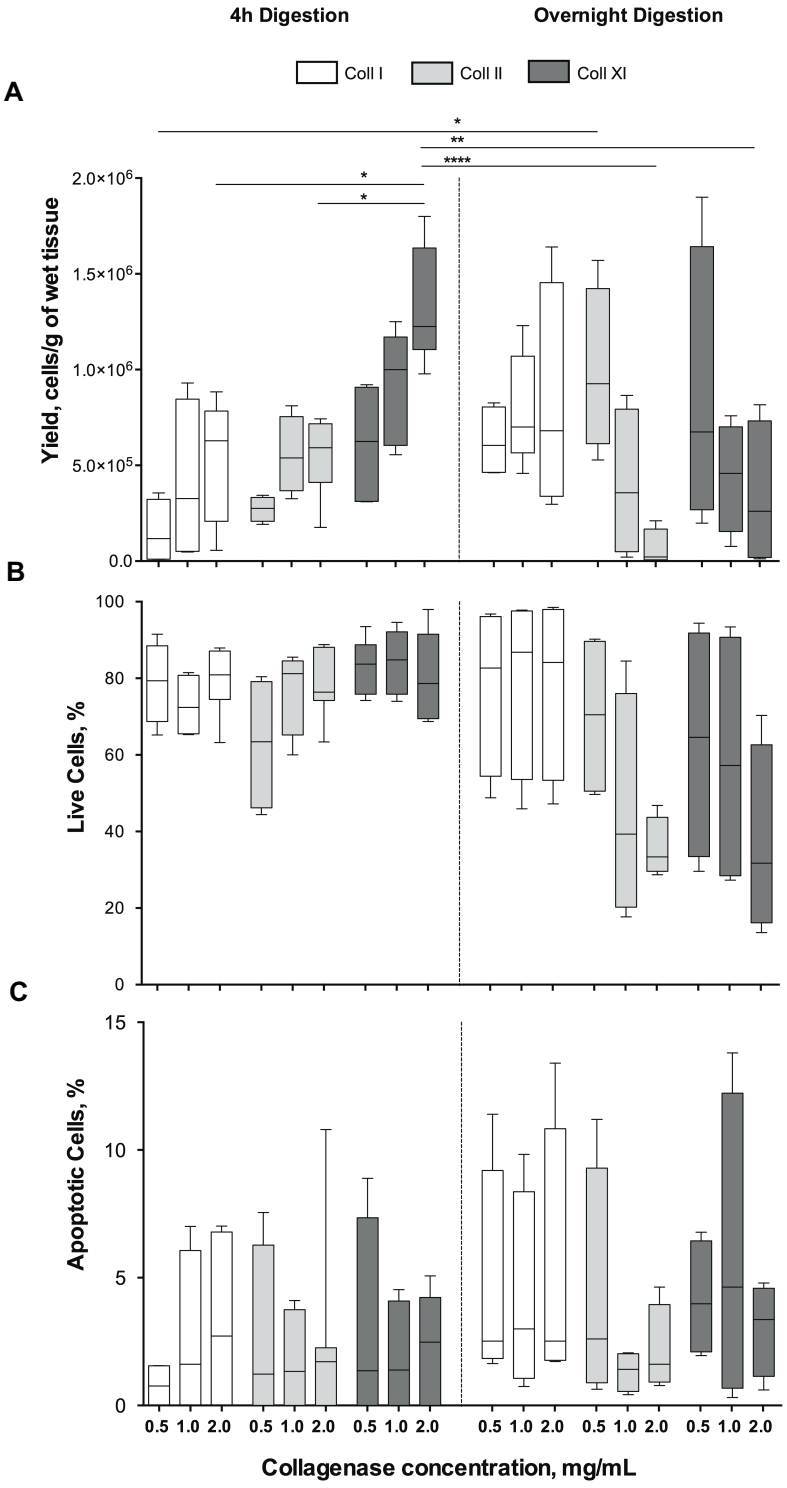

Figure 2.1: Effect of collagenase (Coll) type, enzyme concentration and digestion time on bovine nucleus pulposus (bNP) cell isolation. Coll-I (white bars), Coll-II (light grey) and Coll-XI (dark grey) were used at 0.5, 1 or 2 mg/ml to dissociate NP tissue for 4 h or overnight. Cell yield (cells/g of wet tissue) **(A)**, cell viability (% of live cells determined by flow cytometry analysis of propidium iodide stained cells) **(B)**, and cell apoptosis **(C)** in the different conditions were determined. Results are presented as

box plot and whiskers (Min to Max) with horizontal line at median (n=4-8). Results were analysed for statistical differences using non-parametric Kruskal-Wallis and Dunn's multiple comparison tests. (* $p < 0.05$, ** $0.001 < p < 0.01$ and *** $p < 0.001$).

Morphological analysis of bNP cells

In order to characterize bNP cell morphology immediately upon isolation, freshly isolated bNP cells were analysed by IFC, using masks for brightfield images of cells and for fluorescence images of the cytoskeleton and nuclei (Figure 2.2).

Cells area was first quantified based on both brightfield and fluorescence images of cells cytoskeleton (Figure 2.2 B). Quantification on the cytoskeleton staining revealed that bNP cells present an area ranging from 130±17 μm^2 to 138±34 μm^2, independently of the method of tissue digestion. These values were significantly different from the area calculated based on brightfield images, which suggests the presence of a structure surrounding the cell cytoskeleton in most of the cells. In the case of cells dissociated with Coll-XI, the cell area almost doubled (130±17 μm^2 to 235±38 μm^2, for cytoskeleton and brighfield areas, respectively). The presence of a pericellular matrix surrounding the cells was confirmed by staining against type VI collagen (Supplementary Figure 2.1). Thus, cell diameter was analysed based only in images of actin staining (Figure 2.2 C). It was observed that bNP cells have a diameter of approximately 17.3±1.3 µm, not varying with tissue digestion method.

The nuclear to cytoplasmic ratio (N/C, nucleus area/cytoplasm area) of bNP cells, a feature that has been previously linked to the presence of progenitor cells [22], was quantified from the nuclei and actin staining (Figure 2a, second column). The N/C ratio of bNP cells isolated with Coll-I, Coll-II and Coll-XI (2.0 mg/mL, 4 h digestion) ranged from 0.5±0.1 (Coll-II) to 0.6±0.1 (Coll-I and Coll-XI), respectively (Figure 2d up), with no significant differences found between the isolation methods. Thus, the area occupied by the nucleus is about half the cytoplasmic area. Moreover, the distribution of N/C ratio was very narrow within bNP cells (Figure 2.2 D bottom).

In addition, image analysis of bNP cells revealed the presence of putative vesicles within the cytoplasm of these cells (Figure 2.2 E top). The percentage of bNP cells containing vesicles was quantified by using a mask specifically designed to trace bright spots in brightfield images (Figure 2.2 E bottom). The results obtained showed

that around 50-60% of NP cells presented one or more cytoplasmic bright vesicles (0.5-1.5 µm diameter), independently of the digestion protocol used.

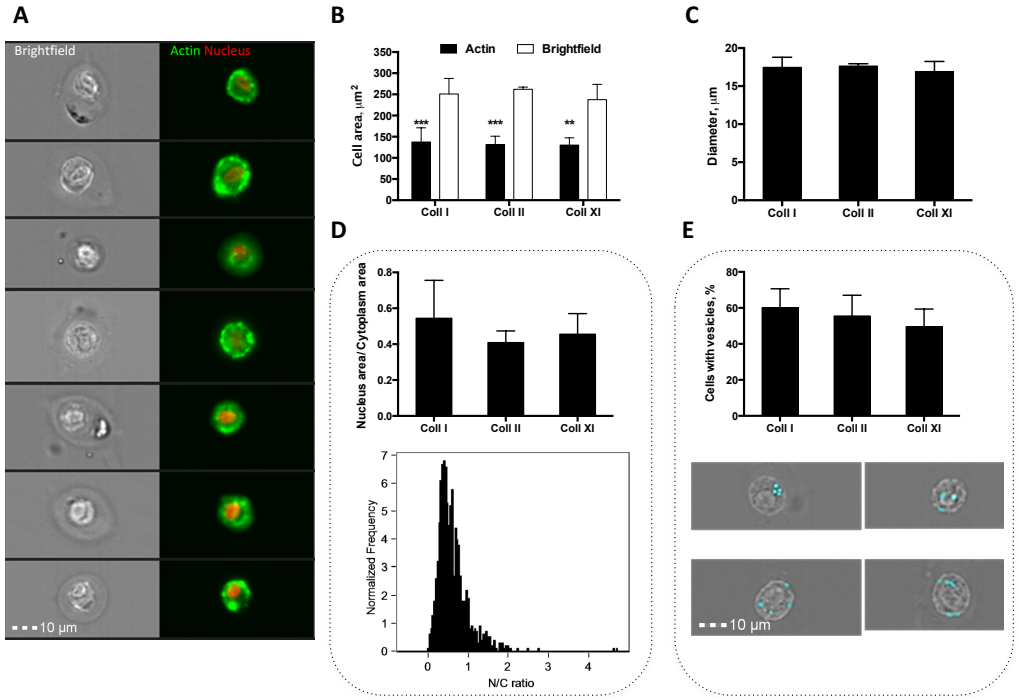

Figure 2.2: Morphological analysis of bNP cells. **A |** Images of bNP cells obtained by Imaging Flow Cytometry (first column: brightfield images of cells; second column: merged fluorescence images of cells stained with phalloidin-FITC (actin, green) and DRAQ5 (nuclei, red); **B |** bNP cells area based on brightfield (white bars) and actin staining (black bars) images of tissue digested with different collagenases: Coll-I, Coll-II and Coll-XI (2.0 mg/mL, 4 h digestion; **C |** bNP cell diameter based on actin staining for tissue digested with the three collagenases; **D |** nuclear to cytoplasmic (N/C) ratio of bNP cells isolated with the three different methods (top), and representative histogram of N/C ratio distribution of bNP cells isolated with Coll-I, 2.0 mg/mL for 4 h (bottom); **E |** Percentage of cells containing one or more vesicles after isolation with the different collagenases - a light blue mask specifically designed to mark and quantify bright vesicles within cells is shown in the bottom brightfield images of cells. Results are presented as Mean±StDev of 3 independent experiments, where a total of 3661 cells for Coll-I, 993 cells for Coll-II and 5385 cells for Coll-XI were analysed. In the case of cell area analysis, groups were compared using a two-way ANOVA (Bonferroni's multiple comparisons test). ** $0.001 < p < 0.01$ and *** $p < 0.001$.

Characterization of bNP cells by flow cytometry

bNP cells freshly isolated with the different collagenases (Coll-I, Coll-II and Coll-XI) were analysed by flow cytometry (Figure 2.3). Discarding PI-positive cells (dead

cells), three subpopulations (P1, P2, P3) of live cells could be consistently identified, based on their size (FSC-H) and auto-fluorescence (in FL3 channel), evidencing a heterogeneous cell population within bovine NP tissue. The presence of nuclei in these bNP cells was confirmed by DRAQ5 expression (Figure 2.3 C).

The subpopulations were distinguishable by: i) small cells with high auto-fluorescence (P1); ii) large cells with high auto-fluorescence (P2); and iii) median sized cells with low auto-fluorescence (P3) (Figure 2.3 A). The frequency of each subpopulation obtained with the different isolation methods was assessed (Figure 2.3 B). P2 is the most abundant subpopulation within bNP cells, with frequencies of 45-62% (Coll-I), 48-65% (Coll-II) and 66-68% (Coll-XI). The P1 subset is less frequent: 32-47% (Coll-I), 29-50% (Coll-II) and 25-28% (Coll-XI). Lastly, P3 is the least frequent subpopulation (<10%): 4-8% (Coll-I), 3-6% (Coll-II) and 5-8% (Coll-XI). Different concentrations of Coll-XI lead to the same distribution of the three populations. The 3 subpopulations were also identified in old bovine animals (>10 years) but with different ratio: lower P3 and higher P1 percentages were observed (Supplementary Figure 2.2).

Based on the higher cell yield obtained and consistency on the subpopulations observed, subsequent assays were performed with cells obtained by 4 h digestion with Coll-XI at 2.0 mg/mL.

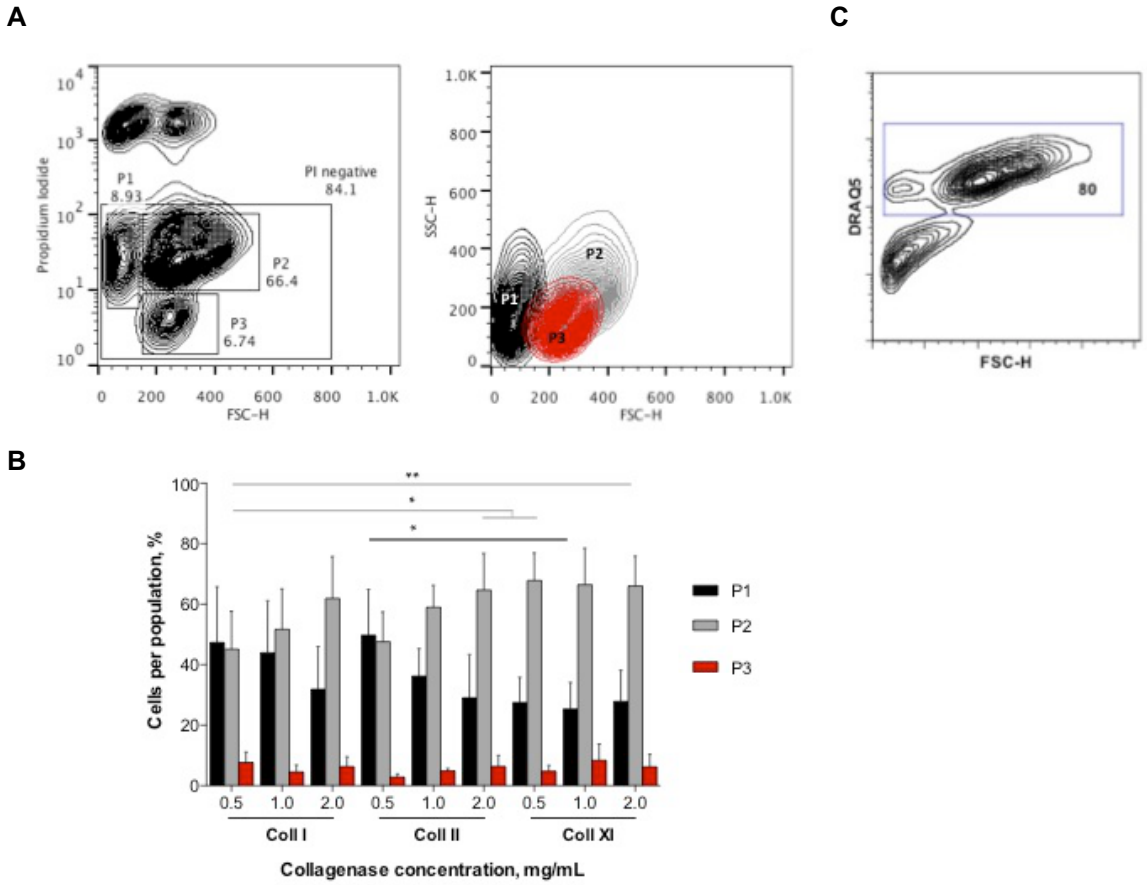

Figure 2.3: Identification of subpopulations of bNP cells, based on size and auto-fluorescence, by flow cytometry. A | Contour plots of freshly isolated bNP cells: PI expression versus forward scatter-height (FSC-H) (left) and side scatter-height (SSC-H) versus FSC-H (right). Three subpopulations of live cells (P1, P2, and P3) could be consistently identified, with distinct size and auto-fluorescence. **B |** Percentages of cells in P1, P2, and P3 subpopulations after NP digestion with Coll-I, Coll-II, and Coll-XI (0.5, 1.0, and 2.0 mg/mL, 4 h digestion). Results are presented as mean – SD (n = 4–8), and analysed for statistical differences using non-parametric Kruskal–Wallis and Dunn's multiple-comparison tests. *p < 0.05 and **0.001 < p < 0.01; **C|** PI and DRAQ5 staining of bNP cells on isolation. Around 80% of all events are DRAQ5 positive (n=5). Colour images available online at www.liebertpub.com/tea

Senescence analysis of bNP cells by flow cytometry

The senescence of bNP cells was analysed by beta-galactosidade activity and its distribution within P1, P2 and P3 sub-populations was assessed (Figure 2.4). The data collected showed that the bulk bNP cell senescence ranges from 13 to 71 %. When analysing in more detail, no senescent cells could be observed within sub population P1, while P2 and P3 present 60±7 % and 56±48 % of cell senescence,

respectively. When cell senescence ($C_{12}FDG^{+}$) vs viable cells (PI^{-}) is analysed, it is clear the existence of 2 populations with senescent cells but with distinct levels of auto-fluorescence (Figure 2.4, first line).

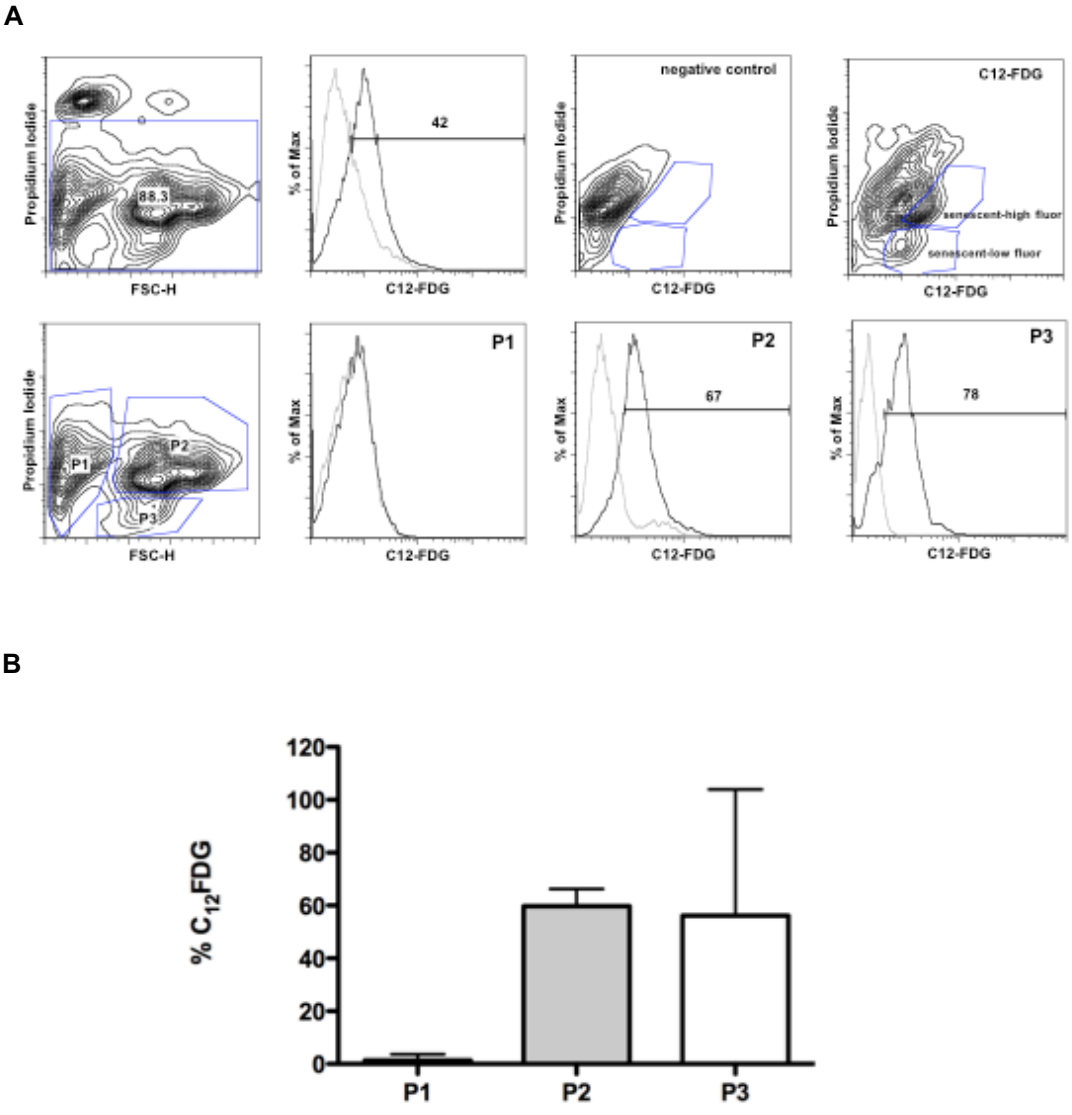

Figure 2.4: Senescence analysis of bNP cells. Freshly isolated bNP cells were incubated with $C_{12}FDG$, a fluorescent substrate for beta-galactosidase. A | The fluorescence intensity of $C_{12}FDG$ cell in whole population of bNP cells is represented in the first line for a representative donor. The second line illustrates the intensity of $C_{12}FDG$ cells for subpopulations P1, P2 and P3. $C_{12}FDG$ was assessed in FL1 channel. The cells were also stained with Propidium Iodide (FL3 channel), to exclude dead cells. **B |** Quantification of $C_{12}FDG$ expression on bNP cells supopulations, P1, P2 and P3. Results are presented as Mean±StDev (n=3 independent donors).

Phenotypic characterization of bNP cells by flow cytometry

To go further on bNP cells characterization, the phenotype of these cells was analysed by flow cytometry. A panel of markers for bNP cells was analysed (Table 2.2).

Expression of each marker in the whole bNP cell population was quantified (Figure 5). Brachyury expression was quantified by IFC, through which it was also possible to validate its correct intra-nuclear localization. The majority of bNP cells were CD29+ (87.7±4 %) and Brachyury+ (90.8±5 %). Intermediate amounts of cells expressing CD44 (18.6±5 %) and CD146 (22.3±8 %) were detected, while only low percentages of hematopoietic-lineage markers, CD45 (8.3±4 %) and CD34 (2.3±1 %), were identified.

A

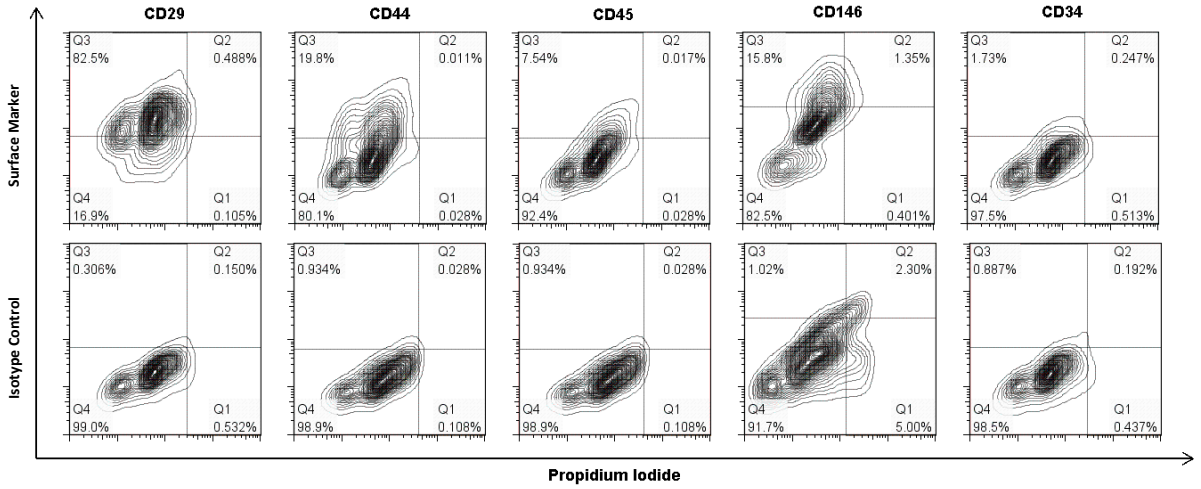

B

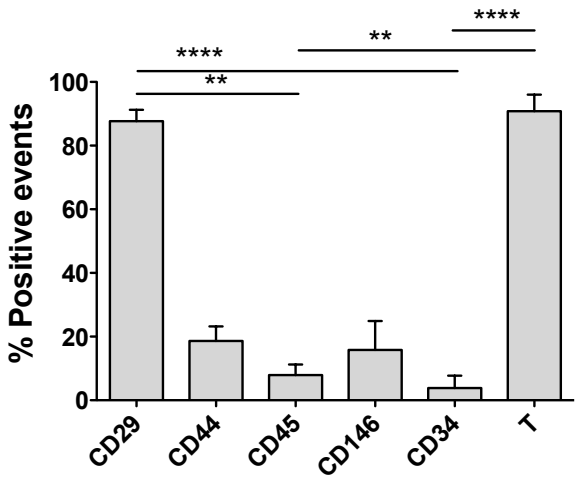

Figure 2.5: Phenotypic analysis of freshly isolated bovine nucleus pulposos (bNP) cells, obtained after digestion with ColI-XI (2.0 mg/mL, 4 h). A | Flow cytometry contour plots of CD29, CD44, CD45, CD146 and CD34 expression of live bNP cells (propidium iodide negative). Gates were established according to respective isotype controls (bottom). B | Graph shows the mean percentage of live cells expressing each of the markers described, after subtracting the respective isotype control. Results are presented as Mean±StDev (n=5-7) and statistical differences were assessed using non-parametric Kruskal-Wallis and Dunn's multiple comparison tests, (** $0.001 < p < 0.01$ and **** $p < 0.0001$). T: Brachyury, transcription factor quantified by imaging flow cytometry.

In addition, expression of each marker was analysed in P1, P2 and P3 subpopulations (Figure 6). The frequency of Brachyury+ cells within the three subpopulations was not analysed, since the detection of this transcription factor could not be simultaneously performed with PI staining, and almost all bNP cells were Brachyury+ (Figure 5). P2, the most frequent subpopulation of bNP cells, was characterized by a large number of cells expressing CD29 (98±2%), some cells expressing CD44 (16±5%) and only a few expressing CD146 (6±4%), CD45 (7±4%) and CD34 (5±8%). P3 (median sized cells with low auto-fluorescence) showed a profile similar to P2, with a high percentage of CD29+ cells (85±7%) and lower number of CD44+ cells (12±7%). However, no cells expressing CD34, CD45 or CD146 were detected in P3. Finally, P1, the subpopulation of smaller cells had a significantly higher (**$p<0.025$) percentage of CD44+ cells (49±2%). A higher percentage of cells expressing CD45 (24±13%), CD34 (6±5%) and CD146 (39±17%) was also found within this subset. On the other hand, the frequency of CD29+ cells (33±7%) was significantly lower (***, $p<0.001$) from that found in P2 and P3. Observation of the FSC vs FL3 plots for the cells positive for each marker, leads to a clearer distinction between P2 and P3 (supplementary Figure S3): CD45 and CD146 expression was found in P2 but not in P3 (even though only a small percentage of cells in P2 expresses these molecules).

Table 2.2: Findings in the literature and in this study regarding markers selected to characterize bNP cells phenotype.

Marker	Description	Species	Method	Findings in the literature	Findings in this study
CD29 (β1-integrin)	Cellular adhesion marker.	Human[13, 23, 24], Rabbit[25], Porcine[24], Rat[26]	IHC, FC	Protein expressed by NP cells from degenerated human IVDs and young AF cells, after monolayer expansion. Also present in rabbit and rat IVD and in immature porcine NP and AF.	Detected in more than 80% of bovine NP cells immediately upon isolation.
CD44	Transmembrane protein. Primary hyaluronic acid receptor.	Human[9, 27], Rabbit[28-30], Rat[26, 31]	FC, IHC, RT-PCR	> 80% expression by human $CD24^+$ NP cells and in cells cultured from herniated and degenerated human IVDs, rabbit NP and in the developing and adult rat IVD. mRNA detected in rabbit AF-derived stem cells.	Detected in nearly 20% of bovine NP cells immediately upon isolation. One subpopulation (P1) with significantly higher percentage of CD44+ cells.
CD45	Hematopoietic lineage-restricted surface marker.	Human[9, 27]	FC	Not found in $CD24^+$ NP cells nor in cells from herniated and degenerated IVDs after culture.	Expressed by only 8% bovine NP cells. Subpopulation P1 with higher percentage of CD45+ cells. Expressed only by cells from P1 and P2.
CD146 (MCAM or MUC18)	Glycoprotein. Marker for vascular endothelial cells, smooth muscle cells, pericytes and mesenchymal stem cells.	Human[9]	FC	Not found in $CD24^+$ NP cells after culture.	Expressed by more than 20% of bovine NP cells. Expressed only by cells from subpopulations P1 and P2.
CD34	Transmembrane protein. Marker for hematopoietic progenitors and vascular endothelial cells.	Human [9, 26, 27, 32-35]	IHC, FC	Detected in blood vessels in degenerated IVDs. Also found in healthy AF and in NP obtained by surgery. Not found in $CD24^+$ NP cells, nor in cells from herniated and degenerated IVD tissues after culture.	Expressed by around 2% of bovine NP cells.
Brachyury (T)	Transcription factor. Marker for notochordal cells and NP cells	Human[36, 37], Rat[38], Mouse[36], Bovine[37], Dog[39]	WB, FC, IHC, RT-PCR, qPCR	Expressed in NP from degenerated human IVD. mRNA expression by AF and NP cells from normal and degenerated IVDs and in bovine NP cells. 15% expression by NP cells from 1m old rats. High expression in the developing mouse NP (not found in AF or cartilage endplates). Decreased expression with aging and degeneration in chondrodystrophic dogs.	Expressed by more than 90% bovine NP cells.

NP: Nucleus Pulposus; **AF:** Annulus Fibrosus; **IHC:** Immunohistochemistry; **FC:** Flow Cytometry; WB: Western Blot; **RT-PCR:** Reverse Transcription-Polymerase Chain Reaction; **qPCR:** quantitative Polymerase Chain Reaction

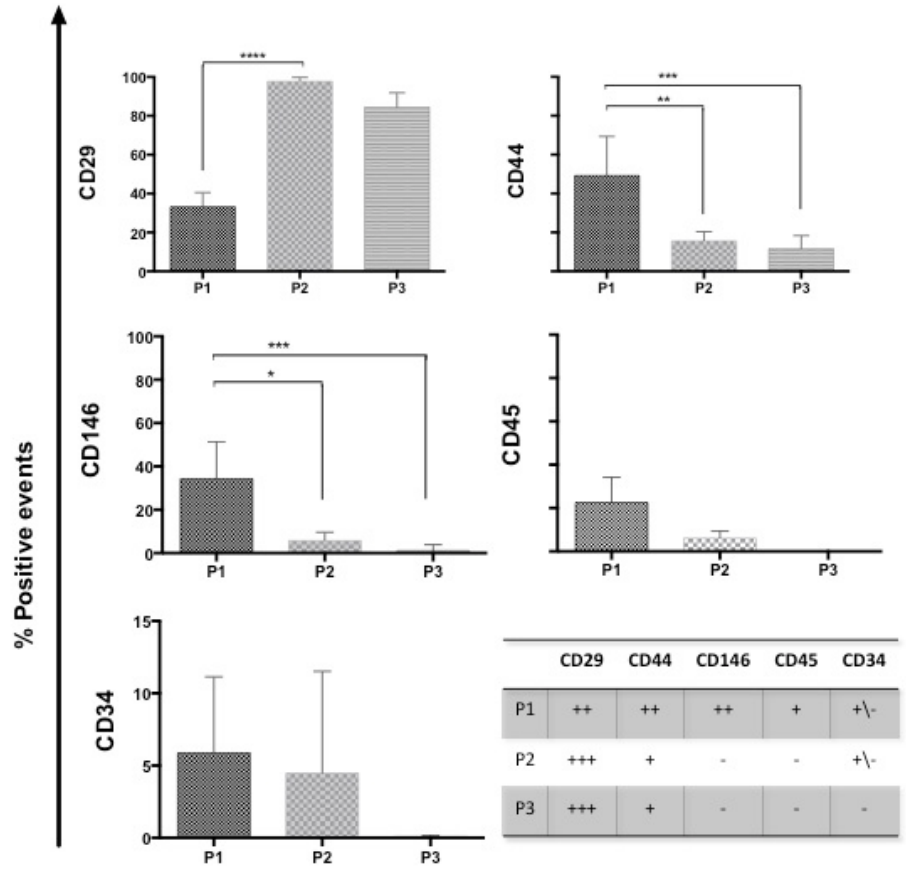

Figure 2.6: Expression of the cell surface markers CD29, CD44, CD45, CD146 and CD34 within P1, P2 and P3 sub-populations, after dead cells exclusion by propidium iodide (PI) staining. Results are presented as Mean±StDev (n=4-7) and were analysed for statistical differences using non-parametric Kruskal-Wallis and Dunn's multiple comparison tests (** $0.001 < p < 0.01$, *** $p < 0.001$ and **** $p < 0.0001$. A comparative summary of the percentages of cells expressing each surface marker for the different subpopulations is presented in the table.

Discussion

Envisaging standardization of NP cell isolation protocols, widely variable within the literature [5, 6, 16-18, 40], bNP digestion was compared for different collagenases. Until now no commercially available formula was designed to digest NP tissue specifically, most likely because it would serve a relatively small, although fast-

growing, community of researchers in this field. Nevertheless, standardization of NP cells isolation method would increase the reliability of results obtained in different labs.

Herein, the results obtained show that bNP 4 h digestion with Coll-XI (2.0 mg/mL) originated higher cell yields than with Coll-I or Coll-II. This suggests that for short-time periods, it is necessary a simultaneous increase of enzymatic activity against both type I and II collagens to better dissociate bNP tissue, although this tissue is known to be enriched in type-II-collagen [41]. Besides being faster, treatment with Coll-XI did not require any additional step of digestion with other enzymes commonly used for NP cell dissociation, such as hyaluronidase [42] or pronase, known to negatively affect the expression of surface markers on AC chondrocytes [43]. On the other hand, for longer digestion time periods (overnight), Coll-I revealed to be a better option than Coll-XI, originating higher cell yields and increased cell viability. Surprisingly, Col II digestion at this longer time period caused very high cell death, suggesting that with prolonged time of exposure digestion of type-II-collagen is more aggressive than type I collagen. In all conditions tested, cell viability was below values usually reported (>95%) [40], which may be due to the higher accuracy of the PI-exclusion method, when compared with the commonly used trypan blue dye exclusion assay.

Morphology of bNP cells after isolation was analysed by IFC, a technique that provides high-resolution images of thousands of cells in flow, and analyses a wider array of cellular parameters [22], when compared with confocal and electron microscopy, traditionally used to characterize IVD cells [44, 45]. bNP cells presented a N/C ratio around 0.5 and an area of 120-130 μm^2, in agreement with the mean surface area of bovine IVD cells previously reported on freshly isolated cells [6]. Moreover, a structure surrounding bNP cell membrane was detected, resembling a pericellular matrix-like structure, frequently described in chondrons in AC [46], and also reported in human and rat IVD cells [47, 48]. As expected, this structure stained positive for the ECM protein type VI collagen [41]. Interestingly, the presence of bright vesicle-like structures (0.5-1.5 μm diameter) was detected in 60% of bNP cells. Other authors have already reported the existence of cell vesicles in IVD cells: i) 1-20 μm vesicles were described in NP progenitors, i.e. NC, from non-chondrodystrophic mongrel dogs [49]; ii) 20 nm-100 μm lipid droplets were described in mature human

NP cells' cytoplasm [50]; and iii) <1 μm size vesicles were recently described in human NP cells [51]. Additionally, it has been suggested that cell communication between NP cells can be mediated by these membrane-bound microvesicles [51].

Three subpopulations of bNP cells (P1, P2, P3) were consistently identified by flow cytometry, based on different sizes and auto-fluorescence. NP cells auto-fluorescence was very recently described and related with cell necrosis and subsequent loss of mitochondrial membranes integrity, which could expose flavoproteins to oxidation, causing a blue-green shift in cells auto-fluorescence [52]. Nevertheless, the auto-fluorescence described herein was exclusive to live cells, i.e. PI-negative events. Furthermore, the senescence of each subpopulation of bNP cells was analysed by detecting β-galactosidase activity [53]. Results showed that bNP cells present a level of senescence around 40%. In the literature β-galactosidase-positive cells ranged from 8 to 95%, increasing with patients age and passage number [54]. Here, no senescent cells were observed in P1, while both P2 and P3 presented higher senescence (approximately 70-80%). Both populations include senescent cells while showing different auto-fluorescence levels, thus excluding the possibility that P2 and P3 populations are only one subset of cells in a different senescent state. Hence, the three subpopulations could instead be at different metabolic states, or at different stages of differentiation, as suggested elsewhere [7, 55]. Interestingly, three subpopulations of human knee meniscus cells (from a fibrocartilaginous tissue as the IVD) have also been described, with similar distribution of auto-fluorescence and size [55]. However, in this case P1 (low size) was discarded, while P2 subpopulation was distinguishable from P3 by the presence of a cell-associated matrix (CAM) (expressing type I and II collagens and aggrecan) [55]. Here, human NP cells obtained from patients with degenerated IVDs, but with contained NP, were also analysed (Supplementary Figure 2.4). However, there was no distinction of subpopulations, but it is unclear if this is due to differences in degenerated versus healthy discs or to differences between species.

Expression of different surface markers was analysed in the 3 populations. Table 2 summarizes the main findings reported here and previously published on expression of these markers in other animal models. Here, high percentages of cells expressing CD29 and Brachyury were detected in bNP cells. CD29 is an anchorage

protein involved in cell adhesion and migration, and its expression was particularly abundant in P2 and P3 subsets. On the other hand, Brachyury is one of the earliest indicators of mesoderm formation during embryonic development. It has been suggested as NP marker in IVD [4, 5] and mostly assessed at mRNA level [5]. Tang et al. reported much less cells expressing Brachyury (~15%) than what was observed in this study (nearly 90%), which may be due to inter-species differences [44]. According to this result we could discard AF contamination in the samples analysed.

In addition, about 20% of bNP cells express CD44, and particularly the P1 subpopulation. This transmembrane protein is a primary HA receptor that also binds to other extracellular proteins, including fibronectin and type I and VI collagens, and plays an important role during chondrogenesis [42]. Importantly, although CD44 cell surface epitope was reported to be especially sensitive to enzymatic digestion [56], herein we assured preservation of CD44 by avoiding hyaluronidase digestion [42].

Concerning CD45 and CD34, low expression of these hematopoietic-lineage markers was found, and more associated with P1 subset, although tissue contamination with blood was not expected. Nevertheless, despite being considered an immune privileged site, it is becoming increasingly evident that inflammatory-like cells [16, 17, 57] or phagocytic cells [16] might be present in IVD. Although CD34 is known as a marker for hematopoietic progenitors [58] and vascular endothelial cells [59], its expression has also been reported in other cell types such as skeletal muscle satellite cells [60], hair follicle keratinocytes [61], hepatic cells [62] and human fibrochondrocytes found within the superficial region of the knee meniscus body [55]. Hence, CD34 expression by itself does not elucidate the origin of the small population described herein, and future studies will be performed to address this, particularly by analysing co-expression with other markers (e.g. CD31 – mature endothelial cells; CD38, CD90 – hematopoietic progenitors). Another study has identified Tie2/Ang-1 expression, usually associated with angiogenesis, in the avascular hNP microenvironment [9]. In fact, although endothelial cells are not expected within the NP, some molecules normally expressed by those cells (e.g. Tie2/Ang-1, vascular endothelial growth factor-A (VEGF-A) and its receptor, membrane-bound vascular endothelial growth factor receptor-1 (mbVEGFR-1)) can also be expressed by NP cells, in response to hypoxic conditions [9, 63].

Interestingly, here, a subset of CD146+ cells was found in bNP, particularly in P1. CD146 has been suggested as a marker for endothelial cells [64], melanoma cells [65], and MSCs [66], but has not been reported in NP cells or cartilage cells before. Its expression has been linked to MSCs multipotency and differentiation potential [67]. Expression of markers as CD146, together with MSCs non-specific markers, such as CD44 or CD73 and absence of blood and endothelial markers has also been linked to the existence of vascular pericytes, cells with multipotency and clonal capability [68]. Although expression of CD146 has not been found in human IVDs [9], here a subset of bNP cells was found to express this marker.

Overall, the P1 subpopulation appears to be a distinguishable subset of bNP cells, enriched in CD146+ and CD44+ cells, while also containing few CD45+ and CD34+ cells. Cells within this subset present a more progenitor-like phenotype than those found in P2 or P3, which due to their CD29 expression, could represent populations with higher migratory capacity. Regarding P2 and P3, senescence does not justify the differences in auto-fluorescence, and CD45 and CD146 expression was found in P2 but not in P3. Thus, the 3 populations described herein can be identified by auto-fluorescence and size or by the combination of markers, but not a single marker.

The data collected with young and old animals suggests morphological changes with aging, with a decrease in P3 subset accompanied by an increase in P1. It is widely known that age affects NP cells morphology and molecular signature [50]. In particular, human/mouse NP progenitor cells identified by Tie2 expression were reported to be exhausted with age [9]. However, whether differences in P1/P2/P3 proportion for animals with different ages correlate with differences in NP cells phenotype is still being addressed.

In summary, this study presents new evidences on the heterogeneity of young NP cells. Future studies will be crucial to understand the contribution of each population for NP repair.

Acknowledgments

This work was financed by FEDER funds through the Programa Operacional

Factores de Competitividade – COMPETE and by Portuguese funds through Fundação para a Ciência e a Tecnologia (FCT) in the framework of PEst-C/SAU/LA0002/2013. MM is recipient of a PhD grant (SFRH/BD/80577/2011) from FCT. CRA and RMG were also funded by North Region Operational Program (ON.2), in the framework of the ‘‘Project on Biomedical Engineering for Regenerative Therapies and Cancer - NORTE-07-0124-FEDER-000005’’, through Quadro de Referência Estratégico Nacional (QREN).” Imaging was performed at the Bioimaging Center for Biomaterials and Regenerative Therapies (b.IMAGE). The authors would like to acknowledge Carnes Landeiro, SA. for kindly providing the bovine tails, and Michiharu Sakurai and Eiichi Momotani for the anti-bovine CD34 antibody.

Improvement of bovine nucleus pulposus cells isolation leads to identification of three phenotypically distinct cell subpopulations

SUPPLEMENTARY INFORMATION

Published in Tissue Engineering Part A 21(15-16):2216-27, 2015

Improvement of bovine nucleus pulposus cells isolation leads to identification of three phenotypically distinct cell subpopulations

Supplementary materials and methods

Collagen type VI staining

Freshly isolated NP cells were permeabilized by incubating for 5 min with PBS/0.2% v/v Triton and blocked by incubating with PBS/BSA 3% for another 5 min on ice. Cells were then stained by incubating with an anti-collagen VI antibody (Santa Cruz, sc-20649) at 10 µg/ml in PBS/BSA 3% for 1.5 h on ice. Cells were then washed three times with PBS and incubated with the secondary antibody Cy3 conjugated anti-rabbit IgG (Jackson Immunoresearch) at 1:500 in PBS/BSA 3% for 1h on ice. Cells were again washed twice with PBS and fixed by incubating for 15 min at room temperature with 4% paraformaldehyde. Finally, cells were washed twice with PBS prior to imaging. For imaging flow cytometry, cells were filtered through a 100µm mesh prior to analysis on an ImageStreamx equipped with a 488nm laser, as described in the main text. Cells were visualized in Channels 1 (brightfield) and 3 (Fluorescence staining). For confocal imaging, 4 µl of cell suspension were placed between a slide and a cover slip. Cells were then imaged with a 40x oil objective with a Leica TCS SP5 II laser scanning confocal microscope (Leica Microsystems).

Isolation of human NP cells

Human NP biopsies were isolated from lumbar IVDs in microdiscectomy surgeries of patients with IVD pathology (that may include disc herniation, degenerative disc disease, spinal stenosis or spondylolisthesis) at Centro Hospitalar S. João under approval of the Hospital Ethics Committee and after patients informed consent. Lumbar IVDs with grade III ou IV according with the Pfirrmann scale were isolated, but only contained fragments of NP were used in this study. Human NP fragments were digested and processed as described for bovine NP.

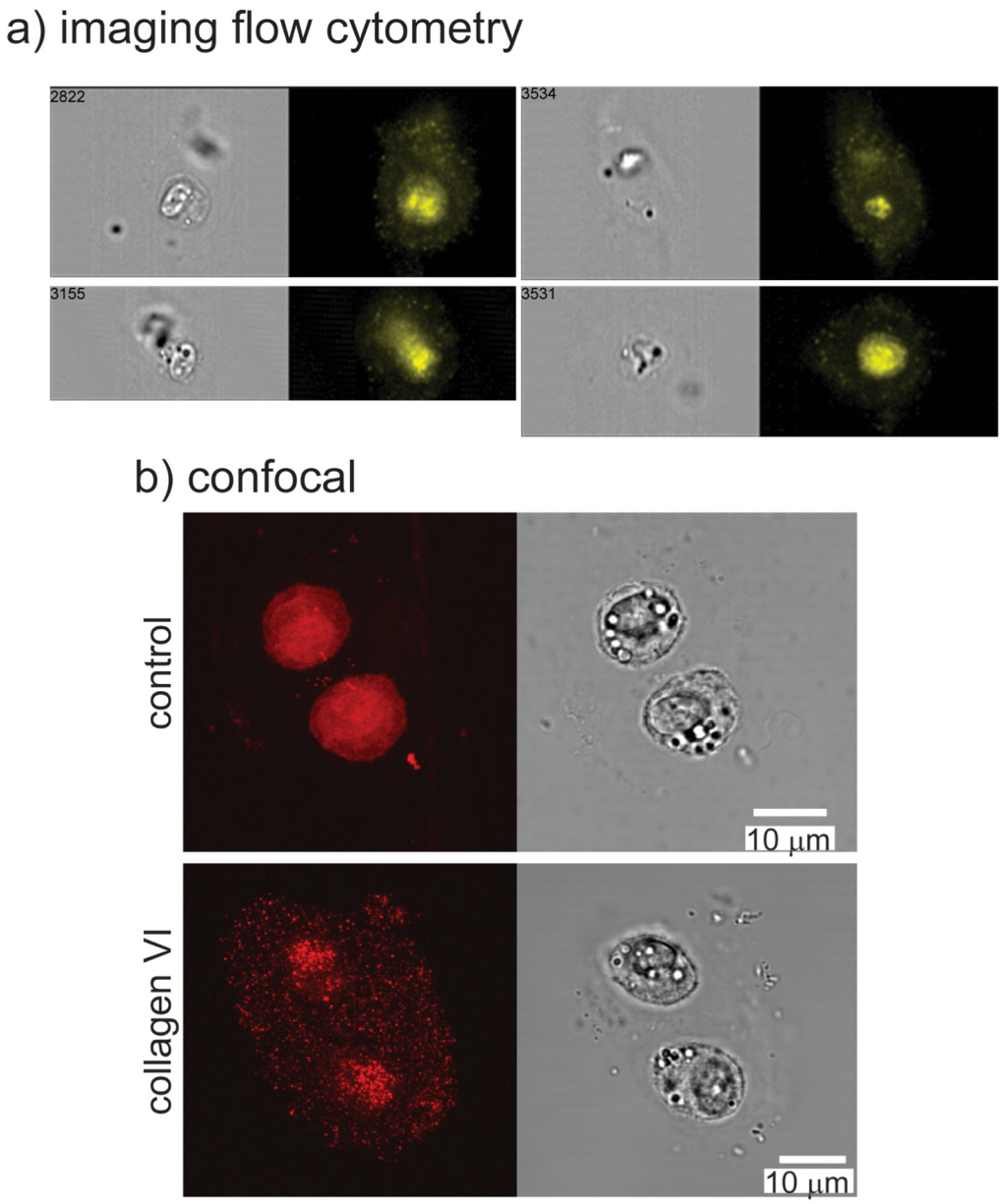

Supplementary Figure 2.1: Expression of type VI collagen on the pericellular matrix of bovine NP cells. Micrographs show brightfield (left) and fluorescence images (right) of freshly isolated bovine NP cells stained against collagen type VI and imaged by imaging flow cytometry **(a)** or confocal microscopy **(b)**. A punctuated staining can be observed located in and outside the cytoplasm of the cells. Fluorescence and brightfield in b show a maximum projection and single slice, respectively. Control refers to cells stained only with the secondary antibody.

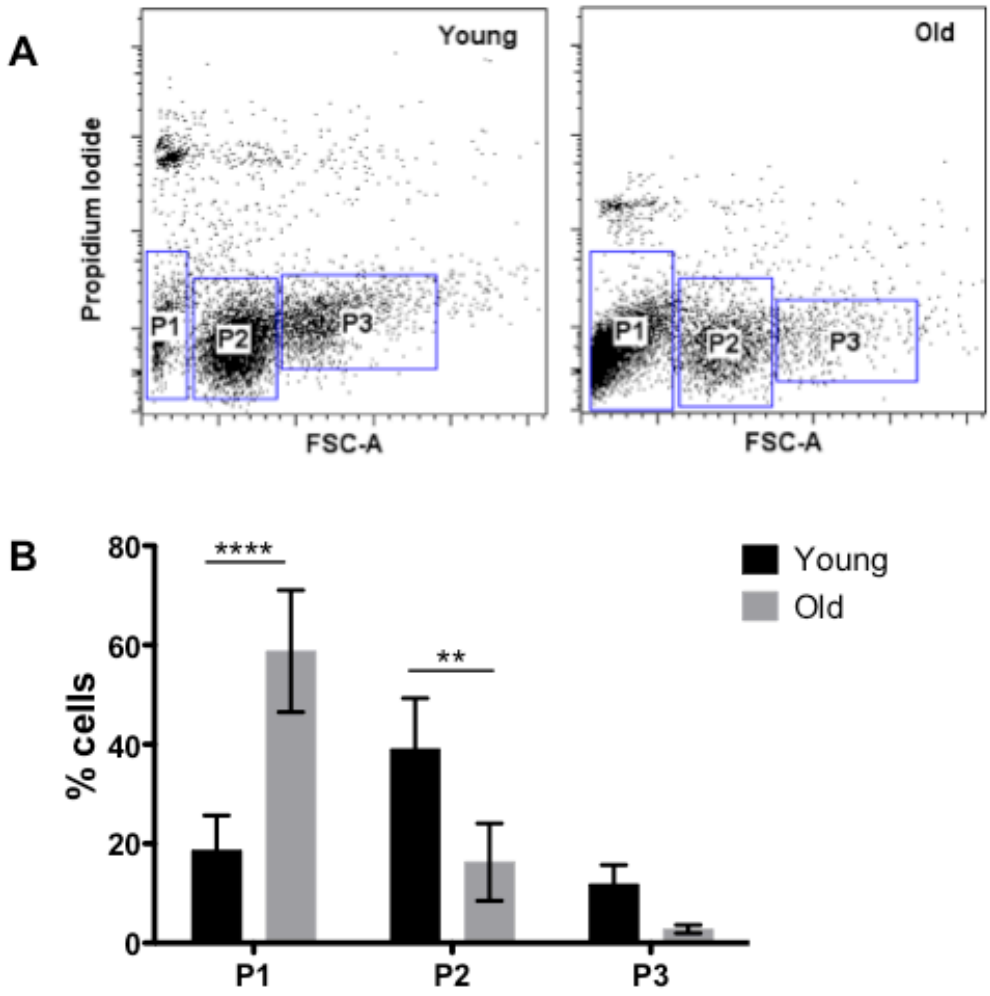

Supplementary Figure 2.2: Comparison of bNP cells size and auto-fluorescence analysed by flow cytometry of young and aged animals. A | Representative dot plots of Propidium Iodide expression versus size (FSC) of bNP cells from young and old animals. **B |** Distribution of P1, P2 and P3 subpopulations in young and old bovine animals. Results are presented as Mean±StDev (n=5 for old animals, n=4-7 for young animals) and were analysed for statistical differences using non-parametric Kruskal-Wallis and Dunn's multiple comparison tests (** $0.001 < p < 0.01$ and **** $p < 0.0001$).

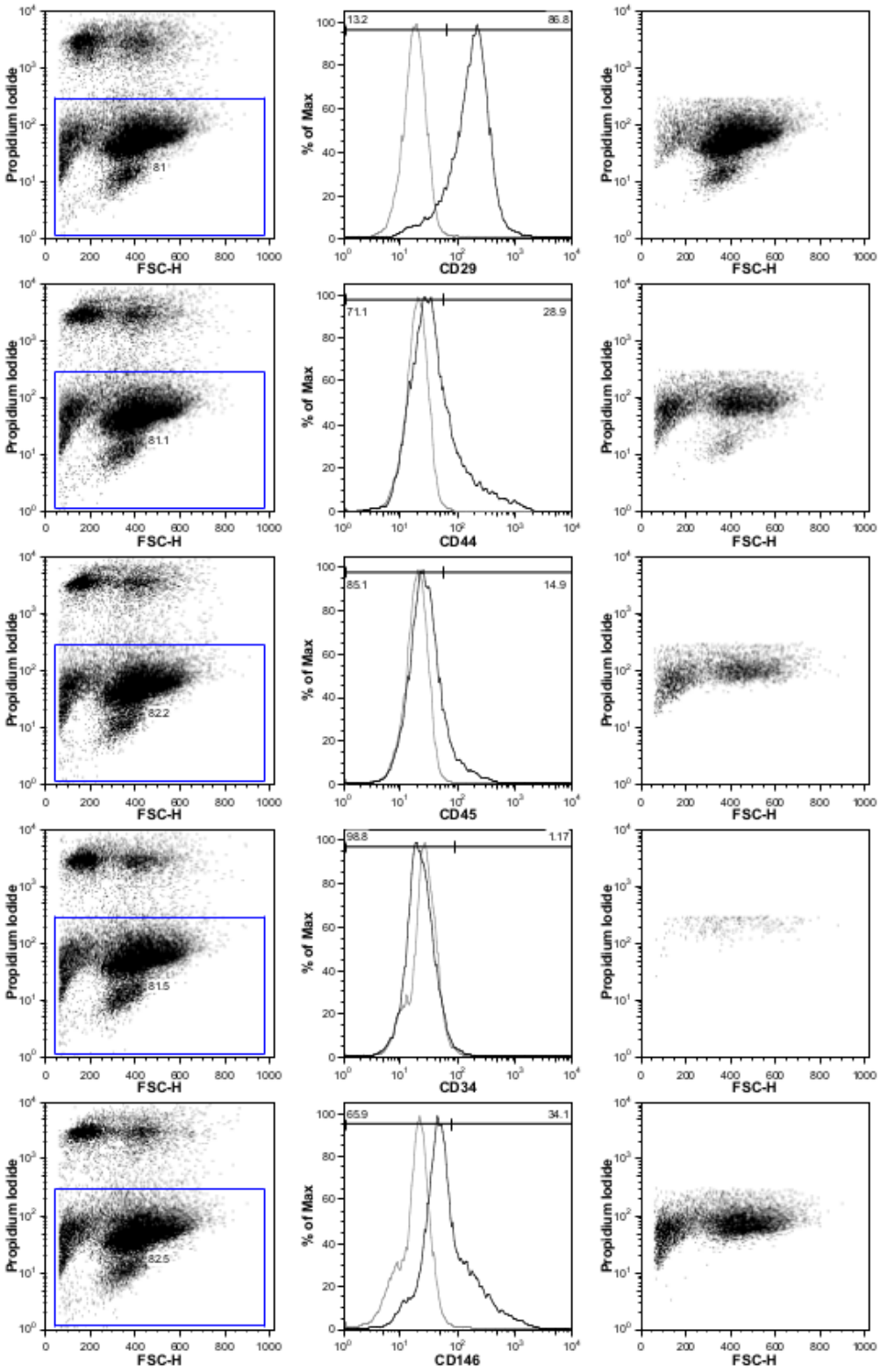

Supplementary Figure 2.3: Representative analysis of the distribution of each analysed marker (CD29, CD44, CD45, CD34 and CD146) within the 3 populations (P1, P2 and P3) of bNP cells.

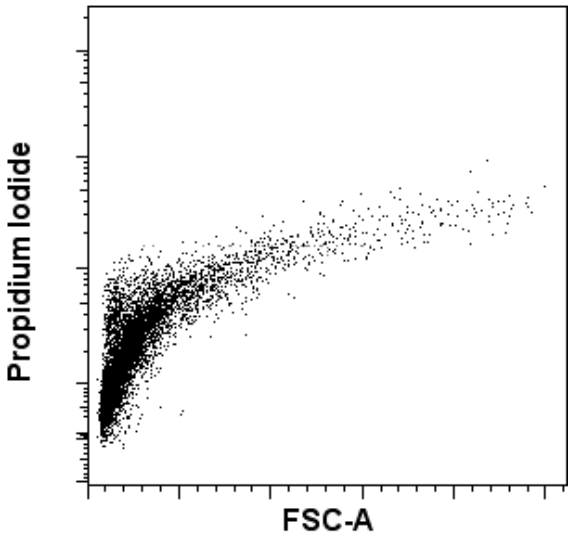

Supplementary Figure 2.4: Representative dot plot of Propidium Iodide expression versus size (FSC) of human NP cells obtained from biopsies of degenerated IVD with contained NP.

References

[1] Hughes, S.P., A.J. Freemont, D.W. Hukins, A.H. McGregor, and S. Roberts (2012) *The pathogenesis of degeneration of the intervertebral disc and emerging therapies in the management of back pain.* J Bone Joint Surg Br, 94(10): p. 1298-304.

[2] Molinos, M., C.R. Almeida, J. Caldeira, C. Cunha, R.M. Goncalves, et al. (2015) *Inflammation in intervertebral disc degeneration and regeneration.* J R Soc Interface, 12(104).

[3] Pereira, C.L., R.M. Goncalves, M. Peroglio, G. Pattappa, M. D'Este, et al. (2014) *The effect of hyaluronan-based delivery of stromal cell-derived factor-1 on the recruitment of MSCs in degenerating intervertebral discs.* Biomaterials.

[4] Henriksson, H.B. and H. Brisby (2012) *Development and Regeneration Potential of the Mammalian Intervertebral Disc.* Cells, tissues, organs.

[5] Minogue, B.M., S.M. Richardson, L.A.H. Zeef, A.J. Freemont, and J.A. Hoyland (2010) *Transcriptional profiling of bovine intervertebral disc cells: implications for identification of normal and degenerate human intervertebral disc cell phenotypes.* Arthritis Research & Therapy, 12(1): p. R22.

[6] Gilson, A., M. Dreger, and J.P. Urban (2010) *Differential expression level of cytokeratin 8 in cells of the bovine nucleus pulposus complicates the search for specific intervertebral disc cell markers.* Arthritis Research & Therapy, 12(1): p. R24.

[7] Risbud, M.V., Z.R. Schoepflin, F. Mwale, R.A. Kandel, S. Grad, et al. (2014) *Defining the phenotype of young healthy nucleus pulposus cells: Recommendations of the Spine Research Interest Group at the 2014 annual ORS meeting.* J Orthop Res.

[8] Brisby, H., N. Papadimitriou, C. Brantsing, P. Bergh, A. Lindahl, et al. (2013) *The presence of local mesenchymal progenitor cells in human degenerated intervertebral discs and possibilities to influence these in vitro: a descriptive study in humans.* Stem Cells Dev, 22(5): p. 804-14.

[9] Illien-Jünger S, P.G., Peroglio M, Benneker LM, Stoddart MJ, Sakai D, Mochida J, Grad S, Alini M. (2012) *Homing of Mesenchymal Stem Cells in Induced Degenerative Intervertebral Discs in a Whole Organ Culture System.* Spine, 37(22): p. 1865-73.

[10] van den Akker, G.G., D.A. Surtel, A. Cremers, R. Rodrigues-Pinto, S.M. Richardson, et al. (2014) *Novel immortal human cell lines reveal subpopulations in the nucleus pulposus.* Arthritis Res Ther, 16(3): p. R135.

[11] Risbud, M.V., A. Guttapalli, T.T. Tsai, J.Y. Lee, K.G. Danielson, et al. (2007) *Evidence for skeletal progenitor cells in the degenerate human intervertebral disc.* Spine (Phila Pa 1976), 32(23): p. 2537-44.

[12] Blanco, J.F., I.F. Graciani, F.M. Sanchez-Guijo, S. Muntion, P. Hernandez-Campo, et al. (2010) *Isolation and characterization of mesenchymal stromal cells from human degenerated nucleus pulposus: comparison with bone marrow mesenchymal stromal cells from the same subjects.* Spine (Phila Pa 1976), 35(26): p. 2259-65.

[13] Feng, G., X. Yang, H. Shang, I.W. Marks, F.H. Shen, et al. (2010) *Multipotential differentiation of human anulus fibrosus cells: an in vitro study.* J Bone Joint Surg Am, 92(3): p. 675-85.

[14] Huang, B., L.T. Liu, C.Q. Li, Y. Zhuang, G. Luo, et al. (2012) *Study to determine the presence of progenitor cells in the degenerated human cartilage endplates.* Eur Spine J, 21(4): p. 613-22.

[15] Miyazaki, T., S. Kobayashi, K. Takeno, A. Meir, J. Urban, et al. (2009) *A phenotypic comparison of proteoglycan production of intervertebral disc cells isolated from rats, rabbits, and bovine tails; which animal model is most suitable to study tissue engineering and biological repair of human disc disorders?* Tissue Eng Part A, 15(12): p. 3835-46.

[16] Jones, P., L. Gardner, J. Menage, G.T. Williams, and S. Roberts (2008) *Intervertebral disc cells as competent phagocytes in vitro: implications for cell death in disc degeneration.* Arthritis research & therapy, 10(4): p. R86.

[17] Nerlich, A.G., C. Weiler, J. Zipperer, M. Narozny, and N. Boos (2002) *Immunolocalization of phagocytic cells in normal and degenerated intervertebral discs.* Spine, 27(22): p. 2484-2490.

[18] Smith, L.J., J.A. Chiaro, N.L. Nerurkar, D.H. Cortes, S.D. Horava, et al. (2011) *Nucleus pulposus cells synthesize a functional extracellular matrix and respond to inflammatory cytokine challenge following long-term agarose culture.* European cells & materials, 22: p. 291-301.

[19] Wuertz, K., J.P. Urban, J. Klasen, A. Ignatius, H.J. Wilke, et al. (2007) *Influence of extracellular osmolarity and mechanical stimulation on gene expression of intervertebral disc cells.* Journal of orthopaedic research : official publication of the Orthopaedic Research Society, 25(11): p. 1513-22.

[20] Sakurai, M., T. Furusawa, M. Ikeda, H. Hikono, S. Shimizu, et al. (2006) *Anti-bovine CD34 monoclonal antibody reveals polymorphisms within coding region of the CD34 gene.* Exp Hematol, 34(7): p. 905-13.

[21] Debacq-Chainiaux, F., J.D. Erusalimsky, J. Campisi, and O. Toussaint (2009) *Protocols to detect senescence-associated beta-galactosidase (SA-betagal) activity, a biomarker of senescent cells in culture and in vivo.* Nat Protoc, 4(12): p. 1798-806.

[22] Zuba-Surma, E.K., M. Kucia, A. Abdel-Latif, B. Dawn, B. Hall, et al. (2008) *Morphological characterization of very small embryonic-like stem cells (VSELs) by ImageStream system analysis.* J Cell Mol Med, 12(1): p. 292-303.

[23] Bridgen, D.T., C.L. Gilchrist, W.J. Richardson, R.E. Isaacs, C.R. Brown, et al. (2013) *Integrin-mediated interactions with extracellular matrix proteins for nucleus pulposus cells of the human intervertebral disc.* J Orthop Res, 31(10): p. 1661-7.

[24] Nettles, D.L., W.J. Richardson, and L.A. Setton (2004) *Integrin expression in cells of the intervertebral disc.* J Anat, 204(6): p. 515-20.

[25] Henriksson, H.B., E. Svala, E. Skioldebrand, A. Lindahl, and H. Brisby (2012) *Support of concept that migrating progenitor cells from stem cell niches contribute to*

normal regeneration of the adult mammal intervertebral disc: a descriptive study in the New Zealand white rabbit. Spine (Phila Pa 1976), 37(9): p. 722-32.

[26] Risbud, M.V., A. Guttapalli, T.T. Tsai, J.Y. Lee, K.G. Danielson, et al. (2007) *Evidence for skeletal progenitor cells in the degenerate human intervertebral disc.* Spine, 32(23): p. 2537-44.

[27] Marfia, G., S.E. Navone, C. Di Vito, S. Tabano, L. Giammattei, et al. (2015) *Gene expression profile analysis of human mesenchymal stem cells from herniated and degenerated intervertebral discs reveals different expression of osteopontin.* Stem Cells Dev, 24(3): p. 320-8.

[28] Gan, J.C., P. Ducheyne, E. Vresilovic, and I.M. Shapiro (2000) *Bioactive glass serves as a substrate for maintenance of phenotype of nucleus pulposus cells of the intervertebral disc.* J Biomed Mater Res, 51(4): p. 596-604.

[29] Gan, J.C., P. Ducheyne, E.J. Vresilovic, W. Swaim, and I.M. Shapiro (2003) *Intervertebral disc tissue engineering I: characterization of the nucleus pulposus.* Clin Orthop Relat Res, (411): p. 305-14.

[30] Liu, C., Q. Guo, J. Li, S. Wang, Y. Wang, et al. (2014) *Identification of rabbit annulus fibrosus-derived stem cells.* PLoS One, 9(9): p. e108239.

[31] Stevens, J.W., G.L. Kurriger, A.S. Carter, and J.A. Maynard (2000) *CD44 expression in the developing and growing rat intervertebral disc.* Dev Dyn, 219(3): p. 381-90.

[32] Bu, G., S. Hou, D. Ren, Y. Wu, W. Shang, et al. (2012) *Increased expression of netrin-1 and its deleted in colorectal cancer receptor in human diseased lumbar intervertebral disc compared with autopsy control.* Spine (Phila Pa 1976), 37(25): p. 2074-81.

[33] Johnson, W.E., H. Evans, J. Menage, S.M. Eisenstein, A. El Haj, et al. (2001) *Immunohistochemical detection of Schwann cells in innervated and vascularized human intervertebral discs.* Spine (Phila Pa 1976), 26(23): p. 2550-7.

[34] Johnson, W.E., A.M. Patterson, S.M. Eisenstein, and S. Roberts (2007) *The presence of pleiotrophin in the human intervertebral disc is associated with increased vascularization: an immunohistologic study.* Spine (Phila Pa 1976), 32(12): p. 1295-302.

[35] Koike, Y., M. Uzuki, S. Kokubun, and T. Sawai (2003) *Angiogenesis and inflammatory cell infiltration in lumbar disc herniation.* Spine (Phila Pa 1976), 28(17): p. 1928-33.

[36] Risbud, M.V. and I.M. Shapiro (2011) *Notochordal cells in the adult intervertebral disc: new perspective on an old question.* Crit Rev Eukaryot Gene Expr, 21(1): p. 29-41.

[37] Kim, K.W., T.H. Lim, J.G. Kim, S.T. Jeong, K. Masuda, et al. (2003) *The origin of chondrocytes in the nucleus pulposus and histologic findings associated with the transition of a notochordal nucleus pulposus to a fibrocartilaginous nucleus pulposus in intact rabbit intervertebral discs.* Spine (Phila Pa 1976), 28(10): p. 982-90.

[38] Tang, X., L. Jing, and J. Chen (2012) *Changes in the molecular phenotype of nucleus pulposus cells with intervertebral disc aging.* PLoS One, 7(12): p. e52020.

[39] Smolders, L.A., B.P. Meij, F.M. Riemers, R. Licht, R. Wubbolts, et al. (2012) *Canonical Wnt signaling in the notochordal cell is upregulated in early intervertebral disk degeneration.* J Orthop Res, 30(6): p. 950-7.

[40] Horner, H.A., S. Roberts, R.C. Bielby, J. Menage, H. Evans, et al. (2002) *Cells from different regions of the intervertebral disc: effect of culture system on matrix expression and cell phenotype.* Spine, 27(10): p. 1018-28.

[41] Roberts, S., J. Menage, V. Duance, S. Wotton, and S. Ayad (1991) *1991 Volvo Award in basic sciences. Collagen types around the cells of the intervertebral disc and cartilage end plate: an immunolocalization study.* Spine, 16(9): p. 1030-8.

[42] Knudson, C.B. (2003) *Hyaluronan and CD44: strategic players for cell-matrix interactions during chondrogenesis and matrix assembly.* Birth Defects Res C Embryo Today, 69(2): p. 174-96.

[43] Diaz-Romero, J., J.P. Gaillard, S.P. Grogan, D. Nesic, T. Trub, et al. (2005) *Immunophenotypic analysis of human articular chondrocytes: changes in surface markers associated with cell expansion in monolayer culture.* J Cell Physiol, 202(3): p. 731-42.

[44] Hunter, C.J., J.R. Matyas, and N.A. Duncan (2004) *Cytomorphology of notochordal and chondrocytic cells from the nucleus pulposus: a species comparison.* J Anat, 205(5): p. 357-62.

[45] Johnson, W.E. and S. Roberts (2003) *Human intervertebral disc cell morphology and cytoskeletal composition: a preliminary study of regional variations in health and disease.* J Anat, 203(6): p. 605-12.

[46] Roberts, S., J. Menage, V. Duance, and S.F. Wotton (1991) *Type III collagen in the intervertebral disc.* The Histochemical journal, 23(11-12): p. 503-8.

[47] Gruber, H.E., J.A. Ingram, and E.N. Hanley, Jr. (2007) *Morphologic complexity of the pericellular matrix in the annulus of the human intervertebral disc.* Biotech Histochem, 82(4-5): p. 217-25.

[48] Cao, L., F. Guilak, and L.A. Setton (2007) *Three-dimensional morphology of the pericellular matrix of intervertebral disc cells in the rat.* J Anat, 211(4): p. 444-52.

[49] Hunter, C.J., S. Bianchi, P. Cheng, and K. Muldrew (2007) *Osmoregulatory function of large vacuoles found in notochordal cells of the intervertebral disc running title: an osmoregulatory vacuole.* Mol Cell Biomech, 4(4): p. 227-37.

[50] Trout, J.J., J.A. Buckwalter, and K.C. Moore (1982) *Ultrastructure of the human intervertebral disc: II. Cells of the nucleus pulposus.* Anat Rec, 204(4): p. 307-14.

[51] Strassburg, S., N.W. Hodson, P.I. Hill, S.M. Richardson, and J.A. Hoyland (2012) *Bi-directional exchange of membrane components occurs during co-culture of mesenchymal stem cells and nucleus pulposus cells.* PLoS One, 7(3): p. e33739.

[52] Dittmar, R., B.G. van Dijk, M.A. van Zandvoort, and K. Ito (2014) *In situ label-free cell viability assessment of nucleus pulposus tissue.* J Orthop Res, 32(4): p. 545-50.

[53] Dimri, G.P., X. Lee, G. Basile, M. Acosta, G. Scott, et al. (1995) *A biomarker that identifies senescent human cells in culture and in aging skin in vivo.* Proc Natl Acad Sci U S A, 92(20): p. 9363-7.

[54] Jeong, S.W., J.S. Lee, and K.W. Kim (2014) *In vitro lifespan and senescence mechanisms of human nucleus pulposus chondrocytes.* Spine J, 14(3): p. 499-504.

[55] Verdonk, P.C., R.G. Forsyth, J. Wang, K.F. Almqvist, R. Verdonk, et al. (2005) *Characterisation of human knee meniscus cell phenotype.* Osteoarthritis Cartilage, 13(7): p. 548-60.

[56] Biddle, A., L. Gammon, B. Fazil, and I.C. Mackenzie (2013) *CD44 staining of cancer stem-like cells is influenced by down-regulation of CD44 variant isoforms and up-regulation of the standard CD44 isoform in the population of cells that have undergone epithelial-to-mesenchymal transition.* PLoS One, 8(2): p. e57314.

[57] Phillips, K.L., N. Chiverton, A.L. Michael, A.A. Cole, L.M. Breakwell, et al. (2013) *The cytokine and chemokine expression profile of nucleus pulposus cells: implications for degeneration and regeneration of the intervertebral disc.* Arthritis Res Ther, 15(6): p. R213.

[58] Pessa-Morikawa, T., M. Niku, and A. Iivanainen (2012) *Fetal bovine bone marrow is a rich source of CD34+ hematopoietic progenitors with myelo-monocytic colony-forming activity.* Dev Comp Immunol, 36(3): p. 572-7.

[59] Lanza, F., L. Healy, and D.R. Sutherland (2001) *Structural and functional features of the CD34 antigen: an update.* J Biol Regul Homeost Agents, 15(1): p. 1-13.

[60] Beauchamp, J.R., L. Heslop, D.S. Yu, S. Tajbakhsh, R.G. Kelly, et al. (2000) *Expression of CD34 and Myf5 defines the majority of quiescent adult skeletal muscle satellite cells.* J Cell Biol, 151(6): p. 1221-34.

[61] Trempus, C.S., R.J. Morris, C.D. Bortner, G. Cotsarelis, R.S. Faircloth, et al. (2003) *Enrichment for living murine keratinocytes from the hair follicle bulge with the cell surface marker CD34.* J Invest Dermatol, 120(4): p. 501-11.

[62] Crosby, H.A., D.A. Kelly, and A.J. Strain (2001) *Human hepatic stem-like cells isolated using c-kit or CD34 can differentiate into biliary epithelium.* Gastroenterology, 120(2): p. 534-44.

[63] Fujita, N., J. Imai, T. Suzuki, M. Yamada, K. Ninomiya, et al. (2008) *Vascular endothelial growth factor-A is a survival factor for nucleus pulposus cells in the intervertebral disc.* Biochem Biophys Res Commun, 372(2): p. 367-72.

[64] Bardin, N., V. Frances, G. Lesaule, N. Horschowski, F. George, et al. (1996) *Identification of the S-Endo 1 endothelial-associated antigen.* Biochem Biophys Res Commun, 218(1): p. 210-6.

[65] Shih, I.M., D.E. Elder, M.Y. Hsu, and M. Herlyn (1994) *Regulation of Mel-CAM/MUC18 expression on melanocytes of different stages of tumor progression by normal keratinocytes.* Am J Pathol, 145(4): p. 837-45.

[66] Covas, D.T., R.A. Panepucci, A.M. Fontes, W.A. Silva, Jr., M.D. Orellana, et al. (2008) *Multipotent mesenchymal stromal cells obtained from diverse human tissues share functional properties and gene-expression profile with CD146+ perivascular cells and fibroblasts.* Exp Hematol, 36(5): p. 642-54.

[67] Russell, K.C., D.G. Phinney, M.R. Lacey, B.L. Barrilleaux, K.E. Meyertholen, et al. (2010) *In vitro high-capacity assay to quantify the clonal heterogeneity in trilineage potential of mesenchymal stem cells reveals a complex hierarchy of lineage commitment.* Stem Cells, 28(4): p. 788-98.

[68] Crisan, M., C.W. Chen, M. Corselli, G. Andriolo, L. Lazzari, et al. (2009) *Perivascular multipotent progenitor cells in human organs.* Ann N Y Acad Sci, 1176: p. 118-23.

Improvement of bovine nucleus pulposus cells isolation leads to identification of three phenotypically distinct cell subpopulations

CHAPTER III

Profiling nucleus pulposus cells aging using a bovine model

Manuscript In preparation

Profiling nucleus pulposus cells aging using a bovine model

Maria Molinos [1-3], Catarina R Almeida[1,2], Graciosa Q. Teixeira[1-4], Raquel M Gonçalves[1,2], Mário A Barbosa[1-3]

[1] i3S - Instituto de Investigação e Inovação em Saúde, Universidade do Porto, Rua Alfredo Allen, 208, 4200-135 Porto, Portugal

[2] INEB - Instituto de Engenharia Biomédica, Universidade do Porto, Portugal

[3] ICBAS - Instituto de Ciências Biomédicas Abel Salazar, Universidade do Porto, Rua de Jorge Viterbo Ferreira n.º 228, 4050-313 Portugal

[4]Institute of Orthopaedic Research and Biomechanics, Center for Musculoskeletal Research, University of Ulm, Ulm, Germany

Abstract

Aging is one of the major etiological factors driving intervertebral disc degeneration. Novel therapies aiming at counteracting age effects will contribute to prevent degenerative disc disease progression.

This work aimed to uncover phenotypic and genotypic alterations that are found in old nucleus pulposus cells as compared to young ones. For that purpose, and in line with previous work from our group, bovine coccygeal discs from young (12 months old) and old (10-16 years old) animals were dissected and primary cells enzymatically isolated from the nucleus pulposus. Using conventional and imaging flow cytometry cells were assessed for a panel of surface receptors (CD29, CD44, CD45, CD146, GD2, Tie2, CD34 and Stro-1), as well as for their subpopulations signature, diameter, prevalence of multinucleated events and bright vesicles content. Genetic expression of proinflammatory cytokines (IL-6 and IL-8), matrix degrading enzymes (MMP1 and 3) and ECM-related proteins (collagen type-II and aggrecan) was evaluated by quantitative real-time reverse transcription–polymerase chain reaction (RT-qPCR).

Cells from elder animals revealed lower percentages of $CD29^+$, $CD44^+$, $CD45^+$ and $Tie2^+$ events, but higher numbers of $GD2^+$ events, a recognised marker for bone marrow mesenchymal stromal (BM-MSC) cells and NP progenitor cells, alongside with a steady prevalence of the MSC marker CD146. Moreover, the subpopulations signature was altered, cells diameter was increased, and the percentage of cell containing bright vesicles was also increased. Finally, Coll II and IL-6 were down-regulated with age.

Overall, we showed the value of bovine nucleus pulposus as a model to study NP cells phenotype in homeostasis and aging. Moreover, novel potential anti-aging targets were identified. All in all, the knowledge gather in this study will hopefully contribute to a better understanding of the mechanisms behind disc degeneration.

Introduction

According to the Lancet Global Burden of disease study 2015, low back pain (LBP) remains the world's leading cause of years leaved with disability, in both developed and developing countries [1], representing a heavy socio-economic impact in modern society [2]. Although the aetiology of LPB is still unclear [3], several reports suggest the existence of a strong positive correlation between degenerative intervertebral disc (IVD) changes, occurring in degenerative disc disease (DDD), and LBP [4-6]. Current treatments for DDD neither address the underlying pathogenesis nor seek to restore IVD's function or to slow down disease progression. Notwithstanding, novel regenerative therapies, born from solid cellular and molecular knowledge of the IVD, are actively being sought [7-9].

Considered the epicentre of IVD degeneration [10], as well as home for progenitor cells [11, 12], the nucleus pulposus (NP) has attracted special attention from the scientific community. During the last decade, various microarray studies have been conducted in order to better define NP cells phenotypic signature, particularly in relation to neighbouring annulus fibrosus (AF) or cartilage endplate (CEP) cells, or to articular cartilage (AC) cells [11, 13-18]. However, the markers reported so far are not exclusive to any of those cell types. Indeed, wide-genome analysis alone is not fulfilling the need for specific cell markers to aid cell-based therapies on restoring an NP-like phenotype [18, 19]. Finally, a consensus paper by Risbud *et al.* has proposed a panel of markers to define the phenotype of young NP cells [20], which were chosen based on their specific expression in young healthy NP cells, relevance to NP physiology, and validation across different species. This work has prompted new immunohistochemical studies, seeking further validation of those markers, and others even less explored, in larger human cohorts [11, 18, 21]. Interestingly, although widely used for cell characterization, flow cytometry (FC) has seldom been used to profile IVD cells. Unlike what is routinely done with blood cells [22], no gating strategy, specific surface markers or Forward-Scatter/Side-Scatter (FCS/SSC) profile has been proposed for these cells yet.

The natural aging process represents one of the major etiological factors responsible for disc degeneration, which seems to affect this organ in a premature manner, when compared to other tissues of the human body [23, 24] (Figure 3.1). Many studies using different animal models have investigated distinct features of disc aging [25-45]. However, the molecular profile alterations of NP cells with age has been poorly monitored and unmatching results are consistently found between microarray data (gene level) and that collected from immunohistochemistry (IHC) or FC (protein) [11, 13, 16, 21, 46-48]. Hence, future research on the phenotypic characterization of IVD cells is warranted, particularly regarding the signature of each subpopulation in terms of its ontogeny, physiology and function, and also concerning its evolution with age and degeneration.

Thus, the aim of this study was to discriminate the cellular and molecular signature changes that occur on old NP cells as opposed to young NP cells from bovine coccygeal IVDs (the latter commonly used to study the molecular phenotype of IVD cells [15, 49-57], and previously characterized by us [58]), namely in terms of expression of mesenchymal-related (CD29, CD44, CD146 and Stro-1), hematopoietic (CD45 and CD34) and NP-progenitor (GD2 and Tie2) markers, morphology, and gene expression profile.

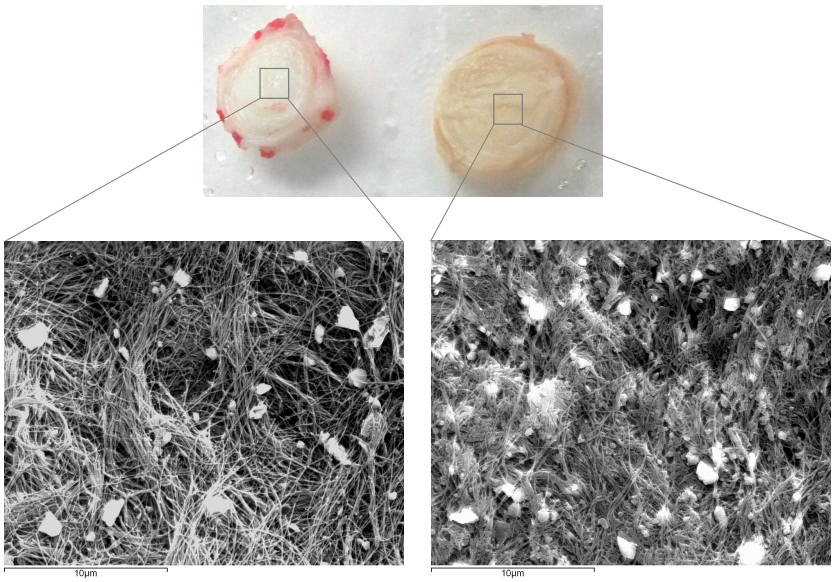

Figure 3.1: Aging of the bovine intervertebral disc. Top image shows one young (12 months old) (left) and one old (16 years old) (right) bovine IVD. Differences are evident both at macroscopic and ultrastructural (bottom scanning electron microscopy (SEM) images) levels. White spots seen in SEM images correspond to calcium deposits, which can be seen already in young animals. In the elder NP ECM fibers are thicker, the number of pores diminishes, and there is an overall disorganized crosslinking/super positioning of fibers. SEM images with permission from Caldeira J.

Materials and Methods

Bovine nucleus pulposus (bNP) cells isolation

Coccygeal IVDs from young (12-month-old) and old (10 to 16 years old) bovine steers were dissected until 3h hours after death. NP was harvested from 7-8 IVDs and cells were isolated according to previously established protocol [58]. Briefly, NP tissue was separated from AF and vertebral endplates with a scalpel blade, and finely chopped. Tissue digestion was performed in Dulbeccos's modified Eagle's medium (DMEM, 21885, Gibco), supplemented with 5% v/v Penicillin Streptomycin (PAA), 10% v/v Amphotericin B. (PAA), 2.5% (v/v) of HEPES Buffer 1 mM (Lonza), 1.5% (v/v) of NaCl 5M and KCl 0.4M solution (to adjust osmolarity to 400 mOsm), 1.3 U/mL DNAse, and collagenase-type-XI (Coll-XI) (C7657, Sigma Aldrich), at 2.0 mg/mL. Tissue/medium ratio was

set at 10% w/v to prevent the pH from dropping below 6.8 during incubation. Tissue was digested for 4-5 h (until complete digestion) in a humidified atmosphere at 37°C/5% CO_2, and under gentle stirring. Finally, ECM contaminants were removed with a 70 µm cell strainer, and cells were resuspended in 10 mL DMEM supplemented with 5% FBS, 1% v/v Penicillin Streptomycin, 0.5 % v/v Amphotericin B, and osmolarity adjusted to 400 mOsm, and left to recover overnight in 15 mL falcon tubes with loosely tightened caps prior to any further analysis.

Characterization of young and old bNP cells phenotype

Cell surface staining. The expression of surface markers (Table 3.1) was analysed by FC immediately upon cells isolation, without fixation, to guaranty dead cells exclusion with PI staining. Firstly, cells were washed with PBS-2% Fetal bovine Serum (FBS) and then incubated with primary antibodies (Table 1), in the same solution, for 1h at RT. In the case of non-conjugated anti-CD34 and anti-GD2 antibodies, cells were additionally incubated in the same conditions with a secondary donkey anti-mouse IgG-AlexaFluor647® antibody, and anti-Stro-1 with a secondary goat anti-mouse IgM-FITC antibody. After labelling, cells were washed with 2mL PBS-2% FBS and run in a FACS Canto (BD). Results were analysed with FlowJo software, version 8.7, as in [58]. Additionally, besides analysing the subpopulations' signature (by considering each subpopulation as a whole, and applying the gates for positive events on each subpopulation individually), the relative distribution of positive events along the distinct subpopulations was also quantified (by applying the subpopulations gates on all positive events for each marker). The two approaches are depicted in Supplementary Figure 3.1.

Table 3.1: Antibodies used in flow cytometry analysis.

Antibodies	Fluorochrome	µg/mL	Clone	Catalog #, Manufacturer
Primary antibodies				
Mouse anti-bovine IgG1,κ CD29	AlexaFluor®488	5µL/10^5cells	TS2/16	303015, Biolegend
Mouse anti-bovine IgG1 CD44	FITC	10	IL-A118	MCA2433F, AbD Serotec
Mouse anti-bovine IgG1 CD45	FITC	10	CC1	MCA832F, AbD Serotec
Mouse anti-human IgG1 CD146	AlexaFluor®647	5	OJ79c	MCA2141A647T, AbD Serotec
Mouse anti-human IgG1 Tie-2	PE	5µL/10^5cells	83715	FAB3131P, R&D Systems
Mouse anti-bovine IgG1 CD34	-	24		Isotype N21, Kindly provided by Sakurai M [59]
Mouse anti-human IgG2a GD2	-	20	14.G2a	554272, BD Pharmigen
Mouse anti-human IgM,λ Stro-1	-	20	STRO-1	14-6688-82, eBioscience
Secondary antibody				
Goat anti-mouse IgM	FITC	5		F0118, R&D Systems
Donkey anti-mouse IgG	AlexaFluor®647	4		A31571, Life Technologies
Isotype controls				
Mouse IgG1, κ	AlexaFluor®488	20	MOPC-21	400132, Biolegend
Mouse IgG1	FITC/R-PE	5µL/10^5cells		M1FP, Life Technologies
Mouse IgG1	AlexaFluor®647	5		sc-24636, Santa Cruz Biotech
Mouse IgG1 k purified	-	20	P3.6.2.8.1	14-4714, eBioscience
Mouse IgG2a,κ purified	-	20	G155-178	556651, BD Pharmigen
Mouse IgM purified	-	20	PFR-03	21275051, Immunotools

Morphology analysis by Imaging Flow Cytometry (IFC). To examine the morphological features of freshly isolated young and old bNP cells, cells were fixed in 4% w/v paraformaldehyde (PFA) at room temperature (RT) for 15 min. and washed with PBS. Shortly prior to acquisition, cells were labelled with DRAQ5 (1:1500 Dil. per $2.0x10^5$ cells, 65-0880, eBioscience), and run on ImageStream^X (IS, Millipore), and analysed with IDEAS® software for cell diameter, prevalence of multinucleated events, mean nuclei number per cell, percentage of cells containing bright vesicles, and mean number of bright vesicles per cell. Gating of cell was performed according to the following sequential steps:

1. DRAQ5+ events selection: plot Area_M01 against Intensity_MC_Ch5
2. Gating of focused events within DRAQ5$^+$ events: plot Gradient RMS_M01_Ch1 histogram

3. Gating of focuced nuclei within DRAQ5$^+$ focused events: plot Gradient RMS_M01_Ch5 histogram

Additionally, specific masks were developed and applied to brightfield and fluorescence images, and respective features were created to characterize cells:
Masks:

- Nuclei: Watershed (Threshold (M05, Nucleus, 50)) - mask applied to clearly identify the nucleus;
- Bright vesicles: Intensity (M01, Brightfield, 1000-4095) - mask designed to mark bright vesicles within cells.

Features:

- Nuclei number: Spot Count (Mask Nuclei) – to quantify the prevalence of multinucleated events and the mean percentage of nuclei per cell;
- Vesicles number: Spot Count (Mask Bright vesicles) - to quantify the prevalence of cell with bright vesicles and the mean percentage of bright vesicles per cell.

Analysis and statistics templates were generated and applied to all samples using Batch Data Files tool. Overlapping of diameter histograms was achieved through compensated image files (.cif) merging.

Gene expression analysis of cells from young and old bNPs

RNA isolation and cDNA synthesis. Gene expression levels were determined by quantitative real-time reverse transcription–polymerase chain reaction (qRT-PCR) as described by Teixeira *et al.* [60] with slight modifications. Briefly, for RNA isolation, NP samples were digested enzymatically, as described above, and cell pellets were recovered by centrifugation at 400 g for 10 min. Total RNA was then extracted from NP cells using ReliaPrep RNA Cell Miniprep System (Promega), according to manufacturer's instructions. Total RNA was quantified using a NanoDrop 1000 spectrophotometer (Thermo Fisher Scientific). Finally, isolated RNA preparations were pre-treated with Turbo DNA-free kit (AM1907, Ambion, Invitrogen) to remove contaminating DNA, and posteriorly 1 µg of RNA from each sample was reverse transcribed into cDNA using

SuperScript III Reverse Transcriptase (18080-093, Invitrogen) completed with oligodeoxythymidine primers (5 μM), random hexamer primers (50 μM), and RNase inhibitor (10 U) in a total volume of 20 μL. The obtained cDNA was diluted at a ratio of 1:4 in RNase-free water (AM9938, Ambion, Invitrogen) and used for qRT-PCR.

Gene expression analysis by quantitative real-time reverse transcription–polymerase chain reaction. Specific primer sets for bovine glyceraldehyde 3-phosphate dehydrogenase (GAPDH), collagen type-II, aggrecan, IL-6 , IL-8 , MMP1, and MMP3 (Table 3.2) were designed using published gene sequences (PubMed, NCBI Entrez Nucleotide Database) and Primer3 software [61], and purchased from Thermo Fisher Scientific. Real-time quantitative polymerase chain reactions (PCR) were conducted on a iQ5 Real-Time PCR Detection System (Biorad), and performed according to the SYBR Green method, in triplicate, in PCR 96-well TW-MT-Plates (Biozym Scientific), under standard conditions. Reaction mixes contained 12.5 mL of Platinum SYBR Green qPCR SuperMix-UDG (Invitrogen) master mix, 0.25 mL of ROX Reference Dye (Invitrogen), 1 mL (0.4 mM) of forward primer, 1 mL (0.4 mM) of reverse primer, 8.25 m L of RNase-free water, and 2 mL of cDNA. For the analysis of the mRNA expression, cloned amplification products were provided and used as standards for qRT-PCR. Statistical analysis was performed on ΔC_t values according to a modified method [62]. The average C_t value of each triplicate measurement of each sample was normalized to the house-keeping gene glyceraldehyde 3-phosphate dehydrogenase (GAPDH) in each sample [$\Delta C_T = C_T$ (gene of interest) - C_T (GAPDH)].

Table 3.2: Bovine primer sets used for qRT-PCR measurements.

Gene	Sequence (forward and reverse primer)	Product length (bp)	NCBI reference sequence
GAPDH	5' -ACC CAG AAG ACT GTG GAT GG-3' 5' -CAA CAG ACA CGT TGG GAG TG-3'	178	XM_001252511
Collagen type-II	5' -CCT GTA GGA CCT TTG GGT CA-3' 5' -ATA GCG CCG TTG TGT AGG AC-3'	145	X02420
Aggrecan	5' -ACA GCG CCT ACC AAG ACA AG-3' 5' -ACG ATG CCT TTT ACC ACG AC-3'	155	NM_173981
IL-6	5' -ACC CCA GGC AGA CTA CTT CT-3' 5' -GCA TCC GTC CTT TTC CTC CA-3'	183	EU276071
IL-8	5' -ATT CCA CAC CTT TCC ACC CC-3' 5' -ACA ACC TTC TGC ACC CAC TT-3'	148	AF232704
MMP-1	5' -ATG CTG TTT TCC AGA AAG GTG G-3' 5' -TCA GGA AAC ACC TTC CAC AGA C-3'	193	NM_174112.1
MMP-3	5' -AAT CAG TTC TGG GCC ATC AG-3' 5' -CTC TGA TTC AAC CCC TGG AA-3'	237	AF069642

GAPDH: glyceraldehyde 3-phosphate dehydrogenase; **IL:** interleukin; **MMP:** metalloprotease; **qRT-PCR:** quantitative real-time reverse transcription–polymerase chain reaction

Statistical Analysis

Statistical analysis was performed using GraphPad Prism version 7.0a for Mac OS X. D'Agostino and Pearson omnibus normality test was used to assess Gaussian distribution of data. Results that follow a normal distribution (whole population's CD29 and CD44 expression) were analysed for statistical differences using parametric one tailed Welch's t test. Results that did not follow a normal distribution were analysed using non-parametric Mann-Whitney one-tailed t-Test or Kruskal-Wallis and Dunn's multiple comparison tests. The cell subpopulations sizes (P1, P2, P3 or P2+P3, and P4), as well as all markers expression within each subpopulation, the average number of nuclei per event and the mean percentage of bright vesicles per event were compared using ordinary two-way ANOVA and Sidak's multi comparisons test. In all cases, a confidence level of at least 95% (*, $p < 0.05$) was considered.

Results

Surface markers expression

To assess the effect of aging on bNP cells surface markers signature, a panel of 8 markers was selected, 5 of which had already been studied in our previous work on young animals [58]. Young bNP cells showed higher percentages of $CD29^+$ (78±15% vs 26±18%, ****p<0.0001, n=16 and 17, respectively), $CD44^+$ (41±18% vs 22±17%, **p<0.01, n=16), $CD45^+$ (16±13% vs 2±3%, **** p<0.0001, n=16) and $Tie2^+$ (86±6% vs 0%, **p<0.01, n=7 and 5, respectively) than old bNP cells. In contrast, GD2 showed increased percentages in elder animals (3±3% vs 9±7%, *p<0.05, n=12 and 10, respectively). Additionally, the percentage of $CD146^+$ cells was maintained with aging (12±11% vs 14±9%), while that of CD34 (0% vs 1±2%) and Stro-1 (2±2% vs 9±13%) was always low, with exception of some older specimens (Figure 3.2 B).

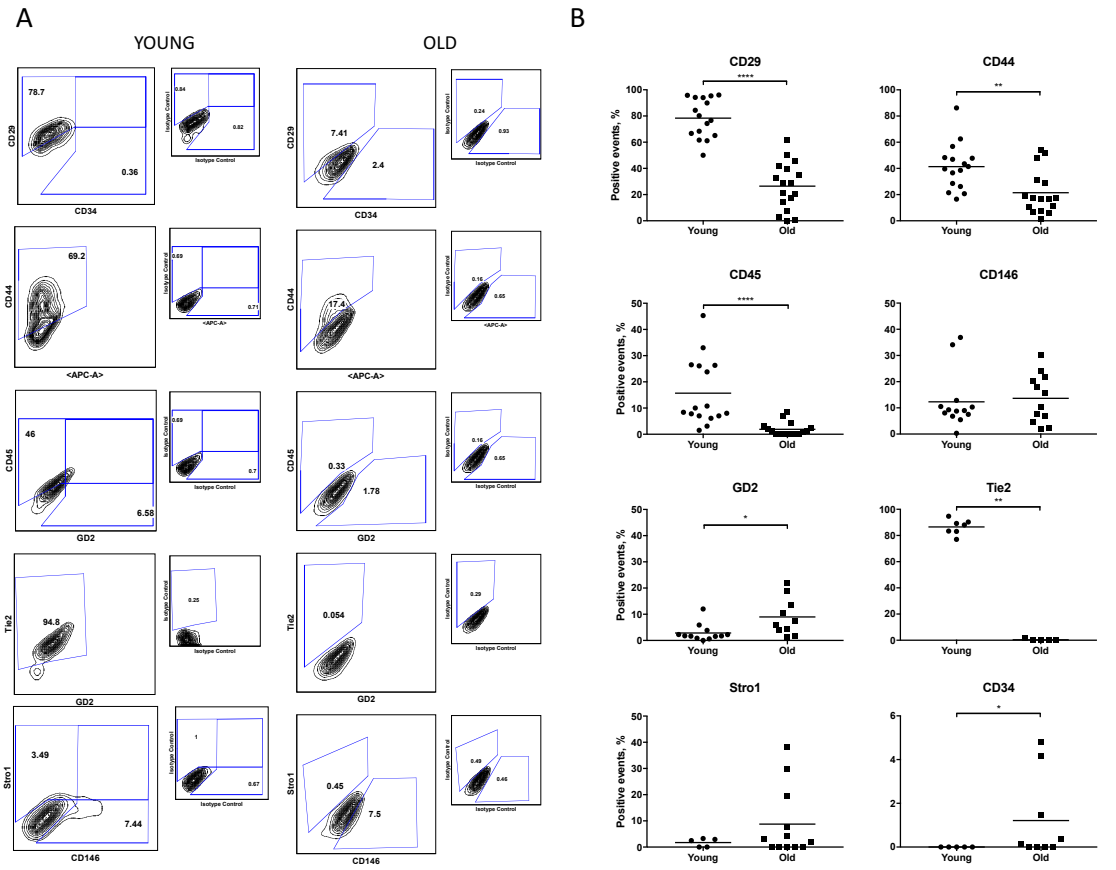

Figure 3.2: Immunophenotypic profile of freshly isolated bovine nucleus pulposus (bNP) cells from young and old animals. A | Flow cytometry contour plots of CD29, CD44, CD45, CD146, GD2, Tie2, CD34 and Stro-1 expression of live bNP cells (propidium iodide negative). Gates were established according to respective isotype controls (top right corners). **B |** Graphs show the mean percentage of live cells expressing each of the markers described, after subtracting the respective isotype control. Statistical differences between young and old cells were assessed using Welch's parametric t-test for CD29 and CD44 and Mann-Whitney non-parametric test for the other markers. P value calculations were based on a one-tailed distribution of data (*p<0.05, **p<0.01 and ****p<0.0001). CD29: n_Y=16, n_O=17; CD44: n_Y=16, n_O=16; CD45: $n_{Y,O}$=16; CD146: n_y=13, n_O=16; GD2: n_Y=12, n_O=10; Tie2: n_Y=7, n_O=5; CD34: n_Y=5, n_O=9; Stro-1: n_Y=5, n_O=12.

After discarding PI positive events (dead cells), different subpopulations of live cells could be consistently identified in both young and old bNPs, in this case four populations (P1, P2, P3, P4), with different size and auto-fluorescence (Figure 3.3 A), similarly to what has been previously published [58]. In young animals, P1 had the lowest percentage of events (7±4% events), which were

small sized and highly auto-fluorescent; P2 was the larger subpopulation (48±8% events), containing medium-sized events with high auto-fluorescence; P3 (9±6% events) also contained medium-sized events, but with low auto-fluorescence, and finally P4 (35±11% events) contained large events with high auto-fluorescence. In old animals, P1 was significantly increased (34±16%, ****p<0.0001), while P3 and P4 were significantly decreased (P3: 6±9%, *p<0.05; P4: 11±4, ****p<0.0001) (Figure 3.3 B).

To verify whether any particular subpopulation could be responsible for the overall age-related profile change in bNP cells (Figure 3.2), the relative distribution of the positive events for each marker along the four subpopulations was quantified (Figure 3.4). In young animals, the majority of positive events for the different markers, with exception of GD2, were found within P2 and P4 subpopulations. However, with increasing age this pattern was altered. Indeed, although the percentage of $CD29^+$ and $CD44^+$ events within P2 increased (41±15% vs 63±14%, n=11 and n=9; 42±8% vs 67±10%, n=12, respectively, ***p<0.001), there was a marked decrease within P4 (50±20% vs 27±12%, n=11 and n=9; 42±11% vs 19±10%, n=12, respectively, ****p<0.0001), most likely responsible for the overall decrease in the prevalence of both markers. Interestingly, while P4 revealed a significant decrease in $CD45^+$ events with age (60±19% vs 30±21%, n=9 and 6, respectively, **p<0.01), again justifying the overall change, P1, containing small-sized events, was enriched in this marker (11±16% vs 41±22%, n=9 and 6, respectively, **p<0.01). Regarding CD146, besides P2 and P3, P1 also contained high percentages of $CD146^+$ events (young: 24±11%, n=9; old: 36±11%, n=8). Notably, no particular changes were found on GD2+ events distribution with aging, although an overall increase in their prevalence was detected in previous analysis. On the other hand, Stro-1 prevalence was increased in P1, P2 and P4 subpopulations with age (5±0% vs 39±8%, ****p<0.0001; 34±1% vs 50±9%, *p<0.05 and 60±0% vs 11±5%, ****p<0.0001, n=2 and 5, respectively) even though no significant alteration was previously detected within the whole cell population. Finally, $CD34^+$ events were

only found in older animals, and were curiously abundant in P1 region (55±5%, n=3).

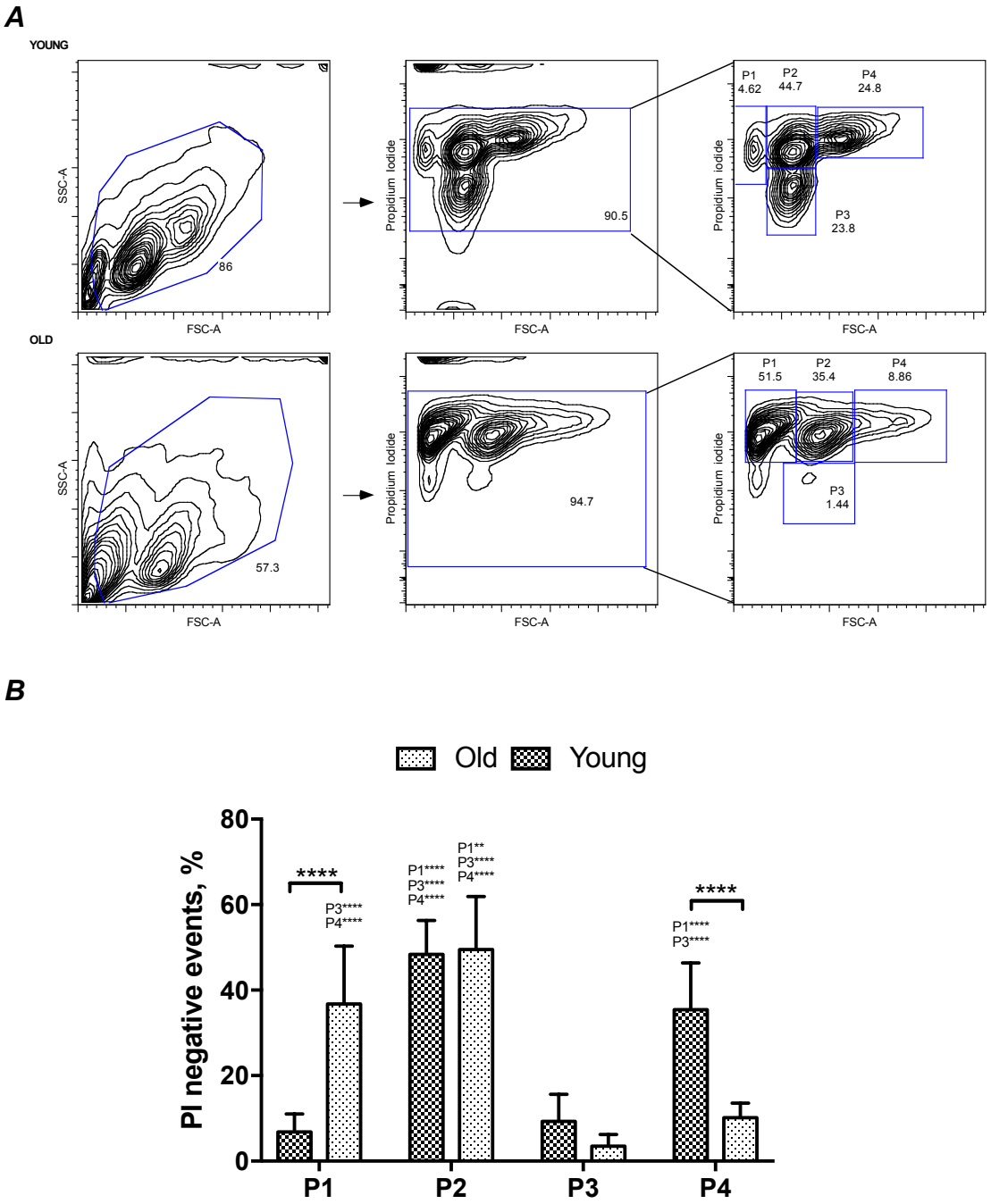

Figure 3.3: Effects of aging on primary bNP cell subpopulations. A | Representative flow cytometry contour plots showing the gating steps applied on cells from young (top) and old (bottom) bNPs to quantify the subpopulations size, based on their distinct size and auto-fluorescence (n=15 and 11, respectively). **B |** Graph shows the mean (± standard deviation) percentage of PI negative events within each subpopulation.

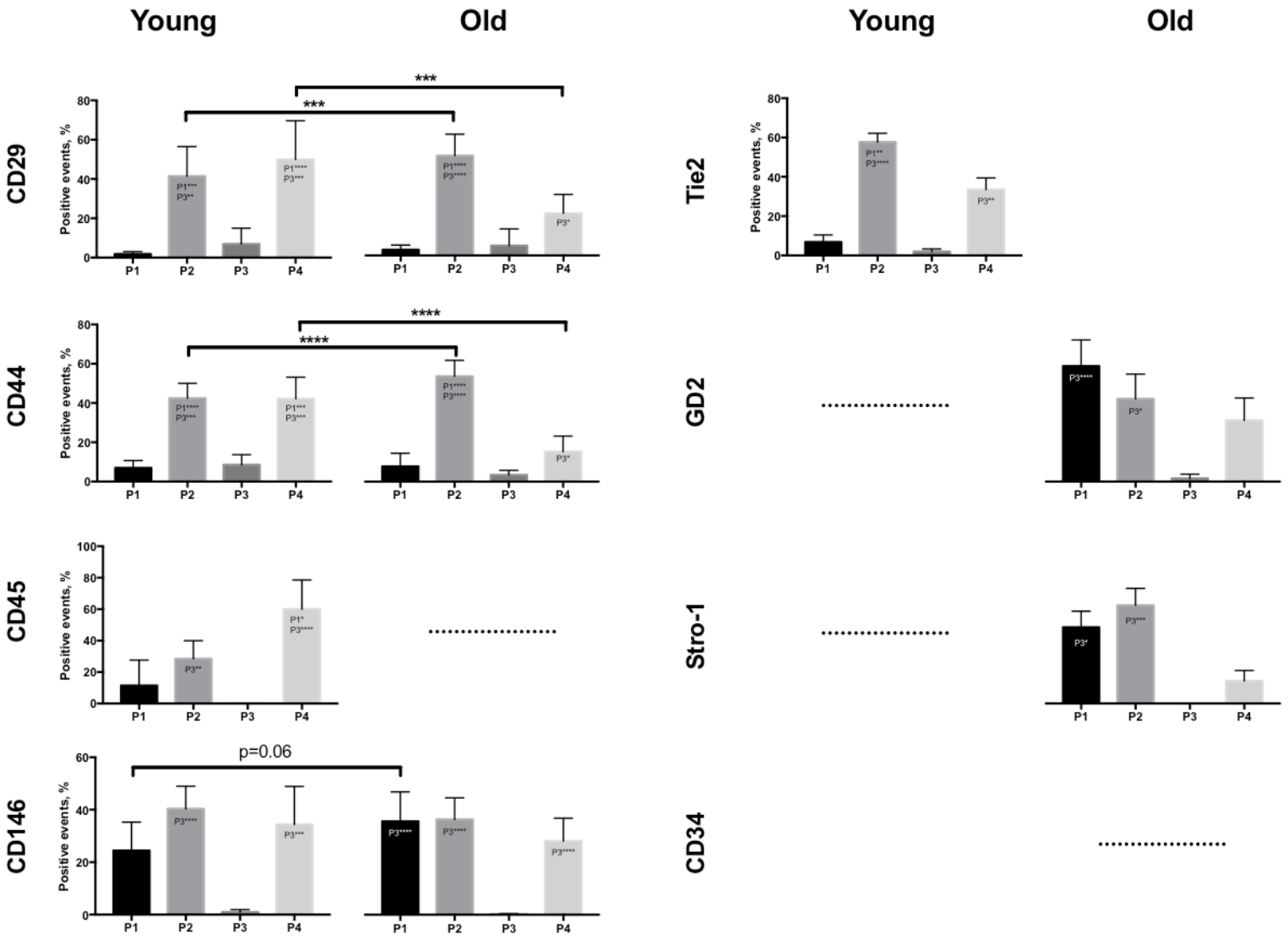
Young
Old
Young
Old
CD29
CD44
CD45
CD146
Tie2
GD2
Stro-1
CD34
Positive events, %
P1
P2
P3
P4
***
****
p=0.06

Figure 3.4: Relative distribution of positive events along the four subpopulations found within young and old bNP. Results from young and old animals were statically compared using a two-way ANOVA and Sidak's multicomparison test, while differences between the subpopulations were analysed using Kruskal-Wallis and Dunn's multicomparison tests or ordinary one-way ANOVA and Sidak's multicomparison test in the case of old $CD146^+$ and young $GD2^+$ cells. Legend inside the columns indicates the subpopulations in relation to which each subpopulation is statistically different, within the same age group. CD29: n_y=11, n_o=9; CD44: $n_{y,0}$=12; CD45: n_y=9; CD146: n_y=9, n_o=8; GD2: n_o=7; Tie2: n_y=7; Stro-1: n_o=5 (*p<0.05; **p<0.01; ***p<0.001 and ****p<0.0001). Note: blank spaces correspond to the cases where overall expression was already low, and a representative number of events (>1000) was not available to proceed with an accurate quantification of subpopulations distribution.

Cell surface receptors expression was further quantified within the different subpopulations from young and old NPs to characterize their signature (Figure 3.5). Table 3.3 resumes the signature of the four cell subpopulations discovered in the young NP, which was additionally supported by previous results regarding CD29, CD44, CD45 and CD34 differential expression across P1, P2 and P3 subpopulations [58]. Importantly, age seemed to negatively affect the expression of CD29 within P4 subpopulation only (95±5% vs 61±39%, n=11 and 10, respectively, *p<0.05), while P1 showed decreased percentages of both $CD44^+$ (50±12% vs 8±11%, n=12, ****p<0.0001) and $CD45^+$ (24±14% vs 6±7, n=10 and 5, respectively, **p<0.01) events. Interestingly, although the overall prevalence of $CD146^+$ events was not altered with age, their prevalence within P1 was significantly decrease (46±13% vs 12±9%, n=9 and 7 respectively, ****p<0.0001), and increased within P4 (16±16% vs 36±21%, n=9 and 7, respectively, **p<0.01), highlighting relevant changes on cells signature, which were otherwise masked.

Table 3.3: Cell surface receptors signature of the four distinct subpopulations found in young bNPs.

	% events	CD29	CD44	CD45	CD146	GD2	Tie2	CD34	Stro-1
P1	7±4	+++	++++	+++	++++	?	++++	-	?
P2	48±8	++++	+++	+	+	?	++++	-	?
P3	9±6	+++	+++	-	-	?	++	-	?
P4	35±11	++++	+++	++	++	?	++++	-	?

Legend: 0%: -; <10%: +; 10-20%: ++; 20-50%: +++; >50%: ++++; ? minimum 1000 events not assured for accurate quantification

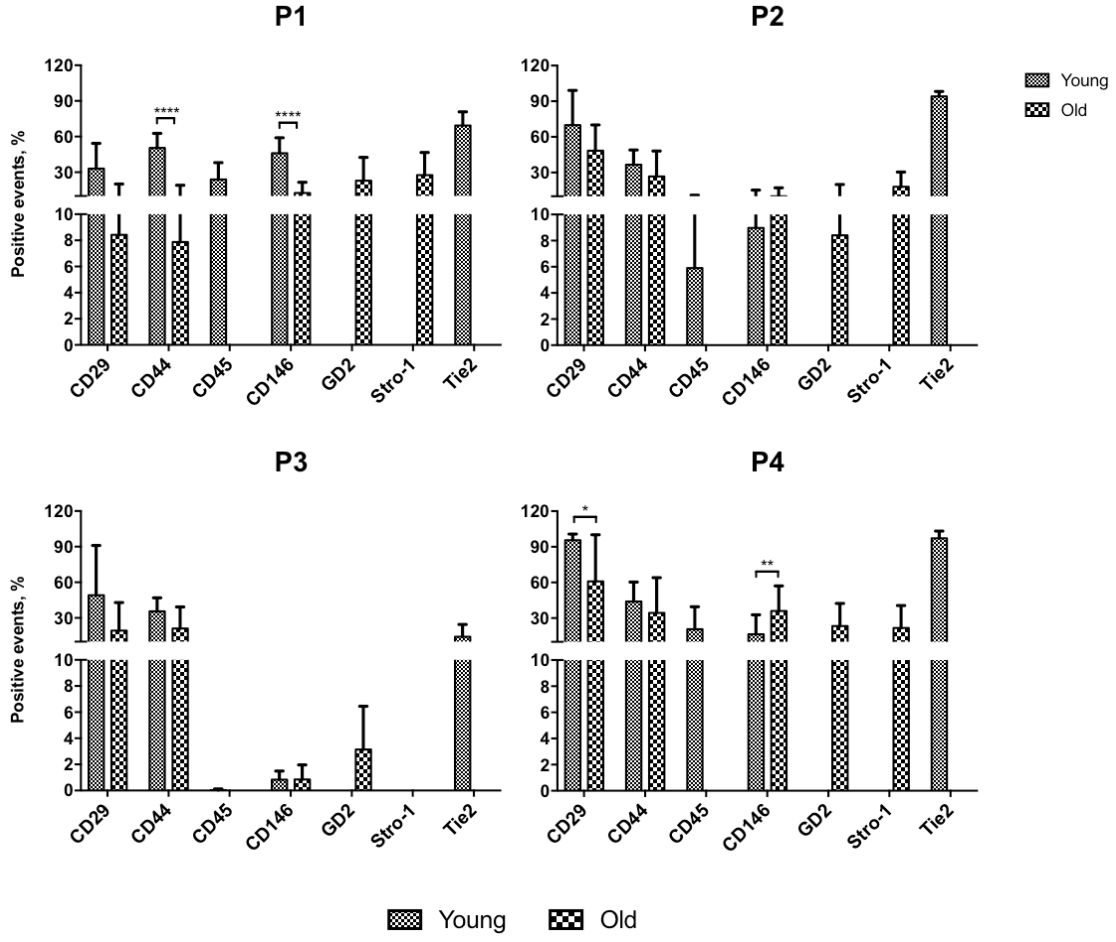

Figure 3.5: Immunophenotypic signature of P1, P2, P3 and P4 cell subpopulations found in young and old bovine NP. Results are presented as mean±standard deviation. Differences between age groups were assessed using a two-way ANOVA and Sidak's multicomparison test.

CD29: n_y=11, n_o=9; CD44: $n_{y,0}$=12; CD45: n_y=9; CD146: n_y=9, n_o=8; GD2: n_o=7; Tie2: n_y=7; Stro-1: n_o=5 (*p<0.05; **p<0.01 and ****p<0.0001). Note: null values correspond to the cases where overall expression was already low, and a representative number of events (>1000) was not available to proceed with an accurate quantification of subpopulations signature.

Morphology analysis of young and old bovine NP cells

Morphological changes with aging in bNP cells from young and old animals were also assessed using IFC. Data from conventional cytometer and from IFC were compared by plotting cells diameter against dark-field intensity (Ch06- the equivalent to SSC). Instead of the four subpopulations previously mentioned, only three could be distinguished in younger animals (Figure 3.4 A), because in conventional FC P2 and P3 are differentiated by their distinct auto-fluorescence when stained with PI, and this did not happen when plotting PI against cells diameter in IFC. Hence, P2 and P3 were analysed as a merged subpopulation. Figure 3.4 B shows examples of brightfield and fluorescence images of cells and their nuclei, respectively, found within each subpopulation. Interestingly, the P2+P3 subpopulation shows a significant decrease with age (74±4% vs 35±13%, ***p<0.001, n=3), while P4 is increased (16±7% vs 49±10%, ***p<0.001, n=3). Contrarily to what was observed by conventional FC, P1 did not reveal alterations with aging in terms of $DRAQ5^+$ events content (Figure 3.4 C). Moreover, an overall shift in cells diameter could be observed with aging (18±1 µm vs 23±2 µm, p<0.05) (Figure 3.5 A). Of note, although no changes were observed in terms of prevalence of multinucleated events (events with more than one $DRAQ5^+$ nuclei), when analysing the subpopulations in particular, P4 showed a significant decrease in the mean number of nuclei per cell with aging (1.887±0.17 nuclei vs 1.156±0.04 nuclei, ****p<0.0001, n=3) (Figure 3.5 B). Finally, the percentage of events containing bright vesicles increased with aging (3.051±0.05 bright vesicles vs 3.317±0.13 bright vesicles), although no particular differences were detected between subpopulations (Figure 3.5 C).

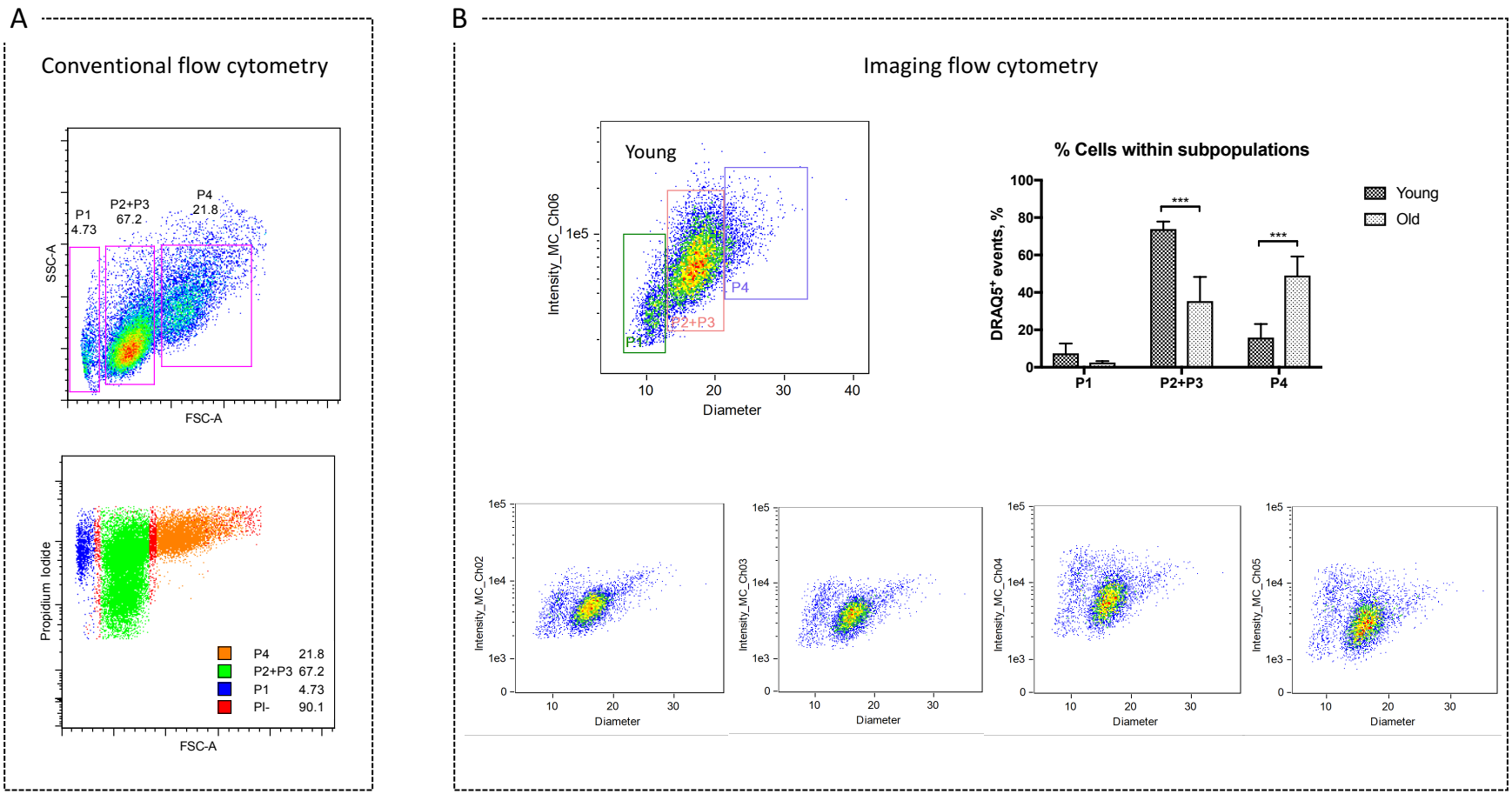
A
Conventional flow cytometry
P1
4.73
P2+P3
67.2
P4
21.8
SSC-A
FSC-A
Propidium Iodide
P4 21.8
P2+P3 67.2
P1 4.73
PI- 90.1
B
Imaging flow cytometry
Young
Intensity_MC_Ch06
Diameter
% Cells within subpopulations
DRAQ5+ events, %
Young
Old
***
P1
P2+P3
P4
Intensity_MC_Ch02
Intensity_MC_Ch03
Intensity_MC_Ch04
Intensity_MC_Ch05

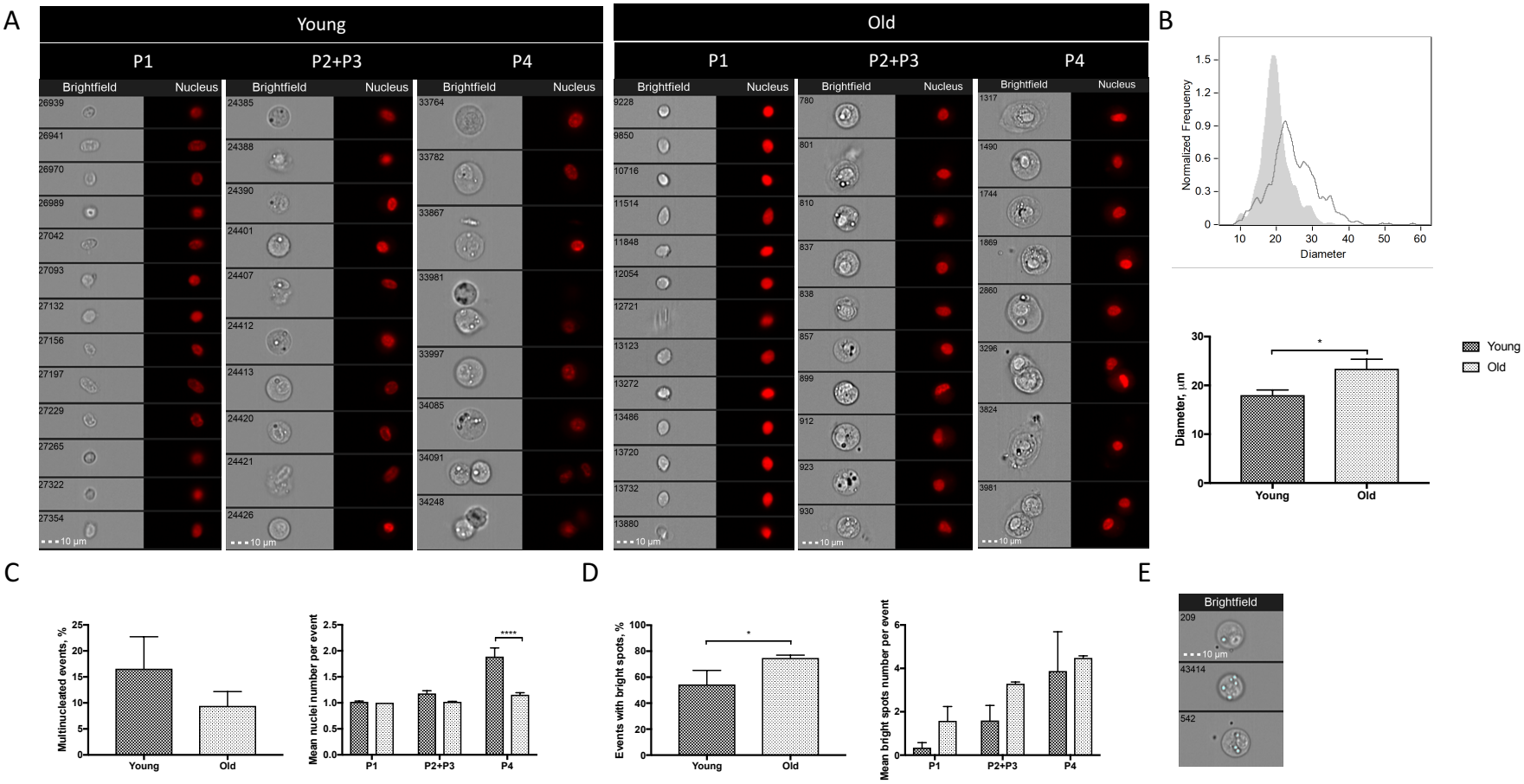
A
Young
Old
P1
P2+P3
P4
Brightfield
Nucleus
10 µm
B
Normalized Frequency
Diameter
Diameter, µm
Young
Old
C
Multinucleated events, %
Mean nuclei number per event
D
Events with bright spots, %
Mean bright spots number per event
E
Brightfield

Figure 3.6: Imaging flow cytometry analysis of young and old bovine NP cells. A | Panel shows conventional FC pseudo-color plots used to identify the subpopulations within the young bNP. Subpopulations P2 and P3 are merged in SSC-A vs FSC-A plots. **B |** IFC analysis of the subpopulations. While dark field intensity (Ch6) vs cells diameter was the equivalent to SSC-A vs FSC-A (top left density plot), no parallel could be established to PI vs FSC-A, as shown in bottom density plots of PI negative cells vs all fluorescence channels available. Top right graph shows the quantification of events distribution within P1, P2+P3 and P4 subpopulations in young and old bNP. Results are presented as mean± standard deviation and statistical differences were analysed using a two-way ANOVA and Sidak's multicomparison test (n=3, ***p<0.001). A total of 17994 DRAQ5+ events were analysed from the three young NPs and 2572 from the three old NPs.

Figure 3.7: Cell Morphology analysis of young and old bNP cells performed with IDEAS software. A | Examples of brightfield and fluorescence (DRAQ5 staining of cells nuclei in red) images of cells found within subpopulations P1, P2+P3 and P4. **B |** Histogram showing diameter distribution of young (filled) and old (line) bNP cells (top), and respective quantification of the average diameter of cells (bottom). **C|** Quantification of the prevalence of multinucleated events and mean nuclei number per cell. **D |** Quantification of the percentage of cells containing more than one bright vesicle and the mean number of bright vesicles per cell. **E |** Examples of brightfield images of cells and respective mask used to analyse bright vesicles (light blue) applied. Results in bars are presented as mean ± standard deviation and were analysed for statistical differences using a non-parametric Mann-Whitney test or a two-way ANOVA and Sidak's multicomparison test (n=3, *p<0.05 and ****p<0.0001). A total of 17994 NP DRAQ5^{+} events were analysed from the three young animals and 2572 from the three old animals.

Gene expression analysis

To evaluate whether the different phenotypic signature of young and old bovine NP cells could impact on cell function, the gene expression of specific NP ECM proteins, proinflammatory markers and MMPs of young and old NP cells was also quantified. Two out of the six genes selected revealed significant changes, namely the ECM protein Coll II (4.3±2 vs 0.4±0.4, **p<0.01, n=6 and 4) and the proinflammatory cytokine IL-8 (0.0169±0.006 vs 0.0061±0.004, **p<0.01, n=6 and 4), whose expression was downregulated with age (Figure 3.6).

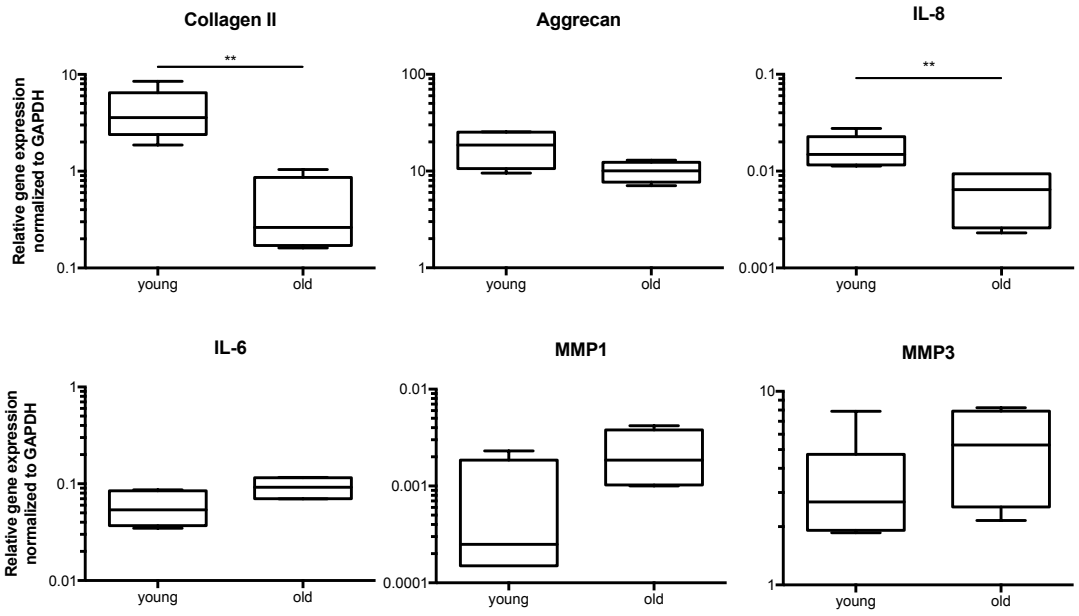

Figure 3.8: Differential gene expression profile of freshly isolated primary young and old bNP cells. Quantitative analysis of relative mRNA expression of ECM components (Coll II and Agg), proinflammatory markers (IL-8 and IL6) and matrix degrading enzymes (MMP1 and -3). Levels of mRNA were normalized to GAPDH. Results are presented as scatter plots, each point representing one animal (n=4-6, **p<0.01, Mann-Whitney test).)

Discussion

Alike every other organ in the human body, the IVD also ages, but in a fast-forward fashion. While people steel feel very young and active in life, the IVD starts to give signs of functional failure and is many times considered the cause, if not the source, of pain and disability. Hence, preventive therapies to address disc degeneration should take place very early in life. This work aimed at pin pointing age-related changes which occur at the NP cell level, in order to inform development of more targeted IVD anti-aging/degeneration therapies. Indeed, differences at the macroscopic level are evident between young and aged IVDs, and this is further reflected on ECM's ultrastructural features (Figure 3.1) and molecular composition, which was further explored within our group [63-66]. On the other hand, the molecular profile of IVD cells aging has been poorly studied. Indeed, to the best of our knowledge, here we report, for the first time in freshly isolated bovine NP cells, a decrease on the

percentage of the surface markers CD29, CD44, CD45 and Tie2 with age, while GD2 prevalence is significantly increased in elder animals.

CD29 (also known as β1-integrin) is an anchorage protein associated with stem cell niches and cell migration via cellular adhesion mechanisms, including cell-to-cell contacts or cell-to-matrix adhesion [67]. Its high prevalence (72-94%), quantified by FC as well, was previously reported in human cells from degenerated NP tissues (age range 21-63 years old), albeit cells were subjected to expansion in liquid culture, which may have favoured the proliferation of subsets enriched in this molecule, thus likely masking the effects of aging. CD44, a transmembrane protein and primary hyaluronic acid receptor, was recently shown to be more expressed in IVD cells from degenerated human tissue (~100%) than from herniated samples (~80%), but no correlation was established with age [68]. Also, the prevalence of $CD44^+$ was much superior than the one we report herein. In this case, cells were cultured until passages 6-8 (to generate IVD-derived mesenchymal stromal cells (MSCs)), and this is known to heavily affect cells phenotype, as reported for articular chondrocytes [69, 70], mouse bone marrow derived MSC precursors [71], and rabbit AF and NP cells [72]. Of note, a previous immunohistochemical study from Stevens *et al.* [73] on the developing and aging rat NP demonstrates a decrease in expression of CD44 associated with increased animals' age and loss of the notochordal cell population. Regarding CD45, although the prevalence of this hematopoietic-lineage marker was highly variable in young animals (1.5-36%), and somehow unexpected, bearing in mind the IVD is only peripherally irrigated, and care was taken to avoid contamination with blood during cells isolation procedure, this result is according to our previous immunophenotypic study, where an average 7% of $CD45^+$ was found in young animals [58]. Interestingly, CD45 was also detected by FC on human samples (~10-15%, n=21) from both degenerated (age range 26-79) and herniated (age range 25-56) tissues, after cell expansion in 2D culture. Importantly, the significant decrease associated with age is further supported by our most recent study with freshly isolated human IVD cells from degenerated discs, where we could not find any expression of CD45 in aged cells (age range 43-69, n=7) [74]. However, we believe that further investigation is required to validate these results by immunohistochemistry to put aside any suspects of contamination with non-endemic cells. Tie2, a recently proposed progenitor cell marker for young and healthy NP cells [20], was highly positive (~85%) in young NP cells as

opposed to old cells, which showed to expression at all. This was according to Sakai *et al.* [12] report stating that nearly 90% of plastic-culture expanded NP cells from young (20 years old) human samples express Tie2, although this expression drops dramatically (<10%) in donors older than 30 years old. Our previous study also revealed no expression of this marker in four donors aged 33, 34, 38 and 66 years old [74]. However, most recently, NP cells from five human donors within the same age range: 37-54, but expanded in pellet culture, revealed an average 14.07 ± 8.3% $Tie2^+$ cells, as evaluated by FC as well [75]. Importantly, the variability of results was high and no correlation was established with donors' age, besides the fact that the effects of the pellet culture on this $Tie2^+$ subset were not explored. Hence, we believe that this result validates bovine NP cells as a good phenotypic aging-model. Interestingly, GD2 followed the opposite tendency to the other markers mentioned so far, with higher percentages of $GD2^+$ cells present in old bovine NPs. This molecule is a component of the plasma membrane found mainly in the nervous system and has been identified before as a marker for bone marrow MSCs [76, 77] and umbilical cord MSCs [76]. Although its expression in primary mouse and human NP cells was reportedly very low (<2%), its increase during liquid culture was correlated with a high proliferative capability in the mouse NP [12]. Hence, bNP cells in old animals may be mounting a damage response, through GD2 signalling, as very recently hypothesised to happen in healer mice IVDs [78]. Finally, it is important to highlight the maintenance of $CD146^+$ events with age, a maker that revealed a pool of chondroprogenitors within late-stage osteoarthritic knee joints, with high clonogenic and multi-differentiation potential [79]. Of note, this was also true for human IVD tissue from degenerate samples [74].

In previous work, we have proven that the NP cell population from young bovine animals is heterogeneous, with the consistent identification of three distinct subpopulations (P1, P2, P3), when cells were plotted in FL3-H vs. FSC-H in FC analysis. Cells within these subpopulations presented different size and auto-fluorescence. Here, by changing the analysis from FSC-H(eight)/SSC-H(eight) to FSC-A(rea)/SSC-A(rea) we were able to identify one other distinct subpopulation, P4, containing large-sized and highly auto-fluorescent events. This is explained by the fact that FSC-A gives full FSC value information of the cell, therefore larger events that were not being detected in previous analysis became now evident and assembled into subpopulation P4. This is of particular importance when profiling NP cell, which are

many times naturally arranged in a chondron [80, 81] or cluster [82, 83] format, and thus should not be discarded as doublets or clumps, but rather considered a native subpopulation. Moreover, we could confirm by IFC that P4 includes both single and multinucleated large events, and surprisingly, is the only subpopulation where the percentage of multinucleated events drops significantly with age. The same reasoning applies to subpopulation P1, which contains much smaller events (~10μm), which are routinely discarded as cell debris. This subset does not stain for PI and contains many DRAQ5$^+$ events (~7%), although only few are calcein positive (0.3%), as evaluated by conventional FC (Supplementary Figure 3.2 A). IFC also reveals some DRAQ5/Actin double positive cells (Supplementary Figure 3.2 B), which further confirms the existence of cells within this subset that should not be disregarded. Interestingly, while FC results show a substantial decrease in subpopulations P3 and P4, and an increase in P1 with age, IFC revealed opposite results for P1 and P4, while P2 and P3, that could not be analyzed in separate, together showed an overall decrease. This could be explained by the clean analysis that IFC allows, through a sequence of gating steps that lead to the ultimate guarantee that we are characterizing cells. Indeed, in conventional FC P1 is most likely including several non-cell events, because for this analysis no specific stain for live cells was used. This had a great influence on the relative percentage of P4 events in old animals, in which the level of contaminating cell debris and ECM breakdown products post cell isolation is much higher. Of note, because the analysis of surface markers expression is based on specific antigen-antibody interactions, the immunophenotyping results are not as highly affected by debris-related auto-fluorescence as the subpopulations distribution analysis, and thus these results should be analyzed independently and not in relation to one another. Steel, it remains clear that the four subpopulations have a distinct signature, and some are more deeply affected by aging than others.

At the genotypic level, there were already some reports on the down-regulation of Coll II both with degeneration, in human NP cells [15], and aging, in bovine NP cells [84]. Interestingly, although in the latter study the age window was rather narrow (9-18 months old), cells as young as 18 months old were unable to reconstitute their ECM to the same extent as the younger cells [84]. This could be a consequence of the high levels of senescent cells present in young NP (8-95%), which we and others have verified before [58, 85], and which are known reduce the secretion of ECM

components, besides arresting cell cycle [86]. Regarding IL-8, while it is reported that human NP cells express this proinflammatory cytokine in homeostasis [87-89] and DDD [89-91], to the best of our knowledge this is the first time that its down-regulation with age in NP cells is reported.

In order to further characterize the four subpopulations identified, preliminary cell sorting experiments were conducted and optimized, using a FACS Aria II sorter, BD, to physically separate cells and determine their gene expression profile. Based on the phenotypic coordinates gathered using flow cytometry, namely cells different size and auto-fluorescence (following PI staining), and CD146 negative expression for P3 subpopulation, we were able to collect the distinct subpopulations with high purity levels (Supplementary Figure 3.3). However, this was a very challenging quest, since several parameters had to be optimized. Besides requiring highly concentrated primary cell suspensions - $5x10^6$ cells per 0.5 mL, and consuming elevated quantities of PI and antibody, the "sticky" nature of events within P2 systematically disturbed the flow, contaminating neighbouring collection tubes. Hence, sorting had to be performed in two stages, to guarantee P2 segregation. This way, good purity levels could be obtained, but cell yields were negatively affected. Indeed, P1 and P3 cell yields were always very low (10^4), representing an additional challenge for RNA extraction. Notwithstanding, gene expression analysis is presently ongoing.

In conclusion, we were able to profile important phenotypic and genotypic alterations that occur in bovine NP cells with age, such as the decrease on $CD29^+$, $CD44^+$, $CD45^+$ and $Tie2^+$ events and increase on $GD2^+$ events, together with a stable expression of CD146, the change in subpopulations prevalence and its surface receptors expression, the shift in cells diameter, the increased number of cells containing bright vesicles, and finally the down-regulation of Coll II and IL-8. Differentiating age-induced from disease-associated modifications will shed light on our understanding of the mechanisms leading to DDD, and we believe that the bovine animal model holds great promise in the further identification of anti-aging targets, towards the prevention of IVD degeneration.

Acknowledgments

This work had the financial support of FCT/MEC through National Funds and, when applicable, co-financed by the FEDER via the PT2020 Partnership Agreement under the 4293 Unit I&D and through European Union funds - Projetos Estruturados de I&D&I - Norte-01-0145-FEDER-000012, Portugal. The authors would like to acknowledge FCT (Fundação para a Ciência e Tecnologia) for funding M.M. Ph.D. grant (SFRH/BD/80577/2011), C.C. Post-Doc grant (SFRH/BDP/87071/2012) and R.M.G. FCT Investigator Starting Grant (IF/00638/2014). The authors also thank María Gómez Lázaro, Principal Technician from the Bioimaging Centre for Biomaterials and Regenerative Therapies (*b.IMAGE*) at i_3S, for the technical hints on Imaging Flow Cytometry data acquisition and analysis, and to Catarina Leitão, from the Translational Cytometry Unit at i_3S, for the continuous support on conventional flow cytometry procedures.

SUPPLEMENTARY INFORMATION

Manuscript in preparation

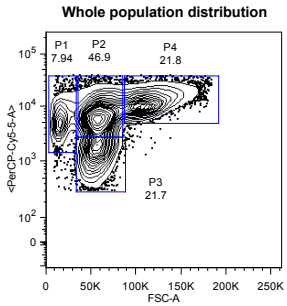

A) Positive events distribution within the 4 subpopulations

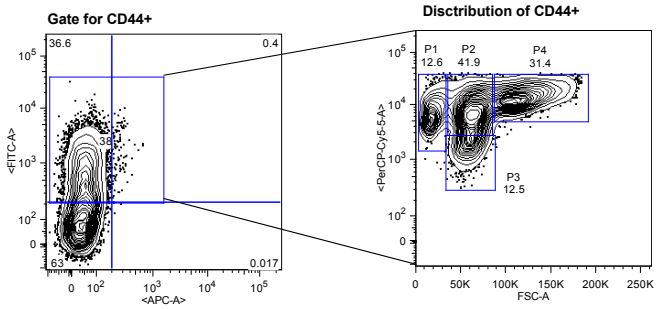

B) Subpopulations signature

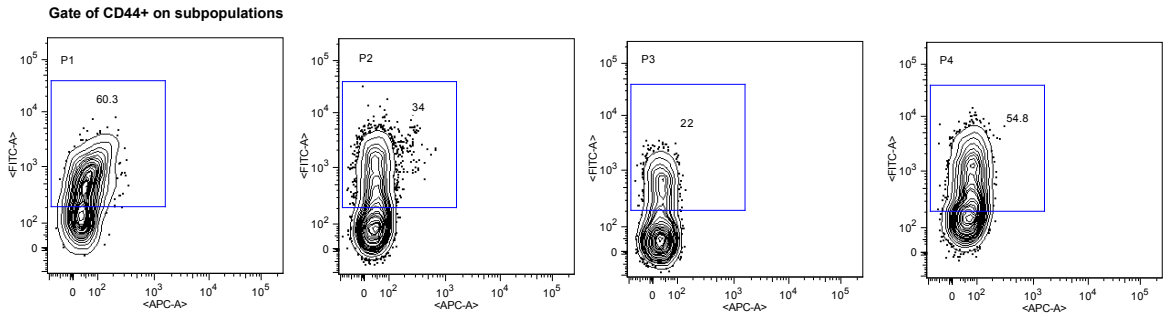

Supplementary Figure 3.1: Schematic showing an example of the normal distribution of PI negative events in PerCP-Cy5-5-A vs FCS-A pseudocolor dot plots, allowing the identification of P1, P2, P3 and P4 subpopulations (top), A) the analysis of the relative distribution of CD44^{+} events along the distinct subpopulations, and B) the quantification of each subpopulations' immunopositivity for CD44 (subpopulation signature), independently of the others.

A

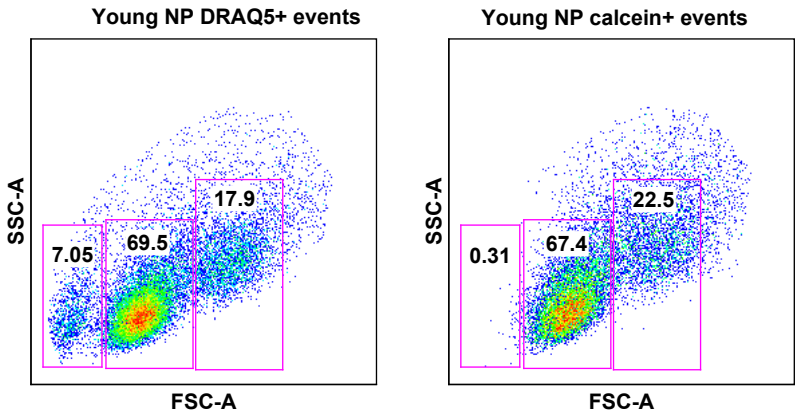

B

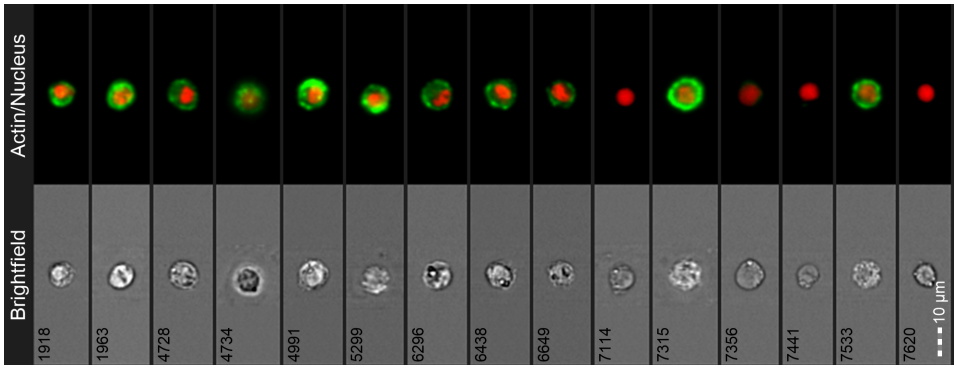

Supplementary Figure 3.2: Analysis of P1 subpopulation. A | Flow cytometry analysis of young and old bNP cells stained with DRAQ5 (binds double stranded DNA) and calcein (enters cells membranes and only fluoresces in live cells). DRAQ5 staining of cells' nuclei showed a subpopulation of small cells (within P1) that does not stain with calcein. However, few green spots can be detected in that area (n=1), and **B|** IFC revealed both $DRAQ5^{+}$ single positive and $DRAQ5^{+}actin^{+}$ double positive cells within P1 subpopulation. For actin staining cells were permeabilized with 0.2% v/v Triton, for 5 min. and washed with PBS, prior to incubation for 20 min at RT, with Phalloidin-AlexaFluor®488 (1:40 Dil. per $2.0x10^{5}$ cells, A12379, Life Technologies) in a PBS-1% w/v bovine serum albumin (BSA) solution, according to manufacturer's instructions.

BD FACSDiva 8.0.1

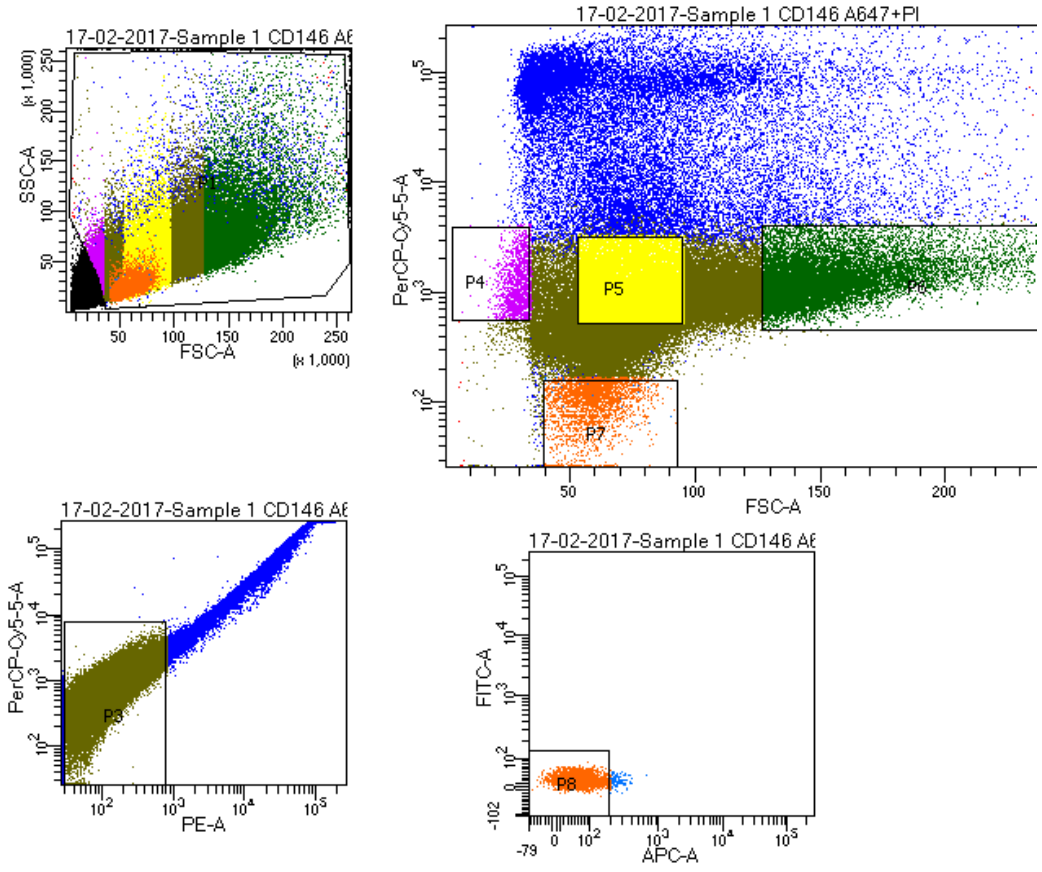

Tube: Sample 1 CD146 A647+PI

Population	#Events	%Parent	%Total
All Events	152,304	####	100.0
P1	115,640	75.9	75.9
P2	115,579	99.9	75.9
P3	87,961	76.1	57.8
P4	1,469	1.3	1.0
P5	32,674	28.3	21.5
P6	13,514	11.7	8.9
P7	2,883	2.5	1.9
P8	2,770	96.1	1.8

Supplementary Figure 3.3: Representative example of cell sorting gating sequence to physically separate P1 (P4 in purple), P2 (P5 in yellow), P3 (P8 in orange, CD146 negative) and P4 (P6 in green) subpopulations for further gene expression profiling.

References

[1] Global Burden of Disease Study, C. (2015) *Global, regional, and national incidence, prevalence, and years lived with disability for 301 acute and chronic diseases and injuries in 188 countries, 1990-2013: a systematic analysis for the Global Burden of Disease Study 2013.* Lancet, 386(9995): p. 743-800.

[2] Maher, C., M. Underwood, and R. Buchbinder (2017) *Non-specific low back pain.* Lancet, 389(10070): p. 736-747.

[3] Olmarker, K., (2014) *Back pain and disc degeneration: are they really linked?*, in *The intervertebral disc: molecular and structural studies of the disc in health and disease*, I.M. Shapiro and M.V. Risbud, Editors. Springer: Wien. p. 261-275.

[4] Schwarzer, A.C., C.N. Aprill, R. Derby, J. Fortin, G. Kine, et al. (1995) *The prevalence and clinical features of internal disc disruption in patients with chronic low back pain.* Spine (Phila Pa 1976), 20(17): p. 1878-83.

[5] Cheung, K.M., J. Karppinen, D. Chan, D.W. Ho, Y.Q. Song, et al. (2009) *Prevalence and pattern of lumbar magnetic resonance imaging changes in a population study of one thousand forty-three individuals.* Spine (Phila Pa 1976), 34(9): p. 934-40.

[6] Teraguchi, M., N. Yoshimura, H. Hashizume, S. Muraki, H. Yamada, et al. (2014) *Prevalence and distribution of intervertebral disc degeneration over the entire spine in a population-based cohort: the Wakayama Spine Study.* Osteoarthritis Cartilage, 22(1): p. 104-10.

[7] Sakai, D. and G.B. Andersson (2015) *Stem cell therapy for intervertebral disc regeneration: obstacles and solutions.* Nat Rev Rheumatol, 11(4): p. 243-56.

[8] Richardson, S.M., G. Kalamegam, P.N. Pushparaj, C. Matta, A. Memic, et al. (2016) *Mesenchymal stem cells in regenerative medicine: Focus on articular cartilage and intervertebral disc regeneration.* Methods, 99: p. 69-80.

[9] Hughes, S.P., A.J. Freemont, D.W. Hukins, A.H. McGregor, and S. Roberts (2012) *The pathogenesis of degeneration of the intervertebral disc and emerging therapies in the management of back pain.* J Bone Joint Surg Br, 94(10): p. 1298-304.

[10] Antoniou, J., T. Steffen, F. Nelson, N. Winterbottom, A.P. Hollander, et al. (1996) *The human lumbar intervertebral disc: evidence for changes in the biosynthesis and denaturation of the extracellular matrix with growth, maturation, aging, and degeneration.* J Clin Invest, 98(4): p. 996-1003.

[11] Richardson, S.M., F.E. Ludwinski, K.K. Gnanalingham, R.A. Atkinson, A.J. Freemont, et al. (2017) *Notochordal and nucleus pulposus marker expression is maintained by sub-populations of adult human nucleus pulposus cells through aging and degeneration.* Sci Rep, 7(1): p. 1501.

[12] Sakai, D., Y. Nakamura, T. Nakai, T. Mishima, S. Kato, et al. (2012) *Exhaustion of nucleus pulposus progenitor cells with aging and degeneration of the intervertebral disc.* Nat Commun, 3: p. 1264.

[13] Lee, C.R., D. Sakai, T. Nakai, K. Toyama, J. Mochida, et al. (2007) *A phenotypic comparison of intervertebral disc and articular cartilage cells in the rat.* European spine journal : official publication of the European Spine Society, the European Spinal Deformity Society, and the European Section of the Cervical Spine Research Society, 16(12): p. 2174-85.

[14] Minogue, B.M., S.M. Richardson, L.A.H. Zeef, A.J. Freemont, and J.A. Hoyland (2010) *Characterization of the human nucleus pulposus cell phenotype and evaluation of novel marker gene expression to define adult stem cell differentiation.* Arthritis & Rheumatism, 62(12): p. 3695-3705.

[15] Minogue, B.M., S.M. Richardson, L.A.H. Zeef, A.J. Freemont, and J.A. Hoyland (2010) *Transcriptional profiling of bovine intervertebral disc cells: implications for identification of normal and degenerate human intervertebral disc cell phenotypes.* Arthritis Research & Therapy, 12(1): p. R22.

[16] Power, K.A., S. Grad, J.P. Rutges, L.B. Creemers, M.H. van Rijen, et al. (2011) *Identification of cell surface-specific markers to target human nucleus pulposus cells:*

expression of carbonic anhydrase XII varies with age and degeneration. Arthritis Rheum, 63(12): p. 3876-86.

[17] Sakai, D., T. Nakai, J. Mochida, M. Alini, and S. Grad (2009) *Differential phenotype of intervertebral disc cells: microarray and immunohistochemical analysis of canine nucleus pulposus and anulus fibrosus.* Spine, 34(14): p. 1448-56.

[18] Thorpe, A.A., A.L. Binch, L.B. Creemers, C. Sammon, and C.L. Le Maitre (2016) *Nucleus pulposus phenotypic markers to determine stem cell differentiation: fact or fiction?* Oncotarget, 7(3): p. 2189-200.

[19] Boyle, E.A., Y.I. Li, and J.K. Pritchard (2017) *An Expanded View of Complex Traits: From Polygenic to Omnigenic.* Cell, 169(7): p. 1177-1186.

[20] Risbud, M.V., Z.R. Schoepflin, F. Mwale, R.A. Kandel, S. Grad, et al. (2015) *Defining the phenotype of young healthy nucleus pulposus cells: recommendations of the Spine Research Interest Group at the 2014 annual ORS meeting.* J Orthop Res, 33(3): p. 283-93.

[21] Tang, X., L. Jing, W.J. Richardson, R.E. Isaacs, R.D. Fitch, et al. (2016) *Identifying molecular phenotype of nucleus pulposus cells in human intervertebral disc with aging and degeneration.* J Orthop Res, 34(8): p. 1316-26.

[22] Streitz, M., T. Miloud, M. Kapinsky, M.R. Reed, R. Magari, et al. (2013) *Standardization of whole blood immune phenotype monitoring for clinical trials: panels and methods from the ONE study.* Transplant Res, 2(1): p. 17.

[23] Boos, N., S. Weissbach, H. Rohrbach, C. Weiler, K.F. Spratt, et al. (2002) *Classification of age-related changes in lumbar intervertebral discs: 2002 Volvo Award in basic science.* Spine (Phila Pa 1976), 27(23): p. 2631-44.

[24] Adams, M.A. and P.J. Roughley (2006) *What is intervertebral disc degeneration, and what causes it?* Spine (Phila Pa 1976), 31(18): p. 2151-61.

[25] Vo, N., H.Y. Seo, A. Robinson, G. Sowa, D. Bentley, et al. (2010) *Accelerated aging of intervertebral discs in a mouse model of progeria.* J Orthop Res, 28(12): p. 1600-7.

[26] Bedore, J., W. Sha, M.R. McCann, S. Liu, A. Leask, et al. (2013) *Impaired intervertebral disc development and premature disc degeneration in mice with notochord-specific deletion of CCN2.* Arthritis Rheum, 65(10): p. 2634-44.

[27] Furukawa, T., K. Ito, S. Nuka, J. Hashimoto, H. Takei, et al. (2009) *Absence of biglycan accelerates the degenerative process in mouse intervertebral disc.* Spine (Phila Pa 1976), 34(25): p. E911-7.

[28] Mason, R.M. and A.J. Palfrey (1984) *Intervertebral disc degeneration in adult mice with hereditary kyphoscoliosis.* J Orthop Res, 2(4): p. 333-8.

[29] Semba, K., K. Araki, Z. Li, K. Matsumoto, M. Suzuki, et al. (2006) *A novel murine gene, Sickle tail, linked to the Danforth's short tail locus, is required for normal development of the intervertebral disc.* Genetics, 172(1): p. 445-56.

[30] Holguin, N., R. Aguilar, R.A. Harland, B.A. Bomar, and M.J. Silva (2014) *The aging mouse partially models the aging human spine: lumbar and coccygeal disc height, composition, mechanical properties, and Wnt signaling in young and old mice.* J Appl Physiol (1985), 116(12): p. 1551-60.

[31] Silberberg, R. and G. Gerritsen (1976) *Aging changes in intervertebral discs and spondylosis in Chinese hamsters.* Diabetes, 25(6): p. 477-83.

[32] Laing, A.C., R. Cox, W. Tetzlaff, and T. Oxland (2011) *Effects of advanced age on the morphometry and degenerative state of the cervical spine in a rat model.* Anat Rec (Hoboken), 294(8): p. 1326-36.

[33] Gruber, H.E., J.A. Ingram, H.J. Norton, and E.N. Hanley, Jr. (2007) *Senescence in cells of the aging and degenerating intervertebral disc: immunolocalization of senescence-associated beta-galactosidase in human and sand rat discs.* Spine (Phila Pa 1976), 32(3): p. 321-7.

[34] Gruber, H.E., B. Gordon, C. Williams, H.J. Norton, and E.N. Hanley, Jr. (2007) *Vertebral endplate and disc changes in the aging sand rat lumbar spine: cross-sectional analyses of a large male and female population.* Spine (Phila Pa 1976), 32(23): p. 2529-36.

[35] Gruber, H.E., B. Gordon, H.J. Norton, J. Kilburn, C. Williams, et al. (2008) *Analysis of cell death and vertebral end plate bone mineral density in the annulus of the aging sand rat.* Spine J, 8(3): p. 475-81.

[36] Moskowitz, R.W., I. Ziv, C.W. Denko, B. Boja, P.K. Jones, et al. (1990) *Spondylosis in sand rats: a model of intervertebral disc degeneration and hyperostosis.* J Orthop Res, 8(3): p. 401-11.

[37] Sowa, G., G. Vadala, R. Studer, J. Kompel, C. Iucu, et al. (2008) *Characterization of intervertebral disc aging: longitudinal analysis of a rabbit model by magnetic resonance imaging, histology, and gene expression.* Spine (Phila Pa 1976), 33(17): p. 1821-8.

[38] Cho, H., S.H. Park, S. Lee, M. Kang, K.A. Hasty, et al. (2011) *Snapshot of degenerative aging of porcine intervertebral disc: a model to unravel the molecular mechanisms.* Exp Mol Med, 43(6): p. 334-40.

[39] Bergknut, N., J.P. Rutges, H.J. Kranenburg, L.A. Smolders, R. Hagman, et al. (2012) *The dog as an animal model for intervertebral disc degeneration?* Spine (Phila Pa 1976), 37(5): p. 351-8.

[40] Wade, K.R., P.A. Robertson, and N.D. Broom (2014) *Influence of maturity on nucleus-endplate integration in the ovine lumbar spine.* Eur Spine J, 23(4): p. 732-44.

[41] Stolworthy, D.K., A.E. Bowden, B.L. Roeder, T.F. Robinson, J.G. Holland, et al. (2015) *MRI evaluation of spontaneous intervertebral disc degeneration in the alpaca cervical spine.* J Orthop Res, 33(12): p. 1776-83.

[42] Lauerman, W.C., R.C. Platenberg, J.E. Cain, and V.F. Deeney (1992) *Age-related disk degeneration: preliminary report of a naturally occurring baboon model.* J Spinal Disord, 5(2): p. 170-4.

[43] Platenberg, R.C., G.B. Hubbard, W.J. Ehler, and C.J. Hixson (2001) *Spontaneous disc degeneration in the baboon model: magnetic resonance imaging and histopathologic correlation.* J Med Primatol, 30(5): p. 268-72.

[44] Duncan, A.E., R.J. Colman, and P.A. Kramer (2011) *Longitudinal study of radiographic spinal osteoarthritis in a macaque model.* J Orthop Res, 29(8): p. 1152-60.

[45] Nuckley, D.J., P.A. Kramer, A. Del Rosario, N. Fabro, S. Baran, et al. (2008) *Intervertebral disc degeneration in a naturally occurring primate model: radiographic and biomechanical evidence.* J Orthop Res, 26(9): p. 1283-8.

[46] Gilson, A., M. Dreger, and J.P. Urban (2010) *Differential expression level of cytokeratin 8 in cells of the bovine nucleus pulposus complicates the search for specific intervertebral disc cell markers.* Arthritis Research & Therapy, 12(1): p. R24.

[47] Tang, X., L. Jing, and J. Chen (2012) *Changes in the molecular phenotype of nucleus pulposus cells with intervertebral disc aging.* PLoS One, 7(12): p. e52020.

[48] Rutges, J., L.B. Creemers, W. Dhert, S. Milz, D. Sakai, et al. (2010) *Variations in gene and protein expression in human nucleus pulposus in comparison with annulus fibrosus and cartilage cells: potential associations with aging and degeneration.* Osteoarthritis and Cartilage, 18(3): p. 416-423.

[49] Gilson, A., M. Dreger, and J.P.G. Urban (2010) *Differential expression level of cytokeratin 8 in cells of the bovine nucleus pulposus complicates the search for specific intervertebral disc cell markers.* Arthritis Research & Therapy, 12(1): p. R24.

[50] Johnson, W.E., S. Stephan, and S. Roberts (2008) *The influence of serum, glucose and oxygen on intervertebral disc cell growth in vitro: implications for degenerative disc disease.* Arthritis Res Ther, 10(2): p. R46.

[51] Stephan, S., W.E. Johnson, and S. Roberts (2011) *The influence of nutrient supply and cell density on the growth and survival of intervertebral disc cells in 3D culture.* Eur Cell Mater, 22: p. 97-108.

[52] Yu, J., P.C. Winlove, S. Roberts, and J.P. Urban (2002) *Elastic fibre organization in the intervertebral discs of the bovine tail.* Journal of anatomy, 201(6): p. 465-75.

[53] Yu, J., U. Tirlapur, J. Fairbank, P. Handford, S. Roberts, et al. (2007) *Microfibrils, elastin fibres and collagen fibres in the human intervertebral disc and bovine tail disc.* J Anat, 210(4): p. 460-71.

[54] Miyazaki, T., S. Kobayashi, K. Takeno, A. Meir, J. Urban, et al. (2009) *A phenotypic comparison of proteoglycan production of intervertebral disc cells isolated from rats, rabbits, and bovine tails; which animal model is most suitable to study tissue engineering and biological repair of human disc disorders?* Tissue Eng Part A, 15(12): p. 3835-46.

[55] Mavrogonatou, E. and D. Kletsas (2010) *Effect of varying osmotic conditions on the response of bovine nucleus pulposus cells to growth factors and the activation of the ERK and Akt pathways.* Journal of Orthopaedic Research, 28(10): p. 1276-1282.

[56] Chujo T, A.H., Akeda K, Miyamoto K, Muehleman C, Attawia M, Andersson G, Masuda K. (2006) *Effects of growth differentiation factor-5 on the intervertebral disc--in vitro bovine study and in vivo rabbit disc degeneration model study.* Spine, 31(25): p. 2909-17.

[57] van den Akker, G.G.H., M.I. Koenders, F.A.J. van de Loo, P. van Lent, E. Blaney Davidson, et al. (2017) *Transcriptional profiling distinguishes inner and outer annulus fibrosus from nucleus pulposus in the bovine intervertebral disc.* Eur Spine J.

[58] Molinos, M., C.R. Almeida, R.M. Goncalves, and M.A. Barbosa (2015) *Improvement of Bovine Nucleus Pulposus Cells Isolation Leads to Identification of Three Phenotypically Distinct Cell Subpopulations.* Tissue Eng Part A, 21(15-16): p. 2216-27.

[59] Sakurai, M., T. Furusawa, M. Ikeda, H. Hikono, S. Shimizu, et al. (2006) *Anti-bovine CD34 monoclonal antibody reveals polymorphisms within coding region of the CD34 gene.* Exp Hematol, 34(7): p. 905-13.

[60] Teixeira, G.Q., A. Boldt, I. Nagl, C.L. Pereira, K. Benz, et al. (2016) *A Degenerative/Proinflammatory Intervertebral Disc Organ Culture: An Ex Vivo Model for Anti-inflammatory Drug and Cell Therapy.* Tissue Eng Part C Methods, 22(1): p. 8-19.

[61] Untergasser, A., I. Cutcutache, T. Koressaar, J. Ye, B.C. Faircloth, et al. (2012) *Primer3--new capabilities and interfaces.* Nucleic Acids Res, 40(15): p. e115.

[62] MacLean, J.J., C.R. Lee, S. Grad, K. Ito, M. Alini, et al. (2003) *Effects of immobilization and dynamic compression on intervertebral disc cell gene expression in vivo.* Spine (Phila Pa 1976), 28(10): p. 973-81.

[63] Caldeira, J., C. Santa, H. Osório, M. Molinos, B. Manadas, et al. (2017) *Matrisome Profiling During Intervertebral Disc Development And Aging.* Scientific Reports, 7(1).

[64] Sarath Babu, N., S. Krishnan, C.V. Brahmendra Swamy, G.P. Venkata Subbaiah, A.V. Gurava Reddy, et al. (2016) *Quantitative proteomic analysis of normal and degenerated human intervertebral disc.* Spine J, 16(8): p. 989-1000.

[65] Ye, D., W. Liang, L. Dai, L. Zhou, Y. Yao, et al. (2015) *Comparative and quantitative proteomic analysis of normal and degenerated human annulus fibrosus cells.* Clin Exp Pharmacol Physiol, 42(5): p. 530-6.

[66] Collin, E.C., M. Kilcoyne, S.J. White, S. Grad, M. Alini, et al. (2016) *Unique glycosignature for intervertebral disc and articular cartilage cells and tissues in immaturity and maturity.* Sci Rep, 6: p. 23062.

[67] Gottschling, S., R. Saffrich, A. Seckinger, U. Krause, K. Horsch, et al. (2007) *Human mesenchymal stromal cells regulate initial self-renewing divisions of hematopoietic progenitor cells by a beta1-integrin-dependent mechanism.* Stem Cells, 25(3): p. 798-806.

[68] Marfia, G., S.E. Navone, C. Di Vito, S. Tabano, L. Giammattei, et al. (2015) *Gene expression profile analysis of human mesenchymal stem cells from herniated and degenerated intervertebral discs reveals different expression of osteopontin.* Stem Cells Dev, 24(3): p. 320-8.

[69] Stewart, M.C., K.M. Saunders, N. Burton-Wurster, and J.N. Macleod (2000) *Phenotypic stability of articular chondrocytes in vitro: the effects of culture models,*

bone morphogenetic protein 2, and serum supplementation. J Bone Miner Res, 15(1): p. 166-74.

[70] Bonaventure, J., N. Kadhom, L. Cohen-Solal, K.H. Ng, J. Bourguignon, et al. (1994) *Reexpression of cartilage-specific genes by dedifferentiated human articular chondrocytes cultured in alginate beads.* Exp Cell Res, 212(1): p. 97-104.

[71] Baustian, C., S. Hanley, and R. Ceredig (2015) *Isolation, selection and culture methods to enhance clonogenicity of mouse bone marrow derived mesenchymal stromal cell precursors.* Stem Cell Res Ther, 6: p. 151.

[72] Sang, C., X. Cao, F. Chen, X. Yang, and Y. Zhang (2016) *Differential Characterization of Two Kinds of Stem Cells Isolated from Rabbit Nucleus Pulposus and Annulus Fibrosus.* Stem Cells Int, 2016: p. 8283257.

[73] Stevens, J.W., G.L. Kurriger, A.S. Carter, and J.A. Maynard (2000) *CD44 expression in the developing and growing rat intervertebral disc.* Dev Dyn, 219(3): p. 381-90.

[74] Molinos, M., C. Cunha, C.R. Almeida, R.M. Goncalves, P. Pereira, et al. (2017) *Age-Correlated Phenotypic Alterations in Cells Isolated from Human Degenerated Intervertebral Discs With Contained Hernias.* Spine (Phila Pa 1976).

[75] Li, X.C., Y. Tang, J.H. Wu, P.S. Yang, D.L. Wang, et al. (2017) *Characteristics and potentials of stem cells derived from human degenerated nucleus pulposus: potential for regeneration of the intervertebral disc.* BMC Musculoskelet Disord, 18(1): p. 242.

[76] Xu, J., W. Liao, D. Gu, L. Liang, M. Liu, et al. (2009) *Neural ganglioside GD2 identifies a subpopulation of mesenchymal stem cells in umbilical cord.* Cell Physiol Biochem, 23(4-6): p. 415-24.

[77] Martinez, C., T.J. Hofmann, R. Marino, M. Dominici, and E.M. Horwitz (2007) *Human bone marrow mesenchymal stromal cells express the neural ganglioside GD2: a novel surface marker for the identification of MSCs.* Blood, 109(10): p. 4245-8.

[78] Zhang, Y., C. Xiong, C.W. Chan, D. Sakai, and D. Chan (2017) *Changes in Nucleus Pulposus Cell Pools in "Healer" Mice for the Repair of Intervertebral Disc Degeneration.* Global Spine Journal, 5(1_suppl): p. s-0035-1554499-s-0035-1554499.

[79] Su, X., W. Zuo, Z. Wu, J. Chen, N. Wu, et al. (2015) *CD146 as a new marker for an increased chondroprogenitor cell sub-population in the later stages of osteoarthritis.* J Orthop Res, 33(1): p. 84-91.

[80] Trout, J.J., J.A. Buckwalter, and K.C. Moore (1982) *Ultrastructure of the human intervertebral disc: II. Cells of the nucleus pulposus.* Anat Rec, 204(4): p. 307-14.

[81] Ciapetti, G., D. Granchi, V. Devescovi, E. Leonardi, T. Greggi, et al. (2012) *Ex vivo observation of human intervertebral disc tissue and cells isolated from degenerated intervertebral discs.* European spine journal : official publication of the European Spine Society, the European Spinal Deformity Society, and the European Section of the Cervical Spine Research Society, 21 Suppl 1: p. S10-9.

[82] Johnson, W.E., S.M. Eisenstein, and S. Roberts (2001) *Cell cluster formation in degenerate lumbar intervertebral discs is associated with increased disc cell proliferation.* Connect Tissue Res, 42(3): p. 197-207.

[83] Sharp, C.A., S. Roberts, H. Evans, and S.J. Brown (2009) *Disc cell clusters in pathological human intervertebral discs are associated with increased stress protein immunostaining.* European spine journal : official publication of the European Spine Society, the European Spinal Deformity Society, and the European Section of the Cervical Spine Research Society, 18(11): p. 1587-94.

[84] Kandel, R.A., D. Hamilton, C. Seguin, S.Q. Li, C. Arana, et al. (2007) *An in vitro tissue model to study the effect of age on nucleus pulposus cells.* Eur Spine J, 16(12): p. 2166-73.

[85] Jeong, S.W., J.S. Lee, and K.W. Kim (2014) *In vitro lifespan and senescence mechanisms of human nucleus pulposus chondrocytes.* Spine J, 14(3): p. 499-504.

[86] Krizhanovsky, V., M. Yon, R.A. Dickins, S. Hearn, J. Simon, et al. (2008) *Senescence of activated stellate cells limits liver fibrosis.* Cell, 134(4): p. 657-67.

[87] Kepler, C.K., D.Z. Markova, F. Dibra, S. Yadla, A.R. Vaccaro, et al. (2013) *Expression and relationship of proinflammatory chemokine RANTES/CCL5 and cytokine IL-1beta in painful human intervertebral discs.* Spine (Phila Pa 1976), 38(11): p. 873-80.

[88] Burke, J.G., G.W. RW, D. Conhyea, D. McCormack, F.E. Dowling, et al. (2003) *Human nucleus pulposis can respond to a pro-inflammatory stimulus.* Spine (Phila Pa 1976), 28(24): p. 2685-93.

[89] Phillips, K.L., N. Chiverton, A.L. Michael, A.A. Cole, L.M. Breakwell, et al. (2013) *The cytokine and chemokine expression profile of nucleus pulposus cells: implications for degeneration and regeneration of the intervertebral disc.* Arthritis Res Ther, 15(6): p. R213.

[90] Burke, J.G., R.W. Watson, D. McCormack, F.E. Dowling, M.G. Walsh, et al. (2002) *Intervertebral discs which cause low back pain secrete high levels of proinflammatory mediators.* J Bone Joint Surg Br, 84(2): p. 196-201.

[91] Ahn, S.H., Y.W. Cho, M.W. Ahn, S.H. Jang, Y.K. Sohn, et al. (2002) *mRNA expression of cytokines and chemokines in herniated lumbar intervertebral discs.* Spine (Phila Pa 1976), 27(9): p. 911-7.

CHAPTER IV

Age-correlated phenotypic alterations in cells isolated from human degenerated intervertebral discs with contained hernias

Article 3
Published in Spine (Phila Pa 1976). 2017 Jul 3
doi: 10.1097/BRS.0000000000002311

Age-correlated phenotypic alterations in cells isolated from human degenerated intervertebral discs with contained hernias

Maria Molinos[1–3], Carla Cunha[1,2], Catarina R. Almeida[1,2,4], Raquel M. Gonçalves[1,2], Paulo Pereira[5,6], Pedro Santos Silva[5], Rui Vaz[1,5,6], Mário A. Barbosa[1–3]

[1] i3S – Instituto de Investigação e Inovação em Saúde, Universidade do Porto, Rua Alfredo Allen, 208, 4200-135 Porto, Portugal

[2] INEB - Instituto de Engenharia Biomédica, Universidade do Porto, Rua Alfredo Allen, 208, 4200-135 Porto, Portugal

[3] ICBAS - Instituto de Ciências Biomédicas Abel Salazar, Universidade do Porto, Rua de Jorge Viterbo Ferreira n.º 228, 4050-313 Porto, Portugal

[4] iBiMED – Instituto de Biomedicina e Departamento de Ciências Médicas, Universidade de Aveiro, Campus Universitário de Santiago, Agra do crasto - edifício 30, 3810-193 Aveiro, Portugal

[5] Departamento de Neurocirurgia, Centro Hospitalar São João, Porto, Portugal | Departamento de Neurociências Clínicas e Saúde Mental, Faculdade de Medicina, Universidade do Porto, Alameda Prof. Hernâni Monteiro, 4200-319 Porto, Portugal

[6] Centro de Neurociências CUF Porto, Estrada da Circunvalação 14341, Porto, Portugal

Abstract

Human intervertebral disc (hIVD) cells were isolated from 41 surgically excised samples and assessed for their phenotypic alterations with age. Towards the design of novel anti-aging strategies to overcome degenerative disc disease (DDD), we investigated age-correlated phenotypic alterations that occur on primary hIVD cells. Although regenerative medicine holds great hope, much is still to be unveiled on IVD cell biology and its intrinsic signalling pathways, which can lead the way to successful therapies for IDD. A greater focus on age-related phenotypic changes at the cell level would contribute to establish more effective anti-aging/degeneration targets. The study was subdivided in four main steps: i) optimization of primary cells isolation technique; ii) high-throughput cell morphology analysis, by imaging flow-cytometry (FC) and subsequent validation by histological analysis; iii) analysis of progenitor cell surface markers expression, by conventional FC; and iv) statistical analysis and correlation of cells morphology and phenotype with donor age. Three subsets of cells were identified based on their diameter: small (SC), large (LC) and super large cells (SLC). The frequency of SCs decreased nearly 50% with age, whereas that of LCs increased nearly 30%. Interestingly, the increased cells size was due to an enlargement of the pericellular matrix (PCM). Moreover, the expression pattern for CD90 and CD73 was a reflexion of age, where older individuals show reduced frequencies of positive cells for those markers. Nevertheless, the elevated percentages of primary positive cells for the mesenchymal stem cells (MSC) marker CD146 found, even in some older donors, bring refreshed hope for the hypothetical activation of the self-renewal potential of the IVD. These findings highlight the remarkable morphological alterations that occur on hIVD cells with aging and degeneration, while reinforcing previous reports on the gradual disappearance of an endogenous progenitor cell population.

Age-correlated phenotypic alterations in cells isolated from human degenerated intervertebral discs with contained hernias

Introduction

Current treatments for DDD fail to address IVD's pathophysiology and to restore its function, and bioengineered sophisticated solutions are still in their infancy, with very few having reached Phase-I clinical trials [1]. In fact, much is still to be unveiled regarding the cell biology of the IVD and its intrinsic signalling pathways. Particularly, a greater knowledge about age-related cellular changes will contribute to establish more effective anti-aging/degeneration targets.

In the adult IVD, chondrocyte-like cells frequently assemble in a fibrous capsule, forming chondrons similar to those found in articular cartilage [2]. It has been suggested that these encircling layers result from accumulation of cellular products, as a consequence of aging [3, 4] with histopathological analysis revealing evident remodeling of the pericelullar matrix (PCM) occurring with age and disease progression [3, 5, 6]. On the other hand, PCM plays an important role in governing the local mechanical environment of chondrocytes and IVD cells [7, 8], as well as in maintaining their phenotype and viability [9, 10].

Despite findings indicating that degenerated human discs may have an endogenous regenerative capacity [11-15], there might be an age-limit for the efficient activation of its cell progenitors [16-18].

The aim of this work was to investigate age-related phenotypic alterations on primary human IVD cells from degenerated tissue. Taking advantage of a multiparameter image analysis tool, that guarantees robust quantitation of morphological features, we correlated IVD cells size, clusters prevalence and PCM area with age, while monitoring changes in expression of known stem cell-related (CD90, CD73, CD105, CD146, CD34, Stro1) and NP-progenitor (GD2 and Tie2) markers.

Materials and methods

Surgical IVD tissue dissection and cell isolation

Degenerated human lumbar IVD fragments, with grade III-IV (Pfirrmann

scale), were isolated from patients undergoing microdiscectomy, after informed consent and ethics committee approval. The surgeries were performed under general anesthesia in a sterile operating room and prophylactic antibiotic therapy with cefazolin 1 g IV was given. Patients were placed in a knee-chest position and a standard posterior approach to the appropriate interlaminar window was undertaken. After removal of the yellow ligament and medial retraction of the nerve root, the disc herniation was exposed. The posterior longitudinal ligament and the annulus fibrosus (AF) were incised and IVD fragments were excised, as deemed necessary by the surgeon. No more disc samples than those considered clinically appropriate were collected. In cases where the disc fragment was in contact with the epidural space or indistinguishable from the AF, the excised tissue was not included in this study. Thus, AF-contained IVD fragments were collected, and cells were isolated by enzymatic digestion, as previously described [19], using one of three enzymatic formulations: collagenase-type-I (Coll-I), collagenase-type-II (Coll-II), or collagenase-type-XI (Coll-XI) (C0130, C6885, and C7657, respectively, Sigma-Aldrich, Sintra, Portugal), at 0.5 mg/mL (more detailed information in Supplementary Methods).

Assessment of yield and viability upon isolation

Immediately upon digestion, cell yield was quantified by trypan blue exclusion and subsequently normalized against initial wet tissue weight. Cell viability was assessed by flow cytometry (FC) (FACS Calibur; BD Immunocytometry Systems, San Jose, CA) upon propidium iodide (PI) staining.

Characterization of cell morphology by imaging flow cytometry (IFC)

Cells from 9 different donors were fixed in 4% w/v paraformaldehyde (PFA) solution at room temperature for 15 min and washed with phosphate-buffered saline (PBS). Cells were labeled with DRAQ5 (1:1500 dil. per 2.0 x 10^5 cells, 65-0880; eBioscience), run on ImageStream^X (IS; Millipore, Billerica, Massachusetts, MA), and analyzed with IDEAS software for: cell diameter,

frequency of small (SC), large (LC) and super large cells (SLC), frequency of single cells and multinucleated events (See Supplementary Figure 4.1 A, B and C: Cell Morphology Analysis Tutorial).

Cells were identified as SC, LC and SLC based on their diameter: 10 μm<SC<20 μm; 20 μm<LC<30 μm and 30 μm<SLC<50 μm. To quantify the percentage of single and multinucleated events, as well as the number of single cells within LC and SLC populations, a specific mask and feature was created and applied to images of DRAQ5 stained nuclei (Supplementary Figure 4.1 B).

To identify the presence of PCM, cells were permeabilized for 5 min with 0.2% Triton and incubated for 20 min at room temperature with Phalloidin-AlexaFluor®488 (1:40 dilution per $2.0x10^5$ cells, A12379; LifeTechnologies, Porto Salvo, Portugal), previously prepared in a PBS-1% w/v bovine serum albumin (BSA) solution, as described in [19]. This allowed the distinction of the cells actin cytoskeleton (cell per se) from the surrounding cell-attached matrix, when merging brightfield images and the fluorescence images of actin staining on IDEAS® software. To further quantify the PCM area, a specific mask was designed (Supplementary Figure 4.1 D).

Histological Analysis

Human IVD fragments were fixed in 10% neutral buffered formalin, processed for paraffin embedding and 5 μm sectioned in a microtome (Leica). Tissue sections throughout the IVD were stained for Alcian blue/Picrosirius red and analyzed by upright optical microscope (Olympus). For each section, delimitation of the area of the pericellular matrix (either proteoglycan- or collagen-rich) was determined for each cluster using ImageJ software. Around 15 sections were analyzed per donor and values were plotted as frequency distribution of the areas obtained in mm^2, using GraphPad Prism.

Analysis of markers expression by flow cytometry (FC)

Expression of surface markers (Table 4.1) was analyzed by conventional

FC, as described in Supplementary Methods.

Statistical Analysis

Statistical analysis was performed using GraphPad-Prism. All tests used are identified in the respective figure legend (additional details in Supplementary Methods).

Table 4.1: Antibodies used in flow cytometry analysis.

	Function	Fluorochrome	µg/mL	Clone	Catalog #, Manufacturer
Primary antibodies					
IgG$_1$ MAH CD34	Marker for hematopoietic progenitors and vascular endothelial cells.	FITC	2.5:50	581 (Class III)	CD34-581-01, Invitrogen
IgG$_1$ MAH CD45	Hematopoietic lineage- restricted surface marker.	PE	3:50	MEM-28	21270454, ImmunoTools
IgG$_1$ MAH Tie2	NP progenitor cell markers [20].	PE	5:50	83715	FAB3131P, R&D Systems
IgG$_{2a}$ MAH GD2		-	2:50	14.G2a	554272, BD Pharmigen™
IgG$_{1,k}$ MAH CD90	Typical MSCs markers.	APC	5:50	eBio5E10	17-0909-41, eBioscience
IgG$_{2a}$ MAH CD105		FITC	3:50	MEM-226	21271053, ImmunoTools
IgG$_1$ MAH CD73		PE	5:50	AD2	550257, BD Pharmigen™
IgM MAH Stro1		-	10:50	STRO-1	MAB1038, R&D Systems
IgG$_1$ MAH CD146	Marker for vascular endothelial cells, smooth muscle cells, pericytes and MSCs.	AlexaFluor®647	5:50	OJ79c	MCA2141A647T, Bio-Rad
Secondary antibodies					
IgM RAM **IgG RAM**		Biotinylated AlexaFluor®647	1:50 1:500		E 0354, Dako
Isotype controls					
Mouse IgG$_1$		FITC/R-PE	2.5:50		M1FP, Invitrogen
Mouse IgG$_1$		AlexaFluor®647	5:50		MCA928A647, Bio-Rad
Mouse IgG1$_{,k}$		APC	5:50	P3.6.2.8.1	17-4714, eBioscience
Mouse IgG$_{2a}$		FITC	3:50		21275523, ImmunoTools
Mouse IgG$_{2a}$		-	2:50	G155-178	556651, BD Pharmigen™

MAH: Mouse anti-Human; **MSCs:** Mesenchymal Stem Cells; **RAM:** Rabbit anti-Mouse

Results

Sample characterization

To characterize the phenotype of primary hIVD cells from degenerated tissue, a total of 41 samples were collected from patients undergoing microdiscectomy – 24 males and 17 females. All samples were collected from disc levels between L3-S1. The donors age ranged from 18 to 66 years old for males (average of 45 ± 11 years old) and from 25 to 77 years old for females (average of 48 ± 13 years old) (Figure 4.1 A), whereas donors' weight ranged from 69 Kg to 110 Kg for males (average of 86 ± 12 Kg) and from 50 Kg to 90 Kg for females (average of 62 ± 10 Kg) (Figure 4.1 B). The weight of collected tissue ranged from 0.2 g to 5.2 g for males (average of 1.7 ± 1.2 g) and from 0.5 g to 8.0 g for females (average 2.8 ± 2.2 g) (Figure 4.1 C). No correlation was found between tissue weight and donors' age or weight (Figure 4.1 C_1 and C_2, respectively).

From the 41 human samples collected, 36 were digested to obtain the IVD cells to: 1) optimize the protocol for primary cells isolation (n=9), 2) analyse cells morphology (n=9), and 3) study cells phenotype by flow cytometry (n=18, of which 2 were discarded after cell isolation, due to insufficient number of cells to be acquired). The remaining 5 tissue samples were formalin fixed for histological validation of the cell morphology analysis performed by IFC.

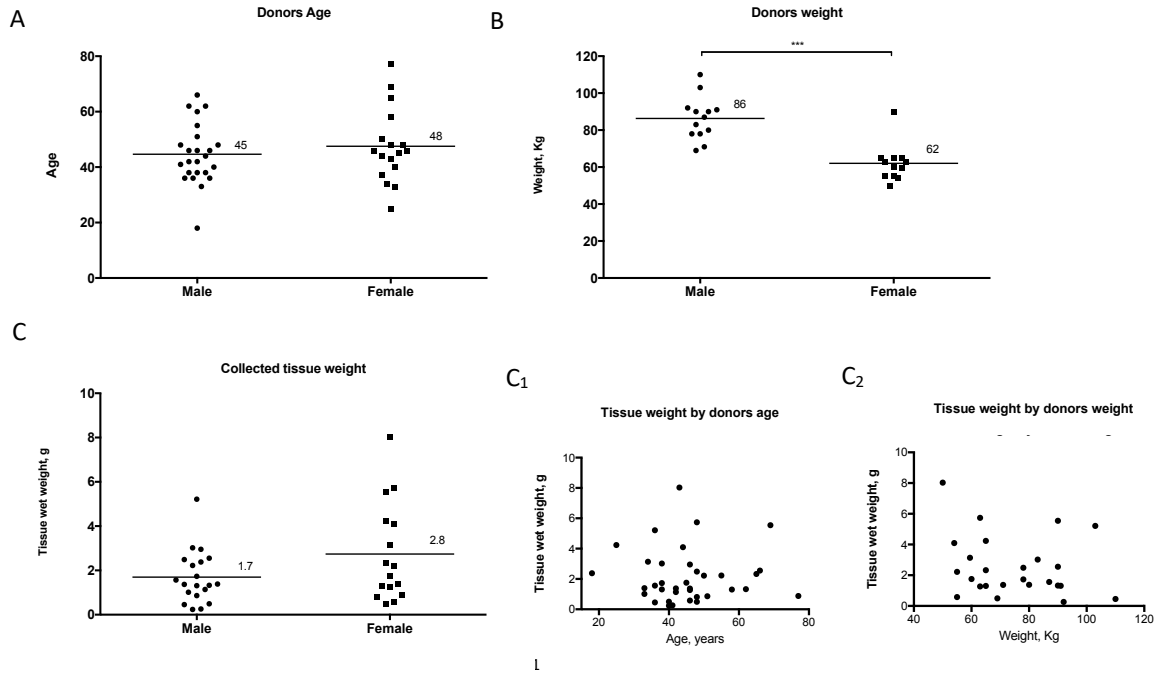

Figure 4.1: Sample characterization. A | Donors age. A total of 41 samples were collected – 24 from male donors and 17 from female donors. **B |** Donors weight by gender. Male donors were heavier than female donors, ***p<0.001 (non-parametric Mann Whitney test). **C |** Collected tissue weight. An average 1.7 g and 2.8 g of tissue was excised from male and female donors, respectively. No correlation was found between collected tissue weight and age **(C_1)** or donors weight **(C_2)**. Line on scattered dot plots presents mean values.

Optimization of cell isolation

Because surgical tissue excised from human degenerated IVDs is normally scarce in cell content, it is important to guarantee that the cell isolation protocol will result in a high yield of viable cells. Three different enzymatic digestion protocols (with Coll-I, -II or -XI, 0.5 mg/ml, overnight) were tested, similarly to what we did previously with bovine NP tissue [19]. Independently of the protocol used, cells viability was always above 90%, as determined by FC (PI negative cells) (Figure 4.2 A). In terms of cell yield, the protocol using Coll-I originated higher cell numbers ((2.6± 2.7) x 10^5 cells/g wet tissue), although no significant differences were detected when comparing to the other protocols used (Coll II:(1.4±1.0) x10^5 and Coll XI:(1.4±0.7) x 10^5 cells/g

wet tissue) (Figure 4.2 B). Thus, subsequent cell isolation procedures were performed using Coll-I. Interestingly, although no correlation was found between the amount of IVD tissue collected from microsurgery and donor age, the cell content (yield) shows a negative correlation (Figure 4.2 C; **p<0.01), suggesting that independently of the isolation method used, age is a heavy counterproductive factor for cell yield.

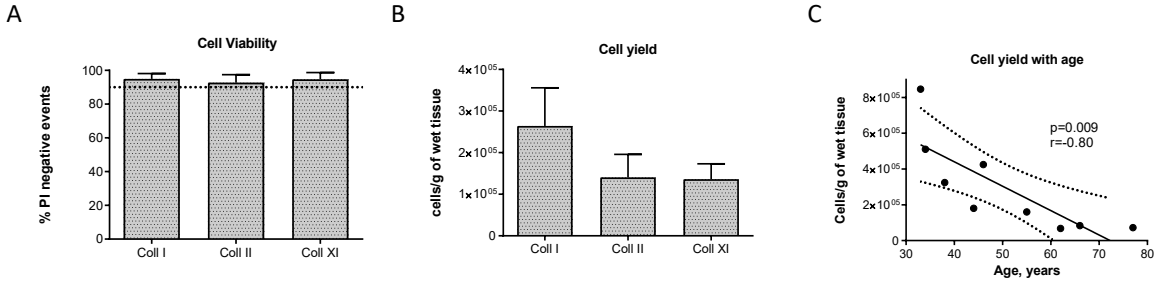

Figure 4.2: Optimization of cell isolation protocol. Three different methods to isolate human primary cells were evaluated, where cells were incubated overnight with either collagenase-type I, -type II or –type XI. **A |** No differences were found in terms of cell viability, as quantified by flow cytometry upon PI staining. All protocols rendered high (>90%) cell viability (Coll I: n=9; Coll II: n=3; Coll XI: n=4). **B |** Tissue overnight digestion with collagenase-type-I allowed the isolation of more cells per g of excised tissue, although this number decreased with donors' age **(C)** (n=9, Pearson r=-0.8, **p<0.01; non-linear regression r^2=0.78). Data on bars are presented as mean ± standard deviation.

Characterization of cellular morphology

In order to characterize the morphology of human degenerated IVD cells, along with its age-related changes, freshly isolated cells were fixed and analyzed by IFC, using masks for brightfield images of cells and for fluorescence images of the cytoskeleton and nuclei (representative analysis tutorial is depicted in Supplementary Figure 4.1).

Analysis of the distribution of the cells diameter with age revealed the presence of small (SC), large (LC) and super large cells (SLC) (Figure 4.3 A), with an average diameter of 16±2 μm, 25±1 μm, and 34±1 μm, respectively (Figure 4.3 B). Representative images of these cells are shown in Supplementary Figure 4.1 C. Overall, the average frequency of SLC (17±14%) was significantly lower (*p<0.05) than the average frequency of SC or LC (39±29% and 43±18%, respectively), although

there was a high variability between donors with ages from 36 to 55 years old. Interestingly, correlation analysis revealed a decrease in SC frequency with age (**p<0.001), while the frequency of LC and SLC increased (**p<0.001 and *p<0.05, respectively) (Figure 4.3 C).

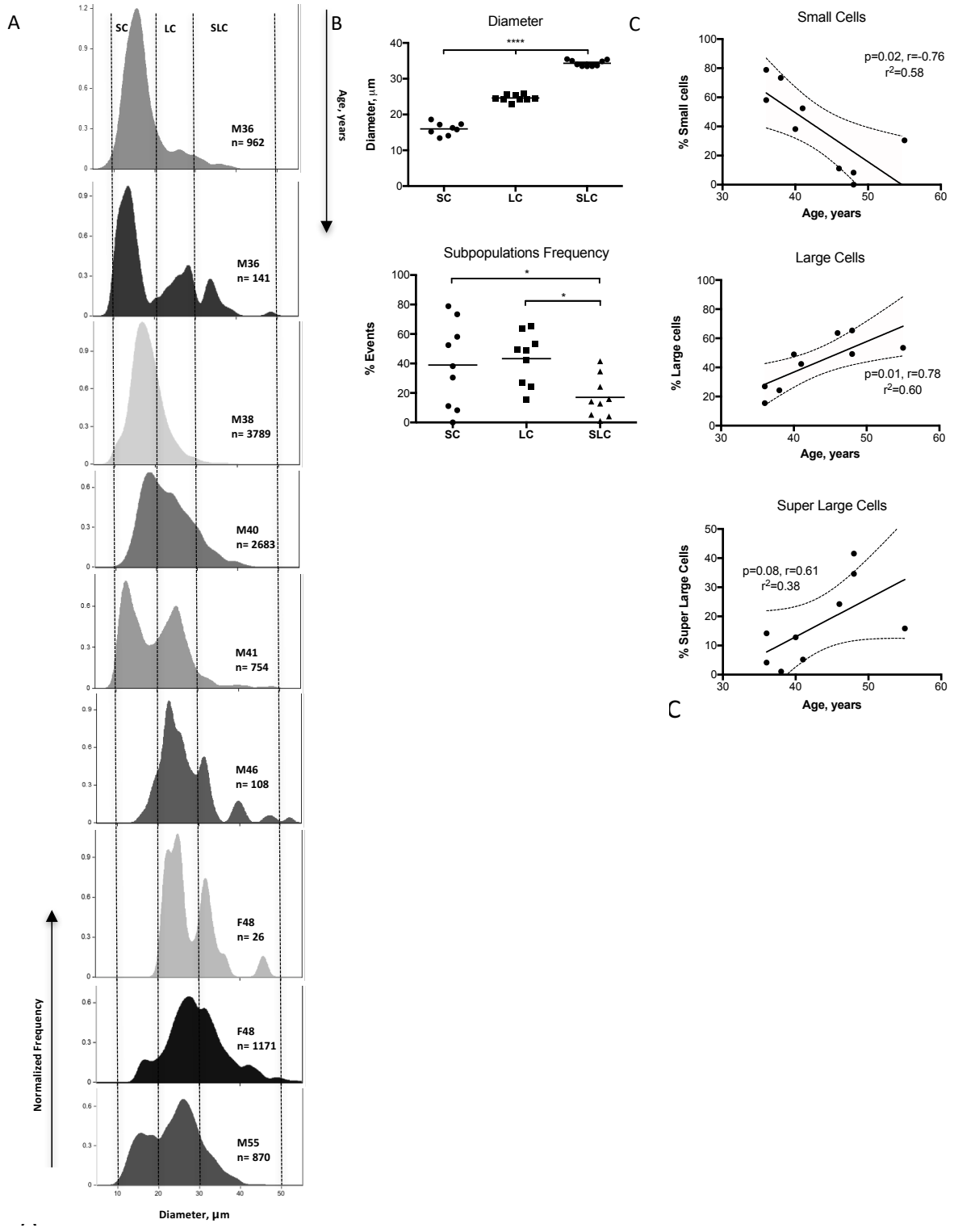

Figure 4.3: The diameter of human IVD cells increases with age. A | Histograms showing the diameter distribution of IVD cells from 9 different donors (left). A shift to the right is visible with increasing age (between 36 (up) and 55 (bottom) years old). Donor age, gender and total number of cells analyzed is indicated on each histogram (bottom right corner). The observation of distinct diameter peaks with

age allowed identification of three cell types based on cells size: Small Cells (SC), Large Cells (LC) and Super Large Cells (SLC). **B |** Average diameter of the gated populations from the same 9 different donors. **C |** Frequency of cells within each gate and its correlation with age. The frequency of cells within SLC population was significantly lower than within SC or LC populations (data analyzed for statistical differences using ordinary one-way ANOVA and Bonferroni's multiple-comparisons test, n=9, *p<0.05, ****p<0.0001). Correlation analysis revealed that SC frequency decreased with age (n=9, one-tailed **p<0.01, Pearson r=-0.76, linear regression r^2=0.58), whereas LC and SLC increased (n=9, one-tailed **p<0.01 and *p<0.05, Pearson r=0.78 and r=0.61, linear regression r^2=0.60 and r^2=0.38, respectively).

The percentage of single and multinucleated events was also quantified for each donor (Figure 4.4 and Supplementary Figure 4.1 B). Interestingly, within the large and SLC populations, the majority of events were single cells: 87±9% and 63±19%, respectively (Figure 4.4 C), although cells had a diameter above 20 µm. Simultaneously, there was no correlation between the prevalence of multinucleated events and age (Figure 4.4 B). Together, these results suggest that the increase on the frequency of LC with age is not due to cell fusion, but is most probably due to an increase of the PCM area surrounding the cells. And indeed, the PCM area of cells within single-SLC population was larger than within the SC (*p<0.05) and single-LC populations (p=0.5) (Figure 4.5).

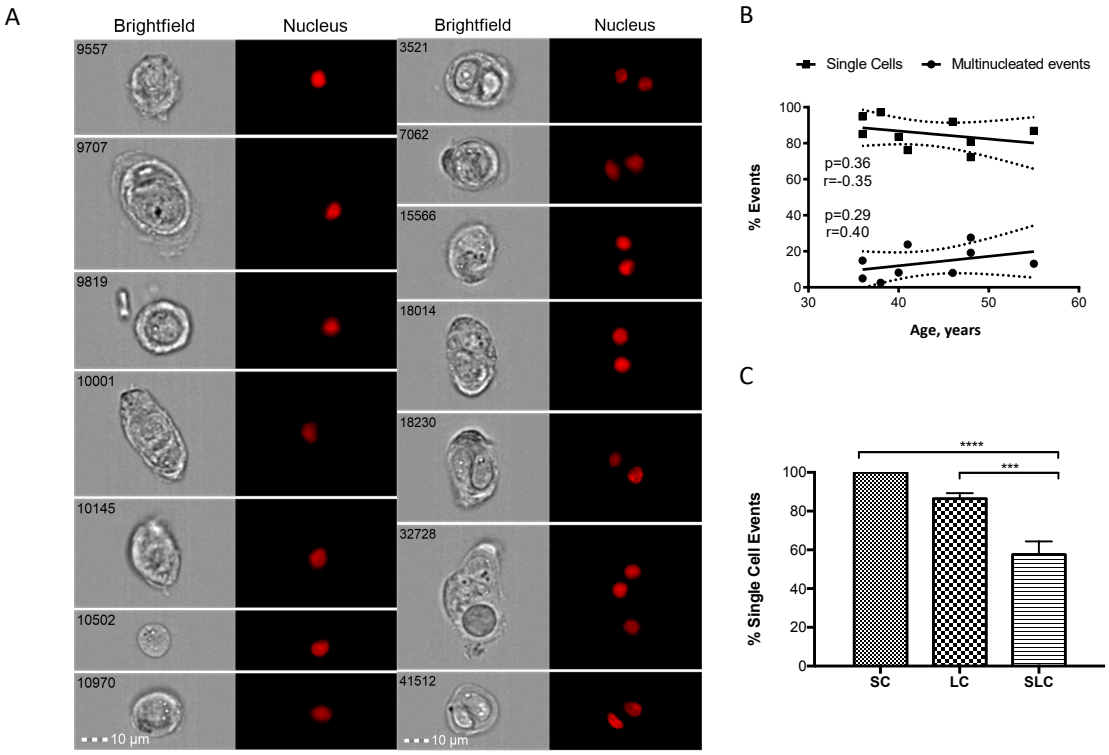

Figure 4.4: Characterization of Large cells. A | Examples of brightfield (left) and fluorescence (right) images of single and multinucleated event and its nuclei. **B |** No correlation between the frequency of single or multinucleated events with age (n=9, p=0.36 and 0.29, respectively). **C |** Quantification of the percentage of single cell events within SC, LC and SLC populations. Only SLC population revealed a significantly lower frequency of single cell events (ordinary one-way ANOVA, Bonferroni's multiple-comparisons test, ***p<0.001, n=9). Hence, LC and SLC (~40%) greater diameter is not necessarily due to cell clustering.

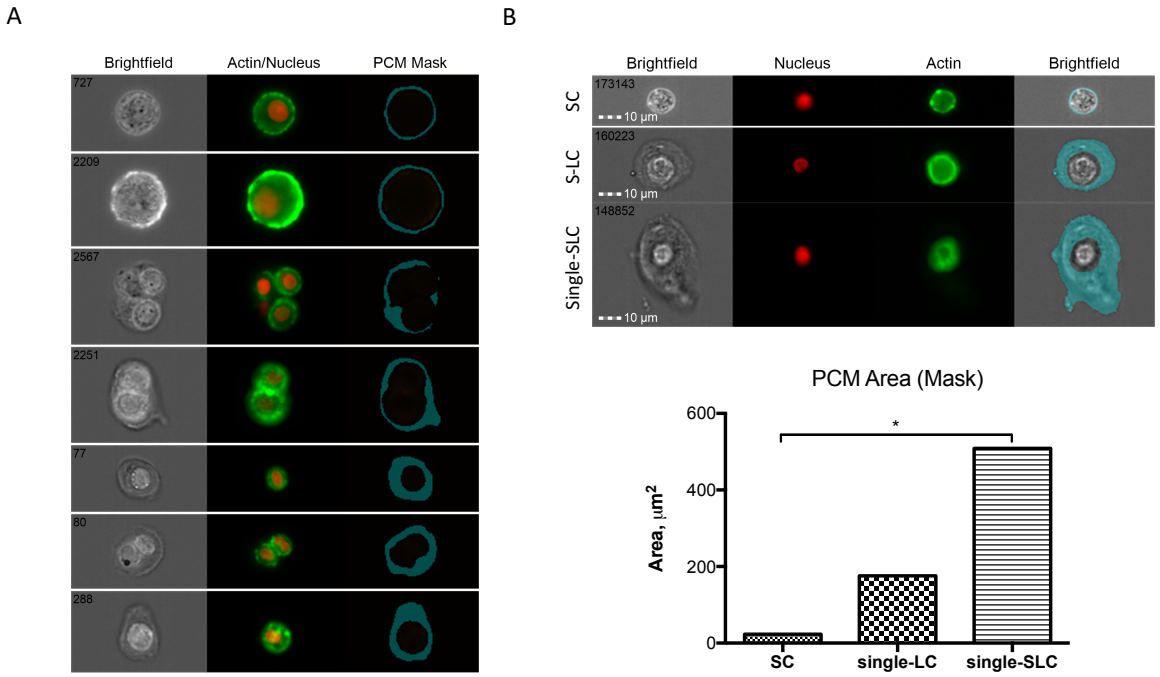

Figure 4.5: Pericellular matrix area quantification. A | Examples of IFC images of IVD cells with various morphologies. The panel shows brightfield images of cells (right), alongside with composite fluorescence images of the respective DRAQ5-stained nuclei and the phalloidin-FITC stained actin (middle). The right column shows the masks (dark green) created to determine the PCM area. Both single- and multinucleated events are surrounded by a PCM. **B |** PCM area was quantified within SC (all were single-cell events), single-LC and single-SLC populations from 3 different donors, with 36, 38 and 41 years old (n=3, Kruskal–Wallis and Dunn's multiple-comparison tests, *p<0.05). LC and SLC cells show an increased diameter due to a greater PCM deposition.

Histological analysis

The morphological analysis performed by IFC was further validated on histological sections of degenerated IVD tissue from 5 donors (ages between 37 and 62 years old), using Alcian blue/Picrosirius red staining, which differentiates the main extracellular components within the tissue, staining collagen in red and proteoglycans in blue, readily allowing the identification of the PCM for each cell cluster. Figure 4.6 A shows the PCM area distribution for the different donors, as quantified from the images represented in Figure 4.6 B, C. This analysis indicates an increase in the prevalence of larger events (corresponding to LC and SLC identified by IFC) with age, especially evident in older donors (60 and 62 years old), accompanied by a decrease in the

frequency of smaller events (SC identified by IFC), resulting in a shift to the right in 60 and 62 years old donor's histograms. This effect on clusters area can be observed in Figure 4.6 B for a younger donor and in Figure 4.6 C for an older donor.

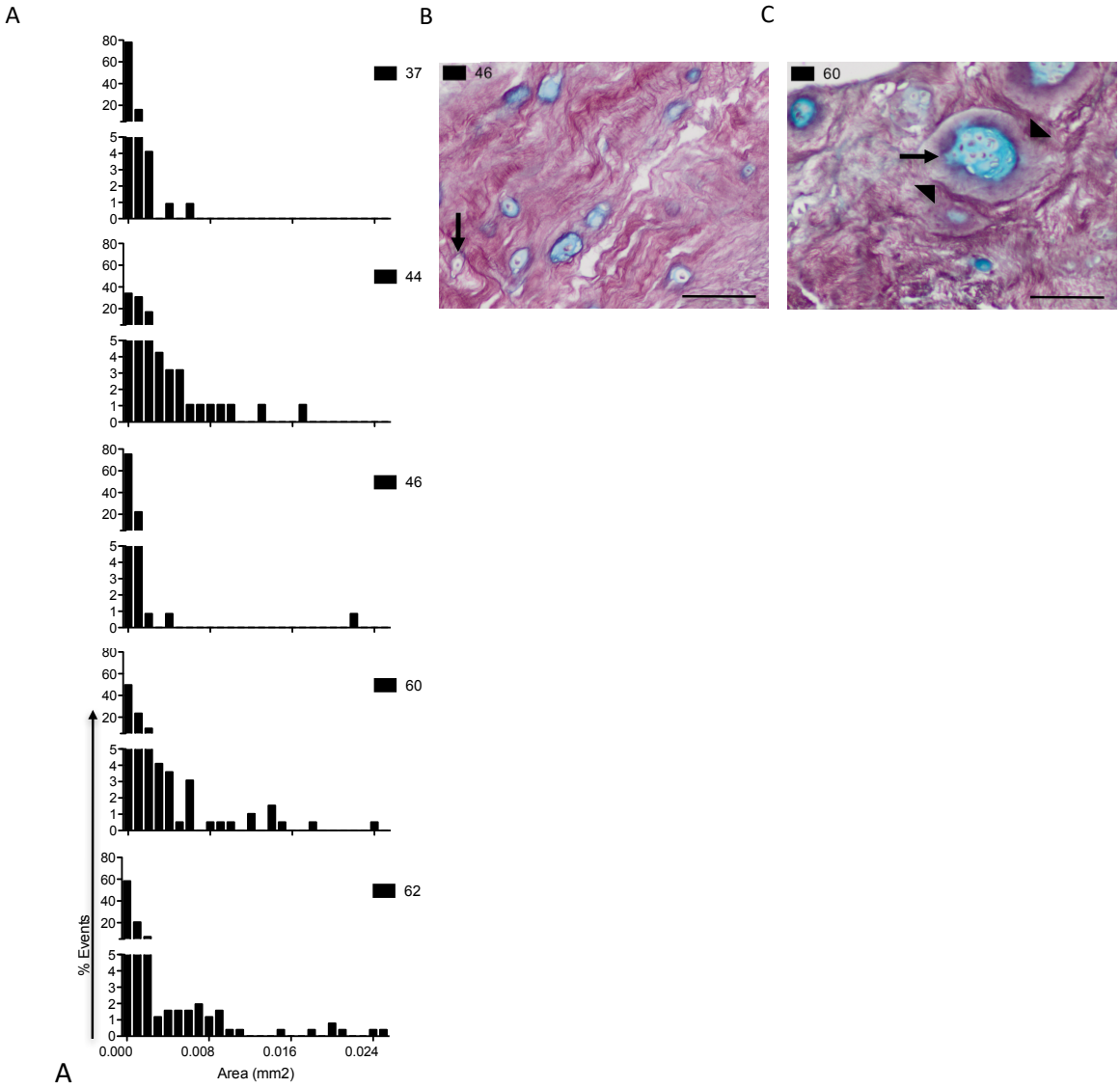

Figure 4.6: Histological analysis of degenerated IVD tissue. A | Histograms showing the distribution of cell clusters area from 5 donors with ages from 37 to 62 years old. There is an increase in the frequency of larger clusters with age. **B, C |** Representative images of Alcian blue/Picrosirius red staining showing small **(B)** and large **(C)** cell clusters producing proteoglycans (Alcian blue) embedded in a collagen matrix (Picrosirius red). In **(B)** a small cell with no PCM (PCM area=0 mm^2) is highlighted (arrow). In **(C)** the proteoglycan-rich pericellular matrix (arrow) is surrounded by a deposition of an outer pericellular collagenous red stained matrix (arrow heads). Scale bars: 100µm.

Analysis of surface markers expression

To assess the correlation between the presence of progenitor-like cells within freshly isolated human IVD cells and aging, expression of 9 surface markers was evaluated (Table 4.1 and Supplementary Figure 4.2). No expression of Tie2, CD45 and CD34 was found, while CD146 expression ranged from 0 to 16%, Stro1 from 0 to 19%, CD90 from 0.3 to 64%, CD73 from 0 to 55%, CD105 from 0 to 17%, and GD2 from 2 to 5% (Figure 4.7 A). A negative correlation was established between the frequency of $CD90^+$ and $CD73^+$ cells and age (Figure 4.7 B, $*p<0.05$), but not for the other markers. These data suggest there is a decrease, but not elimination of progenitor cells with aging. Moreover, seeking to correlate cells size with these markers expression, it was verified that, within the positive events for each marker, there is a smear, containing small and large events, and no distinct subset was found to be more or less prevalent with age (Supplementary Figure 4.3).

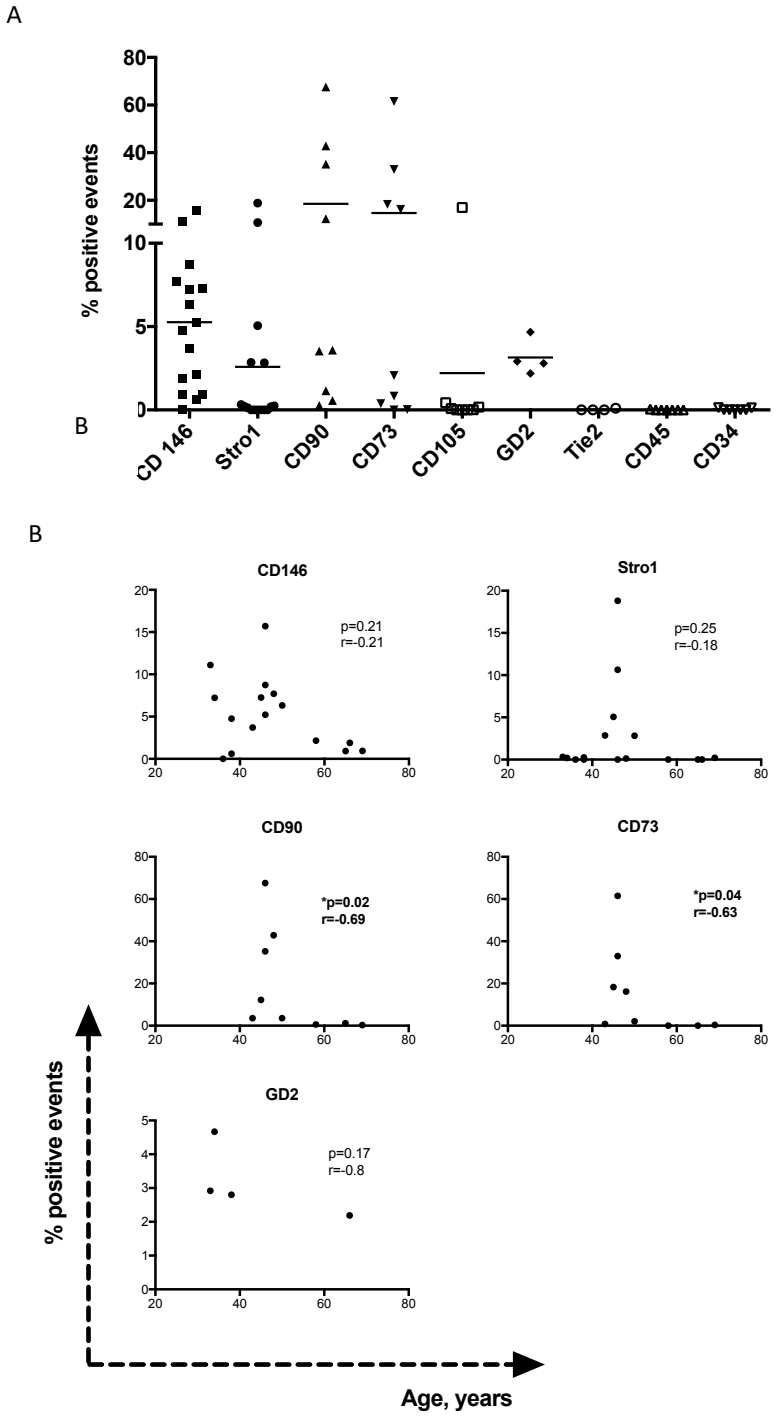

Figure 4.7: Primary human IVD cells phenotype. A | Expression of 9 different cell surface markers. **B |** Age-related changes on the frequency of CD146, Stro1, CD73, CD90 and GD2 positive events. Spearman correlation coefficient analysis revealed a significant decrease of CD90 and CD73 expression with age (n=9, one-tailed *p<0.05, spearman r= -0.69 and r=-0.63, respectively).

Discussion

The aim of this study was to take advantage of available surgical material from microdiscectomy procedures, which in normal circumstances would be discarded as surgical waste, to characterize how IVD degenerated tissue changes with aging. Hence, the material was not collected for research purposes, but as a necessary therapy for the donor. Moreover, in a typical microdiscectomy performed to treat a disc herniation through a posterior approach, at best 30% of the entire disc can be obtained. Indeed, although in anterior and lateral approaches the quantity of material collected may be larger, these are not so common. Nevertheless, the tissue collected was quite homogeneous and representative of the whole degenerated IVD.

Cell isolation techniques should be standardized in order to avoid variability between different studies. Enzymatic digestion is a common procedure to isolate IVD cells, but cell yield is rarely reported, and cells are often expanded in culture prior to FC analysis of cells phenotype [18, 21, 22]. Moreover, pronase pre-treatment is many times applied, not preserving cells with its PCM attached [23]. Here we apply an improved and inexpensive method to efficiently isolate primary hIVD cells, which could be further adopted by other researchers in this field. Of note, a clear negative correlation between cell yield and donor age is evident, supporting previous histological observations on IVD cell depopulation [3].

Morphology of IVD cells was assessed using IFC, a technique that provides high-resolution images of thousands of cells in flow. A clear shift on the distribution of the cells diameter occurred with aging, with a decrease in the frequency of small cells and an increase with that of larger cells. The enlarged cell morphology was due to an increase in the PCM area (Figure 4.5). This effect was previously reported for chondrons in osteoarthritic cartilage [24, 25] and proven to be a consequence of matrix synthesis and/or deposition rather than due to an increase in cell hydration [26]. Theoretically, this alteration may occur following an inflammatory stimulus (e.g. Interleukine-1 [IL-1] exposure), that triggers metalloproteinases (MMPs) upregulation, initiating the destruction of fibrilar collagens around the chondrocyte (diminishing its tensile capacity), while the high intrinsic concentrations of pericellular aggrecan and

hyaluronan ensures the hydrodynamic expansion of the chondron [5]. Of note, even though formation of cell clusters has been previously associated with age and degeneration, we did not find a significant correlation between the frequency of multinucleated events and donors age [27-29]. Histological data validated the results from IFC (Figure 4.6), although a discrepancy in cells size was detected. The maximum area value quantified for cells in flow (from brightfield images of cells with its attached PCM) was about 0.002 mm^2, whereas in the tissue some larger events had a PCM area (including attached collagens and aggrecan) as great as 0.024 mm^2. Nevertheless, this result is in accordance with previous studies using enzymatic digestion to isolate chondrocytes, where the PCM was shown to be substantially reduced in size, due to a loss of some enzyme-sensitive PCM components, such as aggrecan, type II collagen, fibronectin and hyaluronic acid [30-33]. However, chondrocytes enhanced viability, and particularly that of chondrons, when compared to alternative isolation methods, makes enzymatic digestion a better choice [34].

To better understand the consequences of aging on IVD cells, expression of markers for progenitor and inflammatory cells was assessed. Interestingly, the percentage of cells expressing CD73, CD90 were a reflection of age. These findings reinforce previous reports stating that, although mature IVDs may endogenously count on a progenitor cell population [13, 35], its gradual disappearance with aging and degeneration may dictate a limitation in time for its activation [18, 36]. Overall, our results are in accordance to a previous report [30], showing low expression (<1%) of CD105 on primary unexpanded cells from degenerated IVD tissue. As for Stro1, while a low expression profile (<5%) was expected, even in younger individuals [13, 35], here we found some young donors with high $Stro1^+$ numbers (~20%), and others with no expression at all. However, no correlation with age, gender or weight could be determined, that could explain these results. Additionally, CD90 and CD73 expression, which was always below 40% (with the exception of one 46 years old donor, also showing higher expression of CD105, CD146 and Stro1), is different from other studies, where MSC classical markers (including CD105) were expressed by nearly 90% of cells [11, 12, 14, 15]. Nevertheless, in all those studies, cells were expanded prior to acquisition, which might have induced phenotypic alterations, as reported to

occur with articular chondrocytes [37, 38], mouse bone marrow derived MSC precursors [39], and rabbit AF and NP cells [40]. Moreover, Tie2 was not detected, even though others have found around 10% expression in three out of four donors (33-66 years old) [18]. Again, cells were not expanded in this study and the isolation procedure was not the same. Additionally, for GD2 expression, an average 3% expression was detected (n=4, 33-66 years old), whereas others reported only 1% expression in primary hNP cells [18]. We cannot guarantee that these $GD2^+$ are exclusively located in the NP, explaining why we were able to detect higher percentages of these progenitor cell markers in IVD surgical samples (NP+AF tissue). CD146 was also detected in the great majority of samples analysed. We have previously showed that two cell-subsets within the heterogeneous bovine NP cell population were enriched in $CD146^+$ [19]. This protein has been suggested as a marker for endothelial cells, melanoma cells, and MSCs. Interestingly, sorted $CD146^+$ cells isolated from late-stage osteoarthritic knee joints showed high potential of clonogenecity and multi-differentiation, while expressing high levels of MSC-specific surface antigens. Moreover, when compared to adipose-derived MSCs (ADMSCs) and unsorted chondrocytes, this subpopulation showed higher chondrogenesis capacity [41], revealing a pool of chondroprogenitors within the diseased tissue. In contrast, recent work showed that $CD146^+$ were not capable of multipotent differentiation, and were committed to express a contractile phenotype [42]. However, besides distinct species and cell isolation methods used, culture conditions were also different (one-week expansion in normoxia vs three-weeks expansion in hypoxia). Importantly, the frequency of $CD146^+$ cells found herein (0-16%, n=16, mean 6.5%) was much higher than that found in the OA knee (0.01-2.12%, n=6) [41]. We will address the functional characterization of hIVD $CD146^+$ cells in the near future.

In summary, we were able to accurately distinguish three subsets of hIVD cells based on their different sizes, whose frequencies varied significantly with age. Younger individuals showed higher prevalence of small cells (diameter below 20 μm), whereas older donors had more large cells (diameter above 20 μm). Finally, the analysis of specific surface markers expression lead to identification of $CD146^+$ cells within IVD degenerated samples, which supported even further the hypothesis that the

aged/diseased IVD may still have an intrinsic self-repairing potential.

Acknowledgments

This work had the financial support of FCT/MEC through National Funds and, when applicable, co-financed by the FEDER via the PT2020 Partnership Agreement under the 4293 Unit I&D and through European Union funds - Projetos Estruturados de I&D&I - Norte-01-0145-FEDER-000012, Portugal. The authors would like to acknowledge FCT (Fundação para a Ciência e Tecnologia) for funding M.M. Ph.D. grant (SFRH/BD/80577/2011), C.C. Post-Doc grant (SFRH/BDP/87071/2012) and R.M.G. FCT Investigator Starting Grant (IF/00638/2014). The authors also thank María Gómez Lázaro, Principal Technician from the Bioimaging Centre for Biomaterials and Regenerative Therapies (*b.IMAGE*) at i_3S, for the technical hints on Imaging Flow Cytometry data acquisition and analysis, and to Catarina Leitão, from the Translational Cytometry Unit at i_3S, for the continuous support on conventional flow cytometry procedures.

Ethics approval and consent to participate

This study was approved by the Ethical Committee for Health of Hospital de São João, Porto, Portugal, on the 29th September 2011. No reference number was attributed to this process by the mentioned ethical body, as can be verified in the original document uploaded as an additional file together with this manuscript.

SUPPLEMENTARY INFORMATION

Published in Spine (Phila Pa 1976). 2017 Jul 3

Supplementary Methods

Human IVD cell isolation: Briefly, tissue was collected in Dulbecco's modified Eagle's medium (DMEM; 21885 Gibco), supplemented with 10% v/v penicillin–streptomycin (P/S, PAA Laboratories GmbH) and 20% v/v amphotericin B (Amph-B, PAA). Within 3h upon collection, tissue was digested in DMEM supplemented with 5% P/S, 10% Amph-B, 2.5% (v/v) HEPES buffer 1mM (Lonza), 1.5% (v/v) NaCl 5 M and KCl 0.4 M solution (to adjust osmolarity to 400 mOsm), 1.3 U/mL DNAse, and one of three different enzymatic formulations: collagenase-type-I (Coll I), collagenase-type-II (Coll II), or collagenase-type-XI (Coll XI) (C0130, C6885, and C7657, respectively, Sigma Aldrich), at 0.5 mg/mL. All enzymatic preparations contain a mixture of the type I and II forms of the purified collagenase enzyme, differing in their affinity for different substrates as assessed by the manufacturer (www.sigmaaldrich.com/life-science/metabolomics/enzyme-explorer/learning-center/collagenase-guide.html). Tissue/medium ratio was set at 10% w/v to prevent the pH dropping below 6.8 during incubation. Tissue was digested overnight, in a humidified atmosphere at 37°C/5% CO_2, and under gentle stirring. ECM contaminants were filtered with a 70 µm cell strainer.

Analysis of surface markers expression by flow cytometry: Cells were first left to recover from digestion for 30 min in a humidified atmosphere at 37°C/5% CO_2, and then washed with PBS-2% fetal bovine serum (FBS), prior to incubation with primary antibodies (Table 4.1), in the same solution, for 1h at 4°C. In the case of non-conjugated anti-Stro1 antibody, cells were, in addition, incubated with a secondary rabbit anti-mouse-Biotinylated antibody, for 30 min at RT, washed again with PBS-2%FBS and additionally incubated with Streptavidin-APC (BD Pharmigen, #554067; dilution 1:1000) for 10 min at RT. After labeling, cells were washed with 2 mL PBS-2% FBS, fixed in 1% w/v paraformaldehyde (PFA) solution and run in a FACSCanto II within 24h. Results were analyzed with FlowJo software, Version 8.7. Supplementary Figure 4.2 shows representative dot plots from flow cytometry analysis of surface markers expression.

Statistical Analysis: D'Agostino and Pearson omnibus normality test was used to assess Gaussian distribution of data. Results that did not follow a normal distribution were analyzed for statistical differences using non-parametric Mann-Whitney test (donors age and weight by gender) or Kruskal–Wallis and Dunn's multiple-comparison test (cell viability and yield, surface markers expression and PCM Area). When results followed a Gaussian distribution (collected tissue weight by gender and frequency of single events within LC and SLC gates) an unpaired t test was applied. Finally, cells diameter and SC, LC, SLC populations frequency followed a Gaussian distribution, for which groups were compared using ordinary one-way ANOVA (Bonferroni's multiple-comparisons test). In all cases, a confidence level of at least 95% ($*p < 0.05$) was considered. Correlations with age were analyzed using the Spearman correlation coefficient for non-parametric data (surface markers expression), and the Pearson correlation coefficient for parametric data (cell yield, frequency of SC, LC, SLC, and single and multinucleated events). Data is plotted as linear correlation (straight line) ± 5% confidence intervals (dashed curves), also presenting the assigned correlation coefficient "r" and p value.

Supplementary Figures

A – LIVE CELLS GATING

1) Gate DRAQ5 positive events

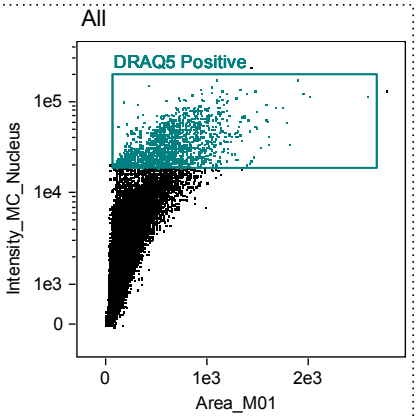

Area_M01, Intensity_MC_Nucleus

Population	Count	%Gated
All	86266	100
DRAQ5 Positive	1618	1.88

2) Gate Focused events

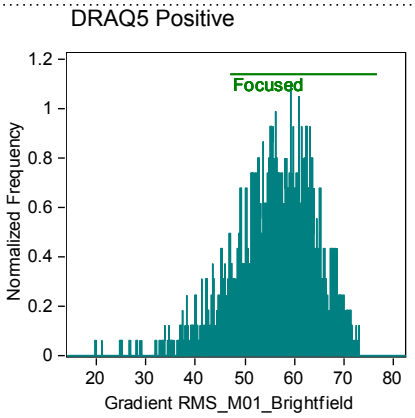

Gradient RMS_M01_Brightfield

Population	Count	%Gated
DRAQ5 Positive	1618	100
Focused & DRAQ5 Positive	1403	86.7

3) Gate focused-nuclei events

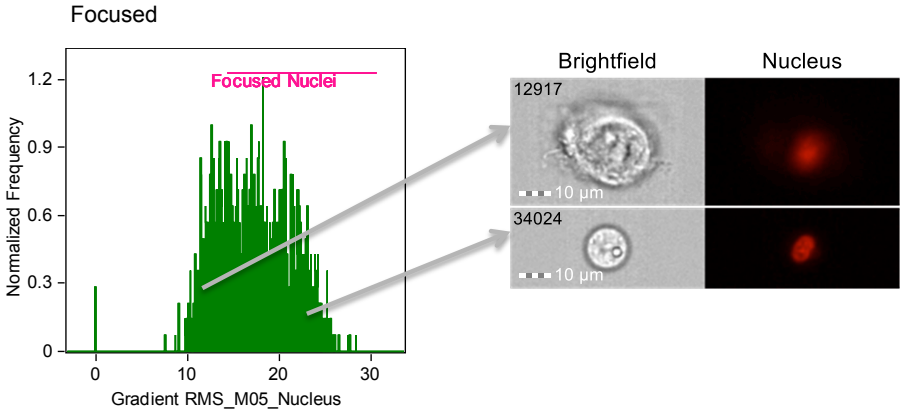

Gradient RMS_M05_Nucleus

Population	Count	%Gated
Focused & DRAQ5 Positive	1403	100
Focused Nuclei & Focused &...	977	69.6

B – SINGLE AND MULTINUCLEATED EVENTS GATING

1) Nuclei mask and "Nuclei Number" feature

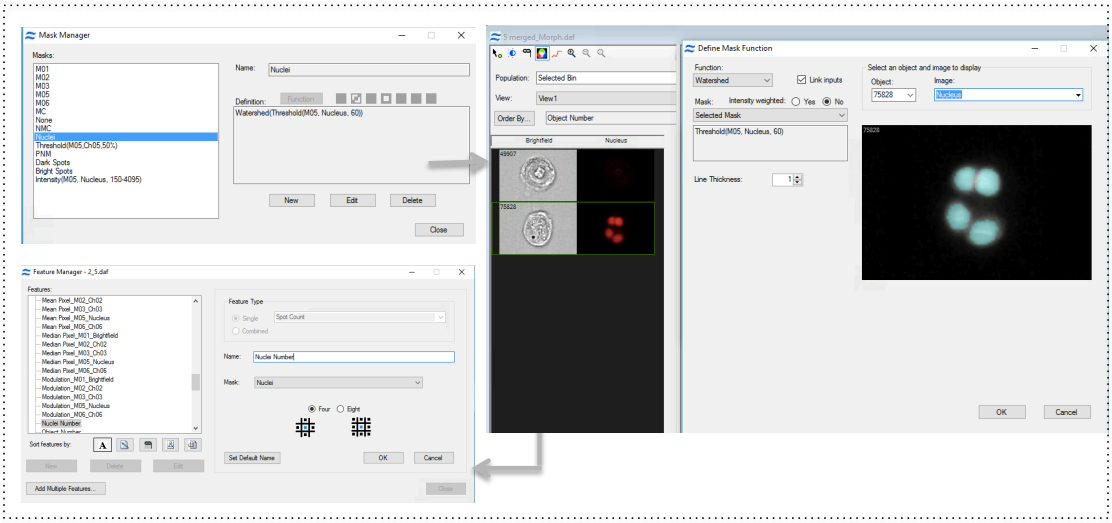

2) Single and Multinucleated events

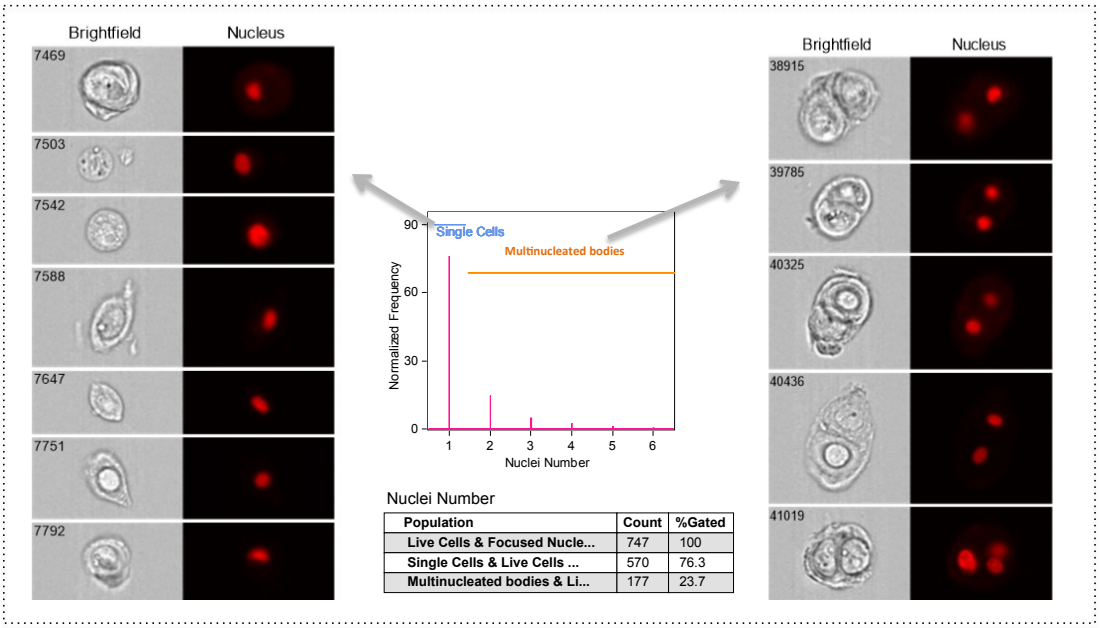

Nuclei Number

Population	Count	%Gated
Live Cells & Focused Nucle...	747	100
Single Cells & Live Cells ...	570	76.3
Multinucleated bodies & Li...	177	23.7

C – DIAMETER GATING

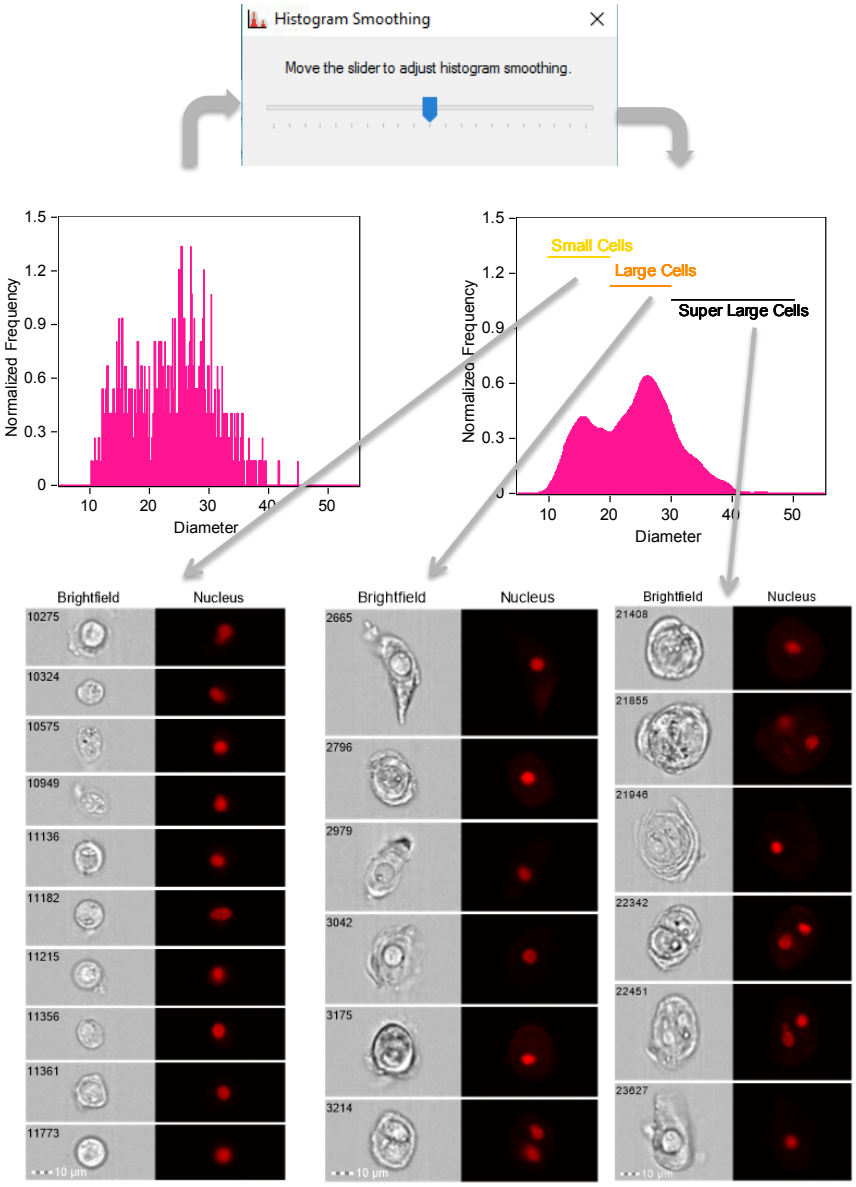

Population	Count	%Gated	Mean	Std. Dev.
Live Cells & Focused Nucle...	747	100	23.78	6.661
Small Cells & Live Cells &...	234	31.3	15.82	2.392
Large Cells & Live Cells &...	388	51.9	25.42	2.659
Super Large Cells & Live C...	123	16.5	33.69	2.855

D – PERICELLULAR MATRIX MORPHOLOGY

PCM mask and "PCM Area" feature

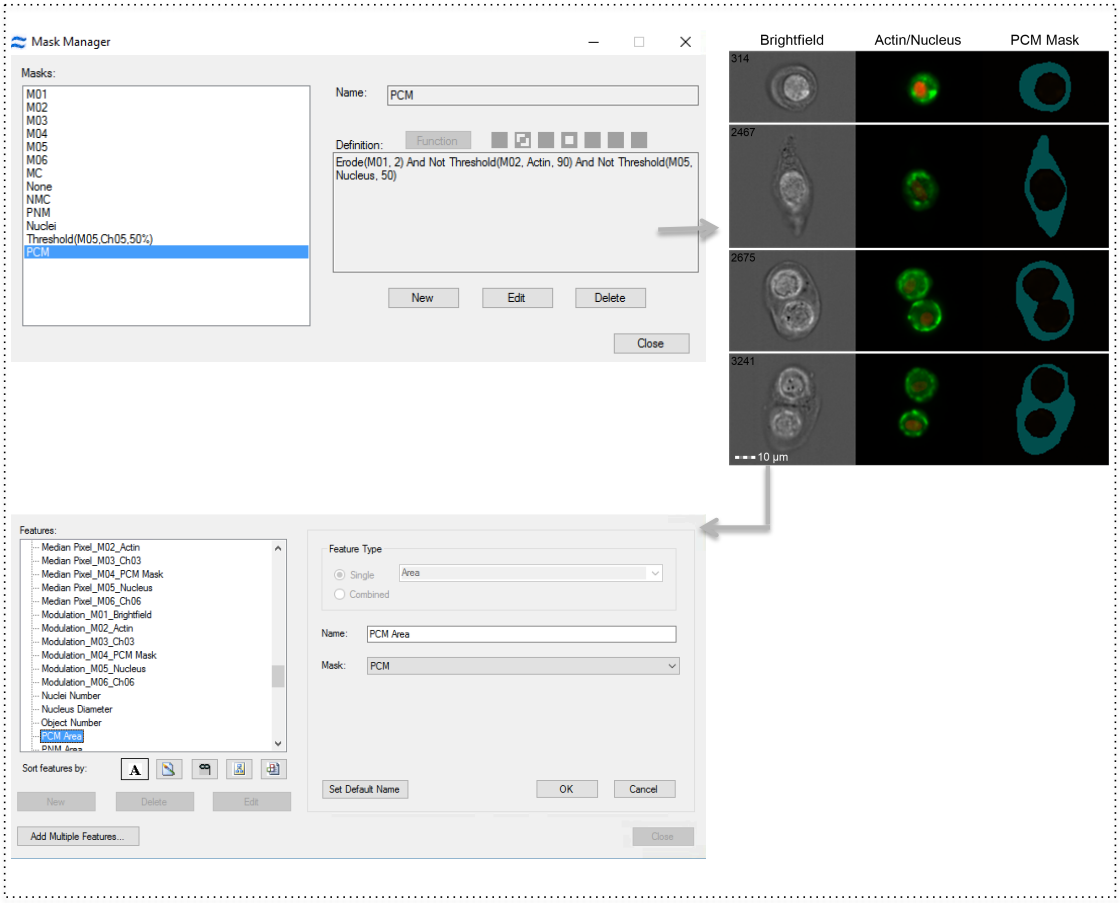

Supplementary Figure 4.1: Imaging flow cytometry morphological analysis flow chart. A | Live cells gating procedure. **B |** Gating of single and multinucleated events, by creating mask for cells nuclei and a feature to calculate the number of nuclei within each live cell. **C |** Diameter histogram analysis, smoothing, and subpopulations fractioning by cell size in Small Cells (SC), Larger Cells (LC) and Super Large Cells (SLC). **D |** Pericellular Matrix morphology analysis by creating specific mask based on the subtraction of nuclei and actin fluorescent images from brightfield images of whole cells, and a feature to calculate PCM area.

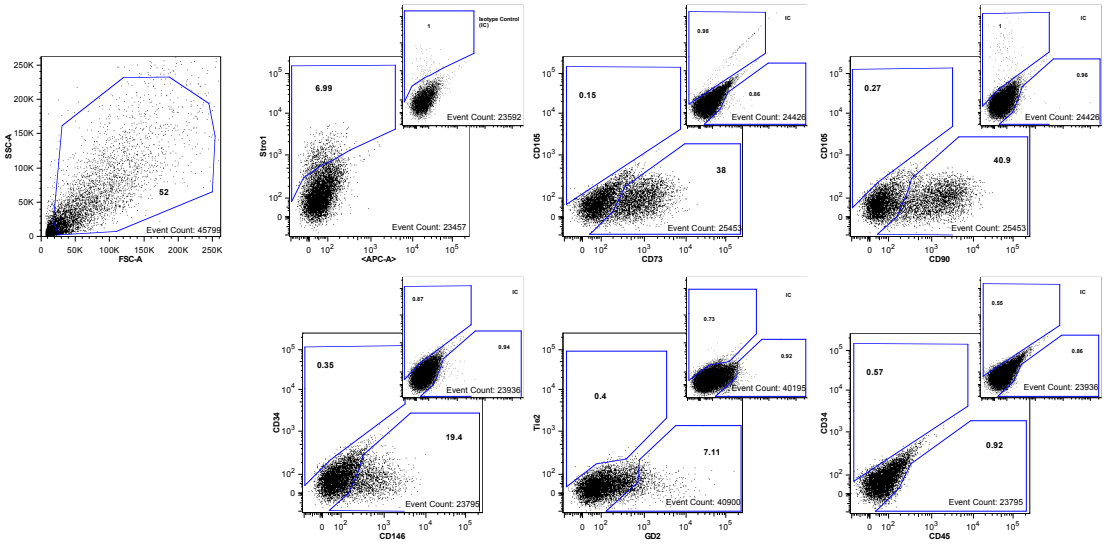

Supplementary Figure 4.2: Representative dot plots from conventional flow cytometry analysis of Stro1, CD146, CD90, CD73 and GD2 surface markers expression.

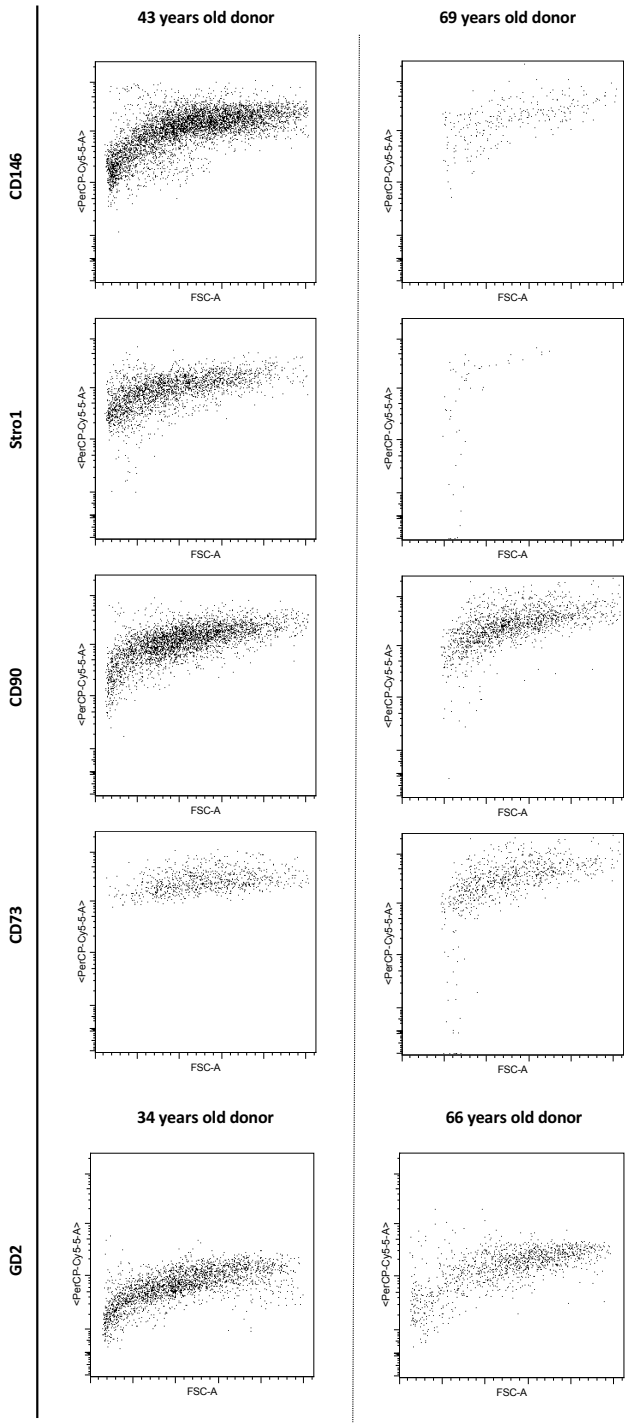

Supplementary Figure 4.3: Representative dot plots of Stro1, CD146, CD90, CD73 and GD2 positive events plotted as PerCp-Cy5-5-A/FSC-A (unused fluorochrome), to evaluated cells distribution regarding their auto-fluorescence. A smear is detected for all markers, hampering the distinction of different cell subsets.

References

[1] Sakai, D. and G.B. Andersson (2015) *Stem cell therapy for intervertebral disc regeneration: obstacles and solutions.* Nat Rev Rheumatol, 11(4): p. 243-56.

[2] Roberts, S., S. Ayad, and P.J. Menage (1991) *Immunolocalisation of type VI collagen in the intervertebral disc.* Annals of the rheumatic diseases, 50(11): p. 787-91.

[3] Trout, J.J., J.A. Buckwalter, and K.C. Moore (1982) *Ultrastructure of the human intervertebral disc: II. Cells of the nucleus pulposus.* Anat Rec, 204(4): p. 307-14.

[4] Gruber, H.E. and E.N. Hanley, Jr. (2002) *Ultrastructure of the human intervertebral disc during aging and degeneration: comparison of surgical and control specimens.* Spine (Phila Pa 1976), 27(8): p. 798-805.

[5] Poole, C.A. (1997) *Articular cartilage chondrons: form, function and failure.* J Anat, 191 (Pt 1): p. 1-13.

[6] Roberts, S., J. Menage, V. Duance, S. Wotton, and S. Ayad (1991) *1991 Volvo Award in basic sciences. Collagen types around the cells of the intervertebral disc and cartilage end plate: an immunolocalization study.* Spine (Phila Pa 1976), 16(9): p. 1030-8.

[7] Youn, I., J.B. Choi, L. Cao, L.A. Setton, and F. Guilak (2006) *Zonal variations in the three-dimensional morphology of the chondron measured in situ using confocal microscopy.* Osteoarthritis and cartilage / OARS, Osteoarthritis Research Society, 14(9): p. 889-97.

[8] Cao, L., F. Guilak, and L.A. Setton (2007) *Three-dimensional morphology of the pericellular matrix of intervertebral disc cells in the rat.* Journal of anatomy, 211(4): p. 444-52.

[9] Kvist, A.J., A. Nystrom, K. Hultenby, T. Sasaki, J.F. Talts, et al. (2008) *The major basement membrane components localize to the chondrocyte pericellular matrix--a*

cartilage basement membrane equivalent? Matrix biology : journal of the International Society for Matrix Biology, 27(1): p. 22-33.

[10] Vonk, L.A., B.Z. Doulabi, C. Huang, M.N. Helder, V. Everts, et al. (2010) *Preservation of the chondrocyte's pericellular matrix improves cell-induced cartilage formation.* Journal of cellular biochemistry, 110(1): p. 260-71.

[11] Blanco, J.F., I.F. Graciani, F.M. Sanchez-Guijo, S. Muntion, P. Hernandez-Campo, et al. (2010) *Isolation and characterization of mesenchymal stromal cells from human degenerated nucleus pulposus: comparison with bone marrow mesenchymal stromal cells from the same subjects.* Spine (Phila Pa 1976), 35(26): p. 2259-65.

[12] Feng, G., X. Yang, H. Shang, I.W. Marks, F.H. Shen, et al. (2010) *Multipotential differentiation of human anulus fibrosus cells: an in vitro study.* J Bone Joint Surg Am, 92(3): p. 675-85.

[13] Brisby, H., N. Papadimitriou, C. Brantsing, P. Bergh, A. Lindahl, et al. (2013) *The presence of local mesenchymal progenitor cells in human degenerated intervertebral discs and possibilities to influence these in vitro: a descriptive study in humans.* Stem Cells Dev, 22(5): p. 804-14.

[14] Huang, B., L.T. Liu, C.Q. Li, Y. Zhuang, G. Luo, et al. (2012) *Study to determine the presence of progenitor cells in the degenerated human cartilage endplates.* Eur Spine J, 21(4): p. 613-22.

[15] Risbud, M.V., A. Guttapalli, T.T. Tsai, J.Y. Lee, K.G. Danielson, et al. (2007) *Evidence for skeletal progenitor cells in the degenerate human intervertebral disc.* Spine, 32(23): p. 2537-44.

[16] Vo, N.V., R.A. Hartman, P.R. Patil, M.V. Risbud, D. Kletsas, et al. (2016) *Molecular mechanisms of biological aging in intervertebral discs.* J Orthop Res, 34(8): p. 1289-306.

[17] Power, K.A., S. Grad, J.P. Rutges, L.B. Creemers, M.H. van Rijen, et al. (2011) *Identification of cell surface-specific markers to target human nucleus pulposus cells:*

expression of carbonic anhydrase XII varies with age and degeneration. Arthritis Rheum, 63(12): p. 3876-86.

[18] Sakai, D., Y. Nakamura, T. Nakai, T. Mishima, S. Kato, et al. (2012) *Exhaustion of nucleus pulposus progenitor cells with aging and degeneration of the intervertebral disc.* Nat Commun, 3: p. 1264.

[19] Molinos, M., C.R. Almeida, R.M. Goncalves, and M.A. Barbosa (2015) *Improvement of Bovine Nucleus Pulposus Cells Isolation Leads to Identification of Three Phenotypically Distinct Cell Subpopulations.* Tissue Eng Part A, 21(15-16): p. 2216-27.

[20] Risbud, M.V., Z.R. Schoepflin, F. Mwale, R.A. Kandel, S. Grad, et al. (2015) *Defining the phenotype of young healthy nucleus pulposus cells: recommendations of the Spine Research Interest Group at the 2014 annual ORS meeting.* J Orthop Res, 33(3): p. 283-93.

[21] Tang, X., L. Jing, W.J. Richardson, R.E. Isaacs, R.D. Fitch, et al. (2016) *Identifying molecular phenotype of nucleus pulposus cells in human intervertebral disc with aging and degeneration.* J Orthop Res, 34(8): p. 1316-26.

[22] Turner, S., B. Balain, B. Caterson, C. Morgan, and S. Roberts (2014) *Viability, growth kinetics and stem cell markers of single and clustered cells in human intervertebral discs: implications for regenerative therapies.* Eur Spine J, 23(11): p. 2462-72.

[23] Kuettner, K.E., V.A. Memoli, B.U. Pauli, N.C. Wrobel, E.J. Thonar, et al. (1982) *Synthesis of cartilage matrix by mammalian chondrocytes in vitro. II. Maintenance of collagen and proteoglycan phenotype.* J Cell Biol, 93(3): p. 751-7.

[24] Poole, C.A., A. Matsuoka, and J.R. Schofield (1991) *Chondrons from articular cartilage. III. Morphologic changes in the cellular microenvironment of chondrons isolated from osteoarthritic cartilage.* Arthritis Rheum, 34(1): p. 22-35.

[25] Lee, G.M., T.A. Paul, M. Slabaugh, and S.S. Kelley (2000) *The incidence of enlarged chondrons in normal and osteoarthritic human cartilage and their relative matrix density.* Osteoarthritis Cartilage, 8(1): p. 44-52.

[26] Lee, G.M. and R.F. Loeser (1998) *Interactions of the chondrocyte with its pericellular matrix*
. Cells and Materials, 8: p. 135-149.

[27] Ciapetti, G., D. Granchi, V. Devescovi, E. Leonardi, T. Greggi, et al. (2012) *Ex vivo observation of human intervertebral disc tissue and cells isolated from degenerated intervertebral discs.* European spine journal : official publication of the European Spine Society, the European Spinal Deformity Society, and the European Section of the Cervical Spine Research Society, 21 Suppl 1: p. S10-9.

[28] Sharp, C.A., S. Roberts, H. Evans, and S.J. Brown (2009) *Disc cell clusters in pathological human intervertebral discs are associated with increased stress protein immunostaining.* European spine journal : official publication of the European Spine Society, the European Spinal Deformity Society, and the European Section of the Cervical Spine Research Society, 18(11): p. 1587-94.

[29] Melrose, J. (2016) *A Global Pictorial Assessment of the Intervertebral Disc Cell in Several Species Reveals a Remarkable Biodiversity in this Cell Type which should be taken into Account in Experimental Studies on Intervertebral Disc Repair.* Spine Research, 2(1:13): p. 1-14.

[30] Lee, G.M., C.A. Poole, S.S. Kelley, J. Chang, and B. Caterson (1997) *Isolated chondrons: a viable alternative for studies of chondrocyte metabolism in vitro.* Osteoarthritis Cartilage, 5(4): p. 261-74.

[31] Knight, M.M., J.M. Ross, A.F. Sherwin, D.A. Lee, D.L. Bader, et al. (2001) *Chondrocyte deformation within mechanically and enzymatically extracted chondrons compressed in agarose.* Biochim Biophys Acta, 1526(2): p. 141-6.

[32] Hing, W.A., A.F. Sherwin, and C.A. Poole (2002) *The influence of the pericellular microenvironment on the chondrocyte response to osmotic challenge.* Osteoarthritis Cartilage, 10(4): p. 297-307.

[33] Wang, Q.G., A.J. El Haj, and N.J. Kuiper (2008) *Glycosaminoglycans in the pericellular matrix of chondrons and chondrocytes.* J Anat, 213(3): p. 266-73.

[34] Ross, J.M., A.F. Sherwin, and C.A. Poole (2006) *In vitro culture of enzymatically isolated chondrons: a possible model for the initiation of osteoarthritis.* J Anat, 209(6): p. 793-806.

[35] Henriksson, H., M. Thornemo, C. Karlsson, O. Hagg, K. Junevik, et al. (2009) *Identification of cell proliferation zones, progenitor cells and a potential stem cell niche in the intervertebral disc region: a study in four species.* Spine, 34(21): p. 2278-87.

[36] Yasen, M., Q. Fei, W.C. Hutton, J. Zhang, J. Dong, et al. (2013) *Changes of number of cells expressing proliferation and progenitor cell markers with age in rabbit intervertebral discs.* Acta Biochim Biophys Sin (Shanghai), 45(5): p. 368-76.

[37] Stewart, M.C., K.M. Saunders, N. Burton-Wurster, and J.N. Macleod (2000) *Phenotypic stability of articular chondrocytes in vitro: the effects of culture models, bone morphogenetic protein 2, and serum supplementation.* J Bone Miner Res, 15(1): p. 166-74.

[38] Bonaventure, J., N. Kadhom, L. Cohen-Solal, K.H. Ng, J. Bourguignon, et al. (1994) *Reexpression of cartilage-specific genes by dedifferentiated human articular chondrocytes cultured in alginate beads.* Exp Cell Res, 212(1): p. 97-104.

[39] Baustian, C., S. Hanley, and R. Ceredig (2015) *Isolation, selection and culture methods to enhance clonogenicity of mouse bone marrow derived mesenchymal stromal cell precursors.* Stem Cell Res Ther, 6: p. 151.

[40] Sang, C., X. Cao, F. Chen, X. Yang, and Y. Zhang (2016) *Differential Characterization of Two Kinds of Stem Cells Isolated from Rabbit Nucleus Pulposus and Annulus Fibrosus.* Stem Cells Int, 2016: p. 8283257.

[41] Su, X., W. Zuo, Z. Wu, J. Chen, N. Wu, et al. (2015) *CD146 as a new marker for an increased chondroprogenitor cell sub-population in the later stages of osteoarthritis.* J Orthop Res, 33(1): p. 84-91.

[42] Nakai, T., D. Sakai, Y. Nakamura, T. Nukaga, S. Grad, et al. (2016) *CD146 defines commitment of cultured annulus fibrosus cells to express a contractile phenotype.* J Orthop Res, 34(8): p. 1361-72.

CHAPTER V

General discussion and future perspectives

The original goal of this doctoral thesis was to move forward the basic knowledge on intervertebral disc (IVD) cell biology, particularly focusing on nucleus pulposus (NP) cells, by introducing novel approaches to this field, namely high-throughput methods of cell analysis, as flow cytometry and imaging flow cytometry.

Initially enrolled in the FP7 European Project "Disc Regeneration" (2009-2012) [1], in which our team was committed to develop a biomaterial to regenerate and repair the degenerated IVD, we got inspired by the complex and fundamental bioactive role of this tissue, so poorly characterized back then. Indeed, recent years have been stage for a tremendous growth in this field of research, highlighting the need to better understand the pathophysiological mechanisms behind disc degeneration, towards improved solutions to treat degenerative disc disease (DDD). Major efforts have been put on biological regenerative therapies [2-4], and the number of clinical trials has been rising each year [5, 6]. Still, much is yet to be uncovered regarding IVD cells signature, physiology and function. The deeper we go into these fundamental questions, the safer, more personalized and successful novel regenerative therapies to treat IVD degeneration and associated LBP will become.

In this PhD dissertation, we proposed to thoroughly characterize NP cells in homeostasis and aging. For this purpose, we have started by using the bovine animal model, widely accepted to study the IVD, due to its cellular and biomolecular resemblance to the human scenario [7-12]. Three main objectives were settled: 1) firstly, to establish an improved method for primary bovine NP cells isolation, whose procedure was not consensual among the literature; 2) in a second phase, characterize NP cells phenotypic profile in homeostasis and evaluate age-related changes at protein and gene level; and finally 3) dissect age-correlated phenotypic alterations in primary cells isolated from human degenerated IVDs with contained hernias, to assure the exclusive characterization of endemic NP cell populations, in collaboration with orthopaedic surgeons from a local hospital.

As we stand, the nonexistence of a definitive cell marker or clear phenotypic assays to distinguish NP cells from other cell types, the lack of standardization of NP cell isolation methods [13-18], together with differences in NP markers expression among distinct species, raises questions concerning the proper identification of cell types in IVD, establishment of *in vitro* cell cultures from these cells, and comparison of results obtained from different labs. Establishing standardized methods to profile IVD cell populations will be key to increase reproducibility and reliability of results in this field of research.

Despite the profound impact that cell isolation protocols might have on cells yield, viability and phenotype, no specific formula to digest NP tissue is commercially available nor consensus exists on the most appropriate protocol to isolate IVD cells. Hence, we propose an improved bNP cell isolation protocol, which originates high cell yields and viability, besides being less time-consuming than the gold standard method (overnight enzymatic digestion). Of note, the presented protocol did not require any additional step of digestion with other enzymes commonly used for NP cell dissociation (e.g. hyaluronidase [19] or pronase), known to negatively affect the expression of surface receptors on articular cartilage (AC) chondrocytes [20] and to remove NP and annulus fibrosus (AF) native pericellular matrix (PCM) [21]. However, although no morphological alterations were observed on primary bNP cells with the different protocols, it would be important to monitor their immunophenotypic profile as well.

A recent consensus paper has proposed a panel of markers to define the phenotype of young NP cells [22], which were chosen based on their specific expression in young healthy NP cells, relevance to NP physiology, and validation across different species. This work prompted new studies seeking further validation of those markers (essentially at protein level) in larger human cohorts [23-25]. Herein, to uncover new cell markers we firstly analysed an array of surface receptor antibodies available at our lab, and this led to the identification of new markers on freshly isolated bNP cells, whose profile was altered with age, namely CD29, CD44, CD45, Tie2 and GD2. In the case of cells from human degenerated tissue, the rational had to be different, since we could not guarantee the analysis of NP cells exclusively. Thus, we focused on the regenerative

potential of IVD cells, by monitoring specific progenitor cell markers, and verified that CD90 and CD73 expression was negatively correlated with age. Importantly, we contributed even further to Risbud and colleagues' phenotypic characterization [22] using a unique approach, which combines conventional and imaging flow cytometry (FC and IFC). It was not until recent years that conventional FC began to be applied in the study of IVD cells [23, 24, 26, 27], alternatively or supporting traditional cell characterization methods, such as electron [28, 29] and confocal microscopy [30, 31], and (immuno)histochemistry [32]. This powerful tool records cytomorphometric data from single cells at high-speed (10^5 cells/s), retrieving statistically relevant analysis on cell populations. Additionally, when a specific cell marker is available, the high sensitivity of FC allows identification of very small subpopulations. Notwithstanding, some drawbacks, such as the need to dissociate cells from native tissues, the impossibility to visualize cells in flow and being an expensive piece of equipment, may have been justifying its seldom use. On the other hand, IFC represents one step forward in FC technology, by collecting high-resolution images of thousands of cells in flow, and providing a user-friendly image analyses software (IDEAS®) to assess an even wider array of cellular parameters [33]. Supported by other evidences on the heterogeneous cell population found within the bovine NP tissue [23, 34-38], this was the first attempt ever made to systematically profile young and healthy NP cells using flow cytometry, similar to what has been done for blood cells [39]. Interestingly, in the first part of this study, using a BD FACSCalibur™ flow cytometer we could consistently identify three distinct subpopulations within young bNPs, solely based on their size and auto-fluorescence (label-free analysis). However, in the second part of the work, as we upgraded to a more efficient flow cytometer (BD FACSCanto™ II system), a fourth subpopulation was detected, due to the analysis transition from forward scatter-height (FSC-H) to forward scatter-area (FSC-A). Crucially, a differential expression of cell surface receptors was found among these subpopulations. Also important was the complementation with IFC robust analysis, which ultimately guaranteed the characterization of live cells and not image-orphaned events only. This is particularly relevant when dealing with primary cells

suspensions, which inevitably include many cell debris and ECM breakdown products. Indeed, in cell suspensions from older animals and degenerated human tissues this was even more evident. However, in order to discriminate the specific role that each subpopulation might play in IVD regeneration and repair, future functional studies are required.

With possible exception of genetics, age is perhaps the factor most strongly associated with dis degeneration [40]. The clear correlation between age and disc degeneration has been observed since the early XX century [41]. While some degenerative findings may be detected already in childhood [42], their increase in frequency and severity is most reported from 20 years old on [43]. Thus, counter-acting detrimental age effects on IVD integrity should be the first-in-line therapeutic to address IVD degeneration. In this sense, profiling age-associated changes on IVD cells phenotype would help to identify potential targets to prevent IVD accelerated degeneration and painfully disabling IVD disease progression. Inspired by this hypothesis, and in line with another work from our team [44], the second part of this thesis focused on the differences found between bNP cells from young and old coccygeal discs. Herein, we showed an age-associated decrease in the prevalence of mesenchymal stromal cells (MSC)-related (CD29 and CD44), hematopoietic (CD45) and NP-progenitor (Tie2) markers in bNP cells. A negative correlation had already been established between Tie2 and age in cells from degenerated human tissues [45], supporting the idea that, although the NP may exhibit an endogenous regenerative potential, there might be a limit in time for its activation. Interestingly, our study revealed an increase in the percentage of $GD2^+$ cells (reported NP-progenitor marker as well [45]) with age, along with a stable expression of CD146 (MSC marker). This brought renewed hope on NP cells capability to respond to age-provoking damage on cells and its surrounding microenvironment, although further functional validation of this potential is also needed.

Finally, we had the exciting opportunity to collaborate with orthopaedic surgeons from Centro Hospitalar de São João (University of Porto) and to apply the same rational of previous chapters on IVD cells isolated from patients undergoing microdiscectomy. This task was particularly challenging for several

reasons. Firstly, because the discussed exclusion criteria (contained hernias only and tissue collection from the deepest zone possible, avoiding major blood contamination) implied a strong commitment from the clinical staff. Secondly, due to the unpredictable nature of the sample (e.g. variable age, tissue weight and integrity), which was additionally generally scarce in cell content and technically impossible to classify as NP, AF or CEP tissue (as far as we are aware this can only be achieved by immunohistochemistry [25] and/or by rough macroscopic dissection [23, 46]). The restricted access to patient's radiographic examinations was also a limitation of this study, not allowing sample stratification by degenerative grade (e.g. using a magnetic resonance imaging (MRI) classification systems for lumbar disc degeneration; Pfirrman Scale [47]), and consequently any correlation between the alterations registered and the grade of degeneration. Here, we began by seeking validation of the cell isolation protocol established for the bovine animal model in Chapter II, but the fact that surgeries were only performed in the evening technically prevented the use of the 4h digestion protocol to rescue fresh primary cells. As such, an alternative method had to be used, which rendered equivalent high levels of cell viability, but cell yields were always much lower. Interestingly, a negative correlation was found between cell yield and age, leading to the conclusion that not only the digestion method, but also age may have a deep negative impact on this parameter, critical for both flow cytometry analysis and *in vitro* cultures of IVD-representative cell populations. Aging effects on hIVD cells were also evident on MSC-related surface receptors CD90 and CD73, which, as somehow expected, showed a negative correlation with age. Surprisingly however, CD146 was not age-correlated and was found in practically all samples analyzed, as well as GD2, two recognized progenitor cell markers [48, 49]. However, the most striking age-dependent alteration recorded, and for the first time quantified, was cells average diameter shift, which dissected to the subpopulation level by IFC morphology analysis, revealed that aging induces the overall deposition of a large PCM around hIVD cells, similar to what has been hypothesized to occur with osteoarthiritic chondrons, following an inflammatory stimulus (e.g. Interleukine-1 [IL-1] exposure) [50]. Notwithstanding, and despite the molecular constitution of

this encapsulating structure is apparently well determined [9, 28, 32, 51, 52], the effects it might have on cell-cell or cell-ECM interactions are still unknown. Interestingly, the specific effects of aging on NP cells microenvironment (matrisome) are also being explored by our team, and putative effectors for disc regeneration have already been identified [44]. Combining cells signature and matrisome mapping data from young healthy discs may constitute a more efficient strategy to face the complex interconnected cascade of degenerative events occurring in IDD.

Overall, the findings presented in this dissertation may better inform future therapies aiming to 1) re-establish homeostasis, through the recapitulation of healthy NP cells signature and/or reversion of age-dependent degenerative changes, or 2) to enhance endogenous repair by progenitor cells activation. Recapitulation of healthy NP cells signature could be achieved either by gene- or cell-based approaches. Indeed, seeking to mitigate the degenerative process and also to enhance tissue regeneration, gene therapies have successfully introduced anabolic genes on IVD cells, such as growth and differentiation factor-5, BMPs, transforming growth factor-beta (TGF-β) and Sox-9[53]. This strategy could also be applied to promote over expression of CD29 and CD44, two important mediators of cell-matrix interactions and MSC markers [19, 54-57], or GD2, Tie2 and CD146 progenitor cell-related surface receptors, which may have a fundamental role in IVD repair [45, 48, 49, 58, 59]. On the other hand, cell-based approaches could enrich therapeutic cell suspensions on cells positive for those markers and repopulate the NP. Focusing on age-specific degenerative changes, one could also promote the downregulation of collagen-VI production (its main constituent) as a hypothetical approach to avoid extensive PCM deposition. Finally, activating the native regenerative cell machinery could be achieved by *in situ* delivery of key bioactive molecular cues [60].

Taken together, the results described in this dissertation represent a scientific contribution to a better understanding of nucleus pulposus cell biology, both in homeostasis and aging. Moreover, potential anti-aging molecular targets for novel therapies were highlighted, that ideally would help to mitigate age-related disc disease.

References

[1] CORDIS. *FP7-NMP 213904 DISC REGENERATION: Novel biofunctional high porous polymer scaffolds and techniques controlling angiogenesis for the regeneration and repair of the degenerated intervertebral disc*. 2012 [cited 2017 14th September]; Available from: http://cordis.europa.eu/project/rcn/88873_en.html.

[2] Sakai, D. and G.B. Andersson (2015) *Stem cell therapy for intervertebral disc regeneration: obstacles and solutions.* Nat Rev Rheumatol, 11(4): p. 243-56.

[3] Richardson, S.M., G. Kalamegam, P.N. Pushparaj, C. Matta, A. Memic, et al. (2016) *Mesenchymal stem cells in regenerative medicine: Focus on articular cartilage and intervertebral disc regeneration.* Methods, 99: p. 69-80.

[4] Hughes, S.P., A.J. Freemont, D.W. Hukins, A.H. McGregor, and S. Roberts (2012) *The pathogenesis of degeneration of the intervertebral disc and emerging therapies in the management of back pain.* J Bone Joint Surg Br, 94(10): p. 1298-304.

[5] Sakai, D. and J. Schol (2017) *Cell therapy for intervertebral disc repair: Clinical perspective.* Journal of Orthopaedic Translation, 9: p. 8-18.

[6] Pennicooke, B., Y. Moriguchi, I. Hussain, L. Bonssar, and R. Hartl (2016) *Biological Treatment Approaches for Degenerative Disc Disease: A Review of Clinical Trials and Future Directions.* Cureus, 8(11): p. e892.

[7] Illien-Junger, S., B.A. Walter, J.E. Mayer, A.C. Hecht, and J. Iatridis, (2014) *Intervertebral disc culture models and their applications to study pathogenesis and repair*, in *The intervertebral disc: molecular and structural studies of the disc in health and disease*, I.M. Shapiro and M.V. Risbud, Editors. Springer Vienna. p. 353-371.

[8] Oshima, H., H. Ishihara, J.P. Urban, and H. Tsuji (1993) *The use of coccygeal discs to study intervertebral disc metabolism.* J Orthop Res, 11(3): p. 332-8.

[9] Roberts, S., J. Menage, V. Duance, S. Wotton, and S. Ayad (1991) *1991 Volvo Award in basic sciences. Collagen types around the cells of the intervertebral disc and cartilage end plate: an immunolocalization study.* Spine (Phila Pa 1976), 16(9): p. 1030-8.

[10] Ishihara, H., D.S. McNally, J.P. Urban, and A.C. Hall (1996) *Effects of hydrostatic pressure on matrix synthesis in different regions of the intervertebral disk.* J Appl Physiol (1985), 80(3): p. 839-46.

[11] Ohshima, H., J.P. Urban, and D.H. Bergel (1995) *Effect of static load on matrix synthesis rates in the intervertebral disc measured in vitro by a new perfusion technique.* Journal of orthopaedic research : official publication of the Orthopaedic Research Society, 13(1): p. 22-9.

[12] Maroudas, A., R.A. Stockwell, A. Nachemson, and J. Urban (1975) *Factors involved in the nutrition of the human lumbar intervertebral disc: cellularity and diffusion of glucose in vitro.* J Anat, 120(Pt 1): p. 113-30.

[13] Gilson, A., M. Dreger, and J.P. Urban (2010) *Differential expression level of cytokeratin 8 in cells of the bovine nucleus pulposus complicates the search for specific intervertebral disc cell markers.* Arthritis Research & Therapy, 12(1): p. R24.

[14] Jones, P., L. Gardner, J. Menage, G.T. Williams, and S. Roberts (2008) *Intervertebral disc cells as competent phagocytes in vitro: implications for cell death in disc degeneration.* Arthritis research & therapy, 10(4): p. R86.

[15] Nerlich, A.G., C. Weiler, J. Zipperer, M. Narozny, and N. Boos (2002) *Immunolocalization of phagocytic cells in normal and degenerated intervertebral discs.* Spine, 27(22): p. 2484-2490.

[16] Smith, L.J., J.A. Chiaro, N.L. Nerurkar, D.H. Cortes, S.D. Horava, et al. (2011) *Nucleus pulposus cells synthesize a functional extracellular matrix and respond to inflammatory cytokine challenge following long-term agarose culture.* European cells & materials, 22: p. 291-301.

[17] Horner, H.A., S. Roberts, R.C. Bielby, J. Menage, H. Evans, et al. (2002) *Cells from different regions of the intervertebral disc: effect of culture system on matrix expression and cell phenotype.* Spine, 27(10): p. 1018-28.

[18] Minogue, B.M., S.M. Richardson, L.A.H. Zeef, A.J. Freemont, and J.A. Hoyland (2010) *Transcriptional profiling of bovine intervertebral disc cells: implications for identification of normal and degenerate human intervertebral disc cell phenotypes.* Arthritis Research & Therapy, 12(1): p. R22.

[19] Knudson, C.B. (2003) *Hyaluronan and CD44: strategic players for cell-matrix interactions during chondrogenesis and matrix assembly.* Birth Defects Res C Embryo Today, 69(2): p. 174-96.

[20] Diaz-Romero, J., J.P. Gaillard, S.P. Grogan, D. Nesic, T. Trub, et al. (2005) *Immunophenotypic analysis of human articular chondrocytes: changes in surface markers associated with cell expansion in monolayer culture.* J Cell Physiol, 202(3): p. 731-42.

[21] Vonk, L.A., B.Z. Doulabi, C. Huang, M.N. Helder, V. Everts, et al. (2010) *Preservation of the chondrocyte's pericellular matrix improves cell-induced cartilage formation.* Journal of cellular biochemistry, 110(1): p. 260-71.

[22] Risbud, M.V., Z.R. Schoepflin, F. Mwale, R.A. Kandel, S. Grad, et al. (2015) *Defining the phenotype of young healthy nucleus pulposus cells: recommendations of the Spine Research Interest Group at the 2014 annual ORS meeting.* J Orthop Res, 33(3): p. 283-93.

[23] Richardson, S.M., F.E. Ludwinski, K.K. Gnanalingham, R.A. Atkinson, A.J. Freemont, et al. (2017) *Notochordal and nucleus pulposus marker expression is*

maintained by sub-populations of adult human nucleus pulposus cells through aging and degeneration. Sci Rep, 7(1): p. 1501.

[24] Tang, X., L. Jing, W.J. Richardson, R.E. Isaacs, R.D. Fitch, et al. (2016) *Identifying molecular phenotype of nucleus pulposus cells in human intervertebral disc with aging and degeneration.* J Orthop Res, 34(8): p. 1316-26.

[25] Thorpe, A.A., A.L. Binch, L.B. Creemers, C. Sammon, and C.L. Le Maitre (2016) *Nucleus pulposus phenotypic markers to determine stem cell differentiation: fact or fiction?* Oncotarget, 7(3): p. 2189-200.

[26] Chen, J., W. Yan, and L.A. Setton (2006) *Molecular phenotypes of notochordal cells purified from immature nucleus pulposus.* Eur Spine J, 15 Suppl 3: p. S303-11.

[27] Tang, X., L. Jing, and J. Chen (2012) *Changes in the molecular phenotype of nucleus pulposus cells with intervertebral disc aging.* PLoS One, 7(12): p. e52020.

[28] Trout, J.J., J.A. Buckwalter, and K.C. Moore (1982) *Ultrastructure of the human intervertebral disc: II. Cells of the nucleus pulposus.* Anat Rec, 204(4): p. 307-14.

[29] Trout, J.J., J.A. Buckwalter, K.C. Moore, and S.K. Landas (1982) *Ultrastructure of the human intervertebral disc. I. Changes in notochordal cells with age.* Tissue Cell, 14(2): p. 359-69.

[30] Hunter, C.J., J.R. Matyas, and N.A. Duncan (2004) *Cytomorphology of notochordal and chondrocytic cells from the nucleus pulposus: a species comparison.* J Anat, 205(5): p. 357-62.

[31] Johnson, W.E. and S. Roberts (2003) *Human intervertebral disc cell morphology and cytoskeletal composition: a preliminary study of regional variations in health and disease.* J Anat, 203(6): p. 605-12.

[32] Gruber, H.E., J.A. Ingram, and E.N. Hanley, Jr. (2007) *Morphologic complexity of the pericellular matrix in the annulus of the human intervertebral disc.* Biotech Histochem, 82(4-5): p. 217-25.

[33] Samsel, L., P.K. Dagur, N. Raghavachari, C. Seamon, G.J. Kato, et al. (2013) *Imaging flow cytometry for morphologic and phenotypic characterization of rare circulating endothelial cells.* Cytometry B Clin Cytom, 84(6): p. 379-89.

[34] van den Akker, G.G., D.A. Surtel, A. Cremers, R. Rodrigues-Pinto, S.M. Richardson, et al. (2014) *Novel immortal human cell lines reveal subpopulations in the nucleus pulposus.* Arthritis Res Ther, 16(3): p. R135.

[35] Weiler, C., A.G. Nerlich, R. Schaaf, B.E. Bachmeier, K. Wuertz, et al. (2010) *Immunohistochemical identification of notochordal markers in cells in the aging human lumbar intervertebral disc.* European Spine Journal, 19(10): p. 1761-1770.

[36] Gilson, A., M. Dreger, and J.P.G. Urban (2010) *Differential expression level of cytokeratin 8 in cells of the bovine nucleus pulposus complicates the search for specific intervertebral disc cell markers.* Arthritis Research & Therapy, 12(1): p. R24.

[37] Tanaka, M., D. Sakai, A. Hiyama, F. Arai, D. Nakajima, et al. (2017) *Evidence of Nonnotochordal Origin in Chondrocyte-like Cells of the Nucleus Pulposus Appearing in Early Stage Disk Degeneration in the Mouse Model.* Global Spine Journal.

[38] Rodrigues-Pinto, R., S.M. Richardson, and J.A. Hoyland (2014) *An understanding of intervertebral disc development, maturation and cell phenotype provides clues to direct cell-based tissue regeneration therapies for disc degeneration.* Eur Spine J, 23(9): p. 1803-14.

[39] Streitz, M., T. Miloud, M. Kapinsky, M.R. Reed, R. Magari, et al. (2013) *Standardization of whole blood immune phenotype monitoring for clinical trials: panels and methods from the ONE study.* Transplant Res, 2(1): p. 17.

[40] Battie, M.C., T. Videman, J. Kaprio, L.E. Gibbons, K. Gill, et al. (2009) *The Twin Spine Study: contributions to a changing view of disc degeneration.* The spine journal : official journal of the North American Spine Society, 9(1): p. 47-59.

[41] Wang, Y. and M.C. Battie, (2014) *Epidemiology of lumbar disc degeneration*, in *The intervertebral disc: molecular and structural studies of the disc in health and disease*, I.M. Shapiro and M.V. Risbud, Editors. Springer: Wien. p. 139-156.

[42] Boos, N., S. Weissbach, H. Rohrbach, C. Weiler, K.F. Spratt, et al. (2002) *Classification of age-related changes in lumbar intervertebral discs: 2002 Volvo Award in basic science.* Spine (Phila Pa 1976), 27(23): p. 2631-44.

[43] Battie, M.C., T. Videman, and E. Parent (2004) *Lumbar disc degeneration: epidemiology and genetic influences.* Spine (Phila Pa 1976), 29(23): p. 2679-90.

[44] Caldeira, J., C. Santa, H. Osório, M. Molinos, B. Manadas, et al. (2017) *Matrisome Profiling During Intervertebral Disc Development And Aging.* Scientific Reports, 7(1).

[45] Sakai, D., Y. Nakamura, T. Nakai, T. Mishima, S. Kato, et al. (2012) *Exhaustion of nucleus pulposus progenitor cells with aging and degeneration of the intervertebral disc.* Nat Commun, 3: p. 1264.

[46] Wang, H., Y. Zhou, T.W. Chu, C.Q. Li, J. Wang, et al. (2016) *Distinguishing characteristics of stem cells derived from different anatomical regions of human degenerated intervertebral discs.* Eur Spine J, 25(9): p. 2691-704.

[47] Pfirrmann, C.W., A. Metzdorf, M. Zanetti, J. Hodler, and N. Boos (2001) *Magnetic resonance classification of lumbar intervertebral disc degeneration.* Spine (Phila Pa 1976), 26(17): p. 1873-8.

[48] Xu, J., W. Liao, D. Gu, L. Liang, M. Liu, et al. (2009) *Neural ganglioside GD2 identifies a subpopulation of mesenchymal stem cells in umbilical cord.* Cell Physiol Biochem, 23(4-6): p. 415-24.

[49] Su, X., W. Zuo, Z. Wu, J. Chen, N. Wu, et al. (2015) *CD146 as a new marker for an increased chondroprogenitor cell sub-population in the later stages of osteoarthritis.* J Orthop Res, 33(1): p. 84-91.

[50] Poole, C.A. (1997) *Articular cartilage chondrons: form, function and failure.* J Anat, 191 (Pt 1): p. 1-13.

[51] Roberts, S., S. Ayad, and P.J. Menage (1991) *Immunolocalisation of type VI collagen in the intervertebral disc.* Annals of the rheumatic diseases, 50(11): p. 787-91.

[52] Roberts, S., J. Menage, V. Duance, and S.F. Wotton (1991) *Type III collagen in the intervertebral disc.* The Histochemical journal, 23(11-12): p. 503-8.

[53] Gazit, Z., N. Kimelman-Bleich, and O. Mizrahi, (2014) *Gene therapy approaches for disc regeneration*, in *The intervertebral disc: molecular and structural studies of the dis in health and disease*, M.V. Risbud and I.M. Shapiro, Editors. Springer. p. 385-400.

[54] Henriksson, H.B., E. Svala, E. Skioldebrand, A. Lindahl, and H. Brisby (2012) *Support of concept that migrating progenitor cells from stem cell niches contribute to normal regeneration of the adult mammal intervertebral disc: a descriptive study in the New Zealand white rabbit.* Spine, 37(9): p. 722-32.

[55] Kurtis, M.S., B.P. Tu, O.A. Gaya, J. Mollenhauer, W. Knudson, et al. (2001) *Mechanisms of chondrocyte adhesion to cartilage: role of beta1-integrins, CD44, and annexin V.* J Orthop Res, 19(6): p. 1122-30.

[56] Stevens, J.W., G.L. Kurriger, A.S. Carter, and J.A. Maynard (2000) *CD44 expression in the developing and growing rat intervertebral disc.* Dev Dyn, 219(3): p. 381-90.

[57] Knudson, W. and R.F. Loeser (2002) *CD44 and integrin matrix receptors participate in cartilage homeostasis.* Cell Mol Life Sci, 59(1): p. 36-44.

[58] Martinez, C., T.J. Hofmann, R. Marino, M. Dominici, and E.M. Horwitz (2007) *Human bone marrow mesenchymal stromal cells express the neural ganglioside GD2: a novel surface marker for the identification of MSCs.* Blood, 109(10): p. 4245-8.

[59] Zhang, Y., C. Xiong, C.W. Chan, D. Sakai, and D. Chan (2017) *Changes in Nucleus Pulposus Cell Pools in "Healer" Mice for the Repair of Intervertebral Disc Degeneration.* Global Spine Journal, 5(1_suppl): p. s-0035-1554499-s-0035-1554499.

[60] Ko, I.K., S.J. Lee, A. Atala, and J.J. Yoo (2013) *In situ tissue regeneration through host stem cell recruitment.* Exp Mol Med, 45: p. e57.

ANNEXES

TISSUE ENGINEERING: Part A
Volume 21, Numbers 15 and 16, 2015

DOI: 10.1089/ten.tea.2014.0461

termis
Tissue Engineering
& Regenerative Medicine
International Society

ORIGINAL ARTICLE

Improvement of Bovine Nucleus Pulposus Cells Isolation Leads to Identification of Three Phenotypically Distinct Cell Subpopulations

Maria Molinos, Msc,[1–3] Catarina R. Almeida, PhD,[1,2]
Raquel M. Gonçalves, PhD,[1,2] and Mário A. Barbosa, PhD[1–3]

Objective: Strategies to promote intervertebral disc (IVD) regeneration have been hindered by the lack of knowledge of IVD fundamental cellular/molecular components. One of the key points to be addressed is the characterization of nucleus pulposus (NP) cell population(s). This study establishes an improved method for bovine NP (bNP) cell isolation, whose procedure is still not consensual among the literature, allowing a thorough characterization of cell (sub)populations that exist in the young NP.
Methods: bNP was digested with distinct enzymes (collagenase-type-I, collagenase-type-II, and collagenase-type-XI) at different concentrations (0.5, 1.0, and 2.0 mg/mL), for 4 and 19 h. Cell yield, viability/apoptosis, and morphology were analyzed by flow cytometry and imaging flow cytometry. Identification of cell subpopulations within NP and its phenotype was investigated by assessing expression of CD29, CD44, CD45, CD34, CD146, and Brachyury.
Results: It was found that bNP cells present a similar morphology independently of the digestive enzyme used. However, cell yield was greatly improved by Coll-XI (2 mg/mL) treatment for a short digestion period. Interestingly, three subpopulations, with different sizes and auto-fluorescence, were consistently identified by flow cytometry. And crucially, differential expression of cell markers was found among these subpopulations.
Conclusion: This study demonstrated that collagenase-type-XI is an efficient enzyme that is used for digesting bNP. And most importantly, three phenotypically distinct subpopulations of cells where identified within the bNP. Such knowledge is key for a better understanding of NP cell biology and its potential endogenous regenerative capacity.

Introduction

The intervertebral disc (IVD) is a complex and bioactive structure within the spine. Continuous multidirectional mechanical forces allied to aging activate degenerative pathways in the IVD, which are responsible for many disabling back diseases, and, ultimately, imply a heavy socioeconomic impact.

Current treatments include rest, anti-inflammatory medication, physical therapy, and, as a last resort, spinal fusion, total disc replacement, or discectomy. These treatments focus on symptomatic management and do not address the underlying pathophysiology of the diseased tissue, resulting in long-term suboptimal outcomes. Alternative strategies, such as cell-based therapies, growth factor injection, gene therapy, and tissue engineering, aiming at stopping or reducing degeneration of the IVD, or at promoting its regeneration, are being pursued.[1,2] Recently, our group has shown that delivery of a chemoattractor in the IVD can recruit mesenchymal stem cells toward the nucleus pulposus (NP), which opened new perspectives for IVD regenerative strategies.[3] However, success of current strategies has been hindered by the lack of knowledge on the cellular and molecular components of the IVD.

Cells in the adult IVD are usually divided in two populations, according to the different embryonic origin of the tissue where they reside: (1) the fibroblast-like cells in the annulus fibrosus (AF), which develop from the somites (sclerotome), and (2) the chondrocyte-like cells in the NP, which derive from the notochord (both mesenchyme-derived tissues).[4] NP cells share typical markers of extracellular matrix (ECM) with AF cells or articular cartilage (AC) cells, such as type-II-collagen, aggrecan, and versican.[5] Expression of specific NP markers has been also described but is species dependent. For

[1]Instituto de Investigação e Inovação em Saúde (i3S), Universidade do Porto, Porto, Portugal.
[2]Instituto de Engenharia Biomédica (INEB) and [3]Instituto de Ciências Biomédicas Abel Salazar (ICBAS), Universidade do Porto, Porto, Portugal.

instance, bovine NP (bNP) cells express synaptosomal-associated protein, 25 kDa (SNAP25), tenomodulin (TNMD), and cytokeratin-8 (CK8),[5,6] while human NP cells express carbonic anhydrase-12 (CA12), paired box 1 (PAX-1), haemoglobin β–chain (HBB), and ovostatin 2 (OVOS2). Rat NP cells exclusively express CD24, while rabbit NP cells express type V collagen, matrix Gla protein (MGP), and Htra serine peptidase 1 (Htra1). Most recently, a selection of markers has been proposed to define the phenotype of NP cells.[7]

Cells isolated from degenerated and non-degenerated human discs can differentiate into adipogenic, osteogenic, and chondrogenic lineages, indicating that the IVD may include progenitor cells within its population.[8–14] In addition, expression of markers associated with progenitors (e.g., Tie2, GD2, Stro-1, Oct3/4, CD105, CD90, and Notch-1) suggests that precursor cell populations might be present within degenerated human discs.[8,9] These findings indicate that degenerated human discs may count on an endogenous regenerative capacity, although the exact nature and origin of the participating cells remains unknown.

Bovine IVDs have been proposed as a suitable model to study Tissue Engineering and biological repair of human IVD,[15] and many studies have been published culturing bovine IVD cells as a model.[3,5,6,16–18] However, the non-existence of a definitive cell marker or clear phenotypic assays to distinguish NP cells from other cell types, the lack of standardization of NP cell isolation methods, together with differences in NP marker expression among distinct species, raise questions regarding the proper identification of cell types in IVD, establishment of *in vitro* cell cultures from these cells, and comparison of results obtained from different labs. A more standardized characterization of cell populations within IVD, and particularly in NP, is crucial when studying biological phenomena that might contribute to both IVD degeneration and its potential regenerative capacity.

Hence, in this study, a bovine model was used to evaluate different isolation methods of NP cells. A new isolation method was explored, guarantying high cell yield and viability. Moreover, bNP cell morphology and phenotypic expression was thoroughly characterized immediately after isolation by image analysis and flow cytometry.

Materials and Methods

bNP cell isolation

Caudal IVDs from 10- to 13 month-old bovine steers were dissected until 3 h after death. NP was harvested from 7 to 8 IVDs. With a scalpel blade, NP was separated from AF and vertebral endplates and finely chopped. Tissue digestion was performed in Dulbecco's modified Eagle's medium (DMEM; 21885 Gibco), supplemented with 5% v/v penicillin–streptomycin (PAA Laboratories GmbH), 10% v/v amphotericin B (PAA), 2.5% (v/v) of HEPES buffer 1 mM (Lonza), 1.5% (v/v) of NaCl 5 M and KCl 0.4 M solution (to adjust osmolarity to 400 mOsm), 1.3 U/mL DNAse, as described elsewhere,[19] and one of three different enzymatic formulations: collagenase-type-I (Coll-I), collagenase-type-II (Coll-II), or collagenase-type-XI (Coll-XI) (C0130, C6885, and C7657, respectively, Sigma Aldrich), at different concentrations (0.5, 1.0, and 2.0 mg/mL). All enzymatic preparations contain a mixture of the type I and II forms of the purified collagenase enzyme, which differ in their affinity for different substrates, as assessed by the manufacturer (www.sigmaaldrich.com/life-science/metabolomics/enzyme-explorer/learning-center/collagenase-guide.html).

Tissue/medium ratio was set at 10% w/v to prevent the pH dropping below 6.8 during incubation. Tissue was digested for 4 h (minimum time required to totally digest tissue from at least one of the protocols used) or 19 h (overnight digestion—tissue totally digested in all protocols), in a humidified atmosphere at 37°C/5% CO_2, and under gentle stirring. ECM contaminants were filtered with a 70 μm cell strainer.

Assessing bNP cell yield, viability, and apoptosis

Immediately on digestion, cell yield was quantified by trypan blue exclusion and subsequently normalized by wet tissue weight. Cell viability and apoptosis were assessed by flow cytometry (FACS Calibur; BD Immunocytometry Systems), using FITC-Annexin V Apoptosis Detection Kit I (556547; eBioscience), according to the manufacturer's instructions.

Characterization of bNP cell morphology by imaging flow cytometry

To examine the morphological features of freshly isolated NP cells, cells were fixed in 4% w/v paraformaldehyde (PFA) at room temperature for 15 min, washed with phosphate-buffered saline (PBS), and permeabilized with 0.2% v/v Triton, for 5 min. After washing again with PBS, cells were incubated for 20 min at room temperature, with Phalloidin-AlexaFluor®488 (1:40 dil. per 2.0×10^5 cells, A12379; Life Technologies), previously prepared in a PBS-1% w/v bovine serum albumin solution, according to the manufacturer's instructions. Shortly before acquisition, cells were labeled with DRAQ5 (1:1500 dil. per 2.0×10^5 cells, 65-0880; eBioscience), run on ImageStream^X (IS; Millipore), and analyzed with IDEAS software for cell area, diameter, nuclear/cytoplasm ratio, and presence of vesicles. To quantify the percentage of cells with bright vesicles and the nuclear-to-cytoplasmic ratio, specific masks were developed and applied to brightfield and fluorescence images:

—Morphology (M01, Bightfield): mask applied to calculate cell area based on brightfield;
—Morphology (M02, Actin): to calculate cell area based on actin staining;
—Erode (M05, 5): to calculate nucleus area;
—Spot (M01, Brightfield, Bright, 34, 1): mask designed to mark bright vesicles within cells.

Characterization of bNP cell phenotype

Cell surface staining. The expression of surface markers (Table 1) was analyzed by flow cytometry immediately on cell isolation, without fixation, to guarantee exclusion of dead cells with propidium iodide (PI) staining. First, cells were left to recover from digestion for 30 min in a humidified atmosphere at 37°C/5% CO_2. Cells were then washed with PBS-2% fetal bovine serum (FBS) and incubated with primary antibodies (Table 1), in the same solution, for 1 h at room temperature. In the case of non-conjugated anti-CD34

Table 1. Antibodies Used in Flow Cytometry Analysis

	Fluorochrome	*μg/mL*	*Clone*	*Catalog no, manufacturer*
Primary antibodies				
Mouse anti-bovine CD29	AlexaFluor®488		TS2/16	303015, Biolegend
Mouse anti-bovine CD44	FITC	10	IL-A118	MCA2433F, AbD Serotec
Mouse anti-bovine CD45	FITC	10	CC1	MCA832F, AbD Serotec
Mouse anti-human CD146	AlexaFluor®647	5	OJ79c	MCA2141A647T, AbD Serotec
Mouse anti-bovine CD34	—	24		Isotype N21, kindly provided by Sakurai M[44]
Mouse anti-human Brachyury	FITC	20	3E4.2	FCMAB302F, Millipore
Secondary antibody				
Goat anti-mouse IgG	AlexaFluor488	20		A-11017, Life Technologies™
Isotype controls				
Mouse IgG1 k	AlexaFluor488	10	MOPC-21	400132, Biolegend
Mouse IgG1 control	FITC	10	PPV-06	21275513, Immunotools
Mouse IgG1	AlexaFluor647	5		sc-24636, Santa Cruz Biotechnology
Mouse IgG1 k purified		20	P3.6.2.8.1	14-4714, eBioscience

antibody, cells were, in addition, incubated with a secondary goat anti-mouse-AlexaFluor488 antibody, in the same conditions. After labeling, cells were washed with 2 mL PBS-2% FBS and run in FACSCalibur. Results were analyzed with FlowJo software, Version 8.7.

Intracellular staining. To quantify brachyury intracellular expression, cells were fixed in 4% w/v PFA at room temperature for 15 min and permeabilized with 0.2% v/v Triton for 5 min. Cells were then incubated with FITC-conjugate anti-Brachyury antibody, for 1 h at 4°C, after which they were washed with PBS-2% FBS and analyzed by imaging flow cytometry (IFC).

Cell senescence analysis by flow cytometry. The senescence of bNP cells was analyzed by the detection of beta-galactosidase activity by flow cytometry, as described by Debacq-Chainiaux *et al.*[20] Briefly, bNP cells were treated with Bafilomycin A1 (100 nM) for 1 h in fresh culture medium at 37°C, 5% CO_2, to induce lysossomal alkalinization. Then, the substrate dodecanoylaminofluorescein di-β-D-galactopyranoside (C_{12}FDG, 33 μM) was added to the cell suspension and incubated during 1–2 h. This substrate, when hydrolyzed by beta-gal, becomes fluorescent. After incubation, the cells were washed in ice-cold PBS, stained with PI, and analyzed by flow cytometry in an FACSCalibur. C_{12}FDG was detected on the FL1 channel. Negative controls of bNP cells incubated only with Bafilomycin A1 or with C_{12}FDG were also performed. The data collected were analyzed in FlowJo vs 8.7 software.

Statistical analysis

Statistical analysis was performed using GraphPad Prism version 6.0a for Mac OS X. D'Agostino and Pearson omnibus normality test was used to assess Gaussian distribution of data. Results that did not follow a normal distribution (cell yield, viability, apoptosis, cell subpopulations sizes [P1, P2, and P3], and marker expression) were analyzed for statistical differences using non-parametric Kruskal–Wallis and Dunn's multiple-comparison tests. In the case of cell morphology data, which followed a Gaussian distribution, groups were compared using a two-way ANOVA (Bonferroni's multiple-comparisons test). In all cases, a confidence level of at least 95% ($^*p < 0.05$) was considered.

Results

Isolation of bNP cells

In order to characterize bNP cells, the cell isolation procedure was first optimized. For that, three different commercially available collagenase formulations were tested: (1) Coll-I, the formulation most used in the literature; (2) Coll-II, a mixture with augmented activity of type-II-collagenase; and (3) Coll-XI, with augmented activity of both type I and II collagenases. The effect of enzyme concentration (0.5, 1, and 2 mg/mL) and tissue digestion time (4 h and overnight) on cell yield, viability, and apoptosis were addressed (Fig. 1).

For shorter digestion periods (4 h), cell yield increased in a concentration-dependent manner with digestion by Coll-XI. In particular, the median cell yield obtained with Coll-XI digestion (2.0 mg/mL) ($[1.2 \pm 0.5] \times 10^6$ cells/mg of wet tissue) was significantly higher ($^*p < 0.05$) than with Coll-I ($[6.3 \pm 5.8] \times 10^5$ cells/mg of wet tissue) or Coll-II ($[5.9 \pm 3.1] \times 10^5$ cells/mg of wet tissue) (Fig. 1a, left). With a longer period of digestion (overnight), no significant differences could be found between the protocols tested, with a high variability being observed (Fig. 1a, right). However, lower cell yields were observed at higher enzyme concentrations (except for Coll-I). In particular, overnight digestion with Coll-II at 2.0 mg/mL resulted in a drop in cell yield to $0.2 \pm 1.6 \times 10^5$ cells/mg wet tissue.

In terms of cell viability, there was also an increase (79–85%) when using Coll-XI, for shorter incubation periods, and independently of enzyme concentration. Cell viability after 4 h digestion with different collagenases ranged from (1) 72% ± 15% to 81% ± 13% for Coll-I; (2) 63% ± 33% to 81% ± 19% for Coll-II; and (3) 79% ± 22% to 85% ± 16% for Coll-XI (Fig. 1b, right). With prolonged digestion time, cell viability showed a decrease, with exception of protocols using Coll-I, with viability around 80% (Fig. 1b, right). Finally, the median percentage of apoptotic cells stood majorly below 5%, with no obvious differences between formulations (Fig. 1c).

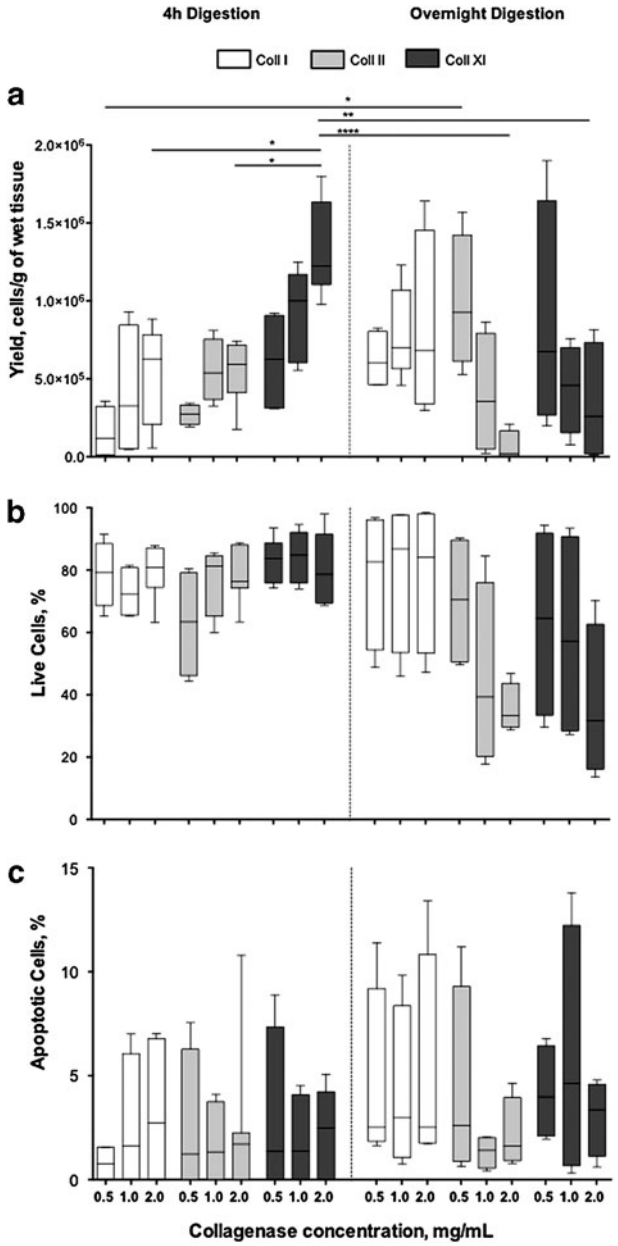

FIG. 1. Effect of collagenase (Coll) type, enzyme concentration, and digestion time on bovine nucleus pulposus (bNP) cell isolation. Coll-I (*white bars*), Coll-II (*light gray*), and Coll-XI (*dark gray*) were used at 0.5, 1, or 2 mg/mL to dissociate NP tissue for 4 h or overnight. Cell yield (cells/g of wet tissue) **(a),** cell viability (% of live cells determined by flow cytometry analysis of propidium iodide [PI] stained cells) **(b),** and cell apoptosis **(c)** in the different conditions were determined. Results are presented as box plot and *whiskers* (min to max) with horizontal line at median ($n = 4$–8). Results were analyzed for statistical differences using non-parametric Kruskal–Wallis and Dunn's multiple-comparison tests (*$p < 0.05$, **$0.001 < p < 0.01$ and ***$p < 0.001$).

Morphological analysis of bNP cells

In order to characterize bNP cell morphology immediately on isolation, freshly isolated bNP cells were analyzed by IFC, using masks for brightfield images of cells and for fluorescence images of the cytoskeleton and nuclei (Fig. 2).

Cells area was first quantified based on both brightfield and fluorescence images of cell cytoskeleton (Fig. 2b). Quantification on the cytoskeleton staining revealed that bNP cells present an area ranging from $130 \pm 17\,\mu m^2$ to $138 \pm 34\,\mu m^2$, independently of the method of tissue digestion. These values were significantly different from the area calculated based on brightfield images, which suggests the presence of a structure surrounding the cell cytoskeleton in most of the cells. In the case of cells dissociated with Coll-XI, the cell area almost doubled ($130 \pm 17\,\mu m^2$ to $235 \pm 38\,\mu m^2$, for cytoskeleton and brighfield areas, respectively). The presence of a pericellular matrix surrounding the cells was confirmed by staining against type VI collagen (Supplementary Fig. S1; Supplementary Data are available online at www.liebertpub.com/tea). Thus, cell diameter was analyzed based only on images of actin staining (Fig. 2c). It was observed that bNP cells have a diameter of $\sim 17.3 \pm 1.3\,\mu m$, not varying with the tissue digestion method.

The nuclear-to-cytoplasmic ratio (N/C, nucleus area/cytoplasm area) of bNP cells, a feature that has been previously linked to the presence of progenitor cells,[21] was quantified from the nuclei and actin staining (Fig. 2a, second column). The N/C ratio of bNP cells isolated with Coll-I, Coll-II, and Coll-XI (2.0 mg/mL, 4 h digestion) ranged from 0.5 ± 0.1 (Coll-II) to 0.6 ± 0.1 (Coll-I and Coll-XI), respectively (Fig. 2d, up), with no significant differences found between the isolation methods. Thus, the area occupied by the nucleus is about half the cytoplasmic area. Moreover, the distribution of N/C ratio was very narrow within bNP cells (Fig. 2d, down).

In addition, image analysis of bNP cells revealed the presence of putative vesicles within the cytoplasm of these cells (Fig. 2e, up). The percentage of bNP cells containing vesicles was quantified by using a mask specifically designed to trace bright spots in brightfield images (Fig. 2e, down). The results obtained showed that around 50–60% of NP cells presented one or more cytoplasmic bright vesicles (0.5–1.5 μm diameter), independently of the digestion protocol used.

Characterization of bNP cells by flow cytometry

bNP cells freshly isolated with the different collagenases (Coll-I, Coll-II, and Coll-XI) were analyzed by flow cytometry (Fig. 3). Discarding PI-positive cells (dead cells), three subpopulations (P1, P2, and P3) of live cells could be consistently identified, based on their size (forward scatter-height [FSC-H]) and auto-fluorescence (in FL3 channel), evidencing a heterogeneous cell population within bNP tissue. The presence of nuclei in these bNP cells was confirmed by DRAQ5 expression (Fig. 3c).

The subpopulations were distinguishable by (1) small cells with high auto-fluorescence (P1); (2) large cells with high auto-fluorescence (P2); and (3) median sized cells with low auto-fluorescence (P3) (Fig. 3a). The frequency of each subpopulation obtained with the different isolation methods was assessed (Fig. 3b). P2 is the most abundant subpopulation within bNP cells, with frequencies of 45–62% (Coll-I), 48–65% (Coll-II), and 66–68% (Coll-XI). The P1 subset is less frequent: 32–47% (Coll-I), 29–50% (Coll-II), and 25–28% (Coll-XI). Lastly, P3 is the least frequent subpopulation (<10%): 4–8% (Coll-I), 3–6% (Coll-II), and

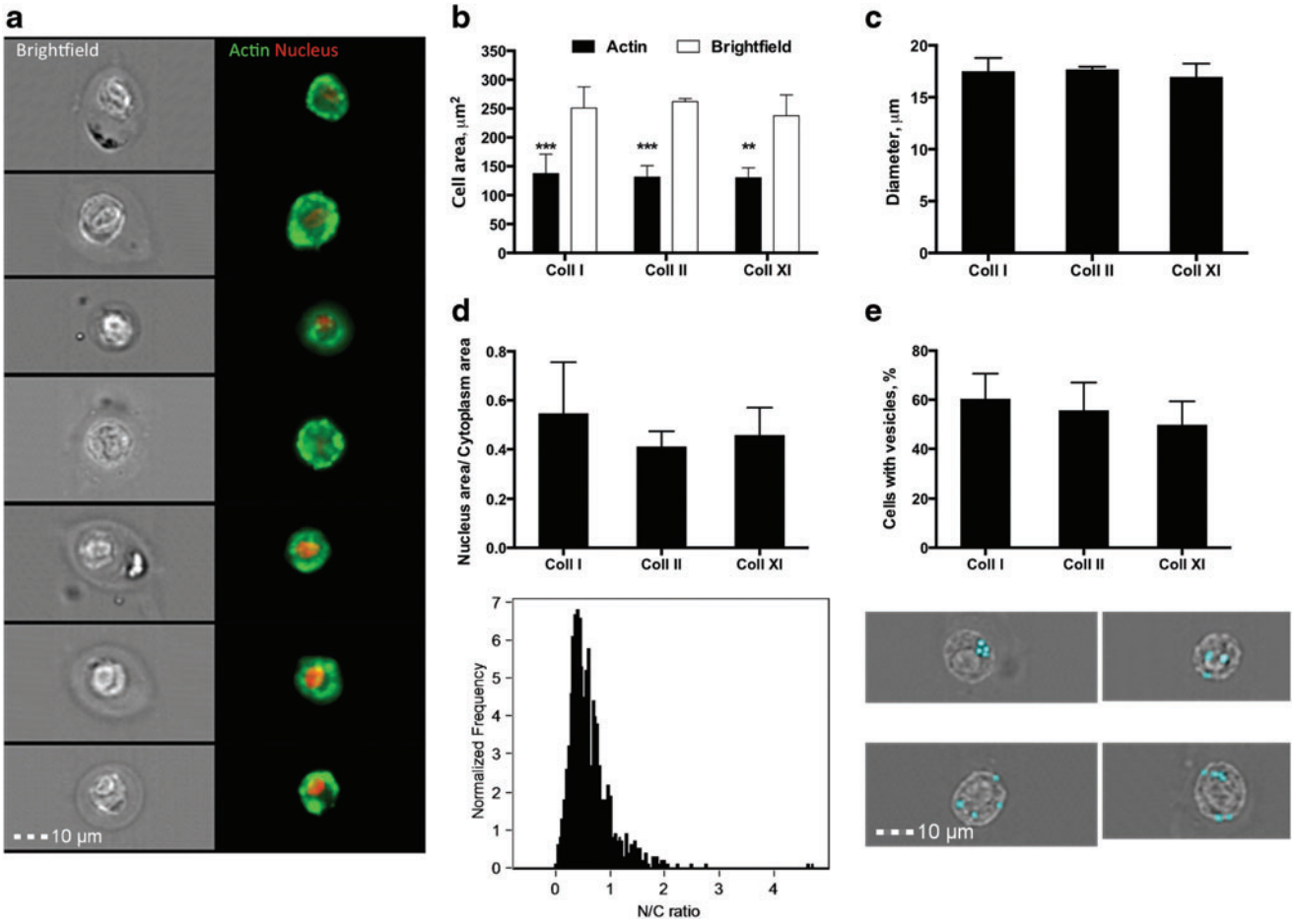

FIG. 2. Morphological analysis of bNP cells. **(a)** Images of bNP cells obtained by Imaging Flow Cytometry (*first column*: brightfield images of cells; *second column*: merged fluorescence images of cells stained with phalloidin-FITC (actin, *green*) and DRAQ5 (nuclei, *red*); **(b)** bNP cell area based on brightfield (*white bars*) and actin staining (*black bars*) images of tissue digested with different collagenases: Coll-I, Coll-II, and Coll-XI (2.0 mg/mL, 4 h digestion); **(c)** bNP cell diameter based on actin staining for tissue digested with the three collagenases; **(d)** nuclear-to-cytoplasmic (N/C) ratio of bNP cells isolated with the three different methods (*top*), and representative histogram of N/C ratio distribution of bNP cells isolated with Coll-I, 2.0 mg/mL for 4 h (*bottom*); **(e)** Percentage of cells containing one or more vesicles after isolation with the different collagenases—a *light blue mask* specifically designed to mark and quantify bright vesicles within cells is shown in the bottom brightfield images of cells. Results are presented as mean ± SD of three independent experiments, where a total of 3661 cells for Coll-I, 993 cells for Coll-II, and 5385 cells for Coll-XI were analyzed. In the case of cell area analysis, groups were compared using a two-way ANOVA (Bonferroni's multiple-comparisons test). $^{**}0.001 < p < 0.01$ and $^{***}p < 0.001$. Color images available online at www.liebertpub.com/tea

5–8% (Coll-XI). Different concentrations of Coll-XI lead to the same distribution of the three populations. The three subpopulations were also identified in old bovine animals (>10 years) but with a different ratio: Lower P3 and higher P1 percentages were observed (Supplementary Fig. S2).

Based on the higher cell yield obtained and consistency of the subpopulations observed, subsequent assays were performed with cells obtained by 4 h digestion with Coll-XI at 2.0 mg/mL.

Senescence analysis of bNP cells by flow cytometry

The senescence of bNP cells was analyzed by beta-galactosidade activity and its distribution within P1, P2, and P3 subpopulations was assessed (Fig. 4). The data collected showed that the bulk bNP cell senescence ranges from 13% to 71%. When analyzing in greater detail, no senescent cells could be observed within sub population P1, while P2 and P3 present 60% ± 7% and 56% ± 48% of cell senescence, respectively. When cell senescence ($C_{12}FDG^{+}$) versus viable cells (PI^{-}) is analyzed, the existence of two populations with senescent cells is clear but with distinct levels of autofluorescence (Fig. 4, first line).

Phenotypic characterization of bNP cells by flow cytometry

To deal with bNP cell characterization further, the phenotype of these cells was analyzed by flow cytometry. A panel of markers for bNP cells was analyzed (Table 2).

Expression of each marker in the whole bNP cell population was quantified (Fig. 5). Brachyury expression was

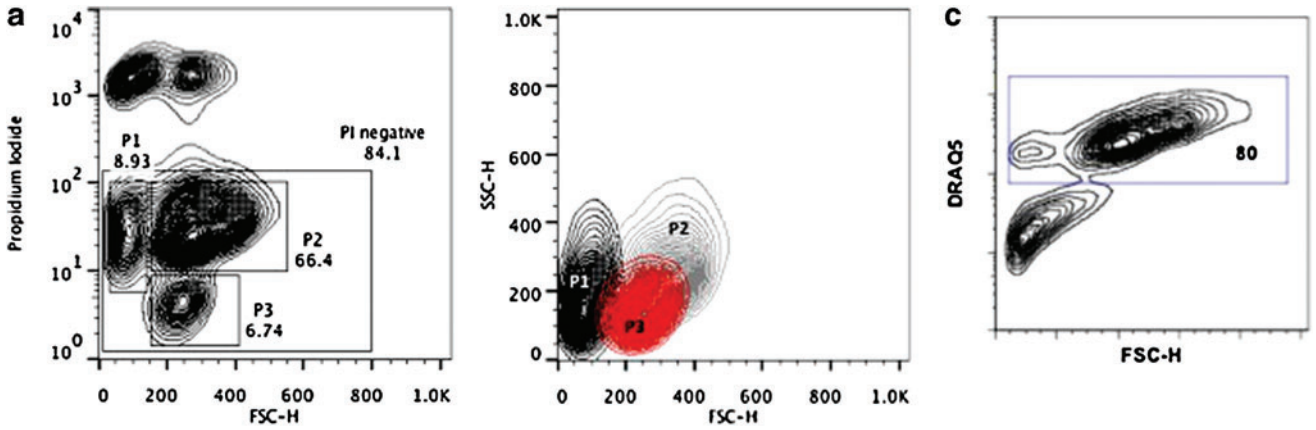

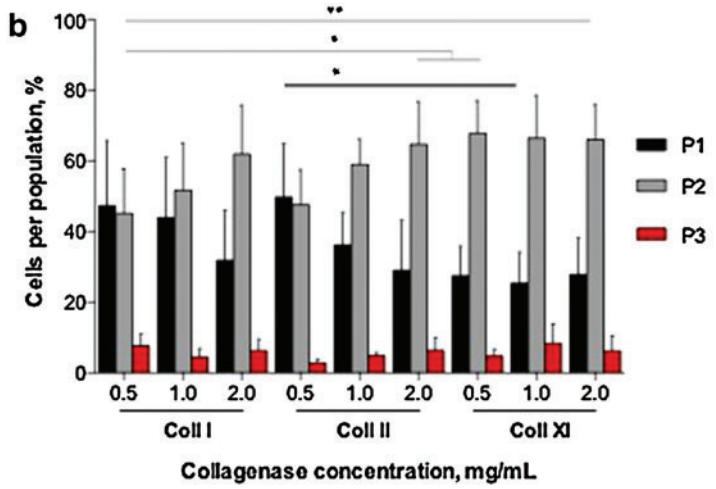

FIG. 3. Identification of subpopulations of bNP cells, based on size and auto-fluorescence, by flow cytometry. **(a)** Contour plots of freshly isolated bNP cells: PI expression versus forward scatter-height (FSC-H) (*left*) and side scatter-height (SSC-H) versus FSC-H (*right*). Three subpopulations of live cells (P1, P2, and P3) could be consistently identified, with distinct size and auto-fluorescence. **(b)** Percentages of cells in P1, P2, and P3 subpopulations after NP digestion with Coll-I, Coll-II, and Coll-XI (0.5, 1.0, and 2.0 mg/mL, 4 h digestion). Results are presented as mean ± SD ($n = 4$–8), and analyzed for statistical differences using non-parametric Kruskal–Wallis and Dunn's multiple-comparison tests. $*p < 0.05$ and $**0.001 < p < 0.01$; **(c)** PI and DRAQ5 staining of bNP cells on isolation. Around 80% of all events are DRAQ5 positive ($n = 5$). Color images available online at www.liebertpub.com/tea

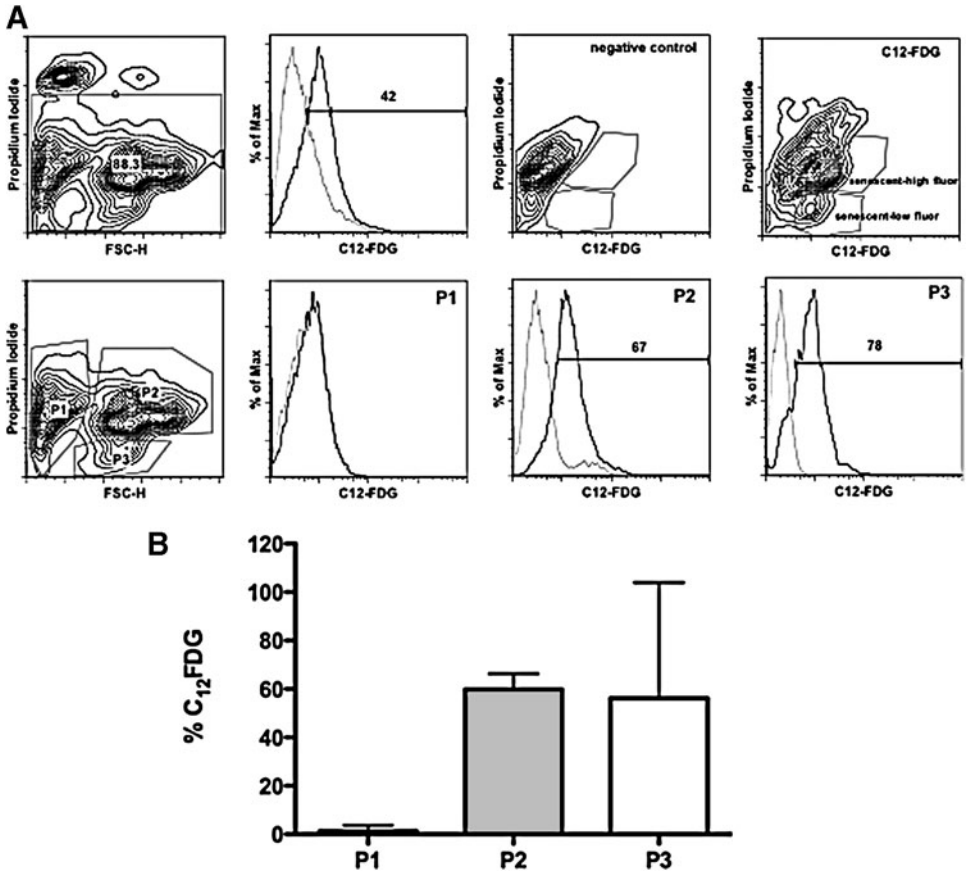

FIG. 4. Senescence analysis of bNP cells. Freshly isolated bNP cells were incubated with C_{12}FDG, a fluorescent substrate for beta-galactosidase. **(A)** The fluorescence intensity of C_{12}FDG cell in the whole population of bNP cells is represented in the *first line* for a representative donor. The *second line* illustrates the intensity of C_{12}FDG cells for subpopulations P1, P2, and P3. C_{12}FDG was assessed in FL1 channel. The cells were also stained with PI (FL3 channel), to exclude dead cells. **(B)** Quantification of C_{12}FDG expression on bNP cell subpopulations, P1, P2, and P3. Results are presented as mean ± SD ($n = 3$ independent donors).

Table 2. Findings in the Literature and in This Study Regarding Markers Selected to Characterize Bovine Nucleus Pulposus Cell Phenotype

Marker	*Description*	*Species*	*Method*	*Findings in the literature*	*Findings in this study*
CD29 (β1-integrin)	Cellular adhesion marker.	Human,[13,51,52] rabbit,[53] porcine,[52] rat[11]	IHC, FC	Protein expressed by NP cells from degenerated human IVDs and young AF cells, after monolayer expansion. Also present in rabbit and rat IVD and in immature porcine NP and AF.	Detected in more than 80% of bNP cells immediately on isolation.
CD44	Transmembrane protein. Primary hyaluronic acid receptor.	Human,[9,54] rabbit,[55–57] rat[11,58]	FC, IHC, RT-PCR	>80% expression by human $CD24^+$ NP cells and in cells cultured from herniated and degenerated human IVDs, rabbit NP, and in the developing and adult rat IVD. mRNA detected in rabbit AF-derived stem cells.	Detected in nearly 20% of bNP cells immediately on isolation. One subpopulation (P1) with significantly higher percentage of $CD44^+$ cells.
CD45	Hematopoietic lineage-restricted surface marker.	Human[9,54]	FC	Not found in $CD24^+$ NP cells nor in cells from herniated and degenerated IVDs after culture.	Expressed by only 8% bNP cells. Subpopulation P1 with higher percentage of $CD45^+$ cells. Expressed only by cells from P1 and P2.
CD146 (MCAM or MUC18)	Glycoprotein. Marker for vascular endothelial cells, smooth muscle cells, pericytes and mesenchymal stem cells.	Human[9]	FC	Not found in $CD24^+$ NP cells after culture.	Expressed by more than 20% of bNP cells. Expressed only by cells from subpopulations P1 and P2.
CD34	Transmembrane protein. Marker for hematopoietic progenitors and vascular endothelial cells.	Human[9,11,54,59–62]	IHC, FC	Detected in blood vessels in degenerated IVDs. Also found in healthy AF and in NP obtained by surgery. Not found in $CD24^+$ NP cells nor in cells from herniated and degenerated IVD tissues after culture.	Expressed by around 2% of bNP cells.
Brachyury (T)	Transcription factor. Marker for notochordal cells and NP cells	Human,[63,64] rat,[65] mouse,[63] bovine,[64] dog[66]	WB, FC, IHC, RT-PCR, qPCR	Expressed in NP from degenerated human IVD. mRNA expression by AF and NP cells from normal and degenerated IVDs and in bNP cells. 15% expression by NP cells from 1 month-old rats. High expression in the developing mouse NP (not found in AF or cartilage endplates). Decreased expression with aging and degeneration in chondrodystrophic dogs.	Expressed by more than 90% bNP cells.

bNP, bovine nucleus pulposus; AF, annulus fibrosus; IHC, immunohistochemistry; FC, flow cytometry; WB, Western blot; RT-PCR, real-time polymerase chain reaction; qPCR, quantitative polymerase chain reaction; IVD, intervertebral disc.

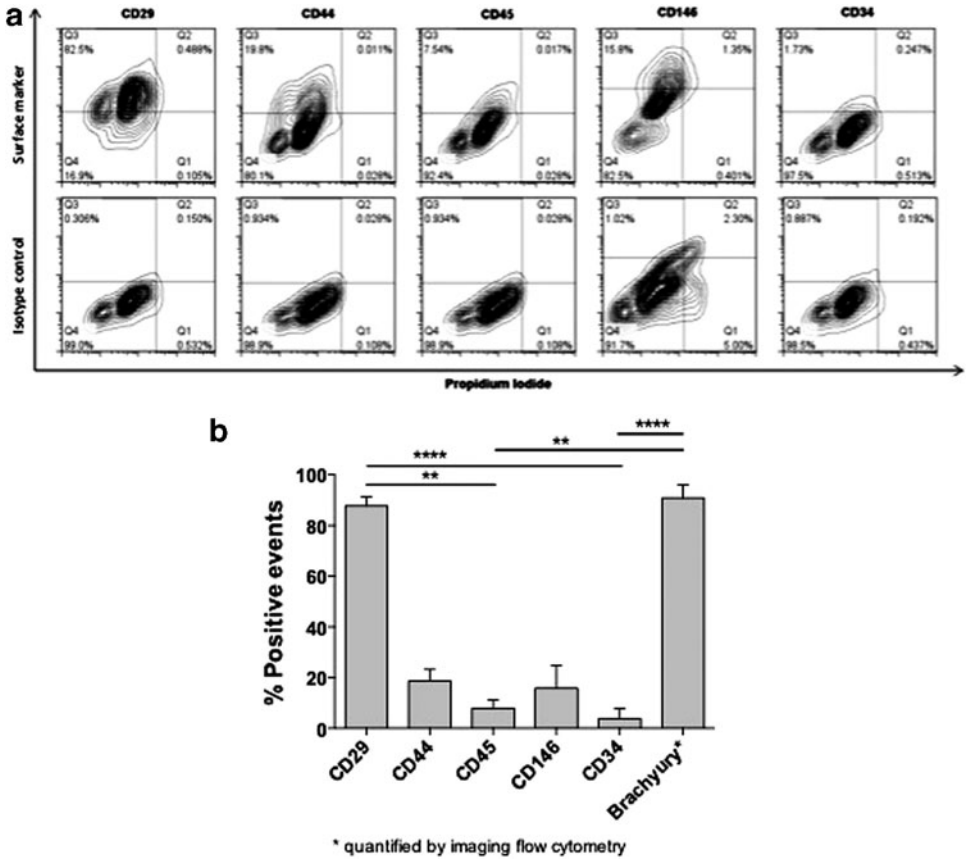

FIG. 5. Phenotypic analysis of freshly isolated bNP cells, obtained after digestion with Coll-XI (2.0 mg/mL, 4 h). **(a)** Flow cytometry contour plots of CD29, CD44, CD45, CD146, and CD34 expression of live bNP cells (PI negative). Gates were established according to respective isotype controls (*bottom*). **(b)** Graph shows the mean percentage of live cells expressing each of the markers described, after subtracting the respective isotype control. Results are presented as mean ± SD ($n = 5$–7), and statistical differences were assessed using non-parametric Kruskal–Wallis and Dunn's multiple-comparison tests (**$0.001 < p < 0.01$ and ****$p < 0.0001$).

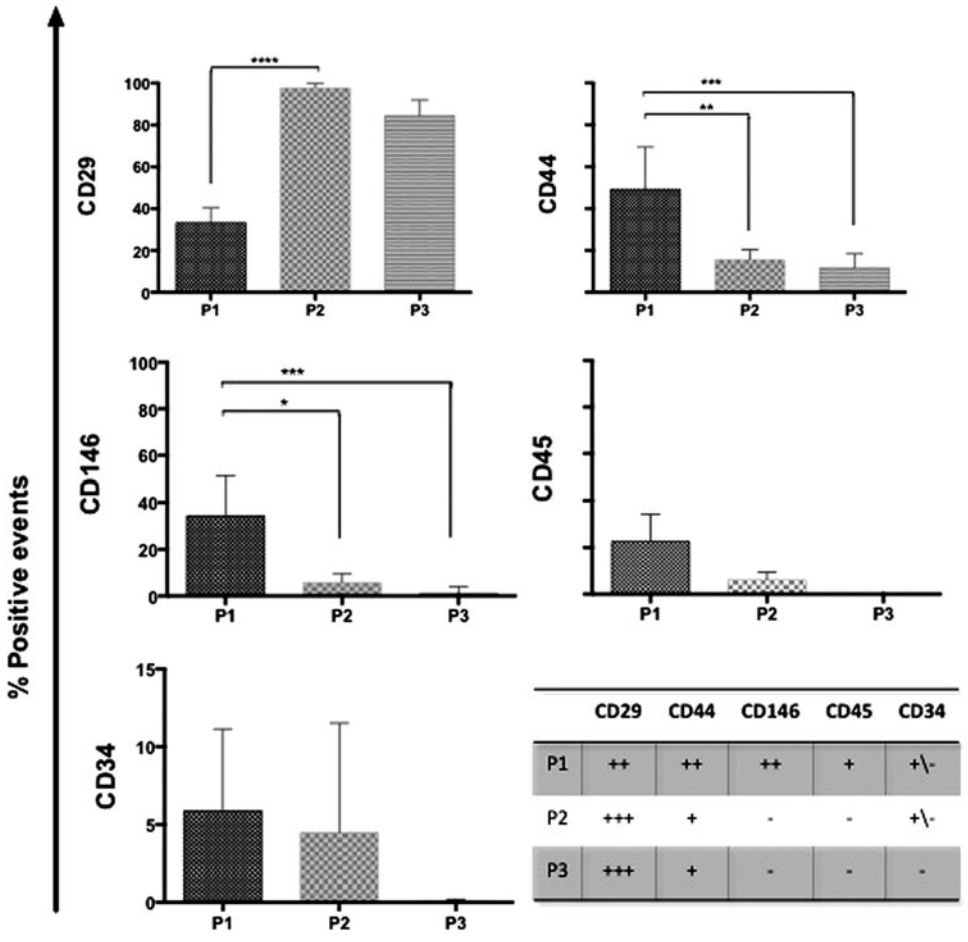

	CD29	CD44	CD146	CD45	CD34
P1	++	++	++	+	+\-
P2	+++	+	-	-	+\-
P3	+++	+	-	-	-

FIG. 6. Expression of the cell surface markers CD29, CD44, CD45, CD146, and CD34 within P1, P2, and P3 subpopulations, after dead cell exclusion by PI staining. Results are presented as mean ± SD ($n = 4$–7) and were analyzed for statistical differences using non-parametric Kruskal–Wallis and Dunn's multiple-comparison tests (*$p < 0.05$, **$0.001 < p < 0.01$, ***$p < 0.001$ and ****$p < 0.0001$). A comparative summary of the percentages of cells expressing each surface marker for the different subpopulations is presented in the table.

quantified by IFC, through which it was also possible to validate its correct intra-nuclear localization. The majority of bNP cells were $CD29^+$ (87.7% ± 4%) and $Brachyury^+$ (90.8% ± 5%). Intermediate amounts of cells expressing CD44 (18.6% ± 5%) and CD146 (22.3% ± 8%) were detected, while only low percentages of hematopoietic-lineage markers, CD45 (8.3% ± 4%) and CD34 (2.3% ± 1%), were identified.

In addition, expression of each marker was analyzed in P1, P2, and P3 subpopulations (Fig. 6). The frequency of $Brachyury^+$ cells within the three subpopulations was not analyzed, since the detection of this transcription factor could not be simultaneously performed with PI staining, and almost all bNP cells were $Brachyury^+$ (Fig. 5). P2, the most frequent subpopulation of bNP cells, was characterized by a large number of cells expressing CD29 (98% ± 2%), some cells expressing CD44 (16% ± 5%), and only a few cells expressing CD146 (6% ± 4%), CD45 (7% ± 4%), and CD34 (5% ± 8%). P3 (median-sized cells with low auto-fluorescence) showed a profile similar to P2, with a high percentage of $CD29^+$ cells (85% ± 7%) and lower number of $CD44^+$ cells (12% ± 7%). However, no cells expressing CD34, CD45, or CD146 were detected in P3. Finally, P1, the subpopulation of smaller cells, had a significantly higher ($^{**}p < 0.025$) percentage of $CD44^+$ cells (49% ± 2%). A higher percentage of cells expressing CD45 (24% ± 13%), CD34 (6% ± 5%), and CD146 (39% ± 17%) was also found within this subset. On the other hand, the frequency of $CD29^+$ cells (33% ± 7%) was significantly lower ($^{***}p < 0.001$) than that found in P2 and P3. Observation of the FSC versus FL3 plots for the cells positive for each marker leads to a clearer distinction between P2 and P3 (Supplementary Fig. S3): CD45 and CD146 expression was found in P2 but not in P3 (even though only a small percentage of cells in P2 expresses these molecules).

Discussion

Envisaging standardization of NP cell isolation protocols is widely variable within the literature,[5,6,16–18,22] bNP digestion was compared for different collagenases. Until now, no commercially available formula was designed to digest NP tissue specifically, most likely because it would serve a relatively small, although fast-growing, community of researchers in this field. Nevertheless, standardization of the NP cells isolation method would increase the reliability of results obtained in different labs.

Here, the results obtained show that bNP 4 h digestion with Coll-XI (2.0 mg/mL) originated higher cell yields than with Coll-I or Coll-II. This suggests that for short-time periods, it is necessary to have a simultaneous increase of enzymatic activity against both type I and II collagens to better dissociate bNP tissue, although this tissue is known to be enriched in type-II-collagen.[23] Besides being faster, treatment with Coll-XI did not require any additional step of digestion with other enzymes commonly used for NP cell dissociation, such as hyaluronidase[24] or pronase, known to negatively affect the expression of surface markers on AC chondrocytes.[25] On the other hand, for longer digestion time periods (overnight), Coll-I revealed to be a better option than Coll-XI, originating higher cell yields and increased cell viability. Surprisingly, Col II digestion at this longer time period caused very high cell death, suggesting that with prolonged time of exposure, digestion of type-II-collagen is more aggressive than type I collagen. In all conditions tested, cell viability was below values usually reported (>95%),[22] which may be due to the higher accuracy of the PI-exclusion method, when compared with the commonly used trypan blue dye exclusion assay.

Morphology of bNP cells after isolation was analyzed by IFC, a technique that provides high-resolution images of thousands of cells in flow, and analyses a wider array of cellular parameters,[21] when compared with confocal and electron microscopy, traditionally used to characterize IVD cells.[26,27] bNP cells presented an N/C ratio around 0.5 and an area of 120–130 μm^2, in agreement with the mean surface area of bovine IVD cells previously reported on freshly isolated cells.[6] Moreover, a structure surrounding bNP cell membrane was detected, resembling a pericellular matrix-like structure, frequently described in chondrons in AC,[28] and also reported in human and rat IVD cells.[29,30] As expected, this structure stained positive for the ECM protein type VI collagen.[23] Interestingly, the presence of bright vesicle-like structures (0.5–1.5 μm diameter) was detected in 60% of bNP cells. Other authors have already reported the existence of cell vesicles in IVD cells: (1) 1–20 μm vesicles were described in NP progenitors, that is, NC, from non-chondrodystrophic mongrel dogs[31]; (2) 20 nm–100 μm lipid droplets were described in mature human NP cells' cytoplasm[32]; and (3) <1 μm size vesicles were recently described in human NP cells.[33] In addition, it has been suggested that cell communication between NP cells can be mediated by these membrane-bound microvesicles.[33]

Three subpopulations of bNP cells (P1, P2, and P3) were consistently identified by flow cytometry, based on different sizes and auto-fluorescence. NP cells auto-fluorescence was very recently described and related with cell necrosis and subsequent loss of mitochondrial membranes integrity, which could expose flavoproteins to oxidation, causing a blue-green shift in auto-fluorescence of cells.[34] Nevertheless, the auto-fluorescence described here was exclusive to live cells, that is, PI-negative events. Furthermore, the senescence of each subpopulation of bNP cells was analyzed by detecting β-galactosidase activity.[35] Results showed that bNP cells present a level of senescence of around 40%. In the literature, β-galactosidase-positive cells ranged from 8% to 95%, increasing with patients' age and passage number.[36] Here, no senescent cells were observed in P1, while both P2 and P3 presented higher senescence (~70–80%). Both populations include senescent cells while showing different auto-fluorescence levels, thus excluding the possibility that P2 and P3 populations are only one subset of cells in a different senescent state. Hence, the three subpopulations could instead be at different metabolic states, or at different stages of differentiation, as suggested elsewhere.[7,37] Interestingly, three subpopulations of human knee meniscus cells (from a fibrocartilaginous tissue as the IVD) have also been described, with a similar distribution of auto-fluorescence and size.[37] However, in this case, P1 (low size) was discarded, while the P2 subpopulation was distinguishable from P3 by the presence of a cell-associated matrix (expressing type I and II collagens and aggrecan).[37] Here, human NP cells obtained from patients with degenerated IVDs, but with contained NP, were also analyzed (Supplementary Methods ''Isolation of Human NP cells'', Supplementary Fig. S4). However, there

was no distinction of subpopulations, but it is unclear whether this is due to differences in degenerated versus healthy discs or to differences between species.

Expression of different surface markers was analyzed in the three populations. Table 2 summarizes the main findings reported here and previously published on expression of these markers in other animal models. Here, high percentages of cells expressing CD29 and Brachyury were detected in bNP cells. CD29 is an anchorage protein involved in cell adhesion and migration, and its expression was particularly abundant in P2 and P3 subsets. On the other hand, Brachyury is one of the earliest indicators of mesoderm formation during embryonic development. It has been suggested as an NP marker in IVD[4,5] and is mostly assessed at mRNA level.[5] Tang *et al.* reported much less cells expressing Brachyury ($\sim$15%) than what was observed in this study (nearly 90%), which may be due to inter-species differences.[65] According to this result, we could discard AF contamination in the samples analyzed.

In addition, about 20% of bNP cells express CD44, and particularly the P1 subpopulation. This transmembrane protein is a primary HA receptor that also binds to other extracellular proteins, including fibronectin and type I and VI collagens, and plays an important role during chondrogenesis.[24] Importantly, although CD44 cell surface epitope was reported to be especially sensitive to enzymatic digestion,[38] here we assured preservation of CD44 by avoiding hyaluronidase digestion.[24]

Regarding CD45 and CD34, low expression of these hematopoietic-lineage markers was found, and more associated with P1 subset, although tissue contamination with blood was not expected. Nevertheless, despite being considered an immune privileged site, it is becoming increasingly evident that inflammatory-like cells[16,17,39] or phagocytic cells[16] might be present in IVD. Although CD34 is known as a marker for hematopoietic progenitors[40] and vascular endothelial cells,[41] its expression has also been reported in other cell types such as skeletal muscle satellite cells,[42] hair follicle keratinocytes,[43] hepatic cells,[44] and human fibrochondrocytes found within the superficial region of the knee meniscus body.[37] Hence, CD34 expression by itself does not elucidate the origin of the small population described here, and future studies will be performed to address this, particularly by analyzing co-expression with other markers (e.g., CD31—mature endothelial cells; CD38, CD90—hematopoietic progenitors). Another study has identified Tie2/Ang-1 expression, usually associated with angiogenesis, in the avascular hNP microenvironment.[9] In fact, although endothelial cells are not expected within the NP, some molecules usually expressed by those cells (e.g., Tie2/Ang-1, vascular endothelial growth factor-A [VEGF-A], and its receptor, membrane-bound vascular endothelial growth factor receptor-1 [mbVEGFR-1]) can also be expressed by NP cells, in response to hypoxic conditions.[9,45]

Interestingly, here, a subset of $CD146^+$ cells was found in bNP, particularly in P1. CD146 has been suggested as a marker for endothelial cells,[46] melanoma cells,[47] and MSCs,[48] but had not been reported in NP cells or cartilage cells earlier. Its expression has been linked to MSCs multipotency and differentiation potential.[49] Expression of markers as CD146, together with MSCs non-specific markers, such as CD44 or CD73 and absence of blood and endothelial markers have also been linked to the existence of vascular pericytes, cells with multipotency and clonal capability.[50] Although expression of CD146 has not been found in human IVDs,[9] here a subset of bNP cells was found to express this marker.

Overall, the P1 subpopulation appears to be a distinguishable subset of bNP cells, enriched in $CD146^+$ and $CD44^+$ cells, while also containing few $CD45^+$ and $CD34^+$ cells. Cells within this subset present a more progenitor-like phenotype than those found in P2 or P3, which, due to their CD29 expression, could represent populations with higher migratory capacity. Regarding P2 and P3, senescence does not justify the differences in auto-fluorescence, and CD45 and CD146 expression was found in P2 but not in P3. Thus, the three populations described here can be identified by auto-fluorescence and size or by the combination of markers, but not a single marker.

The data collected with young and old animals suggest morphological changes with aging, with a decrease in P3 subset accompanied by an increase in P1. It is widely known that age affects NP cell morphology and molecular signature.[32] In particular, human/mouse NP progenitor cells identified by Tie2 expression were reported to be exhausted with age.[9] However, whether differences in P1/P2/P3 proportion for animals with different ages correlate with differences in NP cells phenotype is still being addressed.

In summary, this study presents new evidence on the heterogeneity of young NP cells. Future studies will be crucial to understand the contribution of each population for NP repair.

Acknowledgments

This work had the financial support of FCT/MEC through National Funds and was co-financed by the FEDER through the PT2020 Partnership Agreement under the 4293 Unit I&D. M.M. is recipient of a PhD grant (SFRH/BD/80577/2011) from FCT. C.R.A. and R.M.G. were also funded by North Region Operational Program (ON.2), in the framework of the ''Project on Biomedical Engineering for Regenerative Therapies and Cancer—NORTE-07-0124-FEDER-000005,'' through ''Quadro de Referência Estratégico Nacional (QREN).'' Imaging was performed at the Bioimaging Center for Biomaterials and Regenerative Therapies (b.IMAGE). The authors would like to acknowledge Carnes Landeiro, SA, for kindly providing the bovine tails, and Michiharu Sakurai and Eiichi Momotani for the anti-bovine CD34 antibody.

Authors' Contributions

M.M. performed laboratory work, sample collection, data analysis, and statistical analysis; contributed to study design; and drafted the manuscript. C.R.A. and R.M.G. participated in study design and coordination, performed laboratory work, contributed to data analysis and statistical analysis, and critically revised the manuscript for important intellectual content. M.A.B. conceived the study, contributed to its design and coordination, secured funding, and critically revised the manuscript for important intellectual content. All authors read and approved the final manuscript.

Disclosure Statement

No competing financial interests exist.

References

1. Hughes, S.P., *et al.* The pathogenesis of degeneration of the intervertebral disc and emerging therapies in the management of back pain. J Bone Joint Surg Br **94,** 1298, 2012.
2. Molinos, M., *et al.* Inflammation in intervertebral disc degeneration and regeneration. J R Soc Interface **12,** 2015.
3. Pereira, C.L., *et al.* The effect of hyaluronan-based delivery of stromal cell-derived factor-1 on the recruitment of MSCs in degenerating intervertebral discs. Biomaterials **35,** 8144, 2014.
4. Henriksson, H.B., and Brisby, H. Development and regeneration potential of the mammalian intervertebral disc. Cells Tissues Organs **197,** 1, 2012.
5. Minogue, B.M., *et al.* Transcriptional profiling of bovine intervertebral disc cells: implications for identification of normal and degenerate human intervertebral disc cell phenotypes. Arthritis Res Ther **12,** R22, 2010.
6. Gilson, A., Dreger, M., and Urban, J.P. Differential expression level of cytokeratin 8 in cells of the bovine nucleus pulposus complicates the search for specific intervertebral disc cell markers. Arthritis Res Ther **12,** R24, 2010.
7. Risbud, M.V., *et al.* Defining the phenotype of young healthy nucleus pulposus cells: recommendations of the Spine Research Interest Group at the 2014 annual ORS meeting. J Orthop Res **33,** 283, 2014.
8. Brisby, H., *et al.* The presence of local mesenchymal progenitor cells in human degenerated intervertebral discs and possibilities to influence these in vitro: a descriptive study in humans. Stem Cells Dev **22,** 804, 2012.
9. Sakai, D., *et al.* Exhaustion of nucleus pulposus progenitor cells with ageing and degeneration of the intervertebral disc. Nat Commun **3,** 1264, 2012.
10. van den Akker, G.G., *et al.* Novel immortal human cell lines reveal subpopulations in the nucleus pulposus. Arthritis Res Ther **16,** R135, 2014.
11. Risbud, M.V., *et al.* Evidence for skeletal progenitor cells in the degenerate human intervertebral disc. Spine (Phila Pa 1976) **32,** 2537, 2007.
12. Blanco, J.F., *et al.* Isolation and characterization of mesenchymal stromal cells from human degenerated nucleus pulposus: comparison with bone marrow mesenchymal stromal cells from the same subjects. Spine (Phila Pa 1976) **35,** 2259, 2010.
13. Feng, G., *et al.* Multipotential differentiation of human anulus fibrosus cells: an in vitro study. J Bone Joint Surg Am **92,** 675, 2010.
14. Huang, B., *et al.* Study to determine the presence of progenitor cells in the degenerated human cartilage endplates. Eur Spine J **21,** 613, 2012.
15. Miyazaki, T., *et al.* A phenotypic comparison of proteoglycan production of intervertebral disc cells isolated from rats, rabbits, and bovine tails; which animal model is most suitable to study tissue engineering and biological repair of human disc disorders? Tissue Eng Part A **15,** 3835, 2009.
16. Jones, P., *et al.* Intervertebral disc cells as competent phagocytes in vitro: implications for cell death in disc degeneration. Arthritis Res Ther **10,** R86, 2008.
17. Nerlich, A.G., *et al.* Immunolocalization of phagocytic cells in normal and degenerated intervertebral discs. Spine **27,** 2484, 2002.
18. Smith, L.J., *et al.* Nucleus pulposus cells synthesize a functional extracellular matrix and respond to inflammatory cytokine challenge following long-term agarose culture. Eur Cells Mater **22,** 291, 2011.
19. Wuertz, K., *et al.* Influence of extracellular osmolarity and mechanical stimulation on gene expression of intervertebral disc cells. J Orthop Res **25,** 1513, 2007.
20. Debacq-Chainiaux, F., *et al.* Protocols to detect senescence-associated beta-galactosidase (SA-betagal) activity, a biomarker of senescent cells in culture and in vivo. Nat Protoc **4,** 1798, 2009.
21. Zuba-Surma, E.K., *et al.* Morphological characterization of very small embryonic-like stem cells (VSELs) by ImageStream system analysis. J Cell Mol Med **12,** 292, 2008.
22. Horner, H.A., *et al.* Cells from different regions of the intervertebral disc: effect of culture system on matrix expression and cell phenotype. Spine **27,** 1018, 2002.
23. Roberts, S., *et al.* 1991 Volvo Award in basic sciences. Collagen types around the cells of the intervertebral disc and cartilage end plate: an immunolocalization study. Spine **16,** 1030, 1991.
24. Knudson, C.B. Hyaluronan and CD44: strategic players for cell-matrix interactions during chondrogenesis and matrix assembly. Birth Defects Res C Embryo Today **69,** 174, 2003.
25. Diaz-Romero, J., *et al.* Immunophenotypic analysis of human articular chondrocytes: changes in surface markers associated with cell expansion in monolayer culture. J Cell Physiol **202,** 731, 2005.
26. Hunter, C.J., Matyas, J.R., and Duncan, N.A. Cytomorphology of notochordal and chondrocytic cells from the nucleus pulposus: a species comparison. J Anat **205,** 357, 2004.
27. Johnson, W.E., and Roberts, S. Human intervertebral disc cell morphology and cytoskeletal composition: a preliminary study of regional variations in health and disease. J Anat **203,** 605, 2003.
28. Roberts, S., *et al.* Type III collagen in the intervertebral disc. Histochem J **23,** 503, 1991.
29. Gruber, H.E., Ingram, J.A., and Hanley, Jr., E.N. Morphologic complexity of the pericellular matrix in the annulus of the human intervertebral disc. Biotech Histochem **82,** 217, 2007.
30. Cao, L., Guilak, F., and Setton, L.A. Three-dimensional morphology of the pericellular matrix of intervertebral disc cells in the rat. J Anat **211,** 444, 2007.
31. Hunter, C.J., *et al.* Osmoregulatory function of large vacuoles found in notochordal cells of the intervertebral disc running title: an osmoregulatory vacuole. Mol Cell Biomech **4,** 227, 2007.
32. Trout, J.J., Buckwalter, J.A., and Moore, K.C. Ultrastructure of the human intervertebral disc: II. Cells of the nucleus pulposus. Anat Rec **204,** 307, 1982.
33. Strassburg, S., *et al.* Bi-directional exchange of membrane components occurs during co-culture of mesenchymal stem cells and nucleus pulposus cells. PLoS One **7,** e33739, 2012.
34. Dittmar, R., *et al.* In situ label-free cell viability assessment of nucleus pulposus tissue. J Orthop Res **32,** 545, 2014.
35. Dimri, G.P., *et al.* A biomarker that identifies senescent human cells in culture and in aging skin in vivo. Proc Natl Acad Sci U S A **92,** 9363, 1995.
36. Jeong, S.W., Lee, J.S., and Kim, K.W. In vitro lifespan and senescence mechanisms of human nucleus pulposus chondrocytes. Spine J **14,** 499, 2014.
37. Verdonk, P.C., *et al.* Characterisation of human knee meniscus cell phenotype. Osteoarthritis Cartilage **13,** 548, 2005.

38. Biddle, A., *et al.* CD44 staining of cancer stem-like cells is influenced by down-regulation of CD44 variant isoforms and up-regulation of the standard CD44 isoform in the population of cells that have undergone epithelial-to-mesenchymal transition. PLoS One **8,** e57314, 2013.
39. Phillips, K.L., *et al.* The cytokine and chemokine expression profile of nucleus pulposus cells: implications for degeneration and regeneration of the intervertebral disc. Arthritis Res Ther **15,** R213, 2013.
40. Pessa-Morikawa, T., Niku, M., and Iivanainen, A. Fetal bovine bone marrow is a rich source of CD34+ hematopoietic progenitors with myelo-monocytic colony-forming activity. Dev Comp Immunol **36,** 572, 2012.
41. Lanza, F., Healy, L., and Sutherland, D.R. Structural and functional features of the CD34 antigen: an update. J Biol Regul Homeost Agents **15,** 1, 2001.
42. Beauchamp, J.R., *et al.* Expression of CD34 and Myf5 defines the majority of quiescent adult skeletal muscle satellite cells. J Cell Biol **151,** 1221, 2000.
43. Trempus, C.S., *et al.* Enrichment for living murine keratinocytes from the hair follicle bulge with the cell surface marker CD34. J Invest Dermatol **120,** 501, 2003.
44. Crosby, H.A., Kelly, D.A., and Strain, A.J. Human hepatic stem-like cells isolated using c-kit or CD34 can differentiate into biliary epithelium. Gastroenterology **120,** 534, 2001.
45. Fujita, N., *et al.* Vascular endothelial growth factor-A is a survival factor for nucleus pulposus cells in the intervertebral disc. Biochem Biophys Res Commun **372,** 367, 2008.
46. Bardin, N., *et al.* Identification of the S-Endo 1 endothelial-associated antigen. Biochem Biophys Res Commun **218,** 210, 1996.
47. Shih, I.M., *et al.* Regulation of Mel-CAM/MUC18 expression on melanocytes of different stages of tumor progression by normal keratinocytes. Am J Pathol **145,** 837, 1994.
48. Covas, D.T., *et al.* Multipotent mesenchymal stromal cells obtained from diverse human tissues share functional properties and gene-expression profile with CD146+ perivascular cells and fibroblasts. Exp Hematol **36,** 642, 2008.
49. Russell, K.C., *et al.* In vitro high-capacity assay to quantify the clonal heterogeneity in trilineage potential of mesenchymal stem cells reveals a complex hierarchy of lineage commitment. Stem Cells **28,** 788, 2010.
50. Crisan, M., *et al.* Perivascular multipotent progenitor cells in human organs. Ann N Y Acad Sci **1176,** 118, 2009.
51. Bridgen, D.T., *et al.* Integrin-mediated interactions with extracellular matrix proteins for nucleus pulposus cells of the human intervertebral disc. J Orthop Res **31,** 1661, 2013.
52. Nettles, D.L., Richardson, W.J., and Setton, L.A. Integrin expression in cells of the intervertebral disc. J Anat **204,** 515, 2004.
53. Henriksson, H.B., *et al.* Support of concept that migrating progenitor cells from stem cell niches contribute to normal regeneration of the adult mammal intervertebral disc: a descriptive study in the New Zealand white rabbit. Spine (Phila Pa 1976) **37,** 722, 2012.
54. Marfia, G., Navone, S.E., Di Vito, C., *et al.* Gene expression profile analysis of human mesenchymal stem cells from herniated and degenerated intervertebral discs reveals different expression of osteopontin. Stem Cells Dev **24,** 320, 2015.
55. Gan, J.C., Ducheyne, P., Vresilovic, E., and Shapiro, I.M. Bioactive glass serves as a substrate for maintenance of phenotype of nucleus pulposus cells of the intervertebral disc. J Biomed Mater Res **51,** 596, 2000.
56. Gan, J.C., *et al.* Intervertebral disc tissue engineering I: characterization of the nucleus pulposus. Clin Orthop Relat Res **411,** 305, 2003.
57. Liu, C., Guo, Q., Li, J., *et al.* Identification of rabbit annulus fibrosus-derived stem cells. PLoS One **9,** e108239, 2014.
58. Stevens, J.W., Kurriger, G.L., Carter, A.S., and Maynard, J.A. CD44 expression in the developing and growing rat intervertebral disc. Dev Dyn **219,** 381, 2000.
59. Bu, G., Hou, S., Ren, D., Wu, Y., Shang, W., and Huang, W. Increased expression of netrin-1 and its deleted in colorectal cancer receptor in human diseased lumbar intervertebral disc compared with autopsy control. Spine **37,** 2074, 2012.
60. Johnson, W.E., Evans, H., Menage, J., Eisenstein, S.M., El., Haj, A., and Roberts, S. Immunohistochemical detection of Schwann cells in innervated and vascularized human intervertebral discs. Spine **26,** 2550, 2001.
61. Johnson, W.E., Patterson, A.M., Eisenstein, S.M., and Roberts, S. The presence of pleiotrophin in the human intervertebral disc is associated with increased vascularization: an immunohistologic study. Spine **32,** 1295, 2007.
62. Koike, Y., Uzuki, M., Kokubun, S., and Sawai, T. Angiogenesis and inflammatory cell infiltration in lumbar disc herniation. Spine **28,** 1928, 2003.
63. Risbud, M.V., and Shapiro, I.M. Notochordal cells in the adult intervertebral disc: new perspective on an old question. Crit Rev Eukaryot Gene Expr **21,** 29, 2011.
64. Kim, K.W., Lim, T.H., Kim, J.G., *et al.* The origin of chondrocytes in the nucleus pulposus and histologic findings associated with the transition of a notochordal nucleus pulposus to a fibrocartilaginous nucleus pulposus in intact rabbit intervertebral discs. Spine **28,** 982, 2003.
65. Tang, X., Jing, L., and Chen, J. Changes in the molecular phenotype of nucleus pulposus cells with intervertebral disc aging. PLoS One **7,** e52020, 2012.
66. Smolders, L.A., Meij, B.P., Riemers, F.M., *et al.* Canonical Wnt signaling in the notochordal cell is upregulated in early intervertebral disk degeneration. J Orthop Res **30,** 950, 2012.

Address correspondence to:
Mário A. Barbosa, PhD
Instituto de Engenharia Biomédica (INEB)
Universidade do Porto
Rua do Campo Alegre, 823
Porto 4150-180
Portugal

E-mail: mbarbosa@ineb.up.pt

Received: September 8, 2014
Accepted: April 27, 2015
Online Publication Date: July 13, 2015

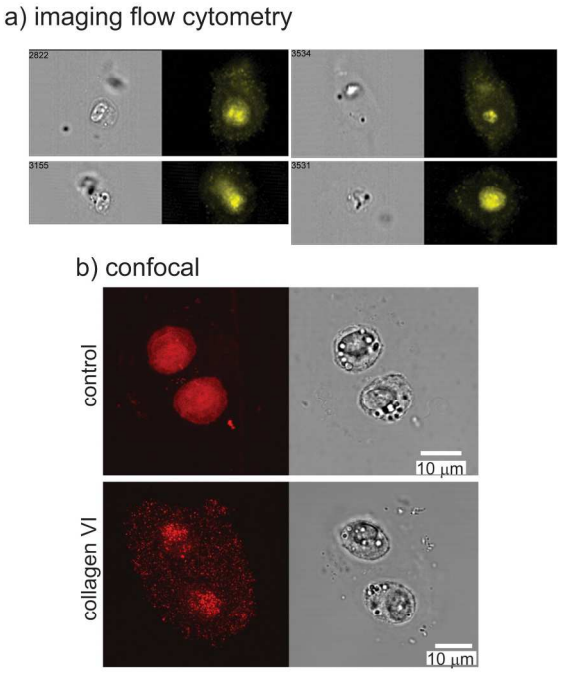

Supplementary Figure S1: Expression of type VI collagen on the pericellular matrix of bovine NP cells. Micrographs show brightfield (left) and fluorescence images (right) of freshly isolated bovine NP cells stained against collagen type VI and imaged by imaging flow cytometry (a) or confocal microscopy (b). A punctuated staining can be observed located in and outside the cytoplasm of the cells. Fluorescence and brightfield in b show a maximum projection and single slice, respectively. Control refers to cells stained only with the secondary antibody.
253x190mm (300 x 300 DPI)

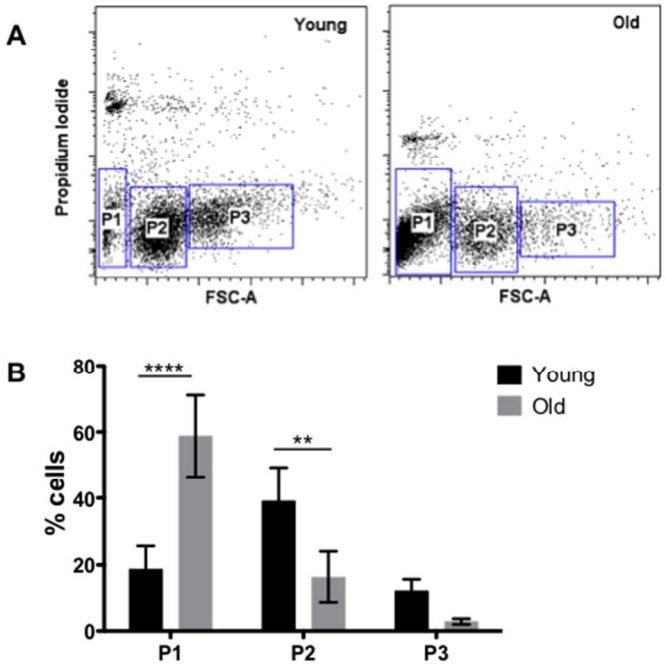

Supplementary Figure S2: Comparison of bNP cells size and auto-fluorescence analysed by flow cytometry of young and aged animals. A) Representative dot plots of Propidium Iodide expression versus size (FSC) of bNP cells from young and old animals. B) Distribution of P1, P2 and P3 subpopulations in young and old bovine animals. Results are presented as Mean±StDev (n=5 for old animals, n=4-7 for young animals) and were analysed for statistical differences using non-parametric Kruskal-Wallis and Dunn's multiple comparison tests (** $0.001 < p < 0.01$ and **** $p < 0.0001$).
60x45mm (300 x 300 DPI)

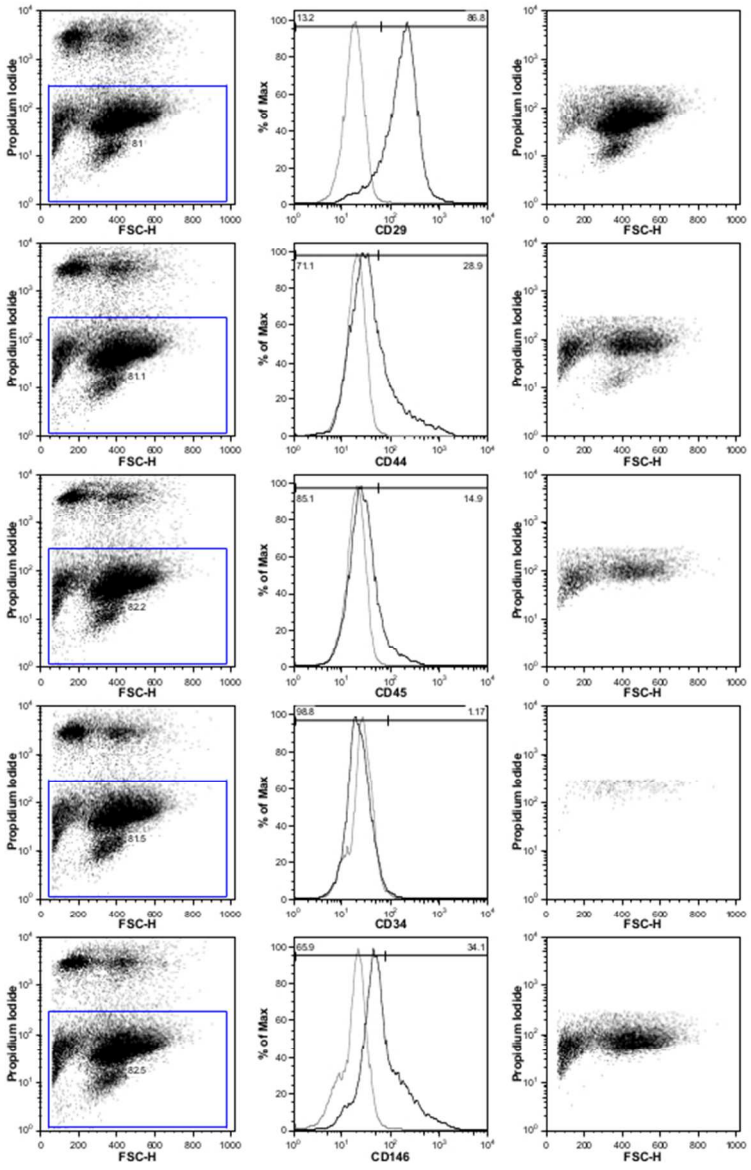

Supplementary Figure S3: Representative analysis of the distribution of each analysed marker (CD29, CD44, CD45, CD34 and CD146) within the 3 populations (P1, P2 and P3) of bNP cells.
141x220mm (100 x 100 DPI)

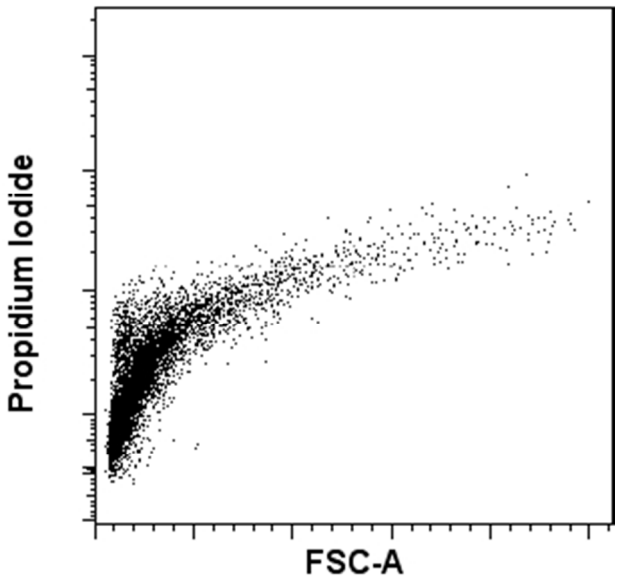

Supplementary Figure S4: Representative dot plot of Propidium Iodide expression versus size (FSC) of human NP cells obtained from biopsies of degenerated IVD with contained NP.
29x27mm (300 x 300 DPI)

INTERFACE

rsif.royalsocietypublishing.org

Review

Cite this article: Molinos M, Almeida CR, Caldeira J, Cunha C, Gonçalves RM, Barbosa MA. 2015 Inflammation in intervertebral disc degeneration and regeneration. *J. R. Soc. Interface* **12**: 20141191.
http://dx.doi.org/10.1098/rsif.2014.1191

Received: 30 October 2014
Accepted: 17 December 2014

Subject Areas:
biomedical engineering, biomaterials

Keywords:
intervertebral disc, degenerative disc disease, inflammation, regeneration, intervertebral disc homeostasis

Author for correspondence:
Mário A. Barbosa
e-mail: mbarbosa@ineb.up.pt

Inflammation in intervertebral disc degeneration and regeneration

Maria Molinos[1,2], Catarina R. Almeida[1], Joana Caldeira[1,3], Carla Cunha[1], Raquel M. Gonçalves[1] and Mário A. Barbosa[1,2]

[1]Instituto de Engenharia Biomédica—INEB, [2]Instituto de Ciências Biomédicas Abel Salazar—ICBAS, and [3]Instituto de Patologia e Imunologia—IPATIMUP, Universidade do Porto, Porto, Portugal

Intervertebral disc (IVD) degeneration is one of the major causes of low back pain, a problem with a heavy economic burden, which has been increasing in prevalence as populations age. Deeper knowledge of the complex spatial and temporal orchestration of cellular interactions and extracellular matrix remodelling is critical to improve current IVD therapies, which have so far proved unsatisfactory. Inflammation has been correlated with degenerative disc disease but its role in discogenic pain and hernia regression remains controversial. The inflammatory response may be involved in the onset of disease, but it is also crucial in maintaining tissue homeostasis. Furthermore, if properly balanced it may contribute to tissue repair/regeneration as has already been demonstrated in other tissues. In this review, we focus on how inflammation has been associated with IVD degeneration by describing observational and *in vitro* studies as well as *in vivo* animal models. Finally, we provide an overview of IVD regenerative therapies that target key inflammatory players.

1. Introduction

Between 70 and 85% of all people have low back pain (LBP) at some time in their life. LBP can limit the activity in people younger than 45, causing a tremendous socio-economic impact [1]. The aetiology of LBP is unclear but in 40% of cases it is related to intervertebral disc (IVD) degeneration [2]. In 90% of sciatica cases, it is also associated with a herniated IVD that compresses a nerve root causing pain [3]. Novel strategies such as gene therapy, growth factor injection, cell-based therapies and tissue engineering approaches are being developed towards impairing degeneration or promoting regeneration of the IVD [4]. However, to achieve full IVD regeneration it is also necessary to recover the biomechanical properties of a native IVD and restore the biological behaviour of resident cells, including production of healthy extracellular matrix (ECM), while ensuring reduction of IVD-associated pain.

Traditionally, inflammation has mostly been seen as detrimental and correlated with disease progression, but it remains unclear whether it is a cause or consequence of IVD degeneration and herniation. A balanced inflammatory response may be required for restoring IVD function as recently suggested for other tissues [5,6]. In this review, we will discuss the inflammatory reaction in IVD, both in homeostasis and IVD degeneration, and comprehensively cover the strategies applied to inflammatory cells and factors targeted towards IVD regeneration.

2. The origin of inflammation in intervertebral disc

Inflammation has mostly been regarded as a response to infection or tissue injury, but the scientific community has been increasingly researching its physiological role in maintaining tissue homeostasis [7]. In general, the mechanisms of inflammation are dependent on the inducing agent and context, with the inflammatory response in the context of infection having been investigated the most. In the infection instigated inflammatory response, plasma and

THE ROYAL SOCIETY PUBLISHING

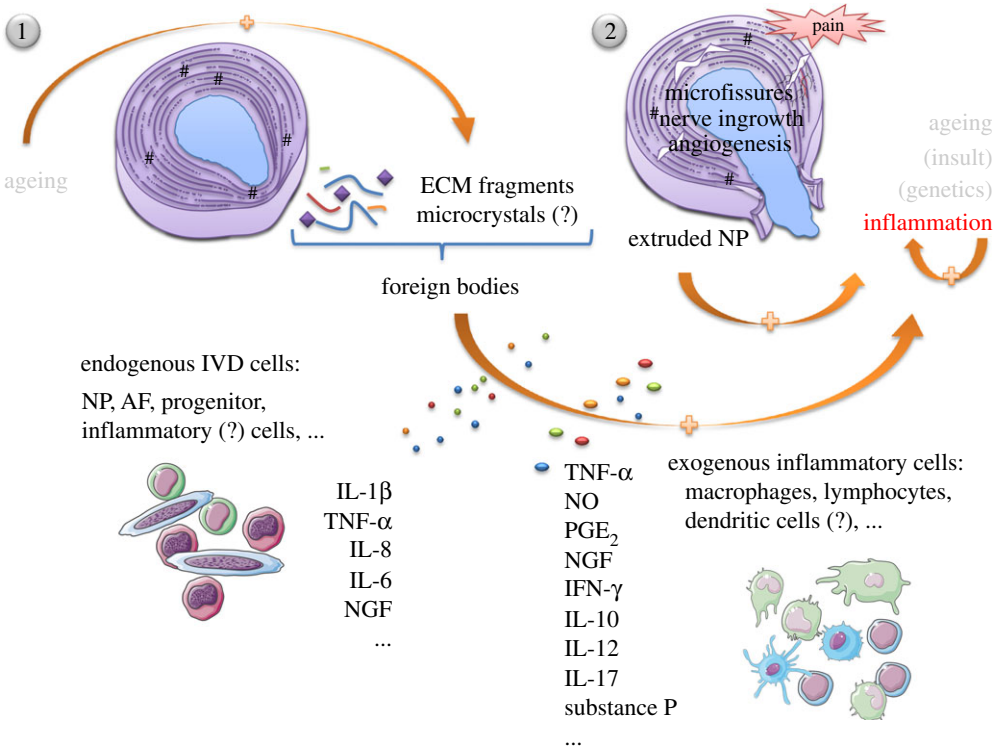

Figure 1. Inflammation in the IVD. It is unclear whether inflammation is the cause or consequence of disc degeneration and herniation, and what may trigger activation and recruitment of different immune cells. The normal ageing process allied to some genetic pre-disposition causes the IVD to degenerate giving rise to profound changes in the ECM—loss of proteoglycan content, dehydration, malnutrition, decrease of native cell population, matrix breakdown and calcifications. In this scenario, the natural response to mechanical loading is compromised and the IVD becomes prone to microfissures and consequent ingrowth of blood and nerve vessels. (1) Disc herniation may also occur when the AF is no longer able to sustain the NP. ECM fragments and microcrystals may internally elicit an inflammatory response, stimulating endogenous IVD cells to produce pro-inflammatory mediators, that will further feed the cascade of tissue degeneration—IL-1β, IL-8, IL-6. (2) NP is recognized as non-self by the immune system. Hence, its exposure (both in microfissures and herniation) may propagate an immunologic response, with recruitment of macrophages, lymphocytes and other possible inflammatory cells, in order to eliminate the foreign body. Discogenic pain has been many times attributed to TNF-α, PGE2, NO and IFN-γ secretion by macrophages, concomitantly with NGF and substance P production, accompanying the processes of nerve ingrowth and angiogenesis inwards the degenerated IVD. Activated B and T lymphocytes are also recruited to the site, contributing to the positive pro-inflammatory feedback loop established. It is not well understood how endogenous IVD cells interact with exogenous inflammatory cells and whether they positively contribute to tissue resorption and regeneration or not. Spontaneous disc regression is currently believed to be a consequence of macrophage activity.

leucocytes are recruited to the site of infection and soluble mediators that lead to recruitment and activation of other cell types are secreted. A complex cascade of events is triggered that eventually leads to clearing infection from the tissue and resolution of inflammation. In response to tissue injury, there also exists a vascular response and an orchestrated recruitment and activation of various cell types. However, the IVD is an avascular tissue and therefore it is unsurprising that the inflammatory response is different in this context.

The process of IVD degeneration implies a cascade of structurally disrupting events, normally starting with declining nutrition of cells within the central IVD, followed by accumulation of cell waste products and degraded matrix molecules. This creates an increasingly acidic environment which further compromises cell viability [8]. Various causes have been hypothesized to play a role in the pathogenesis of degenerative disc disease (DDD), such as endplate calcification, leading to an impairment of normal nutrition routes, excessive mechanical loading, genetic pre-disposition, unhealthy habits, ageing and spine infection [9–16]. Regardless of the cause, inflammation is an omnipresent player, and its association to LBP is clear [17]. Yet, it remains uncertain what may trigger the recruitment of immune cells to IVD and the associated inflammatory response (figure 1).

One hypothesis for the cause of the IVD inflammatory response relies on endogenous factors, such as crystals and ECM breakdown products, which could induce the inflammatory response [7]. Crystal deposits of calcium pyrophosphate dihydrate (CPPD), cuboid microstructures (characterized as magnesium whitlockite) and hydroxyapatite (HA) have been observed in degenerated IVD specimens [15,18–20]. In articular cartilage, regions with crystals showed altered amounts of collagen, calcium-binding proteins, decorin and large proteoglycan content, as well as abnormal pericellular matrix deposition [21,22]. Phagocytosis of crystals present in joints and pericellular tissues can trigger activation of the NOD-like receptor family pyrin domain containing 3 (NALP3) inflammasome. This cytoplasmic multimolecular protein complex regulates activity of caspase-1 and maturation and release of interleukin (IL)-1β [7,23], the latter being commonly found in degenerated IVD [24].

ECM breakdown products generated during tissue dysfunction or damage may also promote an inflammatory response as has been shown in various models [25,26]. The IVD is mostly composed of ECM molecules, including collagens, proteoglycans and other matrix proteins (see table 1 for more information), which are continuously synthesized and degraded by local existing proteases to maintain

Table 1. Main extracellular matrix components of a young and healthy IVD.

name	distribution/localization	putative/possible function
collagens		
fibril-forming collagens		
type I	AF and NP	confers tensile stiffness allowing torsion and flexion [27–30]
type II	AF and NP	confines PG within the matrix to retain more water to allow larger deformations and withstand greater compressive loads [31,32]
type III	NP and outer AF	organizes pericellular environment; allows extensibility of tissue [33–35]
type V	AF and NP (increased in AF cells when compared to NP cells)	regulates fibril diameter (smaller if this collagen is more abundant) influencing mechanical properties [35,36]
type XI [37]	all over, mostly NP	regulates fibril diameter (smaller if this collagen is more abundant) influencing mechanical properties [35,38]
beaded-filament forming collagens		
type VI	all over, mostly NP	helps cell fixation to the matrix and facilitates collagen bundles' sliding and lubrication [39,40]
FACIT collagens		
type IX	NP	maintains matrix integrity [41,42]
type XII	AF	might regulate fibrillogenesis [29,43]
type XIV	AF	might regulate fibrillogenesis [29,43]
proteoglycans		
aggregating PGs		
aggrecan	AF and NP	maintains IVD's osmotic pressure; may act as an anti-angiogenic factor due to its inhibition of endothelial cell migration [40,44,45]
versican	all over, mostly AF	favours the attachment of adjacent lamellae, contributes to resistance to compressive forces and facilitates cell migration, since it is an anti-adhesive molecule [35,40]
non-aggregating PGs		
small leucine-rich proteoglycans (SLRPs)		
decorin	outer AF and fibrillar NP	regulates collagen fibril diameter and spacing, maintaining uniform patterning; GFs' reservoir (TGF-β), modulating ECM metabolism [46–48]
biglycan	outer AF and NP (fibrillar and pericellular region)	GFs' reservoir (TGF-β), modulating ECM metabolism [46,47]
asporin	outer and inner AF, rarely NP	GFs' reservoir (TGF-β), modulating ECM metabolism; may play a major role in modulating chondrocyte matrix homeostasis [49,50]
fibromodulin	AF and NP	regulates collagen fibril diameter and spacing, maintaining uniform patterning; GFs' reservoir (TGF-β), modulating ECM metabolism [44,47]
lumican	AF and NP	regulates collagen fibril diameter and spacing, maintaining uniform patterning [44,51]
prolargin (encoded by PRELP*)	all over, mostly AF	anchors basement membranes to the underlying connective tissue [44,52]
chondroadherin	AF and NP	binds integrin ad collagen; regulates cell metabolism and ECM structure, promoting matrix homeostasis [44,53,54]
osteoglycin/ mimecan	AF and NP	unknown [44]
other matrix proteins		
other PGs		
perlecan	AF and NP	has a role in cell proliferation and differentiation by acting as co-receptor for FGFs; matrix organization and stabilization; role in FGF signalling [40,55]

(*Continued*.)

Table 1. (*Continued.*)

name	distribution/localization	putative/possible function
fibronectin	all over the disc	preserves structural integrity of the ECM; involved in cell adhesion through interaction with integrins [56–58]
elastin	all over the disc	preserves structural integrity of the ECM; helps to regain disc height and shape after deformation [59–61]
COMP	all over, mostly AF	preserves structural integrity of the ECM; binds other matrix proteins and catalyses polymerization of type II collagen fibrils; prevents vascularization of cartilage [62,63]
thrombospondin	AF	preserves structural integrity of the ECM; mediates cell adhesion, matrix–matrix interactions, cell migration and proliferation in other tissues; might prevent vascularization of the tissue; activates TGF-β complex [64,65]

Table 2. Main IVD proteinases.

name	distribution/localization	putative/possible function
aggrecanases		
ADAMTS1, 4, 5, 9 and 15	*ADAMTS1:* NP and AF *ADAMTS4:* low levels NP and AF *ADAMTS5:* low levels NP and AF *ADAMTS9:* NP and AF *ADAMTS15:* low levels NP and AF	degrades aggrecan [66–69], as well as versican, biglycan, fibromodulin, COMP, TSP1, TSP2, nidogen, among other substrates [70]
collagenases		
MMP1, 8 and 13	*MMP1:* low levels, mostly inner AF and NP *MMP8:* low levels *MMP13:* low levels, mostly NP	cleaves fibrillar collagen [66–68]
gelatinases		
MMP2 and 9	*MMP2:* low levels, mostly inner AF and NP *MMP9:* low levels AF and NP	degrades denatured collagen and basement membrane collagen [68]
stromelysin		
MMP3 and 10	*MMP3:* low levels, mostly in the adult NP *MMP10:* only checked in the NP	digests non-collagenous matrix proteins and denatured collagen [66,68,71]
matrilysin		
MMP7	NP and inner AF	degrades aggrecan and collagen type II [72]
other MMPs		
MMP19	AF and NP	cleaves aggrecan, COMP, types I and IV collagen, and fibronectin and acts on tenascin; can interfere with stabilization of capillary-like structures, possibly playing a role in the avascular status of the disc; regulates IGF-mediated proliferation in other tissues by proteolysis of IGFBP3 [73]

homeostasis (table 2) [66,74–76]. However, when an imbalance occurs, degradation products might trigger inflammation. For instance, fibronectin fragments alleviate metalloproteinase (MMP) inhibition and so promote monocyte migration *in vitro* [77]. This certainly facilitates their recruitment into the inflamed region. Fragments of laminin, collagen type XIV and fibrin can also modulate inflammatory cell infiltration and proliferation in other systems [26]. In cartilage explant cultures, fibromodulin fragments are produced following IL-1 stimulation [78]. In different *in vitro* settings, fragments originated from elastin, laminins, collagen (type I and IV), fibronectin, ectactin/nidogen, thrombospondin and hyaluronan also induce protease and cytokine production, independent of their chemotactic activity [79]. Some of the

aforementioned studies were performed in highly vascularized model systems (i.e. cardiovascular, lung or renal tissues). While these systems are very different from healthy adult IVDs, which are largely avascular, their findings might still be of relevance when studying phenomena associated with disc herniation or sequestration, in which blood vessels are much more abundant [80].

It appears that fragment release initiates and propagates the inflammatory response locally. Many of these fragments (e.g. originated from biglycan, fibronectin, hyaluronan) signal through toll-like receptor-2 (TLR2) and/or TLR4 in other model systems [81,82]. TLR4, in particular, is a well-known pattern recognition receptor involved in innate immune responses that has been implicated in inflammatory degeneration [83]. In human IVD cells, hyaluronic acid fragments (fHA) lead to increased mRNA expression levels of inflammatory and catabolic genes IL-1β, IL-6, IL-8, cyclooxygenase (COX)-2, metaloprotease-1 and -13, and IL-6 [84]. However, while IL-6 production is dependent on TLR2 it is independent of TLR4. It should be noted that low and high molecular weight molecules can have different effects, even through the same pathways. For example, high molecular weight hyaluronan protects epithelial cells against pro-apoptotic stimuli through NF-κB activation, in a TLR dependent way. Low molecular weight degradation products can induce inflammation, promoting macrophage mediated production of IL-1β and tumour necrosis factor alpha (TNF-α), through activation of the NF-κB/IκBα complex [82]. It is difficult to assess the overall role of ECM proteins within an immune setting because of their dual roles and because many proteases and a variety of fragments are released simultaneously. This difficulty is exacerbated by the scarcity of *in vivo* data, owing to limitations in the techniques used to detect fragments and immune cells, which are present at low concentrations and are short lived [85].

Numerous studies suggest that the IVD might endogenously include inflammatory-like cells [86,87]. In particular, it has been shown *in vitro* that a population of IVD cells can phagocytize beads and apoptotic bodies [86]. In turn, human surgical non-herniated nucleus pulposus (NP) samples presented a high number of resident CD68+ cells [87]. Furthermore, a recent robust analysis of cytokine/chemokine expression profile of human NP cells has presented clear evidence that NP cells, or at least some of them, are producers of specific inflammation-associated molecules, even in basal conditions (non-degenerated NP) [88]. In addition, infiltrated leukocytes (CD11b-positive cells) were found even in prolapsed IVDs, where NP is supposedly intact and isolated from any vascular source of immune cells [88]. The question of whether these cells could be resident macrophages or macrophage-like cells remains. Although pleiotropic, cytokines and chemokines have three modes of action: (i) stimulating the production of other inflammatory mediators and MMPs, (ii) enhancing matrix degradation, and (iii) recruiting inflammatory cells and activating phagocytosis [89–94]. Together, these effects can contribute to disease progression in the IVD.

It should be stressed that extreme mechanical loading has also been shown to alter ECM properties (through proteinase activation) and promote inflammation, contributing to IVD degeneration [95]. Apart from *in vitro* studies, organ cultures of bovine caudal IVDs have shown that compression induces apoptosis, produces inflammatory mediators and alters matrix integrity, leading to development of the disease [96].

In a more advanced degenerative stage, the well contained and apparently 'sealed' NP (immune privileged) becomes exposed to immune cells, which, responding to an inflammatory stimulus, may arise from newly formed blood vessels that invade pathological clefts and tears found in the annulus fibrosus (AF). Nociceptive nerve fibre ingrowth also accompanies angiogenesis and is believed to be the origin of discogenic pain that actively contributes to LBP [97–100]. Indeed, while the probable sites for focal damage and inflammation are vertebral endplates and AF (the only sites where the IVD is vascularized) [101], the NP is capable of attracting leukocytes and increasing vascular permeability when implanted subcutaneously [100]. An increase in expression of some cytokines and MMPs in herniated IVD may occur when molecules seen as 'non-self' by immune cells become exposed. This may also be linked to the phenomenon of spontaneous regression or disappearance of extruded IVD fragments, which has been attributed to matrix degradation and phagocytosis by recruited/infiltrated macrophages [102–106]. In cases with transligamentous extrusion, which can occur when the NP is potentially more exposed to immune cells, regression occurs [107]. Furthermore, the survival rate of subcutaneously transplanted rat NP cells is higher in immunocompromized NOD mice, and both rat macrophages and NK cells lyse autologous NP cells *in vitro*, indicating that immune cell populations respond to NP tissues [108].

In the next sections, we will review observational, *in vitro* and *in vivo* studies of the inflammatory milieu in IVD.

3. Inflammatory key players in intervertebral disc

3.1. Observational studies

A range of cytokines have been found in human IVDs in varying amounts, depending on whether the IVD is healthy, degenerated or herniated. Table 3 groups by methodology (observational, *in vitro* or pathway analysis) some of the most important studies that have clarified which inflammatory factors are expressed during homeostasis and with degeneration. Importantly, the identity of the cells producing these mediators (i.e. NP cells, AF cells, native IVD cells only, native cells plus infiltrating inflammatory cells) is highlighted.

3.1.1. *Post-mortem* samples

Separating NP from AF tissue upon discectomy is a very challenging task, particularly when dealing with degenerated human IVD tissue. In cases of disc herniation (e.g. extruded, sequestered), the IVD is invaded by other cell types, confounding analysis of molecules released by regions of the IVD. Samples taken *post-mortem*, which are not contaminated by infiltrating inflammatory cells (or at least not to the same extent as herniated discs), are therefore superior when investigating IVD homeostasis. For instance, TNF-α was substantially expressed in autopsy material in fetal/infantile and older adult NP, whereas it was sparsely expressed in adolescent and young adult NP. It was not found in the AF of young adults (below 25 years), but significantly increased in older individuals [24]. Also, calcium-dependent phospholipase A2 (PLA2), a regulator of prostaglandin E2 (PGE_2) production, has been found in both cadaveric and surgical samples, and IVDs of middle-aged cases had higher PLA2

Table 3. Inflammatory mediators found in the human IVD.

mediator	condition	producing cells	references
inflammatory factors that are expressed during homeostasis			
observational studies			
TNF-α	*post-mortem* and non-degenerate samples	IVD cells	[24,71,109]
IL-1β		IVD cells	[71,109–112]
IL-1α, IL-1Ra, IL-1RI, and ICE		NP and AF cells	[112]
IL-6, IL-8, RANTES		AF and NP cells	[110]
NGF		NP and AF cells in monolayer and alginate bead culture	[71,113]
NGF receptor (trkA)		NP and AF cells in monolayer and alginate bead culture	[113]
substance P			[71]
PLA2		NP and AF cells	[114]
CCL3 and CCL4		IVD cells	[115]
NOTCH		IVD cells	[109]
MMPs		IVD cells	[71,92]
inflammatory factors that are expressed with degeneration			
observational studies			
TNF-α	herniations (including subligamentous and transligamentous), protrusion, extrusion, sequestration, spondylosis, scoliosis, degenerated or discogenic pain	IVD cells and infiltrating cells	[24,71,116–121]
IL-1β			[71,111,117,118,120,121]
IL-1α			[117–119]
IL1-Ra, NO			[118]
IL-6			[17,117,118,122]
IL-8			[17,119]
IL-12, IL-17, IFN-γ			[122]
IL-20 (and its receptors)			[90]
IL-10, TGF-β, RANTES			[119]
IL-16, CCL2, CCL7, CXCL8			[88]
substance P			[71,118]
PGE_2			[17,118]
COX-2			[121]
PLA2			[114,121]
NGF			[71]
VEGF, bFGF			[116]
GM-CSF			[117]
CD20, CD45RO, CD68			[107]
MMPs			[71,107,116,118]
in vitro studies			
TNF-α	degenerate, sciatica, discogenic pain, extrusion, sequestration	IVD cells and infiltrating cells treated with different inflammatory stimulus (including IL-1β, TNF-α, substance P, IL-17, IL-20, IFN-γ, LPS) in monolayer or three-dimensional cell culture, or co-cultured with macrophage-like cells, or exposed to high mechanical strain	[95,121,123–125]

(*Continued*.)

Table 3. (*Continued.*)

mediator	condition	producing cells	references
IL-1β	discogenic pain and *post-mortem*		[110,112,124–126]
IL-1α, IL-1Ra, IL-1RI, and ICE	degenerate and *post-mortem*		[112]
IL-6	discogenic pain, scoliosis, sciatica, extrusion, sequestration, degenerate, myelopathy or radiculopathy and *post-mortem*		[89,90,95,110,124,126–129]
IL-8	discogenic pain, scoliosis, sciatica, extrusion, sequestration, degenerate, myelopathy or radiculopathy and *post-mortem*		[90,95,110,124,126–128]
IL-17A	protrusion, extrusion and scoliosis		[123]
IL-15, IFN-γ, CXCL9, TLR-2, TLR-4, MCP-3	*post-mortem*		[95]
RANTES	discogenic pain and *post-mortem*		[110]
MCP-1	discogenic pain, scoliosis, sciatica, extrusion, sequestration and *post-mortem*		[90,95,127]
TFGF-β1	discogenic pain, scoliosis, sciatica and *post-mortem*		[95,127]
substance P	myelopathy or radiculopathy		[126]
bFGF	scoliosis, sciatica and discogenic pain		[127]
PGE_2	degenerate, scoliosis, sciatica and discogenic pain		[89,121,128–130]
COX-2	extruded and sequestrated IVD tissue		[121]
NGF	*post-mortem*		[95,113]
NGF receptor (trkA)	*post-mortem*		[113]
PGF2α	degenerate		[128]
NO	degenerate, scoliosis		[89,124,129,130]
ICAM-1 (CD54)	degenerate and scoliosis		[89]
MMPs	degenerate, non-degenerate, extrusion and sequestration		[90,92,112,130]
NOTCH	protrusion		[109]
pathway analysis			
NF-κB, MAPK and C/EBPβ→ CCL3	discectomy	IVD cells and infiltrating cells	[115]
NF-κB→ADAMTS-4 and -5	DDD and myelopathy	NP and infiltrating cells treated with IL-1β and TNF-α	[131]
NF-κB→Sox9 and collagen type II	spine trauma	IVD cells treated with IL-1	[132]
NF-κB and MAPK→NOTCH pathway	protrusion	NP cells	[109]

activity than those of younger and older subjects, indicating an important physiological role in maintaining homeostasis [114]. Like TNF-α or PLA2, many other inflammatory key players have been localized in non-degenerated human IVD tissue (table 3). Importantly, IVD native enzyme activity has also been studied. It was shown in the intact IVD that IL-1 is a key cytokine mediating IVD matrix degradation, by measuring enzyme activity (*in situ* zymography (ISZ)) against gelatin, collagen II and casein matrices [92]. Also, MMP-10 expression (at mRNA and protein levels) was increased in the symptomatic degenerate IVD, when compared to non-symptomatic one—possibly contributing to matrix degradation and initiation of nociception [71]. An additional perspective is given by studies that identified factors not naturally produced by native IVD cells: immunoreactivity for IL-4, IL-6, IL-12 and interferon (IFN)-γ was modest in surgical IVD tissue, being higher in herniated IVD samples and virtually non-existent in the control

samples taken from *post-mortem* non-degenerated IVDs [122]. The majority of these reports used *post-mortem* IVD samples as healthy controls, exposing the role of IVD native cells in IVD homeostasis. This knowledge is of potential interest for the development of endogenous therapeutic routes to restore homeostasis in DDD.

3.1.2. Degenerated samples

Regarding human degenerated IVD samples, early studies detected the presence of IL-1, intracellular adhesion molecule-1 (ICAM-1), lymphocyte function-associated antigen (LFA) and fibroblast growth factor (FGF) [133]. Immunoreactivity for some cytokines (IL-4, IL-6, IL-12, IFN-γ, TNF-α) seemed modest but evident in herniated and degenerated discs, with substantial macrophage infiltration [116,122]. Also, pathologic discs highly expressed IL-17, suggesting the involvement of Th17 lymphocytes in disc herniation [123]. Others have shown a higher expression of TNF-α, IL-1β, IL-6, IL-8, IL-20, PGE_2 and nitric oxide (NO) in herniated discs [17,90,117]. Some inflammatory key players have also been associated with pain in human IVD: RANTES and IL-1β expression was significantly higher in painful versus painless discs, contrarily to IL-6 and IL-8 [110]. A strong difference was observed in the levels of nerve growth factor (NGF), neurofilament-68, growth-associated protein (GAP)-43, and substance P in invading nerve fibers, in and around the outer layer of uncontained herniated versus spondylotic IVDs [116]. Another study that evaluated 91 cytokine- and chemokine-associated genes in human NP cells showed that NP cells are a source of IL-16, CCL2, CCL7 and CXCL8 [88]. Some of the pro-inflammatory cytokines usually present at increased levels in human degenerated discs, such as IL-1β and TNF-α, may mediate catabolic effects, decreasing proteoglycan production and enhancing MMP expression [71,111,134,135].

3.2. *In vitro* studies

Different *in vitro* studies have focused on studying the sources and role of some inflammatory mediators associated with herniated and degenerated IVD. An increase in IL-6, IL-8 and PGE_2 was observed in control and degenerated human IVD tissues upon lipopolysaccharide (LPS) stimulation [127]. Furthermore, it was shown that substance P, expressed by IVD cells, upregulates IL-1β, IL-6 and IL-8 in both NP and AF, and RANTES and TNF-α in AF only [126]. Also, NP cells were shown to express the CCL3 ligand (also known as macrophage inflammatory protein (MIP)-1α), which is well known for its chemotactic and pro-inflammatory effects, through activation of the MAPK, NF-κB and C/EBP signalling pathways after treatment with IL-1β or TNF-α [115]. These studies suggest a contribution of native IVD cells to the inflammatory milieu. However, others have defended the hypothesis that immune cells, such as macrophages, neutrophils and T cells, can be recruited to degenerated IVD [135]. This hypothesis is supported by evidence that Th17 cells expressing CCR6 are recruited to degenerated IVD by CCL20 secretion from NP [123], and that macrophages can migrate after stimulation with conditioned medium from rat NP cells treated with IL-1β or TNF-α [115].

TNF-α, which is one of the most studied pro-inflammatory molecules, is known to promote aggrecan degradation, disc catabolism and expression of pro-inflammatory cytokines and NGF, without any recovery [136]. TNF-α is an adipokine that has been associated with higher numbers of bovine IVD senescent cells and is therefore implicated with the inability of degenerated IVD to repopulate by itself [137]. Curiously, although many studies have focused on the role of TNF-α in IVD degeneration [136], Hoyland and co-authors suggest instead that IL-1β is the key regulator of matrix degradation in degenerated IVD: IL-1 has greater expression in the IVDs clinically associated with chronic LPB and treatments against IL-1β were shown to inhibit matrix degradation [92]. IL-1 is upregulated in degenerated human discs, inducing MMP7, MMP13 and ADAMTS (a disintegrin and metalloproteinase with thrombospondin motifs)—suggesting a deregulation of the normal IVD homoeostasis [138]. TNF-α blockers had no effect on matrix-degrading activity, suggesting that its upregulation in DDD is not associated with matrix degradation [92] but instead with neighbouring nerve root irritation, which is confirmed by other studies [134,139]. Hence, TNF-α might be contributing to discogenic pain in cases where nerve ingrowth into IVD degenerative fissures occurs [140,141].

3.3. *In vivo* studies

Although some IVD degeneration related inflammatory mediators identified *in vitro* have not yet been studied *in vivo*, recent evidence has shed light on the role of several molecules. The majority of studies have been conducted in rat, rabbit and porcine animal models.

In a rat animal model of IVD herniation, NP exposure led to increased IL-6, TNF-α and IFN-γ levels. Other cytokines (IL-1β, IL-10, IL-1α and IL-2), already increased by the surgical procedure, were not altered [142]. In another study, TNF-α was identified in rat herniated IVDs and associated with radicular pain [139]. Also, a rat model of caudal annular incision demonstrated a transient peak in IL-1β 4 days following injury. This model was characterized by NP size decrease, annular collagen layer disorganization, and cellular metaplasia of annular fibroblasts to chondrocyte-like cells. However, no significant changes in TNF-α or IL-6 were seen [143]. In a lumbar rabbit annular incision model, no alteration in IL-1α or TNF genes was observed in whole IVDs at either one or three weeks after injury [144]. In the same model, IL-1β, transforming growth factor (TGF)-β1 and iNOS (inducible nitric oxide synthase) gene expression increased after three weeks, but decreased between weeks 6 and 12, having a second peak at 24 weeks—possibly showing a long-term pro-inflammatory action [145]. In a rabbit model of IVD herniation, the presence of TNF-α, IL-1β and MCP-1 (which has been demonstrated to be a potent macrophage chemoattractant [146]) was also analysed: TNF-α and IL-1β were detected after day 1 (via immunohistochemistry) followed by MCP-1 3 days post-injury. Infiltrating cells, mainly macrophages, were also observed after day 3 [147]. Interestingly, in a lumbar porcine model of annular incision, a significant increase in IL-8 accompanied by a decrease in IL-1 was observed in IVDs subjected to discectomy at 12 weeks post-injury, while no difference was observed in disc morphology, proteoglycan content, or in levels of IL-6 and TNF-α expression between untreated and injured IVDs. Whereas both IL-1 and IL-8 have pro-inflammatory properties, the authors propose that such discectomy procedure may be capable of initiating a repair response in the IVD, given that expression of IL-8 (an anabolic agent) is increased when the catabolic IL-1 decreases [148].

The TLR4-ligand LPS triggered inflammation when injected in a rat caudal IVD [149]. LPS injection in a rat IVD led to an increase in the levels of IL-1β, TNF-α, HMGB1 (high-mobility group box 1) and MIF (macrophage migration inhibitory factor), which correlated with morphological changes in tissue organization, namely interruption of NP/AF border, contraction of NP shape and decrease of IVD height [149]. Recently, different components of the tissue renin-angiotensin system (tRAS) (angiotensin converting enzyme, Ang II, Ang II receptor type 1, Ang II receptor type 2 and cathepsin D), that contribute to inflammation in many organs, have been found for the first time in the normal rat IVD, at both mRNA and protein levels [150]. However, the association between tRAS and IVD degeneration and its relationship to IVD inflammation has yet to be elucidated.

Most of these *in vivo* studies mainly identify and quantify inflammatory mediators in IVD, but fail to produce a mechanistic explanation of their role in either IVD degeneration or regeneration. One of the reasons for this failure may be the difficulty of unravelling the complex inflammatory mechanisms in injury models of IVD pathology. In this context, animal models of spontaneous IVD degeneration such as the sand rat [151] and both younger chondrodystrophic (with cervical or thoracolumbar IVD disease) and older non-chondrodystrophic (caudal cervical or lumbosacral IVD disease) dogs [152,153] could bring new insights to the clinic. However, as far as we are aware, the inflammatory response has not been addressed in these models. Importantly, differences between species could also bring some intricacy to this issue. For instance, notochordal cells (NC) seem to disappear in the adult human IVD, while in many other species they are retained throughout adulthood [154]. As more models become available, it is central to translate information between species and to interpret the models appropriately to understand in greater depth the process of inflammation.

4. Strategies to target and modulate inflammation towards intervertebral disc regeneration

Promoting IVD regeneration relies on restoring naive IVD properties by: (i) recovering IVD biomechanics, (ii) re-establishing cell biological activity, including production of healthy ECM, and (iii) reducing IVD-associated pain. Biological approaches focusing on IVD regeneration or IVD-associated pain relief begun in the early 1990s, and have since increased in number and diversity as reviewed elsewhere [4].

A well-balanced approach supporting tissue regeneration and control of inflammatory response could be successful in reducing IVD-associated pain. Although the molecular mechanisms behind IVD pathology and inflammatory response remain to be elucidated in detail, some inflammatory-related molecules are key targets of novel therapies in DDD [155,156]. In this section, an overview of the strategies targeting inflammatory mediators towards IVD regeneration will be given.

4.1. Injection of molecules

The more direct approaches to control inflammation in IVD are to inject regulating agents close to the IVD. Example agents are TNF-α blockers, such as infliximab, adalimumab, etanercept [136,157–160], or IL-1 inhibitors, such as IL-1 receptor antagonist (IL-1Ra) [161]. Other TNF-α blockers include a monoclonal antibody tested in herniated IVD patients, who showed less leg and back pain after antibody administration [162], and a p38-TNF-α inhibitor, which was tested in the spine to address neuroinflammation but not specifically for IVD [163]. Other strategies involve injecting corticosteroids into the IVD [164], or the anti-cholesterolemic drug simvastatin [165], which appeared to retard IVD degeneration in animal models.

The therapeutic potential of IL-1Ra for sustained attenuation of IL-1β has also been explored using poly(lactic-*co*-glycolic acid) (PLGA) microspheres as a delivery system [166]. IL-1Ra-PLGA microspheres inhibited NO production in NP cell cultures and partially restored the levels of iNOS, ADAMTS-4, MMP-13, IL-1β, IL-6 and TLR-4, which were increased in the presence in IL-1β [166].

Another candidate to control inflammation in IVDs is COX-2, which regulates PGE_2 synthesis in inflammatory conditions. Epidural injection of COX-2 inhibitors was shown to reduce pain in a rat model of IVD herniation [167]. Another approach uses platelet-rich plasma (PRP) as a therapy for degenerated IVD [168]—PRP was able to rescue chondrocyte degeneration induced by IL-1β and TNF-α [169].

Other approaches to reduce IVD-associated pain have been suggested. Resveratrol, a naturally occurring polyphenol present in red wine, was able to reduce IL-6, IL-8, MMP1, MMP3 and MMP13 expression when injected into the IVD [170]. Rhein (4,5-dihydroxyanthraquinone-2-carboxylic acid), an anthraquinone molecule derived from the rhizome of *Rheum palmatum* that exhibits anti-inflammatory activity and is used in the treatment of osteoarthritis and pain relief, was hypothesized to be a therapeutic agent for IVD through the regulation of IL-1 activity [171]. Fullerol, a derivative from fullerene and known anti-oxidant, retards cellular apoptosis and suppresses dorsal root ganglion (DRG) and neuron TNF-α-induced inflammatory responses, which when incorporated into nanoparticles is relevant for LBP treatment [172].

A very recent and promising approach to target inflammation in IVD is the inhibitor of IκB kinase-β (IKKβ), involved in NF-κB activation. The intradiscal injection of IKKβ reduced the levels of TNF-α, IL-1β and IL-6 of an injured IVD while suppressing high levels of neuropeptides within DRG neurons [173].

Despite good results in other therapeutic areas, injected molecules might be inefficient in DDD due to the short half-life of proteins in solution and the limited effect of a single protein in a complex process such as IVD degeneration [174]. Also, the risk of inducing IVD degeneration by puncturing of the IVD should be considered [175], although more recent studies describe alternative routes for molecule delivery [176]. Furthermore, given the predominantly avascular nature of IVD, systemic delivery of soluble molecules is unlikely to be effective in this situation. This view is supported by the report that the concentration of antibiotics in IVDs was undetectable in the NP of patients with IVD infection under systemic administration of antibiotics [177]. In addition, it has been shown that the rate of diffusion of antibiotics into the IVD is reduced by endplate calcification, increase in IVD size and solute molecular weight [178,179]. Moreover, although some nutrients' diffusion to the NP may occur via the endplates, the short half-life of pharmaceutical drugs or proteins can result in limited therapeutic doses that reach the NP [166].

4.2. Gene therapy

Gene therapy promises more prolonged effects in DDD, by introducing the possibility of locally modulating the expression of a specific gene and the consequent production of its protein [174]. As early as 1997, a study suggested genetic modifications as a therapy for DDD [180]. At that point, a retrovirus vector was proposed to transduce bovine chondrocytic endplate cells with IL-1Ra [180]. Cell transfection resulted in IL-1Ra production in 48 h, and injection of transfected cells in degenerated NP explants considerably reduced expression of several enzymes (such as MMP3) for two weeks after injection. This strategy aims at decreasing IL-1 mediated matrix degradation and stopping DDD progression [181]. *In vivo*, TGF-β1 transfection of rabbit IVD cells also enhanced proteoglycan synthesis for six weeks [182]. In agreement with this result, cells from human degenerated IVD transfected with TGF-β1 increased both proteoglycan and collagen production [183,184].

Gene therapy in a clinical setting may be limited by the safety of the gene transfer vector. Aspects such as exposure to high doses, long-term use, misplaced injections and the possibility of oncogenesis are key concerns when treating a chronic disease like DDD [185]. Progress in the development of more reliable viral vector constructs and in a better control of transgene expression would improve the safety of these therapies. Also, elucidation of molecular mechanisms behind the degenerative process and characterization of cell populations in IVD, as well as their role in ECM production, could bring new advancements to this field [174].

4.3. Cell-based therapies

Several cell-based therapies to stimulate IVD regeneration have been proposed in recent years: haematopoietic stem cells (HSC) [186], fetal spine cells [187], immortalized NP-cell lines [188], autologous IVD chondrocytes [189], embryonic stem cells (SC) [190], induced pluripotent SC [191], olfactory SC [192] and MSCs (derived either from bone marrow [193] or from umbilical cord blood [194]) have all been suggested to have potential for IVD repair/regeneration. NP progenitor cells were isolated from the NP (with approximately 1% frequency) and differentiated into chondrogenic and neurogenic lineages, suggesting potential for IVD regeneration [195]. Besides IVD regeneration, progenitor cells might play a protective role in regulating inflammation in IVD: rabbit NC were shown to reduce the levels of pro-inflammatory cytokines, IL-6 and IL-8, as well as iNOS, in *in vitro* co-cultures of AF cells with macrophages [196].

MSCs are one of the most attractive candidate cell types for IVD regeneration, partly because they could be autologous transplants. In a canine model, MSCs were able to increase collagen type II expression while decreasing cell apoptosis in IVD [197]. In rabbits, MSCs were able to remain in the IVD up to 24 weeks [198]. However, the number of transplanted MSCs is crucial; in the canine model 10^6 MSCs per IVD was ideal, since 10^5 MSCs resulted in decreased cell viability while 10^7 MSCs induced cell apoptosis [197]. Besides MSC multi-differentiation capacity, an associated immuno-modulatory effect has been suggested [199]. MSC role in inflammation is based on their active role as cytokine-release factories that interact directly with injured cells [200]. In this novel scenario, MSCs were shown to secrete IL-1RA in a mouse model of lung injury [201] or produce a potent anti-inflammatory protein (TNF-α stimulated gene/protein 6, TSG-6) in a mouse infarct model [202]. Interestingly, TSG-6 was also identified as a key player in a rat model of corneal injury after MSC systemic administration [203]. After implantation of MSCs into beagle nucleotomized IVDs, the expression of Fas ligand (FasL) (a protein found in other immune privileged sites) was restored. It was suggested that MSCs either differentiated into cells expressing FasL, or stimulated the few remaining NP cells to produce this molecule—thus contributing to the recovery of immune privilege in degenerated IVDs [204]. Although the beneficial effects of these cells have been demonstrated in several models, the mechanisms behind MSC-based therapies are not clear.

In vitro studies showed that MSCs repress IgG production of peripheral blood lymphocytes co-cultured with IVD fragments from the same donors [205]. MSC influence in IVD inflammatory response has not been fully dissected until now due to its multifactorial complexity and time dependence [205]. Human MSCs were able to downregulate gene expression of pro-inflammatory cytokines (IL-3, IL-6, IL-11, IL-15, TNF-α) and MMPs when in co-culture with rat NP cells [198].

In humans, two clinical trials took advantage of autologous MSCs, albeit with controversial results. MSCs were either directly injected in NP [206] or implanted in the IVD after seeding in collagen sponges [207]. In the first case, when MSCs were directly injected in patients diagnosed with DDD, but with preserved external AF and persistent LBP, the lumbar pain was strongly reduced after three months. However, no improvement on IVD height was detected by imaging [206]. Injection of MSCs in degenerated IVDs seems to promote an analgesic effect, due to trophic effects, which can occur quicker than detecting possible regenerative effects [206]. Given this, the authors suggest that the MSCs exhibited immuno-modulatory properties. The second case reports the implantation of MSCs after seeding in collagen sponges [207]. Two years post-surgery, the published results reported relief or disappearance of LBP and improvement of the vacuum phenomenon (gas in the intervertebral space, associated with intervertebral regressive degeneration). However, besides the small number of patients used (two), this study also lacks experimental details such as the controls used and effective number of cells transplanted [207]. More recent studies propose IVD injection of umbilical cord-derived MSCs as a promising therapy to overcome chronic discogenic LBP [208]. In this study, pain and lumbar function were recovered after cell transplantation and preserved over a 2-year follow-up period; however, only two patients were studied. Another recent study injected bone marrow concentrate cells into 26 patients [209]. In the 1-year follow-up study, the majority of the patients showed improvement of pain score and reduced impairment, with only some of them presenting IVD rehydration. The authors emphasize the use of critical unmanipulated cell doses. Usually, MSC-based therapies involve cell expansion *in vitro* to obtain sufficient cell numbers, but this *in vitro* manipulation risks modifying their receptor expression and can introduce contaminants.

One interesting feature of MSCs is their capacity to migrate into injured tissues and participate in the regenerative process, interacting with the surrounding environment through secretion of numerous molecules such as growth factors, cytokines and chemokines [210]. Nevertheless, contrary to leukocyte migration and haematopoietic SC homing, the mechanisms that regulate MSC migration to injured sites

are not well characterized [211]. *In vitro*, in a pro-inflammatory environment stimulated by TNF-α, MSCs migrate towards SDF-1, RANTES and MDC gradients, amongst others [212]. Furthermore, MMPs and their inhibitors have also been shown to enhance MSC migratory capacity [213]. In a recent study, MSCs were recruited *in vitro* by conditioned medium from IVDs cultured under degenerative-simulated conditions [214]. CCL5/RANTES has been identified as a key chemoattractant released by degenerative IVD in organ culture [215]. Moreover, CXCL12/SDF-1 delivery in IVD organ cultures promotes MSC recruitment towards NP, especially if MSCs were harvested from young donors [216]. This does not exclude the possibility that other cytokines involved in IVD degeneration pathogenesis, namely TNF-α and IL-1β, might play a role in regulation of MSC recruitment to the IVD [181]. A hypothetical migration route of high-proliferative cells lateral to the epiphyseal plate and the outer border region of the IVD was recently described [217]—if this route is confirmed, new strategies envisaging IVD regeneration may be attempted.

5. Future perspectives

Recent findings from *in vitro* studies, animal models and clinical trials have started to unveil the role of inflammation in IVD degeneration. However, no evidence for a beneficial role of inflammation in maintaining homeostasis has been presented, owing to the difficulty in studying IVD tissue homeostasis. In other tissues, such as bone [218,219] or cardiovascular tissue [220], the control of inflammation has already proven to be critical in shifting the degeneration/regeneration balance towards regeneration. In particular, our group has focused on modulating inflammation in bone [5,221–224]. Hence, we believe that novel therapies for DDD should aim at restoring the homeostatic inflammatory conditions in the disc, rather than totally inhibiting inflammation, thus enabling endogenous repair mechanisms to operate.

Our group has recently shown that incorporating fibrinogen, a well-known inflammatory protein, into a biomaterial leads to increased bone formation [5]. *In vitro* studies have shown that fibrinogen-modified biomaterial stimulates NK cell-mediated MSC recruitment without affecting the MSC differentiation marker alkaline phosphatase [222]. Moreover, a broad analysis of macrophage-secreted factors showed that fibrinogen modified macrophage response, leading to a downregulation of the expression of inflammatory cytokines and a stimulation in the production of growth factor [224]. Factors such as MIP-1δ, platelet-derived growth factor-BB, bone morphogenetic protein (BMP)-5 and BMP-7 were significantly promoted by fibrinogen [224], which may impact tissue regeneration.

Recent advances in development biology also highlight the crucial role of immune cells. An efficient nuclear reprogramming to obtain induced pluripotent stem (iPS) cells was shown to require activation of an innate response [225] and was achieved via activation of TLR3 in the work of Yamanaka and colleagues [226]. The importance of this finding in physiological situations remains unclear, but it is becoming increasingly evident that activation of the immune response, particularly the innate response, may contribute to regulation of stem cell behaviour [225,227]. Moreover, it has been known for a long time that the post-inflammatory wound repair process recapitulates basic phenomena that occur during embryogenesis [228]. Therefore, future studies should focus on trying to understand what happens early in development, to discover more cues on how to modulate inflammation in a disease situation.

Although diverse studies have presented data on inflammatory key players in IVD, the inherent variability and contradictions arising from the different *in vitro* culture conditions and animal models used in these studies may be hampering translation of the research to a clinical setting. The standardization of methods, the correlation of results with different IVD clinical problems, the use of alternative *ex vivo* models (based on organotypic cultures or bioreactors) and the use of more physiologically accurate *in vivo* models of IVD degeneration could bring further advances to the IVD research field.

For IVD regeneration therapies to succeed, it will be important to address IVD degeneration together with inflammation. Until now, most studies have focused on only one of these two aspects. An integrated strategy, which addresses both the synergistic interplay that exists between the multiple factors associated with IVD degeneration and balances the inflammatory response, could be a step closer to the success of IVD regenerative strategies and bring relief for those suffering from LBP.

References

1. Andersson GB. 1999 Epidemiological features of chronic low-back pain. *Lancet* **354**, 581–585. (doi:10.1016/S0140-6736(99)01312-4)
2. Schwarzer AC, Aprill CN, Derby R, Fortin J, Kine G, Bogduk N. 1995 The prevalence and clinical features of internal disc disruption in patients with chronic low back pain. *Spine* (*Phila Pa 1976*) **20**, 1878–1883. (doi:10.1097/00007632-199509000-00007)
3. Koes BW, Van Tulder MW, Peul WC. 2007 Diagnosis and treatment of sciatica. *Br. Med. J.* **334**, 1313–1317. (doi:10.1136/bmj.39223.428495.BE)
4. Hughes SP, Freemont AJ, Hukins DW, Mcgregor AH, Roberts S. 2012 The pathogenesis of degeneration of the intervertebral disc and emerging therapies in the management of back pain. *J. Bone Joint Surg. Br.* **94**, 1298–1304. (doi:10.1302/0301-620X.94B10.28986)
5. Santos SG *et al*. 2013 Adsorbed fibrinogen leads to improved bone regeneration and correlates with differences in the systemic immune response. *Acta Biomater.* **9**, 7209–7217. (doi:10.1016/j.actbio.2013.04.008)
6. Sun Z, Zhang M, Zhao XH, Zhao ZH, GAO Y, Samartziz D, Wang HQ, Luo ZJ. 2013 Immune cascades in human intervertebral disc: the pros and cons. *Int.J. Clin. Exp. Pathol.* **6**, 1009–1014.
7. Medzhitov R. 2008 Origin and physiological roles of inflammation. *Nature* **454**, 428–435. (doi:10.1038/nature07201)
8. Urban JP, Smith S, Fairbank JC. 2004 Nutrition of the intervertebral disc. *Spine* (*Phila Pa 1976*) **29**, 2700–2709. (doi:10.1097/01.brs.0000146499.97948.52)
9. Moore RJ. 2006 The vertebral endplate: disc degeneration, disc regeneration. *Eur. Spine J.* **15**(Suppl. 3), S333–S337. (doi:10.1007/s00586-006-0170-4)
10. Benneker LM, Heini PF, Alini M, Anderson SE, Ito K. 2005 2004 Young Investigator Award winner: vertebral endplate marrow contact channel

occlusions and intervertebral disc degeneration. *Spine* (*Phila Pa 1976*) **30**, 167–173. (doi:10.1097/01.brs.0000150833.93248.09)

11. Adams MA, Roughley PJ. 2006 What is intervertebral disc degeneration, and what causes it? *Spine* (*Phila Pa 1976*) **31**, 2151–2161. (doi:10.1097/01.brs.0000231761.73859.2c)
12. Battie MC, Videman T, Kaprio J, Gibbons LE, Gill K, Manninen H, Saarela J, Peltonen L. 2009 The Twin Spine Study: contributions to a changing view of disc degeneration. *Spine J.* **9**, 47–59. (doi:10.1016/j.spinee.2008.11.011)
13. Cook CE, Taylor J, Wright A, Milosavljevic S, Goode A, Whitford M. 2013 Risk factors for first time incidence sciatica: a systematic review. *Physiother. Res. Int.* **19**, 65–78. (doi:10.1002/pri.1572)
14. Cheung KM, Karppinen J, Chan D, Ho DWH, Song Y-Q, Sham P, Cheah KSE, Leong JCY, Luk KDK. 2009 Prevalence and pattern of lumbar magnetic resonance imaging changes in a population study of one thousand forty-three individuals. *Spine* (*Phila Pa 1976*) **34**, 934–940. (doi:10.1097/BRS.0b013e3181a01b3f)
15. Hristova GI, Jarzem P, Ouellet JA, Roughley PJ, Epure LM, Antoniou J, Mwale F. 2011 Calcification in human intervertebral disc degeneration and scoliosis. *J. Orthop. Res.* **29**, 1888–1895. (doi:10.1002/jor.21456)
16. Desanto J, Ross JS. 2011 Spine infection/inflammation. *Radiol. Clin. N. Am.* **49**, 105–127. (doi:10.1016/j.rcl.2010.07.018)
17. Burke JG, Watson RW, Mccormack D, Dowling FE, Walsh MG, Fitzpatrick JM. 2002 Intervertebral discs which cause low back pain secrete high levels of proinflammatory mediators. *J. Bone Joint Surg. Br.* **84**, 196–201. (doi:10.1302/0301-620X.84B2.12511)
18. Lee RS, Kayser MV, Ali SY. 2006 Calcium phosphate microcrystal deposition in the human intervertebral disc. *J. Anat.* **208**, 13–19. (doi:10.1111/j.1469-7580.2006.00504.x)
19. Gruber HE, Norton HJ, Sun YB, Hanley EN. 2007 Crystal deposits in the human intervertebral disc: implications. *Spine J.* **7**, 444–450. (doi:10.1016/j.spinee.2006.08.015)
20. Feinberg J, Boachie-Adjei O, Bullough PG, Boskey AL. 1990 The distribution of calcific deposits in intervertebral discs of the lumbosacral spine. *Clin. Orthop. Relat. Res.* **254**, 303–310.
21. Kalya S, Rosenthal AK. 2005 Extracellular matrix changes regulate calcium crystal formation in articular cartilage. *Curr. Opin. Rheumatol.* **17**, 325–329. (doi:10.1097/01.bor.0000160783.14798.10)
22. Masuda I, Ishikawa K, Usuku G. 1991 A histologic and immunohistochemical study of calcium pyrophosphate dihydrate crystal deposition disease. *Clin. Orthop. Relat. Res.* **263**, 272–287.
23. Stutz A, Golenbock DT, Latz E. 2009 Inflammasomes: too big to miss. *J. Clin. Investig.* **119**, 3502–3511. (doi:10.1172/JCI40599)
24. Weiler C, Nerlich AG, Bachmeier BE, Boos N. 2005 Expression and distribution of tumor necrosis factor alpha in human lumbar intervertebral discs: a study in surgical specimen and autopsy controls. *Spine* (*Phila Pa 1976*) **30**, 44–53; discussion 54. (doi:10.1097/01.brs.0000174529.07959.c0)
25. Noble PW. 2002 Hyaluronan and its catabolic products in tissue injury and repair. *Matrix Biol.* **21**, 25–29. (doi:10.1016/S0945-053X(01)00184-6)
26. Vaday GG, Lider O. 2000 Extracellular matrix moieties, cytokines, and enzymes: dynamic effects on immune cell behavior and inflammation. *J. Leukoc. Biol.* **67**, 149–159.
27. Eyre DR, Muir H. 1977 Quantitative analysis of types I and II collagens in human intervertebral discs at various ages. *Biochim. Biophys. Acta* **492**, 29–42. (doi:10.1016/0005-2795(77)90211-2)
28. Eyre DR, Dickson IR, Van Ness K. 1988 Collagen cross-linking in human bone and articular cartilage. Age-related changes in the content of mature hydroxypyridinium residues. *Biochem. J.* **252**, 495–500.
29. Sivan SS, Hayes AJ, Wachtel E, Caterson B, Merkher Y, Maroudas A, Brown S, Roberts S. 2014 Biochemical composition and turnover of the extracellular matrix of the normal and degenerate intervertebral disc. *Eur. Spine J.* **23**(Suppl. 3), S344–S353. (doi:10.1007/s00586-013-2767-8)
30. Eyre DR, Muir H. 1976 Types I and II collagens in intervertebral disc. Interchanging radial distributions in annulus fibrosus. *Biochem. J.* **157**, 267–270.
31. Brinckmann J, Notbohm H, Müller PK. 2005 *Collagen: primer in structure, processing and assembly*, vol. 247, p. 252. Berlin, Germany: Springer.
32. Ippolito E, Ponseti IV. 1981 Juvenile kyphosis: histological and histochemical studies. *J. Bone Joint Surg. Am.* **63**, 175–182.
33. Gruber HE, Ingram JA, Hanley Jr EN. 2007 Morphologic complexity of the pericellular matrix in the annulus of the human intervertebral disc. *Biotech. Histochem.* **82**, 217–225. (doi:10.1080/10520290701713999)
34. Roberts S, Menage J, Duance V, Wotton SF. 1991 Type III collagen in the intervertebral disc. *Histochem. J.* **23**, 503–508. (doi:10.1007/BF01041176)
35. Culav EM, Clark CH, Merrilees MJ. 1999 Connective tissues: matrix composition and its relevance to physical therapy. *Phys. Ther.* **79**, 308–319.
36. Clouet J *et al*. 2009 Identification of phenotypic discriminating markers for intervertebral disc cells and articular chondrocytes. *Rheumatology* **48**, 1447–1450. (doi:10.1093/rheumatology/kep262)
37. Tow BP, Hsu WK, Wang JC. 2007 Disc regeneration: a glimpse of the future. *Clin. Neurosurg.* **54**, 122–128.
38. Mio F *et al*. 2007 A functional polymorphism in COL11A1, which encodes the alpha 1 chain of type XI collagen, is associated with susceptibility to lumbar disc herniation. *Am. J. Hum. Genet.* **81**, 1271–1277. (doi:10.1086/522377)
39. Roberts S, Ayad S, Menage PJ. 1991 Immunolocalisation of type VI collagen in the intervertebral disc. *Ann. Rheum. Dis.* **50**, 787–791. (doi:10.1136/ard.50.11.787)
40. Melrose J, Smith SM, Appleyard RC, Little CB. 2008 Aggrecan, versican and type VI collagen are components of annular translamellar crossbridges in the intervertebral disc. *Eur. Spine J.* **17**, 314–324. (doi:10.1007/s00586-007-0538-0)
41. Eyre DR, Wu JJ, Fernandes RJ, Pietka TA, Weis MA. 2002 Recent developments in cartilage research: matrix biology of the collagen II/IX/XI heterofibril network. *Biochem. Soc. Trans.* **30**, 893–899. (doi:10.1042/BST0300893)
42. Brinckmann J *et al*. 2005 Interleukin 4 and prolonged hypoxia induce a higher gene expression of lysyl hydroxylase 2 and an altered cross-link pattern: important pathogenetic steps in early and late stage of systemic scleroderma? *Matrix Biol.* **24**, 459–468. (doi:10.1016/j.matbio.2005.07.002)
43. Eyre DR, Matsui Y, Wu JJ. 2002 Collagen polymorphisms of the intervertebral disc. *Biochem. Soc. Trans.* **30**, 844–848. (doi:10.1042/BST0300844)
44. Onnerfjord P, Khabut A, Reinholt FP, Svensson O, Heinegard D. 2012 Quantitative proteomic analysis of eight cartilaginous tissues reveals characteristic differences as well as similarities between subgroups. *J. Biol. Chem.* **287**, 18 913–18 924. (doi:10.1074/jbc.M111.298968)
45. Johnson WE, Caterson B, Eisenstein SM, Roberts S. 2005 Human intervertebral disc aggrecan inhibits endothelial cell adhesion and cell migration *in vitro*. *Spine* (*Phila Pa 1976*) **30**, 1139–1147. (doi:10.1097/01.brs.0000162624.95262.73)
46. Gotz W, Barnert S, Bertagnoli R, Miosge N, Kresse H, Herken R. 1997 Immunohistochemical localization of the small proteoglycans decorin and biglycan in human intervertebral discs. *Cell Tissue Res.* **289**, 185–190. (doi:10.1007/s004410050864)
47. Hildebrand A, Romaris M, Rasmussen LM, Heinegård D, Twardzik DR, Border WA, Ruoslahti E. 1994 Interaction of the small interstitial proteoglycans biglycan, decorin and fibromodulin with transforming growth factor beta. *Biochem. J.* **302**, 527–534.
48. Reed CC, Iozzo RV. 2002 The role of decorin in collagen fibrillogenesis and skin homeostasis. *Glycoconj. J.* **19**, 249–255. (doi:10.1023/A:1025383913444)
49. Gruber HE, Ingram JA, Hoelscher GL, Zinchenko N, Hanley Jr EN, Sun Y. 2009 Asporin, a susceptibility gene in osteoarthritis, is expressed at higher levels in the more degenerate human intervertebral disc. *Arthritis Res. Ther.* **11**, R47. (doi:10.1186/ar2660)
50. Kizawa H *et al*. 2005 An aspartic acid repeat polymorphism in asporin inhibits chondrogenesis and increases susceptibility to osteoarthritis. *Nat. Genet.* **37**, 138–144. (doi:10.1038/ng1496)
51. Chakravarti S. 2002 Functions of lumican and fibromodulin: lessons from knockout mice. *Glycoconj. J.* **19**, 287–293. (doi:10.1023/A:1025348417078)
52. Bengtsson E, Morgelin M, Sasaki T, Timpl R, Heinegard D, Aspberg A. 2002 The leucine-rich repeat protein PRELP binds perlecan and collagens and may function as a basement membrane anchor. *J. Biol. Chem.* **277**, 15 061–15 068. (doi:10.1074/jbc.M108285200)

53. Haglund L, Ouellet J, Roughley P. 2009 Variation in chondroadherin abundance and fragmentation in the human scoliotic disc. *Spine* (*Phila Pa 1976*) **34**, 1513–1518. (doi:10.1097/BRS.0b013e3181a8d001)
54. Akhatib B, Onnerfjord P, Gawri R, Ouellet J, Jarzem P, Heinegard D, Mort J, Roughley P, Haglund L. 2013 Chondroadherin fragmentation mediated by the protease HTRA1 distinguishes human intervertebral disc degeneration from normal aging. *J. Biol. Chem.* **288**, 19 280–19 287. (doi:10.1074/jbc.M112.443010)
55. Melrose J, Smith S, Ghosh P, Whitelock J. 2003 Perlecan, the multidomain heparan sulfate proteoglycan of basement membranes, is also a prominent component of the cartilaginous primordia in the developing human fetal spine. *J. Histochem. Cytochem.* **51**, 1331–1341. (doi:10.1177/002215540305101010)
56. Oegema Jr TR, Johnson SL, Aguiar DJ, Ogilvie JW. 2000 Fibronectin and its fragments increase with degeneration in the human intervertebral disc. *Spine* **25**, 2742–2747. (doi:10.1097/00007632-200011010-00005)
57. Kadler KE, Hill A, Canty-Laird EG. 2008 Collagen fibrillogenesis: fibronectin, integrins, and minor collagens as organizers and nucleators. *Curr. Opin. Cell Biol.* **20**, 495–501. (doi:10.1016/j.ceb.2008.06.008)
58. Leiss M, Beckmann K, Giros A, Costell M, Fassler R. 2008 The role of integrin binding sites in fibronectin matrix assembly *in vivo*. *Curr. Opin. Cell Biol.* **20**, 502–507. (doi:10.1016/j.ceb.2008.06.001)
59. Yu J, Fairbank JC, Roberts S, Urban JP. 2005 The elastic fiber network of the anulus fibrosus of the normal and scoliotic human intervertebral disc. *Spine* (*Phila Pa 1976*) **30**, 1815–1820. (doi:10.1097/01.brs.0000173899.97415.5b)
60. Yu J, Winlove PC, Roberts S, Urban JP. 2002 Elastic fibre organization in the intervertebral discs of the bovine tail. *J. Anat.* **201**, 465–475. (doi:10.1046/j.1469-7580.2002.00111.x)
61. Johnson EF, Chetty K, Moore IM, Stewart A, Jones W. 1982 The distribution and arrangement of elastic fibres in the intervertebral disc of the adult human. *J. Anat.* **135**, 301–309.
62. Ishii Y, Thomas AO, Guo XE, Hung CT, Chen FH. 2006 Localization and distribution of cartilage oligomeric matrix protein in the rat intervertebral disc. *Spine* (*Phila Pa 1976*) **31**, 1539–1546. (doi:10.1097/01.brs.0000221994.61882.4a)
63. Rutges J, Creemers LB, Dhert W, Milz S, Sakai D, Mochida J, Alini M, Grad S. 2010 Variations in gene and protein expression in human nucleus pulposus in comparison with annulus fibrosus and cartilage cells: potential associations with aging and degeneration. *Osteoarthritis Cartilage* **18**, 416–423. (doi:10.1016/j.joca.2009.09.009)
64. Gruber HE, Bornstein P, Sage EH, Ingram JA, Zinchenko N, Norton HJ, Hanley EN. 2008 Disruption of the thrombospondin-2 gene alters the lamellar morphology but does not permit vascularization of the adult mouse lumbar disc. *Arthritis Res. Ther.* **10**, R96. (doi:10.1186/ar2483)
65. Dicesare PE, Morgelin M, Mann K, Paulsson M. 1994 Cartilage oligomeric matrix protein and thrombospondin 1. Purification from articular cartilage, electron microscopic structure, and chondrocyte binding. *Eur. J. Biochem.* **223**, 927–937. (doi:10.1111/j.1432-1033.1994.tb19070.x)
66. Le Maitre CL, Freemont AJ, Hoyland JA. 2004 Localization of degradative enzymes and their inhibitors in the degenerate human intervertebral disc. *J. Pathol.* **204**, 47–54. (doi:10.1002/path.1608)
67. Vo NV, Hartman RA, Yurube T, Jacobs LJ, Sowa GA, Kang JD. 2013 Expression and regulation of metalloproteinases and their inhibitors in intervertebral disc aging and degeneration. *Spine J.* **13**, 331–341. (doi:10.1016/j.spinee.2012.02.027)
68. Weiler C, Nerlich AG, Zipperer J, Bachmeier BE, Boos N. 2002 2002 SSE Award Competition in Basic Science: expression of major matrix metalloproteinases is associated with intervertebral disc degradation and resorption. *Eur. Spine J.* **11**, 308–320. (doi:10.1007/s00586-002-0472-0)
69. Pockert AJ, Richardson SM, Le Maitre CL, Lyon M, Deakin JA, Buttle DJ, Freemont AJ, Hoyland JA. 2009 Modified expression of the ADAMTS enzymes and tissue inhibitor of metalloproteinases 3 during human intervertebral disc degeneration. *Arthritis Rheum.* **60**, 482–491. (doi:10.1002/art.24291)
70. Nagase H. 2012 The ADAMTS family of metalloproteinases. In *Extracellular matrix: pathobiology and signalling* (ed. N Karamanos). Berlin, Germany: De Gruyter.
71. Richardson SM, Doyle P, Minogue BM, Gnanalingham K, Hoyland JA. 2009 Increased expression of matrix metalloproteinase-10, nerve growth factor and substance P in the painful degenerate intervertebral disc. *Arthritis Res. Ther.* **11**, R126. (doi:10.1186/ar2793)
72. Le Maitre CL, Freemont AJ, Hoyland JA. 2006 Human disc degeneration is associated with increased MMP 7 expression. *Biotech. Histochem.* **81**, 125–131. (doi:10.1080/10520290601005298)
73. Gruber HE, Ingram JA, Hanley Jr EN. 2005 Immunolocalization of MMP-19 in the human intervertebral disc: implications for disc aging and degeneration. *Biotech. Histochem.* **80**, 157–162. (doi:10.1080/10520290500387607)
74. Feng H, Danfelter M, Stromqvist B, Heinegard D. 2006 Extracellular matrix in disc degeneration. *J. Bone Joint Surg. Am.* **88**(Suppl. 2), 25–29. (doi:10.2106/JBJS.E.01341)
75. Roberts S, Caterson B, Menage J, Evans EH, Jaffray DC, Eisenstein SM. 2000 Matrix metalloproteinases and aggrecanase: their role in disorders of the human intervertebral disc. *Spine* (*Phila Pa 1976*) **25**, 3005–3013. (doi:10.1097/00007632-200012010-00007)
76. Roughley PJ. 2004 Biology of intervertebral disc aging and degeneration: involvement of the extracellular matrix. *Spine* (*Phila Pa 1976*) **29**, 2691–2699. (doi:10.1097/01.brs.0000146101.53784.b1)
77. Marom B, Rahat MA, Lahat N, Weiss-Cerem L, Kinarty A, Bitterman H. 2007 Native and fragmented fibronectin oppositely modulate monocyte secretion of MMP-9. *J. Leukoc. Biol.* **81**, 1466–1476. (doi:10.1189/jlb.0506328)
78. Sztrolovics R, White RJ, Poole AR, Mort JS, Roughley PJ. 1999 Resistance of small leucine-rich repeat proteoglycans to proteolytic degradation during interleukin-1-stimulated cartilage catabolism. *Biochem. J.* **339**, 571–577. (doi:10.1042/0264-6021:3390571)
79. Arroyo AG, Iruela-Arispe ML. 2010 Extracellular matrix, inflammation, and the angiogenic response. *Cardiovasc. Res.* **86**, 226–235. (doi:10.1093/cvr/cvq049)
80. Virri J, Sikk S, Gronblad M, Tolonen J, Seitsalo S, Kankare J, Karaharju EO. 1994 Concomitant immunocytochemical study of macrophage cells and blood vessels in disc herniation tissue. *Eur. Spine J.* **3**, 336–341. (doi:10.1007/BF02200147)
81. Jiang D, Liang J, Noble PW. 2007 Hyaluronan in tissue injury and repair. *Annu. Rev. Cell Dev. Biol.* **23**, 435–461. (doi:10.1146/annurev.cellbio.23.090506.123337)
82. Morwood SR, Nicholson LB. 2006 Modulation of the immune response by extracellular matrix proteins. *Arch. Immunol. Ther. Exp.* **54**, 367–374. (doi:10.1007/s00005-006-0043-x)
83. Abdollahi-Roodsaz S, Joosten LA, Roelofs MF, Radstake TRDJ, Matera G, Popa C, van der Meer JWM, Netea MG, van den Berg WB. 2007 Inhibition of toll-like receptor 4 breaks the inflammatory loop in autoimmune destructive arthritis. *Arthritis Rheum.* **56**, 2957–2967. (doi:10.1002/art.22848)
84. Quero L *et al*. 2013 Hyaluronic acid fragments enhance the inflammatory and catabolic response in human intervertebral disc cells through modulation of toll-like receptor 2 signaling pathways. *Arthritis Res. Ther.* **15**, R94. (doi:10.1186/ar4274)
85. Sorokin L. 2010 The impact of the extracellular matrix on inflammation. *Nat. Rev. Immunol.* **10**, 712–723. (doi:10.1038/nri2852)
86. Jones P, Gardner L, Menage J, Williams GT, Roberts S. 2008 Intervertebral disc cells as competent phagocytes *in vitro*: implications for cell death in disc degeneration. *Arthritis Res. Ther.* **10**, R86. (doi:10.1186/ar2466)
87. Nerlich AG, Weiler C, Zipperer J, Narozny M, Boos N. 2002 Immunolocalization of phagocytic cells in normal and degenerated intervertebral discs. *Spine* **27**, 2484–2490. (doi:10.1097/00007632-200211150-00012)
88. Phillips KL, Chiverton N, Michael AL, Cole AA, Breakwell LM, Haddock G, Bunning RAD, Cross AK, Le Maitre CL. 2013 The cytokine and chemokine expression profile of nucleus pulposus cells: implications for degeneration and regeneration of the intervertebral disc. *Arthritis Res. Ther.* **15**, R213. (doi:10.1186/ar4408)
89. Gabr MA *et al*. 2011 Interleukin-17 synergizes with IFNgamma or TNFalpha to promote inflammatory mediator release and intercellular adhesion

molecule-1 (ICAM-1) expression in human intervertebral disc cells. *J. Orthop. Res.* **29**, 1–7. (doi:10.1002/jor.21206)

90. Huang KY, Lin RM, Chen WY, Lee CL, Yan JJ, Chang MS. 2008 IL-20 may contribute to the pathogenesis of human intervertebral disc herniation. *Spine* (*Phila Pa 1976*) **33**, 2034–2040. (doi:10.1097/BRS.0b013e31817eb872)
91. Smith LJ, Chiaro JA, Nerurkar NL, Cortes DH, Horava SD, Hebela NM, Mauck RL, Dodge GR, Elliott DM. 2011 Nucleus pulposus cells synthesize a functional extracellular matrix and respond to inflammatory cytokine challenge following long-term agarose culture. *Eur. Cell Mater.* **22**, 291–301.
92. Hoyland JA, Le Maitre C, Freemont AJ. 2008 Investigation of the role of IL-1 and TNF in matrix degradation in the intervertebral disc. *Rheumatology* (*Oxf.*) **47**, 809–814. (doi:10.1093/rheumatology/ken056)
93. Seguin CA, Pilliar RM, Roughley PJ, Kandel RA. 2005 Tumor necrosis factor-alpha modulates matrix production and catabolism in nucleus pulposus tissue. *Spine* (*Phila Pa 1976*) **30**, 1940–1948. (doi:10.1097/01.brs.0000176188.40263.f9)
94. Seguin CA, Pilliar RM, Madri JA, Kandel RA. 2008 TNF-alpha induces MMP2 gelatinase activity and MT1-MMP expression in an *in vitro* model of nucleus pulposus tissue degeneration. *Spine* (*Phila Pa 1976*) **33**, 356–365. (doi:10.1097/BRS.0b013e3181642a5e)
95. Gawri R, Rosenzweig DH, Krock E, Ouellet JA, Stone LS, Quinn TM, Haglund L. 2014 High mechanical strain of primary intervertebral disc cells promotes secretion of inflammatory factors associated with disc degeneration and pain. *Arthritis Res. Ther.* **16**, R21. (doi:10.1186/ar4449)
96. Walter BA, Korecki CL, Purmessur D, Roughley PJ, Michalek AJ, Iatridis JC. 2011 Complex loading affects intervertebral disc mechanics and biology. *Osteoarthritis Cartilage* **19**, 1011–1018. (doi:10.1016/j.joca.2011.04.005)
97. Freemont AJ, Watkins A, Le Maitre C, Baird P, Jeziorska M, Knight MTN, Ross ERS, O'Brien JPJ, Hoyland A. 2002 Nerve growth factor expression and innervation of the painful intervertebral disc. *J. Pathol.* **197**, 286–292. (doi:10.1002/path.1108)
98. Melrose J, Roberts S, Smith S, Menage J, Ghosh P. 2002 Increased nerve and blood vessel ingrowth associated with proteoglycan depletion in an ovine anular lesion model of experimental disc degeneration. *Spine* (*Phila Pa 1976*) **27**, 1278–1285. (doi:10.1097/00007632-200206150-00007)
99. Kawakami M, Weinstein JN, Chatani K, Spratt KF, Meller ST, Gebhart GF. 1994 Experimental lumbar radiculopathy. Behavioral and histologic changes in a model of radicular pain after spinal nerve root irritation with chromic gut ligatures in the rat. *Spine (Phila Pa 1976)* **19**, 1795–1802. (doi:10.1097/00007632-199408150-00002)
100. Olmarker K, Blomquist J, Stromberg J, Nannmark U, Thomsen P, Rydevik B. 1995 Inflammatogenic properties of nucleus pulposus. *Spine (Phila Pa 1976)* **20**, 665–669. (doi:10.1097/00007632-199503150-00006)
101. Lotz JC, Ulrich JA. 2006 Innervation, inflammation, and hypermobility may characterize pathologic disc degeneration: review of animal model data. *J. Bone Joint Surg. Am.* **88**(Suppl. 2), 76–82. (doi:10.2106/JBJS.E.01448)
102. Kobayashi S *et al*. 2009 Ultrastructural analysis on lumbar disc herniation using surgical specimens: role of neovascularization and macrophages in hernias. *Spine* (*Phila Pa 1976*) **34**, 655–662. (doi:10.1097/BRS.0b013e31819c9d5b)
103. Ahn SH, Ahn MW, Byun WM. 2000 Effect of the transligamentous extension of lumbar disc herniations on their regression and the clinical outcome of sciatica. *Spine* (*Phila Pa 1976*) **25**, 475–480. (doi:10.1097/00007632-200002150-00014)
104. Ikeda T, Nakamura T, Kikuchi T, Umeda S, Senda H, Takagi K. 1996 Pathomechanism of spontaneous regression of the herniated lumbar disc: histologic and immunohistochemical study. *J. Spinal Disord.* **9**, 136–140. (doi:10.1097/00002517-199604000-00009)
105. Gezici AR, Ergun R. 2009 Spontaneous regression of a huge subligamentous extruded disc herniation: short report of an illustrative case. *Acta Neurochir.* (*Wien*) **151**, 1299–1300. (doi:10.1007/s00701-009-0370-x)
106. Takada T, Nishida K, Maeno K, Kakutani K, Yurube T, Doita M, Kurosaka M. 2012 Intervertebral disc and macrophage interaction induces mechanical hyperalgesia and cytokine production in a herniated disc model in rats. *Arthritis Rheum.* **64**, 2601–2610. (doi:10.1002/art.34456)
107. Matsui Y, Maeda M, Nakagami W, Iwata H. 1998 The involvement of matrix metalloproteinases and inflammation in lumbar disc herniation. *Spine* (*Phila Pa 1976*) **23**, 863–868; discussion 868–869. (doi:10.1097/00007632-199804150-00005)
108. Murai K, Sakai D, Nakamura Y, Nakai T, Igarashi T, Seo N, Murakami T, Kobayashi E, Mochida J. 2010 Primary immune system responders to nucleus pulposus cells: evidence for immune response in disc herniation. *Eur. Cell Mater.* **19**, 13–21.
109. Wang H *et al*. 2013 Inflammatory cytokines induce NOTCH signaling in nucleus pulposus cells: implications in intervertebral disc degeneration. *J. Biol. Chem.* **288**, 16 761–16 774. (doi:10.1074/jbc.M112.446633)
110. Kepler CK, Markova DZ, Dibra F, Yadla S, Vaccaro AR, Risbud MV, Albert TJ, Anderson DG. 2013 Expression and relationship of proinflammatory chemokine RANTES/CCL5 and cytokine IL-1beta in painful human intervertebral discs. *Spine* (*Phila Pa 1976*) **38**, 873–880. (doi:10.1097/BRS.0b013e318285ae08)
111. Le Maitre C, Hoyland J, Freemont A. 2007 Catabolic cytokine expression in degenerate and herniated human intervertebral discs: IL-1beta and TNFalpha expression profile. *Arthritis Res. Ther.* **9**, R77. (doi:10.1186/ar2275)
112. Le Maitre CL, Freemont AJ, Hoyland JA. 2005 The role of interleukin-1 in the pathogenesis of human intervertebral disc degeneration. *Arthritis Res. Ther.* **7**, R732–R745. (doi:10.1186/ar1732)
113. Abe Y, Akeda K, An HS, Aoki Y, Pichika R, Muehleman C, Kimura T, Masuda K. 2007 Proinflammatory cytokines stimulate the expression of nerve growth factor by human intervertebral disc cells. *Spine* (*Phila Pa 1976*) **32**, 635–642. (doi:10.1097/01.brs.0000257556.90850.53)
114. Miyahara K, Ishida T, Hukuda S, Horiike K, Okamoto M, Tojo H. 1996 Human group II phospholipase A2 in normal and diseased intervertebral discs. *Biochim. Biophys. Acta* **1316**, 183–190. (doi:10.1016/0925-4439(96)00023-3)
115. Wang J *et al*. 2013 Tumor necrosis factor alpha- and interleukin-1beta-dependent induction of CCL3 expression by nucleus pulposus cells promotes macrophage migration through CCR1. *Arthritis Rheum.* **65**, 832–842. (doi:10.1002/art.37819)
116. Kokubo Y *et al*. 2008 Herniated and spondylotic intervertebral discs of the human cervical spine: histological and immunohistological findings in 500 en bloc surgical samples. Laboratory investigation. *J. Neurosurg. Spine* **9**, 285–295. (doi:10.3171/SPI/2008/9/9/285)
117. Takahashi H, Suguro T, Okazima Y, Motegi M, Okada Y, Kakiuchi T. 1996 Inflammatory cytokines in the herniated disc of the lumbar spine. *Spine* (*Phila Pa 1976*) **21**, 218–224. (doi:10.1097/00007632-199601150-00011)
118. Kang JD, Georgescu HI, Mcintyre-Larkin L, Stefanovic-Racic M, Donaldson III WF, Evans CH. 1996 Herniated lumbar intervertebral discs spontaneously produce matrix metalloproteinases, nitric oxide, interleukin-6, and prostaglandin E2. *Spine* (*Phila Pa 1976*) **21**, 271–277. (doi:10.1097/00007632-199602010-00003)
119. Ahn SH, Cho YW, Ahn MW, Jang SH, Sohn YK, Kim HS. 2002 mRNA expression of cytokines and chemokines in herniated lumbar intervertebral discs. *Spine* (*Phila Pa 1976*) **27**, 911–917. (doi:10.1097/00007632-200205010-00005)
120. Henriksson H, Thornemo M, Karlsson C, Hägg O, Junevik K, Lindahl A, Brisby H. 2009 Identification of cell proliferation zones, progenitor cells and a potential stem cell niche in the intervertebral disc region: a study in four species. *Spine* **34**, 2278–2287. (doi:10.1097/BRS.0b013e3181a95ad2)
121. Miyamoto H, Saura R, Harada T, Doita M, Mizuno K. 2000 The role of cyclooxygenase-2 and inflammatory cytokines in pain induction of herniated lumbar intervertebral disc. *Kobe J. Med. Sci.* **46**, 13–28.
122. Shamji MF *et al*. 2010 Proinflammatory cytokine expression profile in degenerated and herniated human intervertebral disc tissues. *Arthritis Rheum.* **62**, 1974–1982. (doi:10.1002/art.27444)
123. Zhang W, Nie L, Wang Y, Wang X, Zhao H, Dongol S, Maharjan S, Cheng L. 2013 CCL20 secretion from

the nucleus pulposus improves the recruitment of CCR6-expressing Th17 cells to degenerated IVD tissues. *PLoS ONE* **8**, e66286. (doi:10.1371/journal.pone.0066286)

124. Kim JH, Studer RK, Sowa GA, Vo NV, Kang JD. 2008 Activated macrophage-like THP-1 cells modulate anulus fibrosus cell production of inflammatory mediators in response to cytokines. *Spine* (*Phila Pa 1976*) **33**, 2253–2259. (doi:10.1097/BRS.0b013e318182c35f)
125. Park JY, Kuh SU, Park HS, Kim KS. 2011 Comparative expression of matrix-associated genes and inflammatory cytokines-associated genes according to disc degeneration: analysis of living human nucleus pulposus. *J. Spinal Disord. Tech.* **24**, 352–357. (doi:10.1097/BSD.0b013e3181fee4df)
126. Kepler CK, Markova DZ, Hilibrand AS, Vaccaro AR, Risbud MV, Albert TJ, Anderson DG. 2013 Substance P stimulates production of inflammatory cytokines in human disc cells. *Spine* (*Phila Pa 1976*) **38**, E1291–E1299. (doi:10.1097/BRS.0b013e3182a42bc2)
127. Burke JG, Rw GW, Conhyea D, McCormack D, Dowling FE, Walsh MG, Fitzpatrick JM. 2003 Human nucleus pulposis can respond to a pro-inflammatory stimulus. *Spine* (*Phila Pa 1976*) **28**, 2685–2693. (doi:10.1097/01.BRS.0000103341.45133.F3)
128. Kim JH, Studer RK, Vo NV, Sowa GA, Kang JD. 2009 p38 MAPK inhibition selectively mitigates inflammatory mediators and VEGF production in AF cells co-cultured with activated macrophage-like THP-1 cells. *Osteoarthritis Cartilage* **17**, 1662–1669. (doi:10.1016/j.joca.2009.06.004)
129. Sinclair SM, Shamji MF, Chen J, Jing L, Richardson WJ, Brown CR, Fitch RD, Setton LA. 2011 Attenuation of inflammatory events in human intervertebral disc cells with a tumor necrosis factor antagonist. *Spine* (*Phila Pa 1976*) **36**, 1190–1196. (doi:10.1097/BRS.0b013e3181ebdb43)
130. Studer RK, Vo N, Sowa G, Ondeck C, Kang J. 2011 Human nucleus pulposus cells react to IL-6: independent actions and amplification of response to IL-1 and TNF-alpha. *Spine* (*Phila Pa 1976*) **36**, 593–599. (doi:10.1097/BRS.0b013e3181da38d5)
131. Tian Y, Yuan W, Fujita N, Wang J, Wang H, Shapiro IM, Risbud MV. 2013 Inflammatory cytokines associated with degenerative disc disease control aggrecanase-1 (ADAMTS-4) expression in nucleus pulposus cells through MAPK and NF-kappaB. *Am. J. Pathol.* **182**, 2310–2321. (doi:10.1016/j.ajpath.2013.02.037)
132. Yu ZG, Xu N, Wang WB, Pan SH, Li KS, Liu JK. 2009 Interleukin-1 inhibits Sox9 and collagen type II expression via nuclear factor-kappaB in the cultured human intervertebral disc cells. *Chin. Med. J.* (*Engl.*) **122**, 2483–2488.
133. Doita M, Kanatani T, Harada T, Mizuno K. 1996 Immunohistologic study of the ruptured intervertebral disc of the lumbar spine. *Spine* (*Phila Pa 1976*) **21**, 235–241. (doi:10.1097/00007632-199601150-00015)
134. Bachmeier BE, Nerlich AG, Weiler C, Paesold G, Jochum M, Boos N. 2007 Analysis of tissue distribution of TNF-α, TNF-α-receptors, and the activating TNF-α-converting enzyme suggests activation of the TNF-α system in the aging intervertebral disc. *Ann. NY Acad. Sci.* **1096**, 44–54. (doi:10.1196/annals.1397.069)
135. Risbud MV, Shapiro IM. 2014 Role of cytokines in intervertebral disc degeneration: pain and disc content. *Nat. Rev. Rheumatol.* **10**, 44–56. (doi:10.1038/nrrheum.2013.160)
136. Goupille P, Mulleman D, Paintaud G, Watier H, Valat JP. 2007 Can sciatica induced by disc herniation be treated with tumor necrosis factor alpha blockade? *Arthritis Rheum.* **56**, 3887–3895. (doi:10.1002/art.23051)
137. Purmessur D, Walter BA, Roughley PJ, Laudier DM, Hecht AC, Iatridis J. 2013 A role for TNFalpha in intervertebral disc degeneration: a non-recoverable catabolic shift. *Biochem. Biophys. Res. Commun.* **433**, 151–156. (doi:10.1016/j.bbrc.2013.02.034)
138. Le Maitre CL, Pockert A, Buttle DJ, Freemont AJ, Hoyland JA. 2007 Matrix synthesis and degradation in human intervertebral disc degeneration. *Biochem. Soc. Trans.* **35**, 652–655. (doi:10.1042/BST0350652)
139. Igarashi T, Kikuchi S, Shubayev V, Myers RR. 2000 Exogenous tumor necrosis factor-alpha mimics nucleus pulposus-induced neuropathology: molecular, histologic, and behavioral comparisons in rats. *Spine* **25**, 2975–2980. (doi:10.1097/00007632-200012010-00003)
140. Kauppila LI. 1995 Ingrowth of blood vessels in disc degeneration. Angiographic and histological studies of cadaveric spines. *J. Bone Joint Surg. Am.* **77**, 26–31.
141. Hess A *et al*. 2011 Blockade of TNF-alpha rapidly inhibits pain responses in the central nervous system. *Proc. Natl Acad. Sci. USA* **108**, 3731–3736. (doi:10.1073/pnas.1011774108)
142. Cuellar JM, Borges PM, Cuellar VG, Yoo A, Scuderi GJ, Yeomans DC. 2012 Cytokine expression in the epidural space: a model of non-compressive disc herniation-induced inflammation. *Spine* (*Phila Pa 1976*) **38**, 17–23. (doi:10.1097/BRS.0b013e3182604baa)
143. Rousseau MA, Ulrich JA, Bass EC, Rodriguez AG, Liu JJ, Lotz JC. 2007 Stab incision for inducing intervertebral disc degeneration in the rat. *Spine* (*Phila Pa 1976*) **32**, 17–24. (doi:10.1097/01.brs.0000251013.07656.45)
144. Anderson DG, Izzo MW, Hall DJ, Vaccaro AR, Hilibrand A, Arnold W, Tuan RS, Albert TJ. 2002 Comparative gene expression profiling of normal and degenerative discs: analysis of a rabbit annular laceration model. *Spine* (*Phila Pa 1976*) **27**, 1291–1296. (doi:10.1097/00007632-200206150-00009)
145. Sobajima S, Kompel JF, Kim JS, Wallach CJ, Robertson DD, Vogt MT, Kang JD, Gilbertson LG. 2005 A slowly progressive and reproducible animal model of intervertebral disc degeneration characterized by MRI, X-ray, and histology. *Spine* (*Phila Pa 1976*) **30**, 15–24. (doi:10.1097/00007632-200511150-00023)
146. Baggiolini M, Dewald B, Moser B. 1997 Human chemokines: an update. *Annu. Rev. Immunol.* **15**, 675–705. (doi:10.1146/annurev.immunol.15.1.675)
147. Yoshida M, Nakamura T, Sei A, Kikuchi T, Takagi K, Matsukawa A. 2005 Intervertebral disc cells produce tumor necrosis factor alpha, interleukin-1beta, and monocyte chemoattractant protein-1 immediately after herniation: an experimental study using a new hernia model. *Spine* (*Phila Pa 1976*) **30**, 55–61. (doi:10.1097/01.brs.0000149194.17891.bf)
148. O'Neill CW, Liu JJ, Leibenberg E, Hu SS, Deviren V, Tay BK-B, Chin CT, Lotz JC. 2004 Percutaneous plasma decompression alters cytokine expression in injured porcine intervertebral discs. *Spine J.* **4**, 88–98. (doi:10.1016/S1529-9430(03)00423-6)
149. Rajan N, Bloom O, Maidhof R, Stetson N, Sherry B, Levine M, Chahine NO. 2012 Toll-like receptor 4 (TLR4) expression and stimulation in a model of intervertebral disc inflammation and degeneration. *Spine* (*Phila Pa 1976*) **38**, 1343–1351. (doi:10.1097/BRS.0b013e31826b71f4)
150. Morimoto R, Akeda K, Iida R, Nishimura A, Tsujii M, Obata S, Kasai Y, Uchida A, Sudo A. 2012 Tissue renin-angiotensin system in the intervertebral disc. *Spine* (*Phila Pa 1976*) **38**, E129–E136. (doi:10.1097/BRS.0b013e31827b8c89)
151. Gruber HE, Hanley Jr EN. 2002 Ultrastructure of the human intervertebral disc during aging and degeneration: comparison of surgical and control specimens. *Spine* (*Phila Pa 1976*) **27**, 798–805. (doi:10.1097/00007632-200204150-00004)
152. Bach FC, Willems N, Penning LC, Ito K, Meij BP, Tryfonidou MA. 2014 Potential regenerative treatment strategies for intervertebral disc degeneration in dogs. *BMC Vet. Res.* **10**, 3. (doi:10.1186/1746-6148-10-3)
153. Bergknut N *et al*. 2013 Intervertebral disc disease in dogs—part 1: a new histological grading scheme for classification of intervertebral disc degeneration in dogs. *Vet. J.* **195**, 156–163. (doi:10.1016/j.tvjl.2012.05.027)
154. Alini M *et al*. 2008 Are animal models useful for studying human disc disorders/degeneration? *Eur. Spine J.* **17**, 2–19. (doi:10.1007/s00586-007-0414-y)
155. Roberts S, Butler RC. 2005 Inflammatory mediators as potential therapeutic targets in the spine. *Curr. Drug Targets* **4**, 257–266. (doi:10.2174/1568010053586372).
156. Wuertz K, Vo N, Kletsas D, Boos N. 2012 Inflammatory and catabolic signalling in intervertebral discs: the roles of NF-kappaB and MAP kinases. *Eur. Cell Mater.* **23**, 103–119; discussion 119–120.
157. Genevay S, Viatte S, Finckh A, Zufferey P, Balague F, Gabay C. 2010 Adalimumab in severe and acute sciatica: a multicenter, randomized, double-blind, placebo-controlled trial. *Arthritis Rheum.* **62**, 2339–2346. (doi:10.1002/art.27499)
158. Genevay S, Stingelin S, Gabay C. 2004 Efficacy of etanercept in the treatment of acute, severe sciatica:

a pilot study. *Ann. Rheum. Dis.* **63**, 1120–1123. (doi:10.1136/ard.2003.016451)

159. Olmarker K, Rydevik B. 2001 Selective inhibition of tumor necrosis factor-alpha prevents nucleus pulposus-induced thrombus formation, intraneural edema, and reduction of nerve conduction velocity: possible implications for future pharmacologic treatment strategies of sciatica. *Spine* (*Phila Pa 1976*) **26**, 863–869. (doi:10.1097/00007632-200104150-00007)
160. Okoro T, Tafazal SI, Longworth S, Sell PJ. 2010 Tumor necrosis alpha-blocking agent (etanercept): a triple blind randomized controlled trial of its use in treatment of sciatica. *J. Spinal Disord. Tech.* **23**, 74–77. (doi:10.1097/BSD.0b013e31819afdc4)
161. Muller-Ladner U, Roberts CR, Franklin BN, Gay RE, Robbins PD, Evans CH, Gay S. 1997 Human IL-1Ra gene transfer into human synovial fibroblasts is chondroprotective. *J. Immunol.* **158**, 3492–3498.
162. Autio RA, Karppinen JNiinimäki J, Ojala R, Veeger N, Korhonen T, Hurri H, Tervonen O. 2006 The effect of infliximab, a monoclonal antibody against TNF-α, on disc herniation resorption: a randomized controlled study. *Spine* **31**, 2641–2645. (doi:10.1097/01.brs.0000244616.64962.9e)
163. Tobinick E. 2006 Spinal delivery of p38: TNF-alpha inhibitors. *PLoS Med.* **3**, e511. (doi:10.1371/journal.pmed.0030511)
164. Ragab AA, Woodall Jr JW, Tucci MA, Wingerter SA, Fosnaugh AW, Franklin LN, Benghuzzi HA. 2009 A preliminary report on the effects of sustained administration of corticosteroid on traumatized disc using the adult male rat model. *J. Spinal Disord. Tech.* **22**, 473–478. (doi:10.1097/BSD.0b013e31818d5e55)
165. Zhang H, Wang L, Park JB, Park P, Yang VC, Hollister SJ, La Marca F, Lin C-Y. 2009 Intradiscal injection of simvastatin retards progression of intervertebral disc degeneration induced by stab injury. *Arthritis Res. Ther.* **11**, R172. (doi:10.1186/ar2861)
166. Gorth DJ, Mauck RL, Chiaro JA, Mohanraj B, Hebela NM, Dodge GR, Elliott DM, Smith LJ. 2012 IL-1ra delivered from poly(lactic-co-glycolic acid) microspheres attenuates IL-1β-mediated degradation of nucleus pulposus *in vitro*. *Arthritis Res. Ther.* **14**, R179. (doi:10.1186/ar3932)
167. Kawakami M, Matsumoto T, Hashizume H, Kuribayashi K, Tamaki T. 2002 Epidural injection of cyclooxygenase-2 inhibitor attenuates pain-related behavior following application of nucleus pulposus to the nerve root in the rat. *J. Orthop. Res.* **20**, 376–381. (doi:10.1016/S0736-0266(01)00114-0)
168. Nagae M *et al*. 2007 Intervertebral disc regeneration using platelet-rich plasma and biodegradable gelatin hydrogel microspheres. *Tissue Eng.* **13**, 147–158. (doi:10.1089/ten.2006.0042)
169. Wu C-C, Chen W-H, Zao B, Lai P-L, Lin T-C, Lo H-Y, Shieh Y-H, Wu C-H, Deng W-P. 2011 Regenerative potentials of platelet-rich plasma enhanced by collagen in retrieving pro-inflammatory cytokine-inhibited chondrogenesis. *Biomaterials* **32**, 5847–5854. (doi:10.1016/j.biomaterials.2011.05.002)
170. Wuertz K, Quero L, Sekiguchi M, Klawitter M, Nerlich A, Konno S, Kikuchi S, Boos N. 2011 The red wine polyphenol resveratrol shows promising potential for the treatment of nucleus pulposus-mediated pain *in vitro* and *in vivo*. *Spine* **36**, 1373–1384. (doi:10.1097/BRS.0b013e318221e655)
171. Li H, Liang C, Chen Q, Yang Z. 2011 Rhein: a potential biological therapeutic drug for intervertebral disc degeneration. *Med. Hypotheses* **77**, 1105–1107. (doi:10.1016/j.mehy.2011.09.013)
172. Liu Q, Jin L, Shen FH, Balian G, Li XJ. 2013 Fullerol nanoparticles suppress inflammatory response and adipogenesis of vertebral bone marrow stromal cells—a potential novel treatment for intervertebral disc degeneration. *Spine J.* **13**, 1571–1580. (doi:10.1016/j.spinee.2013.04.004)
173. Kobori S *et al*. 2014 Inhibiting IkappaB kinase-beta downregulates inflammatory cytokines in injured discs and neuropeptides in dorsal root ganglia innervating injured discs in rats. *Spine* (*Phila Pa 1976*) **39**, 1171–1177. (doi:10.1097/BRS.0000000000000374)
174. Vadalà G, Sowa GA, Kang JD. 2007 Gene therapy for disc degeneration. *Expert Opin. Biol. Ther.* **7**, 185–196. (doi:10.1517/14712598.7.2.185)
175. Carragee EJ, Don AS, Hurwitz EL, Cuellar JM, Carrino JA, Herzog R. 2009 2009 ISSLS prize winner: does discography cause accelerated progression of degeneration changes in the lumbar disc: a ten-year matched cohort study. *Spine* (*Phila Pa 1976*) **34**, 2338–2345. (doi:10.1097/BRS.0b013e3181ab5432)
176. Vadala G, Russo F, Pattappa G, Schiuma D, Peroglio M, Benneker LM, Grad S, Alini M, Denaro V. 2013 The transpedicular approach as an alternative route for intervertebral disc regeneration. *Spine* (*Phila Pa 1976*) **38**, E319–E324. (doi:10.1097/BRS.0b013e318285bc4a)
177. Gibson MJ, Karpinski MR, Slack RC, Cowlishaw WA, Webb JK. 1987 The penetration of antibiotics into the normal intervertebral disc. *J. Bone Joint Surg. Br.* **69**, 784–786.
178. Motaghinasab S, Shirazi-Adl A, Urban JP, Parnianpour M. 2012 Computational pharmacokinetics of solute penetration into human intervertebral discs—effects of endplate permeability, solute molecular weight and disc size. *J. Biomech.* **45**, 2195–2202. (doi:10.1016/j.jbiomech.2012.06.033)
179. Ferguson SJ, Ito K, Nolte LP. 2004 Fluid flow and convective transport of solutes within the intervertebral disc. *J. Biomech.* **37**, 213–221. (doi:10.1016/S0021-9290(03)00250-1)
180. Wehling P, Schulitz KP, Robbins PD, Evans CH, Reinecke JA. 1997 Transfer of genes to chondrocytic cells of the lumbar spine. Proposal for a treatment strategy of spinal disorders by local gene therapy. *Spine* **15**, 1092–1097. (doi:10.1097/00007632-199705150-00008)
181. Le Maitre CL, Hoyland JA, Freemont AJ. 2007 Interleukin-1 receptor antagonist delivered directly and by gene therapy inhibits matrix degradation in the intact degenerate human intervertebral disc: an *in situ* zymographic and gene therapy study. *Arthritis Res. Ther.* **9**, R83. (doi:10.1186/ar2282)
182. Nishida K, Kang JD, Gilbertson LG, Moon S-H, Suh J-K, Vogt MT, Robbins PD, Evans CH. 1999 Modulation of the biologic activity of the rabbit intervertebral disc by gene therapy: an *in vivo* study of adenovirus-mediated transfer of the human transforming growth factor beta 1 encoding gene. *Spine* (*Phila Pa 1976*) **24**, 2419–2425. (doi:10.1097/00007632-199912010-00002)
183. Lee YJ, Kong MH, Song KY, Lee KH, Heo SH. 2008 The relation between Sox9, TGF-β1, and proteoglycan in human intervertebral disc cells. *J. Kor. Neurosurg. Soc.* **43**, 149–154. (doi:10.3340/jkns.2008.43.3.149)
184. Tan Y, Hu Y, Tan J. 2003 Extracellular matrix synthesis and ultrastructural changes of degenerative disc cells transfected by Ad/CMV-hTGF-beta 1. *Chin. Med. J.* (*Engl.*) **116**, 1399–1403.
185. Leckie S *et al*. 2012 Injection of AAV2-BMP2 and AAV2-TIMP1 into the nucleus pulposus slows the course of intervertebral disc degeneration in an *in vivo* rabbit model. *Spine* **12**, 7–20. (doi:10.1016/j.spinee.2011.09.011)
186. Haufe SMW, Mork AR. 2006 Intradiscal injection of hematopoietic stem cells in an attempt to rejuvenate the intervertebral discs. *Stem Cells Dev.* **15**, 136–137. (doi:10.1089/scd.2006.15.136)
187. Quintin A, Schizas C, Scaletta C, Jaccoud S, Gerber S, Osterheld MC, Juillerat L, Applegate LA, Pioletti DP. 2008 Isolation and *in vitro* chondrogenic potential of human foetal spine cells. *J. Cell Mol. Med.* **13**, 2559–2569. (doi:10.1111/j.1582-4934.2008.00630.x)
188. Iwashina T, Mochida J, Sakai D, Yamamoto Y, Miyazaki T, Ando K, Hotta T. 2006 Feasibility of using a human nucleus pulposus cell line as a cell source in cell transplantation therapy for intervertebral disc degeneration. *Spine* **31**, 1177–1186. (doi:10.1097/01.brs.0000217687.36874.c4)
189. Hohaus C, Ganey TM, Minkus Y, Meisel HJ. 2008 Cell transplantation in lumbar spine disc degeneration disease. *Eur. Spine J.* **17**(Suppl. 4), S492–S503. (doi:10.1007/s00586-008-0750-6)
190. Sheikh H, Zakharian K, De La Torre RP, Facek C, Vasquez A, Chaudhry GR, Svinarich D, Peter-Cruet MJ. 2009 *In vivo* intervertebral disc regeneration using stem cell-derived chondroprogenitors: laboratory investigation. *J. Neurosurg.* **10**, 265–272. (doi:10.3171/2008.12.SPINE0835)
191. Chen J, Lee EJ, Jing L, Christoforou N, Leong KW, Setton LA. 2013 Differentiation of mouse induced pluripotent stem cells (iPSCs) into nucleus pulposus-like cells *in vitro*. *PLoS ONE* **8**, e75548. (doi:10.1371/journal.pone.0075548)
192. Murrell W, Sanford E, Anderberg L, Cavanagh B, Mackay-Sim A. 2009 Olfactory stem cells can be induced to express chondrogenic phenotype in a rat intervertebral disc injury model. *Spine J.* **9**, 585–594. (doi:10.1016/j.spinee.2009.02.011)
193. Sakai D, Mochida J, Iwashina T, Watanabe T, Nakai T, Ando K, Hotta T. 2005 Differentiation of

mesenchymal stem cells transplanted to a rabbit degenerative disc model: potential and limitations for stem cell therapy in disc regeneration. *Spine* **30**, 2379–2387. (doi:10.1097/01.brs.0000184365.28481.e3)

194. Chon BH, Lee EJ, Jing L, Setton LA, Chen J. 2013 Human umbilical cord mesenchymal stromal cells exhibit immature nucleus pulposus cell phenotype in a laminin-rich pseudo-three-dimensional culture system. *Stem Cell Res. Ther.* **4**, 120. (doi:10.1186/scrt331)
195. Erwin WM, Islam D, Eftekarpour E, Inman RD, Karim MZ, Fehlings MG. 2013 Intervertebral disc-derived stem cells: implications for regenerative medicine and neural repair. *Spine* **38**, 211–216. (doi:10.1097/BRS.0b013e318266a80d)
196. Kim JH, Moon HJ, Lee JH, Kim JH, Kwon TH, Park YK. 2012 Rabbit notochordal cells modulate the expression of inflammatory mediators by human annulus fibrosus cells cocultured with activated macrophage-like THP-1 cells. *Spine* (*Phila Pa 1976*) **37**, 1856–1864. (doi:10.1097/BRS.0b013e3182579434)
197. Serigano K, Sakai D, Hiyama A, Tamura F, Tanaka M, Mochida J. 2010 Effect of cell number on mesenchymal stem cell transplantation in a canine disc degeneration model. *J. Orthop. Res.* **28**, 1267–1275. (doi:10.1002/jor.21147)
198. Miyamoto T, Muneta T, Tabuchi T, Matsumoto K, Saito H, Tsuji K, Sekiya I. 2010 Intradiscal transplantation of synovial mesenchymal stem cells prevents intervertebral disc degeneration through suppression of matrix metalloproteinase-related genes in nucleus pulposus cells in rabbits. *Arthritis Res. Ther.* **12**, R206. (doi:10.1186/ar3182)
199. Yoo K *et al*. 2009 Comparison of immunomodulatory properties of mesenchymal stem cells derived from adult human tissues. *Cell Immunol.* **259**, 150–156. (doi:10.1016/j.cellimm.2009.06.010)
200. Prockop DJ, Oh JY. 2012 Mesenchymal stem/stromal cells (MSCs): role as guardians of inflammation. *Mol. Ther.* **20**, 14–20. (doi:10.1038/mt.2011.211)
201. Ortiz LA, Dutreil M, Fattman C, Pandey AC, Torres G, Go K, Phinney DG. 2007 Interleukin 1 receptor antagonist mediates the antiinflammatory and antifibrotic effect of mesenchymal stem cells during lung injury. *Proc. Natl Acad. Sci. USA* **104**, 11 002–11 007. (doi:10.1073/pnas.0704421104)
202. Lee RH *et al*. 2009 Intravenous hMSCs improve myocardial infarction in mice because cells embolized in lung are activated to secrete the anti-inflammatory protein TSG-6. *Cell Stem Cell* **5**, 54–63. (doi:10.1016/j.stem.2009.05.003)
203. Oh JY, Roddy GW, Choi H, Lee RH, Ylostalo JH, Rosa RH, Prockop DJ. 2010 Anti-inflammatory protein TSG-6 reduces inflammatory damage to the cornea following chemical and mechanical injury. *Proc. Natl Acad. Sci. USA* **107**, 16 875–16 880. (doi:10.1073/pnas.1012451107)
204. Hiyama A, Mochida J, Iwashina T, Omi H, Watanabe T, Serigano K, Tamura F, Sakai D. 2008 Transplantation of mesenchymal stem cells in a canine disc degeneration model. *J. Orthop. Res.* **26**, 589–600. (doi:10.1002/jor.20584)
205. Bertolo A, Thiede T, Aebli N, Baur M, Ferguson S, Stoyanov J. 2011 Human mesenchymal stem cell co-culture modulates the immunological properties of human intervertebral disc tissue fragments *in vitro*. *Eur. Spine J.* **20**, 592–603. (doi:10.1007/s00586-010-1662-9)
206. Orozco L, Soler R, Morera C, Alberca M, Sanchez A, García-Sancho J. 2011 Intervertebral disc repair by autologous mesenchymal bone marrow cells: a pilot study. *Transplantation* **92**, 822–828. (doi:10.1097/TP.0b013e3182298a15)
207. Yoshikawa T, Ueda Y, Miyazaki K, Koizumi M, Takakura Y. 2010 Disc regeneration therapy using marrow mesenchymal cell transplantation: a report of two case studies. *Spine* **35**, E475–E480. (doi:10.1097/BRS.0b013e3181cd2cf4)
208. Pang X, Yang H, Peng B. 2014 Human umbilical cord mesenchymal stem cell transplantation for the treatment of chronic discogenic low back pain. *Pain Phys.* **17**, E525–E530.
209. Pettine KA, Murphy MB, Suzuki RK, Sand TT. 2014 Percutaneous injection of autologous bone marrow concentrate cells significantly reduces lumbar discogenic pain through 12 months. *Stem Cells* **33**, 146–156. (doi:10.1002/stem.1845)
210. Meirelles L, Fontes AM, Covas DT, Caplan AI. 2009 Mechanisms involved in the therapeutic properties of mesenchymal stem cells. *Cytok. Growth Factor Rev.* **20**, 419–427. (doi:10.1016/j.cytogfr.2009.10.002)
211. Karp JM, Leng Teo GS. 2009 Mesenchymal stem cell homing: the devil is in the details. *Cell Stem Cell* **4**, 206–216. (doi:10.1016/j.stem.2009.02.001)
212. Ponte A, Marais E, Gallay N, Langonne A, Delorme B, Herault E, Charboard P, Domenech J. 2009 The *in vitro* migration capacity of human bone marrow mesenchymal stem cells: comparison of chemokine and growth factor chemotactic activities. *Stem Cells* **25**, 1737–1745. (doi:10.1634/stemcells.2007-0054)
213. Tondreau T, Meuleman N, Stamatopoulos B, De Bruyn C, Delforge A, Dejeneffe M, Martiat P, Bron D, Lagneaux L. 2009 *In vitro* study of matrix metalloproteinase/tissue inhibitor of metalloproteinase production by mesenchymal stromal cells in response to inflammatory cytokines: the role of their migration in injured tissues. *Cytotherapy* **11**, 559–569. (doi:10.1080/14653240903051541)
214. Illien-Jünger SPG, Peroglio M, Benneker LM, Stoddart MJ, Sakai D, Mochida J, Grad S, Alini M. 2012 Homing of mesenchymal stem cells in induced degenerative intervertebral discs in a whole organ culture system. *Spine* **37**, 1865–1873. (doi:10.1097/BRS.0b013e3182544a8a)
215. Pattappa G, Peroglio M, Sakai D, Mochida J, Benneker LM, Alini M, Grad S. 2014 CCL5/RANTES is a key chemoattractant released by degenerative intervertebral discs in organ culture. *Eur. Cell Mater.* **27**, 124–136; discussion 136.
216. Pereira CL *et al*. 2014 The effect of hyaluronan-based delivery of stromal cell-derived factor-1 on the recruitment of MSCs in degenerating intervertebral discs. *Biomaterials* **35**, 8144–8153. (doi:10.1016/j.biomaterials.2014.06.017)
217. Henriksson H, Svala E, Skioldebrand E, Lindahl AMD, Brisby H. 2012 Support of concept that migrating progenitor cells from stem cell niches contribute to normal regeneration of the adult mammal intervertebral disc. *Spine* **37**, 722–732. (doi:10.1097/BRS.0b013e318231c2f7)
218. Claes L, Recknagel S, Ignatius A. 2012 Fracture healing under healthy and inflammatory conditions. *Nat. Rev. Rheumatol.* **8**, 133–143. (doi:10.1038/nrrheum.2012.1)
219. Mountziaris PM, Spicer PP, Kasper FK, Mikos AG. 2011 Harnessing and modulating inflammation in strategies for bone regeneration. *Tissue Eng. B* **17**, 393–402. (doi:10.1089/ten.teb.2011.0182)
220. Boccafoschi F, Mosca C, Cannas M. 2012 Cardiovascular biomaterials: when the inflammatory response helps to efficiently restore tissue functionality? *J. Tissue Eng. Regen. Med.* **8**, 253–267. (doi:10.1002/term.1526)
221. Torres AL, Santos SG, Oliveira MI, Barbosa MA. 2013 Fibrinogen promotes resorption of chitosan by human osteoclasts. *Acta Biomater.* **9**, 6553–6562. (doi:10.1016/j.actbio.2013.01.015)
222. Almeida CR, Vasconcelos DP, Goncalves RM, Barbosa MA. 2012 Enhanced mesenchymal stromal cell recruitment via natural killer cells by incorporation of inflammatory signals in biomaterials. *J. R. Soc. Interface* **9**, 261–271. (doi:10.1098/rsif.2011.0357)
223. Oliveira MI, Santos SG, Oliveira MJ, Torres AL, Barbosa MA. 2012 Chitosan drives anti-inflammatory macrophage polarisation and pro-inflammatory dendritic cell stimulation. *Eur. Cell Mater.* **24**, 136–152; discussion 152–153.
224. Maciel J, Oliveira MI, Colton E, McNally AK, Oliveira C, Anderson JM, Barbosa MA. 2014 Adsorbed fibrinogen enhances production of bone- and angiogenic-related factors by monocytes/macrophages. *Tissue Eng. A* **20**, 250–263. (doi:10.1089/ten.tea.2012.0439)
225. Lee J, Sayed N, Hunter A, Au KF,, Wong WH, Mocarski ES, Pera RR, Yakubov E, Cooke JP. 2012 Activation of innate immunity is required for efficient nuclear reprogramming. *Cell* **151**, 547–558. (doi:10.1016/j.cell.2012.09.034)
226. Takahashi K, Tanabe K, Ohnuki M, Narita M, Ichisaka T, Tomoda M, Yamanaka S. 2007 Induction of pluripotent stem cells from adult human fibroblasts by defined factors. *Cell* **131**, 861–872. (doi:10.1016/j.cell.2007.11.019)
227. O'Neill LAJ. 2012 Transflammation: when innate immunity meets induced pluripotency. *Cell* **151**, 471–473. (doi:10.1016/j.cell.2012.10.006)
228. Raghow R. 1994 The role of extracellular matrix in postinflammatory wound healing and fibrosis. *FASEB J.* **8**, 823–831.

Glossary

ADAMTS	A disintegrin and metalloproteinase with thrombospondin motifs
AF	Annulus fibrosus
BMP	Bone morphogenic protein
C/EBPβ	CCAAT/enhancer-binding protein beta
CCL	Chemokine ligand
CEP	Cartilaginous endplates
COX	Cyclooxygenase
CPPD	Calcium pyrophosphate dihydrate
CXCL9	Monokine induced by gamma interferon
DDD	Degenerative disc disease
DRG	Dorsal root ganglion
ECM	Extracellular matrix
FasL	Fas ligand
FGF	Fibroblast growth factor
fHA	Hyaluronic acid fragments
GAG	Glycosaminoglycan
GAP	Growth-associated protein
GDF-1	Growth and differentiation factor-1
GM-CSF	Granulocyte macrophage colony-stimulating factor
HA	Hyaluronic acid
HMGB1	High-mobility group protein box 1
HSC	Haematopoietic stem cells
ICAM-1	Intracellular adhesion molecule-1
ICE	IL-1β-converting enzyme
IFN-γ	Interferon-γ
IKKβ	3-Phosphoinositide-dependent protein kinase-1-mediated IκB kinase β
IL	Interleukin
IL-1Ra	Interleukin-1 receptor antagonist
iNOS	Inducible nitric oxide synthase
iPS	Induced pluripotent stem cells
IVD	Intervertebral disc
LBP	Low back pain
LFA	Lymphocyte function-associated antigen
LPS	Lipopolysaccharide
MAPK	Mitogen-activated protein kinases
MCP	Monocyte chemoattractant protein
MDC	Macrophage-derived chemokine
MIF	Macrophage migration inhibitory factor
MIP	Macrophage inflammatory protein
MMP	Metalloproteinase
mRNA	Messenger ribonucleic acid
MSC	Mesenchymal stromal cells
NALP3	NACHT, LRR and PYD domains-containing protein 3
NC	Notochordal cells
NF-κB	Nuclear factor kappa-light-chain-enhancer of activated B cells
NGF	Nerve growth factor
NLRP3	NOD-like receptor family, pyrin domain containing 3
NO	Nitric oxide
NP	Nucleus pulposus
PGE_2	Prostaglandin E2
PGF2α	Prostaglandin F2 alpha
PLA2	Calcium-dependent phospholipase A2
PLGA	Poly(lactic-co-glycolic acid)
PRP	Platelet-rich plasma
RANTES	Regulated on activation, normal T-cell expressed and secreted
Rhein	4,5-Dihydroxyanthraquinone-2-carboxylic acid
SC	Stem cells
Sox-9	Transcription factor Sox-9
TGF	Transforming growth factor
TGS-6	TNF-α stimulated gene/protein 6
TIMP	Tissue inhibitor of metalloproteinase
TLR	Toll-like receptor
TNF-α	Tumour necrosis factor alpha
TrkA	High affinity NGF receptor
tRAS	Tissue renin-angiotensin system

INTERFACE

rsif.royalsocietypublishing.org

Inflammation in intervertebral disc degeneration and regeneration

Mário Molinos, Catarina R. Almeida, Joana Caldeira, Carla Cunha, Raquel M. Gonçalves and Mário A. Barbosa

J. R. Soc. Interface **12**, 20141191 (2015; Published online 11 February) (doi:10.1098/rsif.2014.1191)

Funding. This work was financed by Portuguese funds through Fundação para a Ciência e a Tecnologia (FCT), in the framework of project UID/BIM/04293/2013. M.M., J.C. and C.C. are also recipients of grants from FCT (SFRH/BD/80577/2011, SFRH/BPD/78187/2011 and SFRH/BPD/87071/2012, respectively).

Addendum

Cite this article: Molinos M, Almeida CR, Caldeira J, Cunha C, Gonçalves RM, Barbosa MA. 2015 Inflammation in intervertebral disc degeneration and regeneration. *J. R. Soc. Interface* **12**: 20150429.
http://dx.doi.org/10.1098/rsif.2015.0429

Received: 13 May 2015
Accepted: 14 May 2015

Author for correspondence:
Mário A. Barbosa
e-mail: mbarbosa@ineb.up.pt

THE ROYAL SOCIETY PUBLISHING

Spine

SPINE Volume 42, Number 00, pp 000–000

BASIC SCIENCE

Age-Correlated Phenotypic Alterations in Cells Isolated from Human Degenerated Intervertebral Discs with Contained Hernias

Maria Molinos, MSc,[*,†,‡] Carla Cunha, PhD,[*,†] Catarina R. Almeida, PhD,[*,†,§] Raquel M. Gonçalves, PhD,[*,†] Paulo Pereira, MD, PhD,[¶,||] Pedro Santos Silva, MD,[¶] Rui Vaz, MD, PhD,[*,¶,||] and Mário A. Barbosa, PhD[*,†,‡]

Study Design. Human intervertebral disc (hIVD) cells were isolated from 41 surgically excised samples and assessed for their phenotypic alterations with age.

Objective. Toward the design of novel anti-aging strategies to overcome degenerative disc disease (DDD), we investigated age-correlated phenotypic alterations that occur on primary hIVD cells.

Summary of Background Data. Although regenerative medicine holds great hope, much is still to be unveiled on IVD cell biology and its intrinsic signaling pathways, which can lead the way to successful therapies for IDD. A greater focus on age-related phenotypic changes at the cell level would contribute to establish more effective anti-aging/degeneration targets.

Methods. The study was subdivided in four main steps: i) optimization of primary cells isolation technique; ii) high-throughput cell morphology analysis, by imaging flow cytometry (FC) and subsequent validation by histological analysis; iii) analysis of progenitor cell surface markers expression, by conventional FC; and iv) statistical analysis and correlation of cells morphology and phenotype with donor age.

Results. Three subsets of cells were identified on the basis of their diameter: small cell (SC), large cell (LC), and super LC (SLC). The frequency of SCs decreased nearly 50% with age, whereas that of LCs increased nearly 30%. Interestingly, the increased cells size was due to an enlargement of the pericellular matrix (PCM). Moreover, the expression pattern for CD90 and CD73 was a reflexion of age, where older individuals show reduced frequencies of positive cells for those markers. Nevertheless, the elevated percentages of primary positive cells for the mesenchymal stem cells (MSCs) marker CD146 found, even in some older donors, refreshed hope for the hypothetical activation of the self-renewal potential of the IVD.

Conclusion. These findings highlight the remarkable morphological alterations that occur on hIVD cells with aging and degeneration, while reinforcing previous reports on the gradual disappearance of an endogenous progenitor cell population.

Key words: aging and degeneration, CD146, chondrons, human IVD cells, pericellular matrix.

Level of Evidence: N/A

Spine 2017;42:xxx-xxx

Current treatments for degenerative disc disease (DDD) fail to address intervertebral disc's (IVD's) pathophysiology and to restore its function, and bioengineered sophisticated solutions are still in their infancy, with very few having reached Phase-I clinical trials.[1] In fact, much is still to be unveiled regarding the cell biology of the IVD and its intrinsic signaling pathways. Particularly, a greater knowledge about age-related cellular changes will contribute to establish more effective anti-aging/degeneration targets.

In the adult IVD, chondrocyte-like cells frequently assemble in a fibrous capsule, forming chondrons similar to those found in articular cartilage.[2] It has been suggested that these encircling layers result from accumulation of cellular products, as a consequence of aging[3,4] with histopathological analysis revealing evident remodeling of the pericelullar matrix (PCM) occurring with age and disease progression.[3,5,6] On the contrary, PCM plays an important role in governing the local mechanical environment of

From the *Institute for Research and Innovation in Health Sciences (i_3S), University of Porto, Porto, Portugal; †Institute for Biomedical Engineering (INEB), University of Porto, Porto, Portugal; ‡Abel Salazar Institute for Biomedical Sciences (ICBAS), University of Porto, Porto, Portugal; §Institute Institute for Biomedicine and Department of Medical Sciences (iBiMED), University of Aveiro, Aveiro, Portugal; ¶Department of Neurosurgery, Centro Hospitalar São João, Porto, Portugal | Department of Clinical Neurosciences and Mental Health, Faculty of Medicine, University of Porto, Porto, Portugal; and ||Neurosciences Center, CUF Porto Hospital, Porto, Portugal.

Acknowledgment date: February 22, 2017. First revision date: April 19, 2017. Acceptance date: June 2, 2017.

The manuscript submitted does not contain information about medical device(s)/drug(s).

This work had the financial support of FCT/MEC through National Funds and, when applicable, cofinanced by the FEDER *via* the PT2020 Partnership Agreement under the 4293 Unit I&D and through European Union funds—Projetos Estruturados de I&D&I - Norte-01-0145-FEDER-000012, Portugal.

Relevant financial activities outside the submitted work: grants.

Address correspondence and reprint requests to Maria Molinos, MSc, i3S, Rua Alfredo Allen, 208, Lab 105.S1, 4200-135 Porto, Portugal; E-mail: maria.molinos@ineb.up.pt

DOI: 10.1097/BRS.0000000000002311

chondrocytes and IVD cells,[7,8] as well as in maintaining their phenotype and viability.[9,10]

Despite findings indicating that degenerated human discs may have an endogenous regenerative capacity,[11–15] there might be an age-limit for the efficient activation of its cell progenitors.[16–18]

The aim of this work was to investigate age-related phenotypic alterations on primary human IVD cells from degenerated tissue. Taking advantage of a multiparameter image analysis tool, which guarantees robust quantitation of morphological features, we correlated IVD cells size, clusters prevalence and PCM area with age, while monitoring changes in expression of known stem cell related (CD90, CD73, CD105, CD146, CD34, Stro1) and NP-progenitor (GD2 and Tie2) markers.

MATERIALS AND METHODS

Surgical IVD Tissue Dissection and Cell Isolation

Degenerated human lumbar IVD fragments, with grade III-IV (Pfirrmann scale), were isolated from patients undergoing microdiscectomy, after informed consent and ethics committee approval. The surgeries were performed under general anesthesia in a sterile operating room and prophylactic antibiotic therapy with cefazolin 1 g IV was given. Patients were placed in a knee-chest position and a standard posterior approach to the appropriate interlaminar window was undertaken. After removal of the yellow ligament and medial retraction of the nerve root, the disc herniation was exposed. The posterior longitudinal ligament and the annulus fibrosus (AF) were incised and IVD fragments were excised, as deemed necessary by the surgeon. No more disc samples than those considered clinically appropriate were collected. In cases where the disc fragment was in contact with the epidural space or indistinguishable from the AF, the excised tissue was not included in this study. Thus, AF-contained IVD fragments were collected, and cells were isolated by enzymatic digestion, as previously described,[19] using one of three enzymatic formulations: collagenase-type-I (Coll-I), collagenase-type-II (Coll-II), or collagenase-type-XI (Coll-XI) (C0130, C6885, and C7657, respectively; Sigma-Aldrich, Sintra, Portugal), at 0.5 mg/ml (more detailed information in Supplemental Methods, http://links.lww.com/BRS/B288).

Assessment of Yield and Viability upon Isolation

Immediately upon digestion, cell yield was quantified by trypan blue exclusion and subsequently normalized against initial wet tissue weight. Cell viability was assessed by flow cytometry (FC) (FACS Calibur; BD Immunocytometry Systems, San Jose, CA) upon propidium iodide (PI) staining.

Characterization of Cell Morphology by Imaging Flow Cytometry (IFC)

Cells from nine different donors were fixed in 4% w/v paraformaldehyde (PFA) solution at room temperature for 15 minutes and washed with phosphate-buffered saline (PBS). Cells were labeled with DRAQ5 (1:1500 dil. per 2.0×10^5 cells, 65-0880; eBioscience), run on ImageStream (IS; Millipore, Billerica, Massachusetts, MA), and analyzed with IDEAS software for: cell diameter, frequency of small cell (SC), large cell (LC), and super large cell (SLC), frequency of single cells and multinucleated events (See Supplemental_Figure1A, B, and C: Cell Morphology Analysis Tutorial, http://links.lww.com/BRS/B289).

Cells were identified as SC, LC, and SLC based on their diameter: $10\,\mu m<SC<20\,\mu m$; $20\,\mu m<LC<30\,\mu m$; and $30\,\mu m<SLC<50\,\mu m$. To quantify the percentage of single and multinucleated events, as well as the number of single cells within LC and SLC populations, a specific mask and feature was created and applied to images of DRAQ5 stained nuclei (Supplemental_Figure1B, http://links.lww.com/BRS/B289).

To identify the presence of PCM, cells were permeabilized for 5 minutes with 0.2% Triton and incubated for 20 minutes at room temperature with Phalloidin-AlexaFluor488 (1:40 dilution per 2.0×10^5 cells, A12379; LifeTechnologies, Porto Salvo, Portugal), previously prepared in a PBS-1% w/v bovine serum albumin (BSA) solution, as described in.[19] This allowed the distinction of the cells actin cytoskeleton (cell per se) from the surrounding cell-attached matrix, when merging brightfield images and the fluorescence images of actin staining on IDEAS software. To further quantify the PCM area, a specific mask was designed (Supplemental_Figure1D, http://links.lww.com/BRS/B289).

Histological Analysis

Human IVD fragments were fixed in 10% neutral buffered formalin, processed for paraffin embedding and 5 μm sectioned in a microtome (Leica). Tissue sections throughout the IVD were stained for Alcian blue/Picrosirius red and analyzed by upright optical microscope (Olympus). For each section, delimitation of the area of the pericellular matrix (either proteoglycan- or collagen-rich) was determined for each cluster using ImageJ software. Around 15 sections were analyzed per donor and values were plotted as frequency distribution of the areas obtained in mm^2, using GraphPad Prism.

Analysis of Markers Expression by Flow Cytometry (FC)

Expression of surface markers (Table 1)[20] was analyzed by conventional FC, as described in Supplemental Methods, http://links.lww.com/BRS/B288.

Statistical Analysis

Statistical analysis was performed using GraphPad-Prism. All tests used are identified in the respective figure legend (additional details in Supplemental Methods, http://links.lww.com/BRS/B288).

RESULTS

Sample Characterization

To characterize the morphology and phenotype of primary hIVD cells from degenerated tissue, a total of 41 samples

TABLE 1. Antibodies used in flow cytometry analysis

	Function	Fluorochrome	μg/mL	Clone	Catalog No., Manufacturer
Primary antibodies					
IgG_1 MAH CD34	Marker for hematopoietic progenitors and vascular endothelial cells	FITC	2.5:50	581 (Class III)	CD34-581-01, Invitrogen
IgG_1 MAH CD45	Hematopoietic lineage-restricted surface marker	PE	3:50	MEM-28	21270454, ImmunoTools
IgG_1 MAH Tie2	NP progenitor cell markers[20]	PE	5:50	83715	FAB3131P, R&D Systems
IgG_{2a} MAH GD2		—	2:50	14.G2a	554272, BD Pharmigen
$IgG_{1,k}$ MAH CD90	Typical MSC markers	APC	5:50	eBio5E10	17-0909-41, eBioscience
IgG_{2a} MAH CD105		FITC	3:50	MEM-226	21271053, ImmunoTools
IgG_1 MAH CD73		PE	5:50	AD2	550257, BD Pharmigen
IgM MAH Stro1		—	10:50	STRO-1	MAB1038, R&D Systems
IgG_1 MAH CD146	Marker for vascular endothelial cells, smooth muscle cells, pericytes, and MSCs	AlexaFluor647	5:50	OJ79c	MCA2141A647T, Bio-Rad
Secondary antibodies					
IgM RAM		Biotinylated	1:50		E 0354, Dako
IgG RAM		AlexaFluor647	1:500		
Isotype controls					
Mouse IgG_1		FITC/R-PE	2.5:50		M1FP, Invitrogen
Mouse IgG_1		AlexaFluor647	5:50		MCA928A647, Bio-Rad
Mouse $IgG_{1,k}$		APC	5:50	P3.6.2.8.1	17-4714, eBioscience
Mouse IgG_{2a}		FITC	3:50		21275523, ImmunoTools
Mouse IgG_{2a}		—	2:50	G155–178	556651, BD Pharmigen^T

MAH indicates mouse anti-human; MSCs, mesenchymal stem cells; RAM, rabbit anti-mouse.

were collected from patients undergoing microdiscectomy—24 males and 17 females. All samples were collected from disc levels between L3 and S1. The donors age ranged from 18 to 66 years for males (average of 45 ± 11 years) and from 25 to 77 years for females (average of 48 ± 13 years) (Figure 1A), whereas donors' weight ranged from 69 to 110 kg for males (average of 86 ± 12 kg) and from 50 to 90 kg for females (average of 62 ± 10 Kg) (Figure 1B). The weight of collected tissue ranged from 0.2 to 5.2 g for males (average of 1.7 ± 1.2 g) and from 0.5 to 8.0 g for females (average 2.8 ± 2.2 g) (Figure 1C). No correlation was found between tissue weight and donors' age or weight (Figure $1C_1$ and C_2, respectively).

From the 41 human samples collected, 36 were digested to obtain the IVD cells to 1) optimize the protocol for primary cells isolation (n = 9), 2) analyze cells morphology (n = 9), and 3) study cells phenotype by FC (n = 18, of which two were discarded after cell isolation, due to insufficient number of cells to be acquired). The remaining five tissue samples were formalin fixed for histological validation of the cell morphology analysis performed by IFC.

Optimization of Cell Isolation

Because surgical tissue excised from human degenerated IVDs is normally scarce in cell content, it is important to guarantee that the cell isolation protocol will result in a high yield of viable cells. Three different enzymatic digestion protocols (with Coll-I, -II, or -XI, 0.5 mg/mL, overnight) were tested, similarly to what we did previously with bovine NP tissue.[19] Independently of the protocol used, cells viability was always above 90%, as determined by FC (PI-negative cells) (Figure 2A). In terms of cell yield, the protocol using Coll-I originated higher cell numbers [$(2.6 \pm 2.7) \times 10^5$ cells/g wet tissue], although no significant differences were detected when comparing to the other protocols used [Coll II: $(1.4 \pm 1.0) \times 10^5$ and Coll XI: $(1.4 \pm 0.7) \times 10^5$ cells/g wet tissue] (Figure 2B). Thus, subsequent cell isolation procedures were performed using Coll-I. Interestingly, although no correlation was found between the amount of IVD tissue collected from microsurgery and donor age, the cell content (yield) shows a negative correlation (Figure 2C; $^{**}P < 0.01$), suggesting that independently of the isolation method used, age is a heavy counterproductive factor for cell yield.

Characterization of Cellular Morphology

In order to characterize the morphology of human degenerated IVD cells, along with its age-related changes, freshly isolated cells were fixed and analyzed by IFC, using masks for bright-field images of cells and for fluorescence images of the cytoskeleton and nuclei (representative analysis tutorial is depicted in Supplemental_Figure 1, http://links.lww.com/BRS/B289).

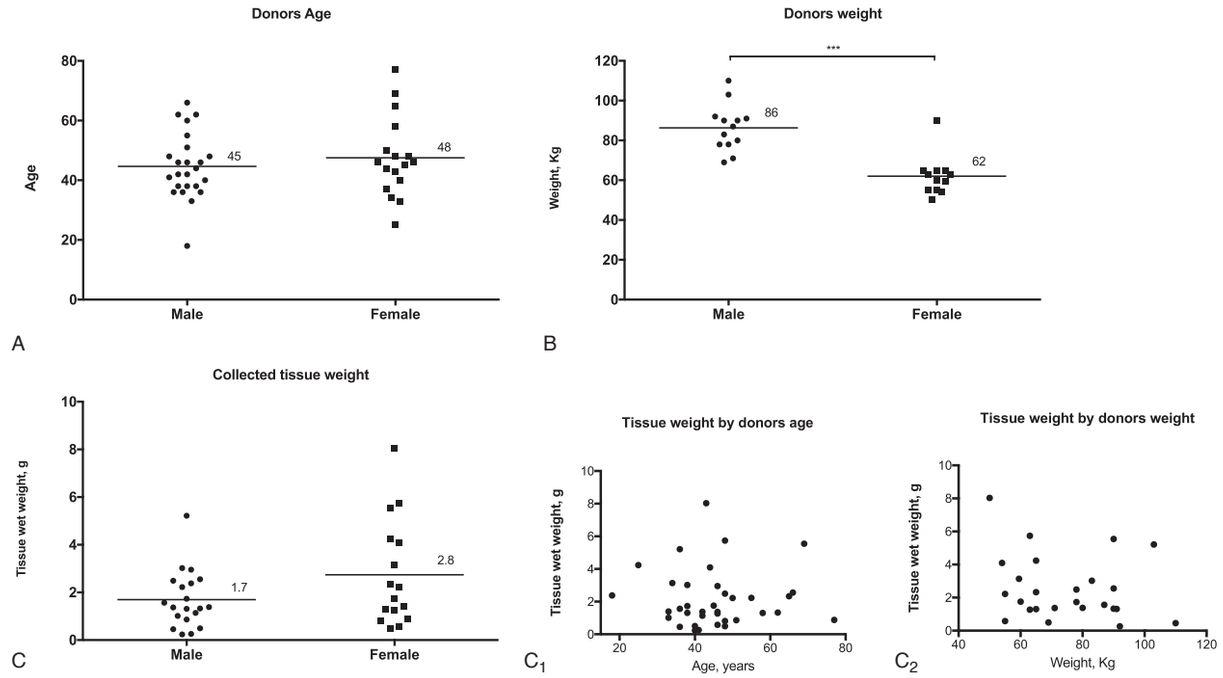

Figure 1. Sample characterization. (A) Donors age. A total of 36 samples were collected—20 from male donors and 16 from female donors. (B) Donors weight by gender. Male donors were heavier than female donors, $^{***}P < 0.001$ (nonparametric Mann-Whitney test). (C) Collected tissue weight. An average 1.7 and 2.8 g of tissue was excised from male and female donors, respectively. No correlation was found between collected tissue weight and age (C_1) or donors weight (C_2). Line on scattered dot plots presents mean values.

Analysis of the distribution of the cells diameter with age revealed the presence of small cell (SC), large cell (LC), and super large cell (SLC) (Figure 3A), with an average diameter of 16 ± 2, 25 ± 1, and 34 ± 1 μm, respectively (Figure 3B). Representative images of these cells are shown in Supplemental_Figure1C, http://links.lww.com/BRS/B289. Overall, the average frequency of SLC ($17 \pm 14\%$) was significantly lower ($^{*}P < 0.05$) than the average frequency of SC or LC ($39 \pm 29\%$ and $43 \pm 18\%$, respectively), although there was a high variability between donors with ages from 36 to 55 years. Interestingly, correlation analysis revealed a decrease in SC frequency with age ($^{**}P < 0.001$), while the frequency of LC and SLC increased ($^{**}P < 0.001$ and $^{*}P < 0.05$, respectively) (Figure 3C).

The percentage of single and multinucleated events was also quantified for each donor (Figure 4A–C and Supplemental_Figure1B, http://links.lww.com/BRS/B289). Interestingly, within the large and SLC populations, the majority of events were single cells: $87 \pm 9\%$ and $63 \pm 19\%$, respectively (Figure 4C), although cells had a diameter above 20 μm. Simultaneously, there was no correlation between the prevalence of multinucleated events and age (Figure 4B). Together, these results suggest that the increase on the frequency of LC with age is not due to cell fusion, but is most probably due to an increase of the PCM area surrounding the cells. And indeed, the PCM area of cells within single-SLC population was larger than within the SC ($^{*}P < 0.05$) and single-LC populations ($P = 0.5$) (Figure 5AB).

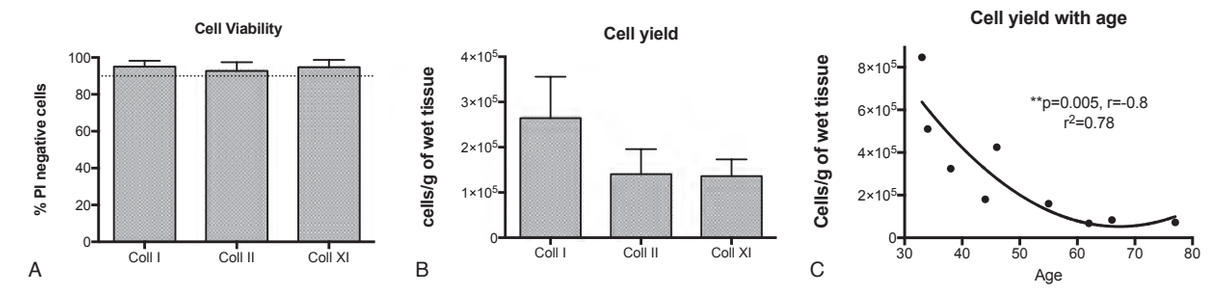

Figure 2. Optimization of cell isolation protocol. Three different methods to isolate human primary cells were evaluated, where cells were incubated overnight with collagenase-type I, -type II, or -type XI. (A) No differences were found in terms of cell viability, as quantified by flow cytometry upon PI staining. All protocols rendered high (>90%) cell viability. (Coll I: n = 9; Coll II: n = 3; Coll XI: n = 4). (B) Tissue overnight digestion with collagenase-type-I allowed the isolation of more cells per g of excised tissue, although this number decreased with donors' age (C) (n = 9, Pearson r = −0.8, $^{**}P < 0.01$; nonlinear regression $r^2 = 0.78$). Data on bars are presented as mean ± standard deviation.

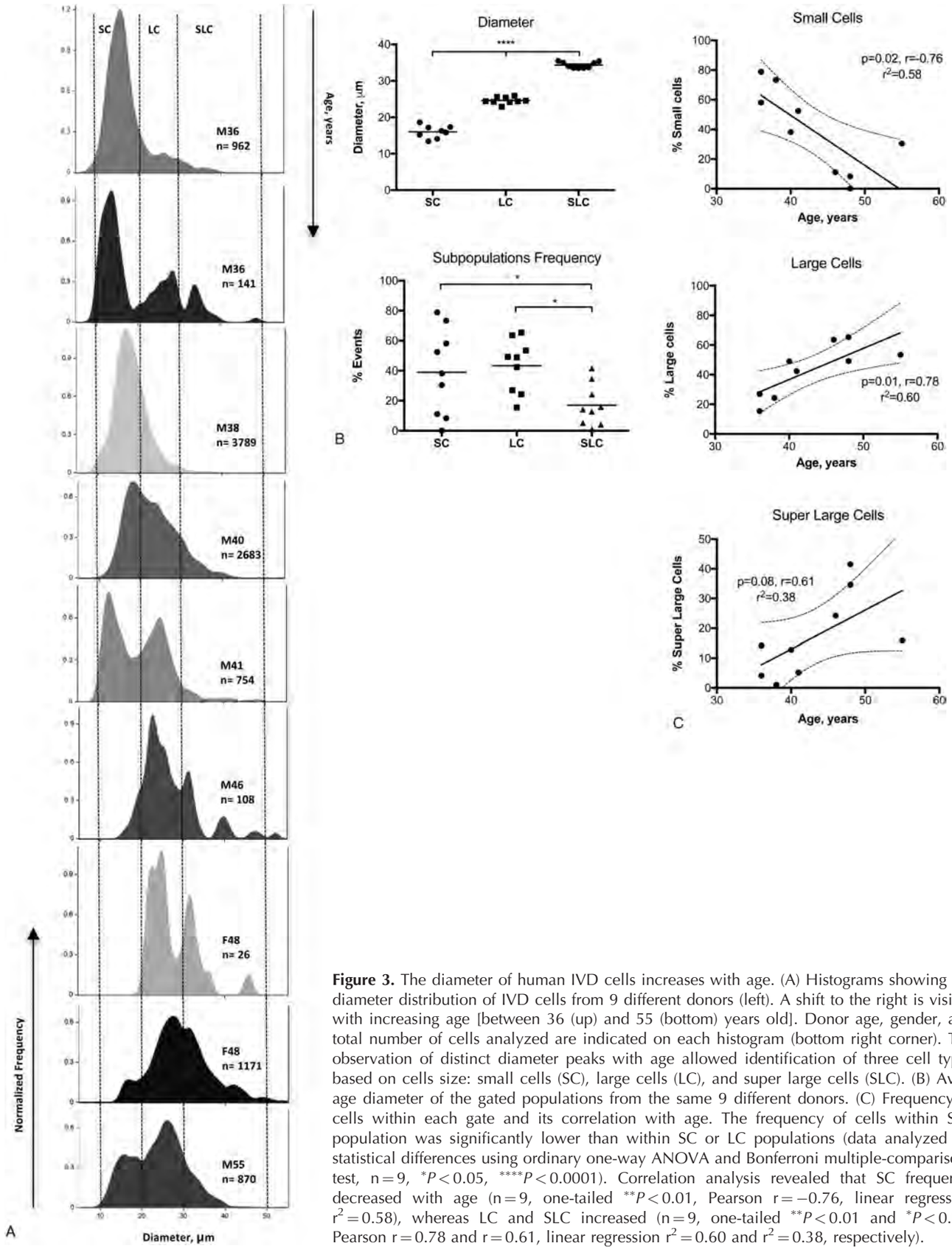

Figure 3. The diameter of human IVD cells increases with age. (A) Histograms showing the diameter distribution of IVD cells from 9 different donors (left). A shift to the right is visible with increasing age [between 36 (up) and 55 (bottom) years old]. Donor age, gender, and total number of cells analyzed are indicated on each histogram (bottom right corner). The observation of distinct diameter peaks with age allowed identification of three cell types based on cells size: small cells (SC), large cells (LC), and super large cells (SLC). (B) Average diameter of the gated populations from the same 9 different donors. (C) Frequency of cells within each gate and its correlation with age. The frequency of cells within SLC population was significantly lower than within SC or LC populations (data analyzed for statistical differences using ordinary one-way ANOVA and Bonferroni multiple-comparisons test, $n = 9$, $^{*}P < 0.05$, $^{****}P < 0.0001$). Correlation analysis revealed that SC frequency decreased with age ($n = 9$, one-tailed $^{**}P < 0.01$, Pearson $r = -0.76$, linear regression $r^2 = 0.58$), whereas LC and SLC increased ($n = 9$, one-tailed $^{**}P < 0.01$ and $^{*}P < 0.05$, Pearson $r = 0.78$ and $r = 0.61$, linear regression $r^2 = 0.60$ and $r^2 = 0.38$, respectively).

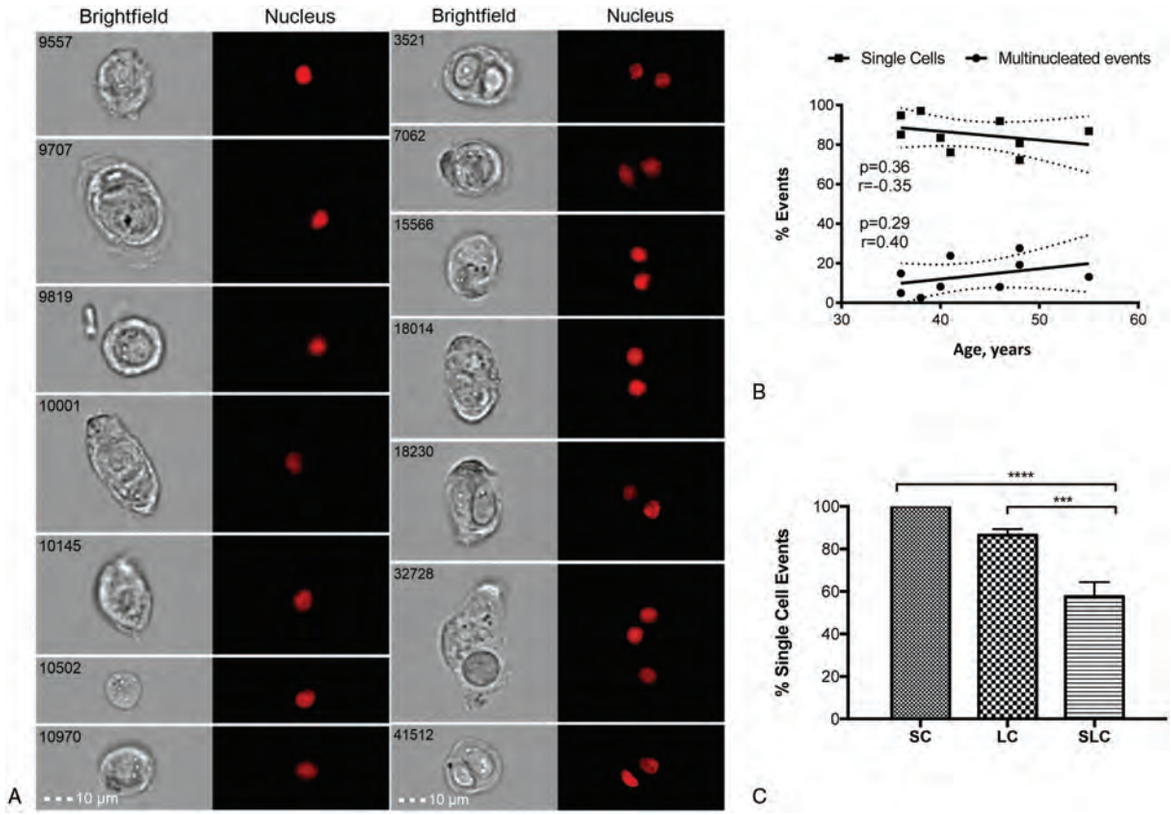

Figure 4. Characterization of large cells. (A) Examples of brightfield (left) and fluorescence (right) images of single and multinucleated event and its nuclei. (B) No correlation between the frequency of single or multinucleated events with age (n = 9, $P = 0.36$ and 0.29, respectively). C) Quantification of the percentage of single cell events within SC, LC, and SLC populations. Only SLC population revealed a significantly lower frequency of single cell events (ordinary one-way ANOVA, Bonferroni multiple-comparisons test, $^{***}P < 0.001$, n = 9). Hence, LC and SLC (~40%) greater diameter is not necessarily due to cell clustering.

Histological Analysis

The morphological analysis performed by IFC was further validated on histological sections of degenerated IVD tissue from five donors (ages between 37 and 62 years), using Alcian blue/Picrosirius red staining, which differentiates the main extracellular components within the tissue, staining collagen in red and proteoglycans in blue, readily allowing the identification of the PCM for each cell cluster. Figure 6A shows the PCM area distribution for the different donors, as quantified from the images represented in Figure 6B, C. This analysis indicates an increase in the prevalence of larger events (corresponding to LC and SLC identified by IFC) with age, especially evident in older donors (60 and 62 years old), accompanied by a decrease in the frequency of smaller events (SC identified by IFC), resulting in a shift to the right in 60 and 62 years old donor's histograms. This effect on clusters area can be observed in Figure 6B for a younger donor and in Figure 6C for an older donor.

Analysis of Surface Markers Expression

To assess the correlation between the presence of progenitor-like cells within freshly isolated human IVD cells and aging, expression of nine surface markers was evaluated (Table 1 and Supplemental Figure 2, http://links.lww.com/BRS/B290). No expression of Tie2, CD45, and CD34 was found, while CD146 expression ranged from 0% to 16%, Stro1 from 0% to 19%, CD90 from 0.3% to 64%, CD73 from 0% to 55%, CD105 from 0% to 17%, and GD2 from 2% to 5% (Figure 7A). A negative correlation was established between the frequency of $CD90^-$ and $CD73^+$ cells and age (Figure 7B, $^*P < 0.05$), but not for the other markers. These data suggest there is a decrease, but not elimination of progenitor cells with aging. Moreover, seeking to correlate cells size with these markers expression, it was verified that, within the positive events for each marker, there is a smear, containing small and large events, and no distinct subset was found to be more or less prevalent with age (Supplemental_Figure 3, http://links.lww.com/BRS/B291).

DISCUSSION

The aim of this study was to take advantage of available surgical material from microdiscectomy procedures, which in normal circumstances would be discarded as surgical waste, to characterize how IVD degenerated tissue changes with ageing. Hence, the material was not collected for research purposes, but as a necessary therapy for the donor. Moreover, in a typical microdiscectomy performed to treat a

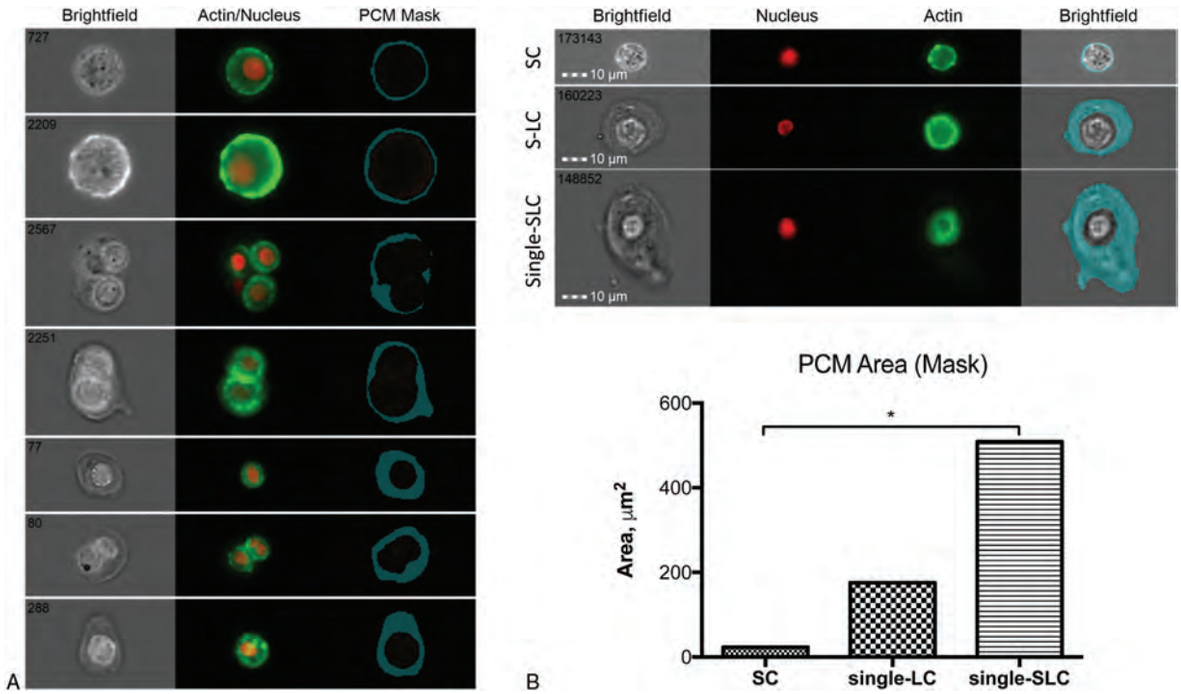

Figure 5. Pericellular matrix area quantification. (A) Examples of IFC images of IVD cells with various morphologies. The panel shows brightfield images of cells (right), alongside with composite fluorescence images of the respective DRAQ5-stained nuclei and the phalloidin-FITC stained actin (middle). The right column shows the masks (dark green) created to determine the PCM area. Both single- and multinucleated events are surrounded by a PCM. (B) PCM area was quantified within SC (all were single-cell events), single-LC, and single-SLC populations from 3 different donors, with 36, 38, and 41 years old ($n = 3$, Kruskal-Wallis and Dunn multiple-comparison tests, $^{*}P < 0.05$). LC and SLC cells show an increased diameter due to a greater PCM deposition.

disc herniation through a posterior approach, at best 30% of the entire disc can be obtained. Indeed, although in anterior and lateral approaches the quantity of material collected may be larger, these are not so common. Nevertheless, the tissue collected was quite homogeneous and representative of the whole degenerated IVD.

Cell isolation techniques should be standardized in order to avoid variability between different studies. Enzymatic digestion is a common procedure to isolate IVD cells, but cell yield is rarely reported, and cells are often expanded in culture before FC analysis of cells phenotype.[18,21,22] Moreover, pronase pre-treatment is many times applied, not preserving cells with its PCM attached.[23] Here, we apply an improved and inexpensive method to efficiently isolate primary hIVD cells, which could be further adopted by other researchers in this field. Of note, a clear negative correlation between cell yield and donor age is evident, supporting previous histological observations on IVD cell depopulation.[3]

Morphology of IVD cells was assessed using IFC, a technique that provides high-resolution images of thousands of cells in flow. A clear shift on the distribution of the cells diameter occurred with aging, with a decrease in the frequency of small cells and an increase with that of larger cells. The enlarged cell morphology was due to an increase in the PCM area (Figure 5). This effect was previously reported for chondrons in osteoarthritic cartilage[24,25] and proven to be a consequence of matrix synthesis and/or deposition rather than due to an increase in cell hydration.[26] Theoretically, this alteration may occur following an inflammatory stimulus [*e.g.*, Interleukine-1 (IL-1) exposure], which triggers metalloproteinases (MMPs) upregulation, initiating the destruction of fibrilar collagens around the chondrocyte (diminishing its tensile capacity), while the high intrinsic concentrations of pericellular aggrecan and hyaluronan ensures the hydrodynamic expansion of the chondron.[5] Of note, even though formation of cell clusters has been previously associated with age and degeneration, we did not find a significant correlation between the frequency of multinucleated events and donors age.[27–29] Histological data validated the results from IFC (Figure 6), although a discrepancy in cells size was detected. The maximum area value quantified for cells in flow (from brightfield images of cells with its attached PCM) was about 0.002 mm^2, whereas in the tissue some larger events had a PCM area (including attached collagens and aggrecan) as great as 0.024 mm^2. Nevertheless, this result is in accordance with previous studies using enzymatic digestion to isolate chondrocytes, where the PCM was shown to be substantially reduced in size, due to a loss of some enzyme-sensitive PCM components, such as aggrecan, type II collagen, fibronectin, and hyaluronic acid.[30–33] However, chondrocytes enhanced viability, and particularly that of chondrons, when compared with alternative isolation methods, makes enzymatic digestion a better choice.[34]

To better understand the consequences of ageing on IVD cells, expression of markers for progenitor and

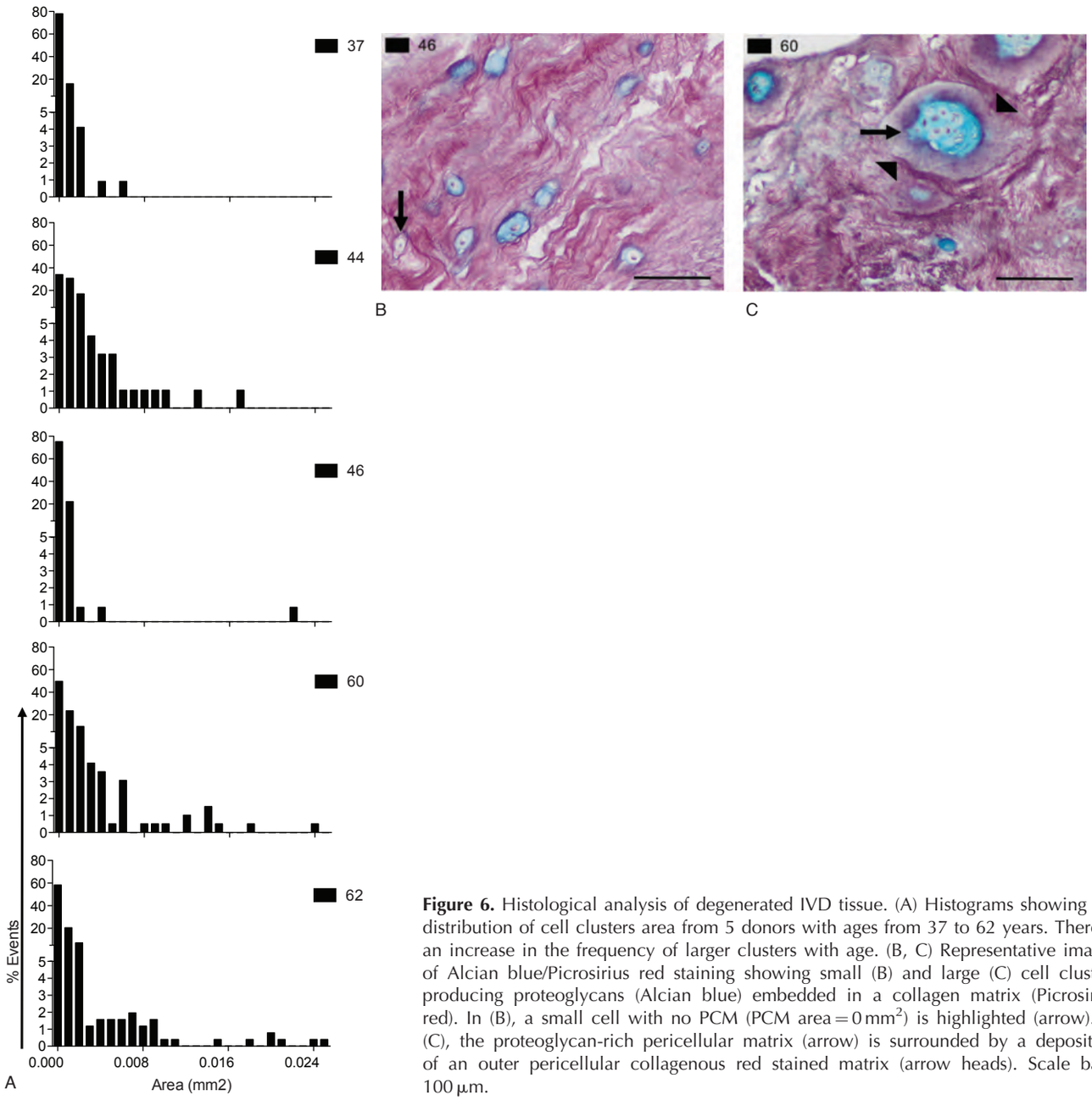

Figure 6. Histological analysis of degenerated IVD tissue. (A) Histograms showing the distribution of cell clusters area from 5 donors with ages from 37 to 62 years. There is an increase in the frequency of larger clusters with age. (B, C) Representative images of Alcian blue/Picrosirius red staining showing small (B) and large (C) cell clusters producing proteoglycans (Alcian blue) embedded in a collagen matrix (Picrosirius red). In (B), a small cell with no PCM (PCM area = 0 mm^2) is highlighted (arrow). In (C), the proteoglycan-rich pericellular matrix (arrow) is surrounded by a deposition of an outer pericellular collagenous red stained matrix (arrow heads). Scale bars: 100 μm.

inflammatory cells was assessed. Interestingly, the percentage of cells expressing CD73, CD90 was a reflection of age. These findings reinforce previous reports stating that, although mature IVDs may endogenously count on a progenitor cell population,[13,35] its gradual disappearance with aging and degeneration may dictate a limitation in time for its activation.[18,36] Overall, our results are in accordance to a previous report,[30] showing low expression (<1%) of CD105 on primary unexpanded cells from degenerated IVD tissue. As for Stro1, while a low expression profile (<5%) was expected, even in younger individuals,[13,35] here we found some young donors with high Stro1$^+$ numbers (~20%), and others with no expression at all. However, no correlation with age, gender, or weight could be determined, which could explain these results. In addition, CD90 and CD73 expression, which was always below 40% (with the exception of one 46 years old donor, also showing higher expression of CD105, CD146, and Stro1), is different from other studies, where MSC classical markers (including CD105) were expressed by nearly 90% of cells.[11,12,14,15] Nevertheless, in all those studies, cells were expanded before acquisition, which might have induced phenotypic alterations, as reported to occur with articular chondrocytes,[37,38] mouse bone marrow derived MSC precursors,[39] and rabbit AF and NP cells.[40] Moreover, Tie2 was not detected, even though others have found around 10% expression in three out of four donors (33–66 years old).[18] Again, cells were not expanded in this study and the isolation procedure was not

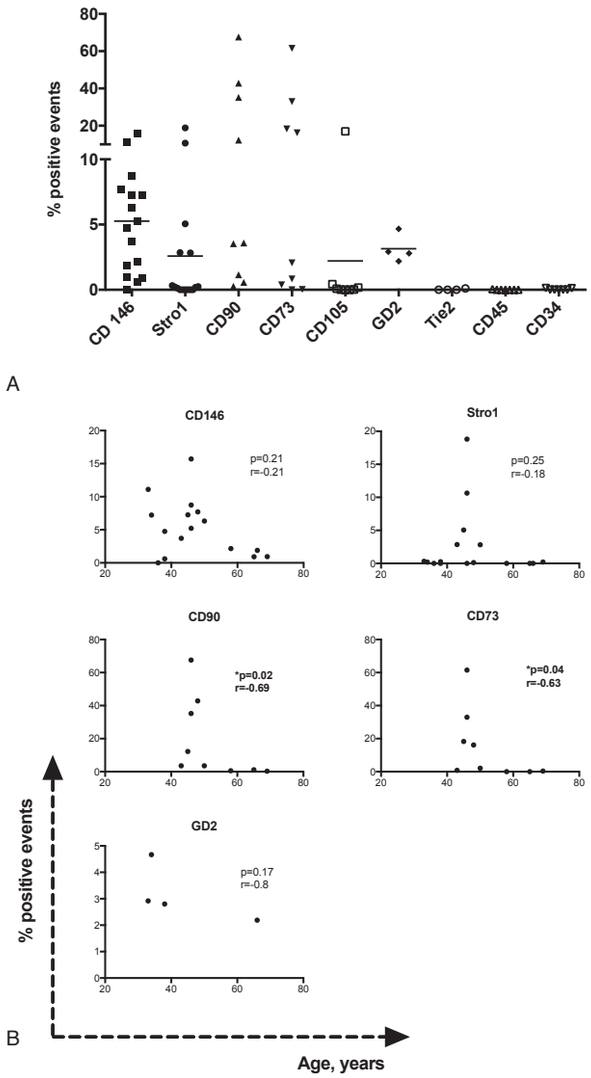

Figure 7. Primary human IVD cells phenotype. (A) Expression of 9 different cell surface markers. (B) Age-related changes on the frequency of CD146, Stro1, CD73, CD90, and GD2-positive events. Spearman correlation coefficient analysis revealed a significant decrease of CD90 and CD73 expression with age (n = 9, one-tailed $^{*}P < 0.05$, Spearman r = −0.69 and r = −0.63, respectively).

the same. In addition, for GD2 expression, an average 3% expression was detected (n = 4, 33–66 years old), whereas others reported only 1% expression in primary hNP cells.[18] We cannot guarantee that these GD2^{+} are exclusively located in the NP, explaining why we were able to detect higher percentages of these progenitor cell markers in IVD surgical samples (NP+AF tissue). CD146 was also detected in the great majority of samples analyzed. We have previously shown that two cell-subsets within the heterogeneous bovine NP cell population were enriched in CD146^{+}.[19] This protein has been suggested as a marker for endothelial cells, melanoma cells, and MSCs. Interestingly, sorted CD146^{+} cells isolated from late-stage osteoarthritic knee joints showed high potential of clonogenecity and multidifferentiation, while expressing high levels of MSC-specific surface antigens. Moreover, when compared with adipose-derived MSCs (ADMSCs) and unsorted chondrocytes, this subpopulation showed higher chondrogenesis capacity,[41] revealing a pool of chondroprogenitors within the diseased tissue. In contrast, recent work showed that CD146^{+} were not capable of multipotent differentiation, and were committed to express a contractile phenotype.[42] However, besides distinct species and cell isolation methods used, culture conditions were also different (1-week expansion in normoxia *vs.* 3-week expansion in hypoxia). Importantly, the frequency of CD146^{+} cells found herein (0–16%, n = 16, mean 6.5%) was much higher than that found in the OA knee (0.01–2.12%, n = 6).[41] We will address the functional characterization of hIVD CD146^{+} cells in the near future.

In summary, we were able to accurately distinguish three subsets of hIVD cells based on their different sizes, whose frequencies varied significantly with age. Younger individuals showed higher prevalence of small cells (diameter below 20 μm), whereas older donors had more large cells (diameter above 20 μm). Finally, the analysis of specific surface markers expression lead to identification of CD146^{+} cells within IVD degenerated samples, which supported even further the hypothesis that the aged/diseased IVD may still have an intrinsic self-repairing potential.

Key Points

- There is a shift in IVD cells size with age and degeneration.
- Younger individuals have higher frequencies of small cells, whereas older individuals have more large cells.
- The increase in cells size is due to an enlargement of its pericellular matrix (PCM).
- There is also an age-associated disappearance of progenitor cell markers within the IVD cell population.
- The expression of the mesenchymal stem cell (MSC) marker CD146 within IVD degenerated samples supports even further the hypothesis that the aged/diseased IVD may still have an intrinsic self-repairing potential.

Acknowledgments

The authors thank María Gómez Lázaro, Principal Technician from the Bioimaging Centre for Biomaterials and Regenerative Therapies (*b.IMAGE*) at i$_3$S, for the technical hints on Imaging Flow Cytometry data acquisition and analysis, and to Catarina Leitão, from the Translational Cytometry Unit at i$_3$S, for the continuous support on conventional flow cytometry procedures.

The authors would like to acknowledge FCT (Fundação para a Ciência e Tecnologia) for funding M.M. Ph.D. grant (SFRH/BD/80577/2011), C.C. Post-Doc grant (SFRH/BDP/87071/2012), and R.M.G. FCT Investigator Starting Grant (IF/00638/2014).

Supplemental digital content is available for this article. Direct URL citations appearing in the printed text are provided in the HTML and PDF version of this article on the journal's Web site (www.spinejournal.com).

References

1. Sakai D, Andersson GB. Stem cell therapy for intervertebral disc regeneration: obstacles and solutions. *Nat Rev Rheumatol* 2015; 11:243–56.
2. Roberts S, Ayad S, Menage PJ. Immunolocalisation of type VI collagen in the intervertebral disc. *Ann Rheum Dis* 1991;50:787–91.
3. Trout JJ, Buckwalter JA, Moore KC. Ultrastructure of the human intervertebral disc: II. Cells of the nucleus pulposus. *Anat Record* 1982;204:307–14.
4. Gruber HE, Hanley EN Jr. Ultrastructure of the human intervertebral disc during aging and degeneration: comparison of surgical and control specimens. *Spine (Phila Pa 1976)* 2002;27: 798–805.
5. Poole CA. Articular cartilage chondrons: form, function and failure. *J Anat* 1997;191:1–13.
6. Roberts S, Menage J, Duance V, et al. 1991 Volvo Award in basic sciences. Collagen types around the cells of the intervertebral disc and cartilage end plate: an immunolocalization study. *Spine (Phila Pa 1976)* 1991;16:1030–8.
7. Youn I, Choi JB, Cao L, et al. Zonal variations in the three-dimensional morphology of the chondron measured in situ using confocal microscopy. *Osteoarthritis Ccartilage* 2006;14:889–97.
8. Cao L, Guilak F, Setton LA. Three-dimensional morphology of the pericellular matrix of intervertebral disc cells in the rat. *J Anat* 2007;211:444–52.
9. Kvist AJ, Nystrom A, Hultenby K, et al. The major basement membrane components localize to the chondrocyte pericellular matrix: a cartilage basement membrane equivalent?. *Matrix Biol* 2008;27:22–33.
10. Vonk LA, Doulabi BZ, Huang C, et al. Preservation of the chondrocyte's pericellular matrix improves cell-induced cartilage formation. *J Cell Biochem* 2010;110:260–71.
11. Blanco JF, Graciani IF, Sanchez-Guijo FM, et al. Isolation and characterization of mesenchymal stromal cells from human degenerated nucleus pulposus: comparison with bone marrow mesenchymal stromal cells from the same subjects. *Spine (Phila Pa 1976)* 2010;35:2259–65.
12. Feng G, Yang X, Shang H, et al. Multipotential differentiation of human anulus fibrosus cells: an in vitro study. *J Bone Joint Surg Am* 2010;92:675–85.
13. Brisby H, Papadimitriou N, Brantsing C, et al. The presence of local mesenchymal progenitor cells in human degenerated intervertebral discs and possibilities to influence these in vitro: a descriptive study in humans. *Stem Cells Dev* 2013;22:804–14.
14. Huang B, Liu LT, Li CQ, et al. Study to determine the presence of progenitor cells in the degenerated human cartilage endplates. *Eur Spine J* 2012;21:613–22.
15. Risbud MV, Guttapalli A, Tsai TT, et al. Evidence for skeletal progenitor cells in the degenerate human intervertebral disc. *Spine* 2007;32:2537–44.
16. Vo NV, Hartman RA, Patil PR, et al. Molecular mechanisms of biological aging in intervertebral discs. *J Orthop Res* 2016;34: 1289–306.
17. Power KA, Grad S, Rutges JP, et al. Identification of cell surface-specific markers to target human nucleus pulposus cells: expression of carbonic anhydrase XII varies with age and degeneration. *Arthritis Rheum* 2011;63:3876–86.
18. Sakai D, Nakamura Y, Nakai T, et al. Exhaustion of nucleus pulposus progenitor cells with ageing and degeneration of the intervertebral disc. *Nat Commun* 2012;3:1264.
19. Molinos M, Almeida CR, Goncalves RM, et al. Improvement of bovine nucleus pulposus cells isolation leads to identification of three phenotypically distinct cell subpopulations. *Tissue Eng Part A* 2015;21:2216–27.
20. Risbud MV, Schoepflin ZR, Mwale F, et al. Defining the phenotype of young healthy nucleus pulposus cells: recommendations of the Spine Research Interest Group at the 2014 annual ORS meeting. *J Orthop Res* 2015;33:283–93.
21. Tang X, Jing L, Richardson WJ, et al. Identifying molecular phenotype of nucleus pulposus cells in human intervertebral disc with aging and degeneration. *J Orthop Res* 2016;34:1316–26.
22. Turner S, Balain B, Caterson B, et al. Viability, growth kinetics and stem cell markers of single and clustered cells in human intervertebral discs: implications for regenerative therapies. *Eur Spine J* 2014;23:2462–72.
23. Kuettner KE, Memoli VA, Pauli BU, et al. Synthesis of cartilage matrix by mammalian chondrocytes in vitro. II. Maintenance of collagen and proteoglycan phenotype. *J Cell Biol* 1982;93: 751–7.
24. Poole CA, Matsuoka A, Schofield JR. Chondrons from articular cartilage. III. Morphologic changes in the cellular microenvironment of chondrons isolated from osteoarthritic cartilage. *Arthritis Rheum* 1991;34:22–35.
25. Lee GM, Paul TA, Slabaugh M, et al. The incidence of enlarged chondrons in normal and osteoarthritic human cartilage and their relative matrix density. *Osteoarthritis Cartilage* 2000;8:44–52.
26. Lee GM, Loeser RF. Interactions of the chondrocyte with its pericellular matrix. *Cells Mater* 1998;8:135–49.
27. Ciapetti G, Granchi D, Devescovi V, et al. Ex vivo observation of human intervertebral disc tissue and cells isolated from degenerated intervertebral discs. *Eur Spine J* 2012;21(Suppl 1):S10–9.
28. Sharp CA, Roberts S, Evans H, et al. Disc cell clusters in pathological human intervertebral discs are associated with increased stress protein immunostaining. *Eur Spine J* 2009;18:1587–94.
29. Melrose J. A global pictorial assessment of the intervertebral disc cell in several species reveals a remarkable biodiversity in this cell type which should be taken into account in experimental studies on intervertebral disc repair. *Spine Res* 2016;2:1–14.
30. Lee GM, Poole CA, Kelley SS, et al. Isolated chondrons: a viable alternative for studies of chondrocyte metabolism in vitro. *Osteoarthritis Cartilage* 1997;5:261–74.
31. Knight MM, Ross JM, Sherwin AF, et al. Chondrocyte deformation within mechanically and enzymatically extracted chondrons compressed in agarose. *Biochim Biophys Acta* 2001;1526:141–6.
32. Hing WA, Sherwin AF, Poole CA. The influence of the pericellular microenvironment on the chondrocyte response to osmotic challenge. *Osteoarthritis Cartilage* 2002;10:297–307.
33. Wang QG, El Haj AJ, Kuiper NJ. Glycosaminoglycans in the pericellular matrix of chondrons and chondrocytes. *J Anat* 2008;213:266–73.
34. Ross JM, Sherwin AF, Poole CA. In vitro culture of enzymatically isolated chondrons: a possible model for the initiation of osteoarthritis. *J Anat* 2006;209:793–806.
35. Henriksson H, Thornemo M, Karlsson C, et al. Identification of cell proliferation zones, progenitor cells and a potential stem cell niche in the intervertebral disc region: a study in four species. *Spine* 2009;34:2278–87.
36. Yasen M, Fei Q, Hutton WC, et al. Changes of number of cells expressing proliferation and progenitor cell markers with age in rabbit intervertebral discs. *Acta Biochim Biophys Sin (Shanghai)* 2013;45:368–76.
37. Stewart MC, Saunders KM, Burton-Wurster N, et al. Phenotypic stability of articular chondrocytes in vitro: the effects of culture models, bone morphogenetic protein 2, and serum supplementation. *J Bone Miner Res* 2000;15:166–74.
38. Bonaventure J, Kadhom N, Cohen-Solal L, et al. Reexpression of cartilage-specific genes by dedifferentiated human articular chondrocytes cultured in alginate beads. *Exp Cell Res* 1994; 212:97–104.
39. Baustian C, Hanley S. Ceredig R: isolation, selection and culture methods to enhance clonogenicity of mouse bone marrow derived

mesenchymal stromal cell precursors. *Stem Cell Res Ther* 2015; 6:151.
40. Sang C, Cao X, Chen F, et al. Differential characterization of two kinds of stem cells isolated from rabbit nucleus pulposus and annulus fibrosus. *Stem Cells Int* 2016;2016: 8283257.
41. Su X, Zuo W, Wu Z, et al. CD146 as a new marker for an increased chondroprogenitor cell sub-population in the later stages of osteoarthritis. *J Orthop Res* 2015;33:84–91.
42. Nakai T, Sakai D, Nakamura Y, et al. CD146 defines commitment of cultured annulus fibrosus cells to express a contractile phenotype. *J Orthop Res* 2016;34:1361–72.

Supplementary Methods

Human IVD cell isolation: Briefly, tissue was collected in Dulbecco's modified Eagle's medium (DMEM; 21885 Gibco), supplemented with 10% v/v penicillin–streptomycin (P/S, PAA Laboratories GmbH) and 20% v/v amphotericin B (Amph-B, PAA). Within 3h upon collection, tissue was digested in DMEM supplemented with 5% P/S, 10% Amph-B, 2.5% (v/v) HEPES buffer 1mM (Lonza), 1.5% (v/v) NaCl 5 M and KCl 0.4 M solution (to adjust osmolarity to 400 mOsm), 1.3 U/mL DNAse, and one of three different enzymatic formulations: collagenase-type-I (Coll I), collagenase-type-II (Coll II), or collagenase-type-XI (Coll XI) (C0130, C6885, and C7657, respectively, Sigma Aldrich), at 0.5 mg/mL. All enzymatic preparations contain a mixture of the type I and II forms of the purified collagenase enzyme, differing in their affinity for different substrates as assessed by the manufacturer (www.sigmaaldrich.com/life-science/metabolomics/enzyme-explorer/learning-center/collagenase-guide.html). Tissue/medium ratio was set at 10% w/v to prevent the pH dropping below 6.8 during incubation. Tissue was digested overnight, in a humidified atmosphere at 37°C/5% CO_2, and under gentle stirring. ECM contaminants were filtered with a 70 µm cell strainer.

Analysis of surface markers expression by flow cytometry: Cells were first left to recover from digestion for 30 min in a humidified atmosphere at 37°C/5% CO_2, and then washed with PBS-2% fetal bovine serum (FBS), prior to incubation with primary antibodies (Table 1), in the same solution, for 1h at 4°C. In the case of non-conjugated anti-Stro1 antibody, cells were, in addition, incubated with a secondary rabbit anti-mouse-Biotinylated antibody, for 30 min at RT, washed again with PBS-2%FBS and additionally incubated with Streptavidin-APC (BD Pharmigen, #554067; dilution 1:1000) for 10 min at RT. After labeling, cells were washed with 2 mL PBS-2% FBS, fixed in 1% w/v paraformaldehyde (PFA) solution and run in a FACSCanto II within 24h. Results were analyzed with FlowJo software, Version 8.7. Supplementary Figure 2 shows representative dot plots from flow cytometry analysis of surface markers expression.

Statistical Analysis: D'Agostino and Pearson omnibus normality test was used to assess Gaussian distribution of data. Results that did not follow a normal distribution were analyzed for statistical differences using non-parametric Mann-Whitney test (donors age and weight by gender) or Kruskal–Wallis and Dunn's multiple-comparison test (cell viability and yield, surface markers expression and PCM Area). When results followed a Gaussian distribution (collected tissue weight by gender and frequency of single events within LC and SLC gates) an unpaired t test was applied. Finally, cells diameter and SC, LC, SLC populations frequency followed a Gaussian distribution, for which groups were compared using ordinary one-way ANOVA (Bonferroni's multiple-comparisons test). In all cases, a confidence level of at least 95% ($*p < 0.05$) was considered. Correlations with age were analyzed using the Spearman correlation coefficient for non-parametric data (surface markers expression), and the Pearson correlation coefficient for parametric data (cell yield, frequency of SC, LC, SLC, and single and multinucleated events). Data is plotted as linear correlation (straight line) ± 5% confidence intervals (dashed curves), also presenting the assigned correlation coefficient "r" and p value.

Supplemental Figure 1: Imaging flow cytometry morphological analysis flow chart. A) Live cells gating procedure. B) Gating of single and multinucleated events, by creating mask for cells nuclei and a feature to calculate the number of nuclei within each live cell. C) Diameter histogram analysis, smoothing, and subpopulations fractioning by cell size in Small Cells (SC), Larger Cells (LC) and Super Large Cells (SLC). D) Pericellular Matrix morphology analysis by creating specific mask based on the subtraction of nuclei and actin fluorescent images from brightfield images of whole cells, and a feature to calculate PCM area.

1) Gate DRAQ5 positive events

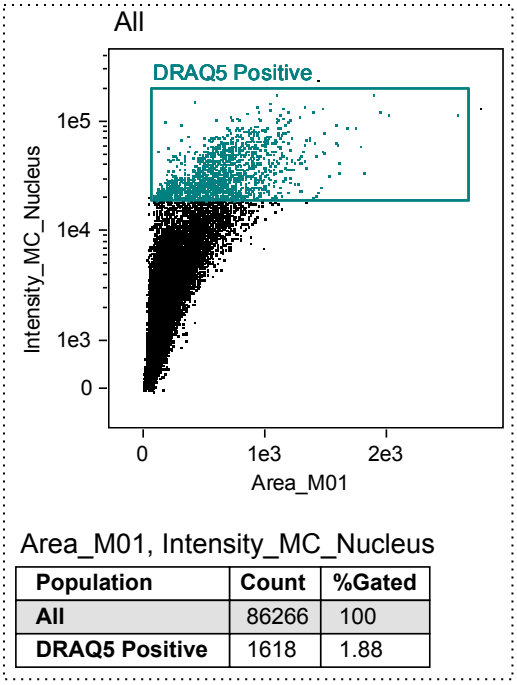

Area_M01, Intensity_MC_Nucleus

Population	Count	%Gated
All	86266	100
DRAQ5 Positive	1618	1.88

2) Gate Focused events

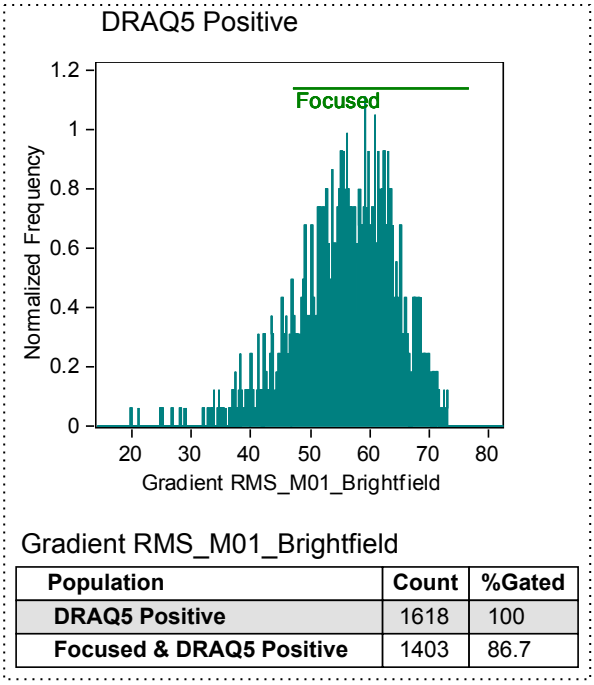

Gradient RMS_M01_Brightfield

Population	Count	%Gated
DRAQ5 Positive	1618	100
Focused & DRAQ5 Positive	1403	86.7

3) Gate focused-nuclei events

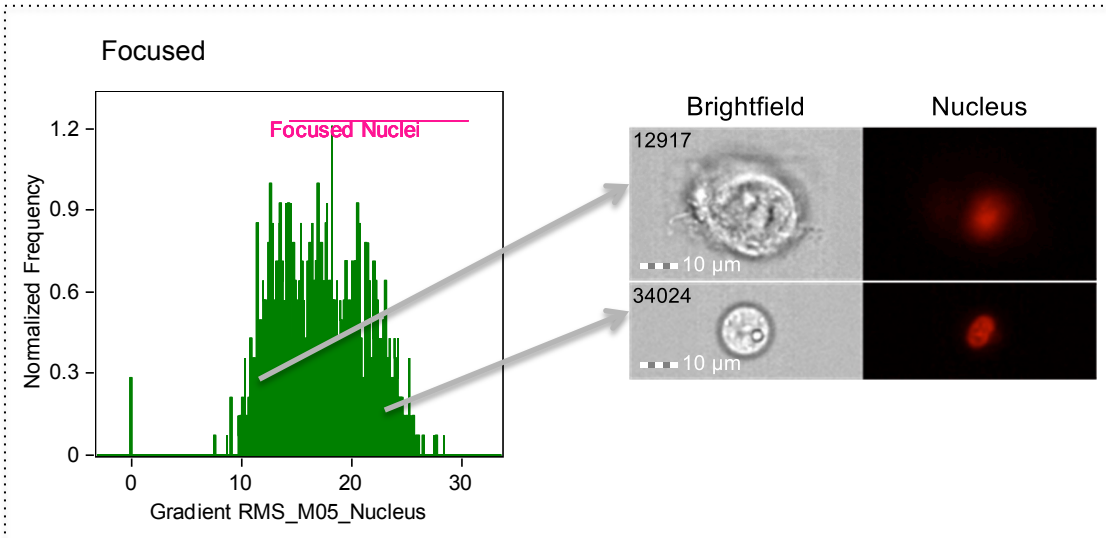

Gradient RMS_M05_Nucleus

Population	Count	%Gated
Focused & DRAQ5 Positive	1403	100
Focused Nuclei & Focused &...	977	69.6

B – Single and multinucleated events gating

1) Nuclei mask and "Nuclei Number" feature

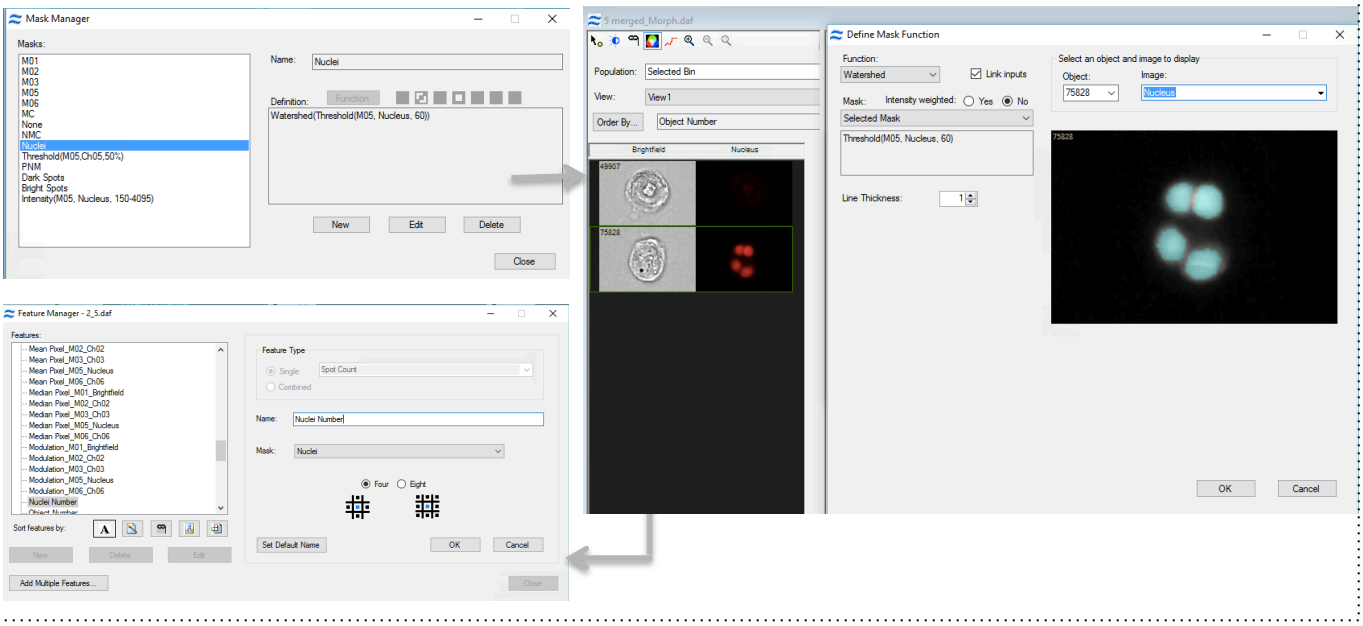

2) Single and Multinucleated events

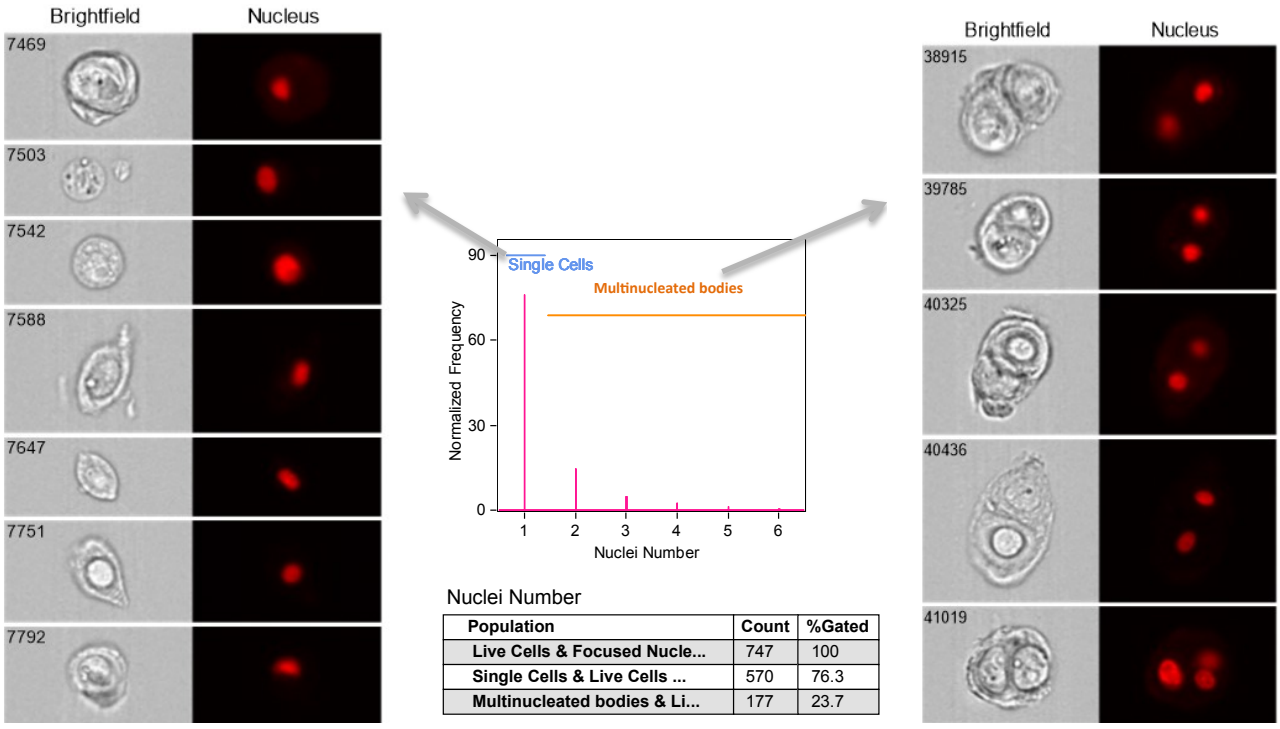

Nuclei Number

Population	Count	%Gated
Live Cells & Focused Nucle...	747	100
Single Cells & Live Cells ...	570	76.3
Multinucleated bodies & Li...	177	23.7

C – Diameter gating

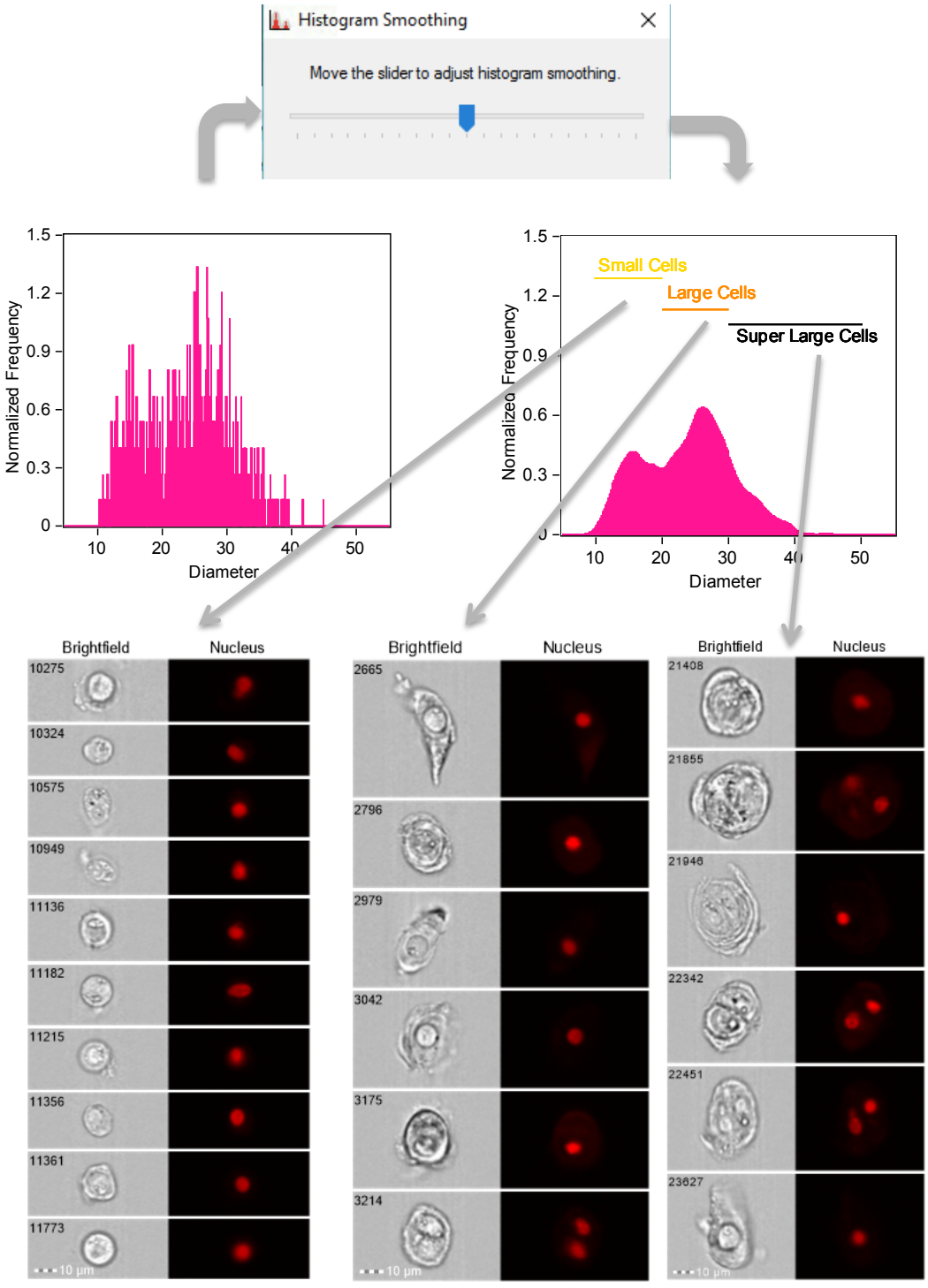

Population	Count	%Gated	Mean	Std. Dev.
Live Cells & Focused Nucle...	747	100	23.78	6.661
Small Cells & Live Cells &...	234	31.3	15.82	2.392
Large Cells & Live Cells &...	388	51.9	25.42	2.659
Super Large Cells & Live C...	123	16.5	33.69	2.855

PCM mask and "PCM Area" feature

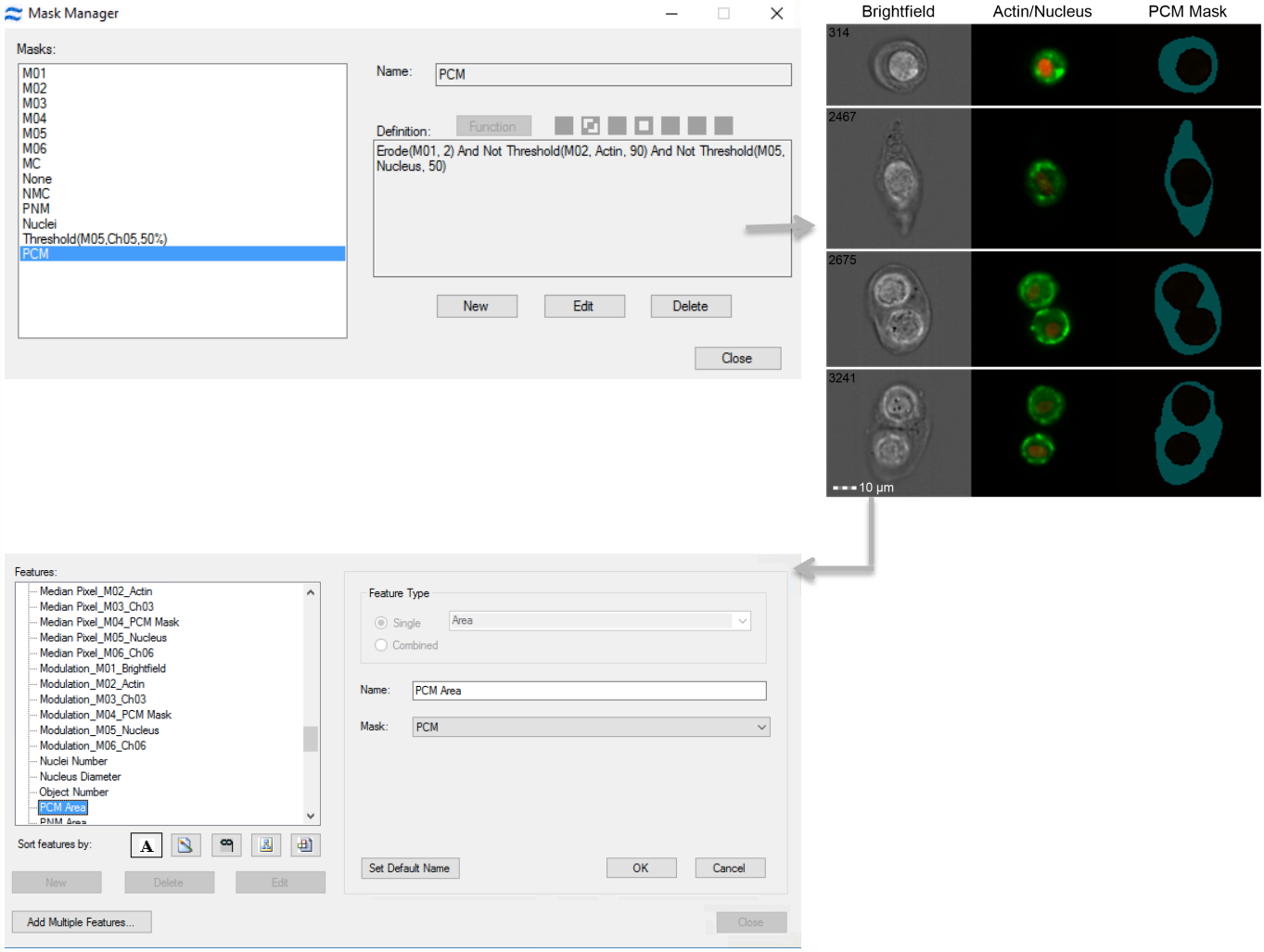

Supplemental Figure 2: Representative dot plots from conventional flow cytometry analysis of Stro1, CD146, CD90, CD73 and GD2 surface markers expression.

Representative dot plots from flow cytometry analysis

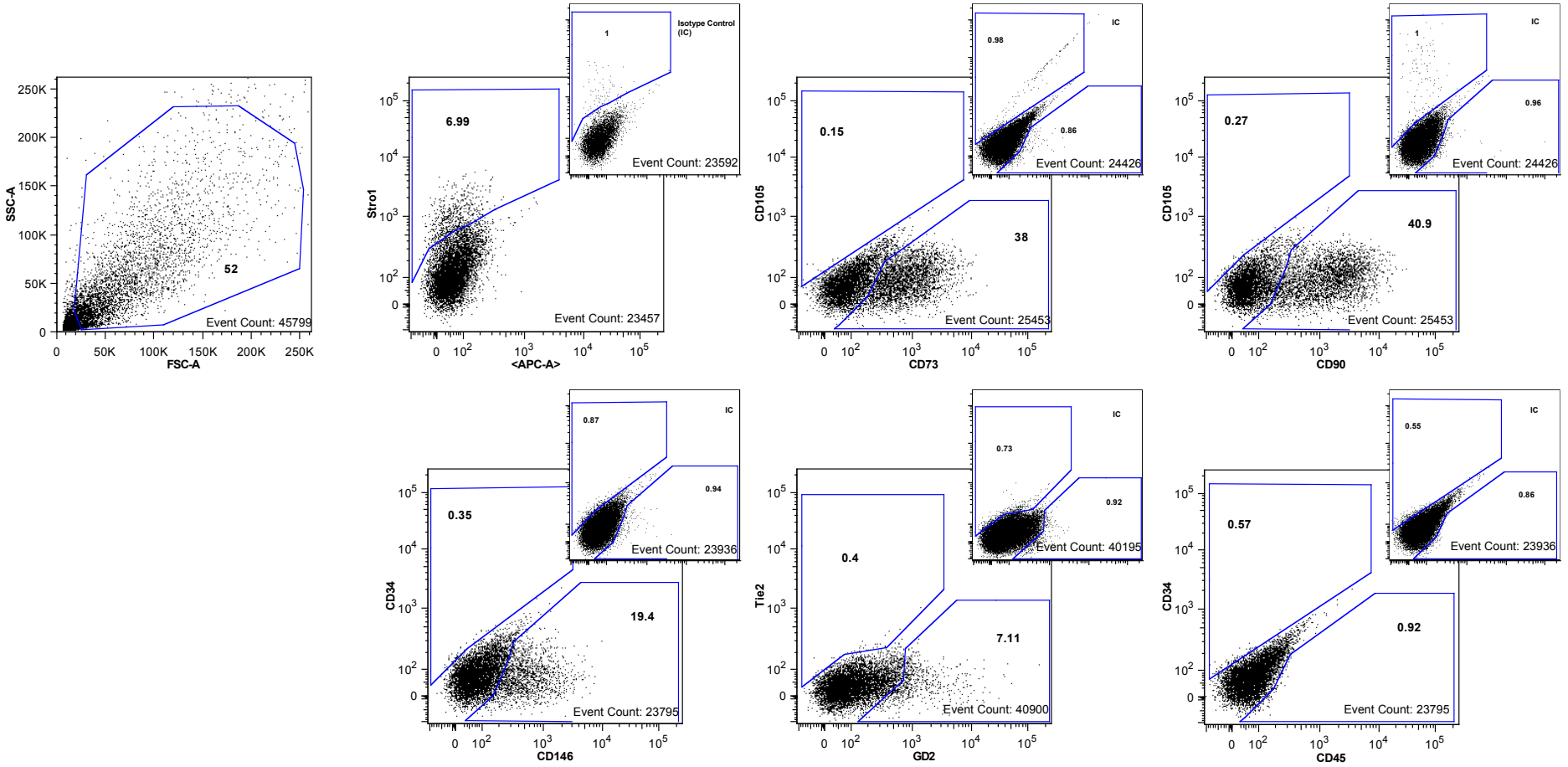

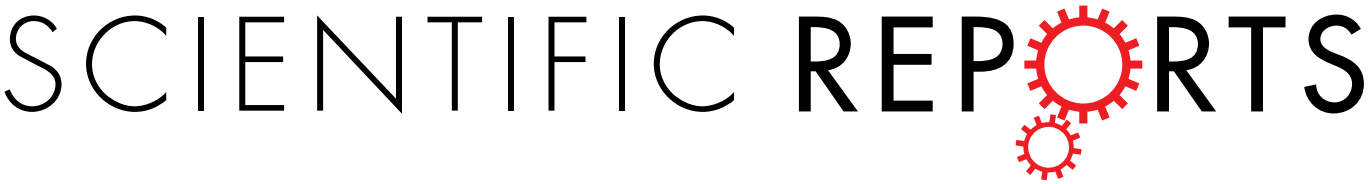

OPEN

Matrisome Profiling During Intervertebral Disc Development And Ageing

Received: 13 January 2017
Accepted: 1 September 2017
Published online: 14 September 2017

Joana Caldeira[1,2,3], Cátia Santa[4,5], Hugo Osório[1,3,6], Maria Molinos[1,2,7], Bruno Manadas[5], Raquel Gonçalves[1,2] & Mário Barbosa[1,2,7]

Intervertebral disc (IVD) degeneration is often the cause of low back pain. Degeneration occurs with age and is accompanied by extracellular matrix (ECM) depletion, culminating in nucleus pulpous (NP) extrusion and IVD destruction. The changes that occur in the disc with age have been under investigation. However, a thorough study of ECM profiling is needed, to better understand IVD development and age-associated degeneration. As so, iTRAQ LC-MS/MS analysis of foetus, young and old bovine NPs, was performed to define the NP matrisome. The enrichment of Collagen XII and XIV in foetus, Fibronectin and Prolargin in elder NPs and Collagen XI in young ones was independently validated. This study provides the first matrisome database of healthy discs during development and ageing, which is key to determine the pathways and processes that maintain disc homeostasis. The factors identified may help to explain age-associated IVD degeneration or constitute putative effectors for disc regeneration.

The intervertebral disc (IVD) is a complex structure capable of resisting spinal compression while allowing motion of intervertebral segments[1,2]. Besides water, it is mainly composed by extracellular matrix (ECM) molecules. These include collagens, proteoglycans (PGs) and other matrix proteins that contribute to the structural and mechanical function of the disc[3,4]. Matrix degrading enzymes are also present to regulate matrix breakdown, maintaining disc homeostasis[5].

A young healthy disc consists of a highly plastic and hydrated region – the nucleus pulposus (NP) – and a network of collagen fibres oriented in sheets around the nucleus – the annulus fibrosus (AF), which provides tensile strength and confines the NP, limiting bulging[6].

During disc degeneration and ageing, significant changes are observed in the IVD at both cell and tissue level. From birth, notochordal cells gradually disappear from the NP[7]. Loss of cell density is accompanied by a shift towards a chondrocyte-like cell population[3], less effective in NP-specific matrix synthesis[8]. Ultimately this results in NP fibrous transformation, from a translucent gel to a more solid and cartilaginous tissue[1] making it difficult to distinguish between NP and AF[6]. Alterations in the composition and mechanical properties of the surrounding environment will in turn influence NP cell function and behaviour, in terms of differentiation, metabolism, proliferation and survival[8].

Along with cellular changes, NP matrix remodeling is also an early step in the ageing process. Apart from overall matrix breakdown caused by MMPs (matrix metalloproteinases) and ADAMTS (a desintegrin and metalloprotease with thrombospondin motifs) overexpression[7], PG and collagen synthesis patterns[9,10], as well as fibre crosslinking[1] are also altered. This inhibits matrix turnover and, together with the already limited repair response, leads to dehydration and progressive ECM disorganization. Furthermore, it promotes mechanical failure, annular tears and many of the characteristic features of disc degeneration[6]. Over time, type II collagen is replaced by

[1]i3S - Instituto de Investigação e Inovação em Saúde, Universidade do Porto, Porto, Portugal. [2]INEB - Instituto de Engenharia Biomédica, Universidade do Porto, Rua Alfredo Allen, 208, 4200-180, Porto, Portugal. [3]IPATIMUP - Institute of Molecular Pathology and Immunology, University of Porto, Rua Júlio Amaral de Carvalho, 45, 4200-135, Porto, Portugal. [4]III – Institute for Interdisciplinary Research, University of Coimbra, Casa Costa Alemão – Pólo II, Rua Dom Francisco de Lemos, 3030-789, Coimbra, Portugal. [5]CNC – Center for Neuroscience and Cell Biology, University of Coimbra, 3004-504, Coimbra, Portugal. [6]Department of Pathology and Oncology, Faculty of Medicine, University of Porto, 4200-319, Porto, Portugal. [7]ICBAS - Instituto de Ciências Biomédicas de Abel Salazar, Universidade do Porto, Rua de Jorge Viterbo Ferreira n. 228, 4050-313, Porto, Portugal. Correspondence and requests for materials should be addressed to J.C. (email: joana.caldeira@ineb.up.pt)

type I collagen in the NP[7] and aggrecan content decreases[3]. Along with structural changes, soluble factors, and cytokines may also be released[11], further affecting cell activity and tissue homoeostasis[7]. The availability of oxygen, nutrients and growth factors[12], and the acidity of the environment, as well as the removal of metabolites, are also influenced by ECM calcification and impermeabilization[7]. With increasing age, this imbalance of the normal homeostatic mechanism impairs normal disc function, particularly in the NP[13], ultimately resulting in reduced disc height, hernia formation and spinal pain, as nerve roots become compressed[2].

Low back pain (LBP) causes disability and life quality deterioration, constituting a tremendous social and economic burden[14]. In more than 40% of the cases, it is triggered by IVD degeneration, which mimics disc ageing but occurs at an accelerated rate[1,7]. Conventional therapies for LBP predominantly involve treatments based on pain modulators and invasive surgeries, like spine fusion or arthroplasty. However, spine surgeries have a high risk of complications associated[15,16], and recurrent interventions are many times needed (15–30% of cases)[17], increasing the personal and financial costs even further[18]. Of note, the underlying pathophysiology is not being addressed, nor is the restoration of IVD's function or the slowing down of disease progression. To date, promising strategies for disc regeneration, based on the maintenance and/or increase of matrix synthesis, are being explored *in vivo*: protein injection[19,20], gene transfer[21,22] and cell implantation[23,24]. Although rapid advances are being made in understanding and regulating the degenerative process, many challenges remain[2].

Understanding IVD pathophysiology (particularly in terms of IVD matrix constituents and their alterations in development and disease) is key to unveil molecular cues that might be used to slow, halt or reverse the age-associated degenerative cascade[2,4].

In this report, we have investigated matrisome changes observed with development and ageing in healthy bovine NPs, with the purpose of validating candidate molecules that might constitute novel therapeutic alternatives to treat IVD degeneration.

Methods

Sample preparation and iTRAQ analysis. Bovine caudal IVDs from foetus (around 7 months of gestation), young (12 months) and old animals (16 to 18 years old) were obtained from the local abattoir and dissected within 3–4 hours after slaughter. The NPs from 7–8 discs from Cd1 to Cd7 or Cd8 were collected as described by Molinos *et al.*[25] and stored at −80 °C in a batch of 500 to 800 mg. For protein extraction, 1100 µL of guanidine extraction buffer were used. Further details on the iTRAQ analysis, including technicalities of protein extraction, precipitation and quantification, reduction, alkylation and trypsin digestion, as well as iTRAQ labelling, sample distribution, fractionation and LC-MS/MS analysis, database searching and protein identification, bioinformatics analysis and candidate selection criteria, can be found as Supplementary Data 1 and Supplementary Table 1. For cell extracts, cells were first isolated by Collagenase Type XI (2 mg/mL) treatment and posteriorly filtered to remove ECM contaminants, as previously reported[25]. Proteins were then extracted using the same guanidine hydrochloride based protocol that was used for whole tissue extracts (Supplementary Data 1). The mass spectrometry proteomics data have been deposited to the ProteomeXchange Consortium via the PRIDE partner repository with the dataset identifiers PXD005616 and PXD004922[26].

Macroscopic characterization and scanning electron microscopy (SEM). For qualitative macroscopic evaluation of the different age groups, IVDs were excised and photographed under an Olympus SZX16 stereomicroscope coupled with a DP71 camera (Olympus, Tokyo, Japan) at 10X magnification.

For SEM analysis, samples were fixed using 2.5% (v/v) glutaraldehyde (Agar Scientific) in 0.1 M sodium cacodylate solution (Sigma) and then stored in sodium cacodylate buffer 0.1 M at 4 °C until further use. IVDs were then dehydrated in serial diluted ethanol solutions of 50, 60, 70, 80, 90, and 99% v/v, being incubated for 10 min in each dilution. Following critical point drying, samples were sputtered-coated with a Au/Pd thin film, using the SPI Module Sputter Coater equipment. Samples were examined at CEMUP (Materials Centre of the University of Porto), using a High resolution Scanning Electron Microscope with X-Ray Microanalysis - JEOL JSM 6301 F/Oxford INCA Energy 350 - at 300X and 5000X magnification. The following parameters (mean fibril diameter, mean pore area, number of pores and number of intersections) were obtained using "DiameterJ", a plugin for ImageJ/FIJI software version 1.46r (NIH) for topographic comparison of samples under study[27].

Western Blotting. Following denaturation for 10 min at 65 °C, protein samples were separated by sodium dodecyl sulphate (SDS) 9% polyacrylamide gel electrophoresis (PAGE), and electroblotted onto a Hybond enhanced chemiluminescence (ECL) membrane (Amersham Biosciences). Antibodies for Collagen Type XII, Collagen Type XIV, Collagen Type XI alpha 2, Fibronectin and Prolargin were used. Further details on blocking solutions, primary and secondary antibodies used, as well as their respective host species, working dilutions and commercial suppliers can be found in Supplementary Table 2.

After ECL detection (Amersham Biosciences), bands were quantified using Quantity One 4.6.8 Software (Bio-Rad) and values were normalized to the total protein loading (density value of each complete lane, obtained after staining of the membrane following immunodetection with Page Blue Protein Staining Solution (ThermoFisher Scientific), using a protocol adapted from Welinder and Ekblad[28]. All samples were run in the same SDS-PAGE gel, and background signal was measured in several different areas of the membrane. Average background signal was then subtracted to the band intensity signal to minimize background variation and interference.

Statistical Analysis. Statistical analysis was performed using non-parametric Mann-Whitney test in GraphPad Prism software 5.0, to compare two groups of non-related samples (e.g. foetus *versus* young or young *versus* old NPs). The parametric distribution of the data was evaluated by D'Agostino and Pearson normality test. Results (from at least three independent biological samples) are expressed as median ± Interquartile Range (IQR)

in box and whiskers plots or as mean ± Standard Error of the Mean (SEM). Values from $p \leq 0.05$ were considered statistically significant.

Results

Structural characterization of different aged IVDs by SEM. At the macroscopic level, several differences could be identified (Fig. 1, left panel). Foetal intervertebral discs (IVDs) consisted of a well-distinguished annulus fibrosus (AF) formed of concentric lamellae delimiting a highly hydrated gel-like nucleus pulposus (NP). During ageing and degeneration, the boundary between AF and NP became less obvious. In addition, discs started looking increasingly dry and fibrous.

Scanning electron microscopy (SEM) has also been optimized, for a more detailed comparison of NP topography from the three different age groups. NP SEM images clearly showed a fine network of randomly oriented fibres (Fig. 1, central and right panels).

Further quantitative characterization of the SEM images obtained for different aged NP samples revealed age-associated changes in matrix architecture. Using DiameterJ, a plugin of ImageJ/Fiji software, we evaluated the following parameters: mean fibre diameter, number of pores, number of intersections and mean pore area (Fig. 1b). Mean fibre diameter of elder (8.826 pixels) NPs was statistically higher than that of the adults (7.482 pxels), whereas no differences were observed between foetal (7.803 pixels) and young NPs. Elder bovine NPs also presented significantly fewer (275.2 pores) but bigger (566.5 pixels^2) pores in comparison to young animals (459 pores and 432.6 pixels^2, respectively) and also less fibre intersections (927 *vs* 1391 intersections). Foetal NP mean pore area (602.6 pixels^2) was also significantly bigger than that of young IVDs.

Optimization of the proteomics workflow. Age-associated protein expression profiles were identified in the first place by the distinct one dimension (1D) SDS-PAGE band signatures obtained. By comparing foetal, young and old NPs, we found that band intensities differed depending on disc age (Fig. 2a). Foetus and young samples presented an enrichment of high molecular weight proteins, between 150 and 250 kDa, where some of the molecules identified were tenascin, collagen type VI and biglycan (Fig. 2a–1F and Y and Supplementary Data 4). This trend was also visible among proteins around 50 kDa that corresponded to actin, link protein (HAPLN1), biglycan and decorin among others (Fig. 2a–6F,Y and O, Supplementary Table 3 and Supplementary Data 4). Noteworthy, we observed that young NPs had increased protein expression levels at around 30 kDa (Fig. 2a–7F,Y,O and 8F,Y,O). These bands corresponded to collagen type II and chondroadherin (Supplementary Table 3 and Supplementary Data 4). Moreover, above 100 kDa a band presented a trend to increase in Young and Old animals when compared to Foetus (Fig. 2a and 3F,Y,O). Fibromodulin, biglycan, aggrecan and cartilage oligomeric matrix protein (COMP) were identified within these bands (Supplementary Table 3 and Supplementary Data 4). In addition, prolargin (PRELP) was only identified in old samples (Fig. 2a–5O, Supplementary Table 3 and Supplementary Data 4) and not in the same molecular weight bands of Foetus or Young animals (Fig. 2a–5F and Y, Supplementary Table 3 and Supplementary Data 4). Nevertheless, the differences detected were only semi-quantitative and the fact that after MS identification of the molecules present in each of the gel bands, protein mixtures were found (Supplementary Table 3 and Supplementary Data 4), made it hard to dissect which were the ones accounting for the observed differences.

For a comprehensive age comparative analysis of the NP matrisome, we used a gel-free MS based high throughput proteomic approach. The first optimization step involved the decision on whether we could use the whole tissue extract or whether decellularization was needed. Comparing the protein band profiles of the whole tissue and of cell extracts obtained using the same buffer, more bands were observed within the cellular rather than the tissue extract. Nevertheless, MS/MS identification showed that the bands corresponding to ECM proteins (namely collagen type II, chondroadherin and mimecan) were mainly present in the tissue extract (Fig. 2b–1w, 2w and 3w, respectively, Supplementary Table 4 and Supplementary Data 5). In fact, most of the disc is made up of water, while ECM and cells represent a very small percentage in terms of tissue volume[12]. For this reason, we did not pursue further the laborious task of improving the decellularization step, given that it brought no added value.

We tested 3 different buffers taken from the literature[29]. For each of them, we evaluated the total number of bovine proteins identified, as well as the number of ECM-associated molecules obtained. For that we took advantage of the Functional Annotation Clustering Tool from DAVID (https://david.ncifcrf.gov/). Qualitative results from Liquid Chromatography coupled to tandem Mass Spectrometry (LC-MS/MS) enabled us to select Guanidine Hydrochloride as the best buffer for our analysis, given that it enabled the identification of more bovine total proteins (146) and, particularly, more ECM molecules (26) than the chondroitinase-containing buffers (Fig. 2c and Supplementary Data 6).

The optimized workflow that was used for sample processing is summarized in Fig. 3. Briefly, NPs were excised from foetal, young and old bovine tails and stored at −80 °C until further use. Samples were then snap frozen in liquid nitrogen and pulverized prior to the 24 hour protein extraction with the 4 M Guanidine Hydrochloride buffer. Protein was then precipitated, quantified, and digested. Following 8-plex isobaric tag for relative and absolute quantitation (iTRAQ) labelling, samples were pooled and fractionated by LC. Finally, the peptide mixture was analysed by LC-MS/MS and protein identification was performed using Protein Pilot. Of note, the labelled samples of each of the two batches were combined into one sample mixture (Batch 1: Y1, Y2, Y3, F1, F2, F3, O Pool, Total Pool; Batch 2: Y1, Y2, Y3, O1, O2, O3, F Pool, Total Pool – Supplementary Data 1 and Supplementary Table 1).

Identification of NP age related proteomic signatures by iTRAQ analysis. PCA-DA plots, obtained with MarkerView, show significant clustering and differentiation among foetus (green), young (blue) and old (red) animals (Supplementary Figure 2a). Despite biological variability within the distinct age groups, and

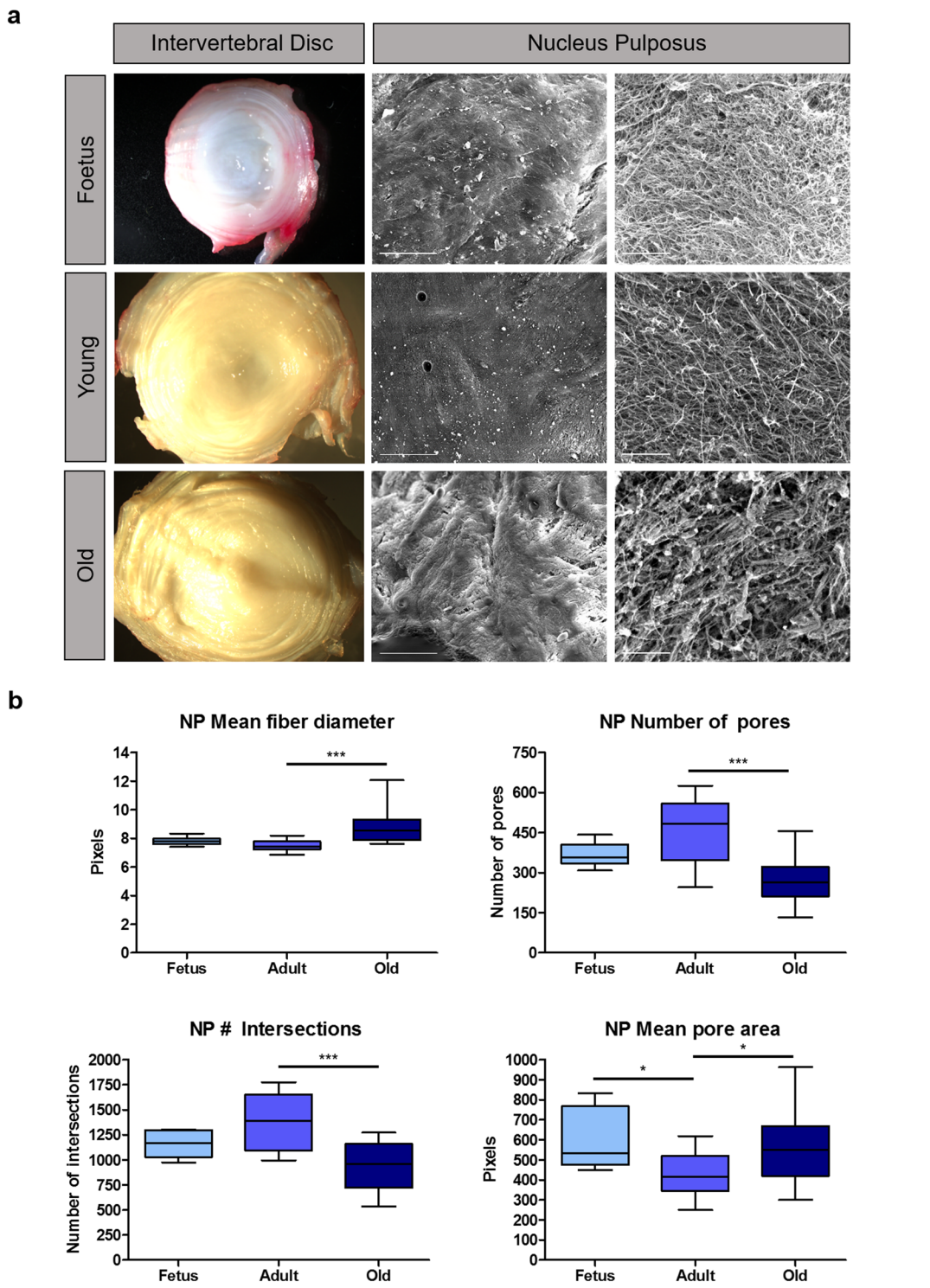

Figure 1. Gross view and topographical characterization of different aged IVDs. (a) - Macroscopic pictures from IVD transversal sections (left panels) and microscopy images from scanning electron microscopy (SEM) (central and right panels, with scale bars representing 200 µm and 10 µm, respectively) of foetal, young and old IVDs are presented. On the right panels are magnifications of the NP, representing the organization of ECM fibres. NP parameters such as mean fibril diameter, mean pore area, number of pores and number of intersections were also plotted regarding each age group (**b**). Box-plot lines represent median and interquartile ranges of the different parameters evaluated. (*) stands for $p \leq 0.05$ (**) for $p \leq 0.01$ and (***) for $p \leq 0.001$, using the non-parametric Mann-Whitney test.

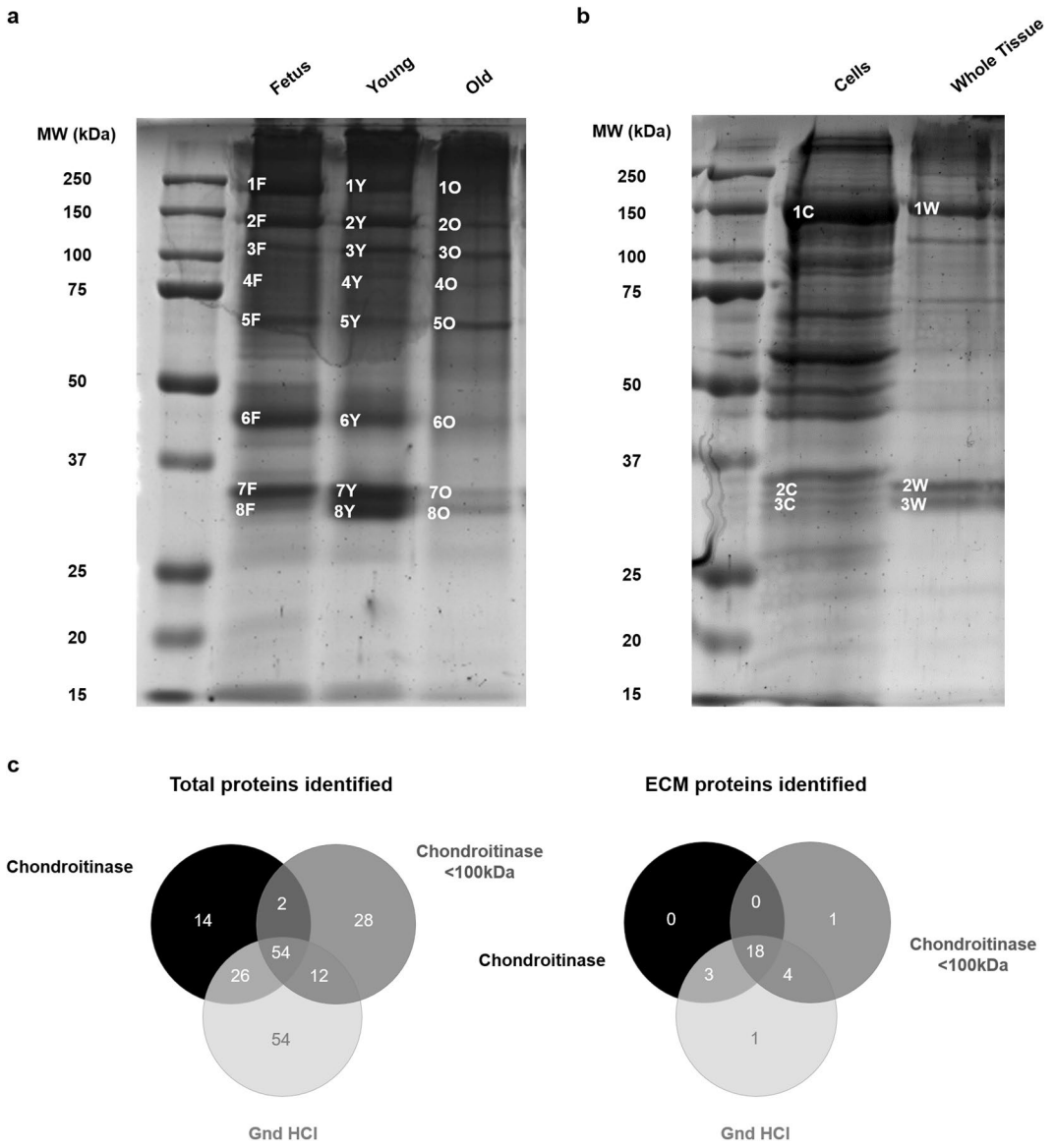

Figure 2. Sample complexity, age-associated SDS-PAGE band profile and extraction buffer evaluation. (**a**) - By comparing the band profiles observed in one dimension (1D) SDS-PAGE gels, for the three distinct age groups, there were already clear differences in the intensity of some of the bands identified by MS + MS/MS. Information on band identification from 1 F to 8 O can be found in Supplementary Table 3. (**b**) - With the same extraction buffer, we observed more bands within the cellular rather than the tissue extract. However, identification by MS + MS/MS (Supplementary Table 4) showed that the bands corresponding to ECM proteins were mainly present in the tissue extract (1 C–COL6A1/COL6A2; 1 W–COL6A1/COL2A1; 2 C–ANXA1/ANXA2/GAPDH; 2 W–COL2A1/CHAD/OGN; 3 C–ANXA8/LDHA; 3 W–CHAD). (**c**) - We compared the number of proteins identified by LC-MS/MS when using distinct buffers recommended from the literature: guanidine hydrochloride buffer (Gnd HCl), the same buffer with a prior chondroitinase 6 h treatment (chondroitinase) and this last condition followed by a centrifugal filtration, using a molecular weight cut-off of 100 kDa (chondroitinase <100 kDa). The extraction buffer with which more proteins in total were identified, and more ECM proteins, in particular, was Gnd HCl.

the fact that iTRAQ data was obtained from two independent runs, the three major groups of samples (Foetus, Young and Old) were well separated from each other, suggesting that NPs from different age sets presented distinct proteomes.

Averaged values of relative protein expression data from iTRAQ based LC-MS/MS (8-plex) assays were subjected to hierarchical clustering with Morpheus software. The heatmap and respective dendrogram generated are represented in Fig. 4a. This supervised analysis was performed by applying Spearman rank standardization. Foetuses were grouped together. Although they were part of the same cluster (showing that they both have similar protein expression profiles), Young and Old animals were also grouped according to their age status. Clustering data analysis demonstrated the ability to conduct global proteomics profiling on NP disc tissues, revealing that

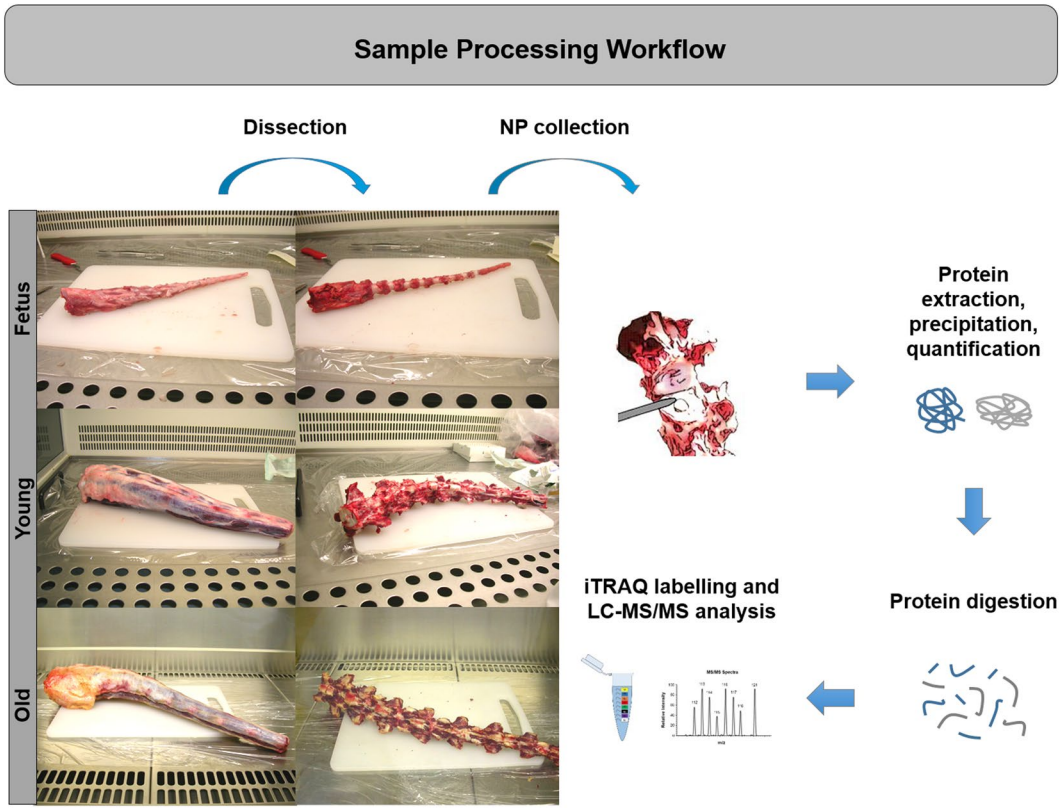

Figure 3. Proteomic sample processing workflow. Bovine caudal IVDs from foetus, young and old animals were dissected within a few hours after slaughter. The NPs were collected and protein was further extracted, precipitated and quantified. After digestion, peptides were marked with isobaric tags for relative and absolute quantitation (iTRAQ) prior to liquid chromatography – tandem mass spectrometry (LC-MS/MS).

significantly different arrays of proteins were expressed depending on the age of the individuals, despite the fact that samples were collected from the same avascular organs in the bovine body.

To explore the biological processes affected by the 77 (out of 161) common proteins identified in all the samples, and thus related to NP function, we performed Gene Ontology (GO) and Pathway term enrichment using the Functional Annotation Clustering Tool from DAVID Database. This allowed us to determine GO and Pathway terms that occurred more frequently than expected by chance. Proteins were then clustered according to functional similarity (Supplementary Tables 5 and 6).

The most significant cluster of proteins, in comparison to *Bos taurus* proteome, included GO terms implicated in extracellular matrix and GAG binding, which was in accordance to what we expected. Interestingly, we also detected a statistically significant group of interactors involved in collagen fibril organization, cartilage and blood vessel development, and also proteins implicated in lipid binding and vesicles. Other statistically significant biological terms that appeared were glycolysis, regulation of phagocytosis, response to wounding, inflammatory response and calcium ion binding, among others. Redoing the analysis concerning pathway term enrichment, we obtained "ECM-receptor interaction", "Focal adhesion" and "integrin signalling".

To integrate known and predicted protein-protein interactions and better understand the relationships between the 77 distinct proteins commonly identified in all 3 age groups, we used STRING (Supplementary Figure 2b).

The interactome obtained highlighted six different clusters marked in same colour circles, broadly representing: cytoskeleton (light green), fibril/collagen organization and skeletal/cartilage development (beige), GAG binding/crosslinking (dark green), glycolysis (red) and vesicle-associated proteins (magenta). Large protein interaction networks illustrated the high degree of connectivity and the presence of promiscuous hub proteins.

Finally, to further highlight correlations between the proteins within each of the 6 main heatmap clusters (cluster 1A, cluster 1B, cluster 2A, cluster 2A', cluster 2B and cluster 2B' – Fig. 4), we performed gene ontology enrichment analysis based on the proteins identified in the different clusters. Among the proteins within cluster 1B (which increase with development and ageing), we found a significant enrichment of Gene Ontology terms related to extracellular matrix, glycosaminoglycan, polyssacharide, carbohydrate, hyaluronic acid and ion binding, as well as cell adhesion and membrane bound organelles. Among the proteins from cluster 2A, there was an enrichment of the term ion binding, whereas among the cluster 2B' (proteins which decrease with development and ageing) there was an enrichment of terms such as melanosomes, cytoplasmic vesicles, collagen fibril organization, blood vessel development, endoplasmic reticulum and also ion binding. No other significantly enriched

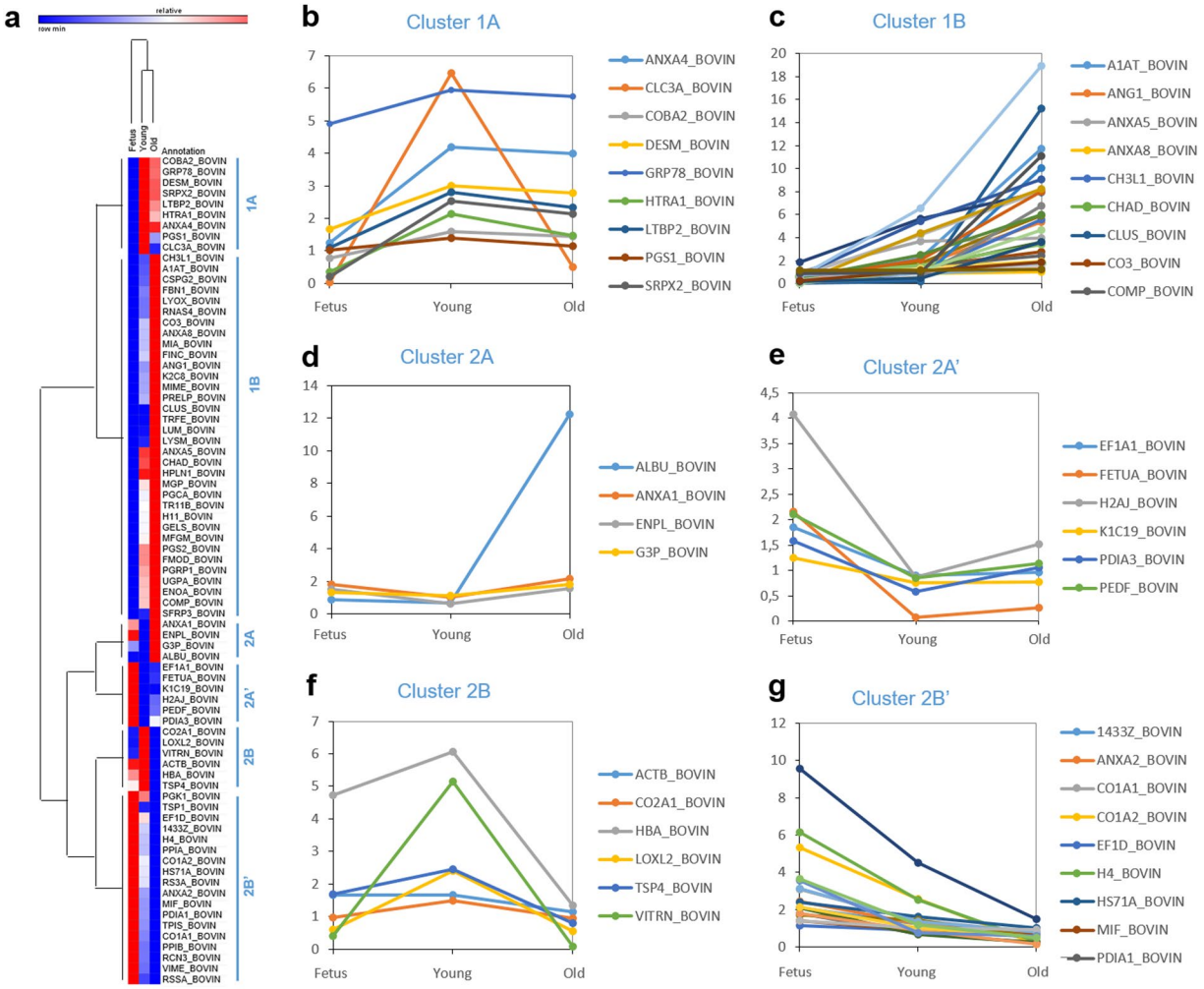

Figure 4. iTRAQ data analysis. (**a**) - Heatmap with the respective dendrogram representing sample-based hierarchical clusters. Average expression levels were represented by colour scale from blue (low) to red (high). In terms of protein expression, there were six main clusters. (**b–g**) - Graphical representation of iTRAQ relative protein expression profiles for the molecules within each of the 6 main clusters: cluster 1 A (**b**), cluster 1B (**c**), cluster 2A (**d**), cluster 2A' (**e**), cluster 2B (**f**) and cluster 2B' (**g**).

GO terms were found for other groups of samples. A detailed list of the enriched GO terms in each cluster can be found in the Supplementary Data 7.

Definition of NP matrisome changes during development and ageing. Given that GO analysis revealed enrichment of several ECM-related categories, we examined the overlap of the NP proteomic signature with the matrisome, a comprehensive list of genes coding for ECM molecules and regulators, which is significantly more comprehensive for data mining and for posing questions relevant to matrix biology than GO terms[30].

Of note, 47% of the genes composing the NP signature encode for matrisomal proteins (Fig. 5a), and ECM-associated molecules. Core matrisomal proteins (64%) are over-represented, particularly in terms of proteoglycans (44%) and glycoproteins (39%). We further defined the NP matrisome as the 36 matrisomal proteins identified in the 3 age groups (relative protein quantification of such molecules is summarized in Fig. 5b).

Candidate validation by Western Blot. The rationale behind the identification of potential age-related matrix components deregulated during NP development and choice of candidates for further investigation was: the analysis of iTRAQ data (e.g. differential protein expression ratio cut-off >1.3 and <0.77 and ProteinPilot protein identification confidence), literature mining concerning promising associations with IVD ageing and degeneration or lack of published data suggesting novel potential candidate biomolecules. Given that most proteins overexpressed in Foetus had not been identified with the highest confidence scores, we decided to further explore additional results obtained by searching the original MS/MS data against the proteomes from all organisms available on Swiss-Prot (results available upon request), instead of only using the *Bos taurus* complete proteome set.

Following these criteria, 5 proteins were selected for further validation: Collagen type XII, Collagen type XIV, Collagen type XI, Prolargin and Fibronectin. To confirm if these NP matrisome candidates were expressed in an age-dependent manner, Western blot analysis was performed (Fig. 6, right panel and Supplementary Figure 3).

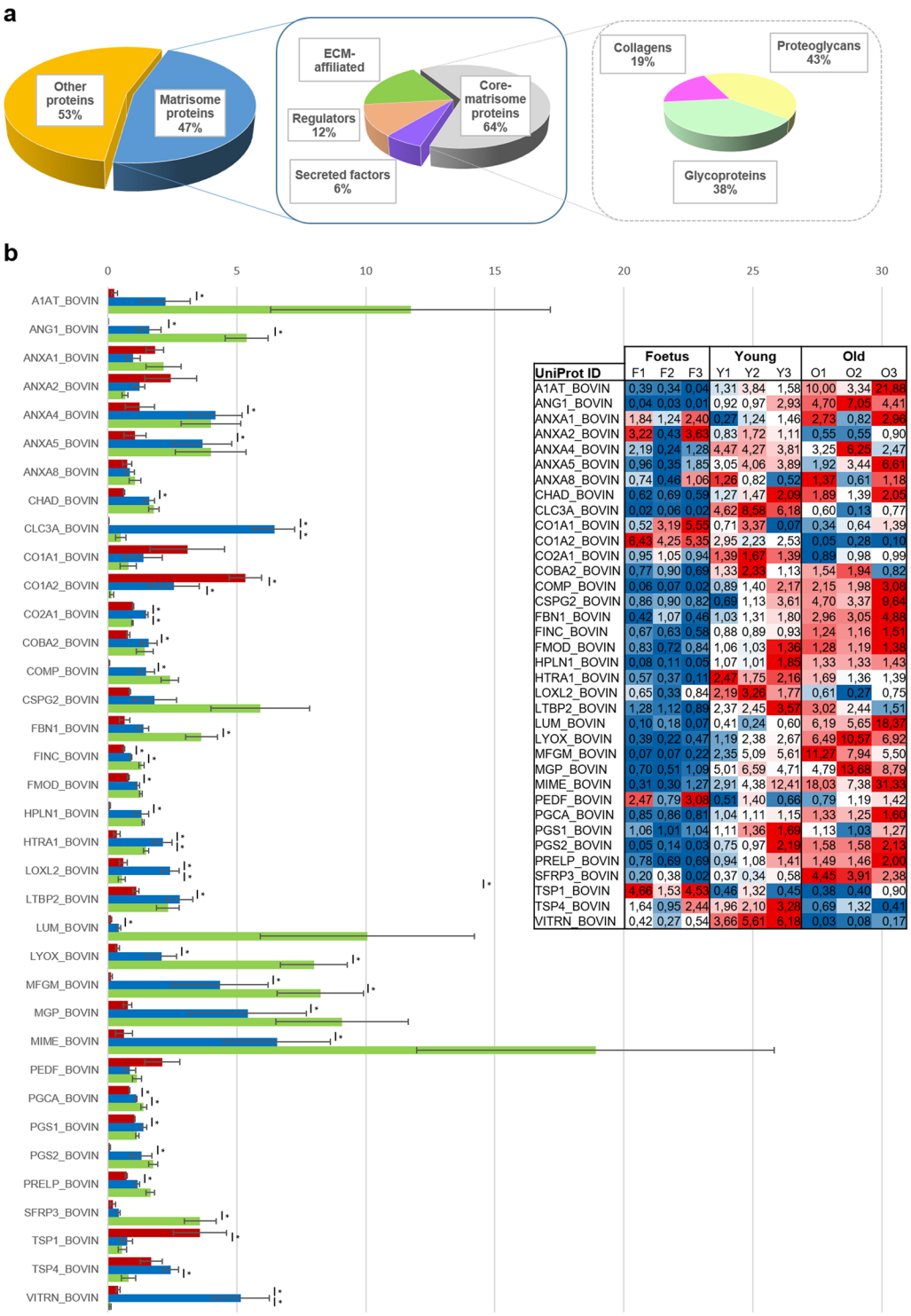

	Foetus			Young			Old		
UniProt ID	F1	F2	F3	Y1	Y2	Y3	O1	O2	O3
A1AT_BOVIN	0,39	0,34	0,04	1,31	3,84	1,58	10,00	3,34	21,88
ANG1_BOVIN	0,04	0,03	0,01	0,92	0,97	2,93	4,70	7,05	4,41
ANXA1_BOVIN	1,84	1,24	2,40	0,27	1,24	1,46	2,73	0,82	2,96
ANXA2_BOVIN	3,22	0,43	3,63	0,83	1,72	1,11	0,55	0,55	0,90
ANXA4_BOVIN	2,19	0,24	1,28	4,47	4,27	3,81	3,25	6,25	2,47
ANXA5_BOVIN	0,96	0,35	1,85	3,05	4,06	3,89	1,92	3,44	6,61
ANXA8_BOVIN	0,74	0,46	1,06	1,26	0,82	0,52	1,37	0,61	1,18
CHAD_BOVIN	0,62	0,69	0,59	1,27	1,47	2,09	1,89	1,39	2,05
CLC3A_BOVIN	0,02	0,06	0,02	4,62	8,58	6,18	0,60	0,13	0,77
CO1A1_BOVIN	0,52	3,19	5,55	0,71	3,37	0,07	0,34	0,64	1,39
CO1A2_BOVIN	6,43	4,25	5,35	2,95	2,23	2,53	0,05	0,28	0,10
CO2A1_BOVIN	0,95	1,05	0,94	1,39	1,67	1,39	0,89	0,98	0,99
COBA2_BOVIN	0,77	0,90	0,69	1,33	2,33	1,13	1,54	1,94	0,82
COMP_BOVIN	0,06	0,07	0,02	0,89	1,40	2,17	2,15	1,98	3,08
CSPG2_BOVIN	0,86	0,90	0,82	0,69	1,13	3,61	4,70	3,37	9,64
FBN1_BOVIN	0,42	1,07	0,46	1,03	1,31	1,80	2,96	3,05	4,88
FINC_BOVIN	0,67	0,63	0,58	0,88	0,89	0,93	1,24	1,16	1,51
FMOD_BOVIN	0,83	0,72	0,84	1,06	1,03	1,36	1,28	1,19	1,38
HPLN1_BOVIN	0,08	0,11	0,05	1,07	1,01	1,85	1,33	1,33	1,43
HTRA1_BOVIN	0,57	0,37	0,11	2,47	1,75	2,16	1,69	1,36	1,39
LOXL2_BOVIN	0,65	0,33	0,84	2,19	3,26	1,77	0,61	0,27	0,75
LTBP2_BOVIN	1,28	1,12	0,89	2,37	2,45	3,57	3,02	2,44	1,51
LUM_BOVIN	0,10	0,18	0,07	0,41	0,24	0,60	6,19	5,65	18,37
LYOX_BOVIN	0,39	0,22	0,47	1,19	2,38	2,67	6,49	10,57	6,92
MFGM_BOVIN	0,07	0,07	0,22	2,35	5,09	5,61	11,27	7,94	5,50
MGP_BOVIN	0,70	0,51	1,09	5,01	6,59	4,71	4,79	13,68	8,79
MIME_BOVIN	0,31	0,30	1,27	2,91	4,38	12,41	18,03	7,38	31,33
PEDF_BOVIN	2,47	0,79	3,08	0,51	1,40	0,66	0,79	1,19	1,42
PGCA_BOVIN	0,85	0,86	0,81	1,04	1,11	1,15	1,33	1,25	1,60
PGS1_BOVIN	1,06	1,01	1,04	1,11	1,36	1,69	1,13	1,03	1,27
PGS2_BOVIN	0,05	0,14	0,03	0,75	0,97	2,19	1,58	1,58	2,13
PRELP_BOVIN	0,78	0,69	0,69	0,94	1,08	1,41	1,49	1,46	2,00
SFRP3_BOVIN	0,20	0,38	0,02	0,37	0,34	0,58	4,45	3,91	2,38
TSP1_BOVIN	4,66	1,53	4,53	0,46	1,32	0,45	0,38	0,40	0,90
TSP4_BOVIN	1,64	0,95	2,44	1,96	2,10	3,28	0,69	1,32	0,41
VITRN_BOVIN	0,42	0,27	0,54	3,66	5,61	6,18	0,03	0,08	0,17

Figure 5. Characterization of the NP matrisome. (**a**) - The pie charts exhibit percentages of identified proteins distributed by matrisome categories. (**b**) - Comparison of the different aged NP matrisome signatures. iTRAQ relative protein expression levels (x axis) are displayed for each of the molecules identified (y axis). Foetal samples are in red, young in blue and old in green. iTRAQ protein quantification scores for individual samples can be found on the embedded table (colour scale from blue – low expression – to red – high expression). In the case of Young animals, the values represent an average of the technical replicates. The non-parametric Mann-Whitney test was used to compare two groups of non-related samples. Standard error of the mean (SEM) is represented as the error bar. (*) stands for $p \leq 0.05$, using the non-parametric Mann-Whitney test.

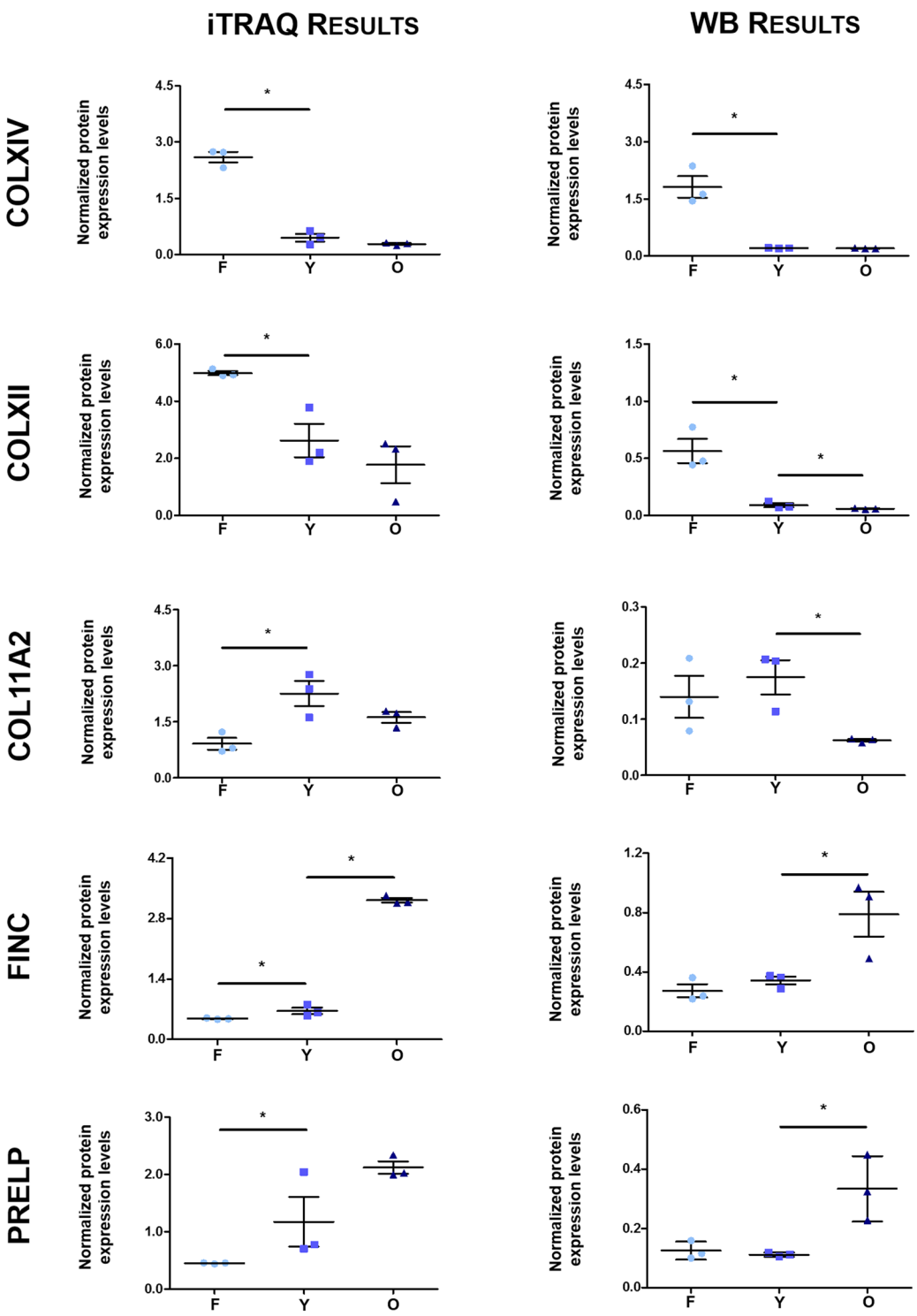

Figure 6. Validation of the candidates' protein expression levels. On the left are the graphics representing normalized protein expression levels from the iTRAQ LC-MS/MS analysis and on the right, of Western Blots (WBs), from Foetus, Young and Old animals. Collagen Type XII (COLXII) and XIV (COLXIV) expression levels are higher in NPs from foetus, Collagen Type 11 (COL11A2) is mostly expressed in Young animals, whereas Fibronectin (FINC) and Prolargin (PRELP) are typical from elder NPs. The non-parametric Mann-Whitney test was used to compare two groups of non-related samples (Foetus *vs* Young and Young *vs* Old). Graphs correspond to the average of protein expression levels obtained by band quantification and subsequent normalization to the total protein loading (Supplementary Figure 3). Standard error of the mean (SEM) is represented as the error bar. (*) stands for $p \leq 0.05$, using the non-parametric Mann-Whitney test.

Collagen type XII and Collagen type XIV were significantly more expressed (6-fold and 9-fold, respectively) in NPs from Foetus rather than from Young animals (0.56 to 0.09 in Collagen type XII and 1.81 to 0.21 in Collagen type XIV). No other relevant protein expression differences were found for Collagen type XIV, when comparing Young and Old samples. Nevertheless, there was also a slight but significant 1.5-fold decrease of Collagen type XII from Young to Old age groups (0.09 to 0.06). Collagen type XI was shown to be expressed at significantly higher levels in Young NPs (0.17) in comparison to Old ones (0.06) and this enrichment at younger stages was also verified by immunofluorescence (Supplementary Figure 4). Fibronectin and Prolargin results reflected a significant (2-fold and 3-fold, respectively) overexpression (from 0.34 to 0.79 in Fibronectin and from 0.11 to 0.33 in Prolargin) only in older tissues. The results of this analysis were consistent with the trends obtained by exploring iTRAQ data (Fig. 6, left panel) and thus highlight the implication of Collagen type XII, Collagen type XIV, Collagen type XI, Prolargin and Fibronectin in age mediated IVD degeneration.

Discussion

Disc degeneration and ageing are intimately associated. While disc ageing is a natural and gradually occurring process, disc degeneration involves more rapid and severe changes. In this study, we aimed to characterize NP proteomic changes that occur with development and ageing and that are closely related to disc degeneration, with a special focus on the ECM. For that, we have used iTRAQ labelling coupled to LC-based tandem mass spectrometry. This technique infers the relative abundance of individual proteins from peptide MS signal intensities and has emerged as an effective tool for quantitative proteomic profiling of complex tissue extracts, like cartilage[31]. SEM analysis and Western blotting also helped us to highlight and validate structural and molecular differences between the different age groups. The significance of our results is summarized as follows: several well-known effector proteins and a number of novel putative players were identified, 5 of which were independently validated.

Recently, proteomic-based studies have risen sharply and have started to be used to characterize normal and/or degenerated disc cells[32,33], secreted factors[34,35] and tissue composition[36], showing promising results. To date, however, limited studies have used proteomic strategies to study IVD matrix composition. One of the few existing studies focuses on the comparison of matrix proteomic signatures in different tissues[37], while another is centred on the identification of cartilage matrix patterns of zonal distribution[38]. To the best of our knowledge, Yee *et al*. were the only ones that dissected ECM changes of human discs in age and degeneration[39]. Nevertheless, they used scoliotic samples as controls, which have been shown to present a gene expression profile that differs from healthy tissues, and signs of calcification that might reflect a premature degenerative process[40,41]. In addition, the age range of non-degenerated samples under study was very limited and not representative of elder individuals.

Unlike existing approaches, we used healthy samples from different age groups, and included, for the first time in this type of analysis, foetal tissue and NPs from very old animals. At the macroscopic level, we demonstrated that tissues, particularly the NP, tend to gradually become less translucent and AF lamellae appears increasingly disorganized, as has been previously reported for degeneration[1]. These observations were supported by SEM analysis through which we thoroughly characterized NP collagen fibres. Mean fibril diameter was reduced in younger samples, indicating that fibrillogenesis was somehow affected at later developmental stages. Fibril organization in elder individuals was also disrupted. Matrix was sparser, with less intersections and reduced numbers of pores, which were bigger in size. Foetal pore area was also larger, possibly due to imbibed water[42]. This may explain the gel-like appearance of foetal NPs and their greater capacity to absorb load and tension.

iTRAQ technology enabled the identification of 161 proteins in total, 77 of which were detected in all samples. From the bioinformatics analysis of the common hits, a few observations were predictable. The highest ranking functional cluster of genes was for those involved in extracellular matrix, which was consistent with the guanidine extraction method selected[43]. Additional cytosolic components equally important for disc homeostasis and function might not have been identified, but these were not the focus of this study. A significant enrichment of other proteins and protein classes like GAG, polysaccharide and carbohydrate binding, collagen fibril organization, blood vessel, skeletal system and cartilage development, as well as glycolysis, was also found and reflected a complex network of interactions, involving more than pure ECM biosynthesis. With regard to response to wounding, its link to disc de- and regeneration has been well established[4]. Interestingly, melanosome regulation and vesicle-mediated transport were also enriched and seem to have a role in embryonic elongation and spine morphogenesis[44].

With respect to pathway term enrichment, ECM-receptor interaction, focal adhesion, integrin and TGF- β signalling, were expected, given that most of these pathways are connected. In most of the tissues, integrin cell surface receptors mediate cell-matrix interactions, which are key to control adhesion, survival and differentiation, among others, in response to environmental cues, like mechanical stimuli[45,46]. Moreover, focal adhesion kinase (FAK) has been shown to be activated in response to strain in non-degenerate disc cells, in an integrin dependent manner[47]. TGF-β can also be activated by integrin signalling, which, in turn, is affected by TGF-β, whose bioavailability is controlled by ECM binding[48] Most of these NP-associated functions might be deregulated not only in development but also during ageing and degeneration.

By assessing the overlap of the NP proteomic signature with a list of nearly 300 ECM and ECM-associated molecules generated by Naba and co-workers[30], we defined the NP matrisome and how it is changed during development and ageing. Meta-analysis of such proteomic data was used to identify potential age-related components deregulated during NP development and select candidates for further investigation. Collagen Type XI, XII, XIV Fibronectin and Prolargin expression profiles were confirmed by Western Blot analysis. Collagen Type XI overexpression in young animals was also validated by immunofluorescence. Moreover, PRELP increase with age was additionally verified by SDS-PAGE band identification. Other proteins like Actin, Collagen Type II, Fibromodulin, Aggrecan and COMP, among others, presented the same trend in iTRAQ analysis as in gel band profiling.

Fibronectin (FN) mediates a wide variety of cellular interactions with the matrix and plays important roles in cell adhesion, migration, growth, differentiation and survival, particularly through integrin interactions[4,46]. It interacts with a broad range of collagens (type I, II, III, IV, V and X)[49] and, in line with our results, FN has been shown to be upregulated in numerous models of disc ageing and degeneration[35,39,50]. Usually, 30 to 40%[51] of the protein content is in the form of fragments from enzymatic cleavage[4,52,53], which in turn promote further degeneration[54]. While excessive FN deposition has been linked to fibrosis[55], polymorphisms have also been associated with disc degeneration[56], given that it mediates collagen deposition and thus preserves matrix structural integrity[57]. FN may also be involved in the clearance of tissue denatured collagen in age and degeneration, or of circulating fibrin after trauma or in inflammation[58,59].

Prolargin (PRELP) is an ECM structural component that anchors the basement membrane to the underlying connective tissue[4]. Apart from binding GAG chains, it also binds type I and type II collagen[60]. PRELP overexpression in mice disrupts collagen fibres (which decrease in content and size), with no influence in fibril diameter[61]. In accordance, we have shown that the matrix of aged samples presented a lower density of fibres, resulting in a reduced number of fibre intersections, as well as in fewer but larger pores. Interestingly, PRELP is absent in neonatal articular cartilage ECM, in contrast to its abundance later in life[62]. This age-related accumulation agrees with our bovine data. In turn, human scoliotic NPs, also present PRELP increase with age[39], whereas in dogs it has been associated with degeneration[35].

Collagen Type XI is a fibril-forming collagen required for embryonic development and its abundance is inversely correlated with fibre diameter[4,63]. This explains our observations (no differences between Foetuses and Young samples, where it is expressed, but an increase in fibre diameter in elder individuals, where it is absent). Apart from having a role in fibrillogenesis (controlling lateral growth of collagen type II fibrils) and in mineralization, Collagen XI also binds PGs, particularly at the cell surface, being important to maintain tissue integrity and cohesion, particularly during matrix remodeling[4,64]. In line with our results, Collagen XI polymorphisms have been associated with disc degeneration[56]. COL11A1 expression levels tend to decrease with the severity of degeneration, at least in part due to MMP-mediated degradation[6,65]. Recent data from Yee *et al*. also seem to indicate that collagen type XI declines in the human scoliotic NPs with ageing, in agreement with our bovine model[39].

Collagen Type XII is a typical collagen-organizer molecule that binds to collagen I containing fibrils, as well as to other matrix proteins, like COMP, modulating fibril organization and mechanical properties[4,66]. It has been suggested to take part in the development of stromal architecture and tissue cohesion[67], particularly by promoting matrix bridges formation essential for network communication[68]. In addition, Collagen XII seems to have a pro-regenerative role, at least in other tissues[69,70].

Collagen Type XIV is a fibril-associated collagen, transiently expressed in several epithelia, including those undergoing rapid remodeling. At later developmental stages, it only persists in the BM, where it co-localizes with Collagen XII[71]. Collagen XIV is thought to control collagen I fibrillogenesis during embryonic development (as has been supported by our results, it inversely correlates with fibril diameter and premature growth), as well as differentiation[4,66,67]. Interestingly, in the chick embryo it is expressed in a gradient around the spinal cord[72]. Like Collagen XII, it is key for the hydration and thickness (and therefore transparency) of tissues[73], supporting our macroscopic observations of a gel-like appearance in foetal NPs. In other settings, type XIV collagen also appears to play a role in regeneration[74,75].

Overall, this study provides the first matrisome database of healthy discs during development and ageing, which is key to determine the pathways and processes required to maintain disc homeostasis. The integrated analysis of the proteomic datasets enabled us to discover novel components and characterize the developmental system in greater detail. The data herein presented may establish a solid foundation for better understanding the complex microenvironment of the IVD. Furthermore, they provide a starting point from which potential biomarkers and pathways that are altered during the dynamic disc degeneration process may be recapitulated or resumed, opening new possibilities for the development of novel therapeutic solutions for the disease. For instance, using these cues to modulate the ECM, recreating a microenvironment similar to early developmental stages, may enable the expansion and differentiation of autologous NP cells *in vivo*. In fact, others have shown that cell-free tissue engineering strategies are sufficient to promote disc regeneration[76]. Alternatively, the same approach could be combined with cell-based therapies currently under study[23,24].

Evidence about the use of bovine coccygeal discs as a model of ageing is still scarce. To date, existing studies have failed to use very old individuals. Nevertheless, a higher incidence of degenerative disc changes has been registered in elder specimens, indicating their clinical relevance[77–79]. In fact, ageing similarities between the two species were found, particularly in terms of extracellular matrix alterations[77].

Moreover, although interspecies differences may naturally occur, bovine coccygeal discs are becoming increasingly accepted tissues for large animal organ culture, majorly because of their large size, low cost and availability. Given the similar aspect ratios, transport distances, and cell content, especially concerning the absence of notochordal cells during adulthood, between bovine and human lumbar discs, and contrarily to what happens in the vast majority of small animal models, they have been proposed as a suitable model to study several aspects of lumbar discs pathobiology[12,79–81]. In particular, comparable types and distribution, synthesis and deposition of extracellular matrix molecules have been found in both human lumbar and bovine coccygeal discs[82–86].

The work herein presented paves the way for future studies using human samples to validate the observed differences and investigating these constituents, thus further elucidating about their functional roles. Importantly, and since it is known that extractability of NP proteins reduces with age due to increased crosslinking and resistance to degradation, particularly concerning the collagen fibrillar network, chemical digestion proposed by Chan and co-workers should also be addressed to analyze the insoluble fractions obtained[39].

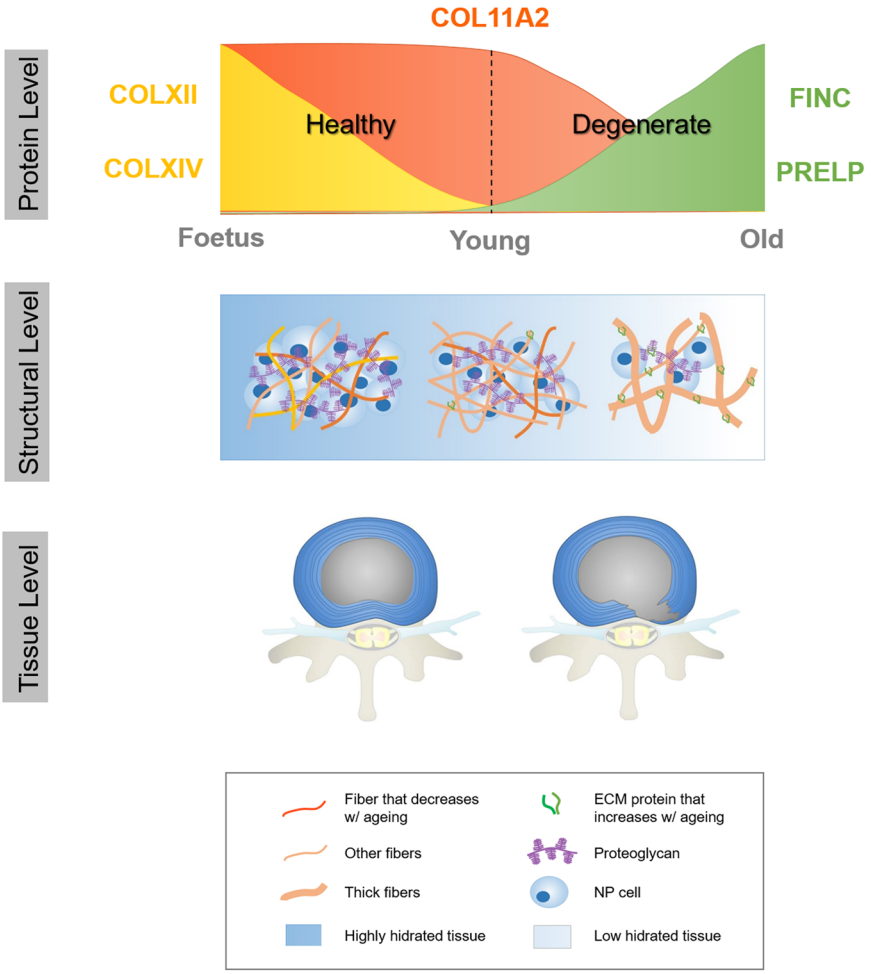

Figure 7. Working model for the changes that occur in the IVD microenvironment with development and ageing. From the foetal stages to adulthood, collagen type XII and XIV expression is lost and only collagen type XI is maintained. With increasing age, there is an enrichment in fibronectin and prolargin. Proteomic alterations are accompanied by matrix remodeling (fibrillogenesis and fibril organization are both affected), concomitant with water loss and a cell population decline. This ultimately causes age-associated degeneration, hernia formation and low back pain.

In addition, reanalysis of this dataset focusing on the numerous cellular proteins identified will be of major importance, given that there are many other proteins equally important for disc homeostasis and function, which are still to be unveiled.

As a model (Fig. 7), we propose that remodeling of NP tissue architecture, which affects IVD mechanical properties and biological function of the tissue, reflects changes that occur in terms of matrix biochemical composition during development and ageing. Integrating information from the protein to the tissue level, taking into account the cell-matrix crosstalk, will provide helpful cues for disc regeneration[26].

References

1. Adams, M. A. & Roughley, P. J. What is intervertebral disc degeneration, and what causes it? *Spine (Phila Pa 1976)* **31**, 2151–2161, https://doi.org/10.1097/01.brs.0000231761.73859.2c (2006).
2. Anderson, D. G. & Tannoury, C. Molecular pathogenic factors in symptomatic disc degeneration. *Spine J* **5**, 260S–266S, https://doi.org/10.1016/j.spinee.2005.02.010 (2005).
3. Roughley, P. J. Biology of intervertebral disc aging and degeneration: involvement of the extracellular matrix. *Spine (Phila Pa 1976)* **29**, 2691–2699 (2004).
4. Molinos, M. *et al.* Inflammation in intervertebral disc degeneration and regeneration. *J R Soc Interface* **12**, 20141191, https://doi.org/10.1098/rsif.2014.1191 (2015).
5. Le Maitre, C. L., Freemont, A. J. & Hoyland, J. A. Localization of degradative enzymes and their inhibitors in the degenerate human intervertebral disc. *J Pathol* **204**, 47–54, https://doi.org/10.1002/path.1608 (2004).
6. Galbusera, F. *et al.* Ageing and degenerative changes of the intervertebral disc and their impact on spinal flexibility. *Eur Spine J* **23**(Suppl 3), S324–332, https://doi.org/10.1007/s00586-014-3203-4 (2014).
7. Colombier, P., Clouet, J., Hamel, O., Lescaudron, L. & Guicheux, J. The lumbar intervertebral disc: from embryonic development to degeneration. *Joint Bone Spine* **81**, 125–129, https://doi.org/10.1016/j.jbspin.2013.07.012 (2014).

8. Hwang, P. Y., Chen, J., Jing, L., Hoffman, B. D. & Setton, L. A. The role of extracellular matrix elasticity and composition in regulating the nucleus pulposus cell phenotype in the intervertebral disc: a narrative review. *J Biomech Eng* **136**, 021010, https://doi.org/10.1115/1.4026360 (2014).
9. Takaishi, H. *et al*. Type-II collagen gene expression is transiently upregulated in experimentally induced degeneration of rabbit intervertebral disc. *J Orthop Res* **15**, 528–538, https://doi.org/10.1002/jor.1100150408 (1997).
10. Cs-Szabo, G. *et al*. Changes in mRNA and protein levels of proteoglycans of the anulus fibrosus and nucleus pulposus during intervertebral disc degeneration. *Spine (Phila Pa 1976)* **27**, 2212–2219, https://doi.org/10.1097/01.BRS.0000029249.02864.5B (2002).
11. Gruber, H. E. & Hanley, E. N. Jr. Analysis of aging and degeneration of the human intervertebral disc. *Comparison of surgical specimens with normal controls. Spine (Phila Pa 1976)* **23**, 751–757 (1998).
12. Maroudas, A., Stockwell, R. A., Nachemson, A. & Urban, J. Factors involved in the nutrition of the human lumbar intervertebral disc: cellularity and diffusion of glucose *in vitro*. *J Anat* **120**, 113–130 (1975).
13. Deyo, R. A. & Weinstein, J. N. Low back pain. *N Engl J Med* **344**, 363–370, https://doi.org/10.1056/NEJM200102013440508 (2001).
14. Waddell, G. Low back pain: a twentieth century health care enigma. *Spine (Phila Pa 1976)* **21**, 2820–2825 (1996).
15. Nasser, R. *et al*. Complications in spine surgery. *J Neurosurg Spine* **13**, 144–157, https://doi.org/10.3171/2010.3.SPINE09369 (2010).
16. Swann, M. C., Hoes, K. S., Aoun, S. G. & McDonagh, D. L. Postoperative complications of spine surgery. *Best Pract Res Clin Anaesthesiol* **30**, 103–120, https://doi.org/10.1016/j.bpa.2016.01.002 (2016).
17. Swartz, K. R. & Trost, G. R. Recurrent lumbar disc herniation. *Neurosurg Focus* **15**, E10 (2003).
18. Onesti, S. T. Failed back syndrome. *Neurologist* **10**, 259–264 (2004).
19. Masuda, K. *et al*. Osteogenic protein-1 injection into a degenerated disc induces the restoration of disc height and structural changes in the rabbit anular puncture model. *Spine (Phila Pa 1976)* **31**, 742–754, https://doi.org/10.1097/01.brs.0000206358.66412.7b (2006).
20. Walsh, A. J., Bradford, D. S. & Lotz, J. C. *In vivo* growth factor treatment of degenerated intervertebral discs. *Spine (Phila Pa 1976)* **29**, 156–163, https://doi.org/10.1097/01.BRS.0000107231.67854.9F (2004).
21. Leckie, S. K. *et al*. Injection of AAV2-BMP2 and AAV2-TIMP1 into the nucleus pulposus slows the course of intervertebral disc degeneration in an *in vivo* rabbit model. *Spine J* **12**, 7–20, https://doi.org/10.1016/j.spinee.2011.09.011 (2012).
22. Yue, B. *et al*. Survivin-TGFB3-TIMP1 Gene Therapy Via Lentivirus Vector Slows the Course of Intervertebral Disc Degeneration in an *In Vivo* Rabbit Model. *Spine (Phila Pa 1976)* **41**, 926–934, https://doi.org/10.1097/BRS.0000000000001474 (2016).
23. Okuma, M., Mochida, J., Nishimura, K., Sakabe, K. & Seiki, K. Reinsertion of stimulated nucleus pulposus cells retards intervertebral disc degeneration: an *in vitro* and *in vivo* experimental study. *J Orthop Res* **18**, 988–997, https://doi.org/10.1002/jor.1100180620 (2000).
24. Sakai, D. *et al*. Differentiation of mesenchymal stem cells transplanted to a rabbit degenerative disc model: potential and limitations for stem cell therapy in disc regeneration. *Spine (Phila Pa 1976)* **30**, 2379–2387 (2005).
25. Molinos, M., Almeida, C. R., Goncalves, R. M. & Barbosa, M. A. Improvement of Bovine Nucleus Pulposus Cells Isolation Leads to Identification of Three Phenotypically Distinct Cell Subpopulations. *Tissue Eng Part A* **21**, 2216–2227, https://doi.org/10.1089/ten.TEA.2014.0461 (2015).
26. Vizcaino, J. A. *et al*. The PRoteomics IDEntifications (PRIDE) database and associated tools: status in 2013. *Nucleic Acids Res* **41**, D1063–1069, https://doi.org/10.1093/nar/gks1262 (2013).
27. Hotaling, N. A., Bharti, K., Kriel, H. & Simon, C. G. Jr. DiameterJ: A validated open source nanofiber diameter measurement tool. *Biomaterials* **61**, 327–338, https://doi.org/10.1016/j.biomaterials.2015.05.015 (2015).
28. Welinder, C. & Ekblad, L. Coomassie staining as loading control in Western blot analysis. *J Proteome Res* **10**, 1416–1419, https://doi.org/10.1021/pr1011476 (2011).
29. Wilson, R. *et al*. Changes in the chondrocyte and extracellular matrix proteome during post-natal mouse cartilage development. *Mol Cell Proteomics* **11**(M111), 014159, https://doi.org/10.1074/mcp.M111.014159 (2012).
30. Naba, A. *et al*. The matrisome: in silico definition and *in vivo* characterization by proteomics of normal and tumor extracellular matrices. *Mol Cell Proteomics* **11**(M111), 014647, https://doi.org/10.1074/mcp.M111.014647 (2012).
31. Wilson, R., Whitelock, J. M. & Bateman, J. F. Proteomics makes progress in cartilage and arthritis research. *Matrix Biol* **28**, 121–128, https://doi.org/10.1016/j.matbio.2009.01.004 (2009).
32. Gilson, A., Dreger, M. & Urban, J. P. Differential expression level of cytokeratin 8 in cells of the bovine nucleus pulposus complicates the search for specific intervertebral disc cell markers. *Arthritis Res Ther* **12**, R24, https://doi.org/10.1186/ar2931 (2010).
33. Ye, D. *et al*. Comparative and quantitative proteomic analysis of normal and degenerated human annulus fibrosus cells. *Clin Exp Pharmacol Physiol* **42**, 530–536, https://doi.org/10.1111/1440-1681.12386 (2015).
34. Purmessur, D. *et al*. Notochordal conditioned media from tissue increases proteoglycan accumulation and promotes a healthy nucleus pulposus phenotype in human mesenchymal stem cells. *Arthritis Res Ther* **13**, R81, https://doi.org/10.1186/ar3344 (2011).
35. Erwin, W. M. *et al*. The biological basis of degenerative disc disease: proteomic and biomechanical analysis of the canine intervertebral disc. *Arthritis Res Ther* **17**, 240, https://doi.org/10.1186/s13075-015-0733-z (2015).
36. Sarath Babu, N. *et al*. Quantitative proteomic analysis of normal and degenerated human intervertebral disc. *Spine J*, https://doi.org/10.1016/j.spinee.2016.03.051 (2016).
37. Onnerfjord, P., Khabut, A., Reinholt, F. P., Svensson, O. & Heinegard, D. Quantitative proteomic analysis of eight cartilaginous tissues reveals characteristic differences as well as similarities between subgroups. *J Biol Chem* **287**, 18913–18924, https://doi.org/10.1074/jbc.M111.298968 (2012).
38. Muller, C. *et al*. Quantitative proteomics at different depths in human articular cartilage reveals unique patterns of protein distribution. *Matrix Biol* **40**, 34–45, https://doi.org/10.1016/j.matbio.2014.08.013 (2014).
39. Yee, A. *et al*. Fibrotic-like changes in degenerate human intervertebral discs revealed by quantitative proteomic analysis. *Osteoarthritis Cartilage* **24**, 503–513, https://doi.org/10.1016/j.joca.2015.09.020 (2016).
40. Grad, S. *et al*. in *Global Spine J*. WO029.
41. Hristova, G. I. *et al*. Calcification in human intervertebral disc degeneration and scoliosis. *J Orthop Res* **29**, 1888–1895, https://doi.org/10.1002/jor.21456 (2011).
42. Riches, P. E., Dhillon, N., Lotz, J., Woods, A. W. & McNally, D. S. The internal mechanics of the intervertebral disc under cyclic loading. *J Biomech* **35**, 1263–1271 (2002).
43. Belluoccio, D. *et al*. Proteomic analysis of mouse growth plate cartilage. *Proteomics* **6**, 6549–6553, https://doi.org/10.1002/pmic.200600191 (2006).
44. Ellis, K., Bagwell, J. & Bagnat, M. Notochord vacuoles are lysosome-related organelles that function in axis and spine morphogenesis. *J Cell Biol* **200**, 667–679, https://doi.org/10.1083/jcb.201212095 (2013).
45. Le Maitre, C. L. *et al*. Altered integrin mechanotransduction in human nucleus pulposus cells derived from degenerated discs. *Arthritis Rheum* **60**, 460–469, https://doi.org/10.1002/art.24248 (2009).
46. Kurakawa, T. *et al*. Functional impact of integrin alpha5beta1 on the homeostasis of intervertebral discs: a study of mechanotransduction pathways using a novel dynamic loading organ culture system. *Spine J* **15**, 417–426, https://doi.org/10.1016/j.spinee.2014.12.143 (2015).
47. Gilbert, H. T., Nagra, N. S., Freemont, A. J., Millward-Sadler, S. J. & Hoyland, J. A. Integrin - dependent mechanotransduction in mechanically stimulated human annulus fibrosus cells: evidence for an alternative mechanotransduction pathway operating with degeneration. *PLoS One* **8**, e72994, https://doi.org/10.1371/journal.pone.0072994 (2013).

48. Margadant, C. & Sonnenberg, A. Integrin-TGF-beta crosstalk in fibrosis, cancer and wound healing. *EMBO Rep* **11**, 97–105, https://doi.org/10.1038/embor.2009.276 (2010).
49. Steffensen, B. *et al.* Fragmentation of fibronectin by inherent autolytic and matrix metalloproteinase activities. *Matrix Biol* **30**, 34–42, https://doi.org/10.1016/j.matbio.2010.09.004 (2011).
50. Yang, F., Leung, V. Y., Luk, K. D., Chan, D. & Cheung, K. M. Injury-induced sequential transformation of notochordal nucleus pulposus to chondrogenic and fibrocartilaginous phenotype in the mouse. *J Pathol* **218**, 113–121, https://doi.org/10.1002/path.2519 (2009).
51. Oegema, T. R. Jr., Johnson, S. L., Aguiar, D. J. & Ogilvie, J. W. Fibronectin and its fragments increase with degeneration in the human intervertebral disc. *Spine (Phila Pa 1976)* **205**, 2742–2747 (2000).
52. Zhang, X., Chen, C. T., Bhargava, M. & Torzilli, P. A. A Comparative Study of Fibronectin Cleavage by MMP-1, −3, −13, and −14. *Cartilage* **3**, 267–277, https://doi.org/10.1177/1947603511435273 (2012).
53. Ruel, N. *et al.* Fibronectin fragments and the cleaving enzyme ADAM-8 in the degenerative human intervertebral disc. *Spine (Phila Pa 1976)* **39**, 1274–1279, https://doi.org/10.1097/BRS.0000000000000397 (2014).
54. Liu, H. F. *et al.* A novel rabbit disc degeneration model induced by fibronectin fragment. *Joint Bone Spine* **80**, 301–306, https://doi.org/10.1016/j.jbspin.2012.07.009 (2013).
55. To, W. S. & Midwood, K. S. Plasma and cellular fibronectin: distinct and independent functions during tissue repair. *Fibrogenesis Tissue Repair* **4**, 21, https://doi.org/10.1186/1755-1536-4-21 (2011).
56. Mayer, J. E. *et al.* Genetic polymorphisms associated with intervertebral disc degeneration. *Spine J* **13**, 299–317, https://doi.org/10.1016/j.spinee.2013.01.041 (2013).
57. McDonald, J. A., Kelley, D. G. & Broekelmann, T. J. Role of fibronectin in collagen deposition: Fab' to the gelatin-binding domain of fibronectin inhibits both fibronectin and collagen organization in fibroblast extracellular matrix. *J Cell Biol* **92**, 485–492 (1982).
58. Antoniou, J. *et al.* The human lumbar intervertebral disc: evidence for changes in the biosynthesis and denaturation of the extracellular matrix with growth, maturation, ageing, and degeneration. *J Clin Invest* **98**, 996–1003, https://doi.org/10.1172/JCI118884 (1996).
59. Pankov, R. & Yamada, K. M. Fibronectin at a glance. *J Cell Sci* **115**, 3861–3863 (2002).
60. Lewis, M. PRELP, collagen, and a theory of Hutchinson-Gilford progeria. *Ageing Res Rev* **2**, 95–105 (2003).
61. Grover, J., Lee, E. R., Mounkes, L. C., Stewart, C. L. & Roughley, P. J. The consequence of PRELP overexpression on skin. *Matrix Biol* **26**, 140–143, https://doi.org/10.1016/j.matbio.2006.10.005 (2007).
62. Melching, L. I. & Roughley, P. J. A matrix protein of Mr 55,000 that accumulates in human articular cartilage with age. *Biochim Biophys Acta* **1036**, 213–220 (1990).
63. Hafez, A. *et al.* Col11a1 Regulates Bone Microarchitecture during Embryonic Development. *J Dev Biol* **3**, 158–176, https://doi.org/10.3390/jdb3040158 (2015).
64. Vaughan-Thomas, A., Young, R. D., Phillips, A. C. & Duance, V. C. Characterization of type XI collagen-glycosaminoglycan interactions. *J Biol Chem* **276**, 5303–5309, https://doi.org/10.1074/jbc.M008764200 (2001).
65. Podrazky, V., Stovickova, J., Novotna, J. & Trnavsky, K. Evidence for the degradation of type XI collagen by bovine intervertebral disc- and articular cartilage extracts. *Biol Chem Hoppe Seyler* **374**, 497–500 (1993).
66. Agarwal, P. *et al.* Collagen XII and XIV, new partners of cartilage oligomeric matrix protein in the skin extracellular matrix suprastructure. *J Biol Chem* **287**, 22549–22559, https://doi.org/10.1074/jbc.M111.335935 (2012).
67. Young, B. B., Zhang, G., Koch, M. & Birk, D. E. The roles of types XII and XIV collagen in fibrillogenesis and matrix assembly in the developing cornea. *J Cell Biochem* **87**, 208–220, https://doi.org/10.1002/jcb.10290 (2002).
68. Izu, Y., Ezura, Y., Koch, M., Birk, D. E. & Noda, M. Collagens VI and XII form complexes mediating osteoblast interactions during osteogenesis. *Cell Tissue Res* **364**, 623–635, https://doi.org/10.1007/s00441-015-2345-y (2016).
69. El-Shabrawi, Y., Kublin, C. L. & Cintron, C. mRNA levels of alpha1(VI) collagen, alpha1(XII) collagen, and beta ig in rabbit cornea during normal development and healing. *Invest Ophthalmol Vis Sci* **39**, 36–44 (1998).
70. Tassava, R. A., Nace, J. D. & Wei, Y. Extracellular matrix protein turnover during salamander limb regeneration. *Wound Repair Regen* **4**, 75–81, https://doi.org/10.1046/j.1524-475X.1996.40113.x (1996).
71. Bader, H. L. *et al.* Zebrafish collagen XIV is transiently expressed in epithelia and is required for proper function of certain basement membranes. *J Biol Chem* **288**, 6777–6787, https://doi.org/10.1074/jbc.M112.430637 (2013).
72. Fukushima, M., Hirano, S. & Tanaka, H. Dorsoventral differential distribution of collagen type XIV around the spinal cord is regulated by the ectoderm. *Dev Growth Differ* **41**, 751–758 (1999).
73. Hemmavanh, C., Koch, M., Birk, D. E. & Espana, E. M. Abnormal corneal endothelial maturation in collagen XII and XIV null mice. *Invest Ophthalmol Vis Sci* **54**, 3297–3308, https://doi.org/10.1167/iovs.12-11456 (2013).
74. Tono-Oka, S., Tanase, S., Miike, T. & Tanaka, H. Transient expression of collagen type XIV during muscle development and its reappearance after denervation and degeneration. *J Histochem Cytochem* **44**, 907–918 (1996).
75. Thorimbert, V., Konig, D., Marro, J., Ruggiero, F. & Jazwinska, A. Bone morphogenetic protein signaling promotes morphogenesis of blood vessels, wound epidermis, and actinotrichia during fin regeneration in zebrafish. *FASEB J* **29**, 4299–4312, https://doi.org/10.1096/fj.15-272955 (2015).
76. Pfeiffer, M. *et al.* Intradiscal application of hyaluronic acid in the non-human primate lumbar spine: radiological results. *Eur Spine J* **12**, 76–83, https://doi.org/10.1007/s00586-002-0478-7 (2003).
77. Demers, C. N., Antoniou, J. & Mwale, F. Value and limitations of using the bovine tail as a model for the human lumbar spine. *Spine (Phila Pa 1976)* **29**, 2793–2799 (2004).
78. Battie, M. C., Videman, T. & Parent, E. Lumbar disc degeneration: epidemiology and genetic influences. *Spine (Phila Pa 1976)* **29**, 2679–2690 (2004).
79. Boos, N. *et al.* Classification of age-related changes in lumbar intervertebral discs: 2002 Volvo Award in basic science. *Spine (Phila Pa 1976)* **27**, 2631–2644, https://doi.org/10.1097/01.BRS.0000035304.27153.5B (2002).
80. Illien-Junger, S., Walter, B. A., Mayer, J. E., Hecht, E. C. & Iatridis, J. C. In *The Intervertebral* Disc (eds I. M. Shapiro & M. V. Risbud) 353-371 (Springer Vienna, 2013).
81. Hansen, H. J. Studies on the pathology of the lumbosacral disc in female cattle. *Acta Orthop Scand* **25**, 161–182 (1956).
82. Oshima, H., Ishihara, H., Urban, J. P. & Tsuji, H. The use of coccygeal discs to study intervertebral disc metabolism. *J Orthop Res* **11**, 332–338, https://doi.org/10.1002/jor.1100110304 (1993).
83. Roberts, S., Menage, J., Duance, V., Wotton, S. & Ayad, S. 1991 Volvo Award in basic sciences. Collagen types around the cells of the intervertebral disc and cartilage end plate: an immunolocalization study. *Spine (Phila Pa 1976)* **16**, 1030–1038 (1991).
84. Sakai, D., Nakai, T., Mochida, J., Alini, M. & Grad, S. Differential phenotype of intervertebral disc cells: microarray and immunohistochemical analysis of canine nucleus pulposus and anulus fibrosus. *Spine (Phila Pa 1976)* **34**, 1448–1456, https://doi.org/10.1097/BRS.0b013e3181a55705 (2009).
85. Ishihara, H., McNally, D. S., Urban, J. P. & Hall, A. C. Effects of hydrostatic pressure on matrix synthesis in different regions of the intervertebral disk. *J Appl Physiol (1985)* **80**, 839–846 (1996).
86. Ohshima, H., Urban, J. P. & Bergel, D. H. Effect of static load on matrix synthesis rates in the intervertebral disc measured *in vitro* by a new perfusion technique. *J Orthop Res* **13**, 22–29, https://doi.org/10.1002/jor.1100130106 (1995).

Acknowledgements

We would like to acknowledge Daniela Silva for running the SEM, as well as Carnes Landeiro, SA and Matadouro e Carnes Linda Rosa, Lda for kindly providing the bovine tails. We are also grateful to Professor Katheleen Keller, Dr. Nick Morris and Dr. Gregory Lunstrum for the collagen XII and XIV antibodies. In addition, we thank Marta Pinto for the technical support on Western Blot troubleshooting, Ana Maria Magalhães and Stefan Mereiter for the tips on sample deglycosylation, as well as Catarina Leite Pereira, Morena Fiordalisi and Graciosa Teixeira for the help with tail dissection. Supported by: The Portuguese Foundation for Science and Technology (FCT) (Projects: PTDC/SAU-NEU/103728/2008, PTDC/NEU-NMC/0205/2012, UID/NEU/04539/2013; Post-Doc grants: SFRH/BPD/78187/2011-JC, SFRH/BD/88419/2012-CS and SFRH/BD/80577/2011-MM; and the Investigator Programme: IF/00638/2014. IPATIMUP is an Associate Laboratory of the Portuguese Ministry of Science, Technology and Higher Education and is partially supported by FCT. This work was co-financed by FEDER - Fundo Europeu de Desenvolvimento Regional funds through the COMPETE 2020 - Operational Programme for Competitiveness and Internationalisation (POCI), Portugal 2020, and by Portuguese funds through FCT—Fundação para a Ciência e a Tecnologia/Ministério da Ciência, Tecnologia e Inovação in the framework of the project "Institute for Research and Innovation in Health Sciences" (POCI-01–0145-FEDER-007274). This work also had the financial support of FCT / MEC through National Funds and, when applicable, co-financed by the FEDER via the PT2020 Partnership Agreement under the 4293 Unit I&D. Last but not least, it was also financed by QREN (Quadro de Referência Estratégica Nacional) and by The National Mass Spectrometry Network (RNEM) (REDE/1506/REM/2005).

Author Contributions

Joana Caldeira—acquisition of data; analysis and interpretation of data; drafting of the manuscript. Cátia Santa—acquisition of data; analysis and interpretation of data. Hugo Osório—acquisition of data; analysis and interpretation of data. Maria Molinos—acquisition of data. Bruno Manadas—provided expertise in proteomics and critical revision of the manuscript for important intellectual content. Raquel Gonçalves—critical revision of the manuscript for important intellectual content. Mário Barbosa—provided expertise in the intervertebral disc field and supervision of the work.

Additional Information

Supplementary information accompanies this paper at https://doi.org/10.1038/s41598-017-11960-0.

Competing Interests: The authors declare that they have no competing interests.

Publisher's note: Springer Nature remains neutral with regard to jurisdictional claims in published maps and institutional affiliations.